Supporting Information

CO_2 capture with post-modified consumer acrylonitrile plastics

Authors: Simon S. Pedersen[1,2]*, Clemens Kaussler[1,2], Ruth Ebenbauer[1,2], Thomas B. Bech[1,2], Riccardo Giovanelli[1–3], Martin L. Henriksen[4], Dennis Wilkens Juhl[2], Niels Christian Nielsen[2], Troels Skrydstrup[1,2]*

Affiliations:

[1]Carbon Dioxide Activation Center (CADIAC), Aarhus University; Gustav Wieds Vej 14, 8000 Aarhus C, Denmark.

[2]Interdisciplinary Nanoscience Center, Department of Chemistry, Aarhus University; Gustav Wieds Vej 14, 8000 Aarhus C, Denmark.

[3]Dipartimento di Chimica "Giacomo Ciamician" Alma Mater Studiorum – Università di Bologna, Via Piero Gobetti 85, 40126 Bologna, Italy.

[4]Department of Biological and Chemical Engineering, Aarhus University; Aabogade 40, 8200 Aarhus N, Denmark.

*Corresponding author. Email: ssp@inano.au.dk, ts@chem.au.dk

Table of Contents

General Information

General Methods: All purchased chemicals were used as received without further purification. Autoclaves were pressurised using a 5000 Multi Reactor System (Parr®) or a Berghof® BR-300 autoclave with hydrogen (99.999% purity) from Air Liquide. The pressure vessels were heated in aluminum blocks specially designed to fit the vessels. Lewatit VP OC 1065 (from now on only referred to as Lewatit) is commercialised by Lanxess® and was purchased through SigmaAldrich as 0.5 mm pellets, which were cryogenically milled to a powder before CO_2-adsorption TGA experiments. All polymer samples, besides SBR1 and one example with ABS1 (10 g scale), were cut to smaller pieces with scissors or a wire cutter prior to reaction. When necessary, solvents were dried according to standard procedures and degassed by bubbling with argon for minimum 30 minutes. Flash column chromatography was carried out on silica gel 60 (230-400 mesh). The solution-state ^{1}H−NMR spectra were recorded at 400 MHz, ^{13}C−NMR spectra were recorded at 101 MHz, and ^{31}P−NMR were recorded at 162 MHz on a Bruker 400 spectrometer. Chemical shifts are reported in ppm relative to solvent residual peak. Coupling patterns in the NMR spectra are abbreviated as follows: s = singlet, d = doublet, t = triplet, q = quartet, quint = quintuplet, sext = sextet, sep = septet, m = multiplet, br = broad, dd = double doublet, dt = double triplet, ddd = double double doublet. NMR spectra are reported as follows: (multiplicity; coupling constant(s) in Hz; integration). HRMS spectra were recorded on a LC TOF (ES) apparatus. GC experiments were conducted using an Agilent 8890 GC System (Column: HP-5 5% Phenyl methyl siloxane, 30 m x 250 µm x 0.25 µm). IR spectra were obtained with a Bruker FTIR Alpha II spectrometer. Elemental analysis (CHNS) was conducted on a EuroVector EA3100, calibrated with acetanilide and sulfanilamide.

Handling of HCN: All reactions with HCN were performed in a two-chamber system, in which gaseous HCN was released in chamber A and utilized in chamber B. The two-chamber system (COWare®) is depicted to the right and is composed of two glass vials (Chamber A and B) connected with a glass tube to allow gas-transfer (Total Volume = 20 mL.). Large scale reactions were conducted with an identical but larger two-chamber system (Total Volume = 100 mL). The chambers can be sealed with a screw cap and a Teflon® coated silicone seal. HCN gas was released from KCN in ethylene glycol dimethyl ether with AcOH at rt.[1] Precise conditions are given in the general procedures.

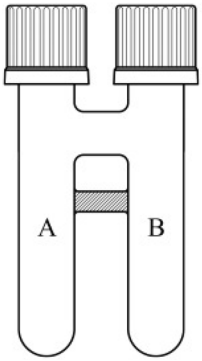

WARNING: Glassware under pressure!

- Glass equipment should always be examined for damages to its surface, which may weaken its strength.
- One must abide to all laboratory safety procedures and always work behind a shield when working with glass equipment under pressure.
- COware is pressure tested to 224 psi (15.4 bar) but should under no circumstances be operated above 60 psi (5 bar).
- Take pre-cautions to toxic HCN gas by only working in a well-ventilated fume-hood!

Thermogravimetric Analysis (TGA)

Decomposition analysis was obtained under a helium atmosphere in a Mettler Toledo TGA/DSC 3+. Sample sizes of 5−12 mg were weighed using an A&D BM-22 microbalance into an Alox 70 µL or Alox 150 µL crucible, which was sealed with a holed Alox lid (**TGA method 1**). The samples were held at 25 °C for 10 min. and then heated at 10 °C min^{-1} from 25 °C to 650 °C under a flow of helium (50 mL/min), after which the atmosphere was changed to air (50 mL/min) to burn off residuals for 30 min. The first derivative of the curve (25 points) was found using the Mettler Toledo StarE software, and the degradation temperature (T_d) was found as the derivative's apex.

CO_2-adsorption/desorption analysis was obtained under various atmosphere combinations in a Mettler Toledo TGA/DSC 3+. The gases used include helium, CO_2, N_2, CO_2/N_2 (10% ± 0.2 mol% CO_2), NO_2 (203 ppm in N_2), and SO_2 (206 ppm in N_2), all at a gas flow of 100 mL/min. For all experiments, an N_2-balance protection gas was also needed (20 mL/min), which could dilute reaction gas concentration to a minor extent, however for simplicity when using e.g. a gas line with 100% CO_2, we report this as adsorption under 100% CO_2. Sample sizes of 5−15 mg were weighed using an A&D BM-22 microbalance into aluminium 100 µL crucibles. Alternatively, an auto-weighing in method by the Mettler Toledo TGA/DSC 3+ was used with pre-weighed sample crucibles. The exact methods used (temperature, time, and gas composition) are listed below for the individual TGA methods.

TGA method 2. 5 *h dry CO_2 capacity (100% CO_2 or 10% CO_2/N_2, 25 °C, 50 °C, or 90 °C)*: The samples were subjected to a flow of helium (100 mL/min) for 10 min at 25 °C and were then heated at 10 °C min^{-1} from 25 °C to 130 °C under a flow of helium (100 mL/min) and then held at 130 °C for 15 min. Thereafter, the samples were cooled to 25 °C by 5 °C min^{-1}, followed by a switch of atmosphere to CO_2 (100%, 100 mL/min) and held as such for 5 h. Hereafter, the atmosphere was changed back to helium (100 mL/min) and the samples were heated at 10 °C min^{-1} from 25 °C to 130 °C under a flow of helium (100 mL/min) and then held at 130 °C for 15 min. Thereafter, the samples were cooled to 50 °C by 5 °C min^{-1}, followed by a switch of atmosphere to CO_2 (100%, 100 mL/min) and held as such for 5 h. Hereafter, the atmosphere was changed back to helium (100 mL/min) and the samples were heated at 10 °C min^{-1} from 50 °C to 130 °C under a flow of helium (100 mL/min) and then held at 130 °C for 15 min. Thereafter, the samples were cooled to 90 °C by 5 °C min^{-1}, followed by a switch of atmosphere to CO_2 (100%, 100 mL/min) and held as such for 5 h. Hereafter, the atmosphere was changed back to helium (100 mL/min) and the samples were heated at 10 °C min^{-1} from 90 °C to 130 °C under a flow of helium (100 mL/min) and then held at 130 °C for 15 min. From here, the method repeats the above using CO_2 (10% in N_2) instead of 100% CO_2.

*Note: For some samples **TGA method 2** was divided into two runs, namely one that measures the adsorption at 25 °C, 50 °C, and 90 °C with 100% CO_2, and another run that measures the adsorption at 25 °C, 50 °C, and 90 °C with 10% CO_2 balanced by N_2.*

TGA method 3. *5 h dry CO_2 capacity (25 °C):* The samples were subjected to a flow of helium (100 mL/min) for 10 min at 25 °C and were then heated at 10 °C min^{-1} from 25 °C to 130 °C under a flow of helium (100 mL/min) and then held at 130 °C for 15 min. Thereafter, the samples were cooled to 25 °C by 5 °C min^{-1} and held at 25 °C for 15 min. followed by a switch of atmosphere to CO_2 (100%, 100 mL/min) and held as such for 5 h. Hereafter, the atmosphere was changed back to helium (100 mL/min) and the samples were heated at 10 °C min^{-1} from 25 °C to 130 °C under a flow of helium (100 mL/min) and then held at 130 °C for 15 min. Thereafter, the samples were cooled to 25 °C by 5 °C min^{-1} and held at 25 °C for 10 min.

TGA method 4. *40 cycles of adsorption-desorption under simulated flue gas conditions (90 °C / 150 °C):* The samples were subjected to a flow of helium (100 mL/min) for 10 min at 25 °C and were then heated at 10 °C min^{-1} from 25 °C to 130 °C under a flow of helium (100 mL/min) and then held at 130 °C for 15 min. Thereafter, the samples were cooled to 90 °C by 5 °C min^{-1} and held at 90 °C for 15 min. followed by a switch of atmosphere to CO_2 (10% in N_2, 100 mL/min) and held as such for 15 min. This was followed by a switch of atmosphere to CO_2 (100%, 100 mL/min) heating at 10 °C min^{-1} from 90 °C to 150 °C and held at that temperature for 15 min. The atmosphere was then switched to helium (100 mL/min) and the samples were cooled at 10 °C min^{-1} from 150 °C to 90 °C, followed by a switch of atmosphere to CO_2 (10% in N_2, 100 mL/min) and held as such for 15 min. The cycle of CO_2 (10% in N_2, 90 °C), CO_2 (100%, 150 °C), and helium (cooling from 150 °C to 90 °C), was then repeated giving in all a total of 40 adsorption-desorption cycles.

TGA method 5. *Helium, 10 h, 150 °C, stress test:* The samples were subjected to a flow of helium (100 mL/min) for 10 min at 25 °C and were then heated at 10 °C min^{-1} from 25 °C to 130 °C under a flow of helium (100 mL/min) and then held at 130 °C for 15 min. Thereafter, the samples were cooled to 25 °C by 10 °C min^{-1} and held at 25 °C for 15 min. followed by a switch of atmosphere to CO_2 (100%, 100 mL/min) and held as such for 5 h. Hereafter, the atmosphere was changed back to helium (100 mL/min) and the samples were heated at 5 °C min^{-1} from 25 °C to 130 °C under a flow of helium (100 mL/min) and then held at 130 °C for 15 min. The samples were then heated at 5 °C min^{-1} from 130 °C to 150 °C followed by 10 hours at 150 °C, and then cooled at 5 °C min^{-1} from 150 °C to 25 °C, held at 25 °C for 15 min., before switching to CO_2 (100%, 100 mL/min) and held as such for 5 h.

TGA method 6. *Air, 10 h, 150 °C, stress test:* The method is identical to **TGA method 5**, only differing in the 10 hour segment, where this method uses compressed air (100 mL/min) instead of helium.

TGA method 7. *CO_2, 10 h, 150 °C, stress test:* The method is identical to **TGA method 5**, only differing in the 10 hour segment, where this method uses CO_2 (100 mL/min) instead of helium.

TGA method 8. *NO_2, 10 h, 25 °C, stress test:* The samples were subjected to a flow of helium (100 mL/min) for 10 min at 25 °C and were then heated at 10 °C min^{-1} from 25 °C to 130 °C under a flow of helium (100 mL/min) and then held at 130 °C for 15 min. Thereafter, the samples were cooled to 25 °C by 10 °C min^{-1} and held at 25 °C for 15 min. followed by a switch of atmosphere to CO_2 (100%, 100 mL/min) and held as such for 5 h. Hereafter, the atmosphere was changed back to helium (100 mL/min) and the samples were heated at 5 °C min^{-1} from 25 °C to 130 °C under a flow of helium (100 mL/min) and then held at 130 °C for 15 min. Thereafter, the samples were cooled to 25 °C by 10 °C min^{-1} and held at 25 °C for 15 min. followed by a switch of atmosphere to NO_2 (203 ppm in N_2, 100 mL/min) and held as such for 10 h. The samples were then heated at 10 °C min^{-1} from 25 °C to 130 °C under a flow of helium (100 mL/min) and then held at 130 °C for 15 min. Thereafter, the samples were cooled to 25 °C by 10 °C min^{-1} and held at 25 °C for 15 min. followed by a switch of atmosphere to CO_2 (100%, 100 mL/min) and held as such for 5 h.

TGA method 9. *SO_2, 10 h, 25 °C, stress test:* Identical to the **TGA method 8**, however using SO_2 (206 ppm in N_2, 100 mL/min) instead of NO_2 (203 ppm in N_2, 100 mL/min).

TGA method 10. *40 cycles stress test:* The samples were subjected to a flow of helium (100 mL/min) for 10 min at 25 °C and were then heated at 10 °C min^{-1} from 25 °C to 130 °C under a flow of helium (100 mL/min) and then held at 130 °C for 15 min. Thereafter, the samples were cooled to 50 °C by 5 °C min^{-1} and held at 50 °C for 15 min. followed by a switch of atmosphere to CO_2 (10% in N_2, 100 mL/min) and held as such for 15 min. This was followed by a switch of atmosphere to CO_2 (100%, 100 mL/min) heating at 10 °C min^{-1} from 50 °C to 150 °C and held at that temperature for 15 min. The atmosphere was then switched to helium (100 mL/min) and the samples were cooled at 10 °C min^{-1} from 150 °C to 50 °C, followed by a switch of atmosphere to CO_2 (10% in N_2, 100 mL/min) and held as such for 15 min. The cycle of CO_2 (10% in N_2, 50 °C), CO_2 (100%, 150 °C), helium (cooling from 150 °C to 50 °C), was then repeated giving in all a total of 40 adsorption-desorption cycles.

TGA method 11. *Desorption study using helium as purge gas:* The samples were subjected to a flow of helium (100 mL/min) for 10 min at 25 °C and were then heated at 10 °C min^{-1} from 25 °C to 130 °C under a flow of helium (100 mL/min) and then held at 130 °C for 15 min. Thereafter, the samples were cooled to 25 °C by 10 °C min^{-1} and held at 25 °C for 15 min. followed by a switch of atmosphere to CO_2 (100%, 100 mL/min) and held as such for 5 h. Hereafter, the atmosphere was changed back to helium (100 mL/min) and the samples were held at 25 °C for 30 min., then heated at 5 °C min^{-1} to 50 °C and held at that temperature for 30 min. This was then repeated for 60 °C, 70 °C, 80 °C, 90 °C, 100 °C, 110 °C, 120 °C, and 130 °C.

TGA method 12. *Desorption study using CO_2 as purge gas:* The samples were subjected to a flow of helium (100 mL/min) for 10 min at 25 °C and were then heated at 10 °C min^{-1} from 25 °C to 130 °C under a flow of helium (100 mL/min) and then held at 130 °C for 15 min. Thereafter, the samples were cooled to 25 °C by 10 °C min^{-1} and held at 25 °C for 15 min. followed by a switch of atmosphere to CO_2 (100%, 100 mL/min) and held as such for 5 h. Hereafter, the samples were heated at 5 °C min^{-1} to 100 °C and held at that temperature for 30 min. This was then repeated for 110 °C, 120 °C, 130 °C, 140 °C, and 150 °C.

TGA method 13. *Temperature-programmed desorption*: The samples were subjected to a flow of helium (100 mL/min) for 10 min at 25 °C and were then heated at 10 °C min^{-1} from 25 °C to 130 °C under a flow of helium (100 mL/min) and then held at 130 °C for 15 min. Thereafter, the samples were cooled to 25 °C by 10 °C min^{-1} and held at 25 °C for 15 min. followed by a switch of atmosphere to CO_2 (100%, 100 mL/min) and held as such for 5 h. Hereafter, the atmosphere was changed back to helium (100 mL/min) and the samples were heated at 1 °C min^{-1} from 25 °C to 150 °C under a flow of helium (100 mL/min).

Note for all TGA graphs: The temperature depicted on the X-axis is the reference temperature, while inflection-, midpoint- and peak values correspond to the sample temperature.

Differential Scanning Calorimetry (DSC)

All substrates and polymers were analysed by TGA/DSC analysis, and with the decomposition analysis method described under "Thermogravimetric Analysis (TGA)", any thermal events besides decomposition and evaporation of volatiles were identified. For simplicity, the DSC curves for such polymers are left out, and only DSC curves for polymers displaying visible glass transitions or melting points are reported. For those samples, specific methods were used to better observe the thermal events:

DSC method 1 (for ABS and SAN polymers): The samples were heated at 5 °C min^{-1} under a flow of helium (50 mL/min) from 25 °C to 300 °C and subsequently cooled to 25 °C by 5 °C min^{-1}. The samples were held at 25 °C for 15 min, and thereafter heated at 5 °C min^{-1} under a flow of helium (50 mL/min) from 25 °C to 300 °C and subsequently cooled to 25 °C by 5 °C min^{-1}. Finally, the samples were held at 25 °C for 15 min. *The glass transitions were best observed during the second heating ramp, due to removal of volatiles during the first heating ramp.*

DSC method 2 (for acrylic textiles): The samples were heated at 5 °C min^{-1} under a flow of helium (50 mL/min) from 25 °C to 350 °C and subsequently cooled to 25 °C by 5 °C min^{-1}. The samples were held at 25 °C for 15 min, and thereafter heated at 5 °C min^{-1} under a flow of helium (50 mL/min) from 25 °C to 350 °C and subsequently cooled to 25 °C by 5 °C min^{-1}. Finally, the samples were held at 25 °C for 15 min. *No glass transitions were observed for these samples but melting points of PA-6 and PET co-polymers were observed during the first heating ramp.*

Cryogenic Milling

All polymer products and some substrates were cryogenically milled using a Retsch® Cryo-mill.

Samples were subjected to 9 cycles of 2 minutes grinding at 30 Hz under cooling with liquid nitrogen. Between grinding cycles, 0.5 min of cooling was applied under 5 Hz frequency. For starting materials and scale-up products, the grinding jar was of a nominal volume of 50.0 mL and two steel balls of Ø15 mm were used. In case of regular $\leq$ 1 g-scale hydrogenation products, the grinding jar was of a nominal volume of 10.0 mL and two steel balls of Ø10 mm were used.

Particle size sieving

If stated specifically, some adsorbents were sieved with a FRITSCH Analysette 3 PRO sieve shaker in combination with Retsch® sieves with apertures 106 µm (mesh 140) and 25 µm (mesh 500), thus collecting a particle sizes range of -140 +500 mesh.

N_2-physisorption (BET)

Nitrogen adsorption and desorption measurements were performed using a Quantachrome iQ2 autosorp instrument at 77 K, after outgassing samples under vacuum for 48 hours at 50 °C using a home-built setup. Approximately 100 mg of each sample was used for each measurement, and the attempts to estimate the BET surface areas were made by considering the straight line through the data points in the p/p0 range of 0.05-0.3.

Analysis of three adsorbent materials, **H-NBR2**, **H-ABS2**, and **H-SAN2**, showed surface area values below the detection limit, thus indicating non-porous materials.

Scanning Electron Microscopy (SEM)

Scanning electron microscopy (SEM) pictures were recorded on a Tescan Clara using its Everhart-Thornley detector. The depth imaging mode was commonly employed with beam currents of 300 pA to 3 nA and acceleration voltages between 5 and 20 kV. Powder samples for SEM imaging were prepared by attaching a few milligrams of polymer product to carbon adhesive discs (Leit tabs), mounted on 12 mm aluminium specimen stubs. Excess powder was removed by tapping and blowing with pressurized air. A platinum coating of 6 nm thickness was then sputtered onto the samples with a Leica EM SCD 500 to minimize charging effects.

^{13}C Cross-Polarisation Magic-Angle-Spinning Nuclear Magnetic Resonance (^{13}C CP/MAS NMR)

All experiments were performed at a 9.4 T magnetic field (400 MHz for ^{1H}) on a Bruker Avance II spectrometer, equipped with a 4 mm HXY MAS probe, and the MAS rate was 15 kHz for all measurements. Carbon spectra (^{1}H–^{13}C CP) were acquired with 512−16384 scans depending on the mobility of the sample, a relaxation delay of 2.5 s and an acquisition time of 15 ms. The ^{1}H 90° pulse was 3.32 µs and the CP contact time was set to 3.5 ms using a 80-100% ramp on the ^{13}C channel and using 50 kHz and 35 kHz rf field strength on the ^{1}H and ^{13}C channels, respectively. The Spinal64 program was used for ^{1}H decoupling during acquisition with an rf field strength of 100 kHz. ^{13}C chemical shifts were referenced against adamantane (38.5 ppm tertiary carbon).

Solubility studies

Unless otherwise stated, the relevant polymer (between 1−5 mg) was added to 1.5−4 mL of solvent and left overnight at room temperature and then determined to be dissolved, swelled, or not dissolved.

Polymer Substrate Characterisation

Nitrile Butadiene Rubber 1 (NBR1, NBR block) was purchased from SigmaAldrich and used without further purification. The label stated a 37–39 wt% acrylonitrile, however we determined the content to be 40 wt% by elemental analysis. Smaller pieces were generated by cutting with scissors and used as such in the catalytic hydrogenation. The polymer was analysed with ^{1}H– and ^{13}C–NMR, solid-state ^{13}C CP/MAS NMR, IR-, TGA-, DSC-, and elemental analysis. Solubility tests were also conducted with several solvents. No thermal events besides decomposition were observed with DSC.

Particle sizes used for the catalytic hydrogenation reactions

Solubility chart

Soluble **Swells** **Not soluble**

$CHCl_3$	Acetone	*i*-PrOH	DMF	DMSO	THF	PhMe	H_2O	MeOH	MeCN

^{1}H–NMR ($CDCl_3$)

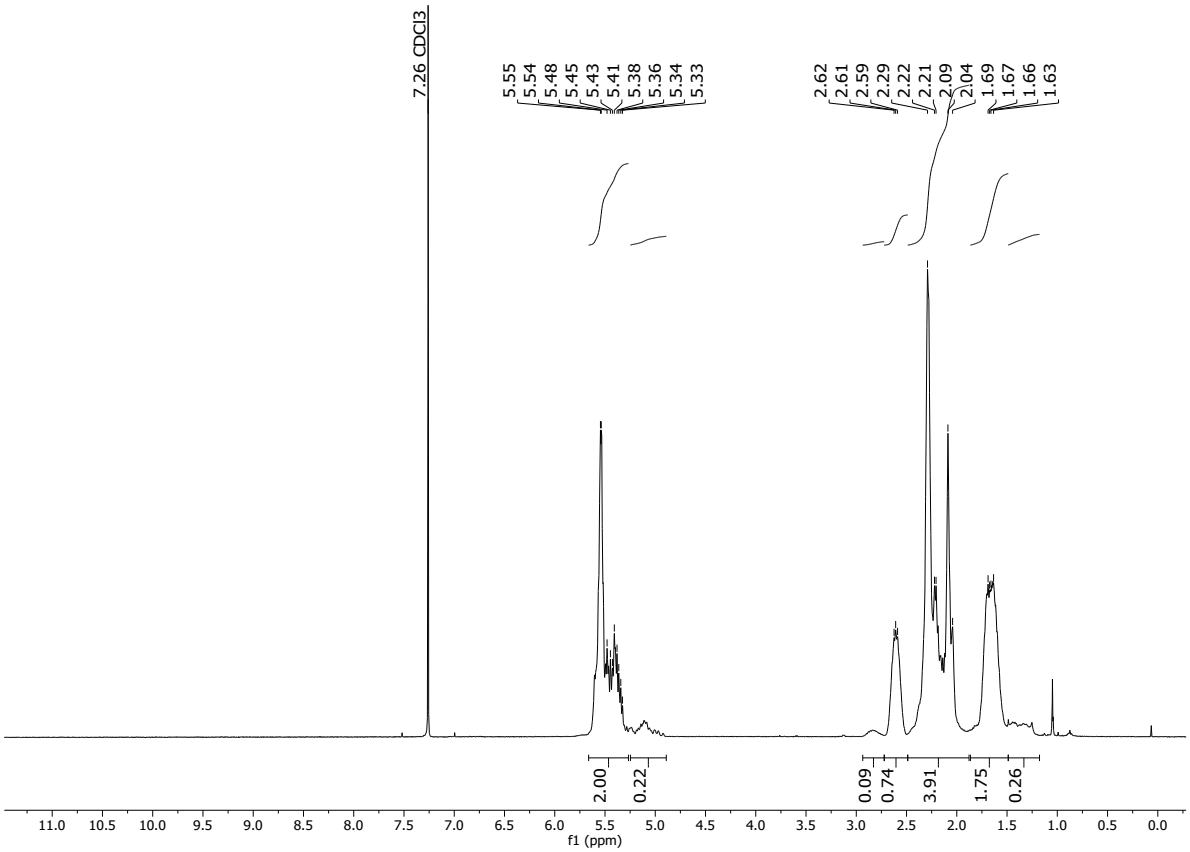

^{13}C–NMR ($CDCl_3$)

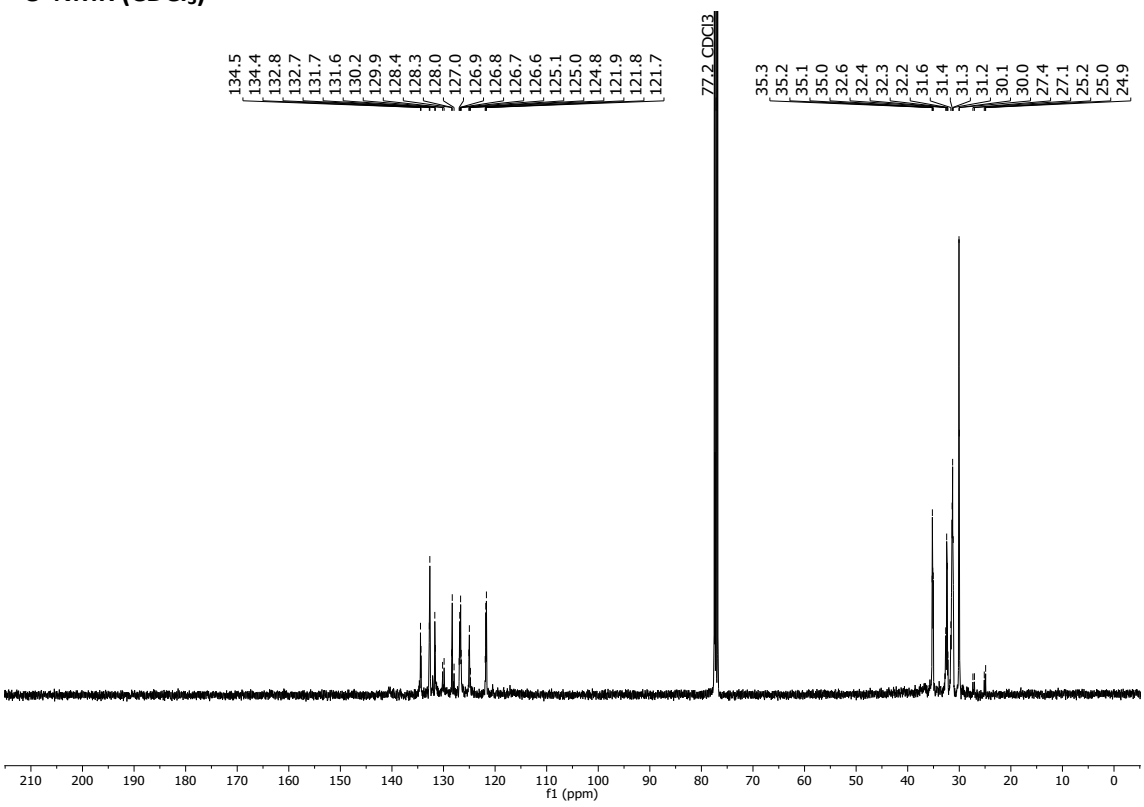

^{13}C CP/MAS NMR (solid-state)

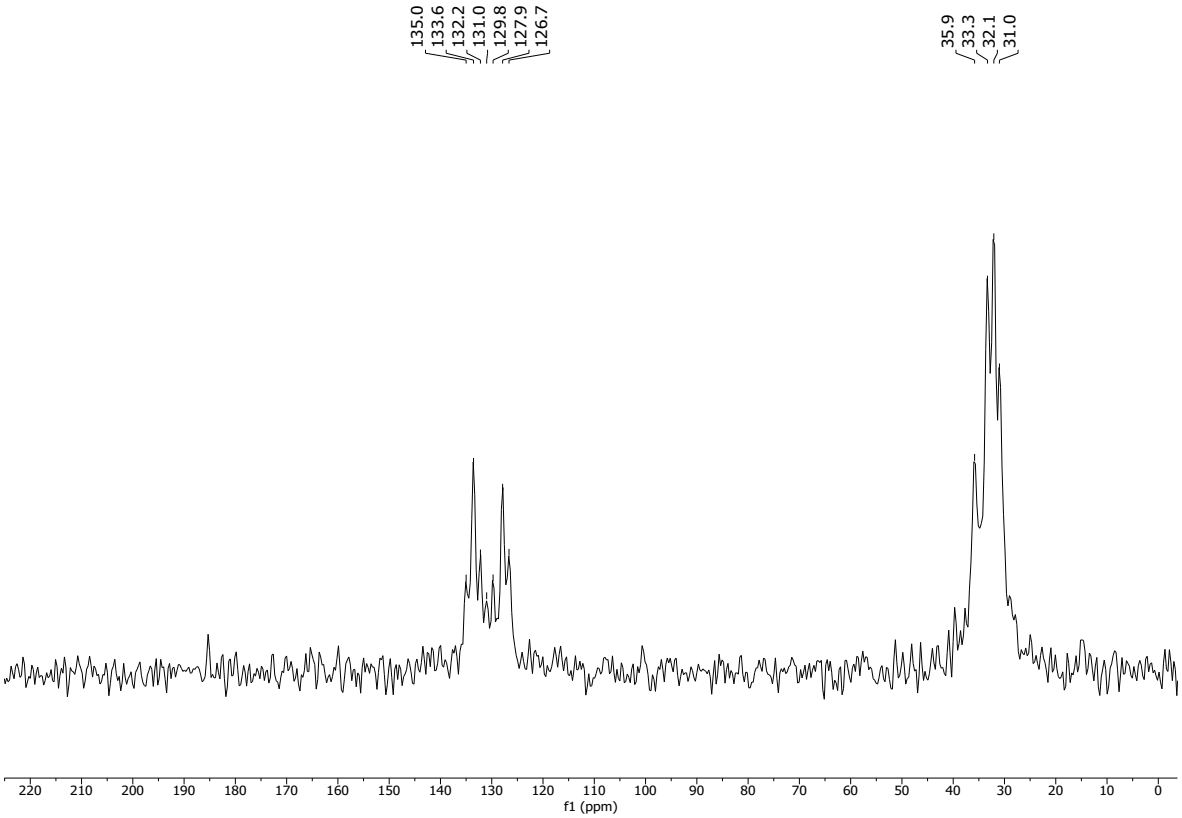

Infrared (IR) Spectroscopic Analysis

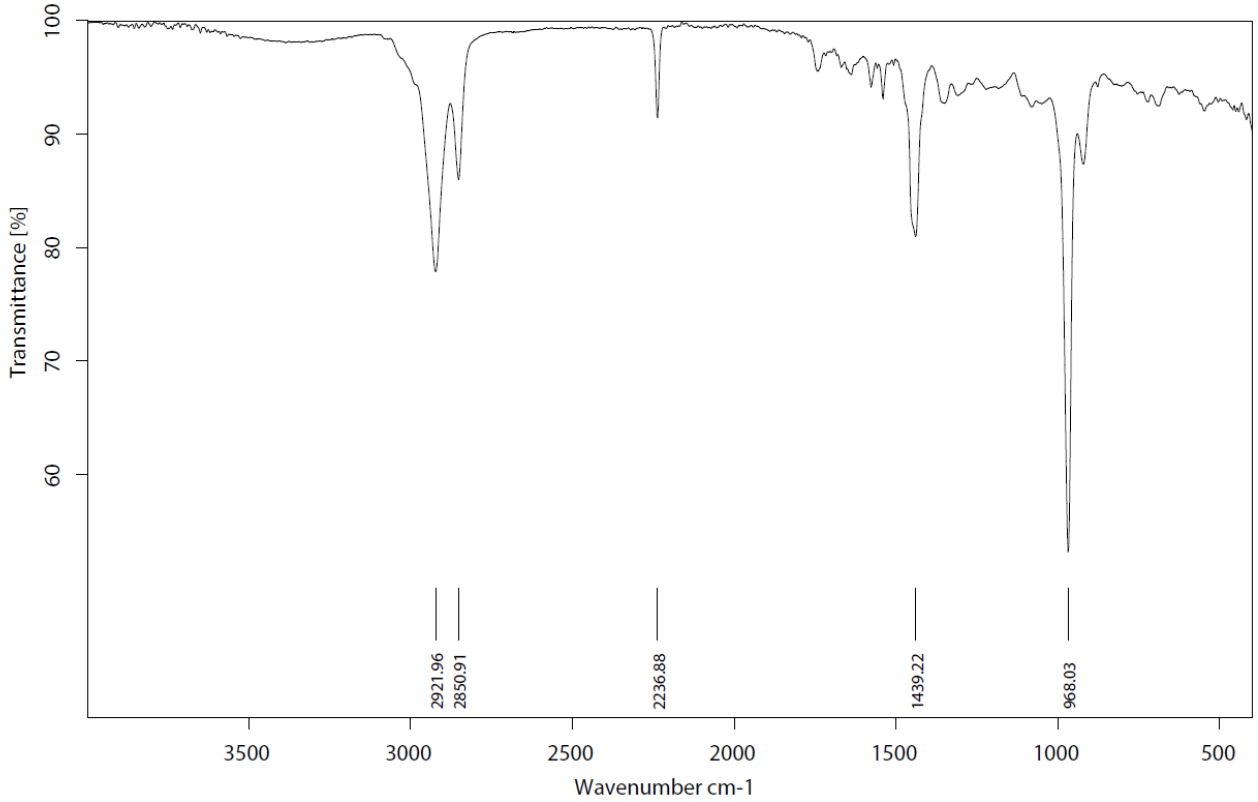

Thermogravimetric Analysis (TGA)

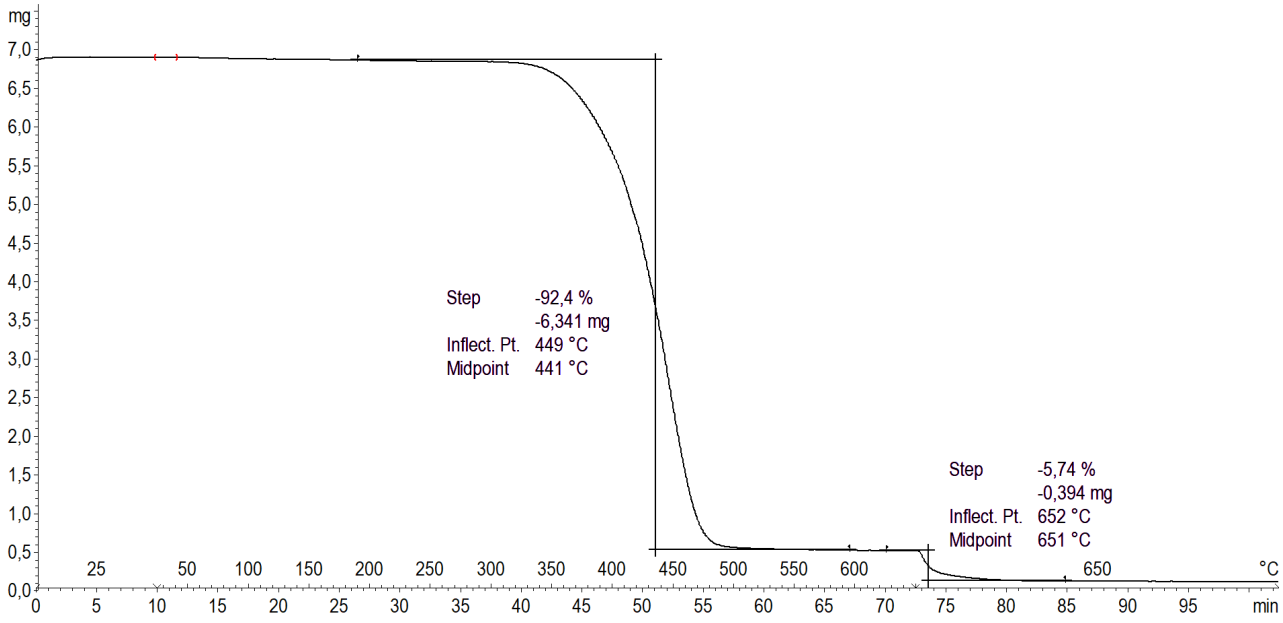

Decomposition graph. The experiment was conducted under He then air (after 650 °C).

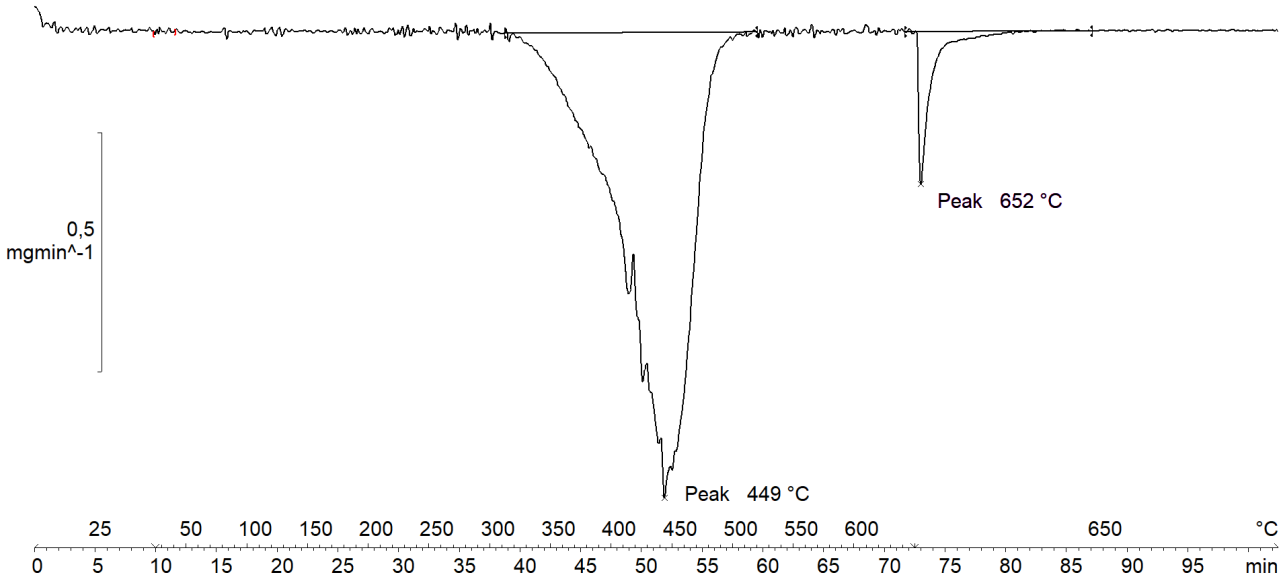

1st derivative of decomposition graph. The experiment was conducted under He then air (after 650 °C).

Decomposition temperature (T_d) = 449 °C.

Elemental Analysis (EA)

N [%]	C [%]	H [%]	S [%]	mmol N/g	C/N ratio	C/H ratio
10.53	**77.78**	**8.69**	**Not detected**	**7.52**	**8.62**	**0.75**

Acrylonitrile weight percentage calculation (AN%):
N% = 10.53
M(N) = 14.0067 g/mol
M(AN) = 53.06 g/mol
$AN\% = \frac{N\%}{M(N)} \cdot M(AN)$ = 40%

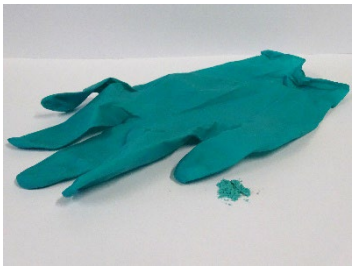

Nitrile Butadiene Rubber 2 (NBR2, Nitrile glove) was purchased from Ansell (glove producer) and used without further purification. Smaller pieces were generated by cutting with scissors or cryogenically milled and used as such in the catalytic hydrogenation or hydrocyanation. The polymer was analysed with solid-state ^{13}C CP/MAS NMR, IR-, TGA-, and elemental analysis. Solubility tests were also conducted with several solvents. Since this is a vulcanised polymer, solution state NMR was not an option. No thermal events besides decomposition were observed with DSC.

Particle size used for the catalytic hydrogenation (run 1 and run 2)

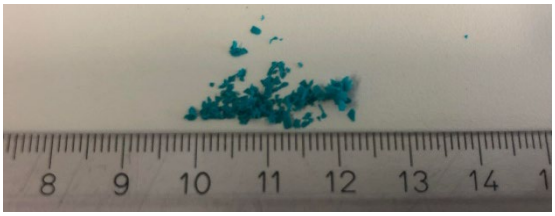

Particle size of NBR2 after cryogenic milling used for hydrogenation reactions (run 3 and run 5) and hydrocyanation reactions

Solubility chart

Soluble **Swells** **Not soluble**

$CHCl_3$	Acetone	*i*-PrOH	DMF	DMSO	THF	PhMe	H_2O	MeOH	MeCN

^{13}C CP/MAS NMR (solid-state)

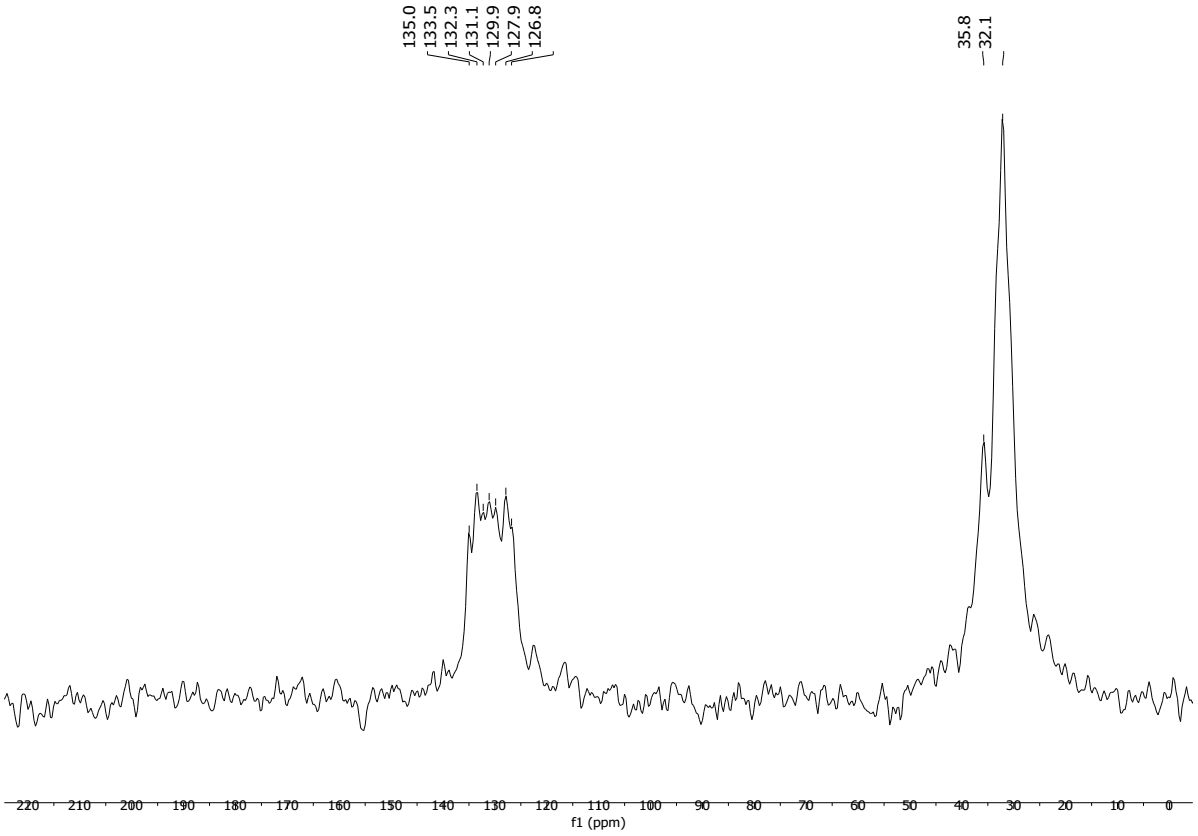

Infrared (IR) Spectroscopic Analysis

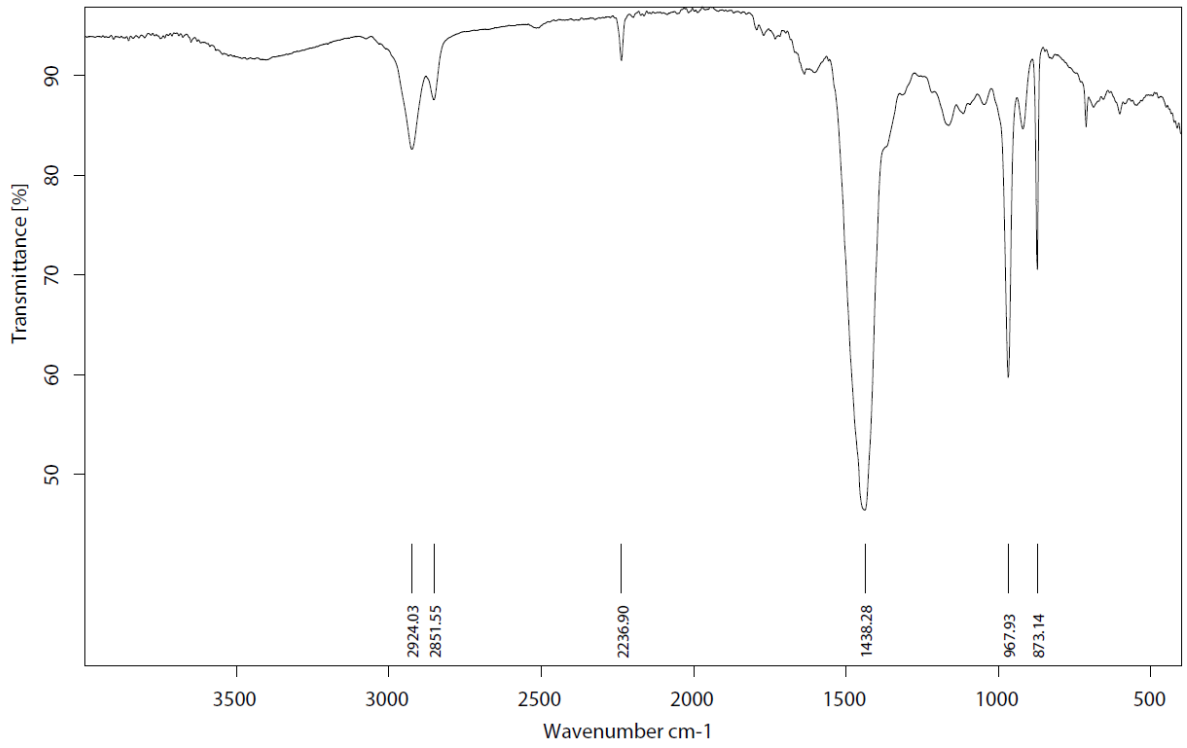

Thermogravimetric Analysis (TGA)

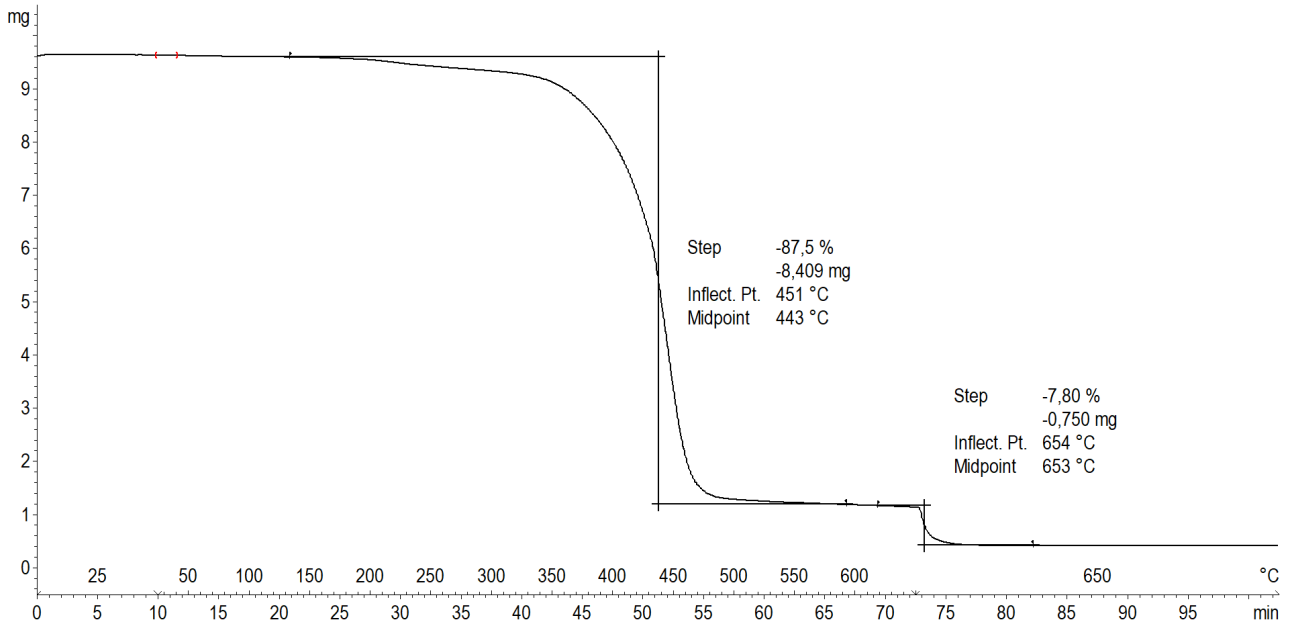

Decomposition graph. The experiment was conducted under He then air (after 650 °C).

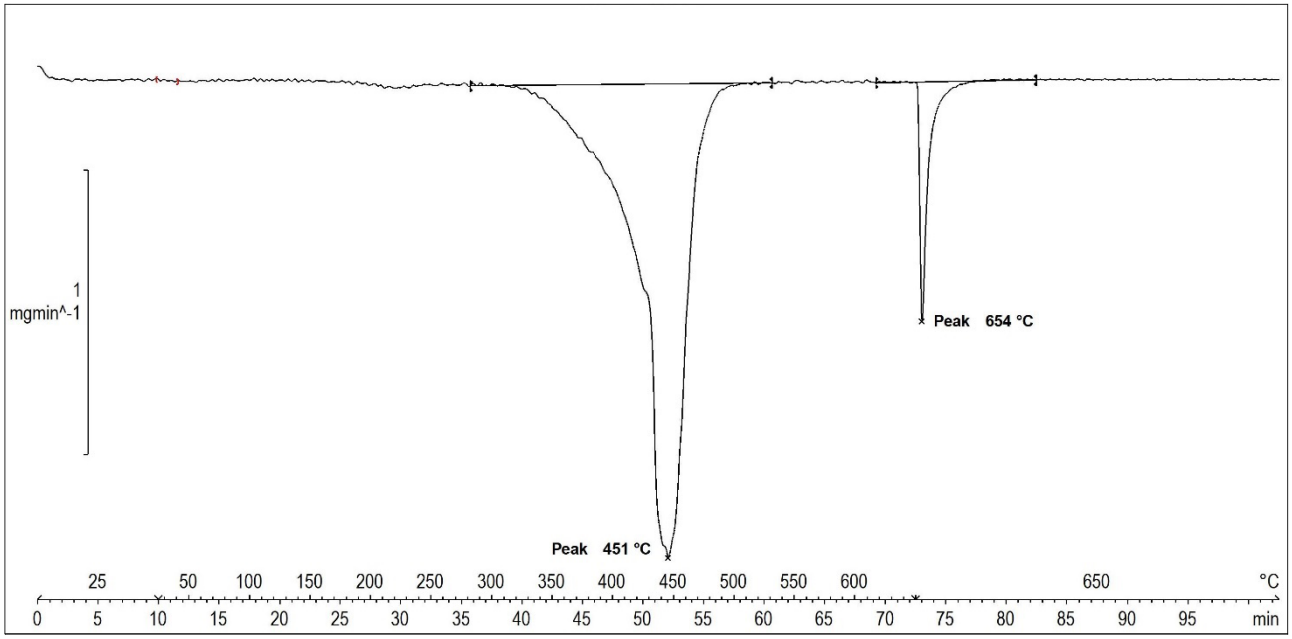

1st derivative of decomposition graph. The experiment was conducted under He then air (after 650 °C).

Decomposition temperature (T_d) = 451 °C.

Elemental Analysis (EA)

N [%]	C [%]	H [%]	S [%]	mmol N/g	C/N ratio	C/H ratio
8.84	74.45	8.40	1.12	6.31	9.82	0.74

Acrylonitrile weight percentage calculation (AN%):
N% = 8.84

M(N) = 14.0067 g/mol
M(AN) = 53.06 g/mol
$AN\% = \frac{N\%}{M(N)} \cdot M(AN)$ = 33%

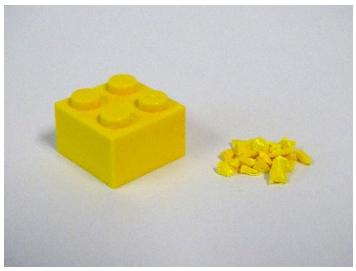

Acrylonitrile Butadiene Styrene 1 (ABS1, LEGO® bricks) was purchased from Føtex (Danish supermarket) and used without further purification. Smaller pieces were generated by cutting with a diagonal cutter and used as such in the catalytic hydrogenation. For the 10 g-scale experiment, the LEGO® bricks were used as is without cutting to smaller pieces. The polymer was analysed with ^{1}H– and ^{13}C–NMR, solid-state ^{13}C CP/MAS NMR, IR, TGA, DSC, and Elemental Analysis. Solubility tests were also conducted with several solvents.

Particle size used for the catalytic hydrogenation reactions

Solubility chart

Soluble **Swells** **Not soluble**

$CHCl_3$	Acetone	*i*-PrOH	DMF	DMSO	THF	PhMe	H_2O	MeOH	MeCN

^{1}H–NMR ($CDCl_3$)

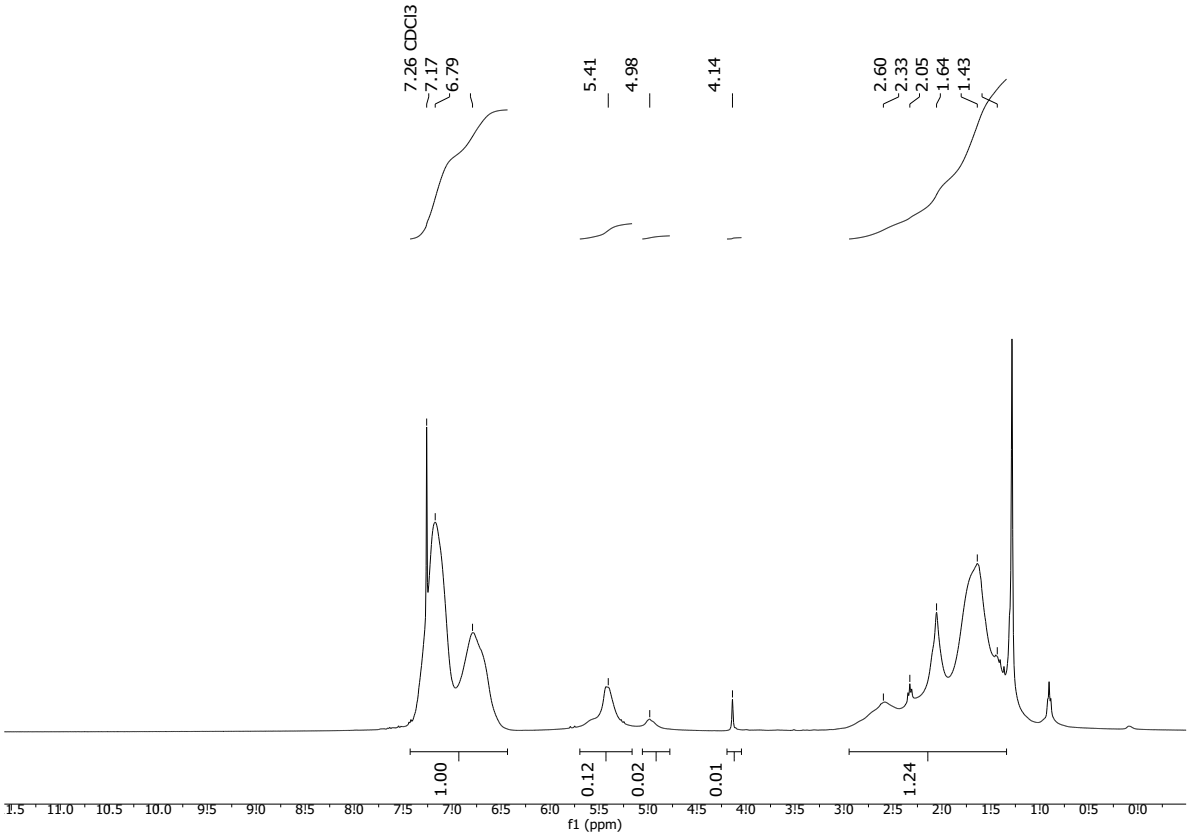

^{13}C–NMR ($CDCl_3$)

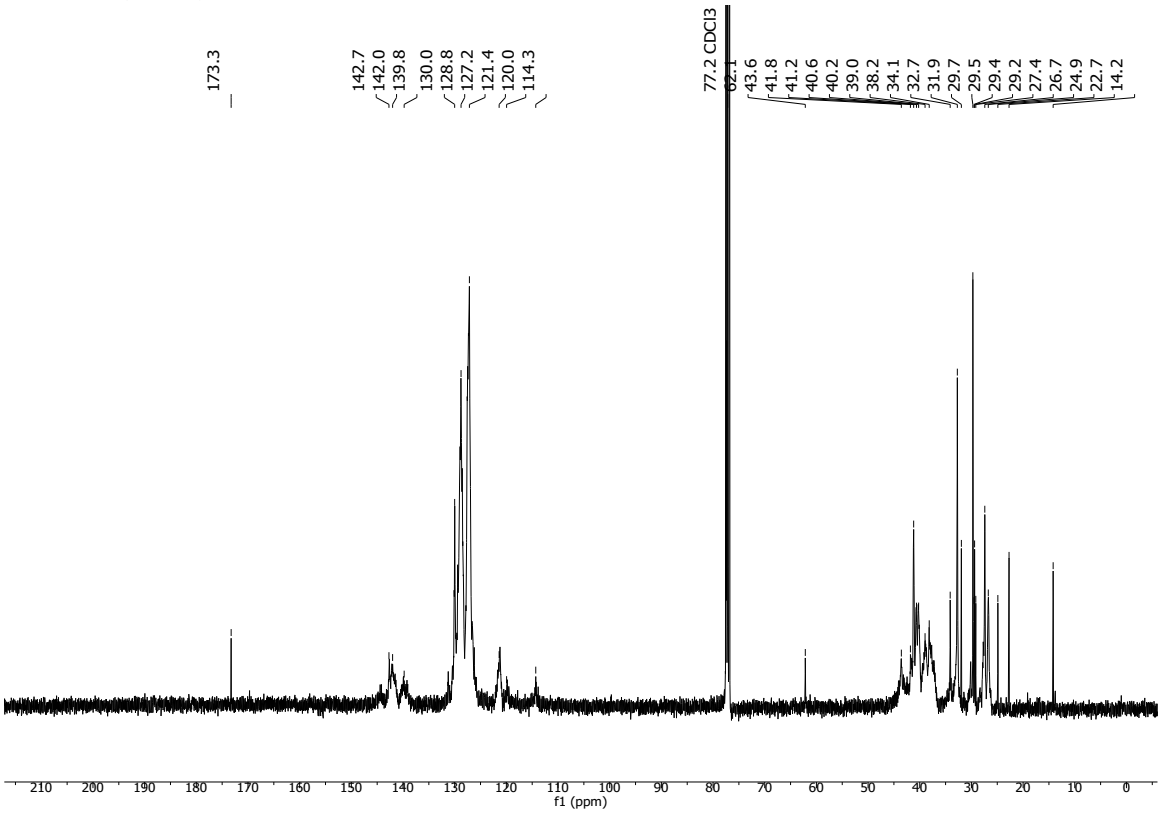

^{13}C CP/MAS NMR (solid-state)

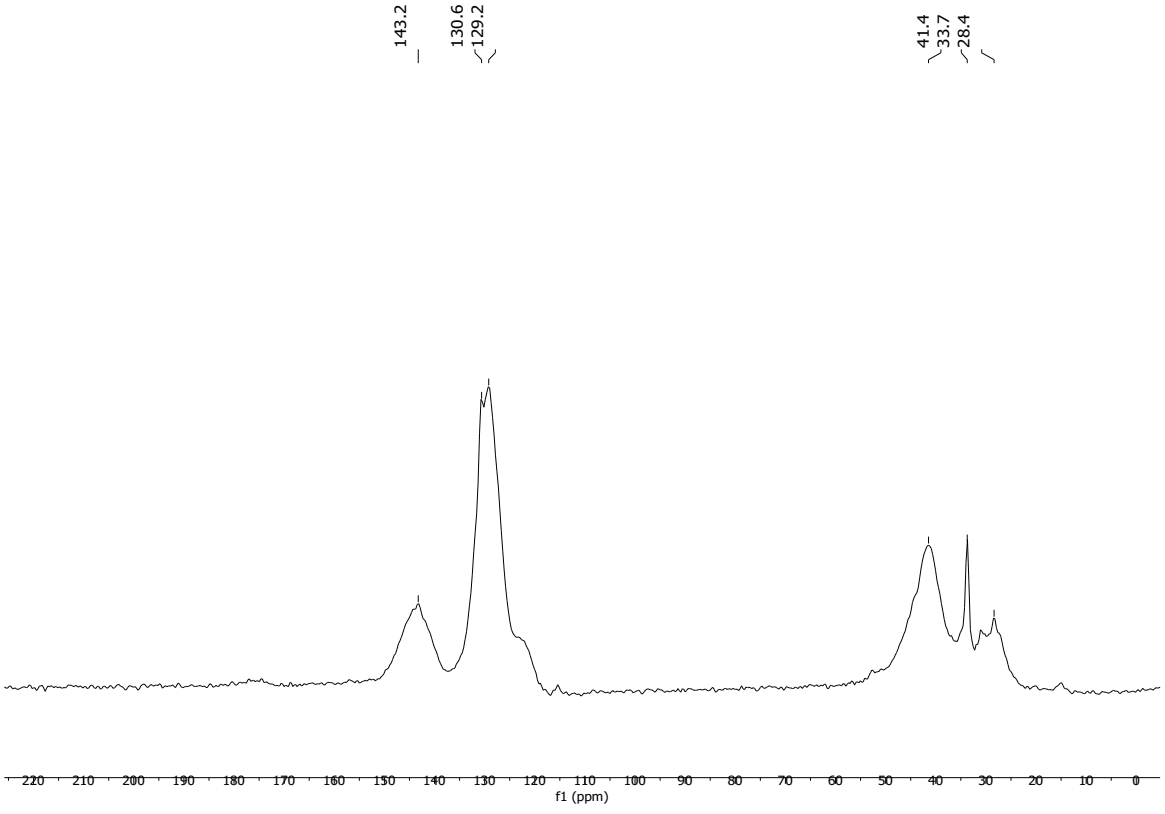

Infrared (IR) Spectroscopic Analysis

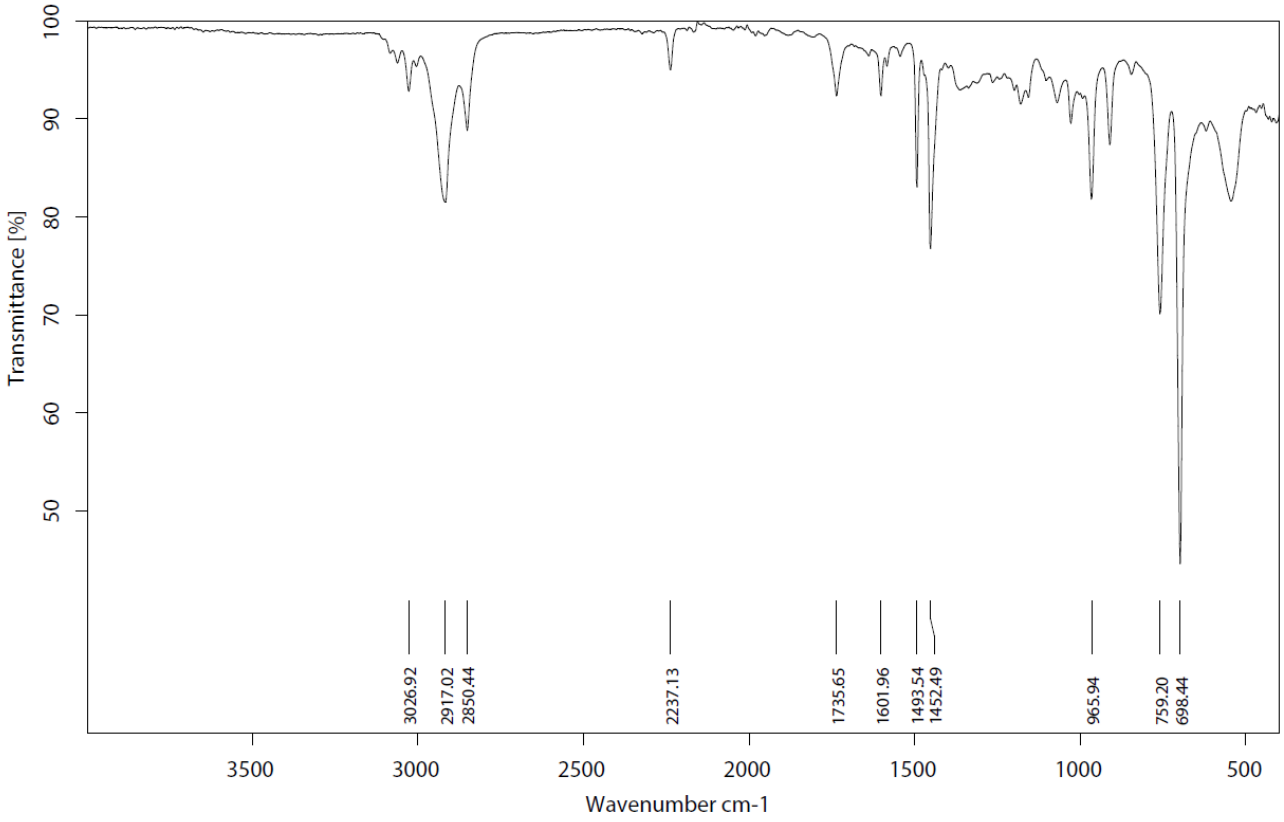

Thermogravimetric Analysis (TGA)

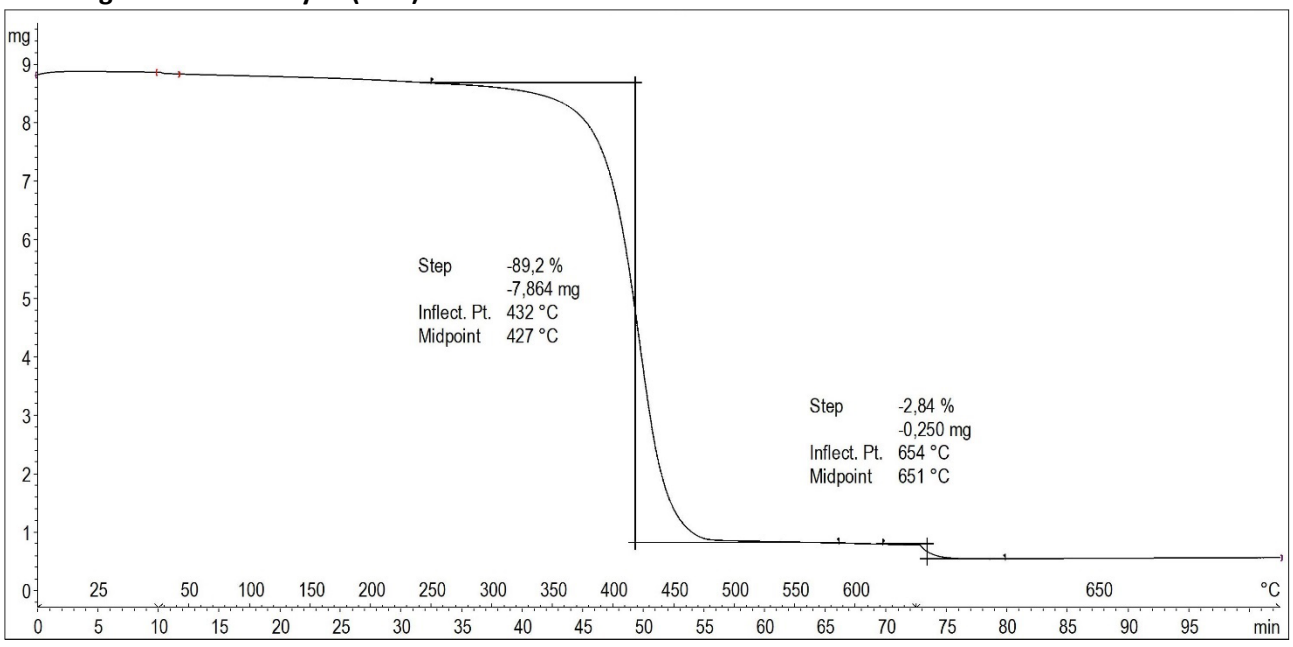

Decomposition graph. The experiment was conducted under He then air (after 650 °C).

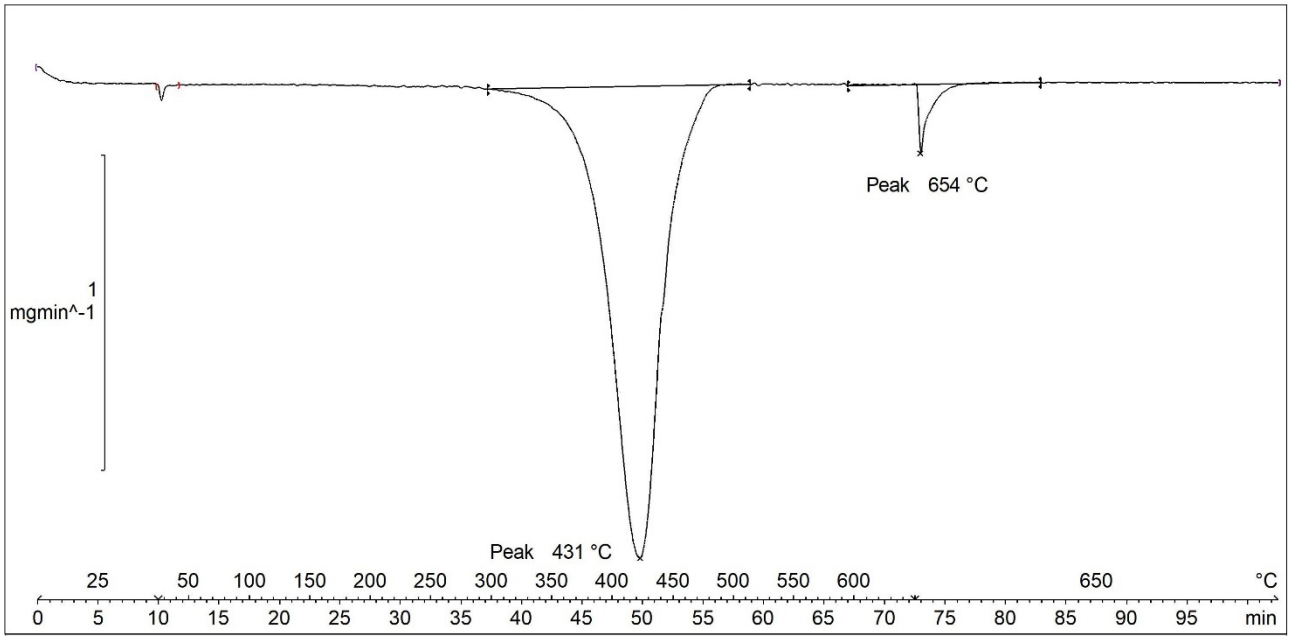

1st derivative of decomposition graph. The experiment was conducted under He then air (after 650 °C).

Decomposition temperature (T_d) = 431 °C.

Differential Scanning Calorimetry (DSC) Analysis

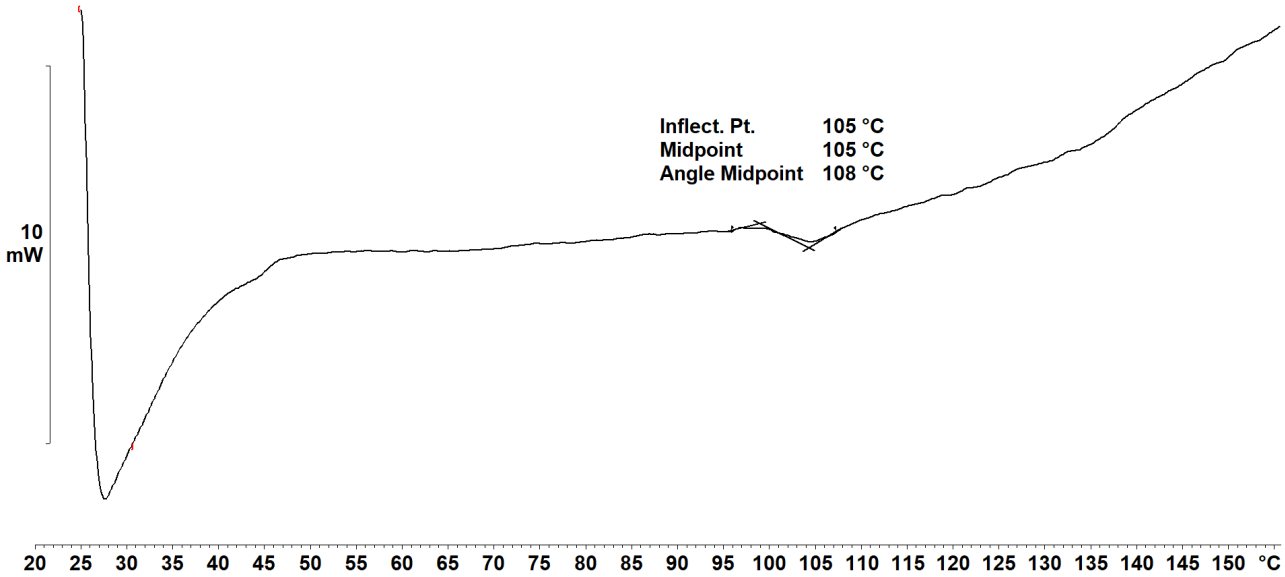

DSC graph.

Glass transition temperature (T_g) = 105 °C.

Elemental Analysis (EA)

N [%]	C [%]	H [%]	S [%]	mmol N/g	C/N ratio	C/H ratio
5.33	84.41	8.15	Not detected	3.80	18.48	0.87

Acrylonitrile weight percentage calculation (AN%):

N% = 5.33

M(N) = 14.0067 g/mol

M(AN) = 53.06 g/mol

$AN\% = \frac{N\%}{M(N)} \cdot M(AN)$ = 20%

Acrylonitrile Butadiene Styrene 2 (ABS2, Fujitsu® keyboard) was acquired from a waste bin and used without further purification. Smaller pieces were generated by cutting with a diagonal cutter and used as such in the catalytic hydrogenation. The polymer was analysed with ^{1}H– and ^{13}C–NMR, solid-state ^{13}C CP/MAS NMR, IR, TGA, DSC, and elemental analysis. Solubility tests were also conducted with several solvents.

Particle size used for the catalytic hydrogenation reactions

Solubility chart

Soluble **Swells** **Not soluble**

$CHCl_3$	Acetone	*i*-PrOH	DMF	DMSO	THF	PhMe	H_2O	MeOH	MeCN

^{1}H–NMR ($CDCl_3$)

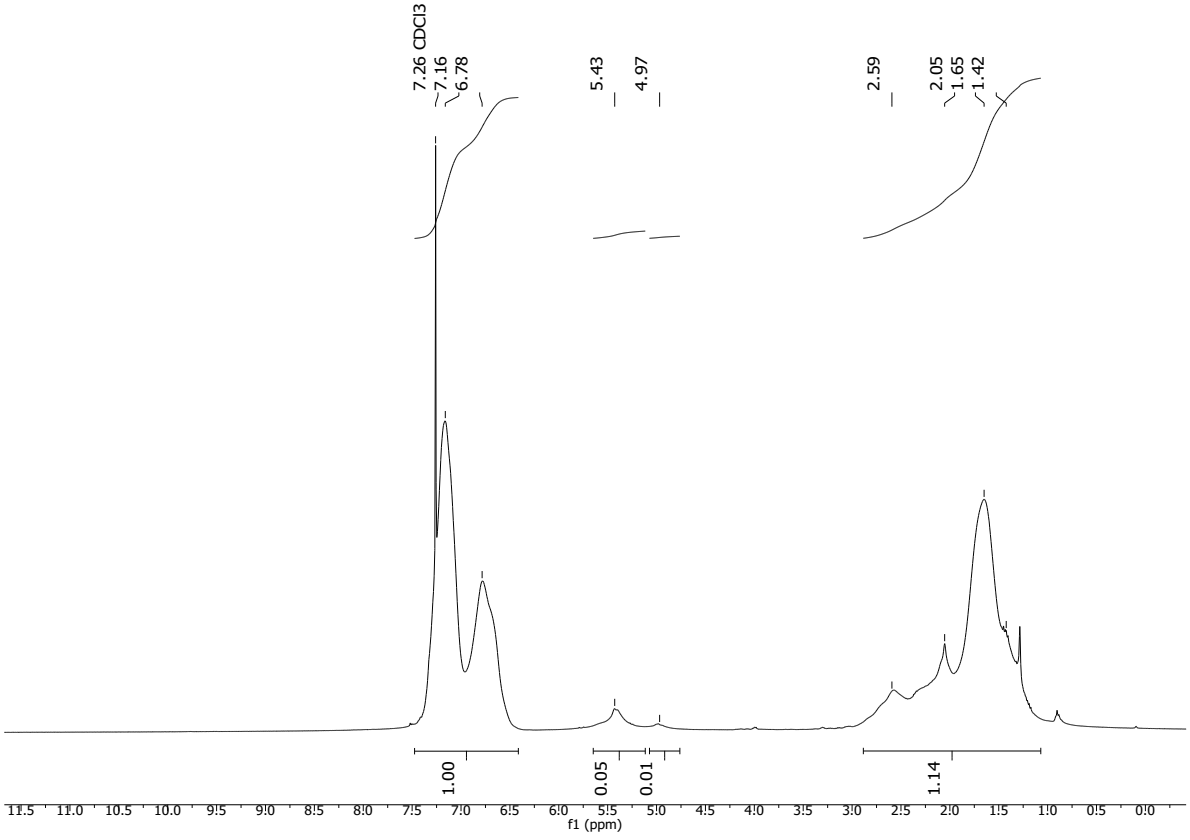

^{13}C–NMR ($CDCl_3$)

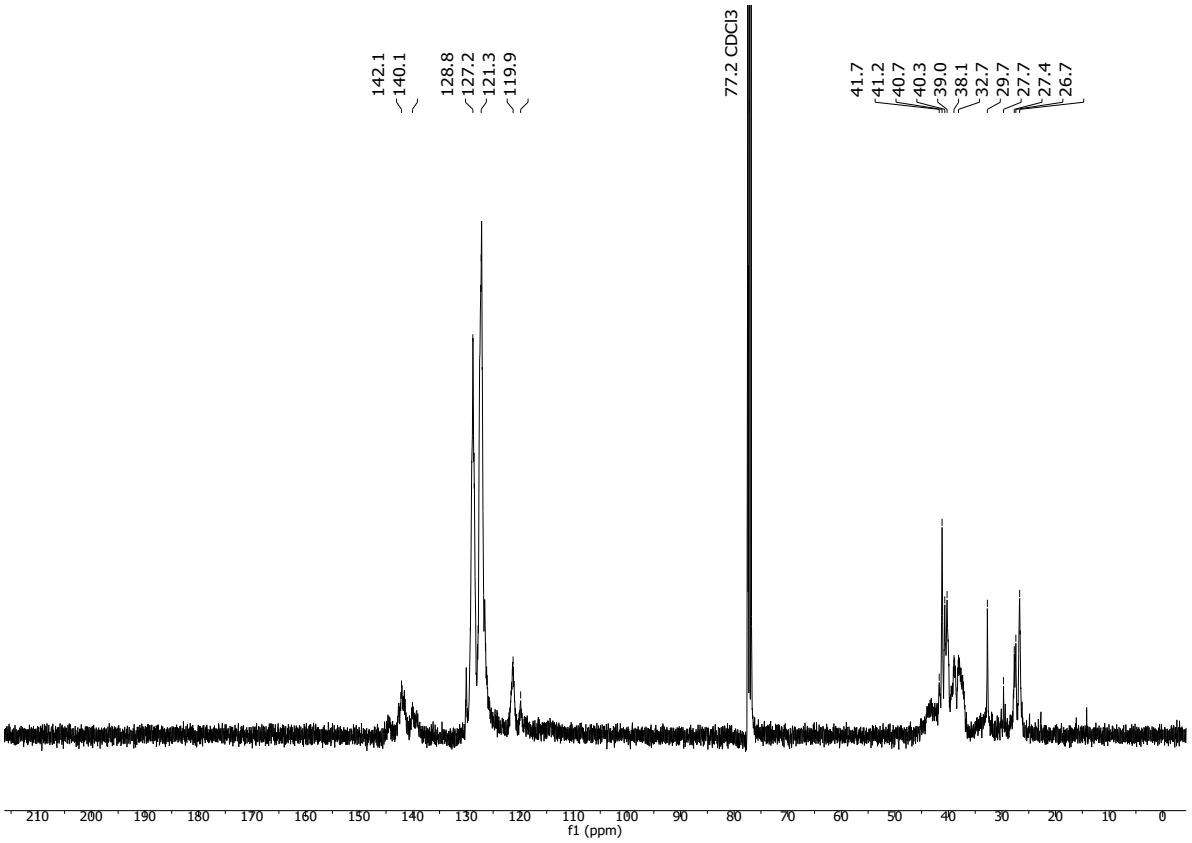

^{13}C CP/MAS NMR (solid-state)

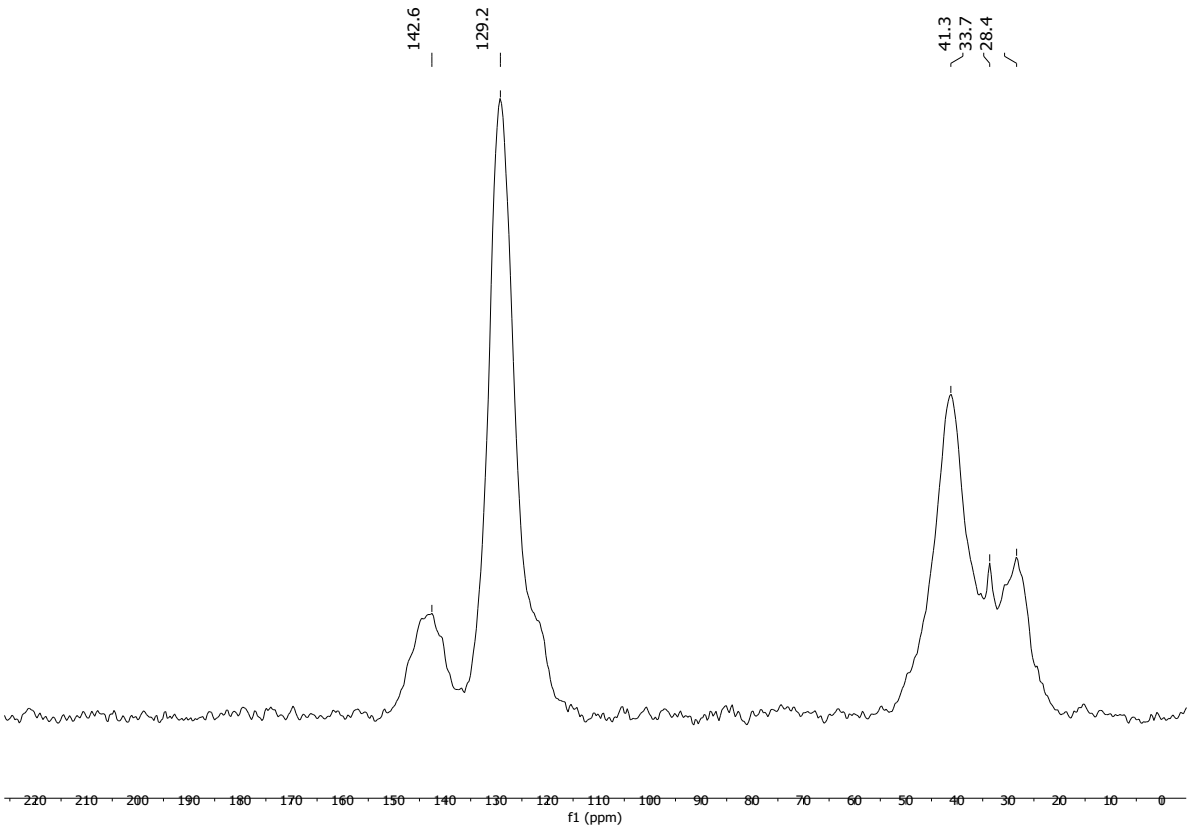

Infrared (IR) Spectroscopic Analysis

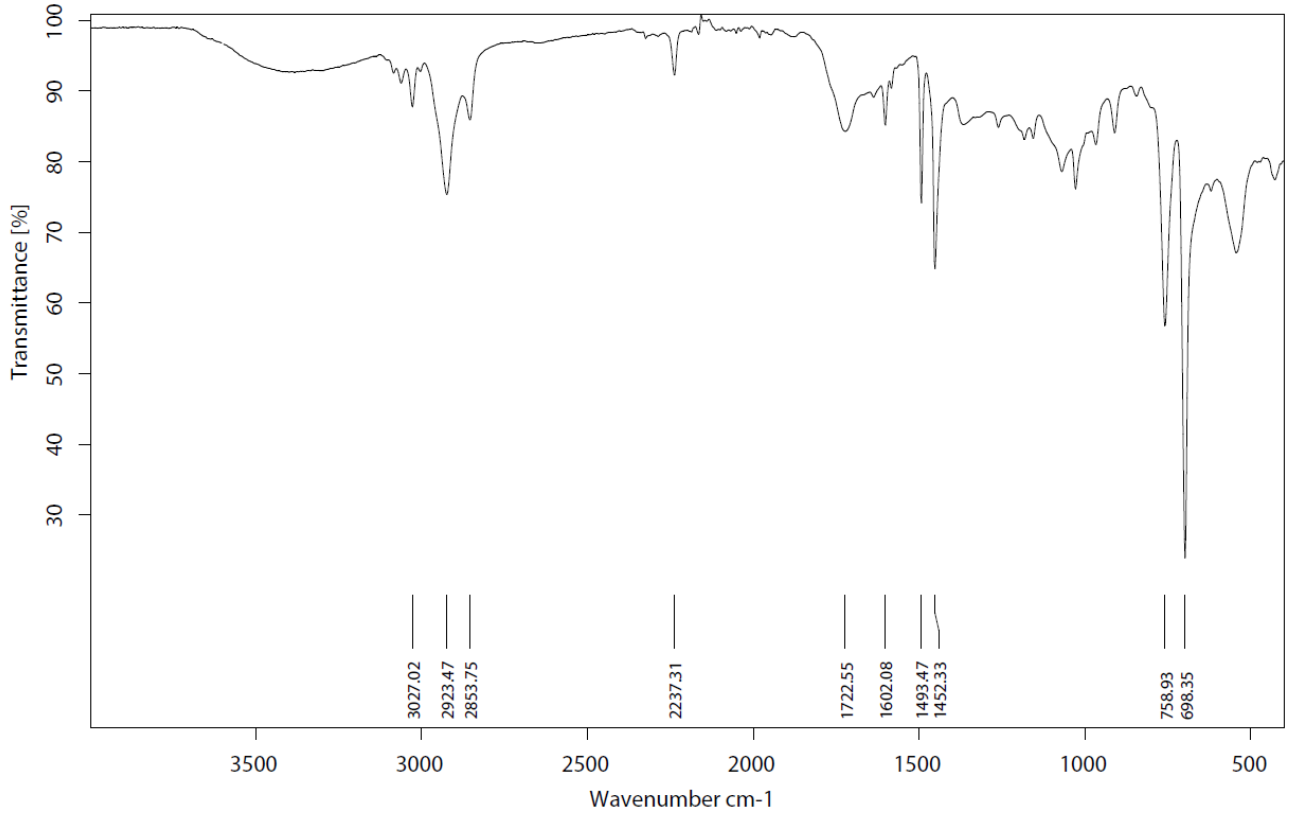

Thermogravimetric Analysis (TGA)

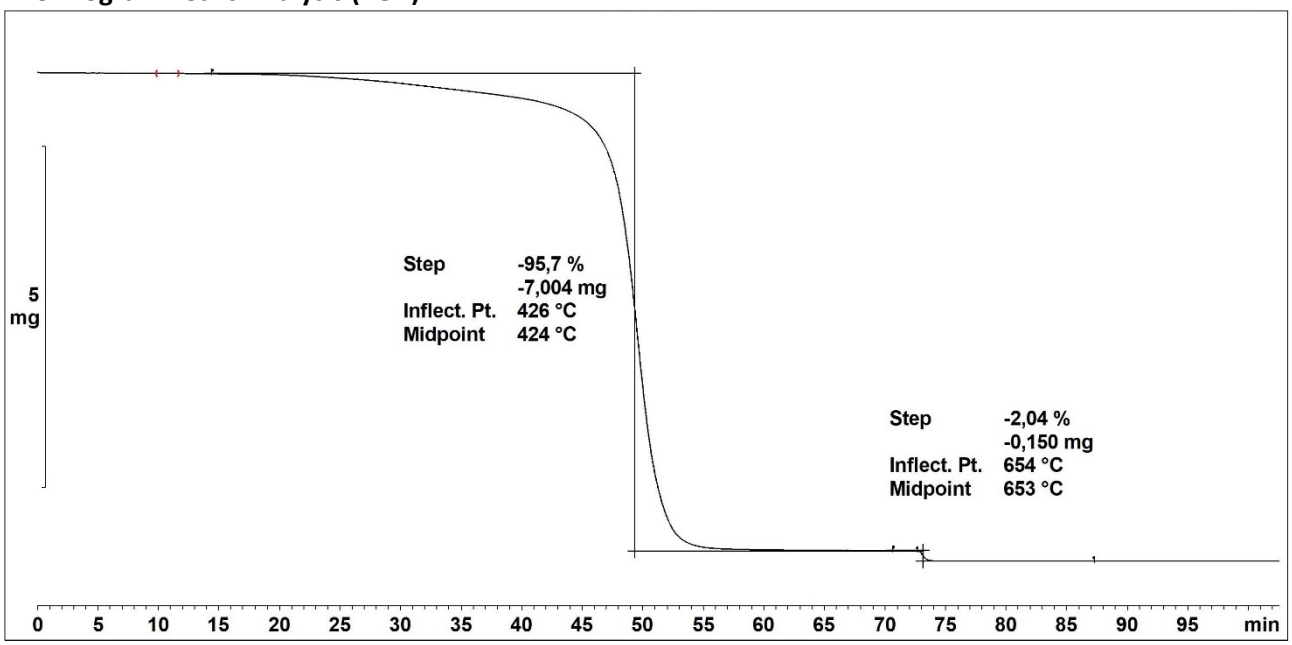

Decomposition graph. The experiment was conducted under He then air (after 650 °C).

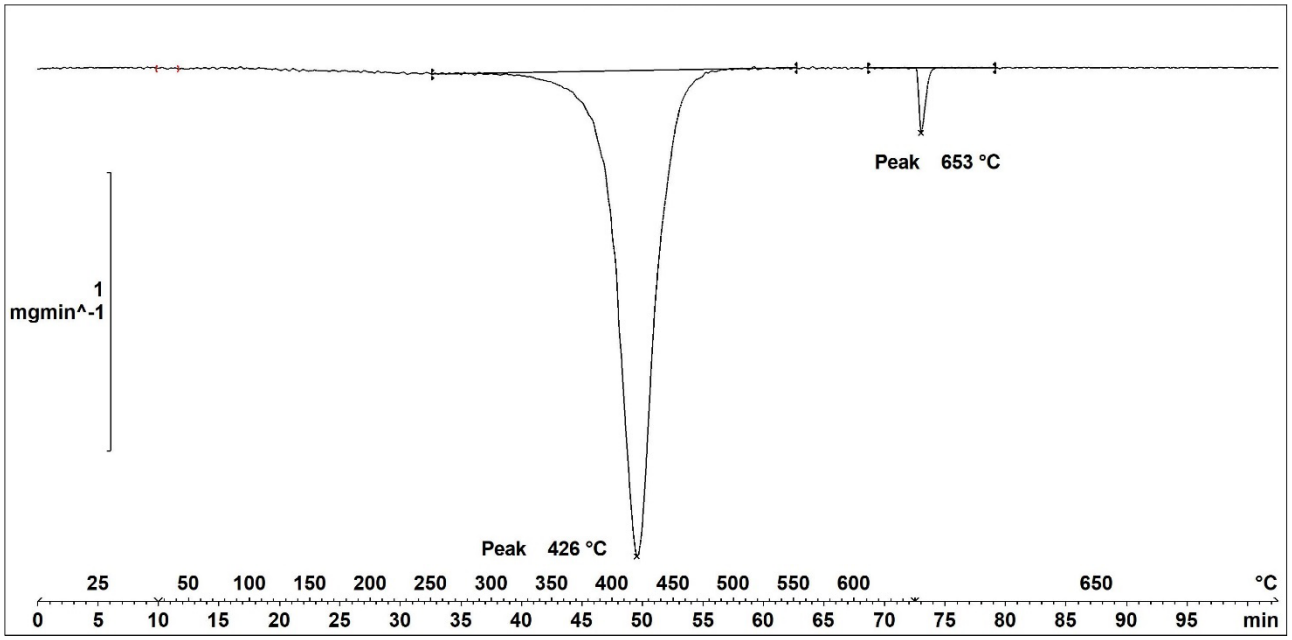

1st derivative of decomposition graph. The experiment was conducted under He then air (after 650 °C).

Decomposition temperature (T_d) = 426 °C.

Differential Scanning Calorimetry (DSC) Analysis

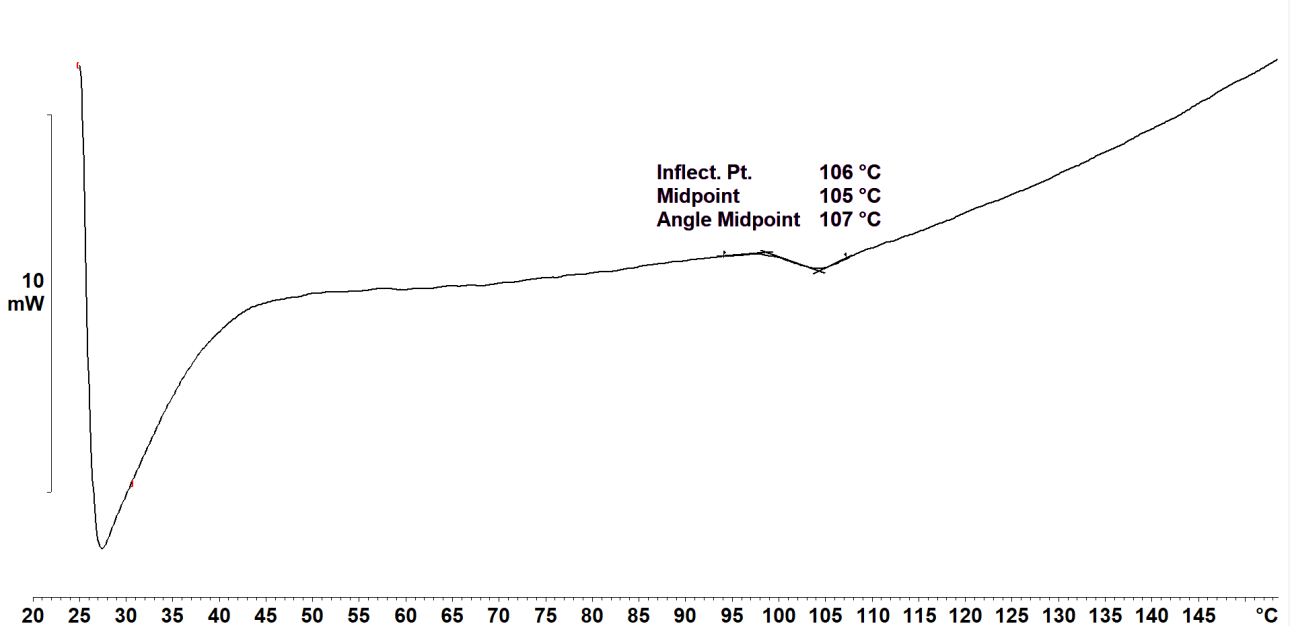

DSC graph.

Glass transition temperature (T_g) = 106 °C.

Elemental Analysis (EA)

N [%]	C [%]	H [%]	S [%]	mmol N/g	C/N ratio	C/H ratio
5.46	82.56	7.75	Not detected	3.90	17.62	0.89

Acrylonitrile weight percentage calculation (AN%):

N% = 5.46

M(N) = 14.0067 g/mol

M(AN) = 53.06 g/mol

$AN\% = \frac{N\%}{M(N)} \cdot M(AN)$ = 21%

Styrene Acrylonitrile 1 (SAN1, Beaker) was purchased from Føtex (Danish supermarket) and used without further purification. Smaller pieces were generated by cutting with a diagonal cutter and used as such in the catalytic hydrogenation. The polymer was analysed with ^{1}H– and ^{13}C–NMR, solid-state ^{13}C CP/MAS NMR, IR, TGA, DSC, and elemental analysis. Solubility tests were also conducted with several solvents.

Particle size used for the catalytic hydrogenation reactions

Solubility chart

Soluble **Swells** **Not soluble**

$CHCl_3$	Acetone	*i*-PrOH	DMF	DMSO	THF	PhMe	H_2O	MeOH	MeCN

^{1}H–NMR ($CDCl_3$)

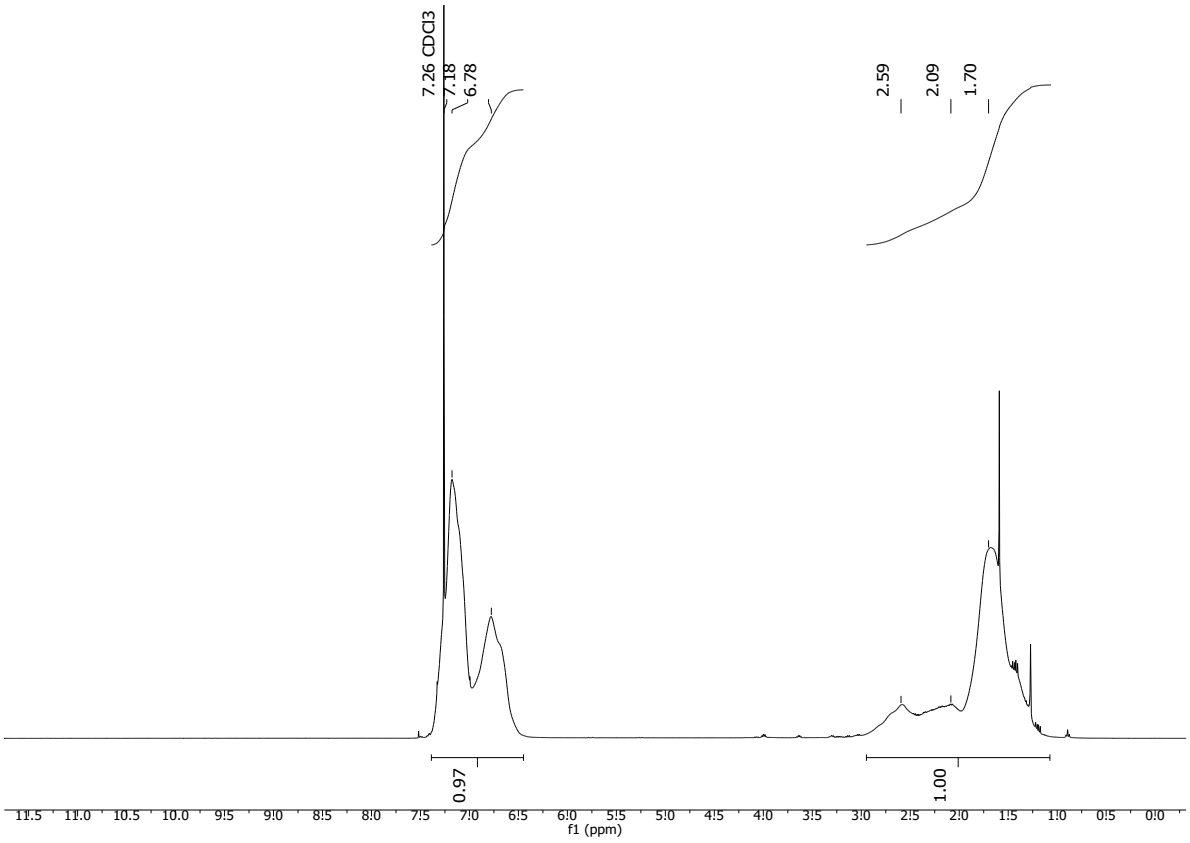

^{13}C–NMR ($CDCl_3$)

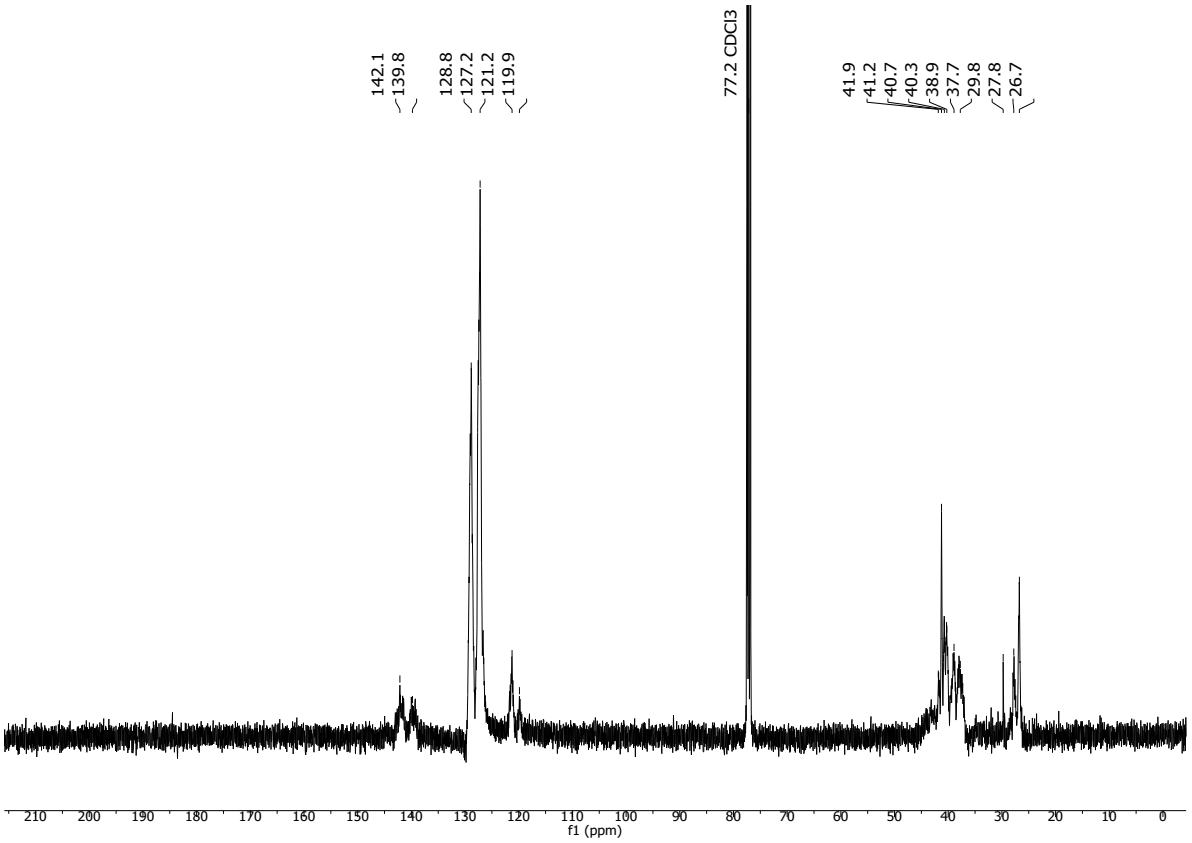

^{13}C CP/MAS NMR (solid-state)

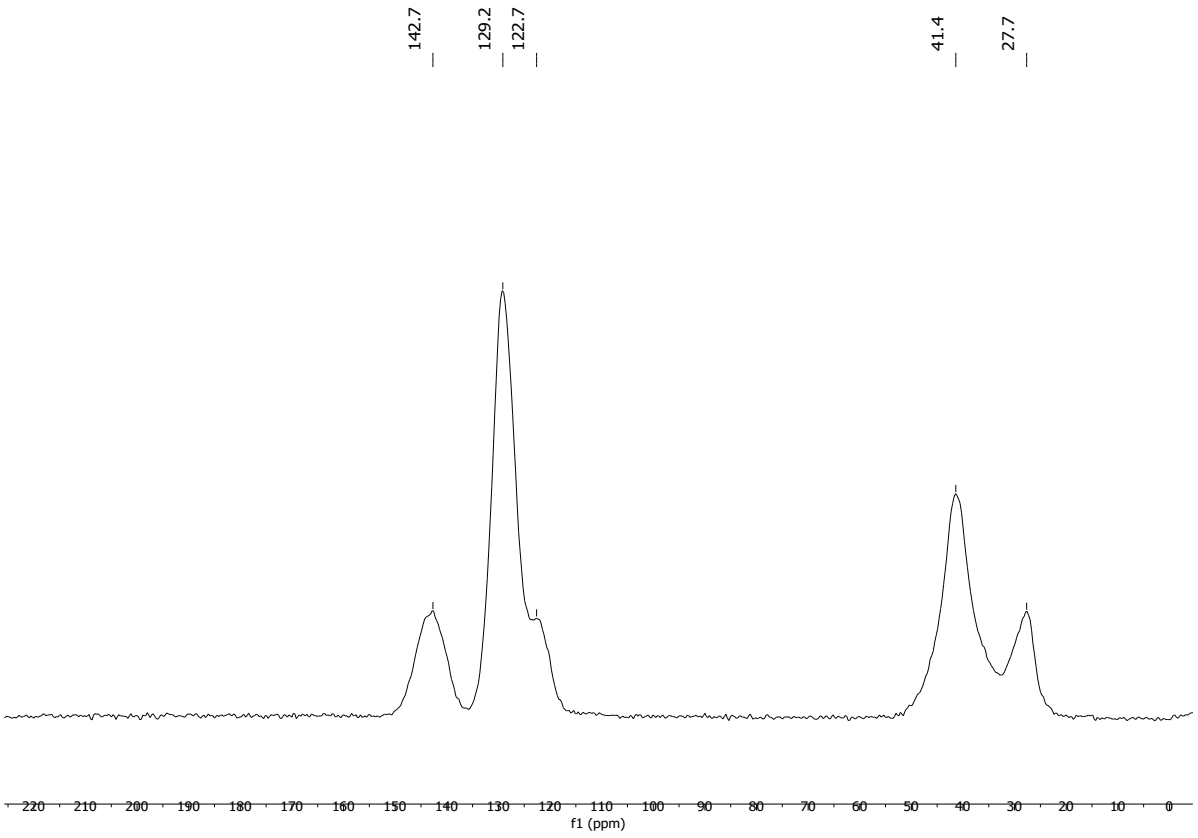

Infrared (IR) Spectroscopic Analysis

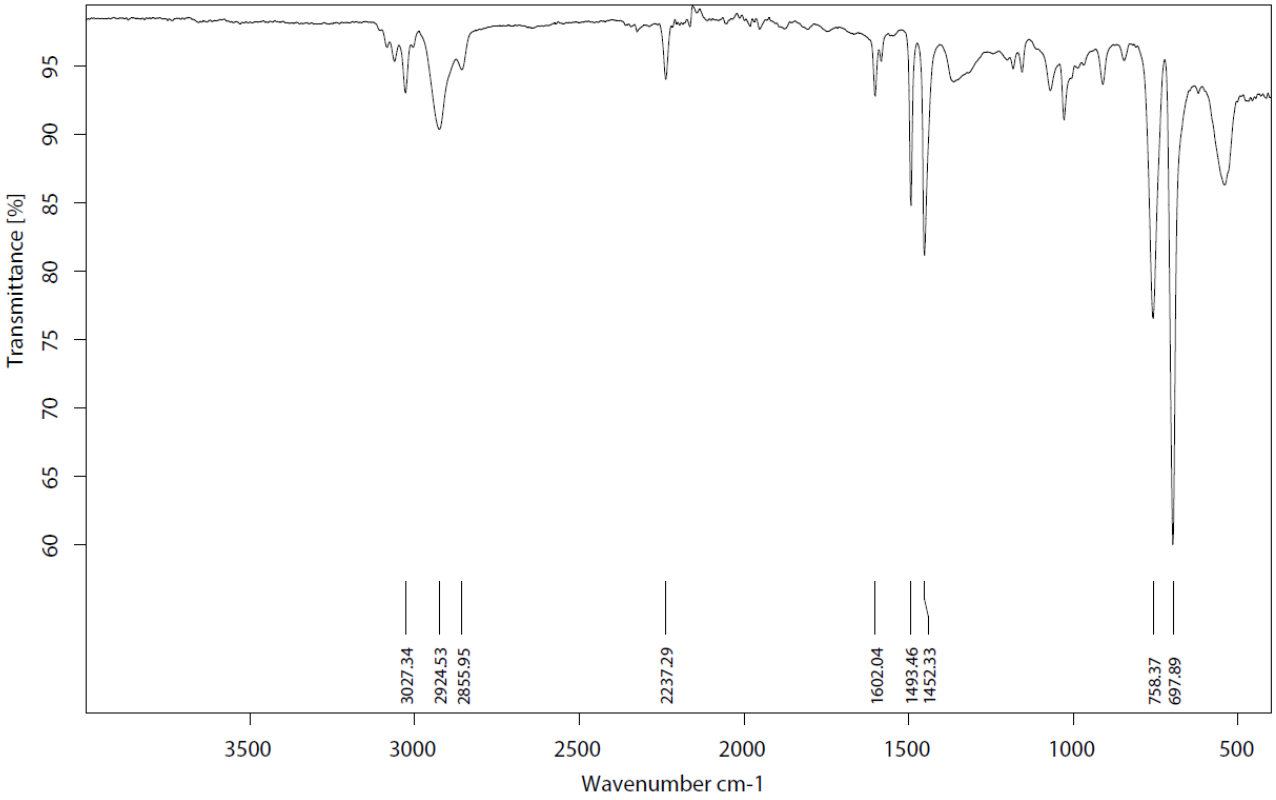

Thermogravimetric Analysis (TGA)

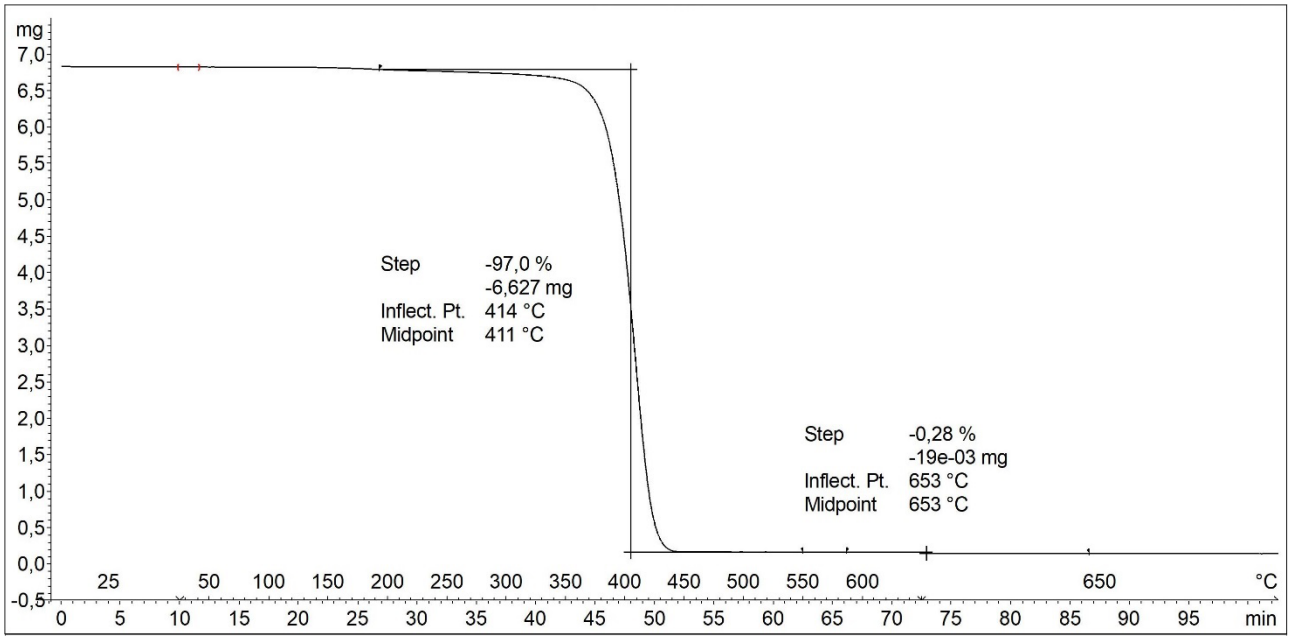

Decomposition graph. The experiment was conducted under He then air (after 650 °C).

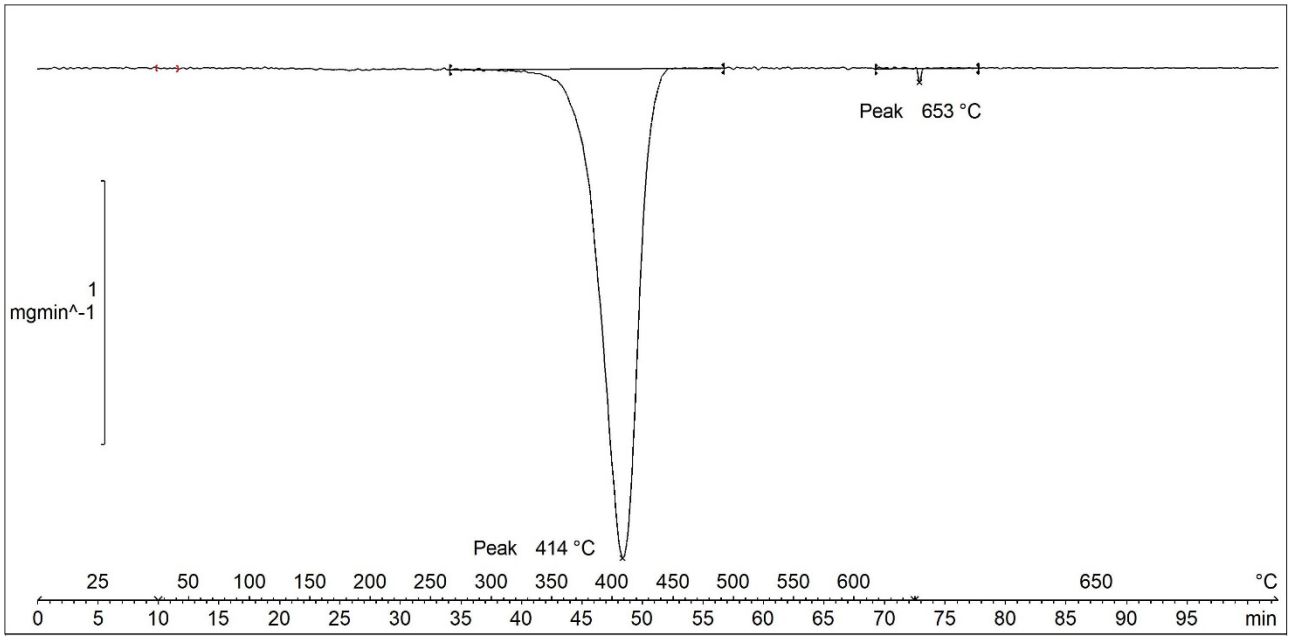

1st derivative of decomposition graph. The experiment was conducted under He then air (after 650 °C).

Decomposition temperature (T_d) = 414 °C.

Differential Scanning Calorimetry (DSC) Analysis

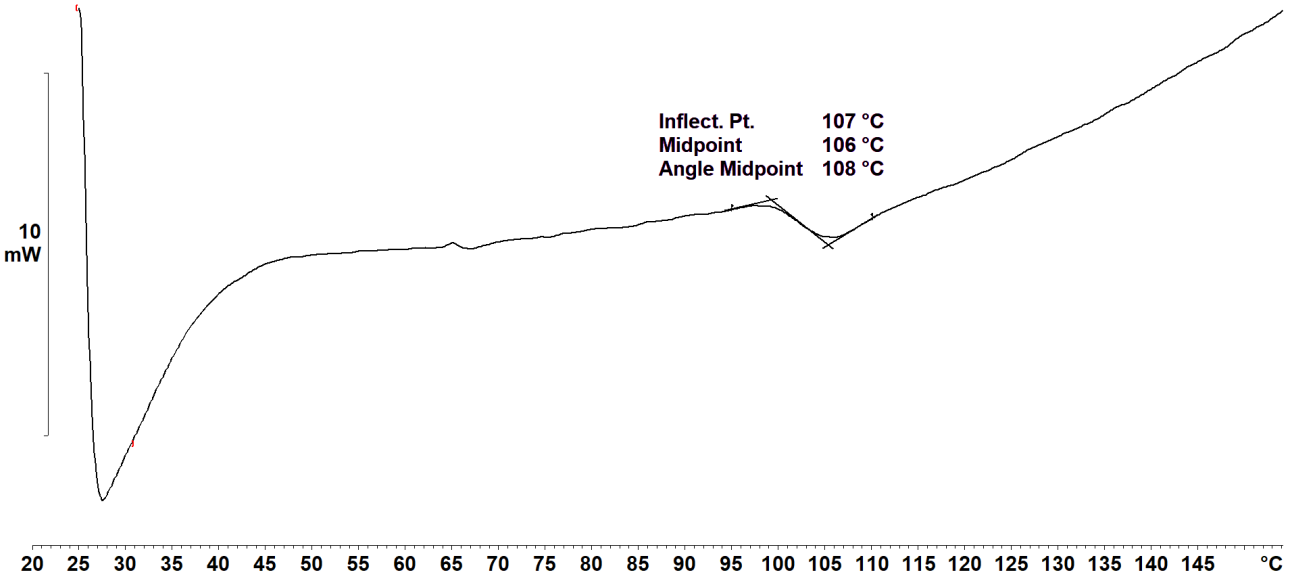

DSC Curve.

Glass transition temperature (T_g) = 107 °C.

Elemental Analysis (EA)

N [%]	C [%]	H [%]	S [%]	mmol N/g	C/N ratio	C/H ratio
6.94	84.36	7.72	Not detected	4.95	14.19	0.92

Acrylonitrile weight percentage calculation (AN%):

N% = 6.94

M(N) = 14.0067 g/mol

M(AN) = 53.06 g/mol

$AN\% = \frac{N\%}{M(N)} \cdot M(AN)$ = 26%

Styrene Acrylonitrile 2 (SAN2, Tandex® toothbrush) was purchased from Matas (Danish store) and used without further purification. Smaller pieces were generated by cutting with a wire cutter and used as such in the catalytic hydrogenation. The polymer was analysed with ^{1}H– and ^{13}C–NMR, solid-state ^{13}C CP/MAS NMR, IR, TGA, DSC, and elemental analysis. Solubility tests were also conducted with several solvents.

Particle size used for the catalytic hydrogenation reactions

Solubility chart

Soluble **Swells** **Not soluble**

$CHCl_3$	Acetone	*i*-PrOH	DMF	DMSO	THF	PhMe	H_2O	MeOH	MeCN

^{1}H–NMR ($CDCl_3$)

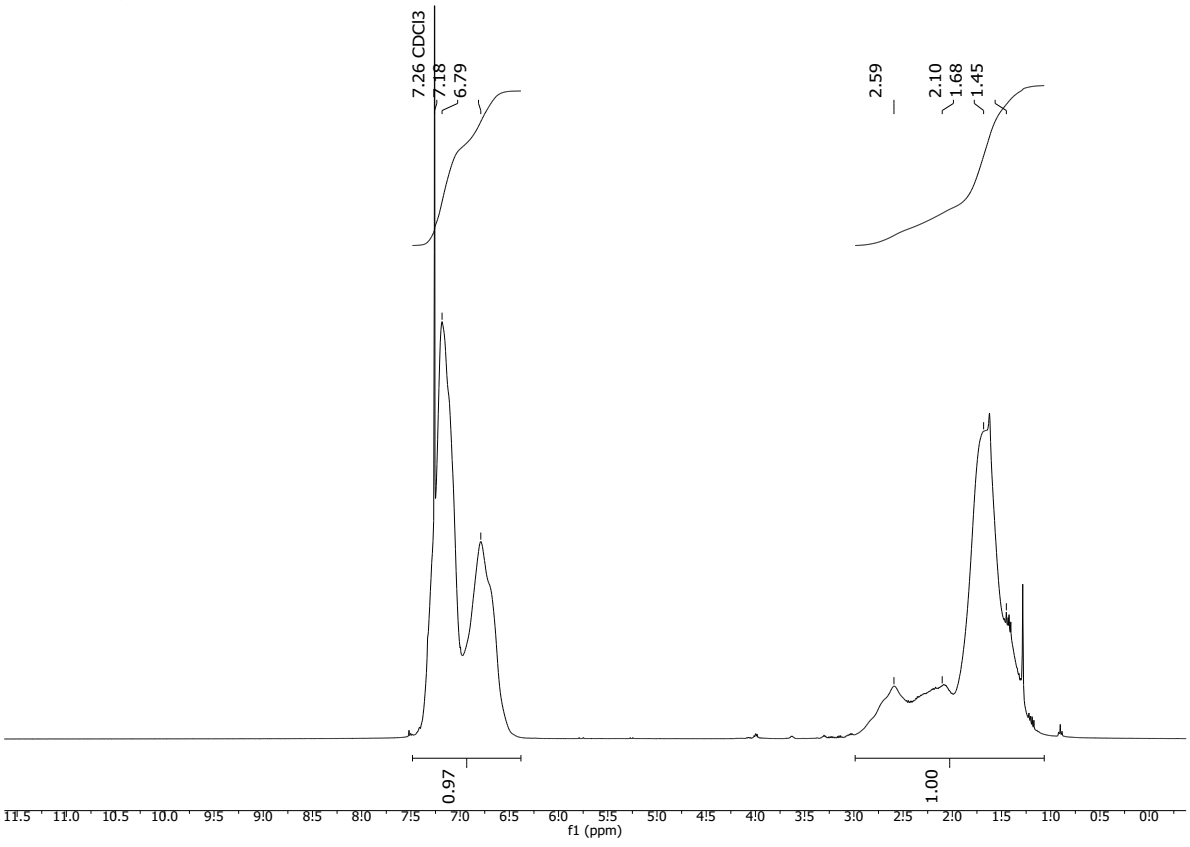

^{13}C–NMR ($CDCl_3$)

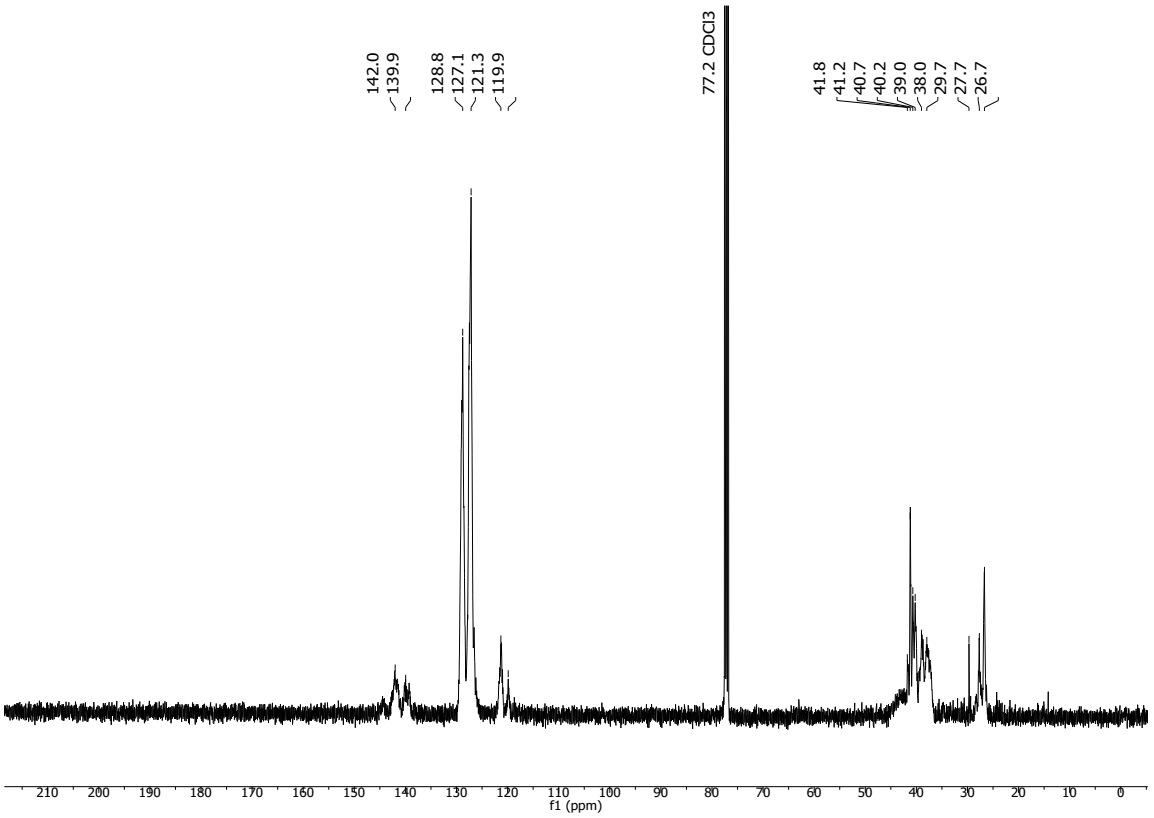

^{13}C CP/MAS NMR (solid-state)

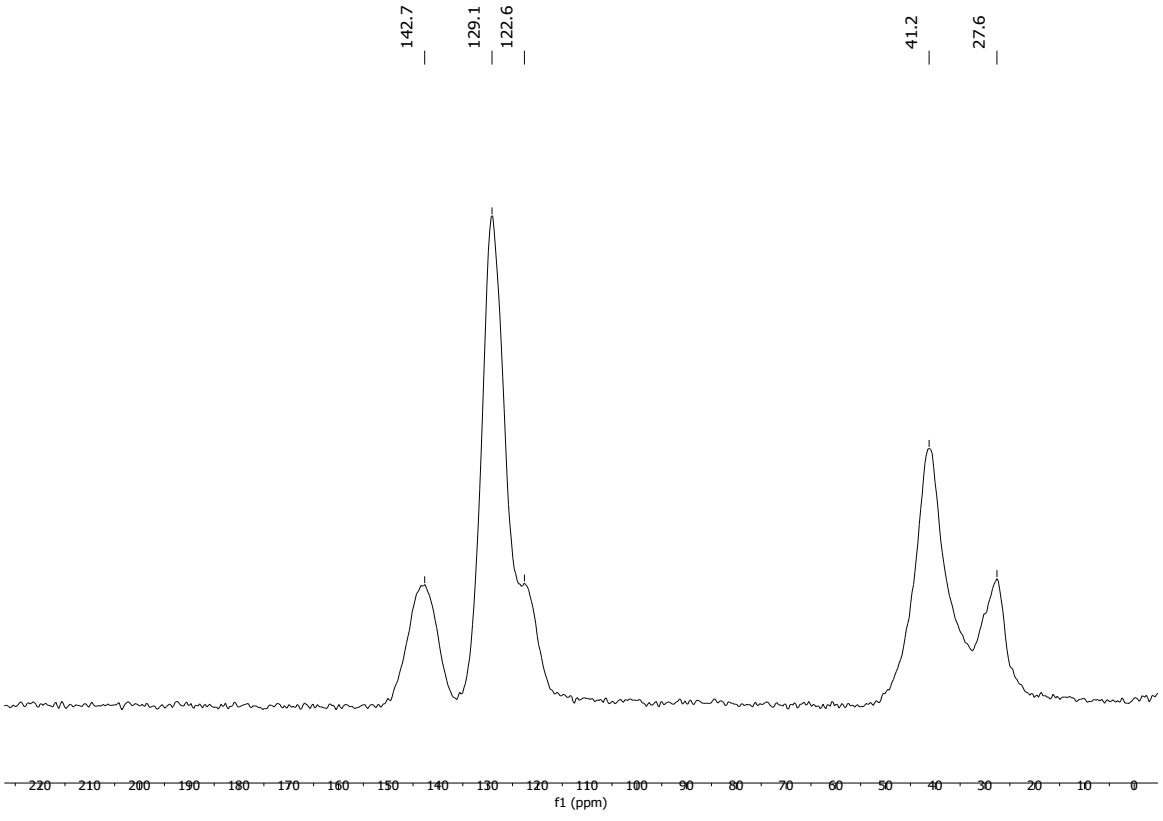

Infrared (IR) Spectroscopic Analysis

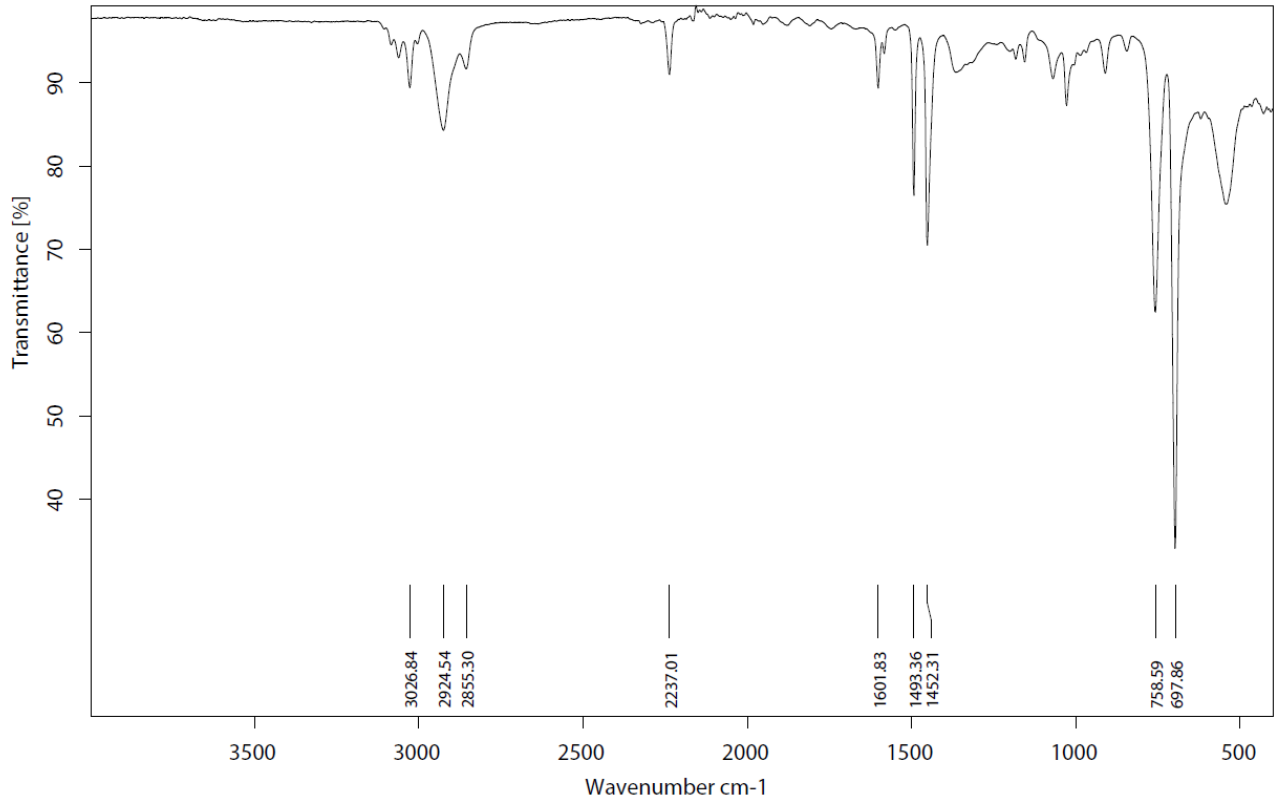

Thermogravimetric Analysis (TGA)

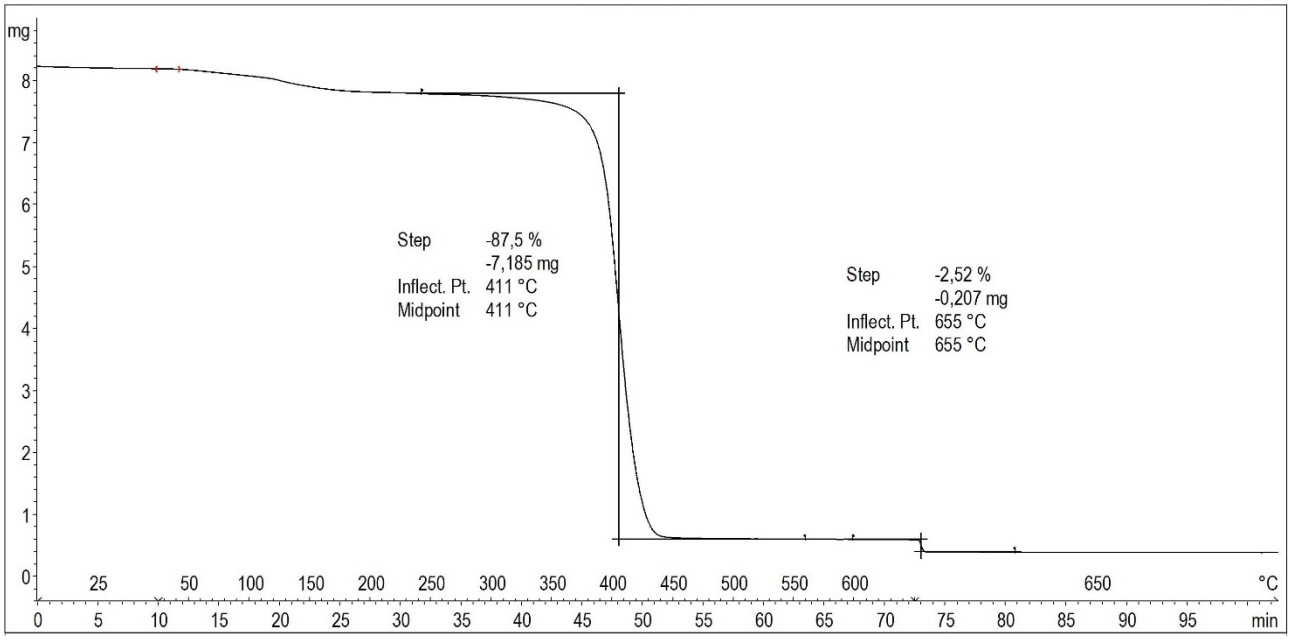

Decomposition graph. The experiment was conducted under He then air (after 650 °C).

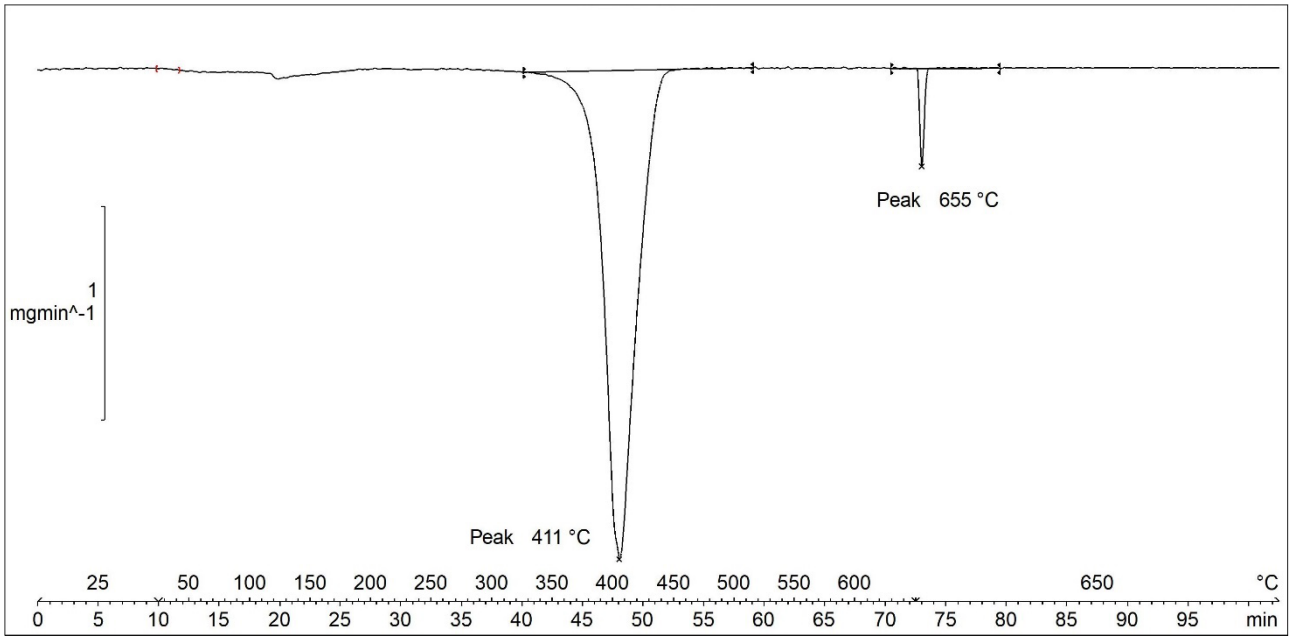

1st derivative of decomposition graph. The experiment was conducted under He then air (after 650 °C).

Decomposition temperature (T_d) = 411 °C.

Differential Scanning Calorimetry (DSC) Analysis

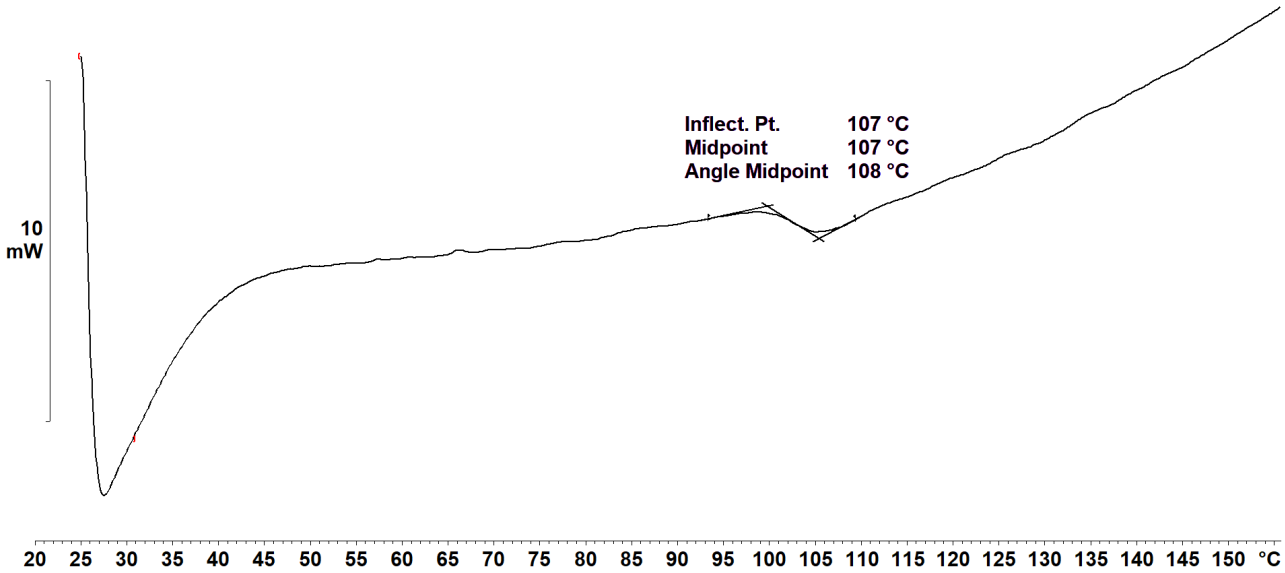

Glass transition temperature (T_g) = 107 °C.

Elemental Analysis (EA)

N [%]	C [%]	H [%]	S [%]	mmol N/g	C/N ratio	C/H ratio
6.82	83.76	7.59	Not detected	4.87	14.32	0.93

Acrylonitrile weight percentage calculation (AN%):
N% = 6.82

M(N) = 14.0067 g/mol
M(AN) = 53.06 g/mol
$AN\% = \frac{N\%}{M(N)} \cdot M(AN)$ = 26%

Acrylic yarn (TEX1, White Yarn) was purchased from Føtex (Danish supermarket) and used without further purification. Smaller pieces were generated by cutting with scissors and used as such in the catalytic hydrogenation. The polymer was analysed with ^{1}H– and ^{13}C–NMR, solid-state ^{13}C CP/MAS NMR, IR, TGA, DSC, and elemental analysis. Solubility tests were also conducted with several solvents.

Fibers used for the catalytic hydrogenation reactions

Solubility chart

Soluble **Swells** **Not soluble**

$CHCl_3$	Acetone	*i*-PrOH	DMF	DMSO	THF	PhMe	H_2O	MeOH	MeCN	GVL*

*Dissolving in GVL (γ-valerolactone) needed heating at 100 °C.

^{1}H–NMR (DMSO-d_6) (Only DMSO-soluble fraction)

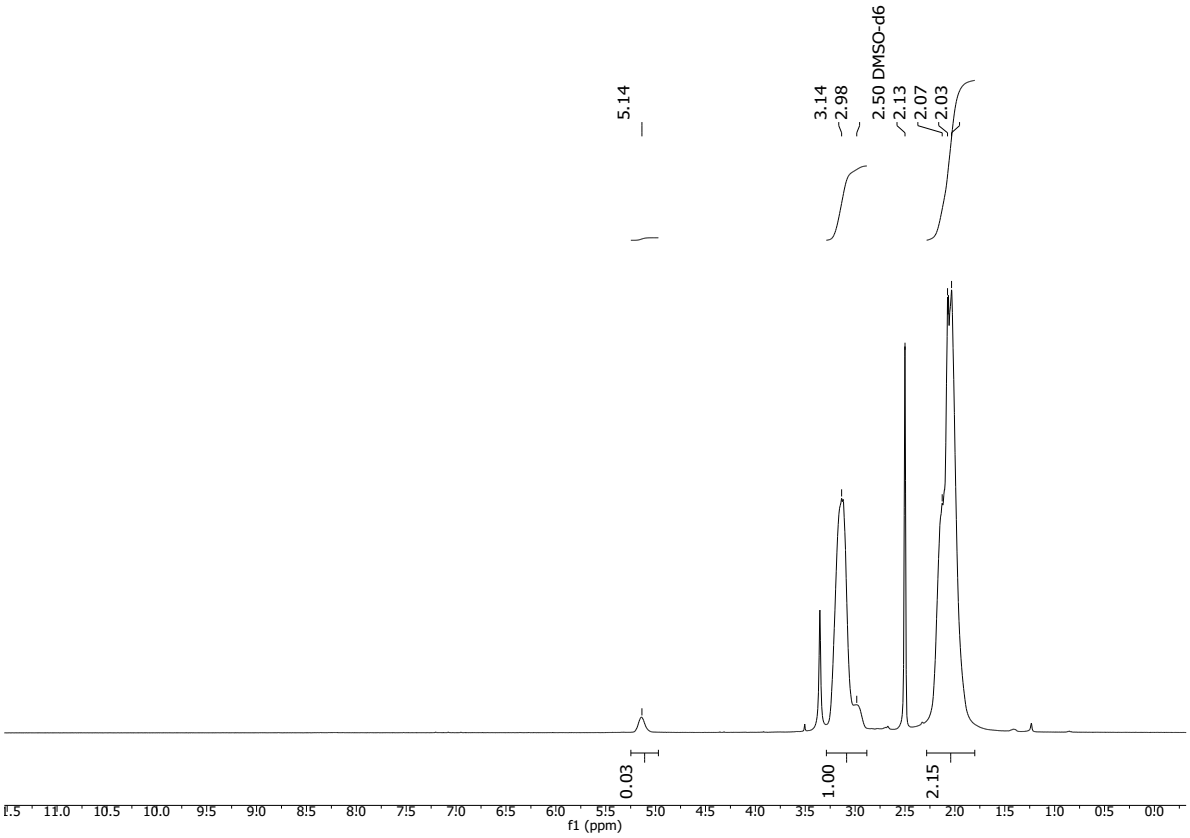

^{13}C–NMR (DMSO-d_6)

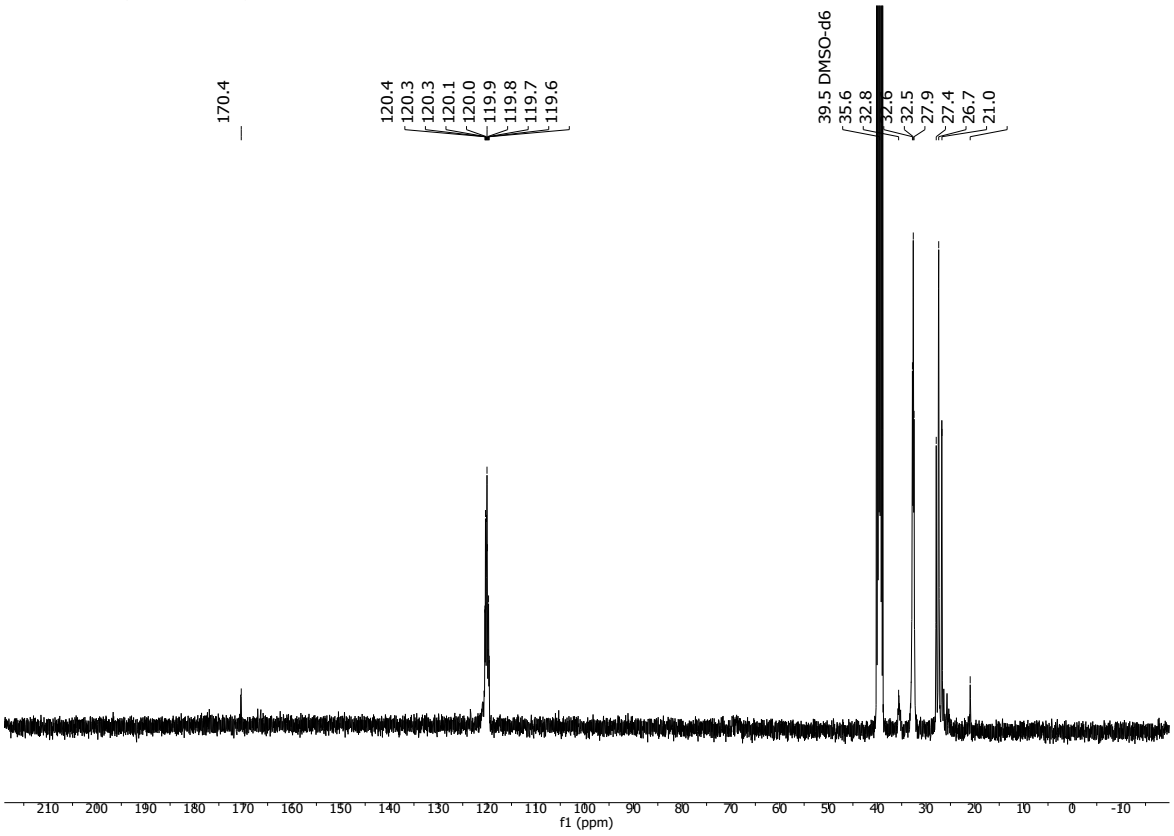

^{13}C CP/MAS NMR (solid-state)

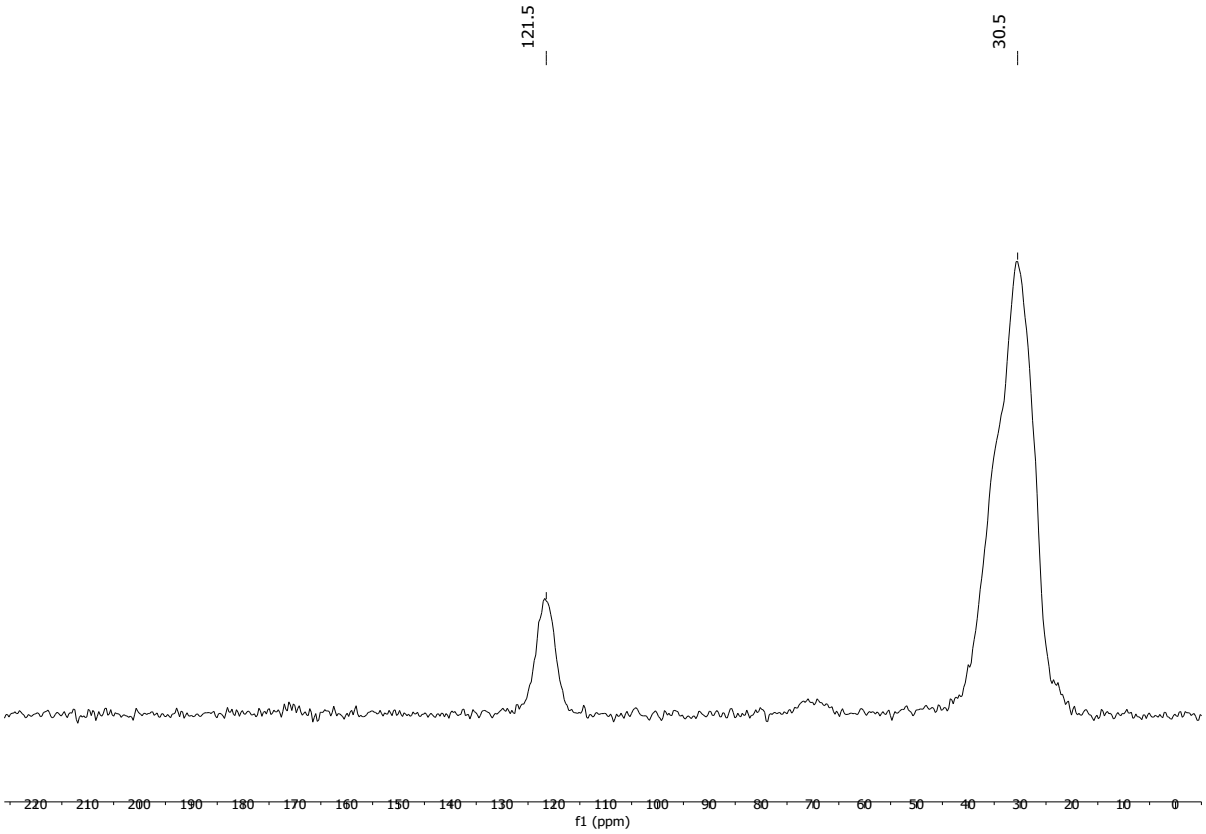

Infrared (IR) Spectroscopic Analysis

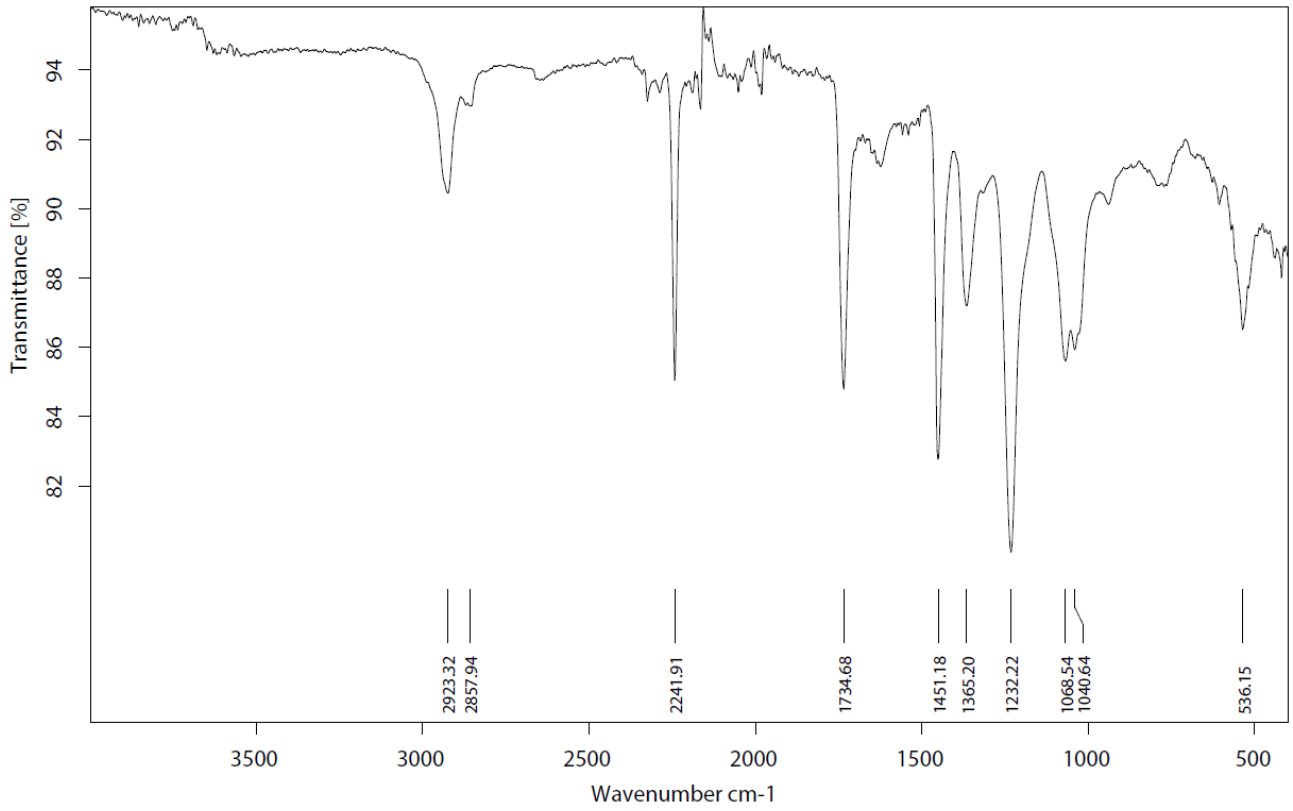

Thermogravimetric Analysis (TGA)

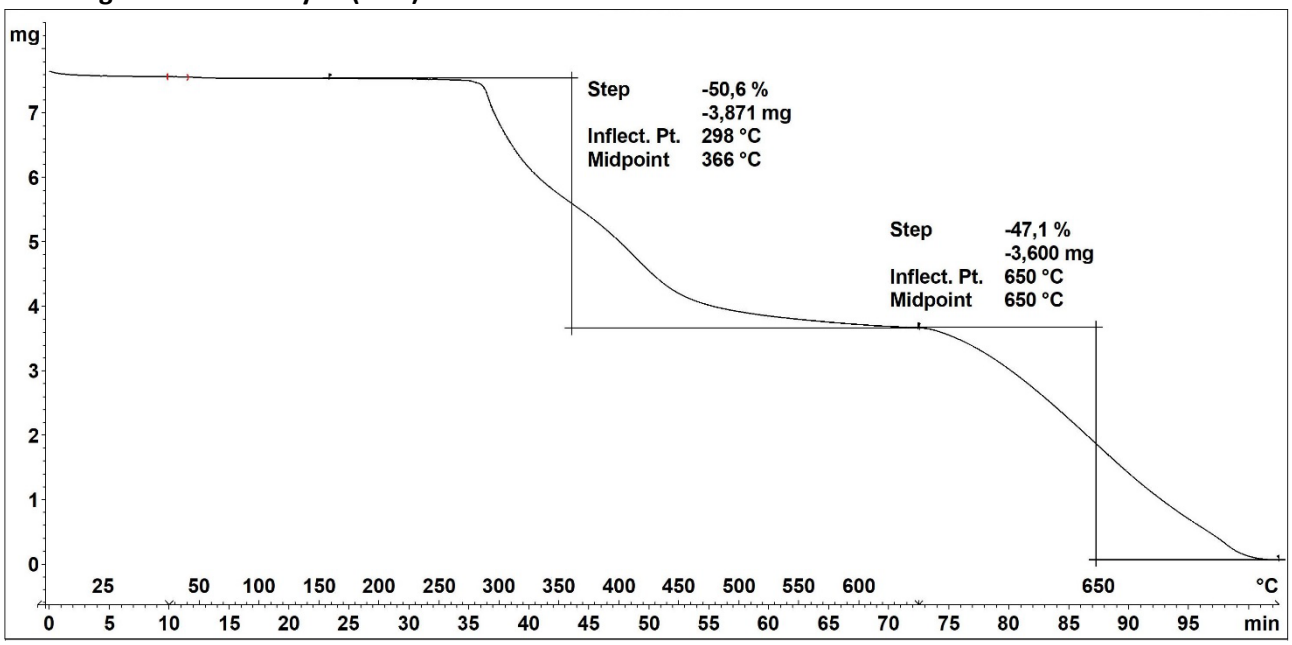

Decomposition graph. The experiment was conducted under He then air (after 650 °C).

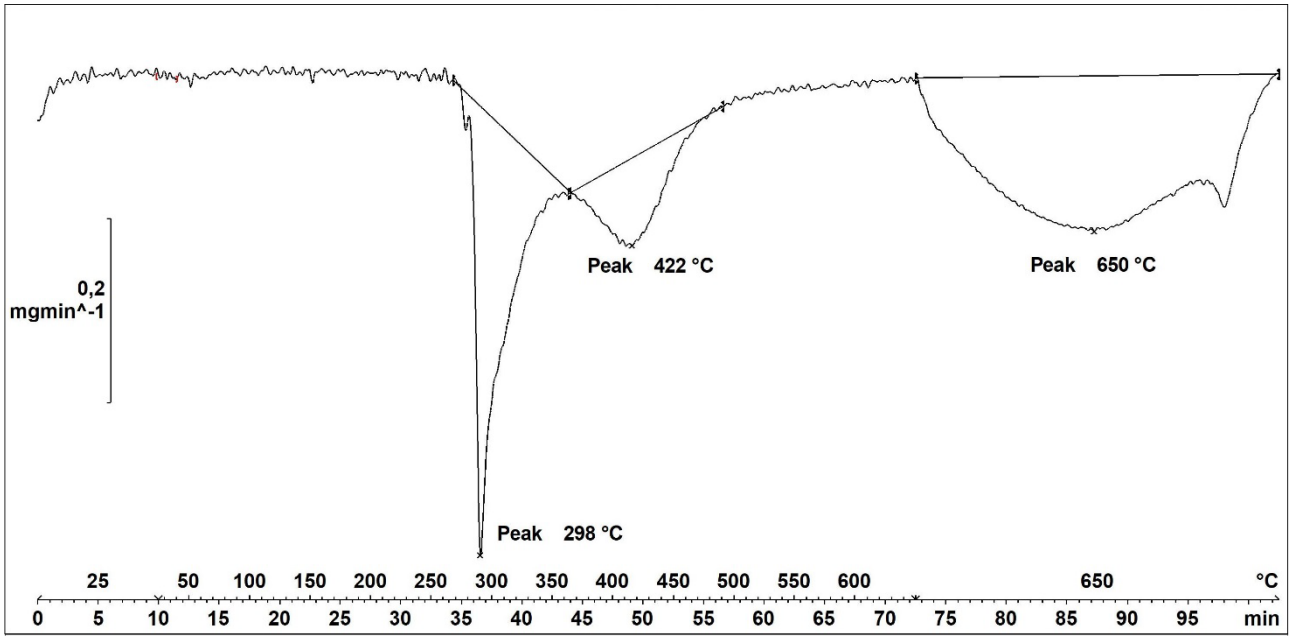

1st derivative of decomposition graph. The experiment was conducted under He then air (after 650 °C).

Decomposition temperature (T_d) = 298 and 422 ^{o}C (two decomposition steps).

Differential Scanning Calorimetry (DSC) Analysis

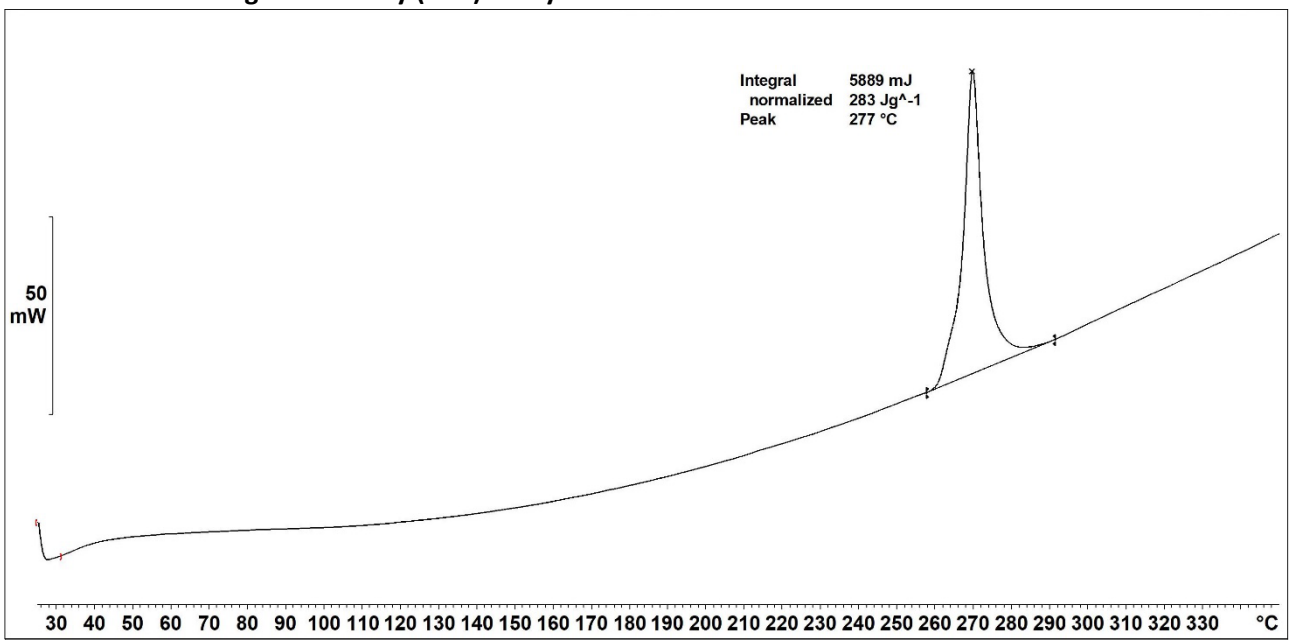

No glass transition or melting point was observed. The peak at 277 °C is due to thermal decomposition.

Elemental Analysis (EA)

N [%]	C [%]	H [%]	S [%]	mmol N/g	C/N ratio	C/H ratio
24.15	65.68	5.92	Not detected	17.24	3.17	0.93

Acrylonitrile weight percentage calculation (AN%):
N% = 24.15

M(N) = 14.0067 g/mol
M(AN) = 53.06 g/mol
$AN\% = \frac{N\%}{M(N)} \cdot M(AN)$ = 91%

Acrylic yarn with poly(amide) (TEX2, Puffy yarn) was purchased from Føtex (Danish supermarket) and used without further purification. Smaller pieces were generated by cutting with scissors and used as such in the catalytic hydrogenation. The polymer was analysed with ^{1}H– and ^{13}C–NMR, solid-state ^{13}C CP/MAS NMR, IR, TGA, DSC, and elemental analysis. Solubility tests were also conducted with several solvents.

Fibers used for the catalytic hydrogenation reactions

Solubility chart

Soluble **Swells** **Not soluble**

$CHCl_3$	Acetone	*i*-PrOH	DMF*	DMSO*	THF	PhMe	H_2O	MeOH	MeCN	GVL*

*Only the acrylic part dissolved and the poly(amide) was left behind as a solid. Dissolving in GVL needed heating at 100 °C.

^{1}H–NMR (DMSO-d_6) (only DMSO-soluble fraction)

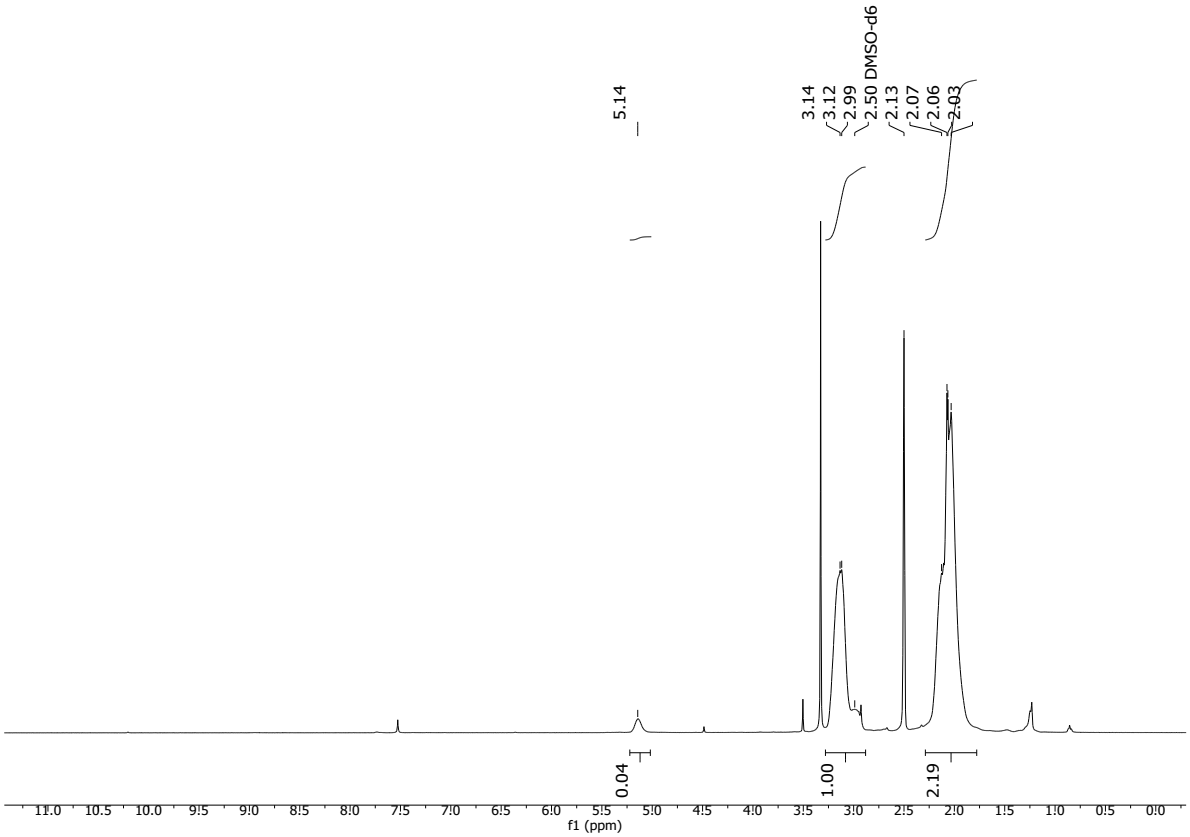

^{13}C–NMR (DMSO-d_6) (only DMSO-soluble fraction)

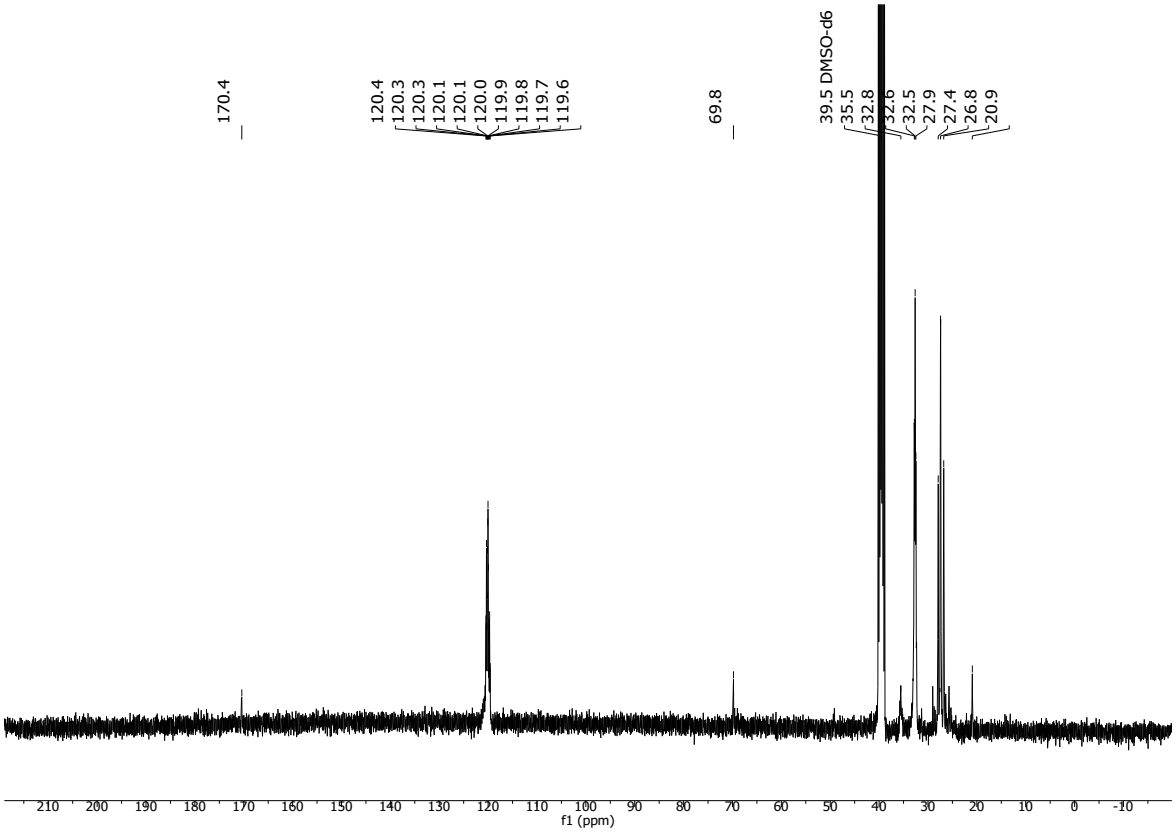

^{13}C CP/MAS NMR (solid-state)

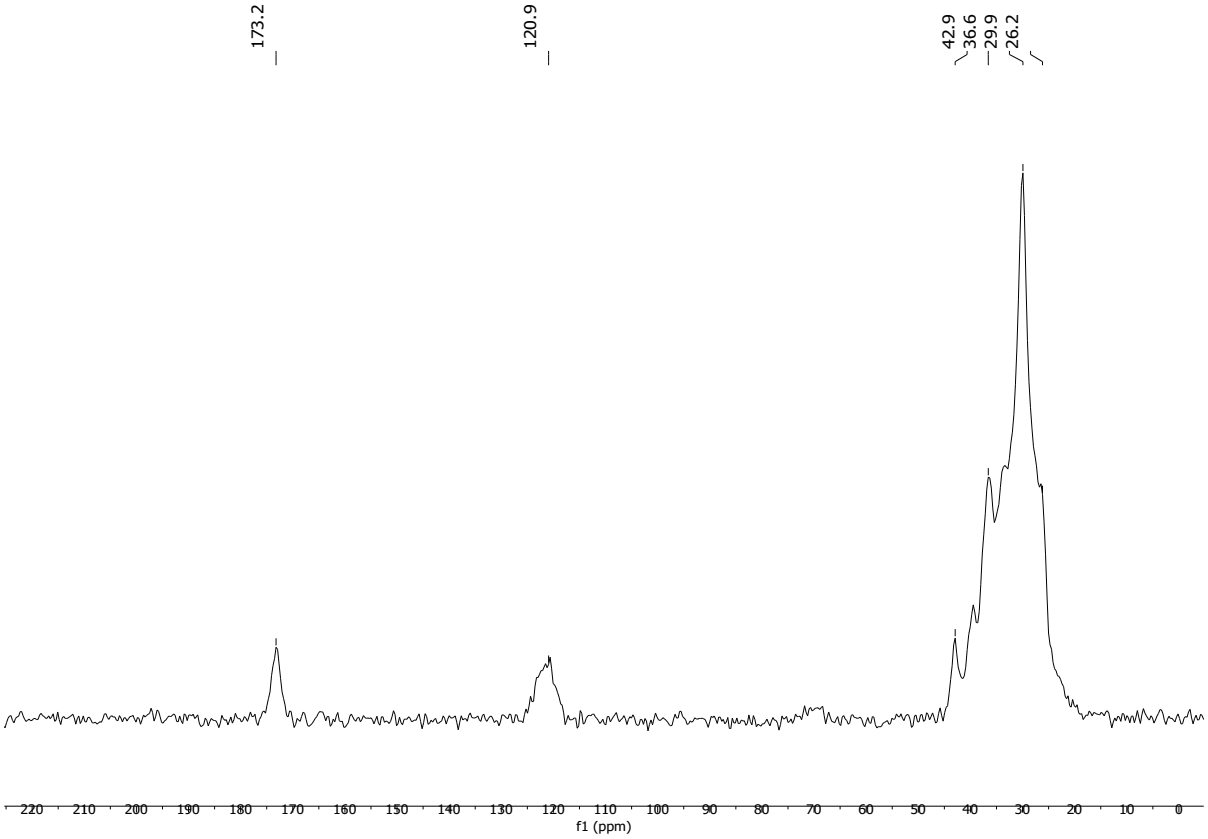

Infrared (IR) Spectroscopic Analysis

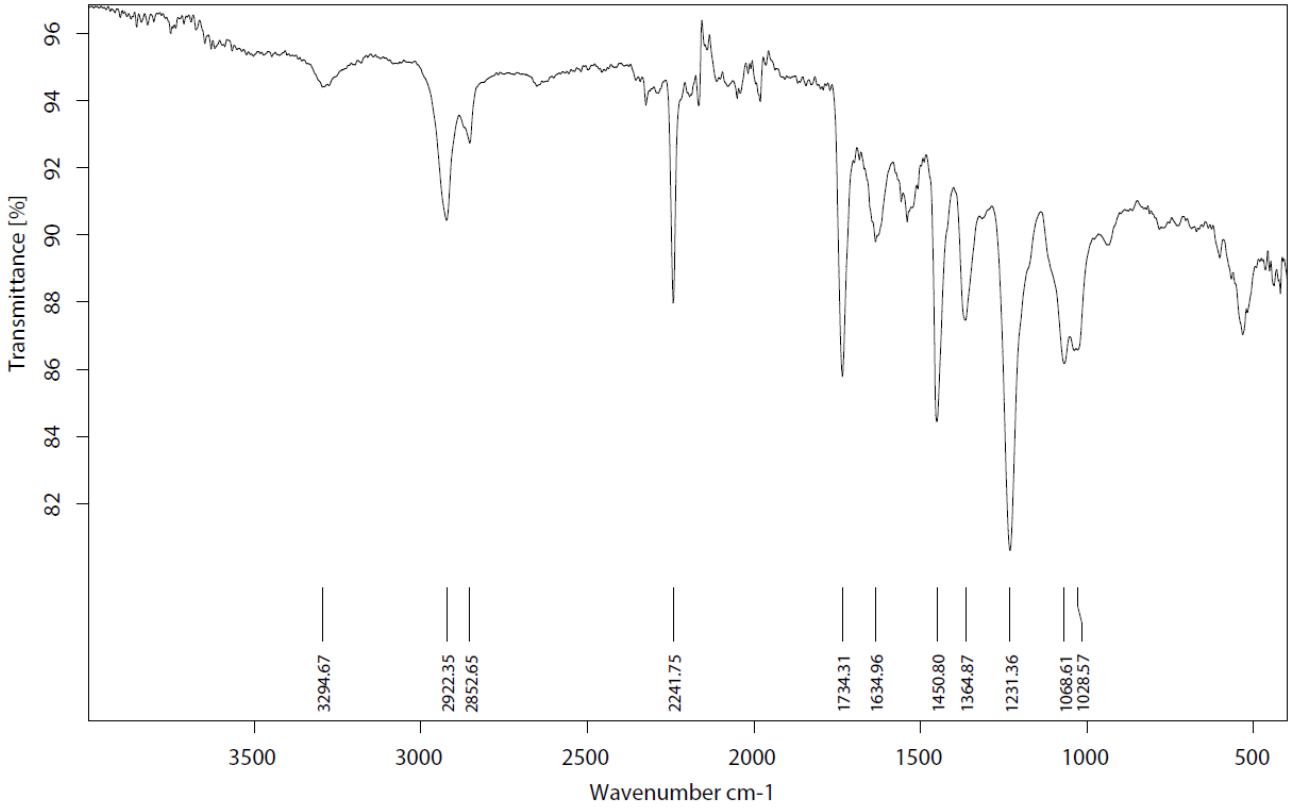

Thermogravimetric Analysis (TGA)

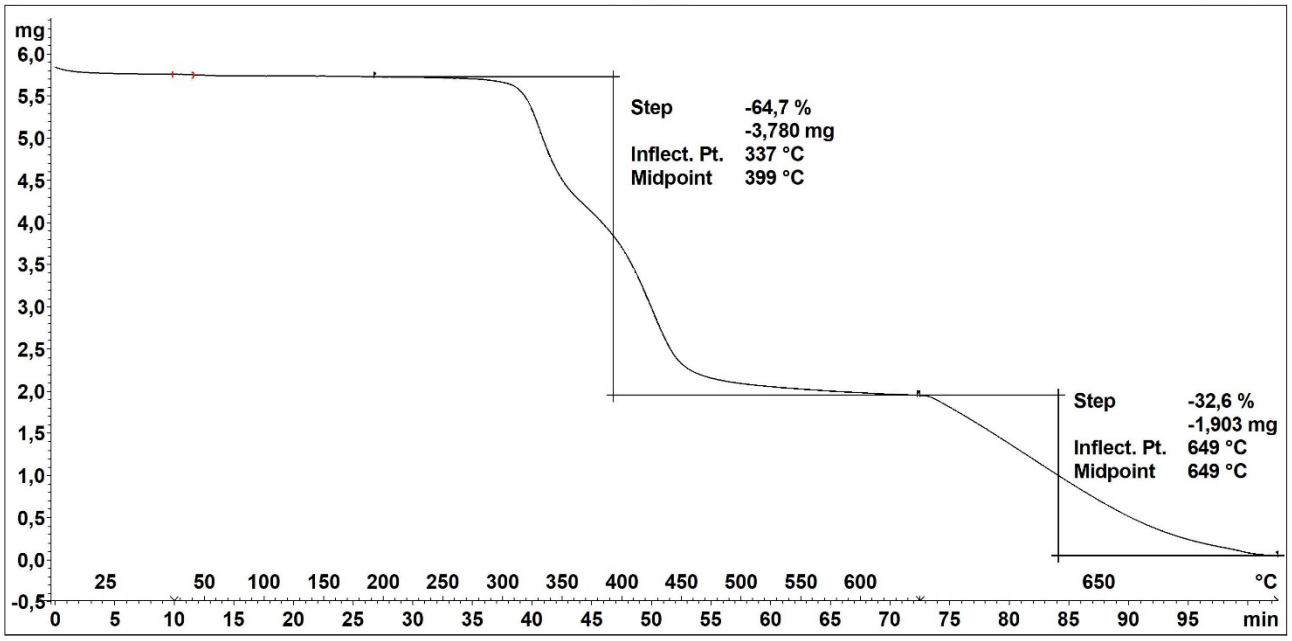

Decomposition graph. The experiment was conducted under He then air (after 650 °C).

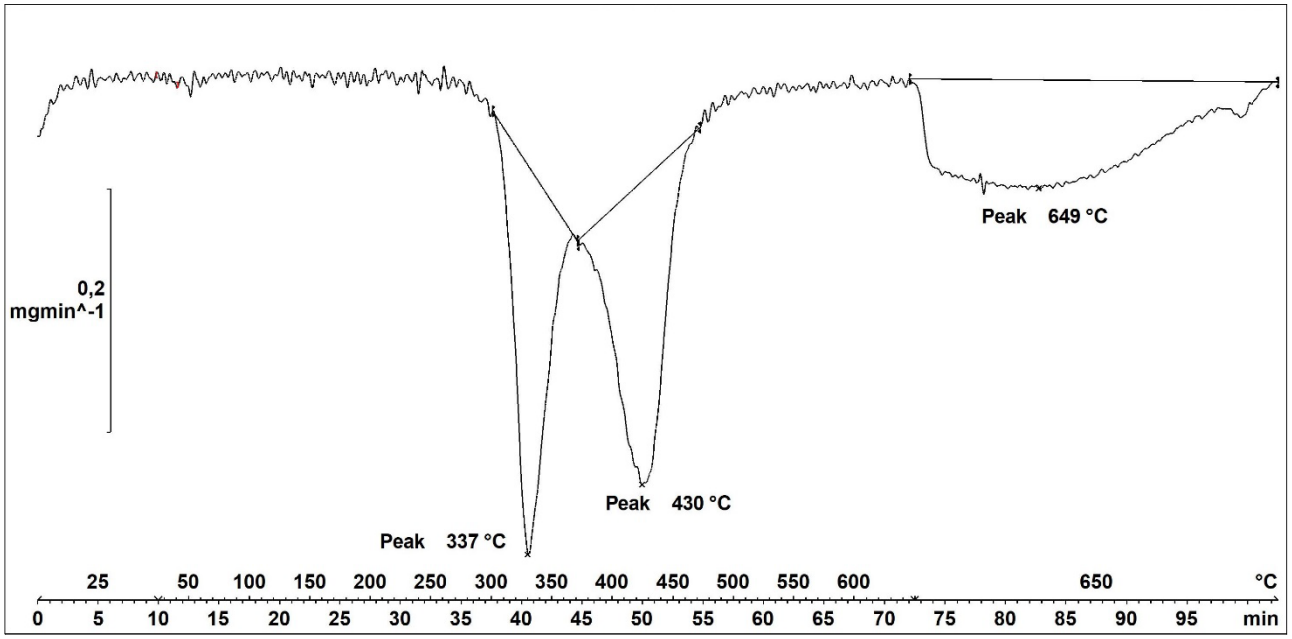

1st derivative of decomposition graph. The experiment was conducted under He then air (after 650 °C).

Decomposition temperature (T_d) = 337 and 430 °C (two decomposition steps).

Differential Scanning Calorimetry (DSC) Analysis

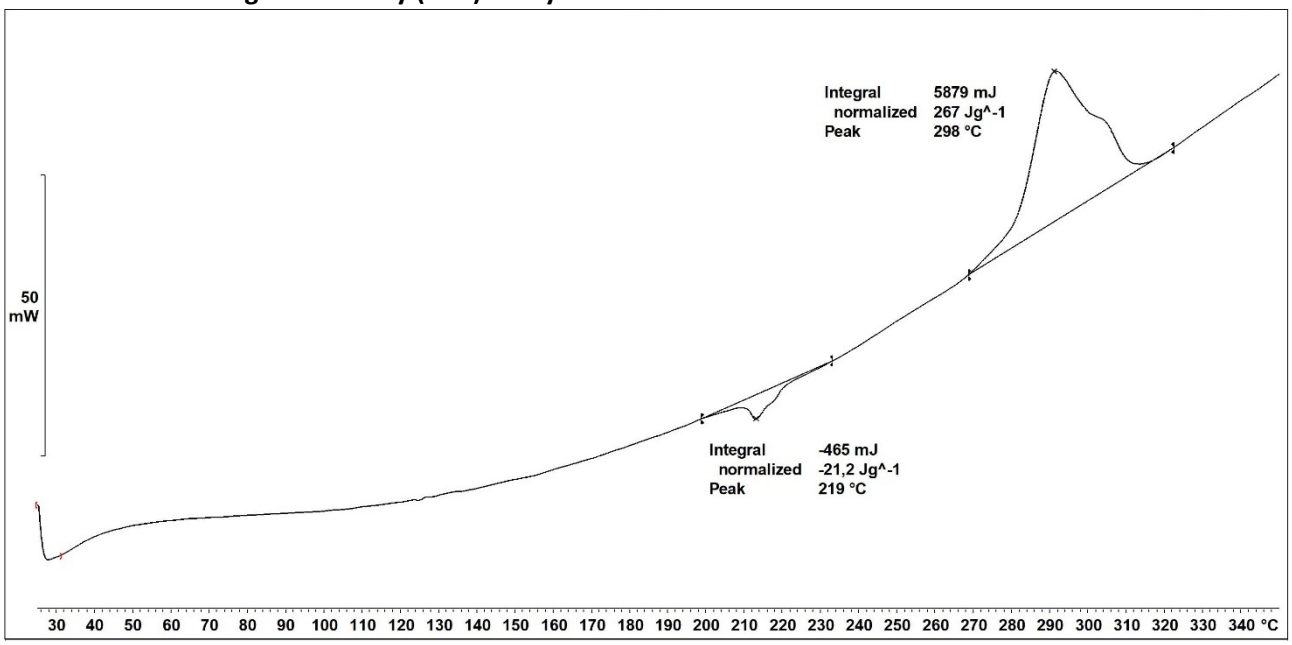

No glass transition was observed. A melting point for poly(amide) is observed at 219 °C, which suggests a PA-6 polymer. The peak at 298 °C is due to thermal decomposition.

Elemental Analysis (EA)

N [%]	C [%]	H [%]	S [%]	mmol N/g	C/N ratio	C/H ratio
20.48	64.87	7.18	Not detected	14.62	3.69	0.76

Acrylonitrile weight percentage calculation based on EA (AN%):
N% = 20.48
M(N) = 14.0067 g/mol
M(AN) = 53.06 g/mol
$AN\% = \frac{N\%}{M(N)} \cdot M(AN)$ = 78%*

*Since this textile consists of both acrylic and poly(amide) co-polymers, the calculation of AN% via the EA result gives a higher percentage due to the nitrogen content of the poly(amide).

Acrylic textile with poly(amide) (TEX3, VRS® Black sock) was purchased from Føtex (Danish supermarket) and used without further purification. Smaller pieces were generated by cutting with scissors and used as such in the catalytic hydrogenation. The polymer was analysed with ^{1}H– and ^{13}C–NMR, solid-state ^{13}C CP/MAS NMR, IR, TGA, DSC, and elemental analysis. Solubility tests were also conducted with several solvents.

Note: Although the hydrogenated **TEX3** was able to adsorb CO_2 as shown by TGA, the adsorption capacities were found to be irregular, thus this sample has been excluded from the main materials scope. However, **TEX3** was still used to prepare **MIX2** (the GVL-extracted acrylic powder, see p. S63).

Solubility chart

Soluble **Swells** **Not soluble**

$CHCl_3$	Acetone	*i*-PrOH	DMF*	DMSO*	THF	PhMe	H_2O	MeOH	MeCN	GVL*

*Only the acrylic part dissolved and the poly(amide) was left behind as a solid. Dissolving in GVL needed heating at 100 °C.

^{1}H–NMR (DMSO-d_6) (Only DMSO-soluble fraction)

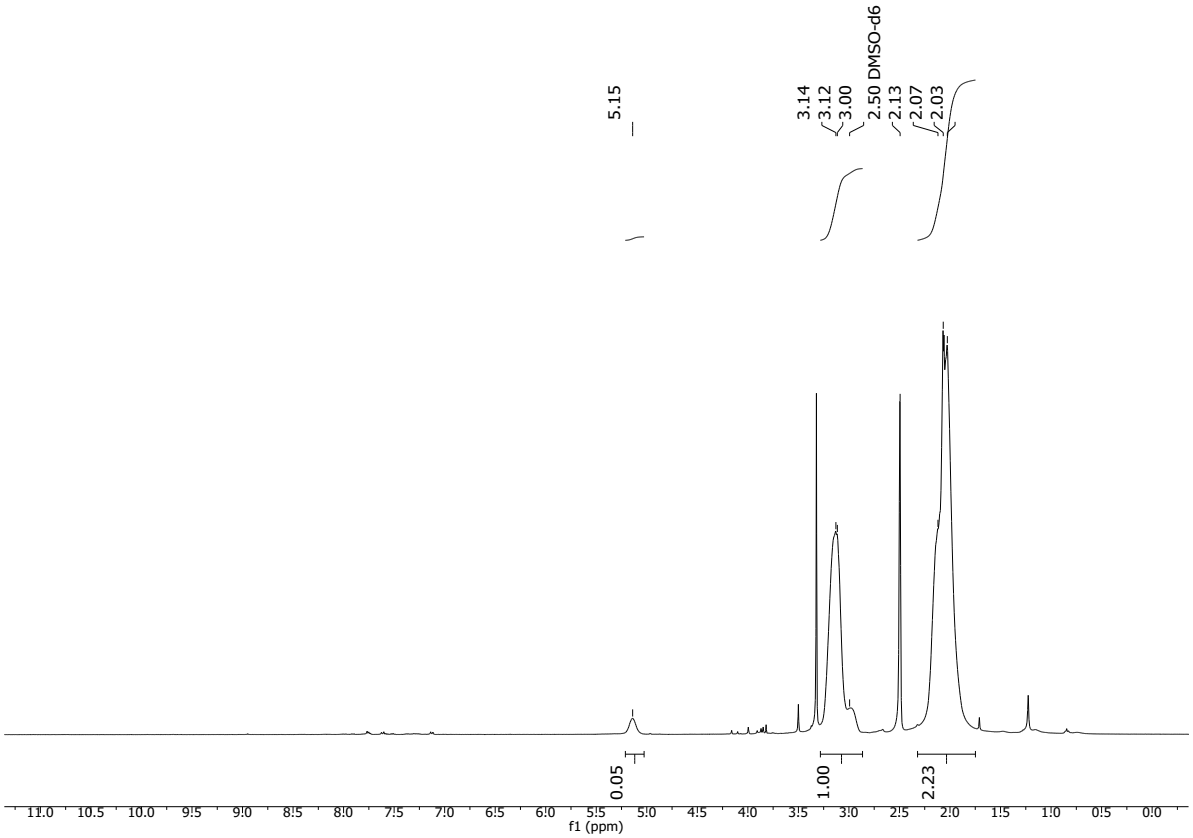

^{13}C–NMR (DMSO-d_6) (only DMSO-soluble fraction)

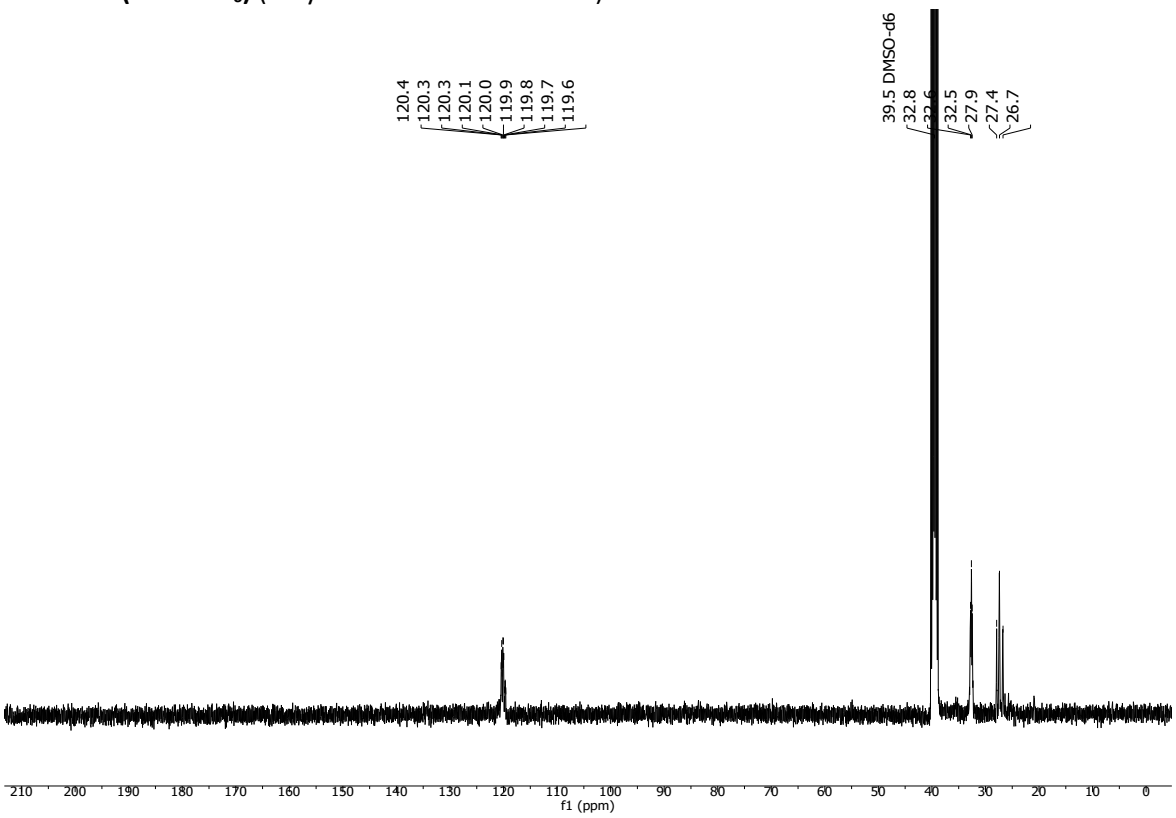

^{13}C CP/MAS NMR (solid-state)

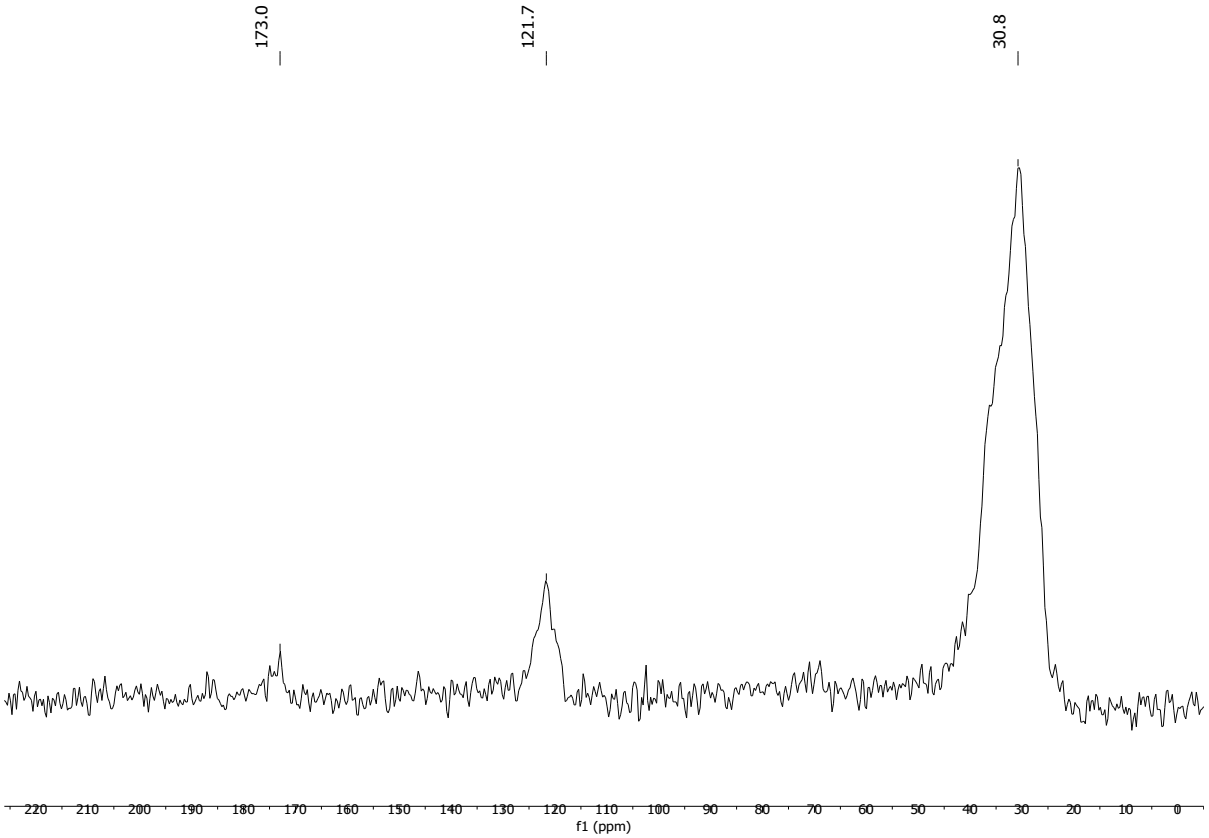

Infrared (IR) Spectroscopic Analysis

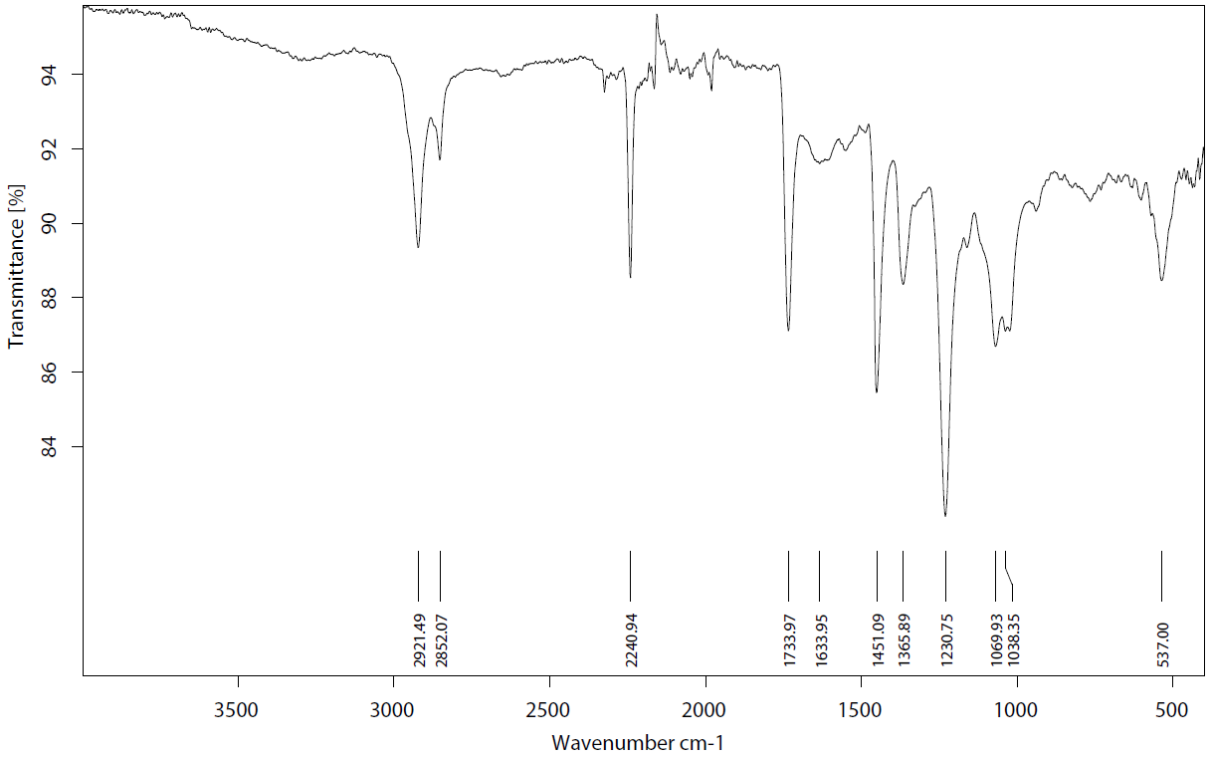

Thermogravimetric Analysis (TGA)

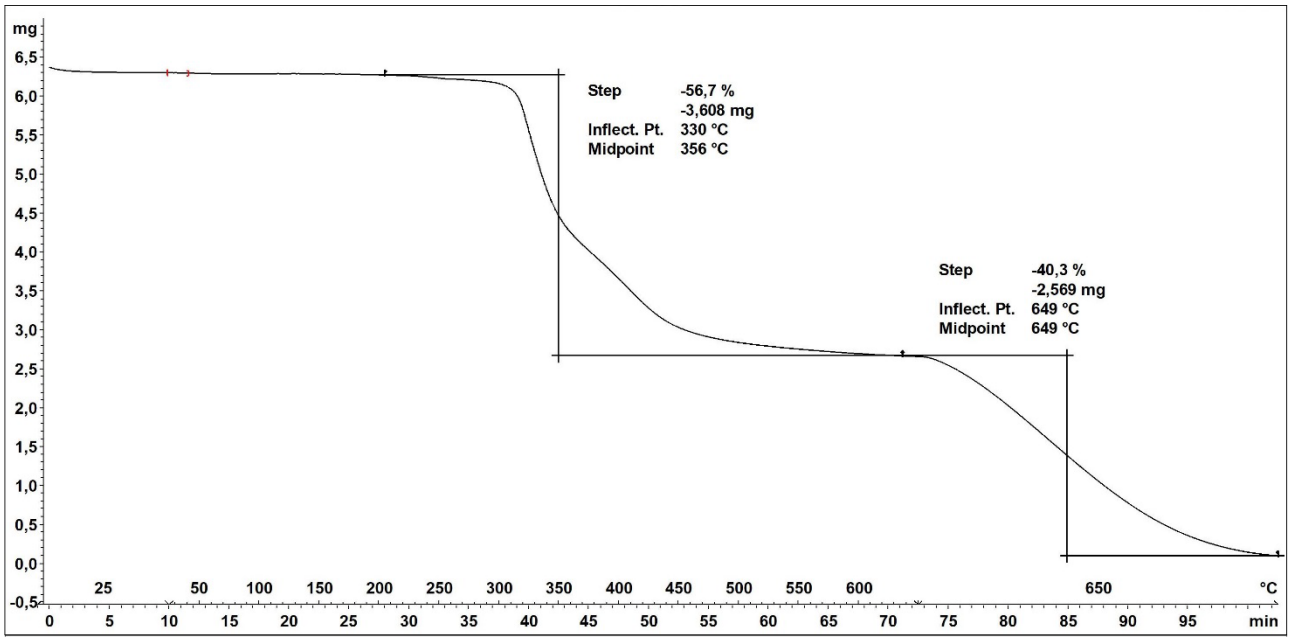

Decomposition graph. The experiment was conducted under He then air (after 650 °C).

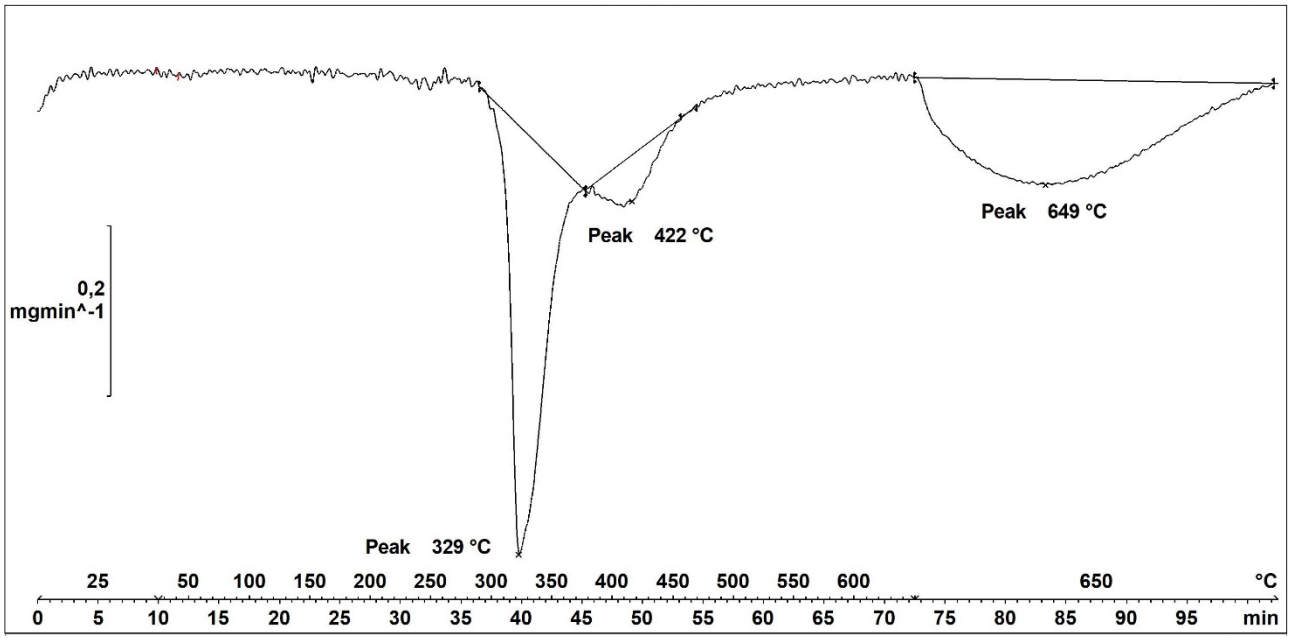

1st derivative of decomposition graph. The experiment was conducted under He then air (after 650 °C).

Decomposition temperature (T_d) = 329 and 422 ^{o}C (two decomposition steps).

Differential Scanning Calorimetry (DSC) Analysis

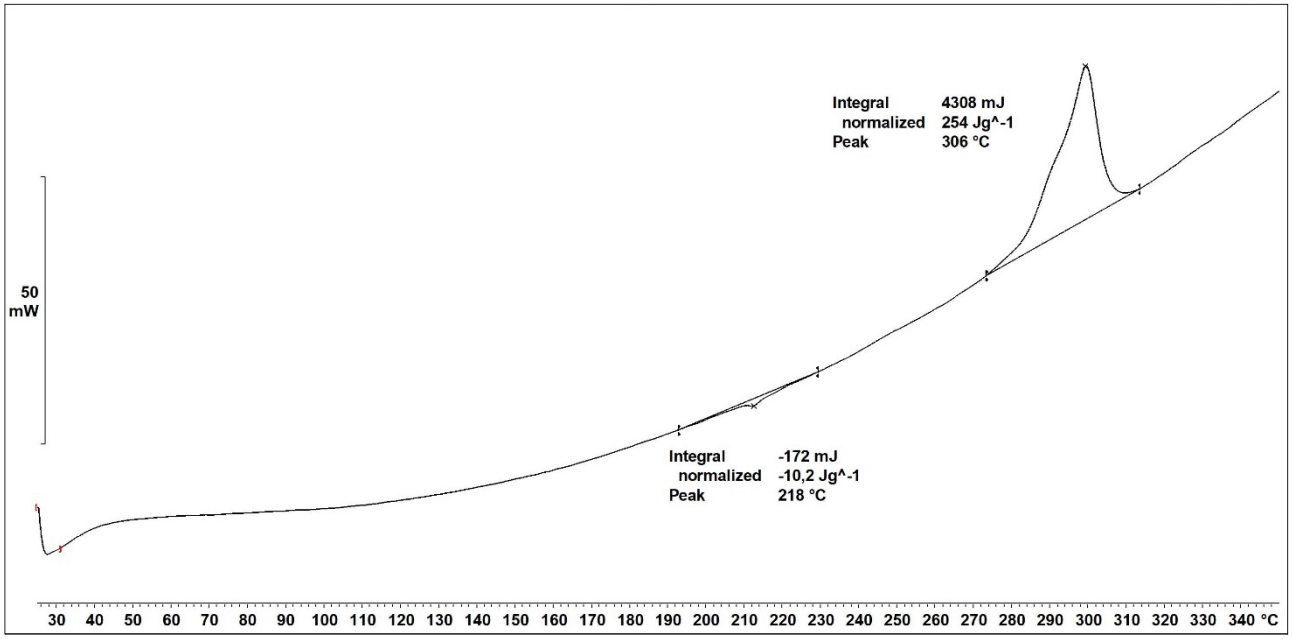

No glass transition was observed. A melting point for poly(amide) is observed at 218 °C, which suggests a PA-6 polymer. The peak at 306 °C is due to thermal decomposition.

Elemental Analysis (EA)

N [%]	C [%]	H [%]	S [%]	mmol N/g	C/N ratio	C/H ratio
23.07	65.48	6.19	Not detected	16.47	3.31	0.89

Acrylonitrile weight percentage calculation based on EA (AN%):
N% = 23.07
M(N) = 14.0067 g/mol
M(AN) = 53.06 g/mol
$AN\% = \frac{N\%}{M(N)} \cdot M(AN)$ = 87%*

*Since this textile consists of both acrylic and poly(amide) fibers, the calculation of AN% via the EA result gives a higher percentage due to the nitrogen content of the poly(amide).

Acrylic textile with Poly(ethylene terephthalate) (TEX4, VRS® White sock) was purchased from Føtex (Danish supermarket) and used without further purification. For simplifying the process, only the white part of the textile was used in the reaction. Smaller pieces were generated by cutting with scissors and used as such in the catalytic hydrogenation. The polymer was analysed with ^{1}H– and ^{13}C–NMR, solid-state ^{13}C CP/MAS NMR, IR, TGA, DSC, and elemental analysis. Solubility tests were also conducted with several solvents.

Note: Although the hydrogenated **TEX4** was able to adsorb CO_2 as shown by TGA, the adsorption capacities were found to be irregular, thus this sample has been excluded from the main materials scope. However, **TEX4** was still used to prepare **MIX2** (the GVL-extracted acrylic powder, see p. S63).

Solubility chart

Soluble **Swells** **Not soluble**

$CHCl_3$	Acetone	*i*-PrOH	DMF*	DMSO*	THF	PhMe	H_2O	MeOH	MeCN	GVL*

*Only the poly(acrylonitrile) polymer dissolves and the poly(ethylene terephthalate) is left behind as a solid. Dissolving in GVL needed heating at 100 °C.

^{1}H–NMR (DMSO-d_6) (Only DMSO-soluble fraction)

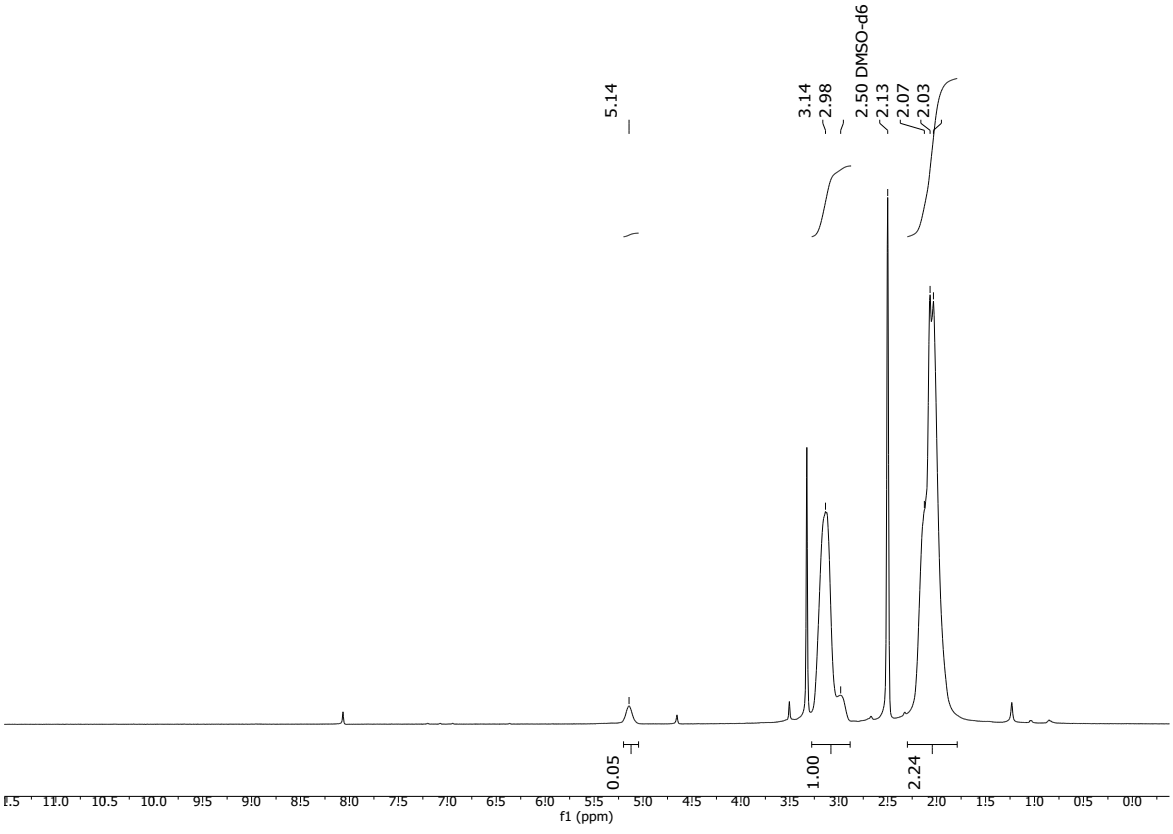

^{13}C–NMR (DMSO-d_6) (only DMSO-soluble fraction)

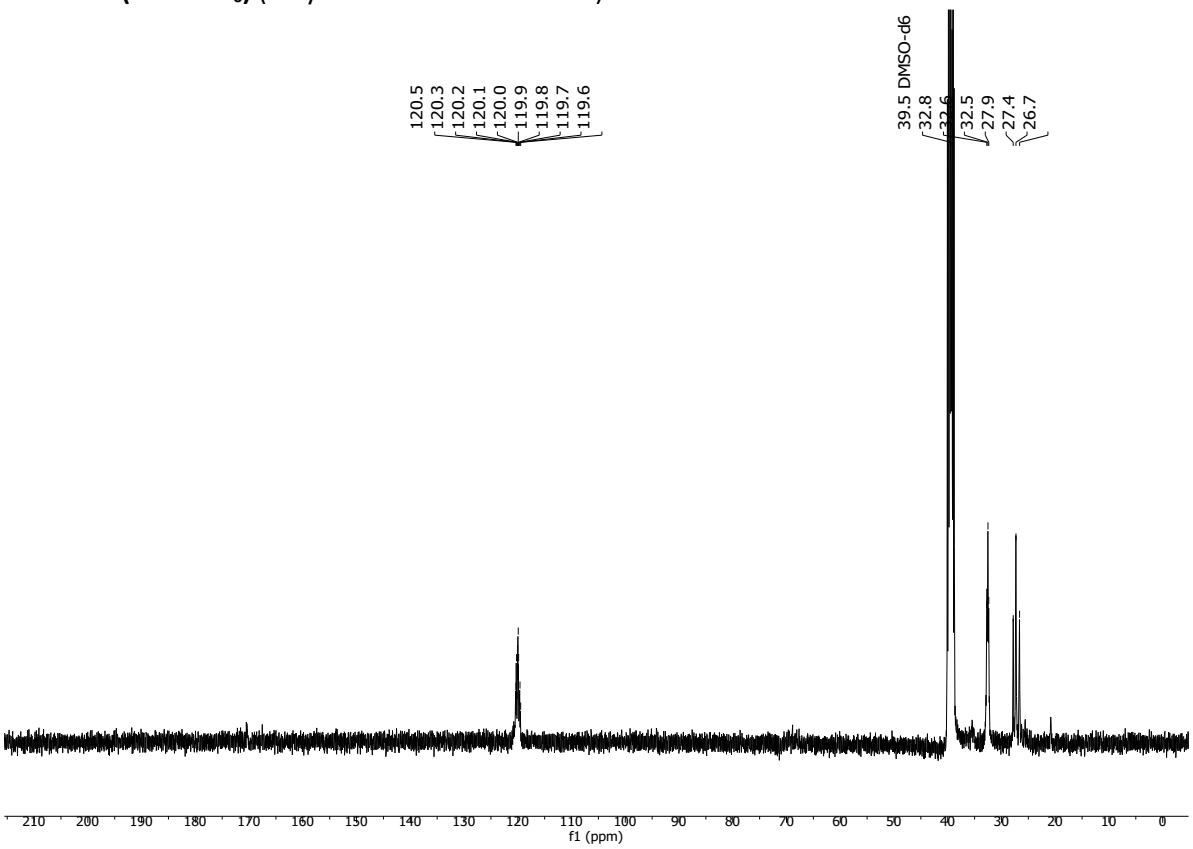

^{13}C CP/MAS NMR (solid-state)

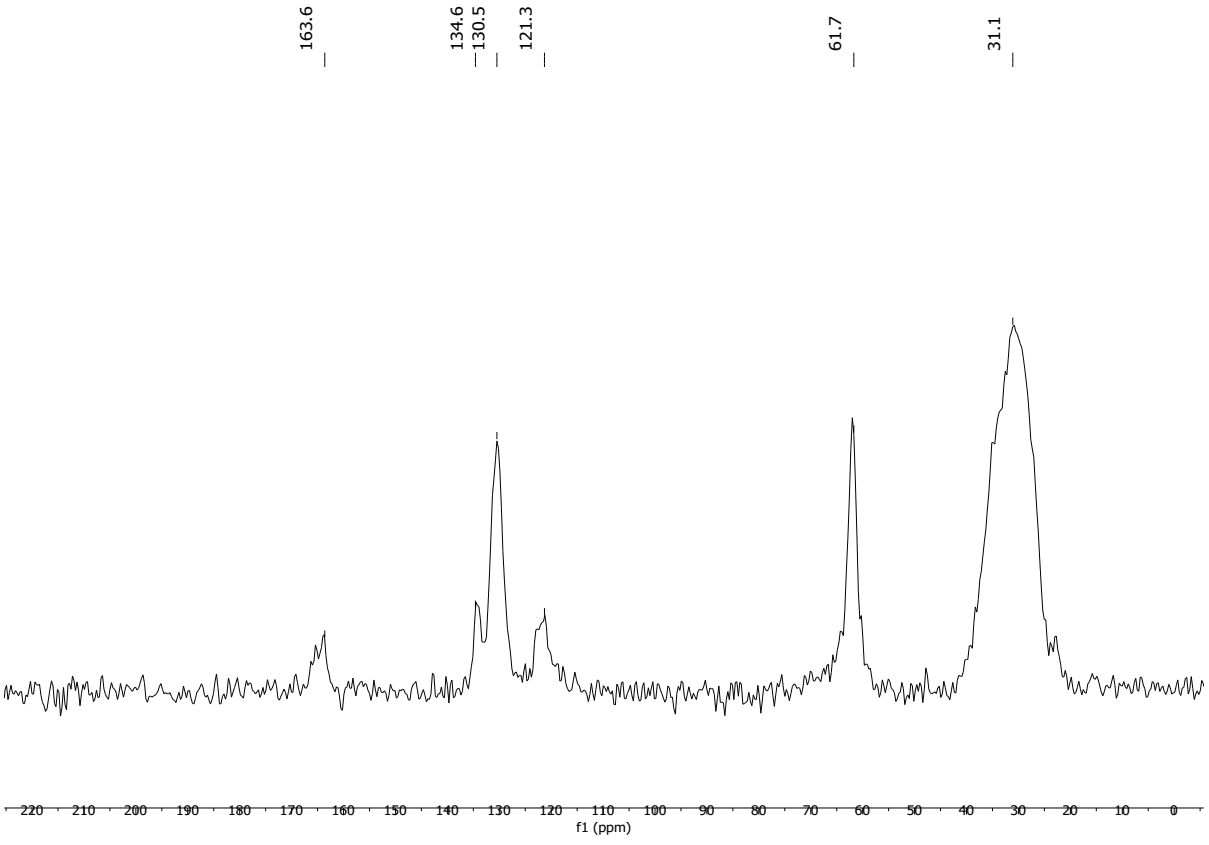

Infrared (IR) Spectroscopic Analysis

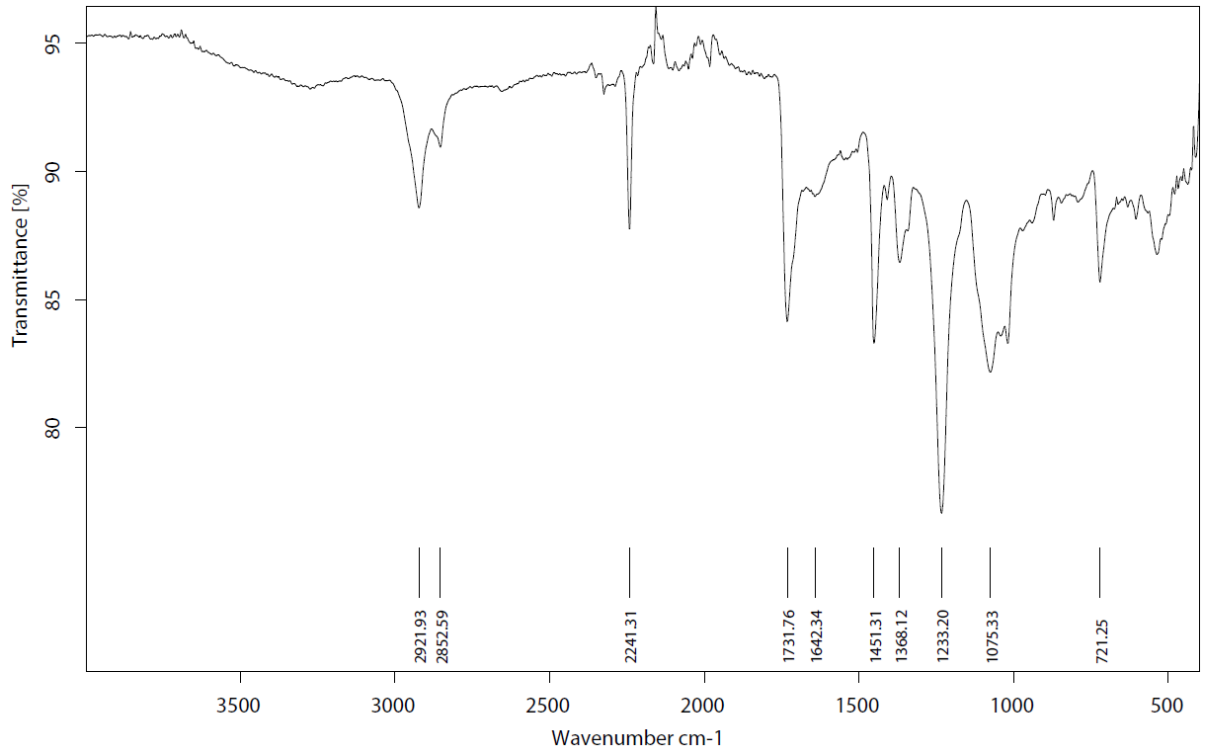

Thermogravimetric Analysis (TGA)

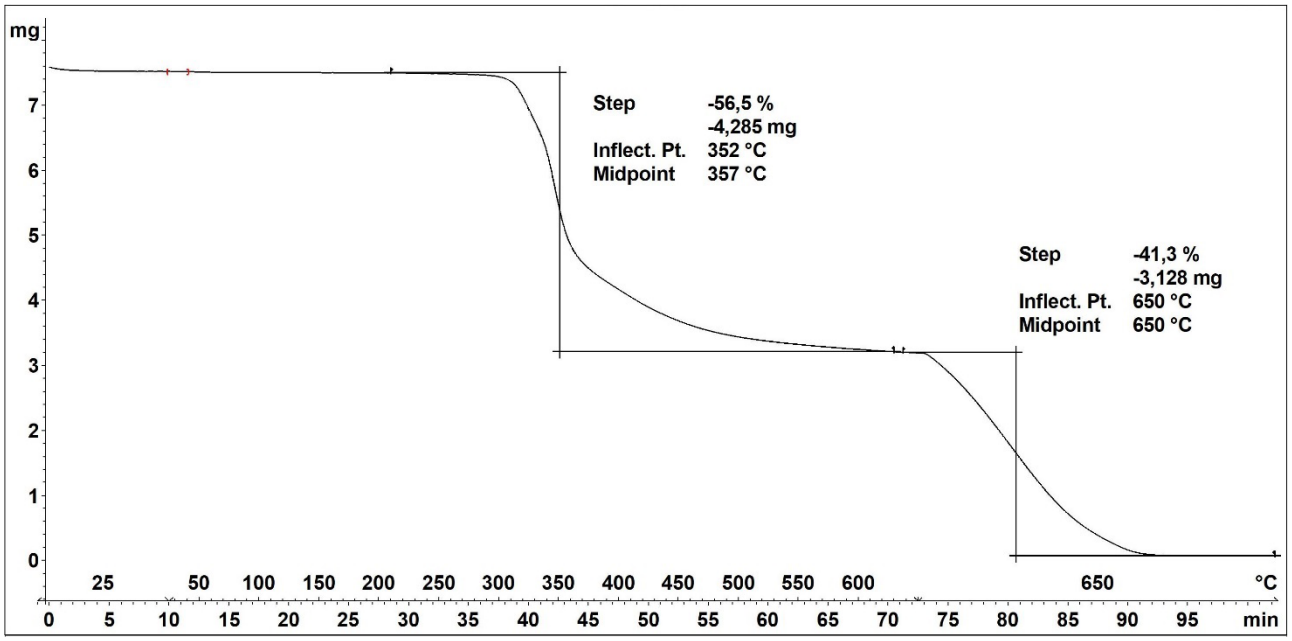

Decomposition graph. The experiment was conducted under He then air (after 650 °C).

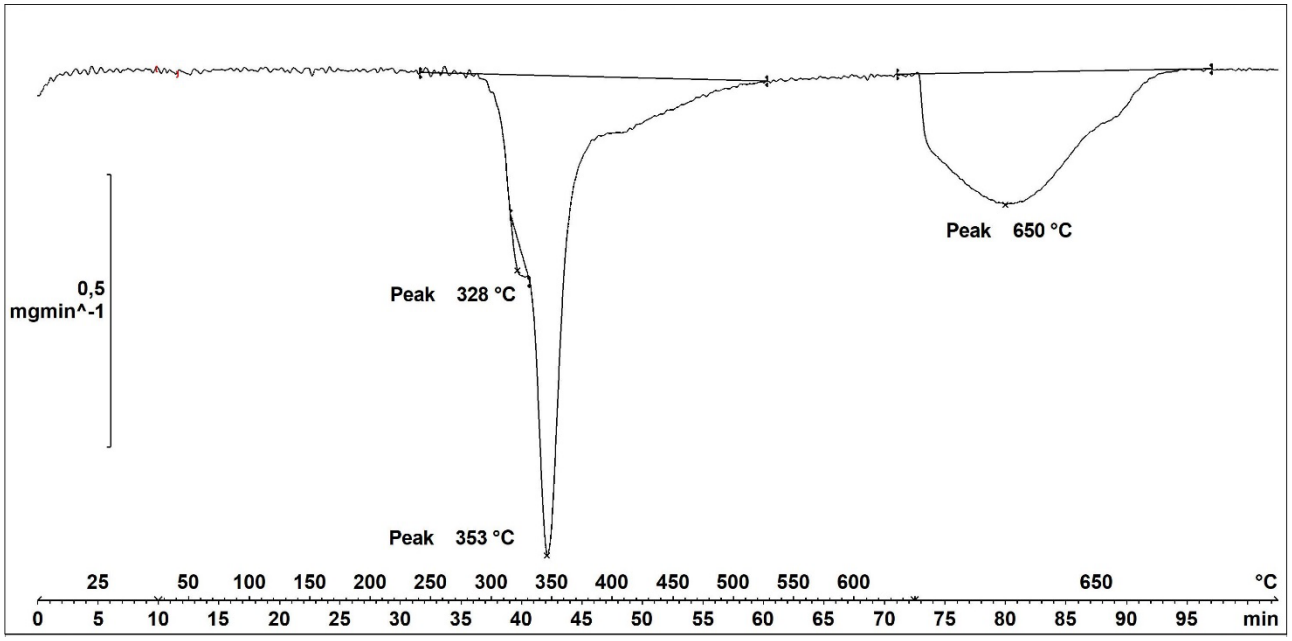

1st derivative of decomposition graph. The experiment was conducted under He then air (after 650 °C).

Decomposition temperature (T_d) = 328 and 353 °C (two decomposition steps).

Differential Scanning Calorimetry (DSC) Analysis

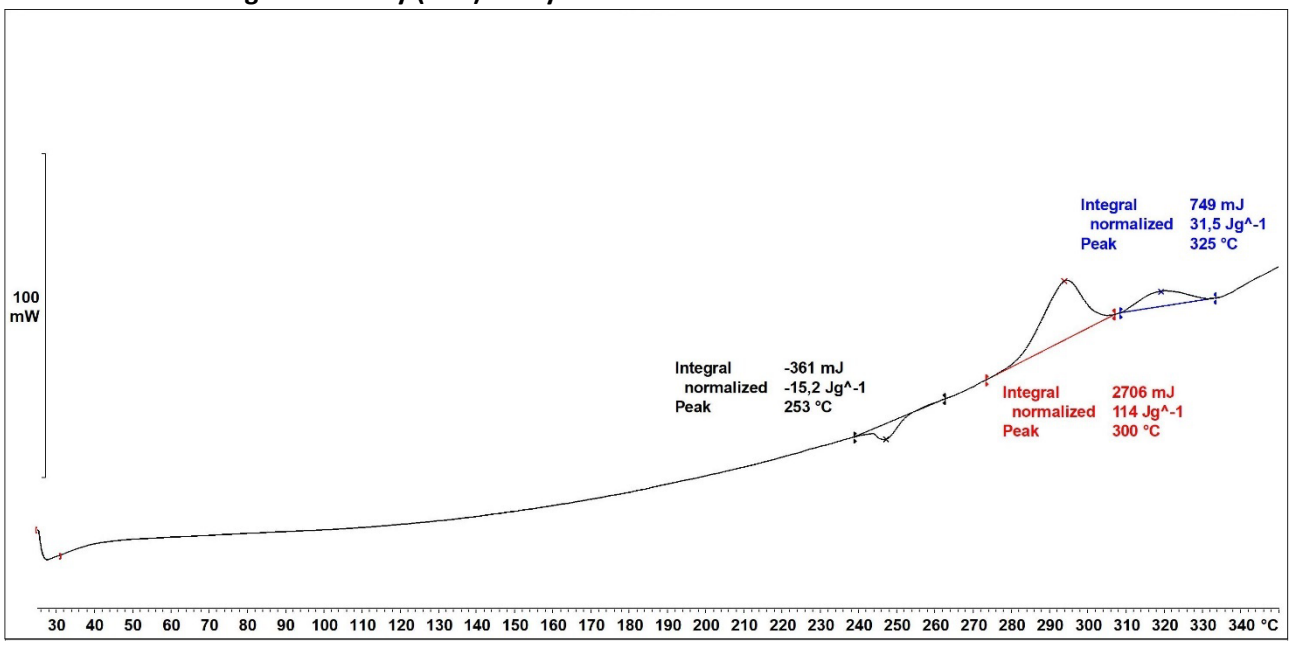

No glass transition was observed. A melting point for poly(ethylene) terephthalate (PET) is observed at 253 °C. The peak at 306 °C and 325 °C is due to thermal decomposition.

Elemental Analysis (EA)

N [%]	C [%]	H [%]	S [%]	mmol N/g	C/N ratio	C/H ratio
15.87	64.33	5.48	Not detected	11.33	4.73	0.99

Acrylonitrile weight percentage calculation based on EA (AN%):

N% = 15.87

M(N) = 14.0067 g/mol

M(AN) = 53.06 g/mol

$AN\% = \frac{N\%}{M(N)} \cdot M(AN)$ = 60%

Styrene Butadiene Rubber 1 (SBR1, SBR pellets, block co-polymer) was purchased from a SigmaAldrich® and used without further purification. This polymer is soluble in the solvent of the hydrocyanation reaction (toluene), thus cutting to smaller pieces was not necessary. The polymer was analysed with ^{1}H– and ^{13}C–NMR, solid-state ^{13}C CP/MAS NMR, IR, TGA, DSC, and elemental analysis. Solubility tests were also conducted with several solvents. According to the label, this polymer contains 30 wt% styrene, thus 70 wt% butadiene. No thermal events besides decomposition were observed with DSC.

Pellet size used for the catalytic hydrocyanation reactions (dissolves in the PhMe solvent**)**

Solubility chart

Soluble **Swells** **Not soluble**

$CHCl_3$	Acetone	*i*-PrOH	DMF	DMSO	THF	PhMe	H_2O	MeOH	MeCN

^{1}H–NMR ($CDCl_3$)

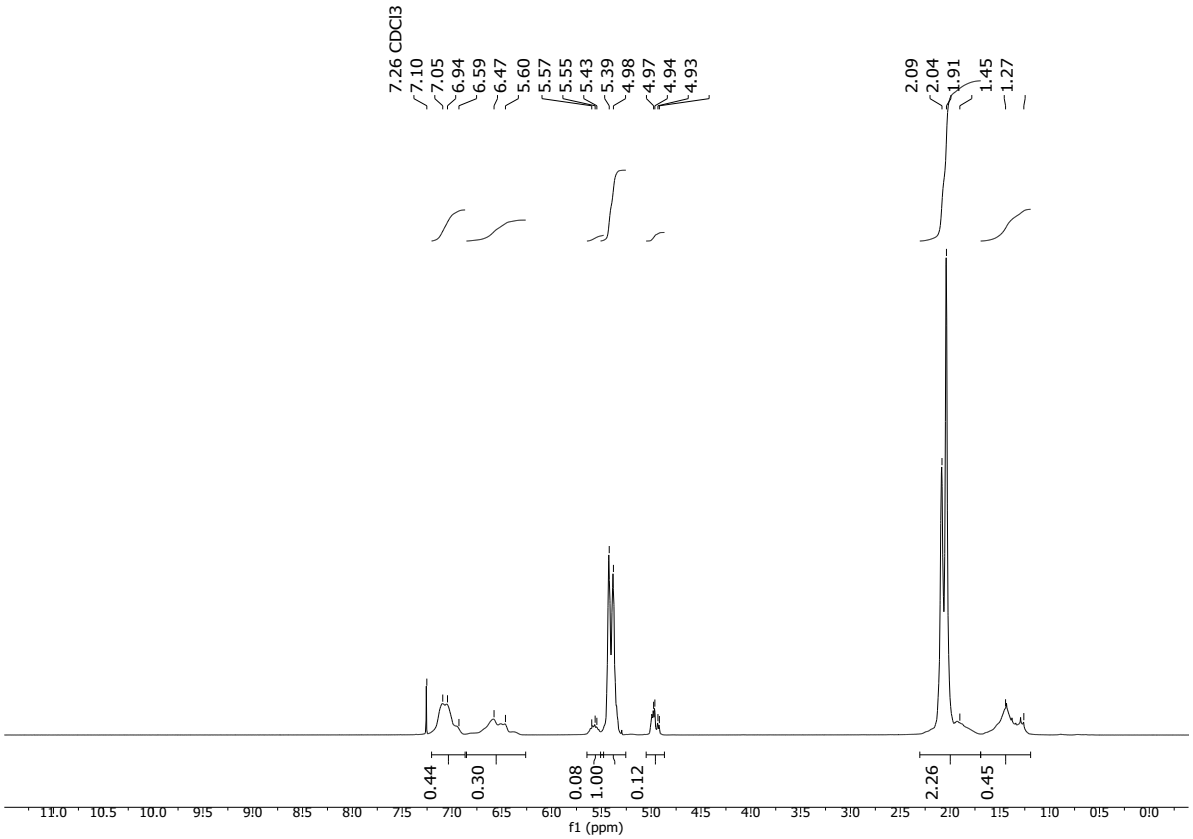

^{13}C–NMR ($CDCl_3$)

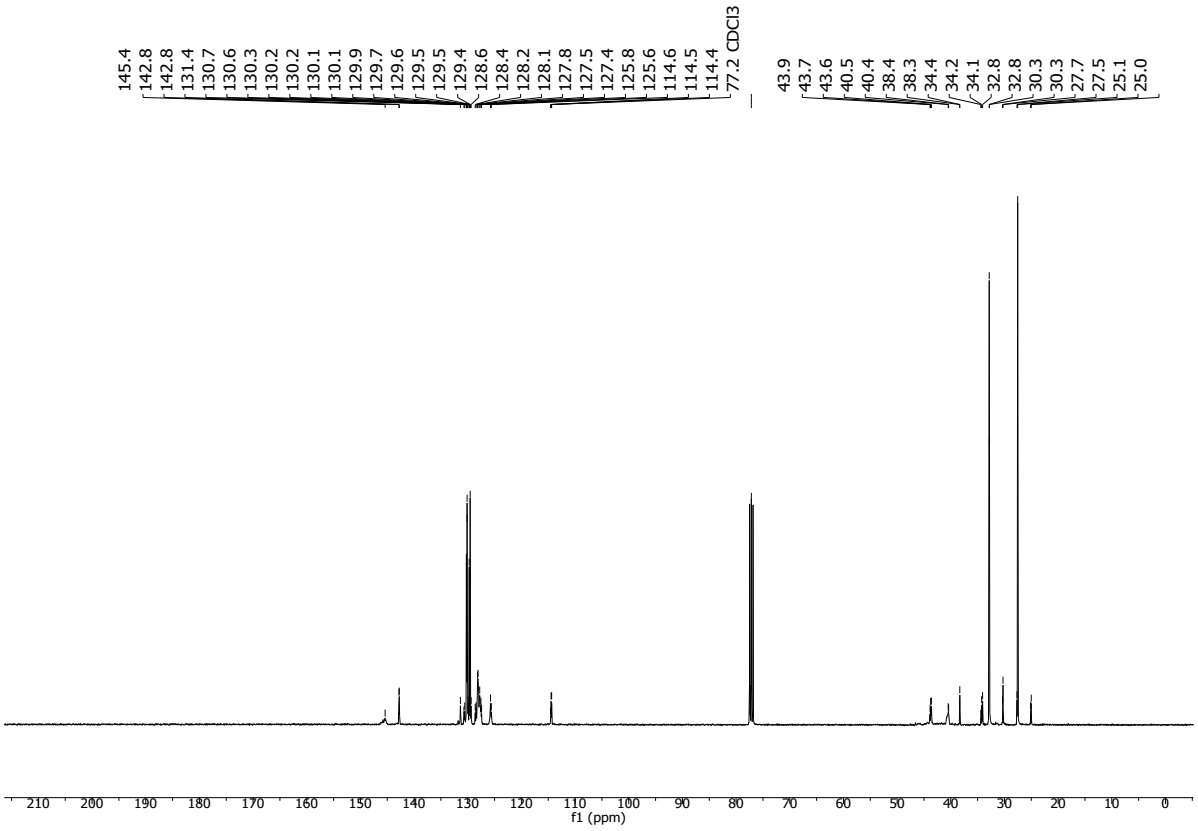

^{13}C CP/MAS NMR (solid-state)

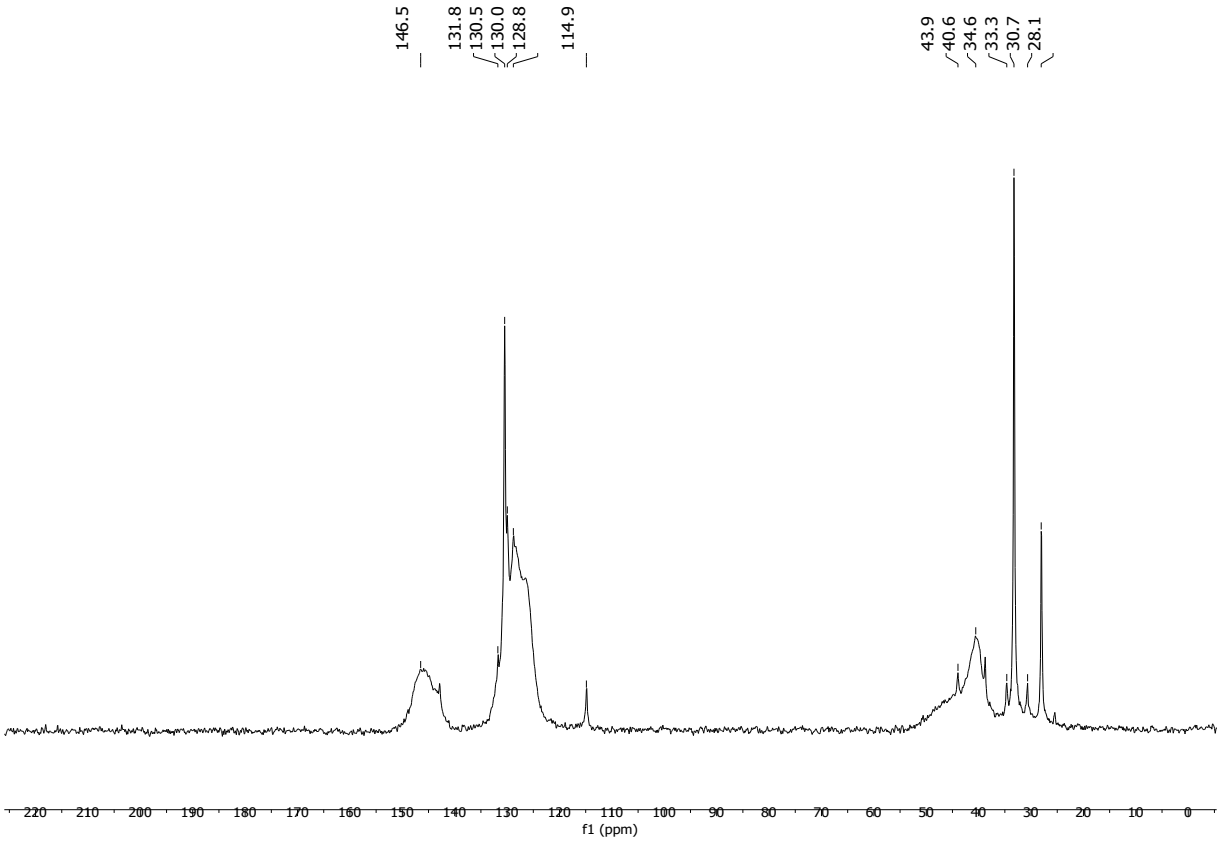

Infrared (IR) Spectroscopic Analysis

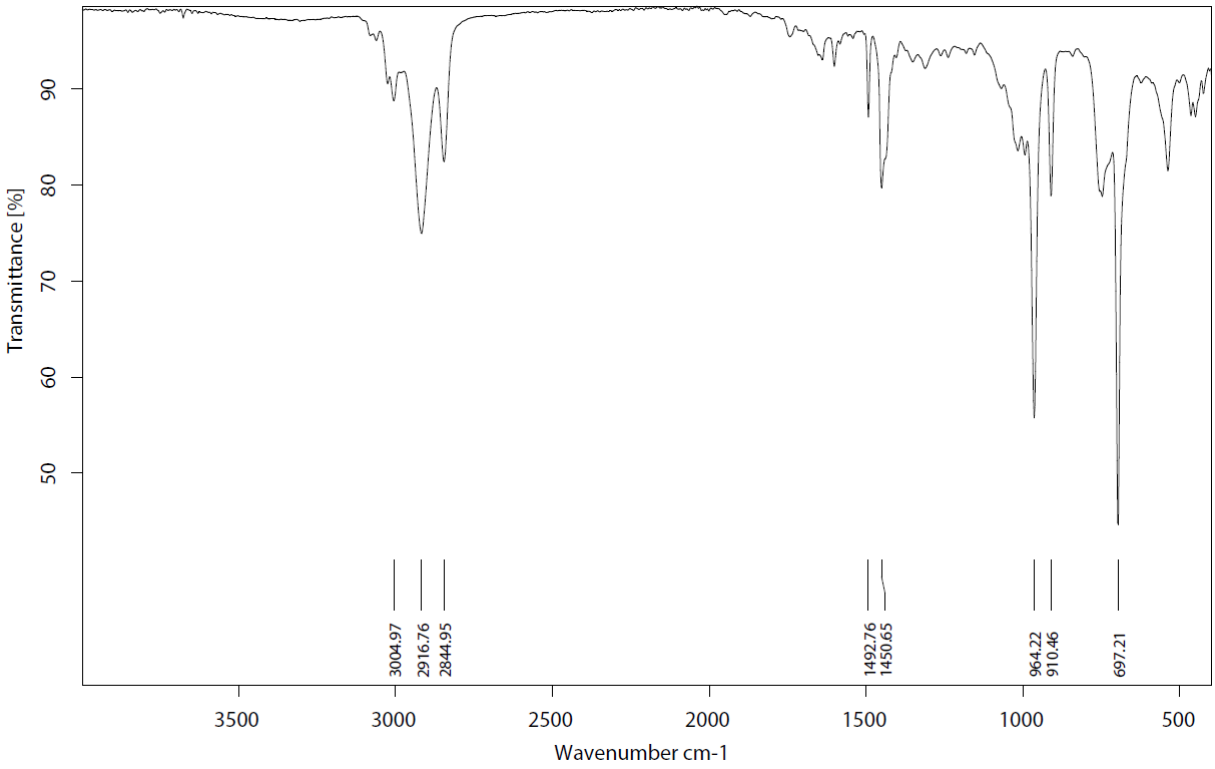

Thermogravimetric Analysis (TGA)

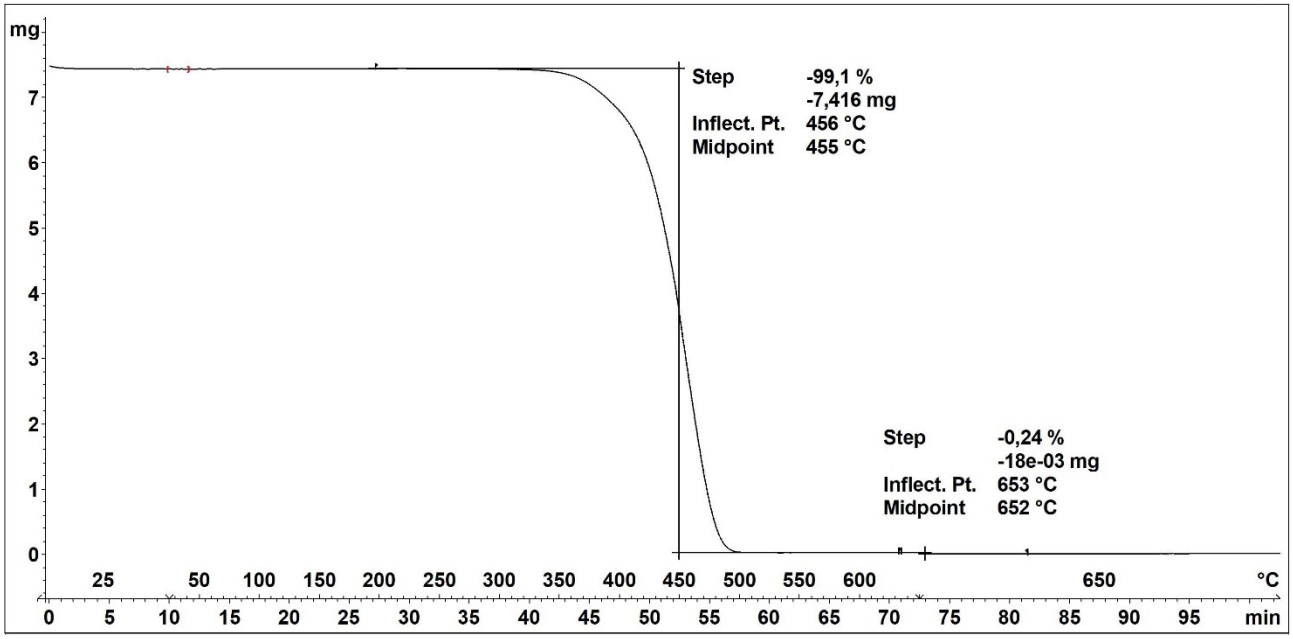

Decomposition graph. The experiment was conducted under He then air (after 650 °C).

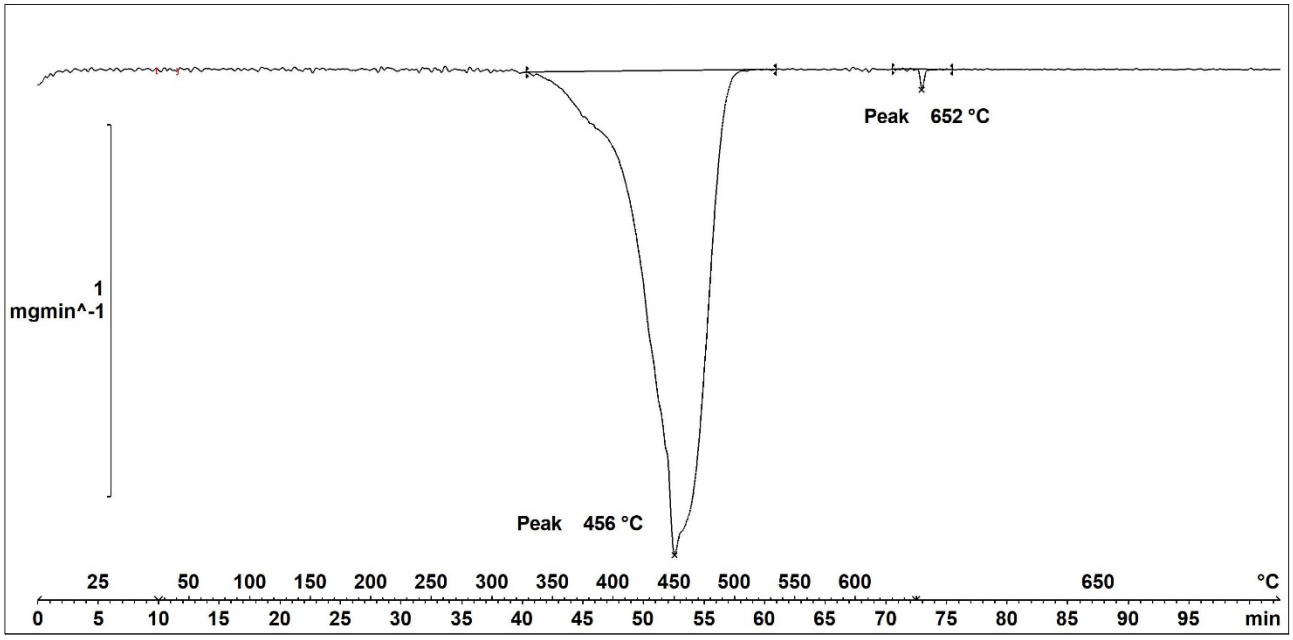

1st derivative of decomposition graph. The experiment was conducted under He then air (after 650 °C).

Decomposition temperature (T_d) = 456 °C.

Elemental Analysis (EA)

N [%]	C [%]	H [%]	S [%]	mmol N/g	C/N ratio	C/H ratio
0.09	89.55	10.62	Not detected	--	--	0.71

Styrene Butadiene Rubber 2 (SBR2, Monki® Shoe sole) was purchased from Blå Kors (Danish secondhand shop) and used without further purification. Smaller pieces were generated by cutting with a wire cutter and used as such in the catalytic hydrocyanation. The polymer was analysed with ^{1}H– and ^{13}C–NMR, solid-state ^{13}C CP/MAS NMR, IR, TGA, DSC, and elemental analysis. Solubility tests were also conducted with several solvents. No thermal events besides decomposition were observed with DSC.

Particle size used for the catalytic hydrocyanation reactions (dissolves in the PhMe solvent**)**

Solubility chart

Soluble **Swells** **Not soluble**

$CHCl_3$*	Acetone	*i*-PrOH	DMF	DMSO	THF*	PhMe*	H_2O	MeOH	MeCN

*Carbon black which is inherent in the material was not dissolved.

^{1}H–NMR ($CDCl_3$)

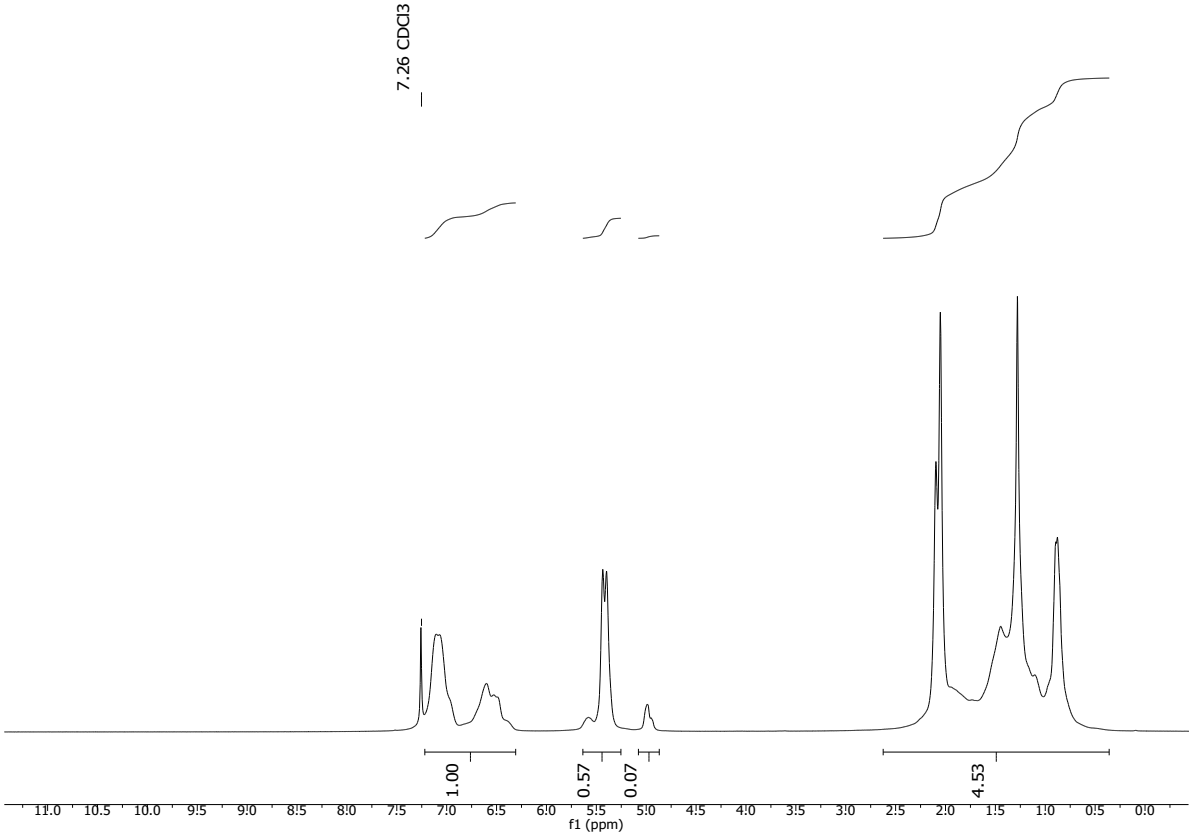

^{13}C–NMR ($CDCl_3$)

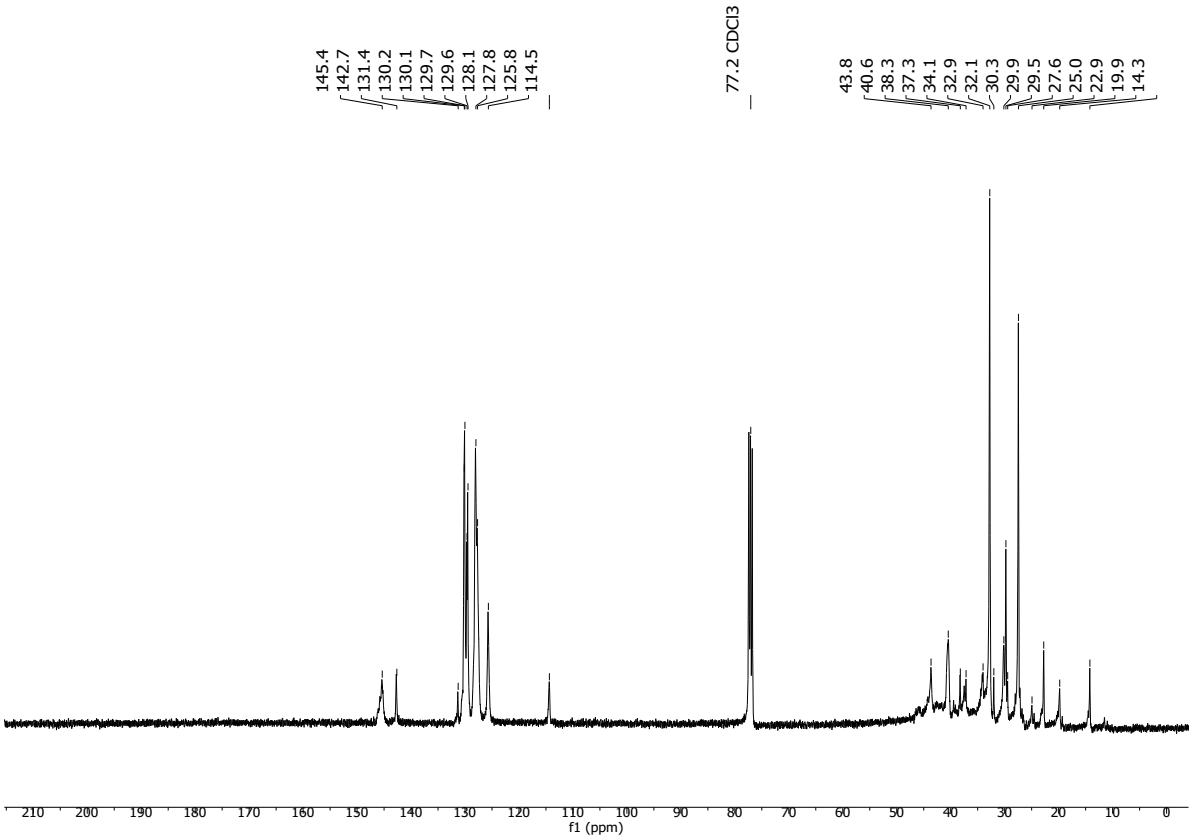

^{13}C CP/MAS NMR (solid-state)

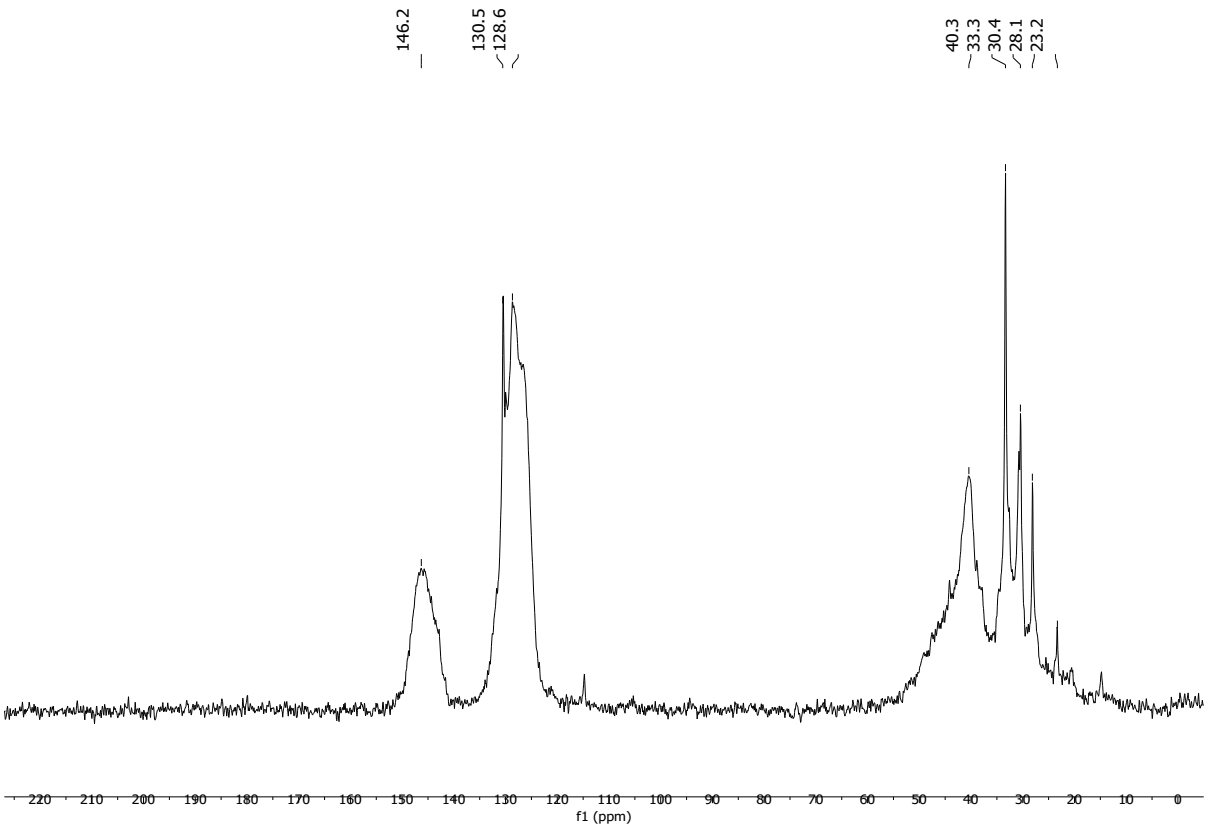

Infrared (IR) Spectroscopic Analysis

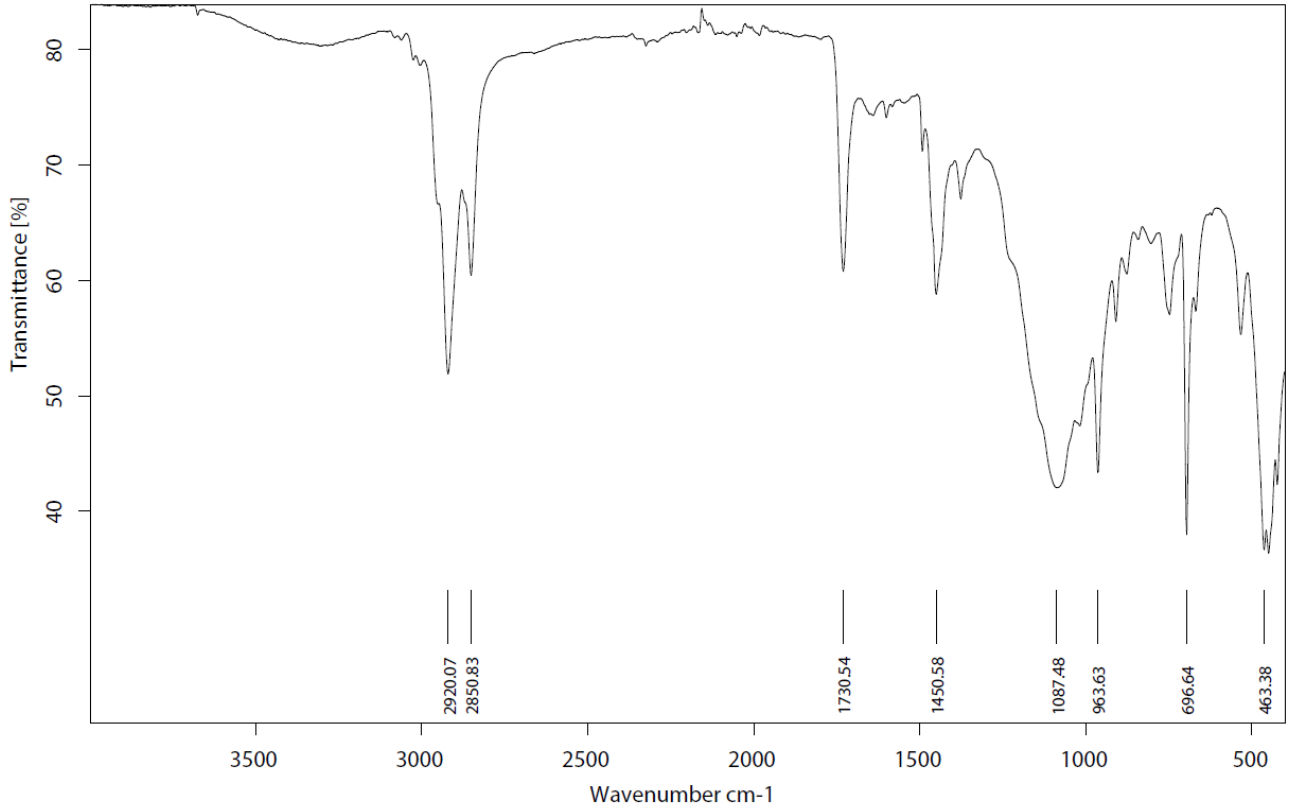

Thermogravimetric Analysis (TGA)

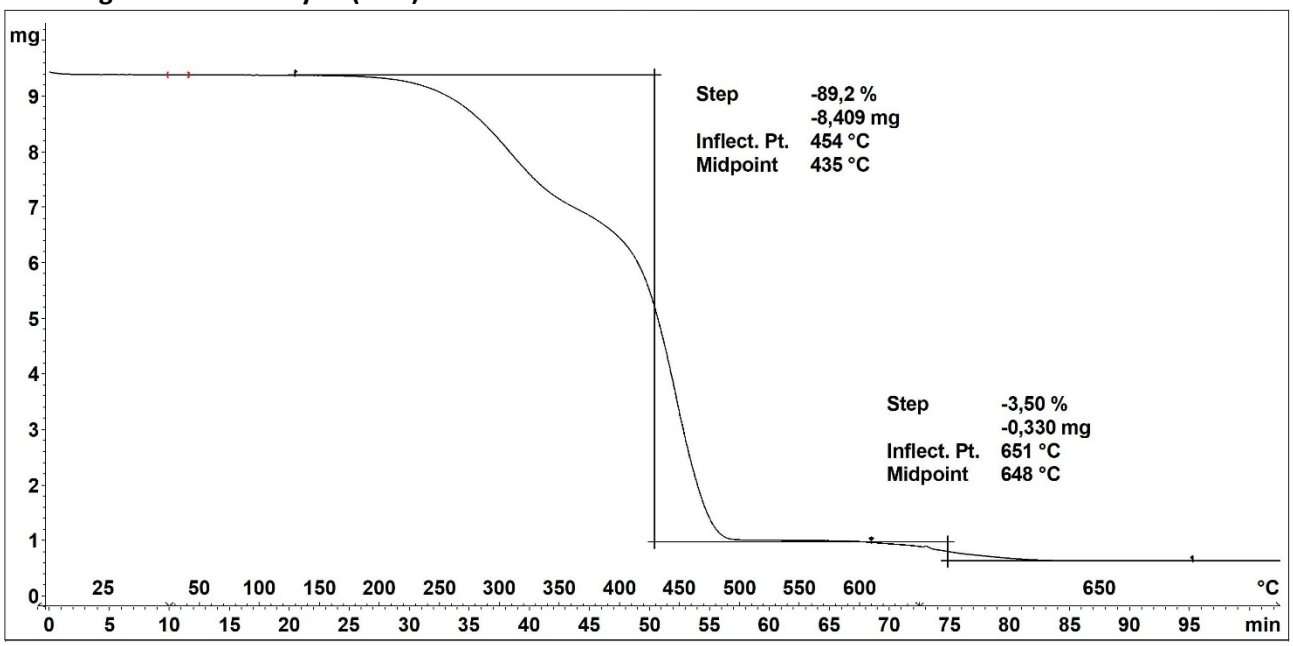

Decomposition graph. The experiment was conducted under He then air (after 650 °C).

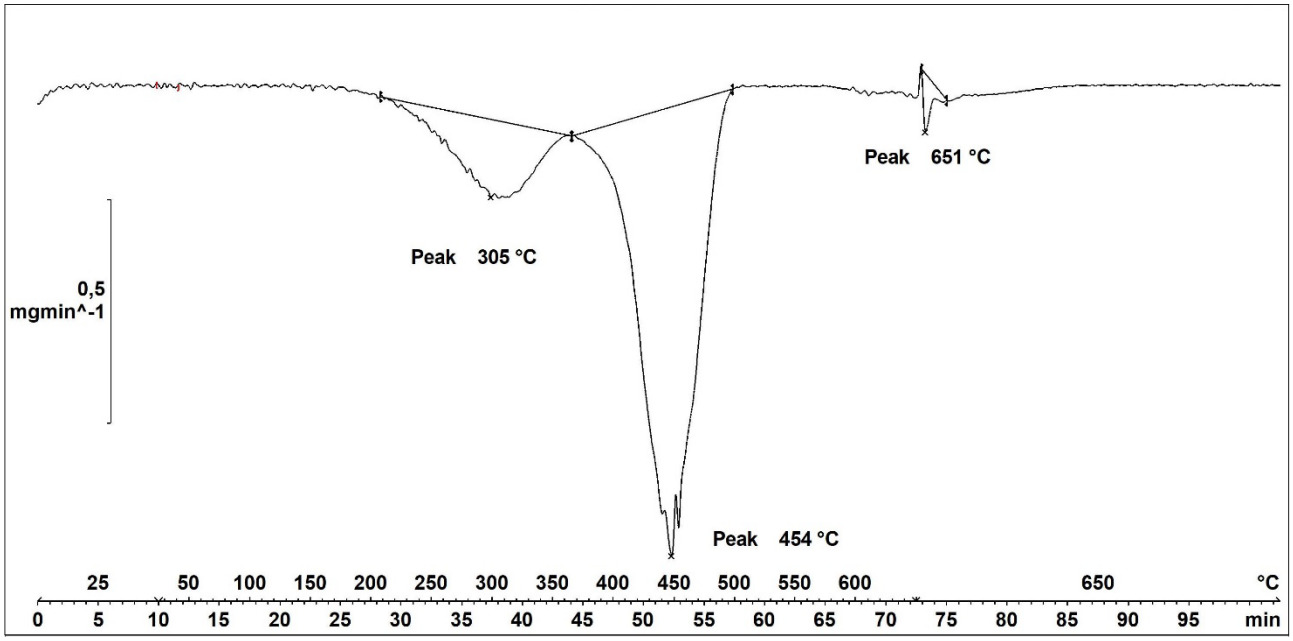

1st derivative of decomposition graph. The experiment was conducted under He then air (after 650 °C).

Decomposition temperature (T_d) = 305 and 454 ^{o}C (two decomposition steps).

Elemental Analysis (EA)

N [%]	C [%]	H [%]	S [%]	mmol N/g	C/N ratio	C/H ratio
0.22	80.30	10.23	Not detected	--	--	0.66

Extraction of Acrylic Polymer from Mixed Textile Waste with γ-Valerolactone (GVL)

GVL-Extracted Acrylic Polymer from mixed textiles (MIX2) was obtained from the acrylic polymer extraction procedure (see below). The dissolution experiment used 7 different fabrics/textiles, which were cut thoroughly with scissors before the addition of GVL. All textiles were obtained from Føtex (Danish supermarket) and used without further purification. Specifically, the textiles used in the experiment were as follows:

1) Yellow cloth (from label: Viscose (82%)/PP (18%)). 201 mg.
2) Grey yarn (from label: Wool (75%)/PET (25%)). 202 mg.
3) Black sock (from label: Cotton (70%)/PET (27%)/Elastane (3%)). 201 mg.
4) White acrylic yarn (**TEX1**, from label: Acrylic (100%), from EA: acrylonitrile% = 91%). 202 mg.
5) Puffy acrylic yarn (**TEX2**, from label: Acrylic (76%)/PA (24%), from EA: acrylonitrile% = 78%*). 200 mg.
6) Black sock (**TEX3**, from label: Acrylic (80%)/PA (20%), from EA: acrylonitrile% = 87%*). 205 mg.
7) White sock (**TEX4**, from label: Acrylic (100%) for the white part of the sock, however, we find that it is composed of 60% acrylonitrile (via elemental analysis) and the rest being PET. 201 mg.

*Acrylonitrile percentages are higher than the actual values since this number is obtained from elemental analysis, which also detects the nitrogen present in the poly(amide) co-polymer of these textiles.

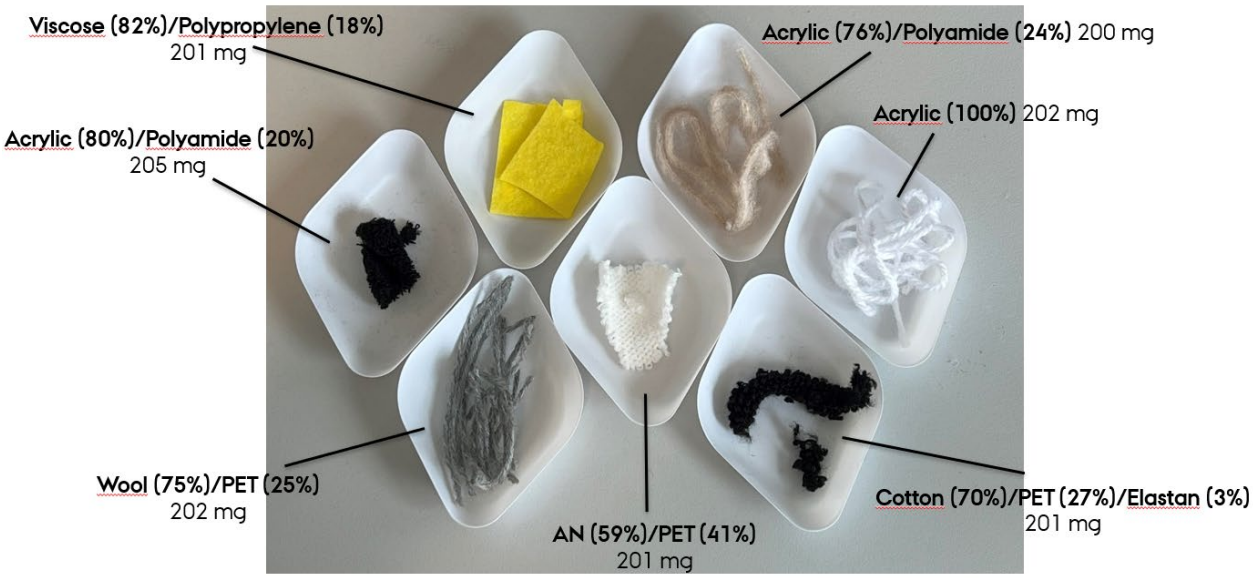

Figure S1. All textile samples that were mixed and used in the GVL-extraction of acrylic polymer.

Procedure for dissolution experiment with GVL:
To the mix of different textiles (in the exact amounts as described above) was added GVL (15 mL), after which the batch was heated under stirring for 15 min. at 150 °C. The batch was left to cool to rt, and hereafter the liquid phase was precipitated in H_2O (30 mL) by dropwise addition through a cotton-packed Pasteur pipette filter to remove solids. The precipitate was now filtered with a Puriflash dryload column (30 mL total volume) and washed extensively with H_2O and afterwards with MeOH. Finally, the precipitate was dried *in vacuo* for 2 days to yield a grey powder (514 mg, 8.2 wt% residual GVL, 471 mg when corrected for residual GVL

determined by ^{1}H–NMR integration with an internal standard). Smaller size particles were generated by crushing the polymer in a mortar using liquid nitrogen cooling.

Particle size used for the catalytic hydrogenation reactions

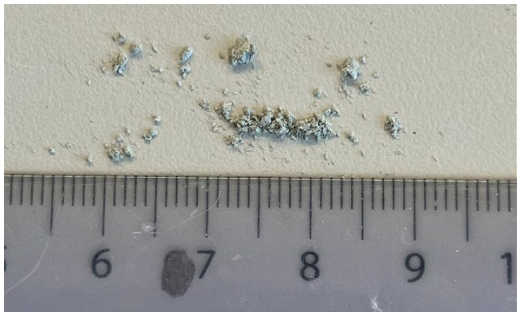

Solubility chart

Soluble **Swells** **Not soluble**

$CHCl_3$	Acetone	*i*-PrOH	DMF	DMSO	THF	PhMe	H_2O	MeOH	MeCN	GVL*

*Soluble when heating to 100 °C.

^{1}H–NMR (DMSO-d_6)

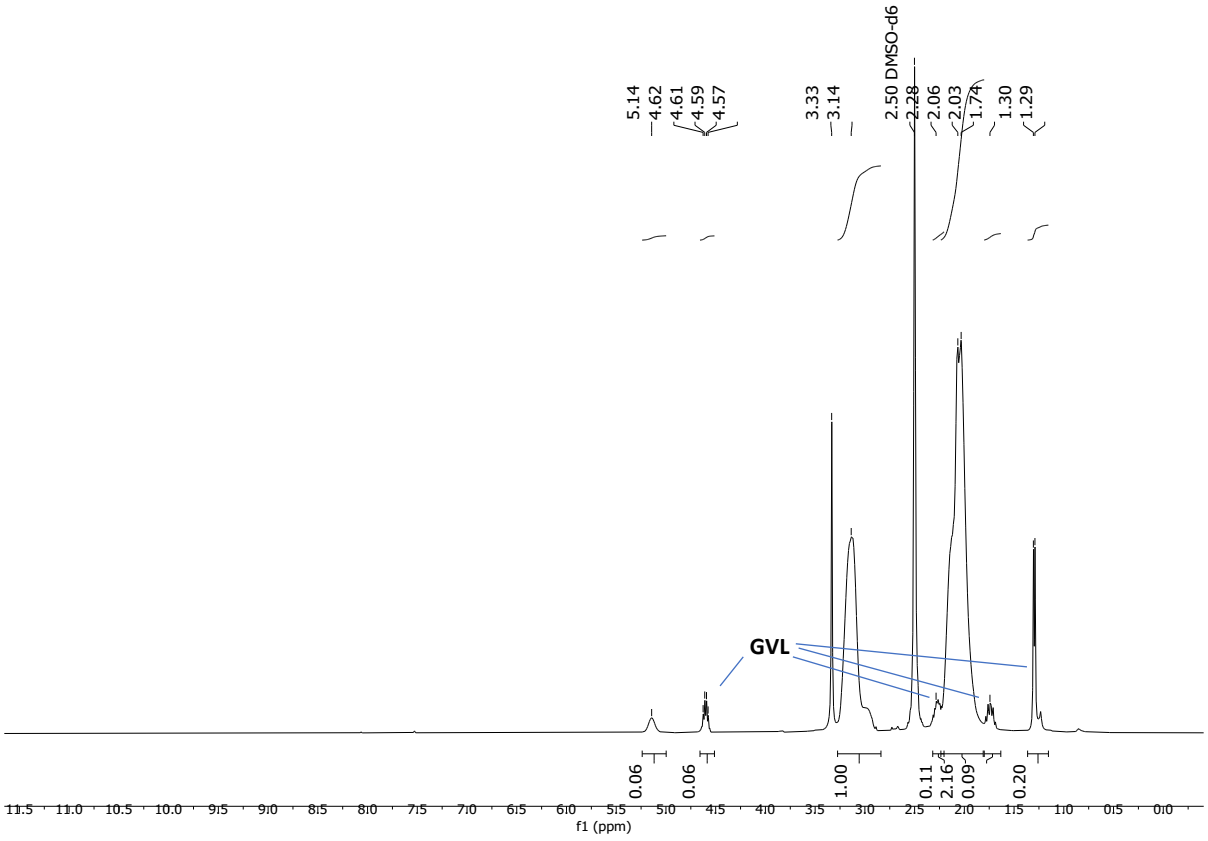

^{13}C–NMR (DMSO-d_6)

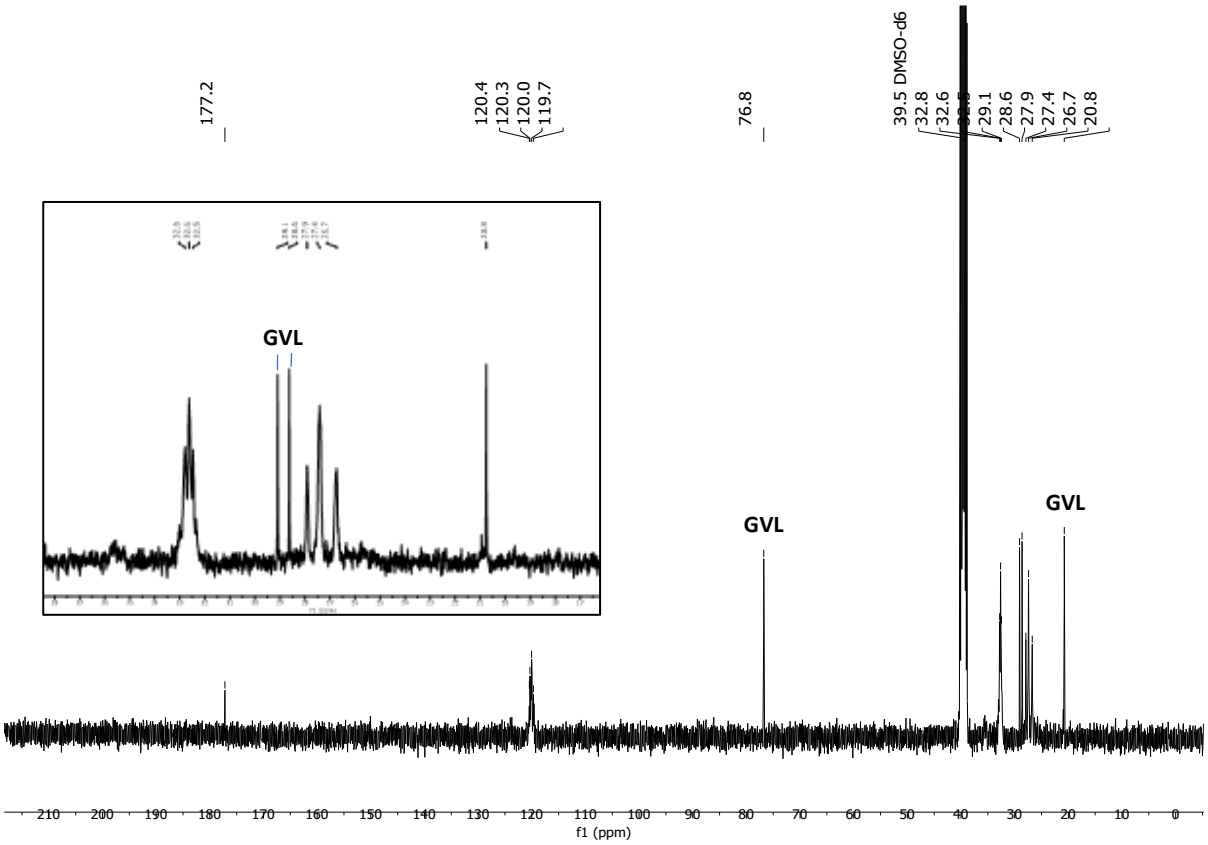

^{13}C CP/MAS NMR (solid-state)

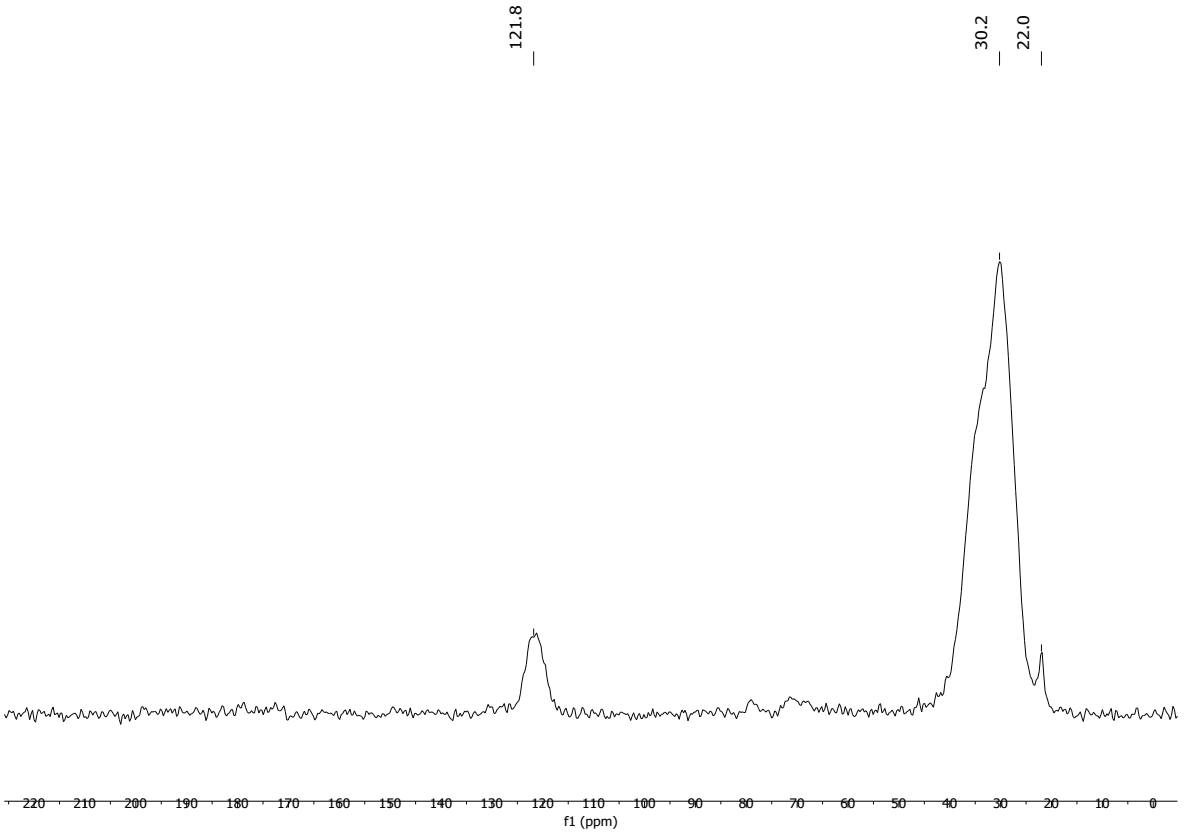

Infrared (IR) Spectroscopic Analysis

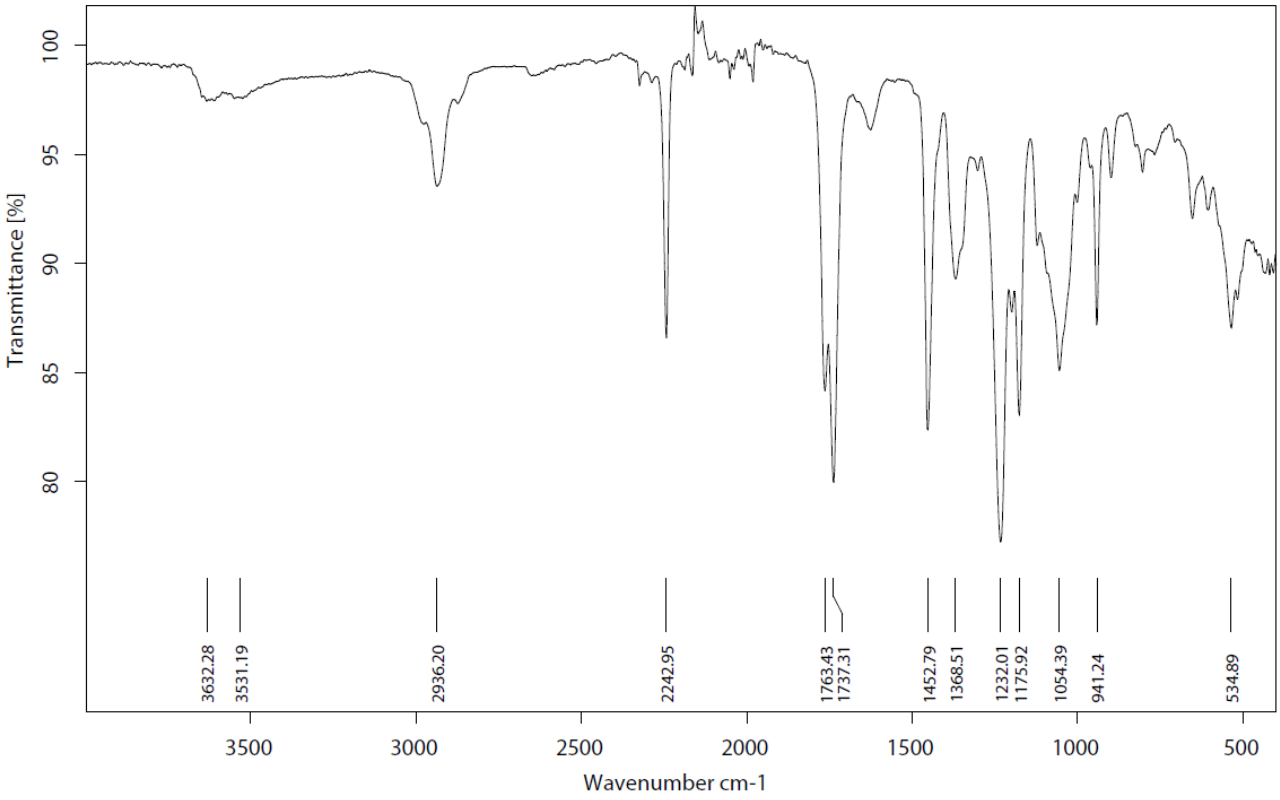

Thermogravimetric Analysis (TGA)

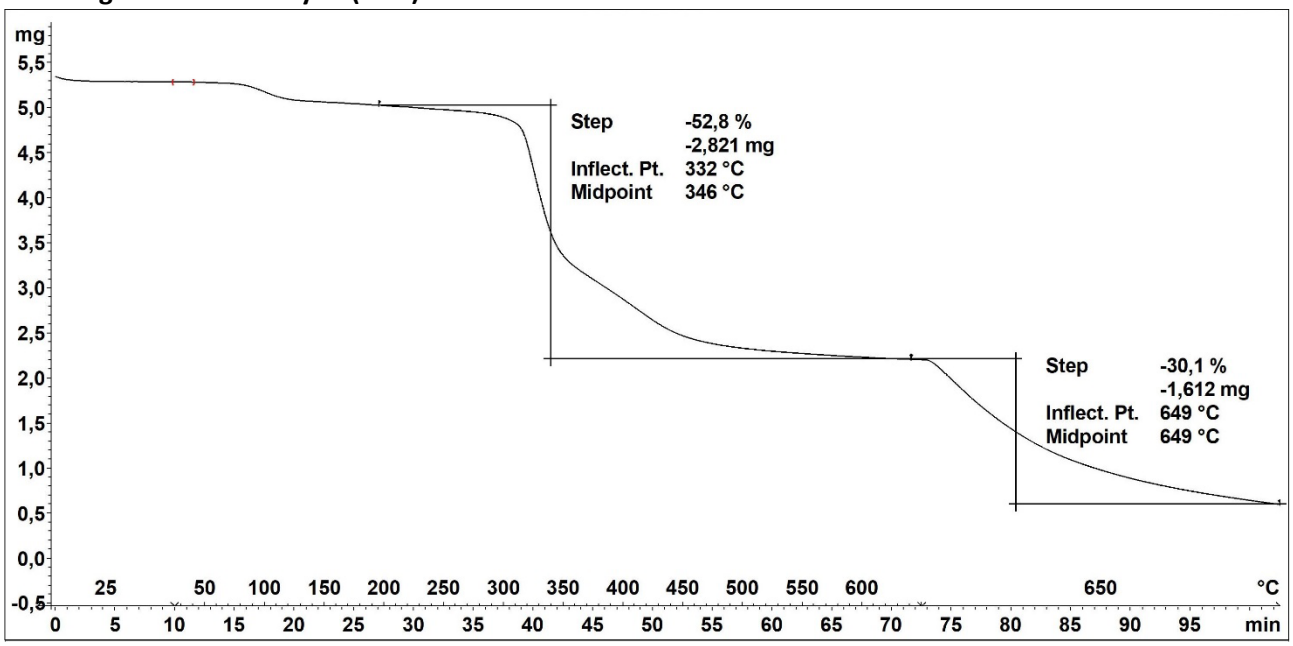

Decomposition graph. The experiment was conducted under He then air (after 650 °C).

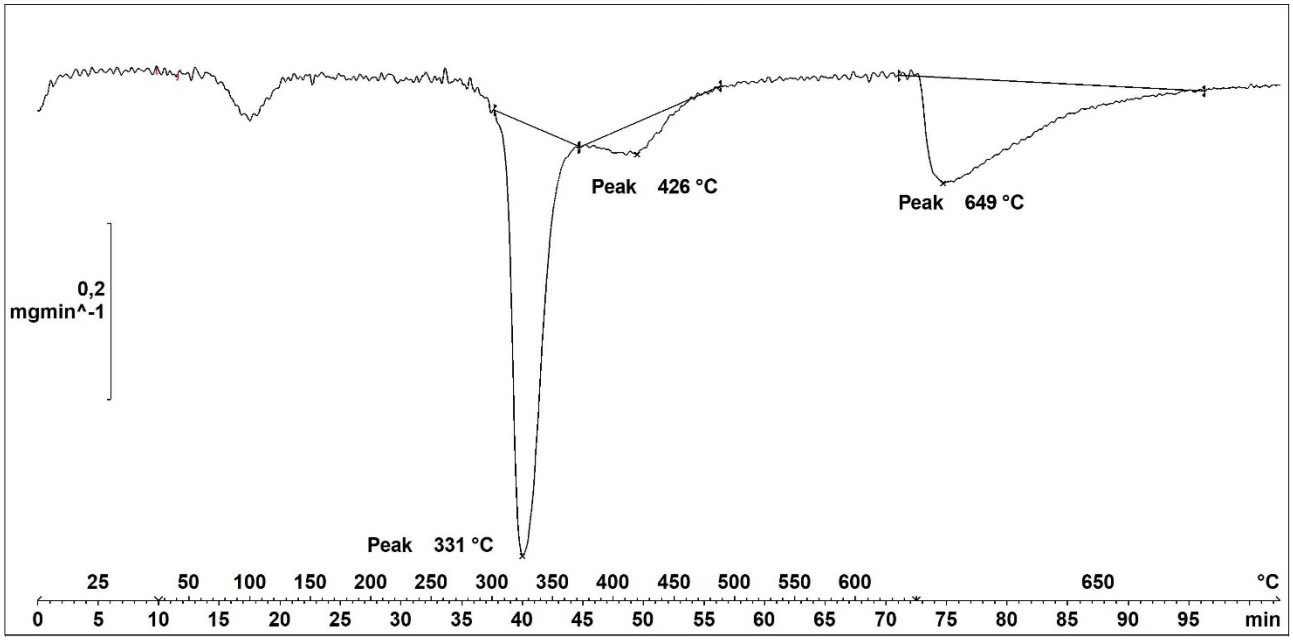

1st derivative of decomposition graph. The experiment was conducted under He then air (after 650 °C).

Decomposition temperature (T_d) = 331 and 426 °C (two decomposition steps).

Differential Scanning Calorimetry (DSC) Analysis

No thermal events besides evaporation of volatiles and decomposition were observed.

Elemental Analysis (EA)

N [%]	C [%]	H [%]	S [%]	mmol N/g	C/N ratio	C/H ratio
22.16	**65.72**	**6.31**	**Not detected**	**15.82**	**3.46**	**0.87**

Acrylonitrile weight percentage calculation based on EA (AN%):

N% = 22.16

M(N) = 14.0067 g/mol

M(AN) = 53.06 g/mol

$AN\% = \frac{N\%}{M(N)} \cdot M(AN)$ = 84%

General Procedures for the Catalytic Hydrogenation of Nitrile Polymers

General Procedure A (Optimisation)

In an argon glove-box, to a glass vial (8 mL total volume) with a stir bar, inserted in a Parr autoclave reactor fitted with a Teflon inlay (30 mL total volume), was added polymer, pre-catalyst, KO*t*Bu, and dry *i*-PrOH. The autoclave was pressurised with H_2 and subsequently heated to the relevant temperature overnight under magnetic stirring. Thereafter, the polymer product was isolated by decanting the reaction solution, and the polymer was then washed with MeOH (3 x 6 mL). Concentration *in vacuo* yielded the amine polymer, which was analysed without further manipulation.

General Procedure B (NBR, ABS, and SAN scope)

In an argon glove-box, to a glass vial (20 mL total volume) with a stir bar, inserted in a Parr autoclave reactor, was added the relevant polymer (1000 mg), Ru-MACHO® (20 mg, 2 wt%, 0.035 mmol), KO*t*Bu (40 mg, 4 wt%, 0.36 mmol), and dry *i*-PrOH (10 mL). The autoclave was pressurised with H_2 (30 bar) and subsequently heated to 80 °C for 24 hours under magnetic stirring. Thereafter, the reaction mixture was concentrated slightly under reduced pressure, then added water (10 mL), mixed by shaking, and decanted. The decanted liquid was added into H_2O (10 mL) in a separate vial and any polymer leftover was isolated and added to the initial vial containing the majority of the polymer. Then the combined solid polymer was added H_2O (15 mL) and sonicated for 1 h, followed by decantation. The polymer was then rinsed and decanted with H_2O (2 x 15 mL). This washing procedure was then subsequently carried out again with toluene. The resulting polymer was dried *in vacuo* o/n and thereafter cut into smaller pieces. The washing procedure with H_2O and toluene was then carried out once more, after which the polymer was dried in vacuo o/n. Lastly, the polymer was then cut into small pieces with scissors, and the resulting particles were then added MeOH (15 mL) and sonicated (10 min.), then filtered using an empty Puriflash dry column (30 mL total volume) and rinsed with MeOH (100 mL) under suction. The washed polymer was then dried in *vacuo* o/n and finally cryogenically milled to give a powder.

General Procedure B2 (10 g scale)

In an argon glove-box, to a Teflon insert (310 mL total volume) equipped with a stir bar, inserted in a Berghof autoclave reactor, was added the relevant polymer (10 g), Ru-MACHO® (200 mg, 2 wt%, 0.350 mmol), KO*t*Bu (400 mg, 4 wt%, 3.60 mmol), and dry *i*-PrOH (100 mL). The autoclave was pressurised with H_2 (30 bar) and subsequently heated to 80 °C for 24 hours under magnetic stirring. Thereafter, the reaction mixture was transferred to a brown flask (250 mL total volume), then added water (100 mL), mixed by shaking, and decanted. The decanted liquid was added into H_2O (100 mL) in a separate flask and any polymer leftover was isolated and added to the initial flask containing the majority of the polymer. Then the combined solid polymer was added PhMe (250 mL) and sonicated for 1 h, followed by decantation. The polymer was then rinsed and decanted with PhMe (2 x 250 mL). This washing procedure was then subsequently carried out again with water and finally toluene again. The resulting polymer was dried *in vacuo* o/n and thereafter cut into smaller pieces. This washing procedure was then carried out once more, after which the polymer was dried in vacuo o/n. Lastly, the polymer was cut into smaller pieces with scissors, and the resulting particles were added MeOH (250 mL) and sonicated (1 h), then collected by suction filtration and rinsed with MeOH (250 mL). The decanted PhMe fractions from the first washing step were added NaOH (1 M, 100 mL), thereby precipitating some additional polymer in suspension. This polymer fraction was subjected to the same washing procedure as with the initial polymer fraction. The washed polymer fractions were then combined and dried in *vacuo* o/n and finally cryogenically milled to give a powder.

General Procedure C (Textile scope)

In an argon glove-box, to a glass vial (4 mL total volume) with a stir bar, inserted in a Parr autoclave reactor fitted with a Teflon inlay (30 mL total volume), was added textile sample (50 mg), [Ru-C6] (see **Figure S6** for complex structure) (10 mg, 20 wt%, 0.022 mmol), KO*t*Bu (8 mg, 16 wt%, 0.08 mmol), and dry *i*-PrOH (2 mL). The autoclave was pressurised with H_2 (50 bar) and subsequently heated to 100 °C for 24 hours under magnetic stirring. Thereafter, the polymer product was isolated by filtration using an empty Puriflash dry column (10 mL total volume) or syringe filter (6 mL total volume), and the polymer was then washed with H_2O (10 mL), PhMe (10 mL), and lastly MeOH (10 mL). The washed polymer was thereafter dried in *vacuo* overnight and then cryogenically milled to give a powder.

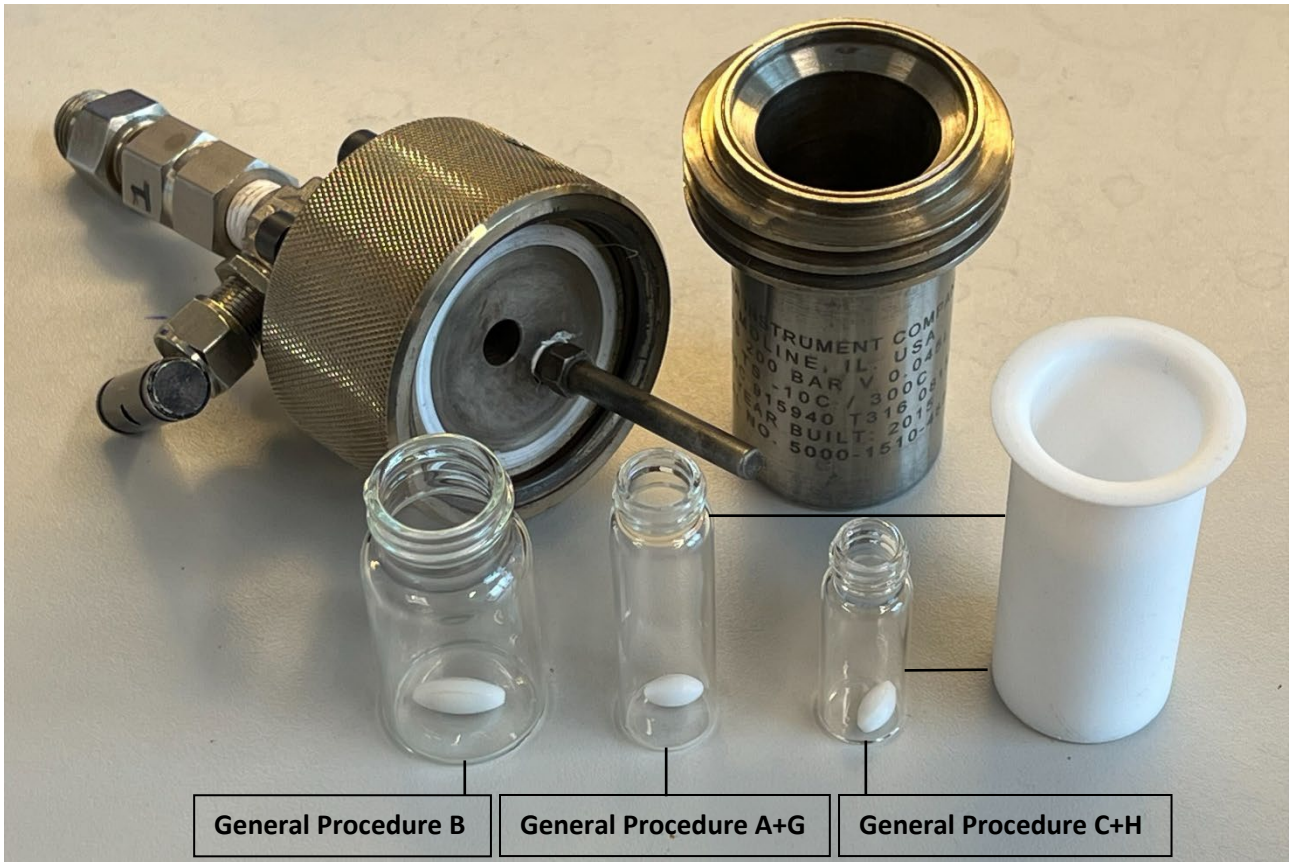

Figure S2. Parr® autoclave setup for General Procedures A, B, C, G, and H. For General Procedures A and G, an 8 mL vial, fitted with a magnetic stir bar, is inserted into the Teflon® inlay, which is then inserted into the autoclave. For General Procedure B, the 20 mL vial, fitted with a magnetic stir bar, is inserted directly into the autoclave without the Teflon® inlay. Lastly, for General Procedure C and H, a 4 mL vial, fitted with a magnetic stir bar, is inserted into the Teflon® inlay, which is then inserted into the autoclave.

Note for General Procedure B: If nitrile is still present in the polymer after hydrogenation, it is likely that the particle size of the substrate was too large in comparison to that depicted in the "Polymer substrate characterisation" section. For some of the polymer materials, such as LEGO® bricks, we noted that the reaction with larger pieces than the ones shown in the "Polymer Substrates" tends to not always yield full nitrile hydrogenation with the General Procedure B. Furthermore, if a low wt% yield is obtained after the washing procedure, we suggest a more careful decantation step, in which one makes sure that no polymer particles are washed away, however, this can be challenging for some of the polymers.

Note for General Procedure C: The small fibers can easily clog the filter used, so in some cases it can be necessary to use a needle to gently de-clog the filter in order to thoroughly wash the polymer with the indicated solvents.

Figure S3. Berghof autoclave setup for the General Procedure B2.

General Procedures for the Hydrocyanation-Hydrogenation of Poly(butadiene) Polymers

General Procedure D (Hydrocyanation optimisation)

In an argon glove-box, to a two-chamber system (20 mL total volume), **SBR1** (50 mg, 70 wt% butadiene, 0.65 mmol butadiene), $Ni(COD)_2$, and ligand were added to chamber A. To chamber B was added KCN and diethylene glycol dimethyl ether. Then, to chamber A was added dry PhMe, and the chamber was sealed with a screwcap fitted with a Teflon®-coated silicone seal and a stabilising PTFE disc. AcOH (9 equiv. to KCN) was then added slowly to the top of the glycol ether layer in chamber B, and was sealed with a screwcap fitted with a Teflon®-coated silicone seal and a stabilising PTFE disc. **(Beware! The AcOH must be added slowly on top of the glycol solvent, otherwise HCN release will occur before the chamber is sealed).** The reaction in chamber A was stirred at the relevant temperature o/n, whereas chamber B was stirred at rt, while placed in a well-ventilated fume-hood. Upon completion, the two-chamber system was cooled down to rt, then opened and left stirring for 20–30 min under good ventilation. The polymer product was then isolated by removing volatiles *in vacuo*, and finally analysed by FT-IR spectroscopic analysis to obtain the intensity ratio of the C≡N band (sp C≡N stretch, 2238 cm^{-1}) to the C=C–H band (sp^2 C–H bending, 968 cm^{-1}).

General Procedure E (Hydrocyanation scope)

In an argon glove-box, to a two-chamber system (100 mL total volume), the relevant polymer substrate (250 mg), $Ni(COD)_2$ (10 wt%, 25 mg, 0.91 mmol), and BiPhePhos (1 equiv./Ni, 72 mg, 0.91 mmol) were added to chamber A. To chamber B was added KCN (1.16 g, 17.8 mmol) and diethylene glycol dimethyl ether (10 mL), and the chamber was sealed with a screwcap fitted with a Teflon®-coated pierceable silicone seal and a stabilising PTFE disc. Then, to chamber A was added dry PhMe (10 mL), and the chamber was sealed with a screwcap fitted with a Teflon®-coated silicone seal and a stabilising PTFE disc. AcOH (8.33 mL) was then added slowly to the top of the glycol ether layer in chamber B, using a syringe, through the pierceable silicone seal. **(Beware! The AcOH must be added slowly on top of the glycol solvent, otherwise HCN release will occur)**. The reaction in chamber A was stirred at 90 °C for 24 h, whereas chamber B was stirred at rt,

while placed in a well-ventilated fume-hood. Upon completion, the two-chamber system was cooled down to rt, then opened and left stirring for 20−30 min under good ventilation. Substrate-specific workup is described in the respective polymer product sections.

General Procedure F ($^{13/12}$C-Hydrocyanation of SBR1)

In an argon glove-box, to a two-chamber system (100 mL total volume), the relevant polymer substrate (250 mg), $Ni(COD)_2$ (10 wt%, 25 mg, 0.91 mmol), and BiPhePhos (1 equiv./Ni, 72 mg, 0.91 mmol) was added to chamber A. To chamber B was added $K^{13}CN$ (232 mg, 3.51 mmol), $K^{12}CN$ (928 mg, 14.3 mmol), and diethylene glycol dimethyl ether (10 mL) and the chamber was sealed with a screwcap fitted with a Teflon®-coated pierceable silicone seal and a stabilising PTFE disc. Then, to chamber A was added dry PhMe (10 mL), and the chamber was sealed with a screwcap fitted with a Teflon®-coated silicone seal and a stabilising PTFE disc. AcOH (8.33 mL) was then added slowly to the top of the glycol ether layer in chamber B, using a syringe, through the pierceable silicone seal. **(Beware! The AcOH must be added slowly on top of the glycol solvent, otherwise HCN release will occur)**. The reaction in chamber A was stirred at 90 °C for 24 h, whereas chamber B was stirred at rt, while placed in a well-ventilated fume-hood. Upon completion, the two-chamber system was cooled down to rt, opened and left stirring for 20−30 min under good ventilation. Substrate-specific workup is described in the respective polymer product sections.

General Procedure G (Hydrogenation of hydrocyanation products)

In an argon glove-box, to a glass vial (8 mL total volume) with a stir bar, inserted in a Parr autoclave reactor fitted with a Teflon inlay (30 mL total volume), was added hydrocyanated polymer (100 mg), RuMACHO® (10 mg, 10 wt%, 0.017 mmol), KO*t*Bu (8 mg, 8 wt%, 0.07 mmol) and dry *i*-PrOH (4 mL). The autoclave was pressurised with H_2 to 30 bar and subsequently heated at 80 °C for 24 h. Thereafter, the polymer product was isolated by filtration using a syringe filter (6 mL total volume), and the polymer was then washed with H_2O (10 mL), PhMe (10 mL), and lastly MeOH (10 mL). The washed polymer was then dried in *vacuo* overnight and then cryogenically milled to give a powder.

General Procedure H (Hydrogenation of hydrocyanation products)

In an argon glove-box, to a glass vial (4 mL total volume) with a stir bar, inserted in a Parr autoclave reactor fitted with a Teflon inlay (30 mL total volume), was added hydrocyanated polymer (50 mg), [Ru-C6] (see **Figure S6** for complex structure) (10 mg, 20 wt%, 0.022 mmol), KO*t*Bu (8 mg, 16 wt%, 0.08 mmol), and dry *i*-PrOH (2 mL). The autoclave was pressurised with H_2 (50 bar) and subsequently heated to 100 °C for 24 hours under magnetic stirring. Thereafter, the polymer product was isolated by filtration using an empty Puriflash dry column (10 mL total volume) or syringe filter (6 mL total volume), and the polymer was then washed with H_2O (10 mL), PhMe (10 mL), and lastly MeOH (10 mL). The washed polymer was thereafter dried in *vacuo* overnight and then cryogenically milled to give a powder.

Figure S4. Two-chamber reaction glassware, stir bars, caps, Teflon disks, and silicone seals used for the 250 mg scale hydrocyanation reactions.

Note for General Procedure D–H: The hydrogenation reaction (general procedures G and H) is highly sensitive to a detected cyanide species (2179 cm^{-1} in FT–IR) that can be present in the hydrocyanation polymer products if the NaOH wash is not carried out or not done sufficiently (as stated in the substrate-specific workups for hydrocyanation reactions in general procedures D–F). If a cyanide band at 2179 cm^{-1} is detected in the hydrocyanated polymer, this needs additional washing with aq. NaOH (2 M), often under ultrasonication, to remove it fully prior to the hydrogenation reaction.

Optimisation of Nitrile Reduction with Nitrile Butadiene Rubber 1 (NBR1)

The optimisation was conducted according to the General Procedure A. To estimate the amine content, a 2-step amidation-deprotection sequence was used. The combined amount of **1** and **2** generated via this method is directly proportional to the combined primary and secondary amine content of the polymer. The amount of **1** and **2** is determined by ^{1}H−NMR integration with an internal standard or by isolation of the combined **1** and **2**. Although this method is useful for insoluble polymers, it is not applicable to the analysis of soluble or semi-soluble polymers, which can be washed out of the syringe filter during the washing step after the initial amidation. Furthermore, this method is likely to only detect surface-accessible amines, thus elemental analysis is a more precise method to quantify amine in a fully reduced sample. However, this Fmoc-based quantification method served well for optimising the reaction conditions with **NBR1**. This quantification method was inspired by a UV-Vis based quantification of **1** for the determination of amine contents in solid phase peptide synthesis resins.[22]

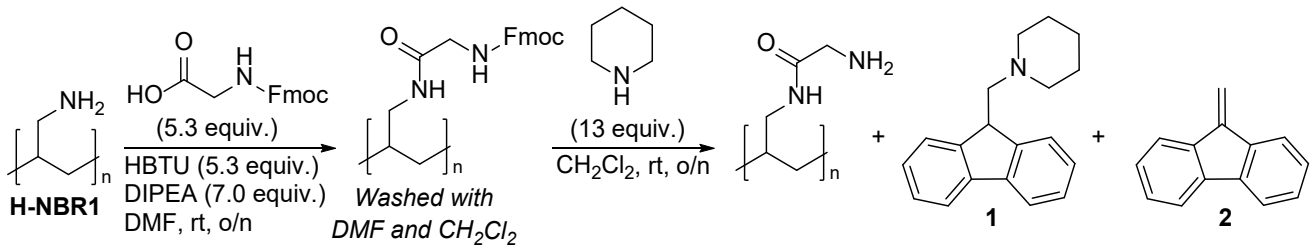

Scheme S1. Fmoc-based amine quantification used for optimisation of **H-NBR1** synthesis.

General Procedure for Fmoc-based amine quantification

To an emptied and capped Puriflash silica column (see **Figure S5**) was added **H-NBR1** (20 mg, 0.151 mmol amine*), Fmoc-Glycine (237 mg, 0.797 mmol, 5.3 equiv.), HBTU (303 mg, 0.799 mmol, 5.3 equiv.), DMF (4 mL), and DIPEA (185 µL, 1.06 mmol, 7.0 equiv.). The column was fitted with a septum and a needle outlet and thereafter stirred o/n at rt. Then the reaction was filtered and washed extensively with DMF and thereafter extensively with CH_2Cl_2. The column was then capped again and added CH_2Cl_2 (4 mL) and piperidine (197 µL, 1.99 mmol, 13 equiv.), after which the column was fitted with a septum and a needle outlet and then stirred o/n at rt. The liquid phase was now transferred to a round-bottomed flask (25 or 50 mL total volume) with a glass pipette, and then the column was washed with CH_2Cl_2 into the RB flask. The solvent was then removed *in vacuo*, and the combined yield of **1** and **2** was determined by ^{1}H–NMR integration using 1,3,5-trimethoxybenzene as an internal standard. Alternatively, the CH_2Cl_2 solution was washed with $NaHCO_3$ (5 x 5 mL) and H_2O (5 mL), dried over Na_2SO_4, filtered through celite and lastly concentrated *in vacuo* to yield a mixture of **1** and **2** as a white solid.

Example from entry 30, **Table S1**: (29.7 mg, white solid). From ^{1}H–NMR spectroscopic analysis, the corrected yield of **1** is 69%, while the corrected yield of **2** is 6%, giving a combined yield of 75%. ^{1}H–NMR (400 MHz, $CDCl_3$) δ_H (ppm) 7.76 (**1**) (d, J = 7.5 Hz, 4H), 7.70 (**1**) (d, J = 7.5 Hz, 4H), 7.37 (**1**) (t, J = 7.3 Hz, 2H), 7.30 (**1**) (dt, J_1 = 7.3 Hz, J_2 = 1.2 Hz, 2H), 6.08 (**2**) (s, 0.17H), 4.05 (**1**) (t, J = 8.1 Hz, 1H), 2.59-2.57 (**1**) (m, 6H), 1.72-1.66 (**1**) (m, 4H), 1.57-1.49 (**1**) (m, 2H). ^{13}C–NMR (100 MHz, $CDCl_3$) δ_C (ppm) 146.9 (**1**), 141.1(**1**), 128.9 (**2**), 127.1 (**2**), 127.1, 126.8 (**1**), 125.6 (**1**), 121.2 (**2**), 119.9 (**2**), 119.8 (**1**), 63.2 (**1**), 55.1 (**1**), 45.0 (**1**), 26.4 (**1**), 24.8 (**1**). ^{1}H–, and ^{13}C–NMR spectroscopic analyses of **1** and **2** are in accordance with literature values.[3,4]

*An assumed amine content based on a theoretical 43 wt% of allylamine monomer present in the **H-NBR1**, which is the maximum wt% allylamine that can be obtained if all nitrile is converted to primary amine.

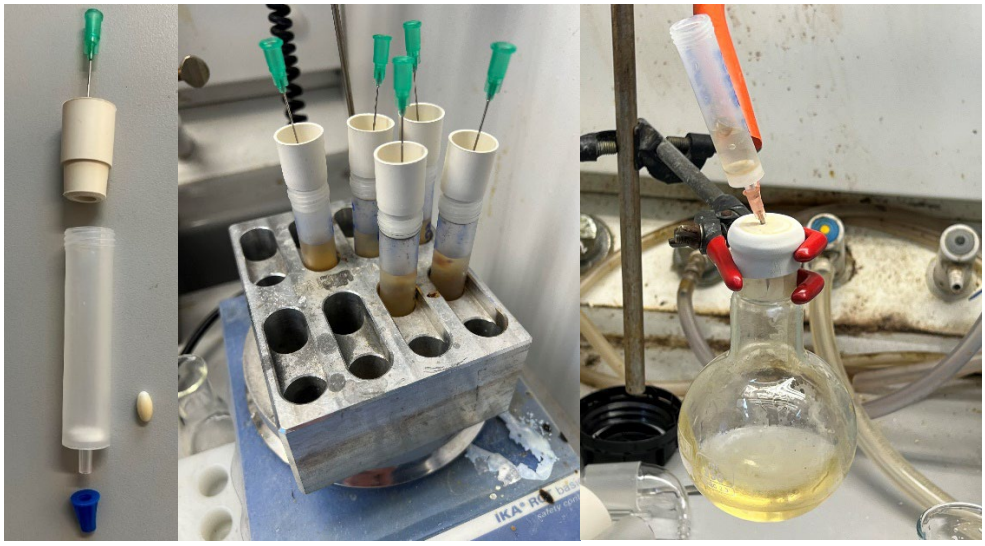

Figure S5. Left picture: Column setup for Fmoc-based amine quantification. Middle picture: Quantification reactions stirring at room temperature. Right picture: Washing the polymer with DMF and CH_2Cl_2 after the initial amidation step (the RB flask is under suction).

Three solid-phase peptide synthesis resins with known amine contents were analysed with the method showing an accuracy of 90–97% (see below). Also conducting the quantification using 20.2 mg **NBR1** (no amine) gave 0% of the products, **1** or **2**, as expected.

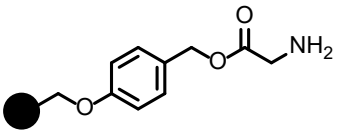

Wang-Gly (after deprotect.)
Amine content: 0.70 mmol/g
fmoc quant: 0.68 mmol/g (**97%**)

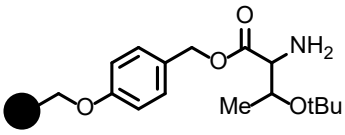

Wang-Thr(OtBu) (after deprotect.)
Amine content: 0.82 mmol/g
fmoc quant: 0.74 mmol/g (**90%**)

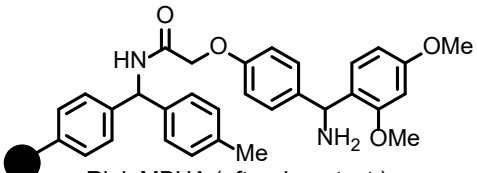

Rink MBHA (after deprotect.)
Amine content: 0.45 mmol/g
fmoc quant: 0.41 mmol/g (**91%**)

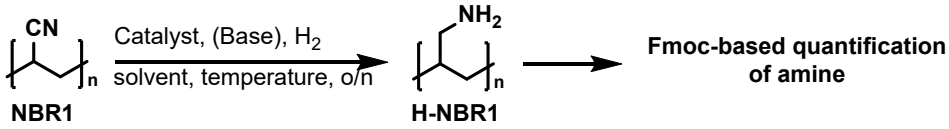

Entry	Pre-catalyst (wt%)	Base	H_2 (bar)	Solvent (mL)	Temp. (°C)	Yield (%)
1	[Ru-C1] (5)	KO*t*Bu (4 equiv/pre-catalyst, 4 wt%)	30	*i*PrOH (2)	70	63
2	[Ru-C1] (5)	No base	30	*i*PrOH (2)	70	0[a]
3	[Ru-C2] (5)	No base	30	*i*PrOH (2)	70	71
4	[Ru-C2] (5)	KO*t*Bu (4 wt%)	30	*i*PrOH (2)	70	74
5	[Ir-C1] (5)	KO*t*Bu (4 equiv/pre-catalyst, 4 wt%)	30	*i*PrOH (2)	70	3
6	[Mn-C1] (5)	KO*t*Bu (4 equiv/pre-catalyst, 5 wt%)	30	*i*PrOH (2)	70	7
7	[Co-C1] (5)	KO*t*Bu (4 equiv/pre-catalyst, 6 wt%)	30	*i*PrOH (2)	70	0[a]
8	[Ru-C3] (5)	KO*t*Bu (4 equiv/pre-catalyst, 5 wt%)	30	*i*PrOH (2)	70	7
9	[Ru-C4] (5)	KO*t*Bu (4 equiv/pre-catalyst, 4 wt%)	30	*i*PrOH (2)	70	67
10	[Ru-C5] (5)	KO*t*Bu (4 equiv/pre-catalyst, 5 wt%)	30	*i*PrOH (2)	70	65
11	[Ru-C6] (5)	KO*t*Bu (4 equiv/pre-catalyst, 5 wt%)	30	*i*PrOH (2)	70	62
12	[Ru-C7] (5)	KO*t*Bu (4 equiv/pre-catalyst, 4 wt%)	30	*i*PrOH (2)	70	3
13	[Ru-C8] (5)	KO*t*Bu (4 wt%)	30	*i*PrOH (2)	70	18
14	[Fe-C1] (5)	KO*t*Bu (4 wt%)	30	*i*PrOH (2)	70	60
15	[Fe-C2] (5)	KO*t*Bu (4 wt%)	30	*i*PrOH (2)	70	31
16	None	KO*t*Bu (4 wt%)	30	*i*PrOH (2)	70	0[a]
17	[Ru-C2] (5)	No base	30	*i*PrOH (1.5) + acetone (0.5)	70	40
18[b]	[Ru-C1] (5)	KO*t*Bu (4 wt%)	30	*i*PrOH (2)	70	63
19	[Ru-C1] (5)	KO*t*Bu (4 wt%)	40	*i*PrOH (2)	70	67
20	[Ru-C1] (5)	KO*t*Bu (4 wt%)	50	*i*PrOH (2)	70	68
21	[Ru-C1] (5)	KO*t*Bu (4 wt%)	30	*i*PrOH (4)	80	74
22	[Ru-C1] (10)	KO*t*Bu (8 wt%)	30	*i*PrOH (4)	80	72
23	[Ru-C1] (20)	KO*t*Bu (16 wt%)	30	*i*PrOH (4)	80	75
24	[Ru-C1] (2)	KO*t*Bu (4 wt%)	30	*i*PrOH (4)	80	76
25	[Ru-C1] (1)	KO*t*Bu (4 wt%)	30	*i*PrOH (4)	80	19
26	[Ru-C1] (2)	KO*t*Bu (2 wt%)	30	*i*PrOH (4)	80	55
27	[Ru-C1] (2)	KO*t*Bu (1 wt%)	30	*i*PrOH (4)	80	7
28[d]	[Ru-C1] (5)	KO*t*Bu (4 wt%)	30	*i*PrOH (4)	80	77
29[d]	[Ru-C1] (5)	KO*t*Bu (4 wt%)	30	*i*PrOH (6)	80	79
30[e]	[Ru-C1] (2)	KO*t*Bu (4 wt%)	30	*i*PrOH (10)	80	[75][c]

Table S1. The nitrile butadiene rubber starting material was used with a random size consisting of most often 2–5 pieces. Yields were obtained by ^{1}H−NMR integration of **1** and **2** after the Fmoc-quantification procedure using 1,3,5-trimethoxybenzene as an internal standard. See **Figure S6** for catalyst abbreviations. [a]Was not analysed with the Fmoc-quantification method but showed no blue color with Kaiser amine test‡, indicative of no reduction. [b]Extra small pieces (see picture below). [c]Indicates the yield after isolation of the mixture of **1** and **2**, and this reported yield is the combined yield of **1** and **2**. [d]Polymer (50 mg). [e]Polymer (1 g). ‡Kaiser test was carried out by adding ~ 5 µL of mix A, then ~ 5 µL of mix B, and finally ~ 5 µL of mix C to a small amount of polymer product (~ 5 mg). A blue-purple color indicates a primary amine due to the formation of Ruhemann's purple. The Kaiser test A, B, and C solutions can be prepared according to a reported procedure.[5]

Concerning footnote b, **Table S1**.

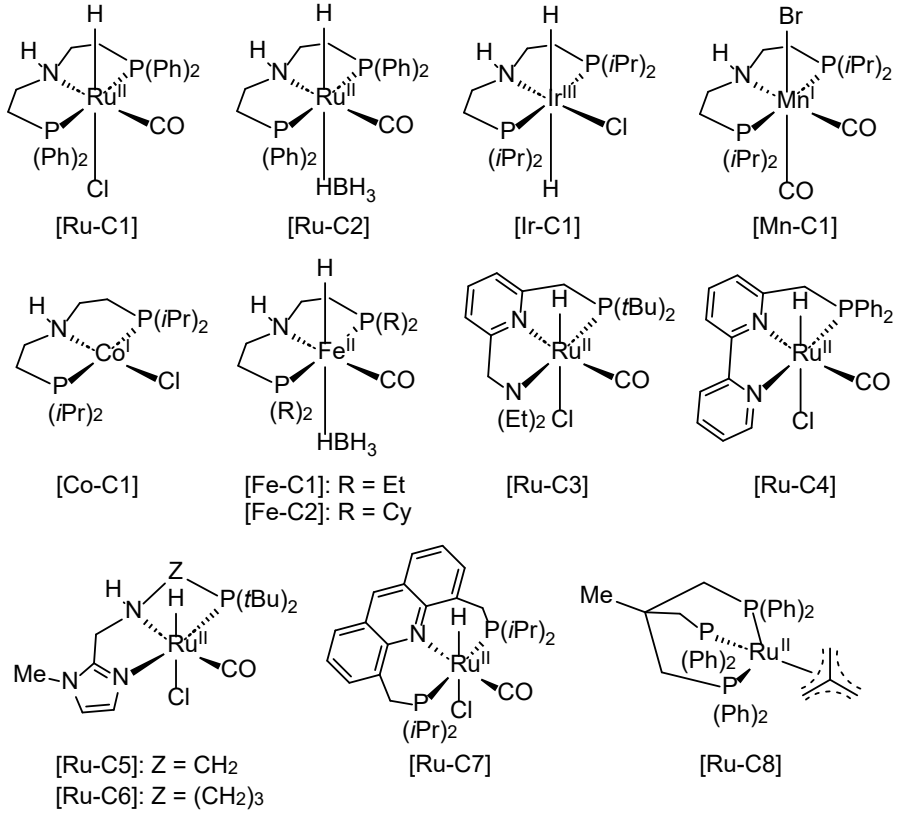

Figure S6. Pre-catalyst abbreviations.

As indicated in the optimisation (**Table S1**), several catalysts are capable of hydrogenating **NBR1** to **H-NBR1**, however, with varying amine yields. The result with [Fe-C1] was promising in the sense that iron is a cheaper and more abundant metal than *e.g.* ruthenium or iridium, however, when we tested another substrate, namely **NBR2** (nitrile glove), there was no nitrile hydrogenation with the [Fe-C1] complex in contrast to [Ru-C1] as observed qualitatively by FT−IR spectroscopic analysis. For this reason, we chose to continue with the [Ru-C1] (RuMACHO®) complex for the further optimisation and substrate scope, but further optimising the reaction with [Fe-C1] or similar iron-based hydrogenation catalysts could be highly interesting as a future prospect.

It was decided to raise the temperature to 80 °C since a preliminary reaction with **ABS1** (LEGO® bricks) showed a full hydrogenation of the nitrile in that case, as evidenced by FT−IR spectroscopic analysis, and this was not the case at 70 °C. The solvent volume was changed from 2 mL to 4 mL since some of the polymer substrates would tend to adhere to the sides of the glass vial above the reaction solution. This problem was mitigated by using 4 mL of solvent.

The amine yield could reach a maximum of 79% and we propose that the Fmoc-based amine quantification is only able to quantify surface-accessible amines, which thus leads to a lower amine yield. Furthermore, we detect a basic gas phase after conducting the hydrogenation reaction (exposing a wetted pH paper to the gas of the autoclave will show a green color, see **Figure S7**). The basic gas phase is likely to be due to ammonia formation from imine-amine crosslinking, which has been observed previously for the same catalytic system.[6] For reaction entries where no amine was detected, e.g. entry 7, **Table S*1***, the gas phase was not found to be basic.

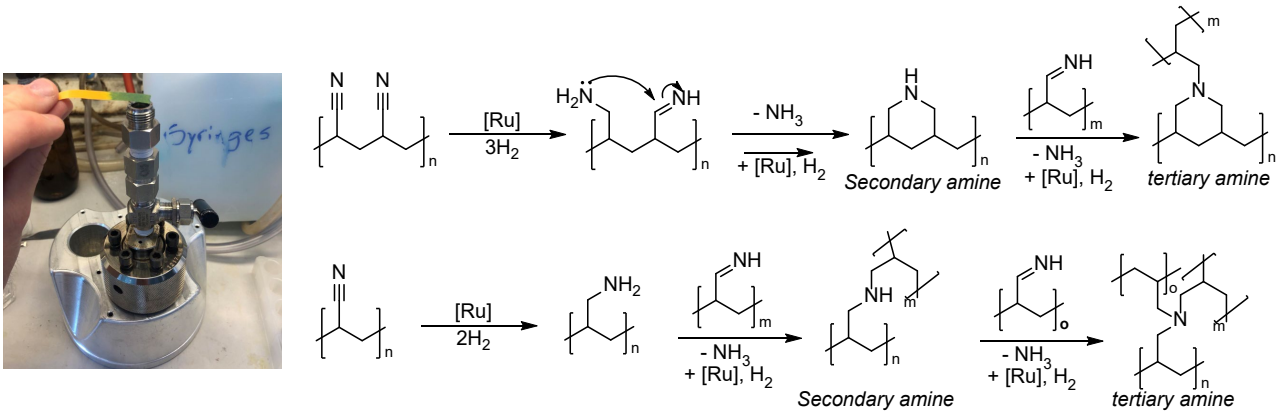

Figure S7. Proposed mechanism for amine-imine crosslinking to form secondary and tertiary amine. In addition, a picture of a pH-test shows a green color when exposed to the gas phase of the autoclave after catalytic hydrogenation of **NBR1**.

From the work of Beller and co-workers, it was found that a low catalyst loading (0.25 mol%), would result in a higher degree of imine-amine crosslinking.[6] We thus studied the amine content of the polymer product after reaction with higher catalyst loadings (10 and 20 wt%, entries 22 and 23, **Table S1**), however, the amine content remained of the same order as with 5 and 2 wt% catalyst loadings. Thus, from the amine contents, the higher catalyst loadings did not seem to have a visible effect on crosslinking, which would result in a higher amine content due a lower degree of NH_3-formation. A catalyst loading of 2 wt% was found to be the lowest possible, as 1 wt% catalyst would result in a sluggish reaction, giving only 19% amine content (entry 25). FT−IR spectroscopic analysis of polymer products from different catalyst loadings (2−20 wt%) also showed near-identical spectra with the exception of the CO signal ~ 1912 cm^{-1} (**Figure S8**).

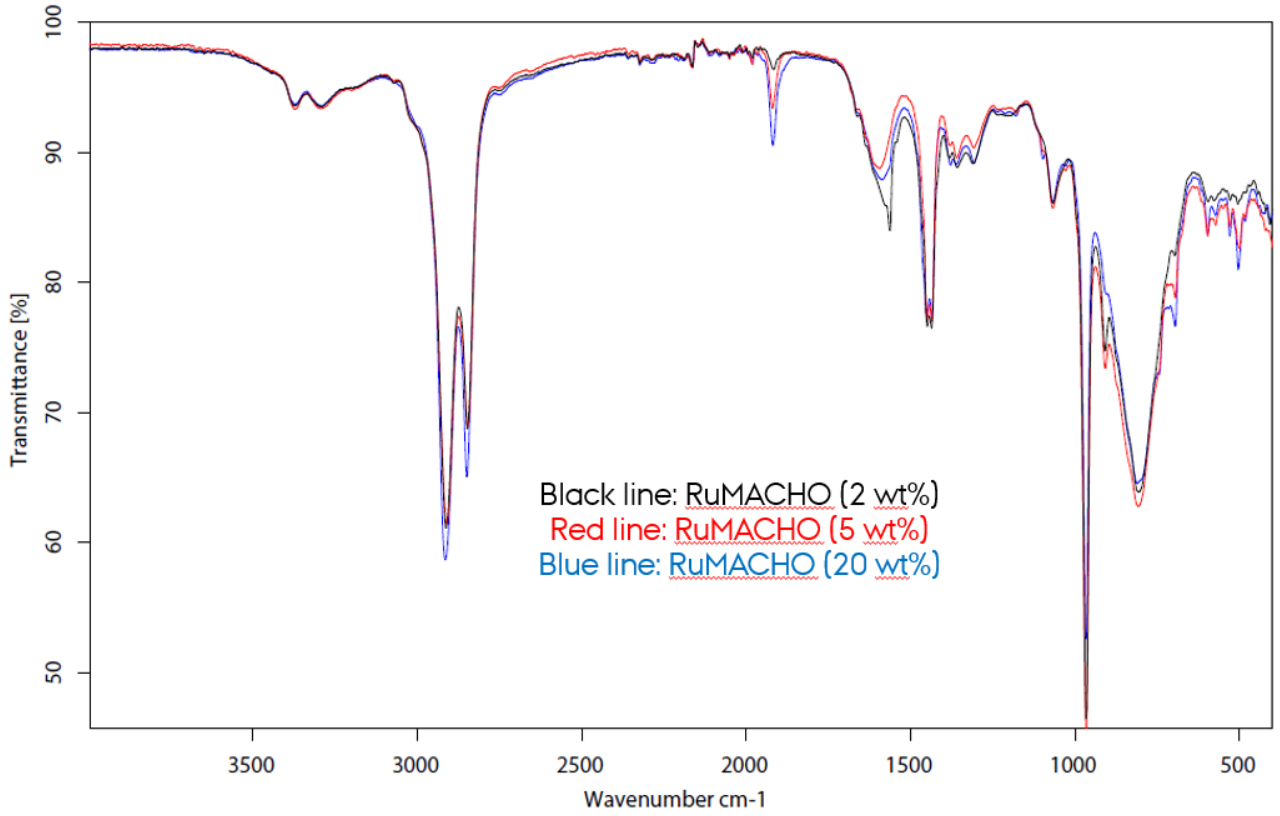

Figure S8. Near-identical spectra for products deriving from different catalyst loadings.

We attempted to further dilute the reaction, as we hypothesised that this could affect the crosslinking degree, however, the amine contents of these reactions (entries 26 and 27, 77−79%) were comparable to the previously observed amine contents. The base loading could be reduced to 2 wt%, however, with a drop in the amine yield (entry 26, 55%). Furthermore, we found that catalytic amounts (2 wt% or higher) of KO*t*Bu helped to swell **NBR1** in the reaction, thus giving a higher surface area for nitrile hydrogenation on the polymer. In comparison, the reaction with 1 wt% KO*t*Bu does not swell the polymer to a large degree, which is reflected in the amine yield (entry 27, 7%).

Finally, we attempted a scale-up reaction using 1 g of **NBR1**, and advantageously found that the solvent volume could be decreased to 10 mL without hampering the amine content of the product (entry 30, 75%).

For all polymer products of the hydrogenation substrate scope we detect a CO band by FT−IR spectroscopic analysis at ~1912−1894 cm^{-1}. This suggests that some of the ruthenium catalyst is deposited or bound to the polymer after the reaction, and for this reason, we employ rigorous washing procedures (see the General Procedures). However, even when washing with a wide selection of solvents (MeCN, DMF, EtOAc, CH_2Cl_2, THF, DMSO, NaOH (2.5M in H_2O), HCl (4M in H_2O)) or conducting Soxhlet extraction overnight to wash the polymer with hot methanol, the CO band could not be removed fully. Potentially, the amines in the polymer could act as covalent or dative ligands to the ruthenium, thus washing with NH_3 (25% in H_2O) or EDTA solution (1 M in H_2O) could work, but this was also not possible to further diminish the CO band.

The NBR, ABS, and SAN polymers, which are central to this study, also holds styrene and/or butadiene monomers besides acrylonitrile. We thus examined the reaction outcome of a model compound **3**, consisting of both phenyl groups and an internal alkene, mimicking styrene and butadiene monomers. Under reaction

conditions similar to the optimised conditions, we could observe a partial hydrogenation of the alkene to an alkane product (observable by GC−MS), while the phenyl groups were not hydrogenated (**Scheme S2**).

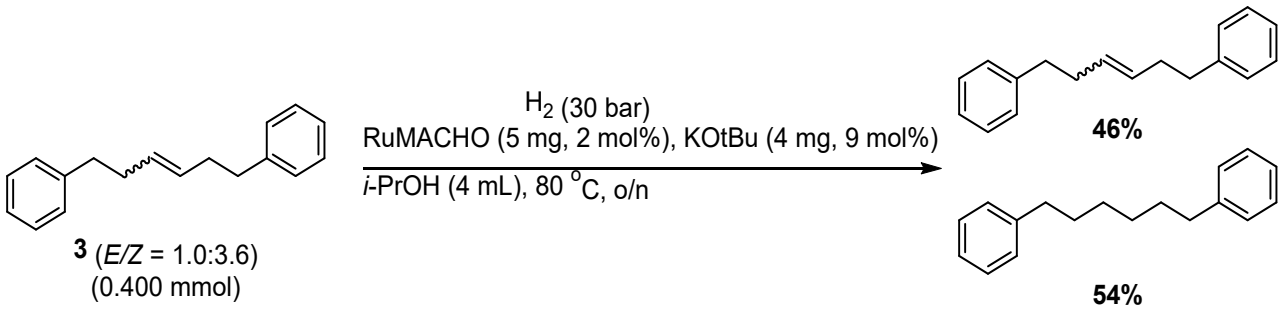

3 (*E/Z* = 1.0:3.6)
(0.400 mmol)

Scheme S2. Reaction of styrene-butadiene model compound **3** under the catalytic hydrogenation conditions. Conversion percentages are based on the ratio of GC−MS FID values.

Synthesis of model compound **3**:
In an argon glove-box, to a pressure flask (50 mL total volume) was added Hoveyda-Grubbs 2nd Gen (3 mol%, 251 mg, 0.399 mmol), 1,4-benzoquinone (10 mol%, 140 mg, 1.33 mmol) and but-3-en-1-ylbenzene (2.0 mL, 13 mmol). Ethylene gas formation was observed, and the reaction was left standing for 5 minutes, after which the flask was sealed with a screwcap fitted with a Teflon®-coated pierceable silicone seal and a stabilising PTFE disc. To the flask was then added degassed and dry CH_2Cl_2 (12 mL) through the pierceable seal with a syringe and the contents were stirred at 55 °C for 3 days. After cooling to rt, the reaction mixture was filtered through celite, while washing with CH_2Cl_2 and then purified by flash column chromatography (Pentane) to yield the product as a colorless liquid (668 mg, 42%). The *E/Z*-ratio was determined to be 1.0:3.6 from ^{1}H−NMR analysis. ^{1}H−NMR (400 MHz, $CDCl_3$) δ_H (ppm) 7.31−7.27 (m, 4H), 7.22−7.17 (m, 6H), 5.51−5.48 (m, 1.5H), 5.48−5.43 (m, 0.4H), 2.67 (t, *J* = 7.0 Hz, 3.2H), 2.59 (t, *J* =7.1 Hz, 0.8H), 2.34−2.29 (m, 4H). ^{13}C−NMR (100 MHz, $CDCl_3$) δ_C (ppm) 142.2, 142.2, 130.2, 129.6, 128.6, 128.5, 128.4, 125.9, 125.9, 36.2, 36.0, 34.6, 29.3. NMR spectroscopic analysis is in accordance with literature values.[7]

Optimisation of Nitrile Reduction with Acrylic Textiles

Although the optimised reaction conditions were successful in the hydrogenation of NBR, ABS, and SAN samples, this proved not to be the case for the hydrogenation of acrylic fibers. Thus, a new optimisation of reaction conditions was carried out (**Table S2**), with the acrylic fiber substrates **TEX1**−**TEX4**. For this optimisation, Kaiser amine testing and FT−IR spectroscopic analysis were used to evaluate the hydrogenated polymer products. [RuC6] was prepared according to a literature procedure.[8]

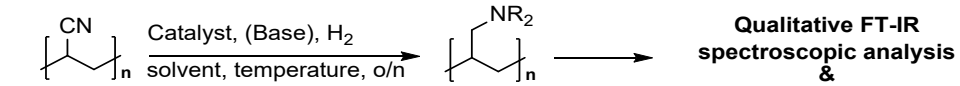

TEX1 – TEX4
(100 mg)

H-TEX1 – H-TEX4
R = H or alkyl

Entry	Substrate (100 mg)	Pre-catalyst (wt%)	Base (wt%)	H_2 (bar)	Solvent (mL)	Temp. (°C)	Kaiser test	FT-IR C≡N reduction
1	**TEX1**	[Ru-C1] (5)	KO*t*Bu (4)	30	*i*-PrOH (5)	70	Neg.	No
2	**TEX2**	[Ru-C1] (5)	KO*t*Bu (4)	30	*i*-PrOH (5)	70	Neg.	No
3	**TEX3**	[Ru-C1] (5)	KO*t*Bu (4)	30	*i*-PrOH (5)	70	Neg.	No
4	**TEX4**	[Ru-C1] (5)	KO*t*Bu (4)	30	*i*-PrOH (5)	70	Neg.	No
5	**TEX4**	[Ru-C2] (5)	None	30	*i*-PrOH (5)	70	Neg.	No
6[a]	**TEX4**	[Ru-C1] (5)	KO*t*Bu (4)	30	*i*-PrOH (5)	70	Neg.	No
7	**TEX4**	[Ru-C1] (5)	KO*t*Bu (4)	30	*i*-PrOH/DMF (4:1, 5)	70	Neg.	No
8	**TEX4**	[Ru-C1] (5)	KO*t*Bu (4)	30	DMF (5)	70	Neg.	No
9	**TEX4**	[Ru-C1] (5)	KO*t*Bu (4)	30	DMSO (5)	70	Neg.	No
10	**TEX4**	[Ru-C1] (5)	KO*t*Bu (4)	30	Glyme (5)	70	Neg.	No
11	**TEX4**	[Ru-C1] (5)	KO*t*Bu (4)	30	MeCN (5)	70	Neg.	No
12	**TEX4**	[Ru-C1] (5)	KO*t*Bu (4)	30	THF (5)	70	Neg.	No
13	**TEX4**	[Ru-C1] (5)	KO*t*Bu (4)	30	*i*-PrOH/DMSO (1:1, 5)	70	Neg.	No
14	**TEX4**	[Ru-C1] (5)	KO*t*Bu (4)	30	*i*-PrOH/DMF (9:1, 5)	70	Neg.	No
15	**TEX4**	[Ru-C1] (5)	KO*t*Bu (4)	30	*i*-PrOH (5)	100	Neg.	No
16	**TEX1**	[Ru-C1] (5)	KO*t*Bu (4)	30	MeOH (5)	70	Neg.	No
17	**TEX1**	[Ru-C1] (5)	KO*t*Bu (4)	30	EtOH (5)	70	Neg.	No
18	**TEX1**	[Ru-C1] (5)	KO*t*Bu (4)	30	DMF (5)	70	Neg.	No
19	**TEX1**	[Ru-C1] (5)	KO*t*Bu (4)	30	*i*-PrOH/DMF (1:1, 5)	70	Neg.	No
20	**TEX1**	[Ru-C1] (5)	KO*t*Bu (4)	30	*i*-PrOH/DMF (7:1, 5)	70	Neg.	No
21	**TEX1**	[Ru-C1] (5)	KO*t*Bu (4)	30	*i*-PrOH/DMSO (1:1, 5)	70	Neg.	No
22	**TEX1**	[Ru-C1] (5)	KO*t*Bu (4)	30	*i*-PrOH (5)	150	Neg.	No
23	**TEX1**	[Ru-C1] (5)	KO*t*Bu (4)	30	*i*-PrOH (5)	200	Neg.	No
24[b]	**TEX1**	[Ru-C1] (5)	KO*t*Bu (4)	30	*i*-PrOH (5)	70	Neg.	No
25[b]	**TEX1**	[Ru-C1] (5)	KO*t*Bu (4)	30	*i*-PrOH (5)	150	Neg.	No
26[b]	**TEX1**	[Ru-C1] (5)	KO*t*Bu (4)	30	*i*-PrOH (5)	200	Neg.	No
27	**TEX1**	[Ru-C1] (50)	KO*t*Bu (40)	30	*i*-PrOH (5)	200	Neg.	No
28	**TEX1**	[Ru-C4] (5)	KO*t*Bu (4)	30	*i*-PrOH (5)	70	Neg.	No
29	**TEX1**	[Ru-C5] (5)	KO*t*Bu (4)	30	*i*-PrOH (5)	70	Neg.	No
30	**TEX1**	[Ru-C6] (5)	KO*t*Bu (4)	30	*i*-PrOH (5)	70	Pos.	Yes
31	**TEX1**	[Ru-C6] (10)	KO*t*Bu (4)	30	*i*-PrOH (5)	70	Pos.	Yes
32	**TEX1**	[Ru-C6] (10)	KO*t*Bu (4)	50	*i*-PrOH (5)	70	Pos.	Yes
33	**TEX1**	[Ru-C6] (10)	KO*t*Bu (4)	50	*i*-PrOH (5)	100	Pos.	Yes
34	**TEX1**	[Ru-C6] (20)	KO*t*Bu (4)	50	*i*-PrOH (5)	100	Pos.	Yes

Table S2. [a]The polymer substrate was washed extensively with H_2O, EtOH, and acetone, prior to the reaction. [b]**TEX1** was dissolved in DMF and precipitated with H_2O, then dried in vacuo prior to the reaction.

The positive result (entry 30) was further optimised using qualitative FT−IR spectroscopic analysis (**Figure S9**). Close to full consumption of the nitrile band (2242 cm^{-1}) required higher temperature (100 °C), higher H_2-pressure (50 bar), and a higher catalyst loading (20 wt%). With these conditions we observed the highest qualitative conversion. A catalyst loading of 20 wt% [RuC6] corresponds to 2.5 mol% in relation to the molar amount of acrylonitrile monomers in **TEX1** (AN (wt%) = 91).

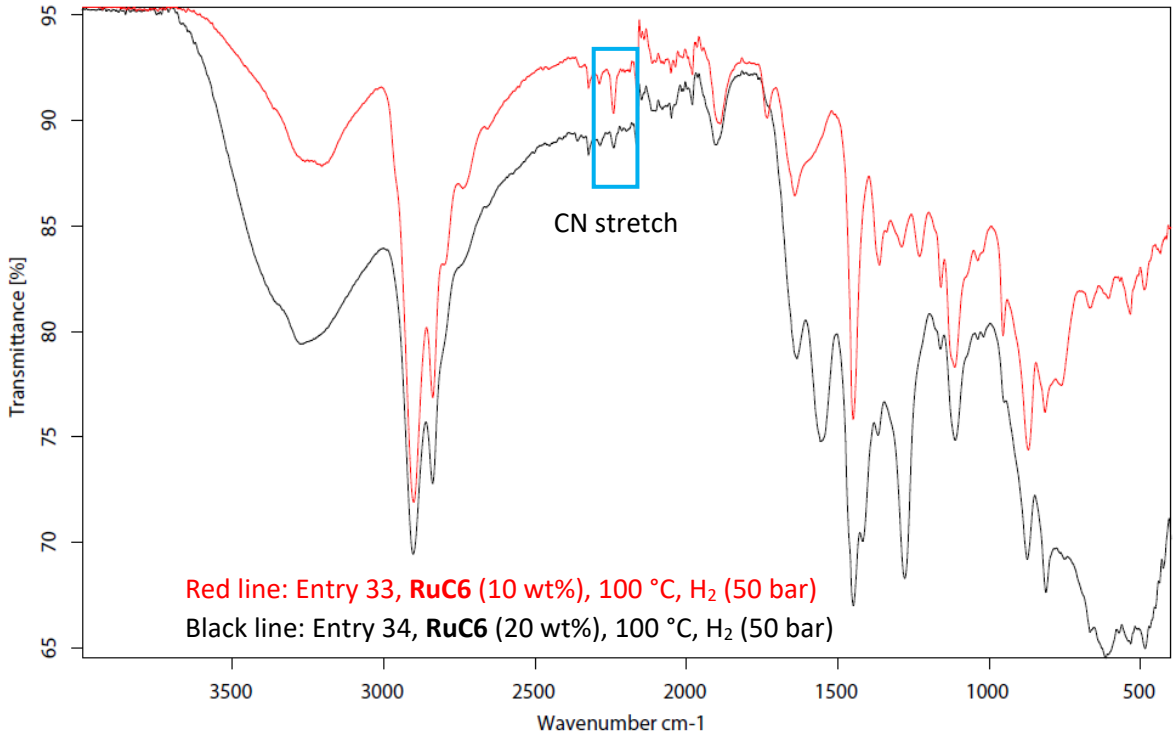

Figure S9. FT−IR-based qualitative optimisation of nitrile hydrogenation for acrylic fiber substrate **TEX1**.

Although the IR-spectroscopic analysis suggests close to full hydrogenation of nitrile, we do observe leftover nitrile from ^{13}C CP/MAS NMR spectroscopic analysis as well as chemical shifts corresponding to secondary amines (see characterisation of hydrogenated textile substrates, pp. S145−S173). We hypothesise that the reaction is only surface-active and does not hydrogenate the bulk of the acrylic fibers in contrast to NBR, ABS and SAN substrates, while the higher concentration of acrylonitrile monomers leads to a higher degree of secondary amine. Furthermore, these observations can explain the lower amine efficiencies obtained from CO_2-adsorption experiments using TGA (see e.g. **Table S5**).

Optimisation of Poly(butadiene) Hydrocyanation and Regioselectivity Study

The optimisation of poly(butadiene) hydrocyanation was conducted with the polymer substrate **SBR1**, which contains 30 wt% styrene (according to the label), thus a 70 wt% butadiene content. We found that obtaining yields by ^1H−NMR integration with an internal standard was challenging due to a crowded spectrum, thus we decided to use an FT−IR-based quantification method for the measure of hydrocyanation conversion. For each reaction, the polymer product was analysed by FT−IR spectroscopic analysis to obtain the intensity ratio of the C≡N band (sp C≡N stretch, 2238 cm^{-1}) to the C=C−H band (sp^2 C−H bending, 968 cm^{-1}) (**Table S3**).

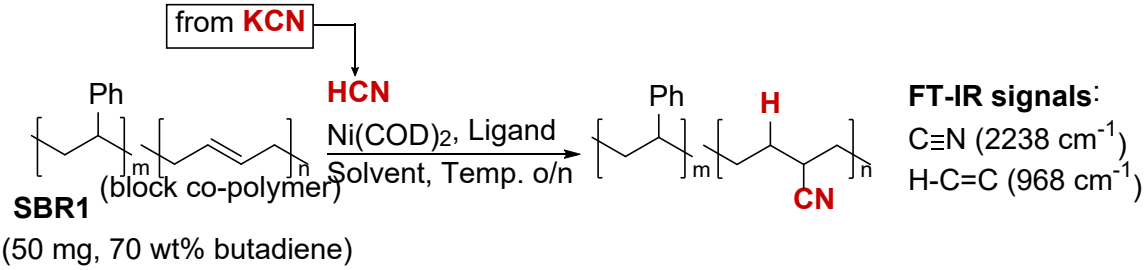

SBR1

(50 mg, 70 wt% butadiene)

Entry	$Ni(COD)_2$ (wt%)	Ligand (equiv/[Ni])	HCN (equiv/olefin)	Solvent (mL)	Temp. (°C)	C≡N/H-C=C (FT-IR ratio %)
1	5	$P(OMe)_3$ (4)	1.1	PhMe (2)	70	-
2	5	$P(OPh)_3$ (4)	1.1	PhMe (2)	70	-
3	5	Xantphos (2)	1.1	PhMe (2)	70	4
4	5	P(*o*-tolyl)$_3$ (4)	1.1	PhMe (2)	70	-
5	5	DPEPhos (2)	1.1	PhMe (2)	70	-
6	5	Xantphos (1)	1.1	PhMe (2)	70	5
7	5	DIOP (1)	1.1	PhMe (2)	70	8
8	5	L1 (1)	1.1	PhMe (2)	70	-
9	5	Cy_2-Xantphos (1)	1.1	PhMe (2)	70	-
10	5	*Rac*-BINAP (1)	1.1	PhMe (2)	70	-
11	20	Xantphos (1)	1.1	PhMe (2)	70	10
12	5	BiPhePhos (1)	1.1	PhMe (2)	70	12
13	5	BiPhePhos (1)	2.2	PhMe (2)	70	18
14	5	BiPhePhos (1)	3.3	PhMe (2)	70	23
15	5	BiPhePhos (1)	1.1	PhMe (2)	90	15
16	5	BiPhePhos (1)	3.3	PhMe (2)	90	25
17	5	BiPhePhos (1)	3.3	*o*-xylene (2)	110	24
18	5	BiPhePhos (1)	4.4	PhMe (2)	90	26
19	5	BiPhePhos (1)	5.5	PhMe (2)	90	27
20	10	BiPhePhos (1)	5.5	PhMe (2)	90	32
21	20	BiPhePhos (1)	5.5	PhMe (2)	90	34
22	10	BiPhePhos (1)	AC (3)	PhMe (2)	90	22
23	10	BiPhePhos (1)	AC (5)	PhMe (2)	90	20
24[a]	10	BiPhePhos (1)	5.5	PhMe (2)	90	38
25	10	BiPhePhos (2)	5.5	PhMe (2)	90	31
26	10	BiPhePhos (1)	5.5	PhMe (1)	90	33
27[b]	10	BiPhePhos (1)	5.5	PhMe (10)	90	31

Table S3. The styrene butadiene rubber starting material was used with a random size consisting of most often 2–3 pieces. AC = acetone cyanohydrin (reaction was conducted in a COtube (one reaction chamber instead of a two-chamber reactor). [a]Was reacted for 4 days. [b]250 mg of **SBR1**.

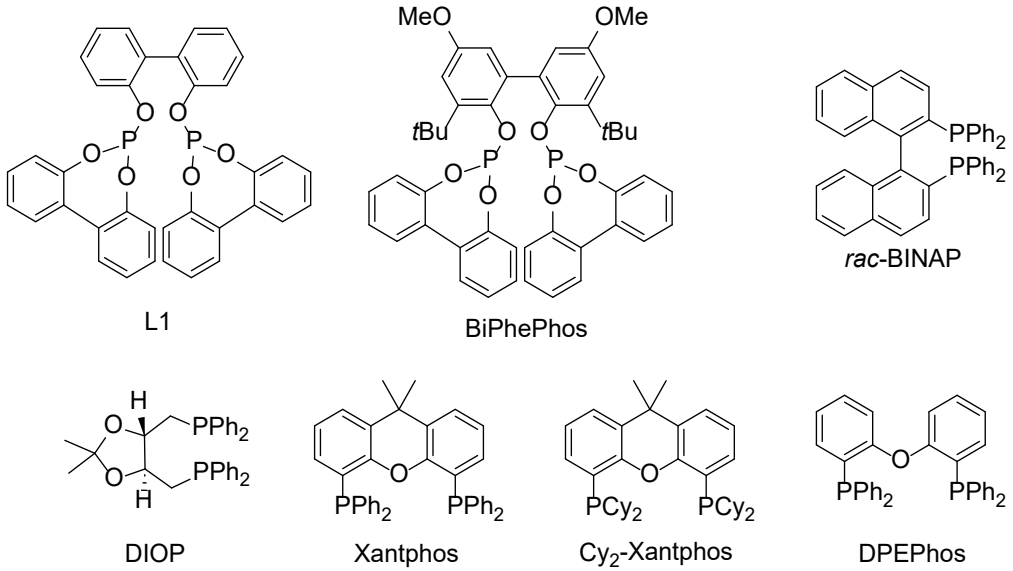

Figure S10. Structures of ligand abbreviations in **Table S3**.

Through a ligand screening, we observed the product nitrile band by FT−IR spectroscopic analysis with Xantphos, DIOP, and BiPhePhos, of which the latter gave the highest CN/C=C-H ratio of 12% (entry 12). Raising the amount of HCN (2.2 and 3.3 equiv. per butadiene) led to higher CN/C=C-H ratios of 18−23% (entries 13 and 14). Also, by raising the temperature to 90 °C, a higher CN/C=C-H ratio of 25% could be achieved (entry 16), however, increasing the temperature to 110 °C did not achieve a higher ratio yielding 24% (entry 17). For that reaction, *o*-xylene was used as the solvent to prevent evaporation of the toluene solvent to the other chamber B of the two-chamber system, which is kept at rt. Raising the equivalents of HCN per butadiene to 5.5 gave a small increment in the IR-ratio (27%, entry 20), and higher catalyst loadings of 10 and 20 wt% $Ni(COD)_2$ gave slightly higher IR-ratios of 32−34% (entries 21 and 22). We decided to continue with 10 wt% catalyst loading, since the ratio increase of using 20 wt% catalyst was not significant. Instead of conducting the reaction with *ex situ* generated HCN in a two-chamber system, we attempted the use of acetone cyanohydrin also, which has been reported previously for hydrocyanation of internal olefins,[9−11] although, for these reactions, the IR-ratio was lower (20−22%, entries 22 and 23). The best IR-ratio was obtained when conducting the reaction for 4 days giving an IR-ratio of 38%, however, for the hydrocyanation substrate scope we prefer a reaction time of 24 h, since there is not a significant difference in the IR-ratios (32% for 1 day, and 38% for 4 days). Then, we attempted the reaction with 2 equivalents of BiPhePhos per $Ni(COD)_2$ which gave an indifferent IR-ratio of 31% (entry 25), and this was also the case when concentrating the reaction to 1 mL of toluene solvent (33%, entry 26). It is preferable however, to use 2 mL of toluene solvent, because the polymer substrates are less prone to deposit on the sides of the reaction chamber over the solvent layer when stirring the reaction. Finally, we were successful in scaling up the reaction to 250 mg of **SBR1**, which resulted in an IR-ratio of 31%. ^{1}H−NMR spectroscopic analysis of the hydrocyanated product **HCN-SBR1** shows a significantly reduced alkene area (5.25–5.75 ppm) when comparing with the starting material **SBR1** (see the hydrocyanation products section, p. S166).

Elemental analysis shows an average N-content of 5.68 mmol/g in **HCN-SBR1** products, thus corresponding to a 44% yield compared to the molar amount of butadiene derived from its 70 wt% content in **SBR1**.

Hydrocyanation reactions with model compounds

Due to the successful optimisation of poly(butadiene) hydrocyanation with polymer substrate **SBR1**, we decided to investigate the regioselectivity of the reaction, as the olefin substrates commonly undergo

migration to become conjugated or to an alkyl chain end.[9–11] For this purpose, we tested the SBR model compound **3** under the hydrocyanation conditions, which resulted in a 98% isolated yield of the migratory hydrocyanation benzyl cyanide product **4** (see below).

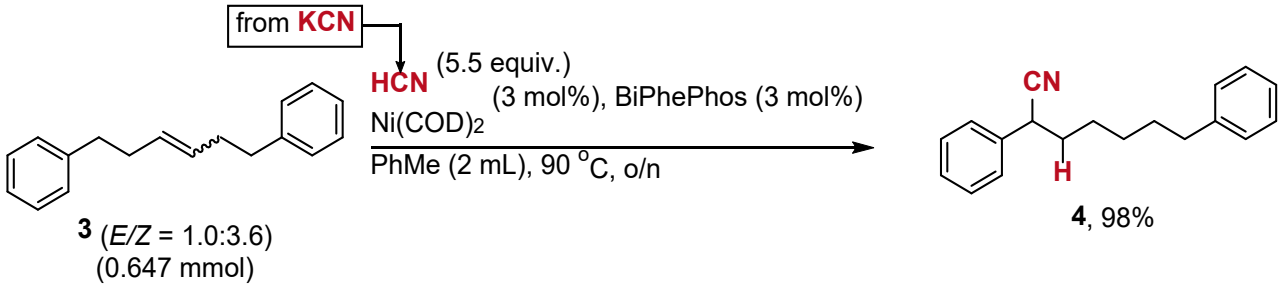

Scheme S3. Hydrocyanation of styrene-butadiene model compound **3**.

This suggests that for styrene-butadiene polymers, a migration of the olefin to the styrene position occurs prior to hydrocyanation, however, this model compound lacks the benzylic alkyl substitution that would be present in a styrene-butadiene polymer and only features one olefin. Thus, we synthesised styrene-butadiene model compound **6**, which more closely resembles styrene-butadiene due to the benzylic methyl substituents. From the hydrocyanation of **6**, a complex product mixture was observed with GC-MS, showing full conversion of the starting material to mono-hydrocyanation products. Thus, with the benzylic alkyl branching and the extra olefin in model compound **6**, the reaction seems to be less selective, favoring different nitrile regioisomers.

Synthesis of **4**:
In an argon glove-box to chamber A of a two-chamber system was added $Ni(COD)_2$ (3 mol%, 5 mg, 0.02 mmol), BiPhePhos (3 mol%, 14 mg, 0.018 mmol), PhMe (2 mL), and *E/Z*-1,6-diphenylhex-3-ene (**2**) (153 mg, 0.647 mmol). The chamber was sealed with a screwcap fitted with a Teflon®-coated silicone seal and a stabilising PTFE disc. To chamber B of the two-chamber system was added KCN (5.5 equiv., 232 mg, 3.56 mmol), ethylene glycol dimethyl ether (2 mL), and lastly AcOH (45 equiv., 1.7 mL, 29 mmol) slowly on top of the solvent. **(Beware! The AcOH must be added slowly on top of the glycol solvent, otherwise HCN release will occur)**. The chamber was sealed with a screwcap fitted with a Teflon®-coated silicone seal and a stabilising PTFE disc. The reaction in chamber A was stirred at 90 °C o/n, whereas chamber B was kept at rt, while placed in a well-ventilated fume-hood. Upon completion, the two-chamber system was cooled down to rt, then opened and left stirring for 20−30 min under good ventilation. The reaction mixture was concentrated onto celite and purified by flash column chromatography (Pentane to pentane/EtOAc 9:1) to yield 2,7-diphenylheptanenitrile (**3**) as a colorless oil (167 mg, 98%). ^{1}H−NMR (400 MHz, $CDCl_3$) δ_H (ppm) 7.40−7.26 (m, 7H), 7.20−7.15 (m, 3H), 3.76 (dd, J_1 = 8.4 Hz, J_2 = 6.2 Hz, 1H), 2.60 (t, J = 7.6 Hz, 2H), 1.97−1.81 (m, 2H), 1.67−1.33 (m, 6H). ^{13}C−NMR (100 MHz, $CDCl_3$) δ_C (ppm) 142.5, 136.1, 129.2, 128.5, 128.4, 128.1, 127.3, 125.9, 121.0, 37.5, 35.9, 35.9, 31.2, 28.6, 27.0. HRMS $C_{19}H_{22}N^+$ [M + H$^+$]: calcd 264.1747, found 264.1748. Values are in accordance with literature.[12]

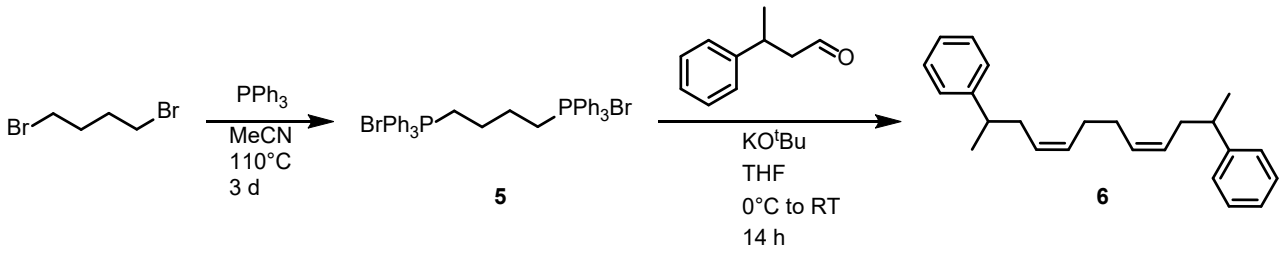

Scheme S4. Synthesis of model compound **6**.

Synthesis of **5**:
In an argon-filled glovebox, to a 50 mL pressure flask was added 1,4-dibromobutane (1.0 equiv., 1.08 g, 5.00 mmol), triphenylphosphine (2.1 equiv., 2.75 g, 10.5 mmol) and dry MeCN (21 mL). The flask was sealed with a screwcap and taken outside the glovebox. After stirring at 110 °C for 3 days, the precipitate was collected by filtration and washed with EtOAc. Recrystallization of the precipitate from boiling EtOAc/MeOH yielded the pure product butane-1,4-diylbis(triphenylphosphonium) bromide (**5**) as a colorless solid (3.35 g, 89%). ^{1}H−NMR (400 MHz, CD_3OD) δ 7.94 – 7.68 (m, 30H), 3.70 – 3.51 (m, 4H), 2.06 – 1.89 (m, 4H). ^{13}C−NMR (101 MHz, CD_3OD) δ 136.3 (d, *J* = 3.1 Hz), 134.9 (d, *J* = 10.3 Hz), 131.6 (d, *J* = 12.8 Hz), 119.6 (d, *J* = 86.6 Hz), 24.4 (dd, *J* = 18.5, 3.7 Hz), 22.4 (d, *J* = 52.3 Hz). ^{31}P−NMR (162 MHz, CD_3OD) δ (ppm) 23.6. Values are in accordance with literature.[13]

Synthesis of **6**:
In an argon-filled glovebox, compound **5** (1.1 equiv., 2.51 g, 3.33 mmol) and potassium *tert*-butoxide (2.2 equiv., 741 mg, 6.66 mmol) were suspended in dry THF (3.5 mL) in a 5 mL flask and then sealed with a screwcap fitted with a Teflon®-coated pierceable silicone seal and a stabilising PTFE disc. Outside the glovebox, the orange suspension was cooled to 0 °C with an ice bath for 1 h before adding 3-phenylbutyraldehyde (2.0 equiv., 889 mg, 890 µL, 6.00 mmol) with a syringe. The reaction was allowed to warm up to room temperature and stirred overnight. Then, the reaction mixture was quenched with saturated NH_4Cl solution, and the aqueous layer was extracted with CH_2Cl_2 (4 x 10 mL). The combined organic layers were dried over Na_2SO4, filtered and the solvent was removed under reduced pressure. The product was purified by flash column chromatography (0-10% EtOAc in Heptane) to yield the product dodeca-4,8-diene-2,11-diyldibenzene (**6**) as a colorless oil (781 mg, 82%). ^{1}H NMR (400 MHz, $CDCl_3$) δ_H (ppm) 7.34 – 7.28 (m, 4H), 7.25 – 7.16 (m, 6H), 5.45 – 5.24 (m, 4H), 2.77 (h, *J* = 7.0 Hz, 2H), 2.40 – 2.26 (m, 4H), 2.07 – 1.92 (m, 4H), 1.29 (d, *J* = 6.9 Hz, 6H). ^{13}C NMR (101 MHz, $CDCl_3$) δ_C (ppm) 147.3, 130.4, 128.4, 127.1, 126.0, 40.2, 36.1, 27.5, 21.6. HRMS $C_{24}H_{13}^{+}$ [M + H^{+}]: calculated 319.2421, found 319.2426.

Hydrocyanation with model compound 6

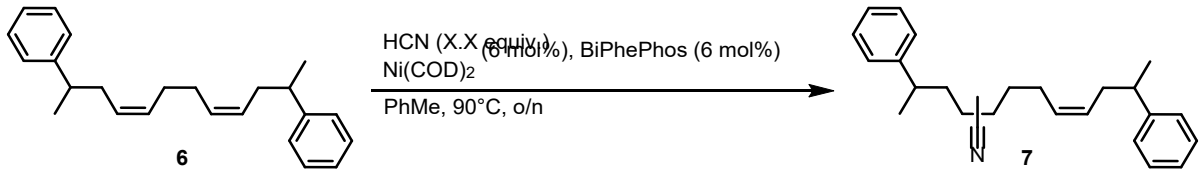

Entry	Two-chamber volume (mL)	**6** (mmol)	KCN (mmol)	HCN (mmol/mL)	PhMe (mL)	Substrate conc. (M)	AcOH (mL)	EGDME (mL)
6-E1	20	0.324	1.78 (2.75 equiv/olefin)	0.089	2.00	0.16	1.7	2.0
6-E2	100	0.8	8.8 (5.5 equiv/olefin)	0.088	2.47	0.32	4.2	4.9
6-E3	100	0.8	17.6 (11 equiv/olefin)	0.176	2.47	0.32	8.4	9.9

Table S4. The experimental procedure is equal to the General Procedure E although with the adjustments provided in the table above. EGDME = Ethylene glycol dimethyl ether.

Due to the formation of multiple hydrocyanation and isomerised olefin (side)products, the outcome of the reaction was only evaluated by mass spectroscopic analyses.

6-E1

According to GC-MS spectroscopic analysis, full conversion of the starting material (**6**) was observed. The chromatogram indicated a mono-hydrocyanation product (m/z 345).

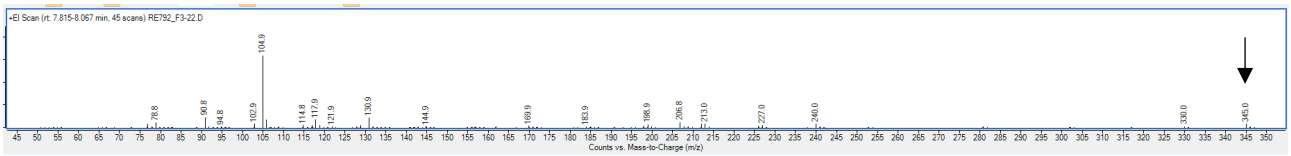

6-E2

According to GC-MS spectroscopic analysis, full conversion of the starting material was observed, and the crude chromatogram was visibly the same as in **6-E1** (m/z 345).

From high-resolution mass spectrometry, the mono-hydrocyanation product mass was observed as well: $C_{25}H_{32}N^+$ [M + H^+]: calculated 346.2530, found 346.2532. However, no mass for a doubly hydrocyanated product was observed.

NMR comparison of product batch (top) vs. starting material (bottom, compound 6): The spectra show conversion of the olefinic signals at ~ 5.4 ppm.

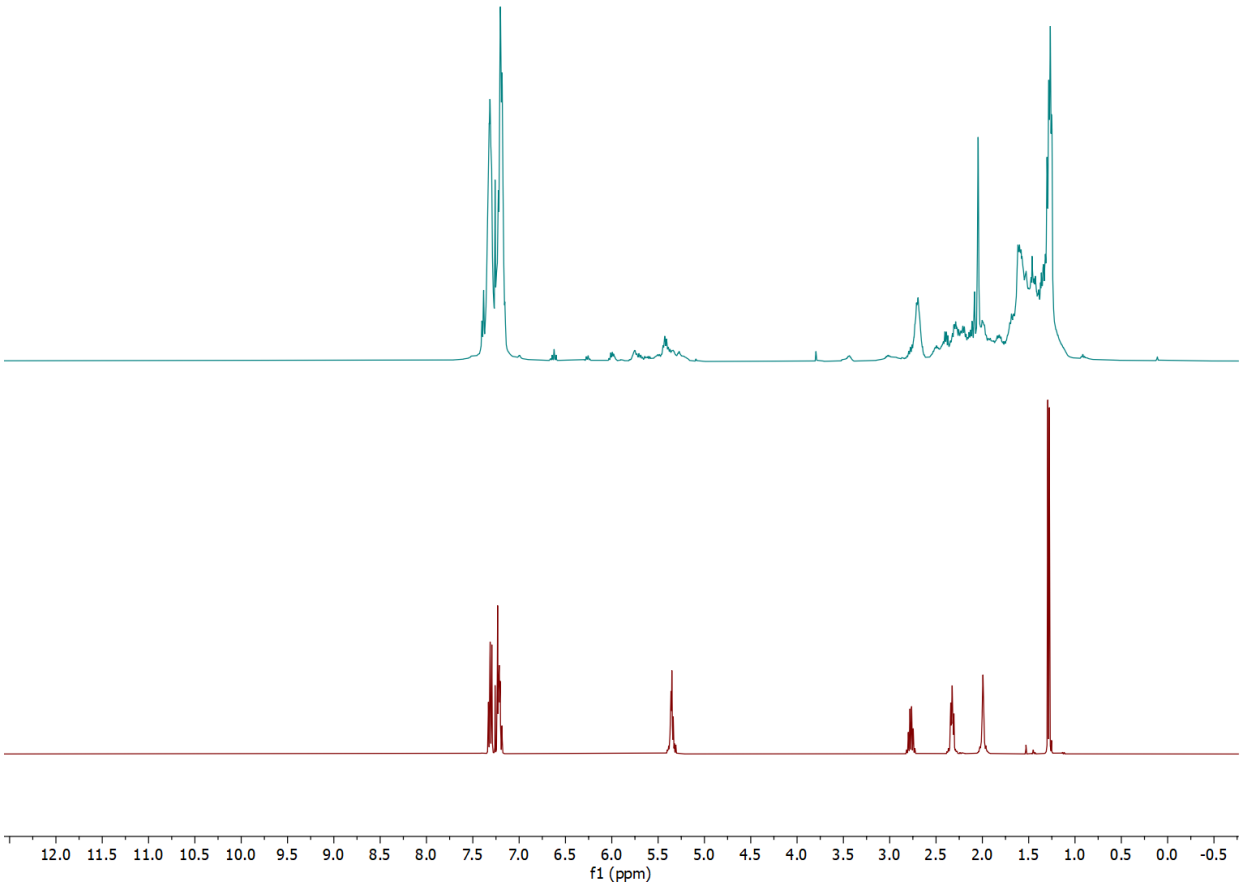

6-E3

According to GC-MS spectroscopic analysis, full conversion of the starting material was observed, and the crude chromatogram was the same as for **6-E1** and **6-E2** (monohydrocyanation product visible as m/z 345).

Post-Modification of Amine Polymer Products with *N*-Boc-Aziridine

O-Tosyl-*N*-Boc-ethanolamine was synthesised according to a previously published procedure,[14] and additionally purified by filtration over a short plug of silica with ethyl acetate elution. *N*-Boc-aziridine was obtained by intramolecular cyclisation of *O*-Tosyl-*N*-Boc-ethanolamine following a modified literature procedure,[15] purifying the product by distillation over crushed KOH (20−30 mbar / 32−38 °C head temperature) and silica plug filtration instead of column chromatography.

O-Tosyl-N-Boc-ethanolamine (7.0 g, 22 mmol, 1.0 equiv.) was dissolved in dry THF (110 mL) to give a clear, yellowish solution. Potassium *tert*-butoxide (2.8 g, 25 mmol, 1.1 equiv.) was added to the stirred solution in one portion. Thin layer chromatographic analysis (1:4 Ethyl acetate/pentane) confirmed full conversion after 1 h and the reaction was quenched by the addition of water (40 mL). Extraction with Et_2O (3 x 100 mL), drying over anhydrous Na_2SO_4, filtration and rotary evaporation (40 °C / 70 mbar) yielded a liquid crude product. This was distilled over two freshly crushed KOH pellets at 80 °C, and fractions were collected at 20−30 mbar / 32−38 °C (head temperature). This biphasic mixture was then filtered over a short silica plug with diethyl ether to give the pure title compound as a clear, colorless liquid (1.0 g, 7.0 mmol, 32%). ^{1}H-NMR (400 MHz, $CDCl_3$) δ_H (ppm) 2.14 (s, 4H), 1.45 (s, 9H). ^{13}C-NMR (100 MHz, $CDCl_3$) δ_C (ppm) 163.0, 81.3, 28.0, 25.9.

General Procedure I

Polymer (100 mg) was weighed into a 10 mL pressure tube and added *N*-Boc-aziridine (1.35 equiv. with respect to the polymer's estimated amine-content, based on the elemental analysis of pre-hydrogenated polymer). The mixture was then suspended in dry acetonitrile (7 mL). After flushing with argon, the pressure tube was closed and heated to 90 °C for 100 h under vigorous stirring. The Boc-protected intermediate was separated by centrifuge-assisted decantation, washed with acetonitrile (6 mL), dried under high vacuum overnight, and analysed by IR and Kaiser test. Boc-deprotection of this polymer was achieved by adding HCl/dioxane (4 M, 5 mL) to 80−180 mg of the intermediate product at -78 °C and letting the reaction mixture thaw under stirring overnight. After centrifugation and decantation, the product hydrochloride was washed with water (8 mL) and methanol (8 mL). The obtained solid was resuspended in ethanol (2 mL) and then aq. NaOH (1 M, 1 mL) was added dropwise at -78 °C. Washing with water (2 x 8 mL), methanol (8 mL), and diethyl ether (8 mL) as well as drying under high vacuum overnight afforded the functionalised polymer.

Polymer Products from Hydrogenation of NBR, ABS, and SAN

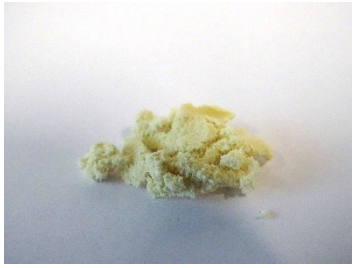

Hydrogenated Nitrile Butadiene Rubber 1 (H-NBR1) was synthesised according to the General Procedure B from substrate **NBR1** (NBR block) and was obtained in weight yields of 942 mg, 94 wt% and 941 mg, 94 wt%, respectively, from two independent runs (94 wt% on average). The polymer was analysed with solid-state ^{13}C CP/MAS NMR, IR-, TGA-, DSC-, and elemental analysis. Solubility tests were also conducted with several solvents. No thermal events besides decomposition were observed with DSC.

Particle size after cryogenic milling used for CO_2 adsorption-desorption experiments

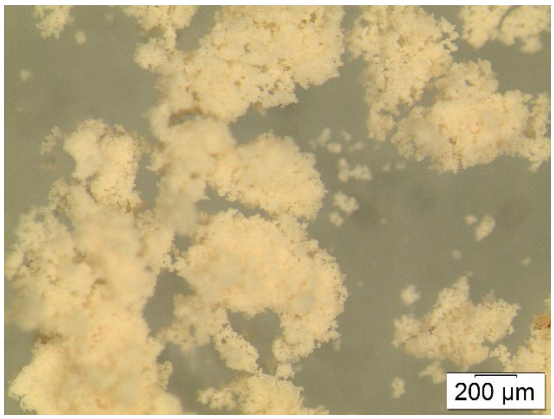

Solubility chart

Soluble **Swells** **Not soluble**

$CHCl_3$	Acetone	*i*-PrOH	DMF	DMSO	THF	PhMe	H_2O	MeOH	MeCN

^{13}C CP/MAS NMR (solid-state)

*Solid-state ^{13}C–NMR of **H-NBR1** (run 1):*

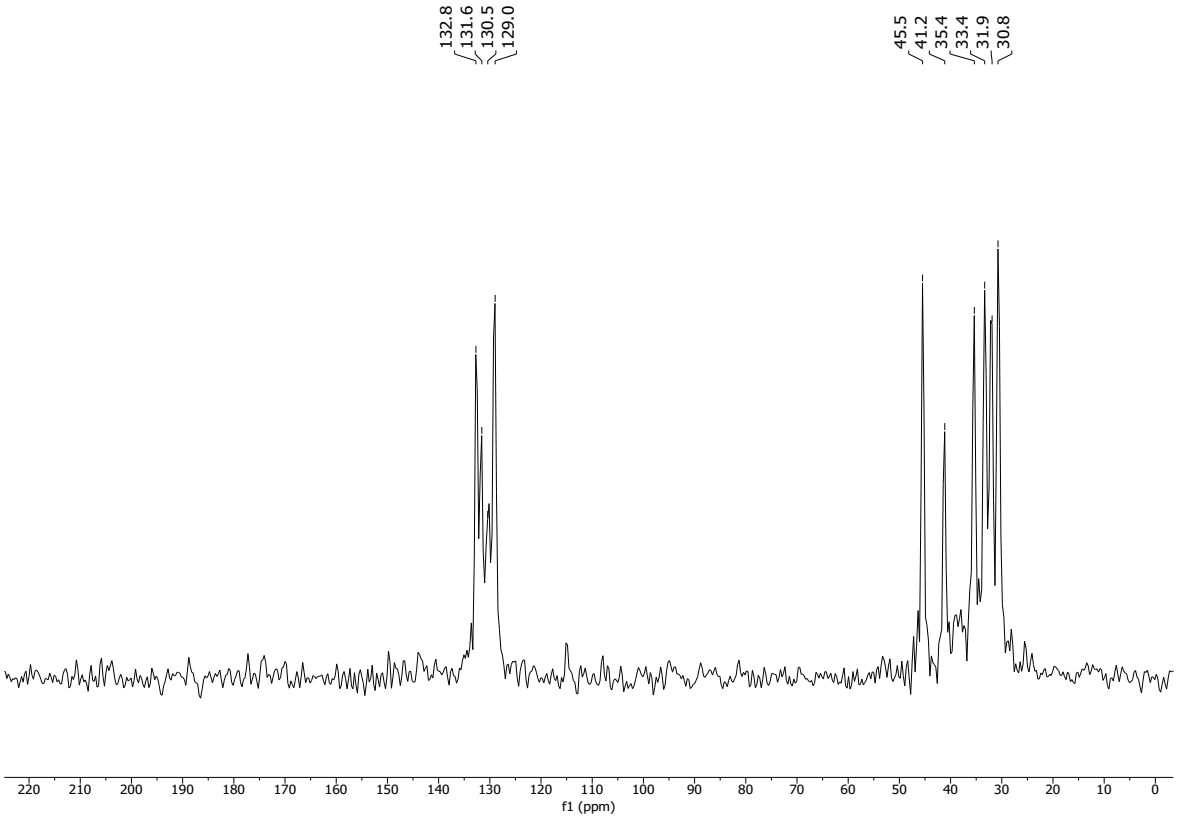

*Solid-state ^{13}C–NMR of **H-NBR1** (run 2):*

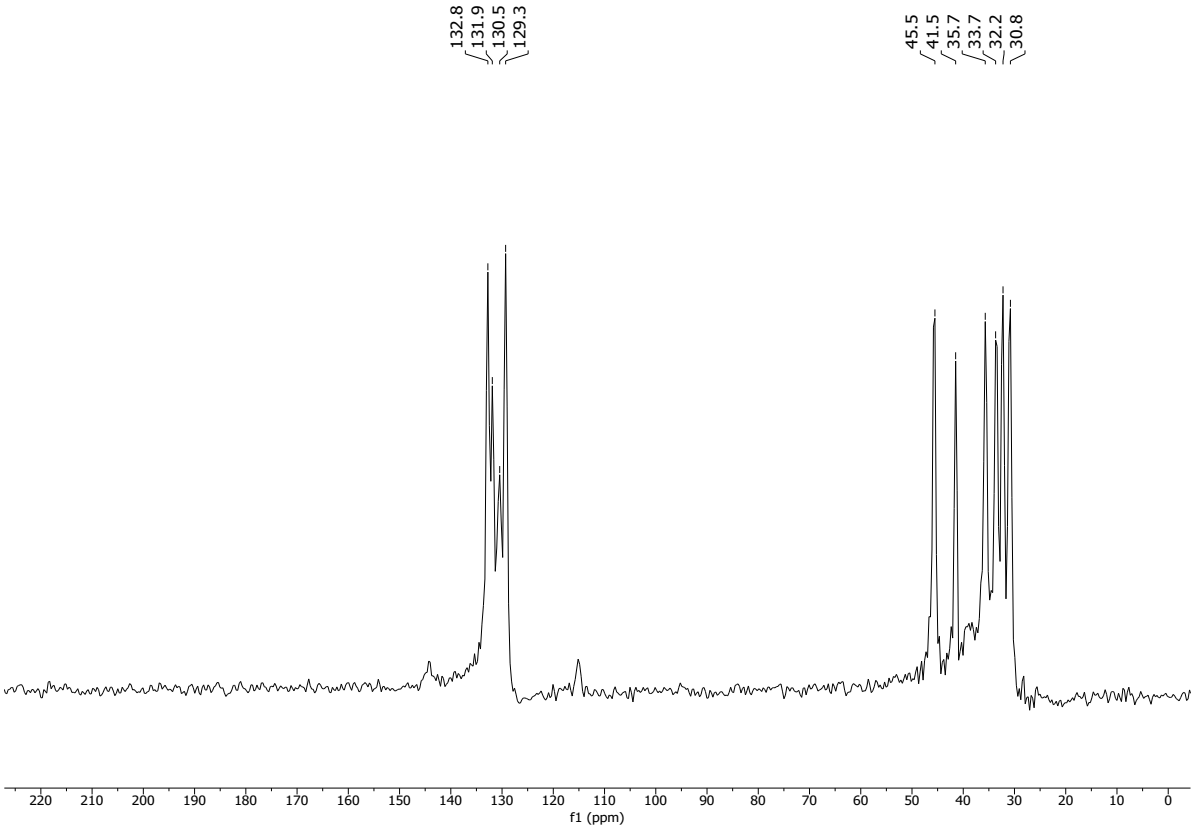

*Solid-state ^{13}C–NMR stacked spectra of **H-NBR1** (run 1, **brown**) and **NBR1** (substrate, **light blue**):*

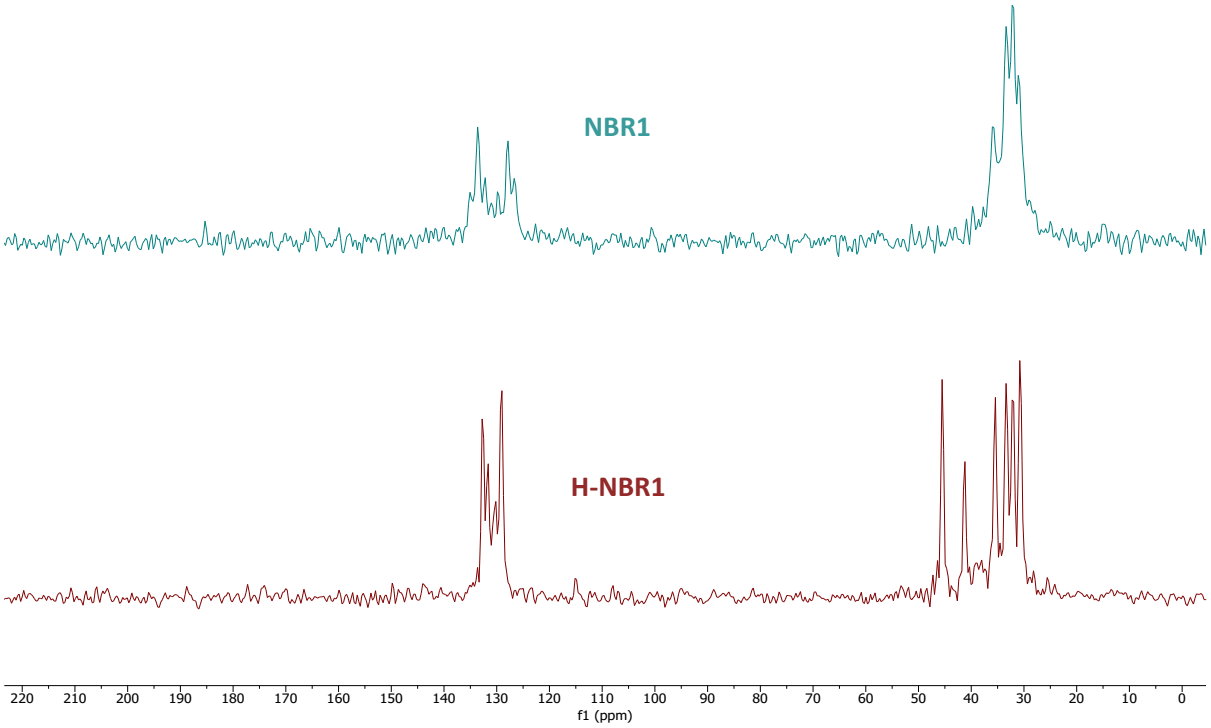

Infrared (IR) Spectroscopic Analysis

*IR-spectrum of **H-NBR1** (run 1):*

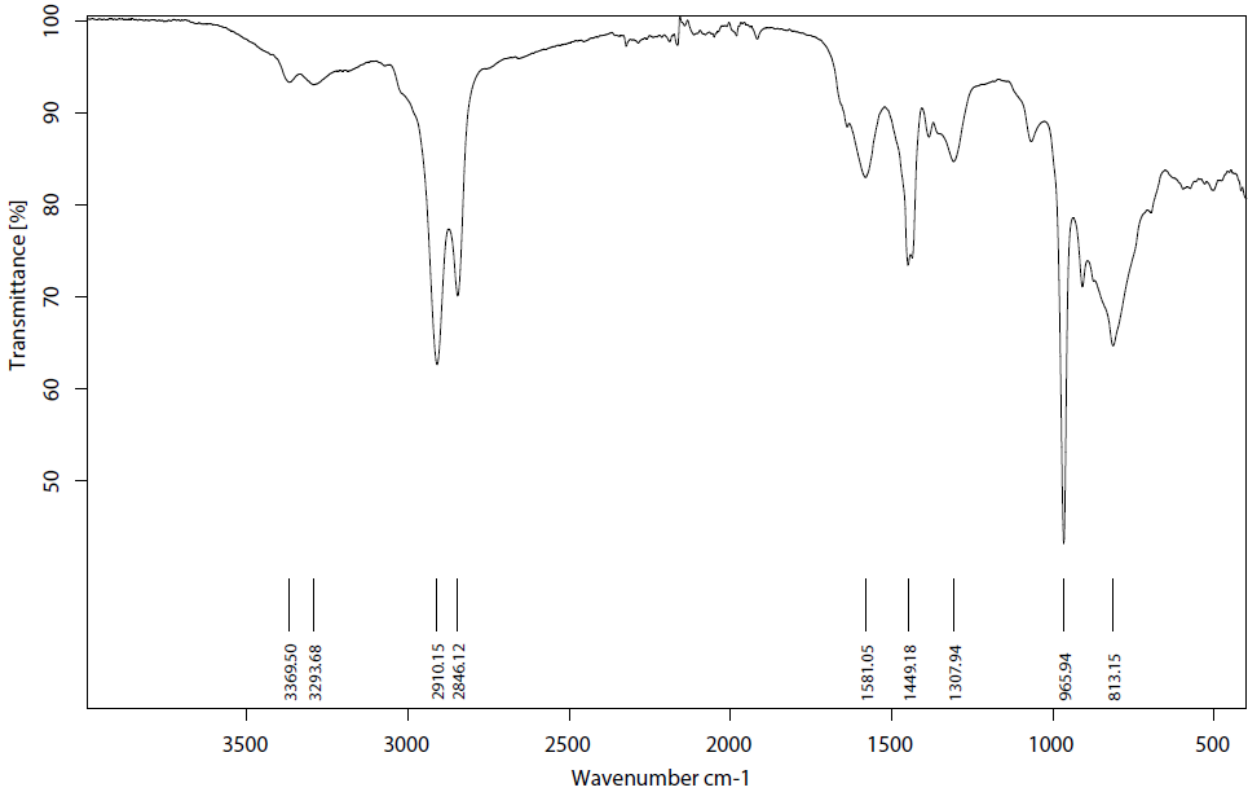

*IR-spectrum of **H-NBR1** (run 2):*

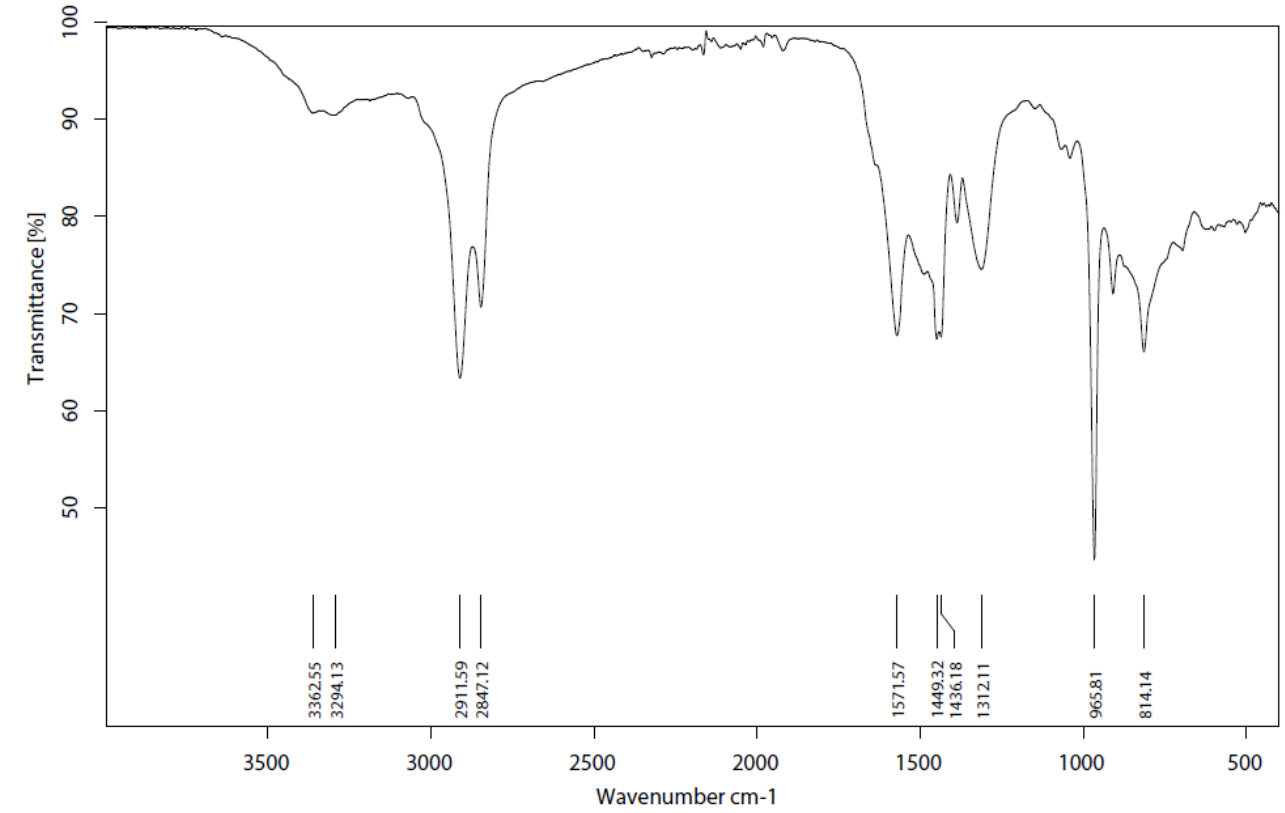

*IR-spectrum overlay of **H-NBR1** (run 1, **black**) and **NBR1** (substrate, **red**):*

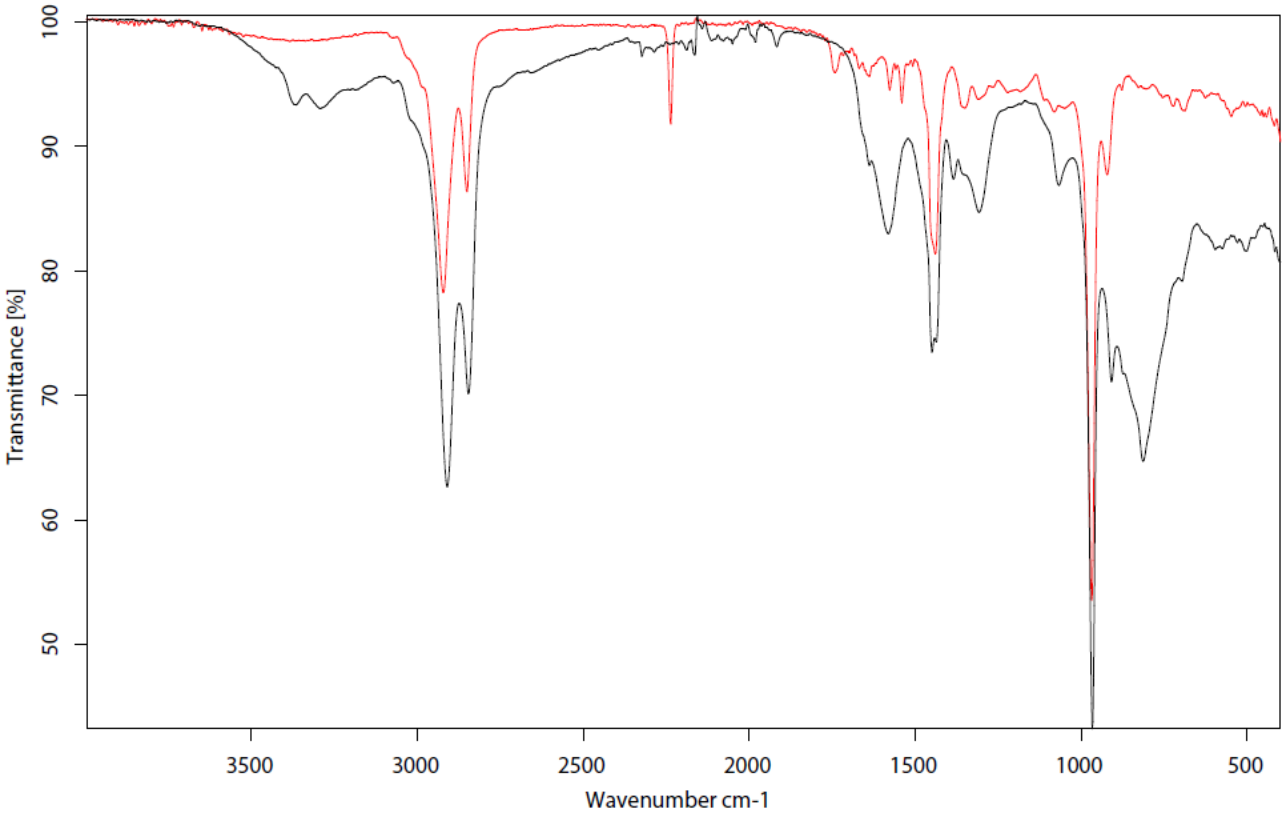

Thermogravimetric Analysis (TGA)

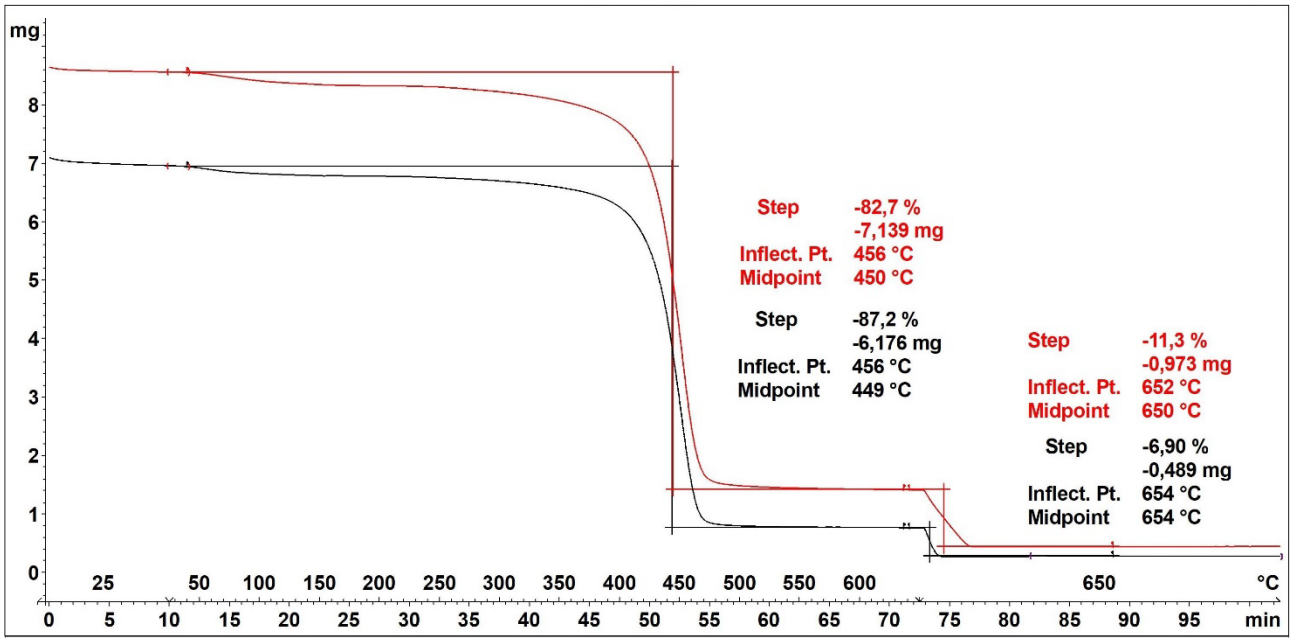

Decomposition graph. The experiment was conducted under He then air (after 650 °C). The black curve is the result from run 1, while the red curve is for run 2.

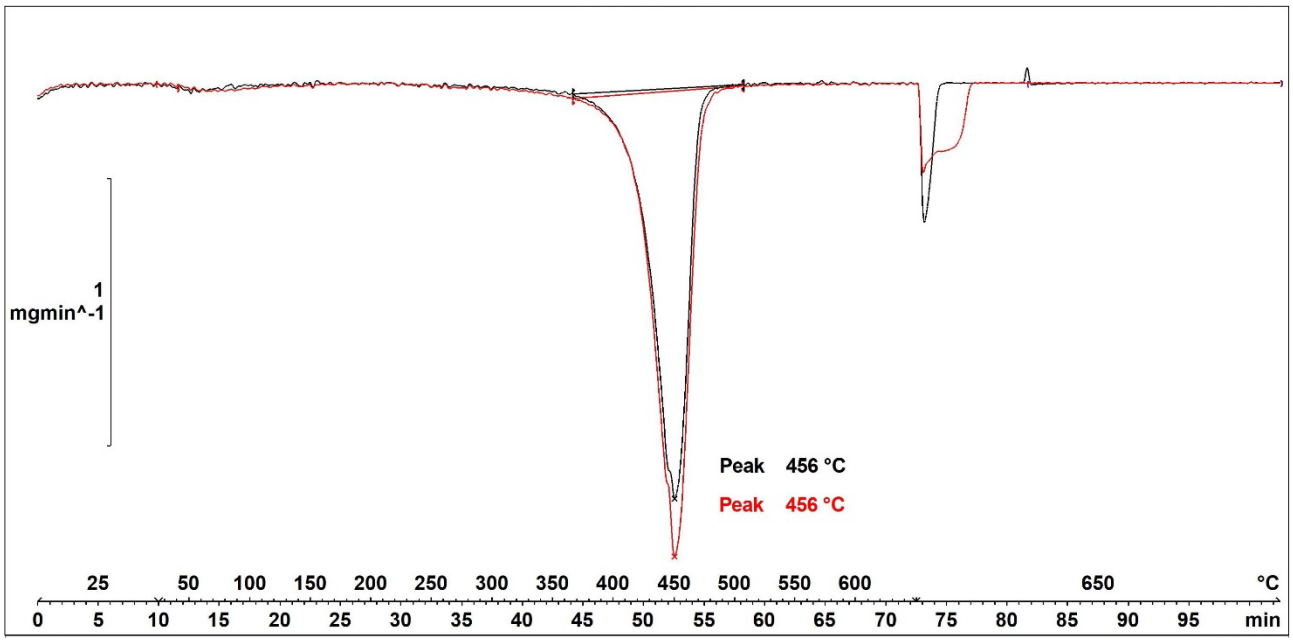

1st derivative of decomposition graph. The experiment was conducted under He then air (after 650 °C). The black curve is the result from run 1, while the red curve is for run 2.

Decomposition temperature (T_d) = 456 °C.

CO_2-adsorption analysis by thermogravimetric analysis

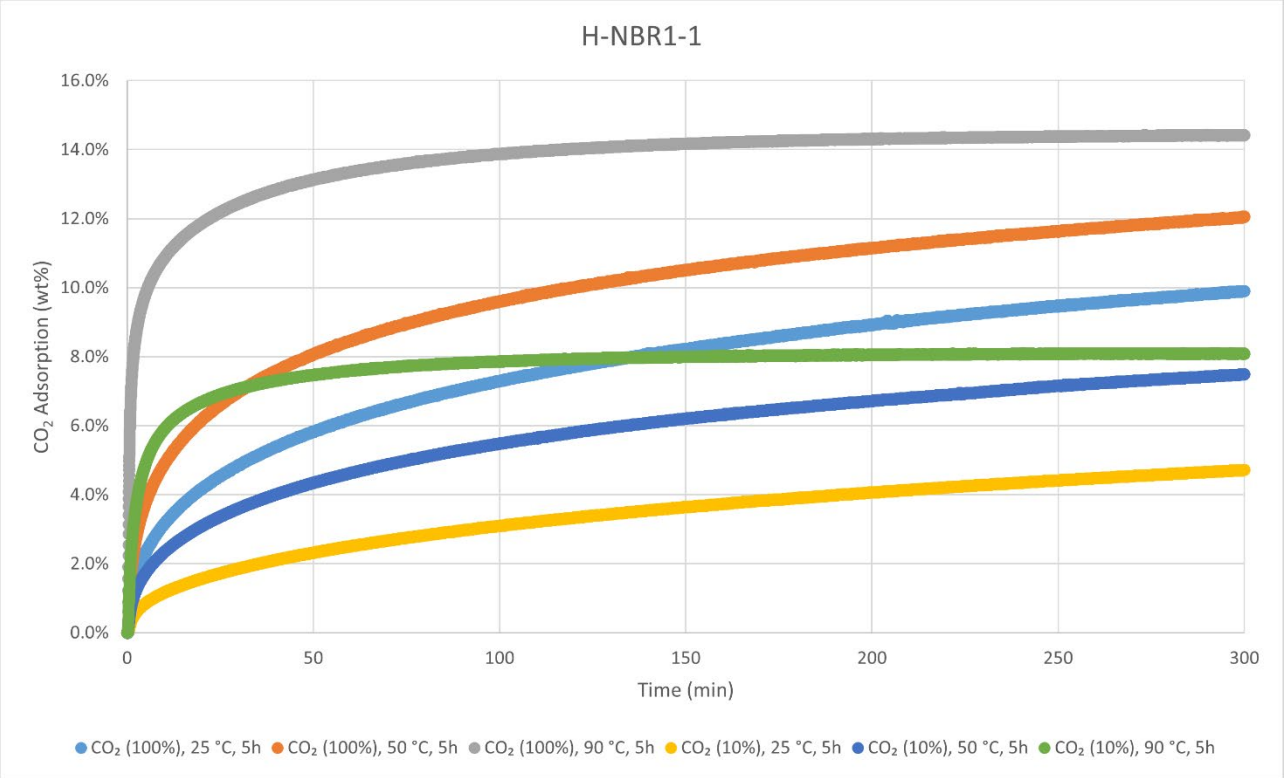

CO_2 adsorption using **TGA method 2** (measurement of product batch from run 1: H-NBR1-1).

HNBR1-1	wt%	mmol/g
CO_2 (100%), 25 °C, 5h	9.9%	2.25
CO_2 (100%), 50 °C, 5h	12.1%	2.74
CO_2 (100%), 90 °C, 5h	14.4%	3.28
CO_2 (10%), 25 °C, 5h	4.7%	1.07
CO_2 (10%), 50 °C, 5h	7.5%	1.70
CO_2 (10%), 90 °C, 5h	8.1%	1.84

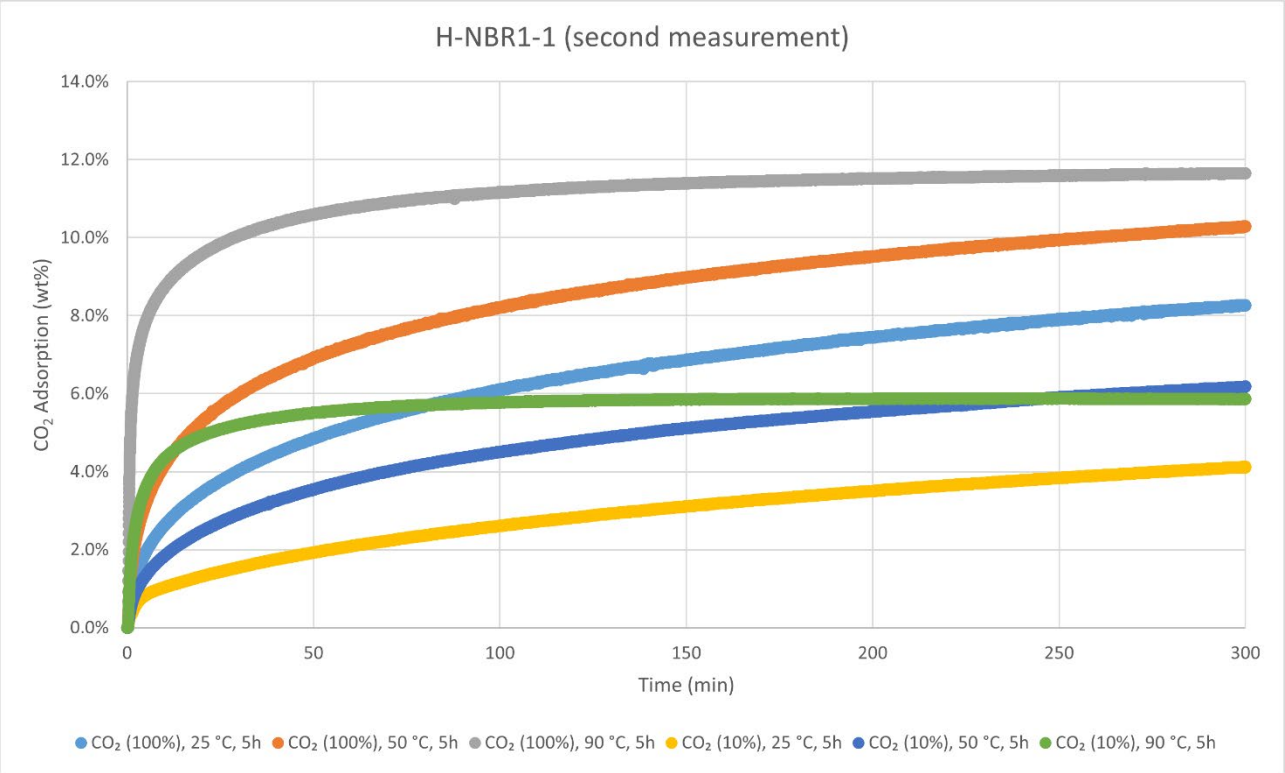

CO_2 adsorption using **TGA method 2** (a second measurement of product batch from run 1: H-NBR1-1).

HNBR1-1 (2nd measurement)	wt%	mmol/g
CO_2 (100%), 25 °C, 5h	8.3%	1.88
CO_2 (100%), 50 °C, 5h	10.3%	2.34
CO_2 (100%), 90 °C, 5h	11.7%	2.65
CO_2 (10%), 25 °C, 5h	4.1%	0.94
CO_2 (10%), 50 °C, 5h	6.2%	1.41
CO_2 (10%), 90 °C, 5h	5.9%	1.33

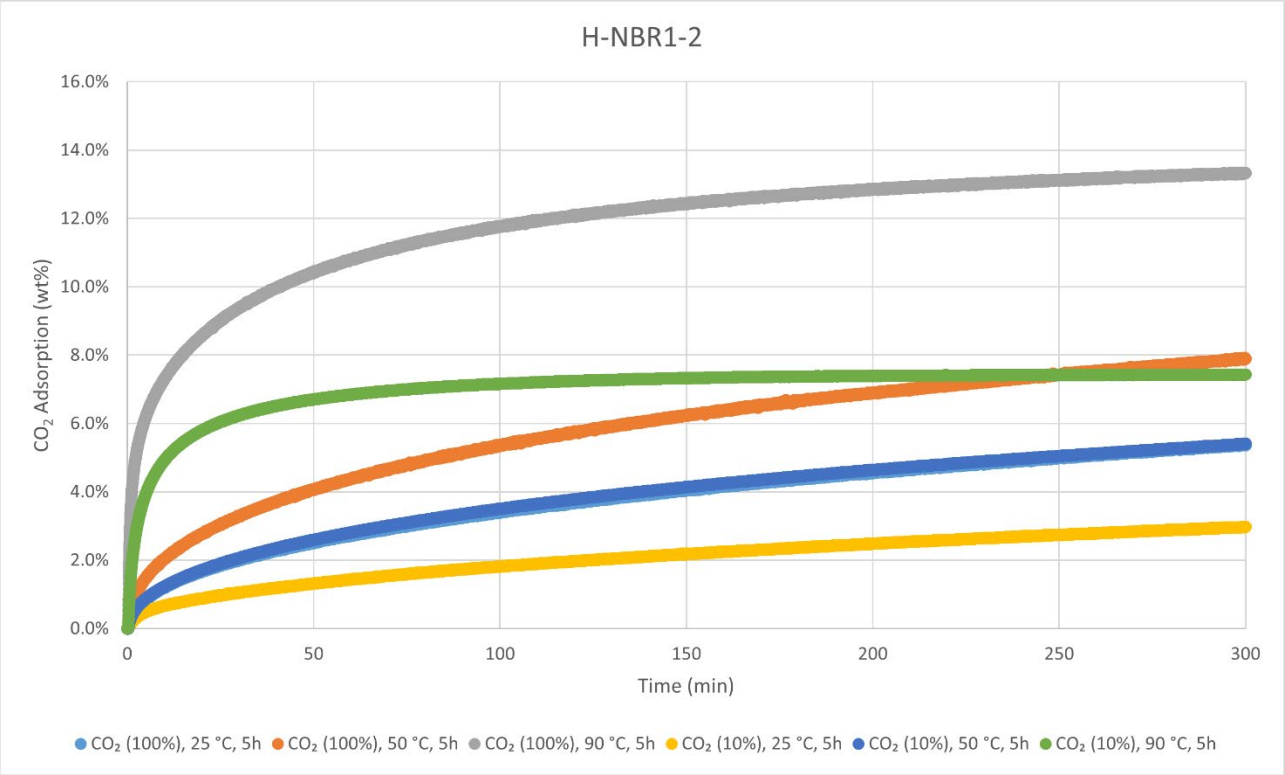

CO_2 adsorption using **TGA method 2** (measurement of product batch from run 2: H-NBR1-2).

HNBR1-2	wt%	mmol/g
CO_2 (100%), 25 °C, 5h	5.4%	1.22
CO_2 (100%), 50 °C, 5h	7.9%	1.79
CO_2 (100%), 90 °C, 5h	13.3%	3.03
CO_2 (10%), 25 °C, 5h	3.0%	0.68
CO_2 (10%), 50 °C, 5h	5.4%	1.23
CO_2 (10%), 90 °C, 5h	7.4%	1.69

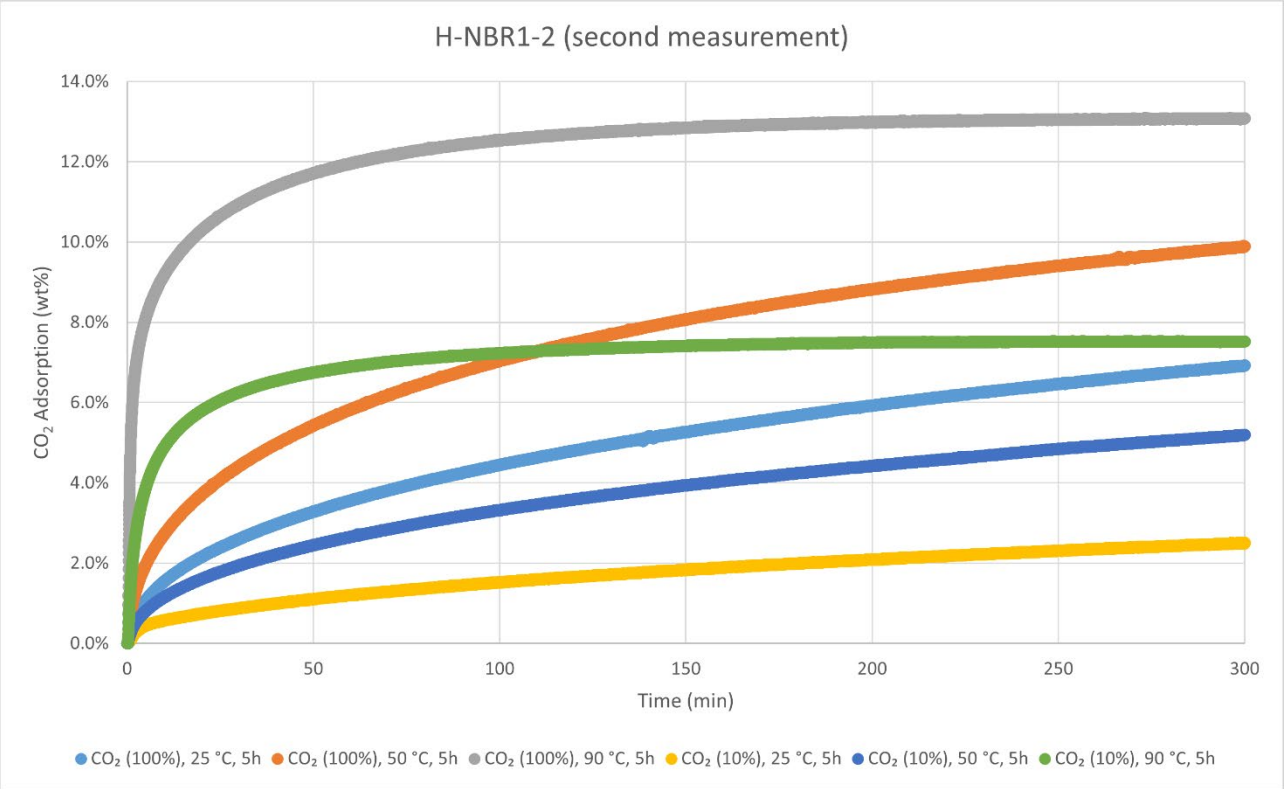

CO_2 adsorption using **TGA method 2** (a second measurement of product batch from run 2: H-NBR1-2).

HNBR1-2 (2nd measurement)	wt%	mmol/g
CO_2 (100%), 25 °C, 5h	6.9%	1.57
CO_2 (100%), 50 °C, 5h	9.9%	2.25
CO_2 (100%), 90 °C, 5h	13.1%	2.97
CO_2 (10%), 25 °C, 5h	2.5%	0.57
CO_2 (10%), 50 °C, 5h	5.2%	1.18
CO_2 (10%), 90 °C, 5h	7.5%	1.71

Elemental Analysis (EA)

	N [%]	C [%]	H [%]	S [%]	mmol N/g	C/N ratio	C/H ratio
run 1	**9.31**	**73.57**	**10.90**	**Not detected**	**6.64**	**9.22**	**0.57**
run 2	**9.58**	**74.00**	**11.25**		**6.84**	**9.00**	**0.55**

Reaction of H-NBR1 with $^{13}CO_2$

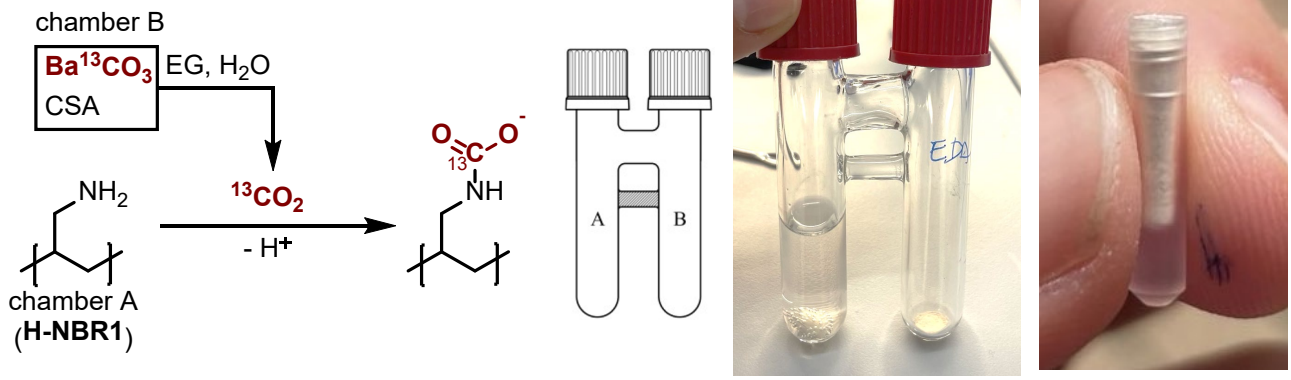

Figure S11. $^{13}CO_2$-labelling experiment for ^{13}C CP/MAS NMR analysis.

In a two-chamber flask (total volume 18 mL) 20 mg of the polymer sample was added to chamber A and a magnetic stir bar, $Ba^{13}CO_3$ (1 equiv., 147 mg, 0.741 mmol) and camphorsulfonic acid (CSA, 2 equiv., 348 mg, 1.50 mmol) to chamber B. The amount of $Ba^{13}CO_3$ was calculated to provide 1 bar of $^{13}CO_2$ within the flask. After sealing both sides with a pierceable screw cap, 2 mL of ethylene glycol (EG) were added to chamber B with a syringe. Then, 0.7 mL of water was layered on top of the ethylene glycol with a syringe and the flask was placed on a magnetic stirrer. $^{13}CO_2$ release was instantly observed and the white suspension turned transparent within 15 min. The glassware was kept at room temperature for 5 h for the adsorption of $^{13}CO_2$ by the polymer. Then, the two-chamber reactor system was opened and the polymer was transferred into a Kel-F insert, compressed and closed with the sealing screw before placing it in a regular 4 mm rotor.

*Solid-state ^{13}C–NMR of **H-NBR1** after being subjected to $^{13}CO_2$ gas (The 164.5 ppm peak is assigned to the ^{13}C-enriched carbamate based on previous reports):*[16,17]

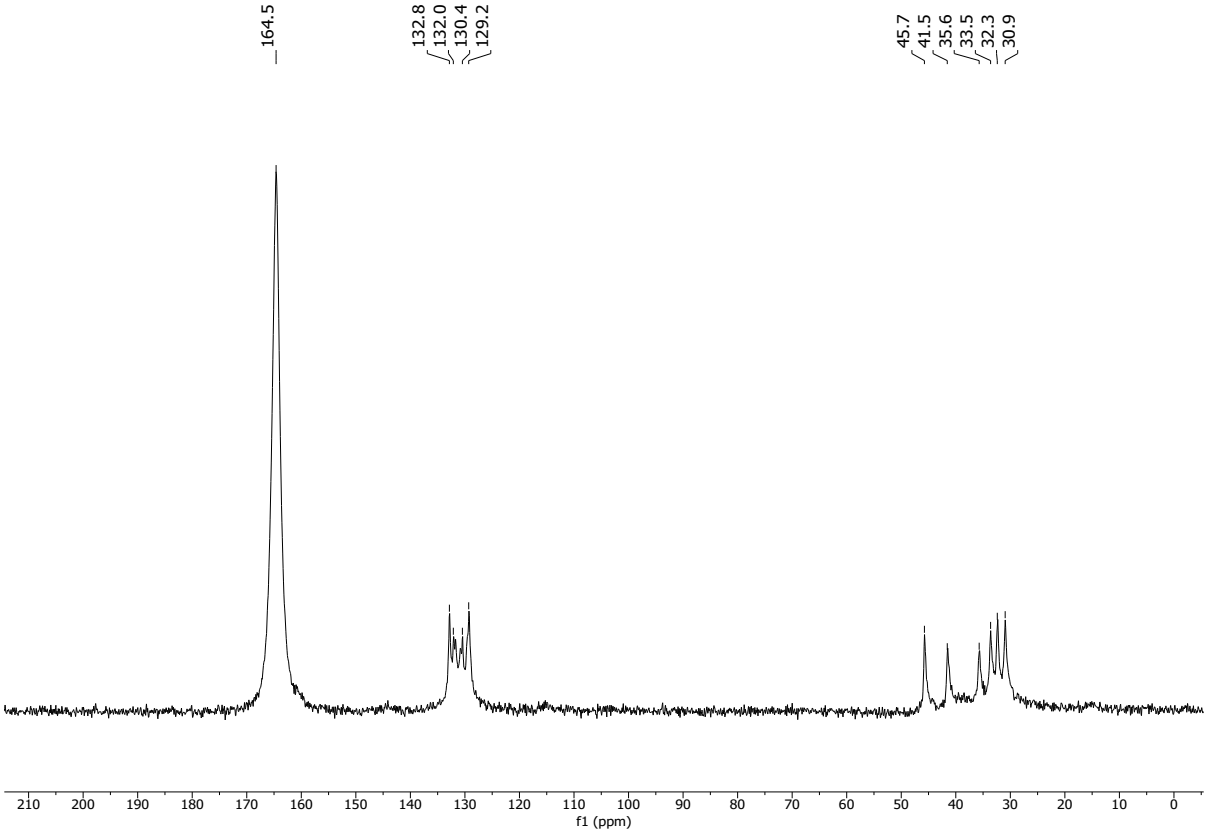

Hydrogenated Nitrile Butadiene Rubber 2 (H-NBR2) was synthesised according to the General Procedure B but using RuMACHO (10 wt%, 100 mg) and KO*t*Bu (8 wt%, 80 mg) instead since lower catalyst loadings did not give full nitrile reduction at the 1 g scale. The reaction was carried out with substrate **NBR2** (nitrile glove) and was obtained in weight yields of 975 mg, 97 wt% and 924 mg, 92 wt%, respectively, from two independent runs. A third reaction using cryogenically milled **NBR2** starting material was also conducted yielding 899 mg (90 wt%). To further support the discussion on the reproducibility of CO_2-capacity with **H-NBR2** (see below), two further reactions were set up: Run 4 with a weight yield of 894 mg, 89 wt% and run 5 (cryogenically milled starting material like run 3) yielding 934 mg, 93 wt%. Thus, the average of these 5 reactions is 92 wt%. For simplicity, only the full characterisation of two runs is reported. The polymer was analysed with solid-state ^{13}C CP/MAS NMR, IR-, TGA-, DSC-, and elemental analysis. Solubility tests were also conducted with several solvents. No thermal events besides decomposition were observed with DSC.

Particle size of H-NBR2 after cryogenic milling used for CO_2 adsorption-desorption experiments

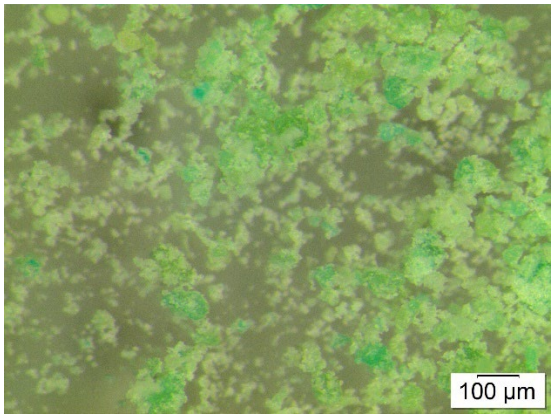

Solubility chart

Soluble **Swells** **Not soluble**

$CHCl_3$	Acetone	*i*-PrOH	DMF	DMSO	THF	PhMe	H_2O	MeOH	MeCN

^{13}C CP/MAS NMR (solid-state)

*Solid-state ^{13}C–NMR of **H-NBR2** (run 1):*

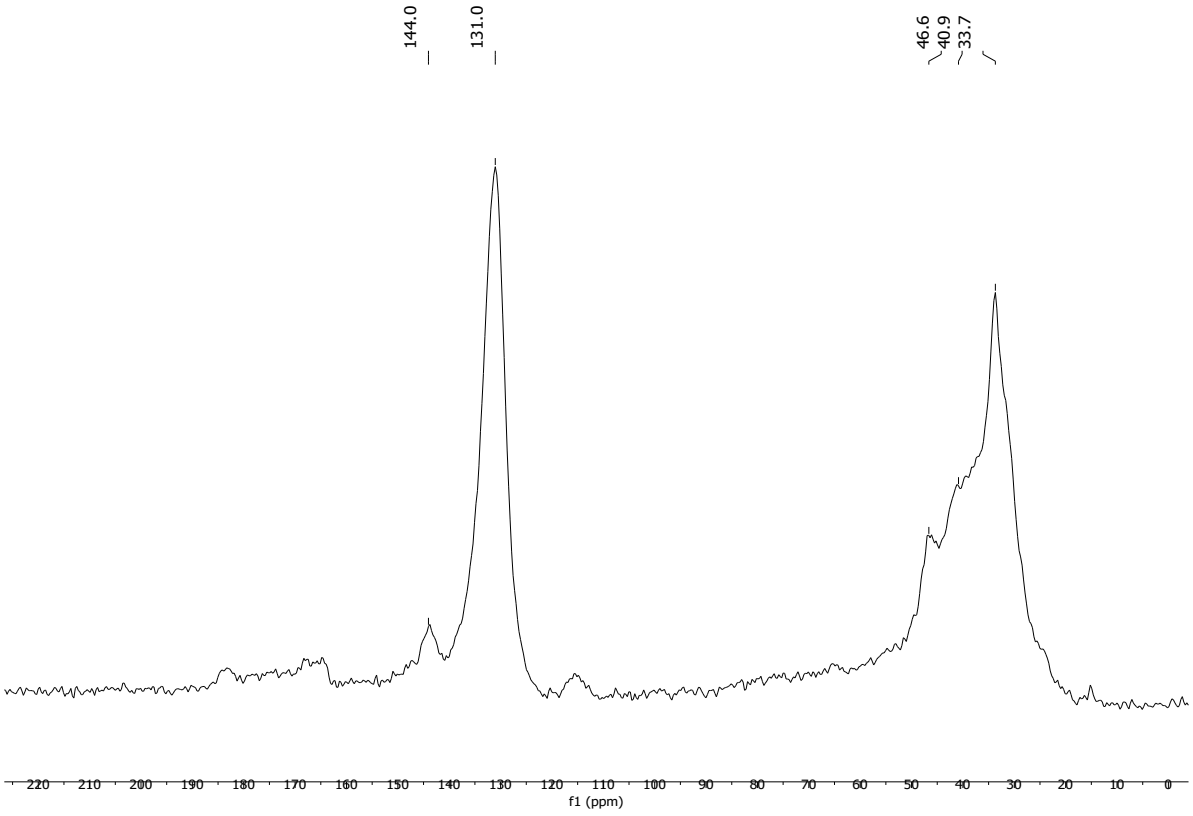

*Solid-state ^{13}C–NMR of **H-NBR2** (run 2):*

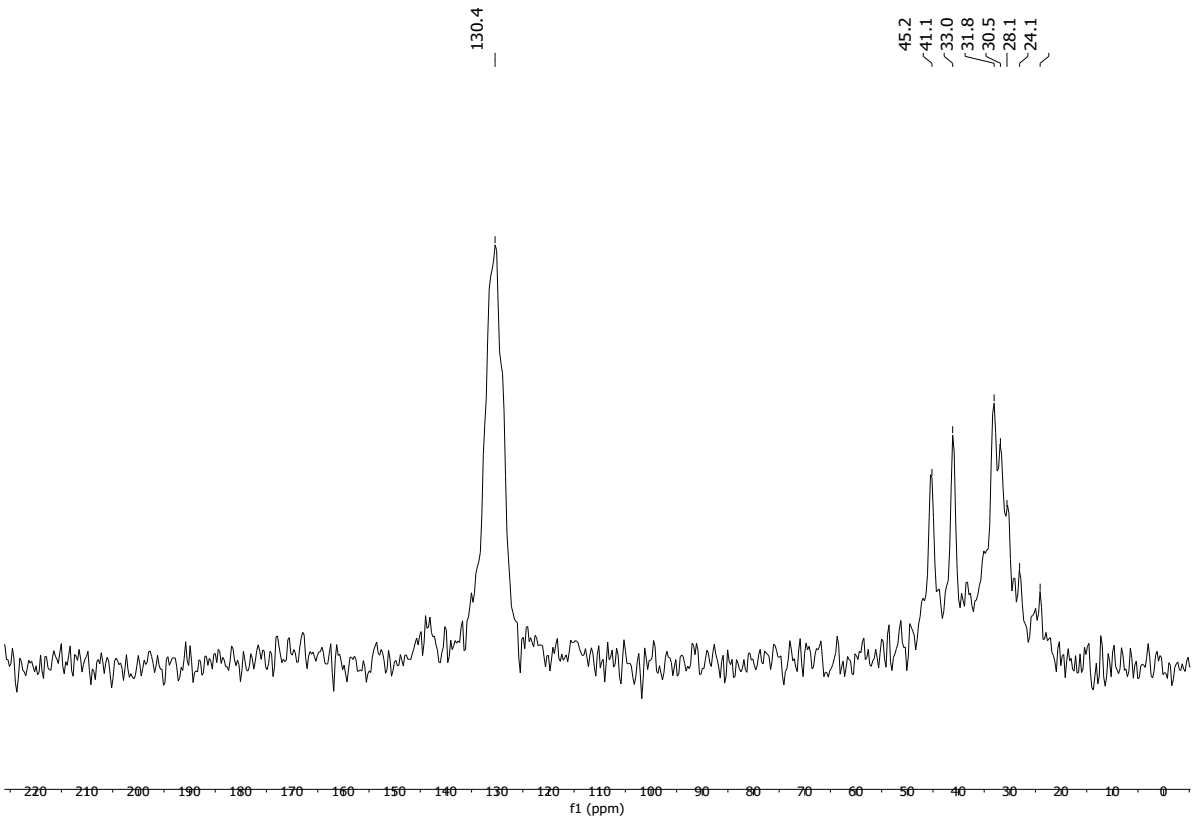

*Stacked solid-state ^{13}C–NMR of **H-NBR2** (run 2, **brown**) with **NBR2** (substrate, **light blue**):*

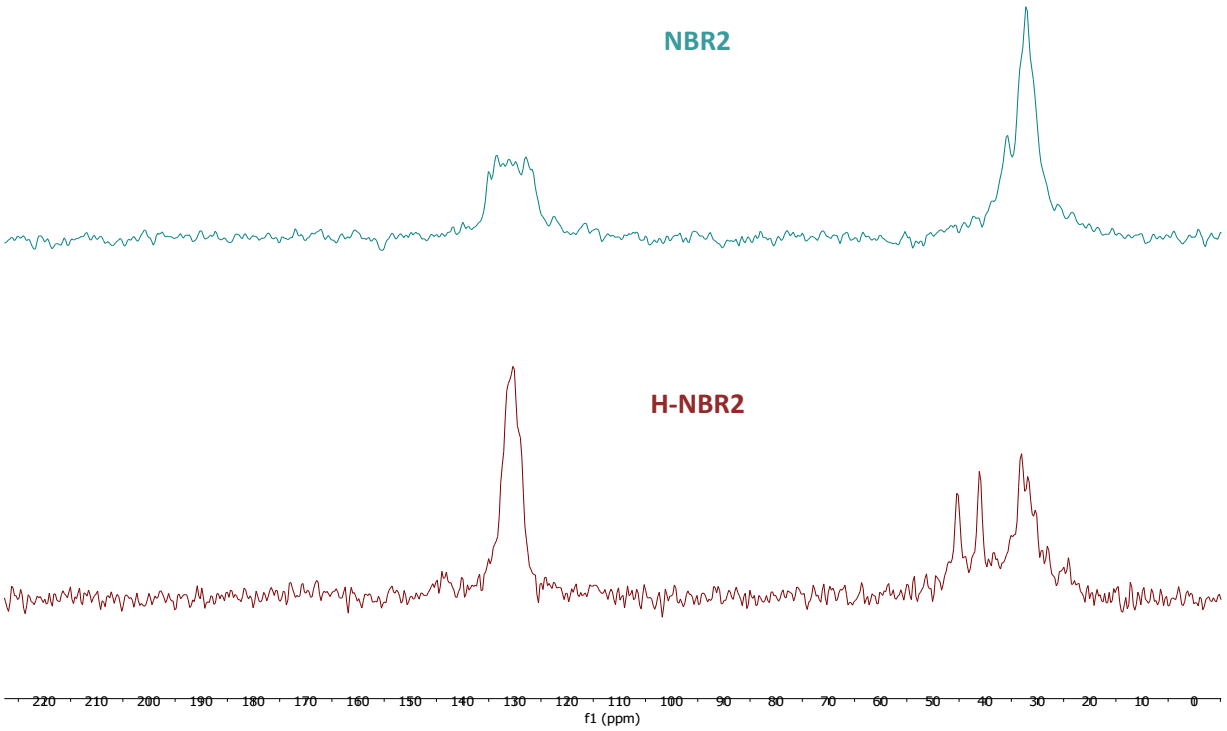

Infrared (IR) Spectroscopic Analysis

*IR-spectrum of **H-NBR2** (run 1):*

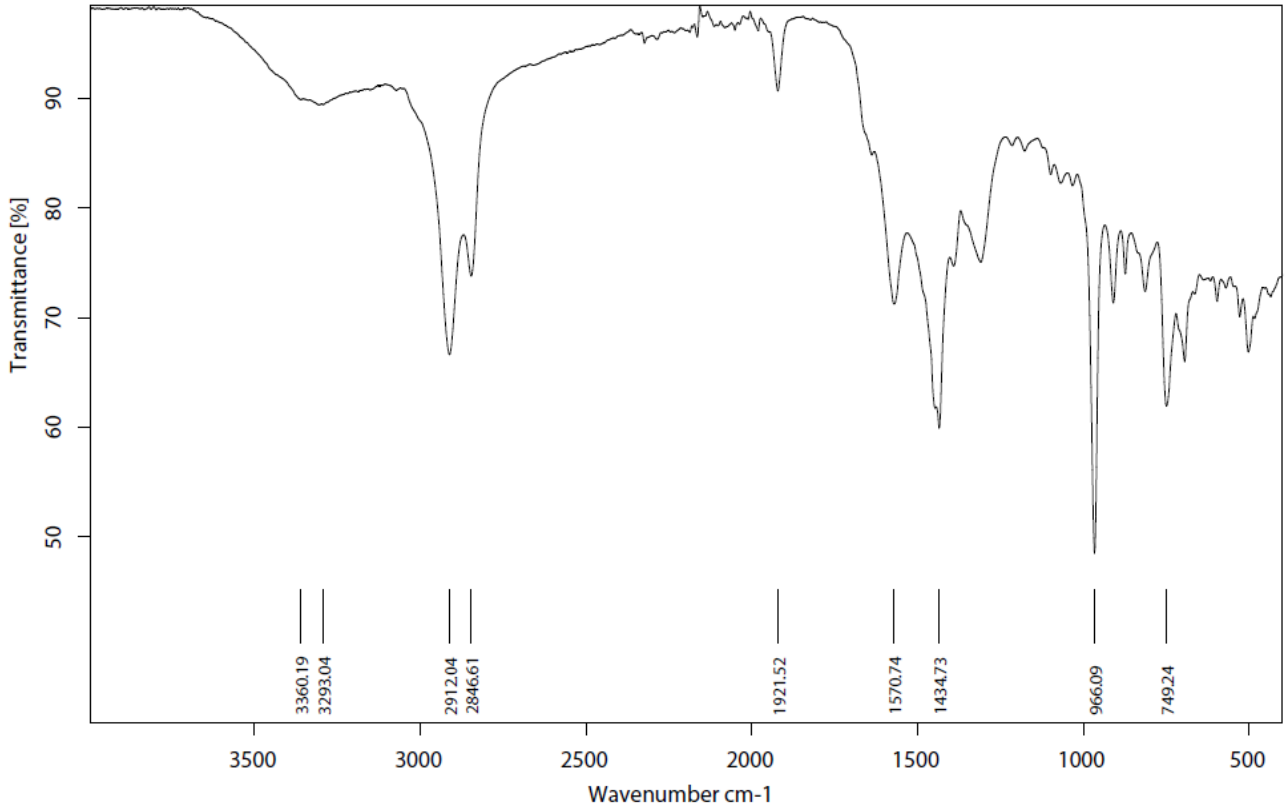

*IR-spectrum of **H-NBR2** (run 2):*

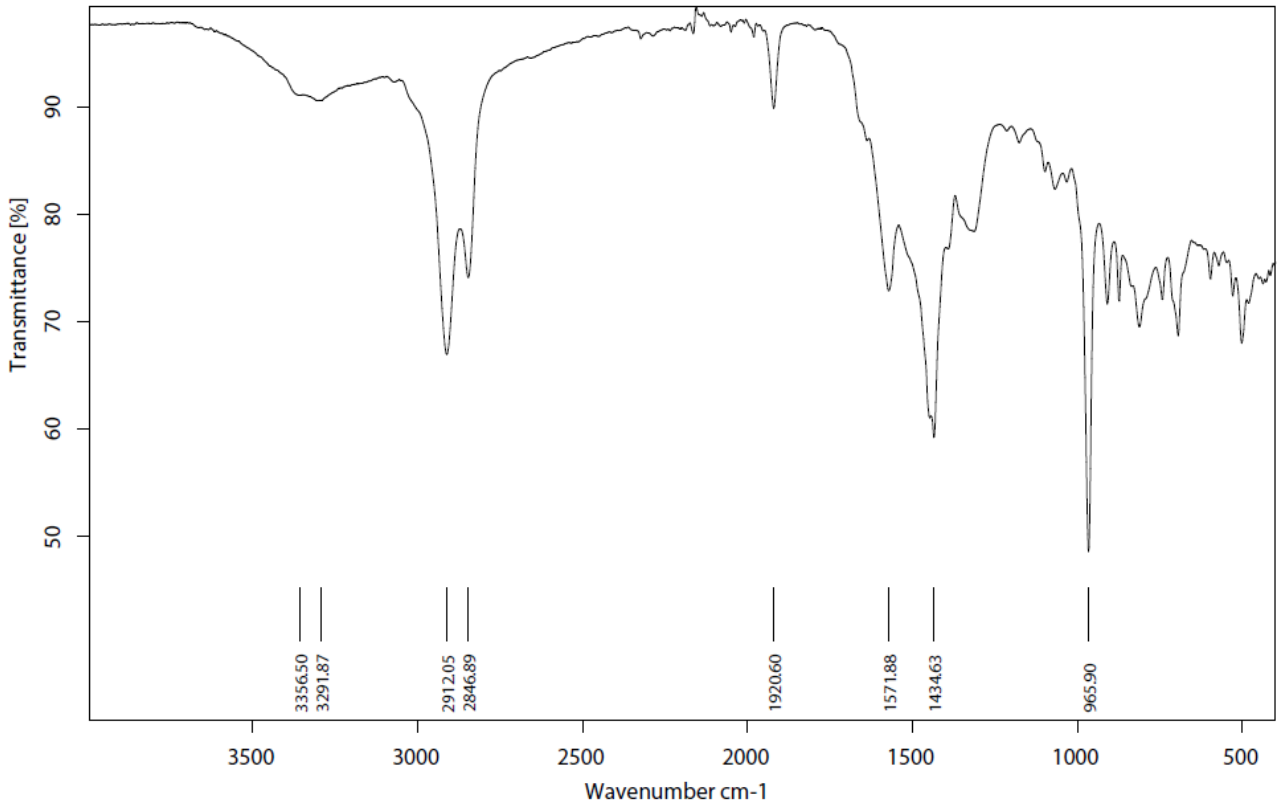

*IR-spectrum of **H-NBR2** (run 3 – from cryogenically milled **NBR2** substrate):*

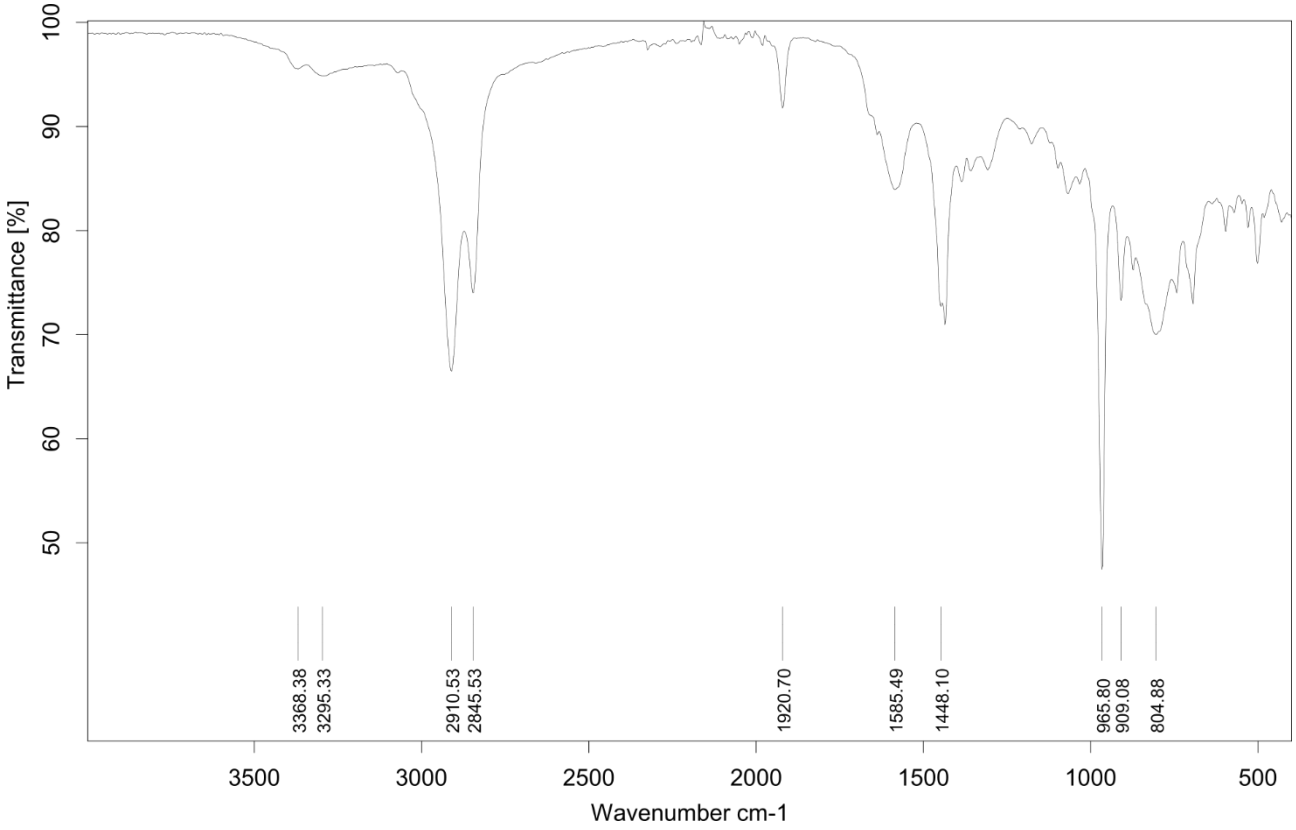

*IR-spectrum overlay of **H-NBR2** (run 1, **black**) and **NBR2** (substrate, **red**):*

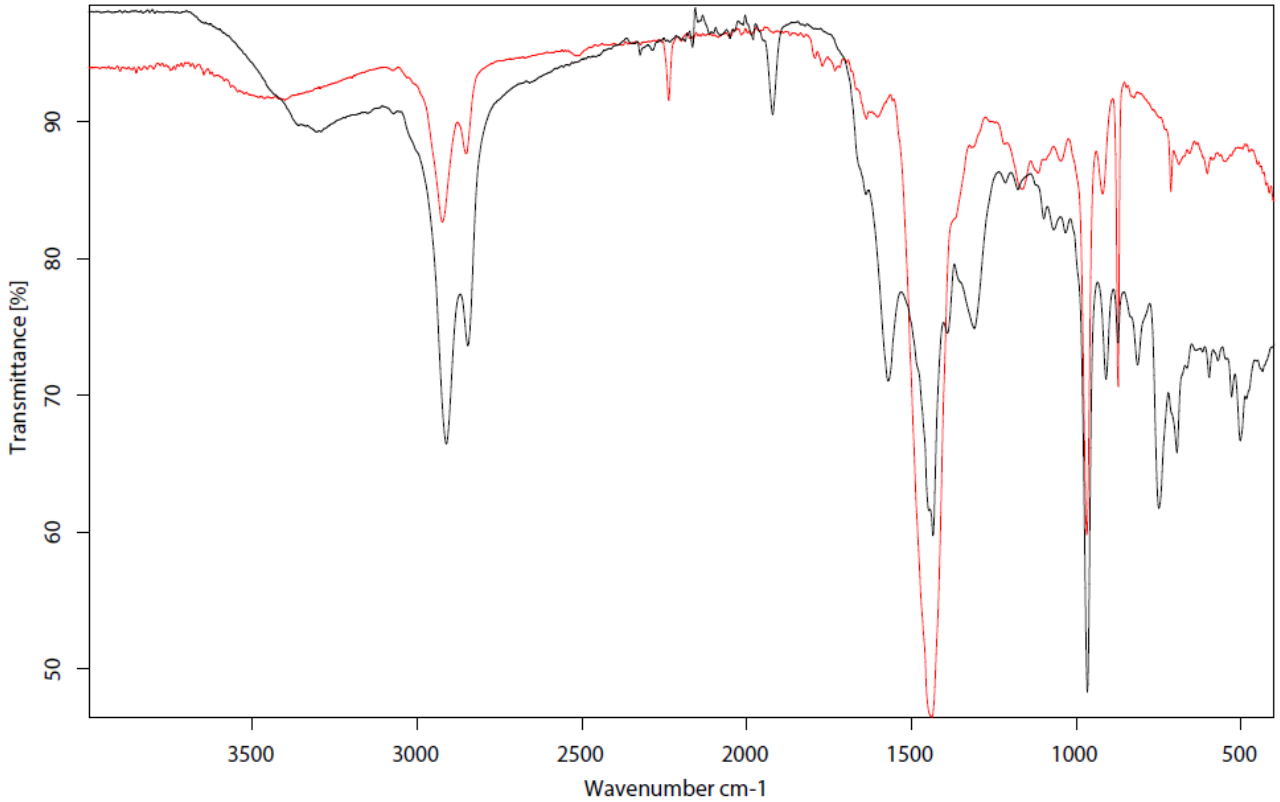

Thermogravimetric Analysis (TGA)

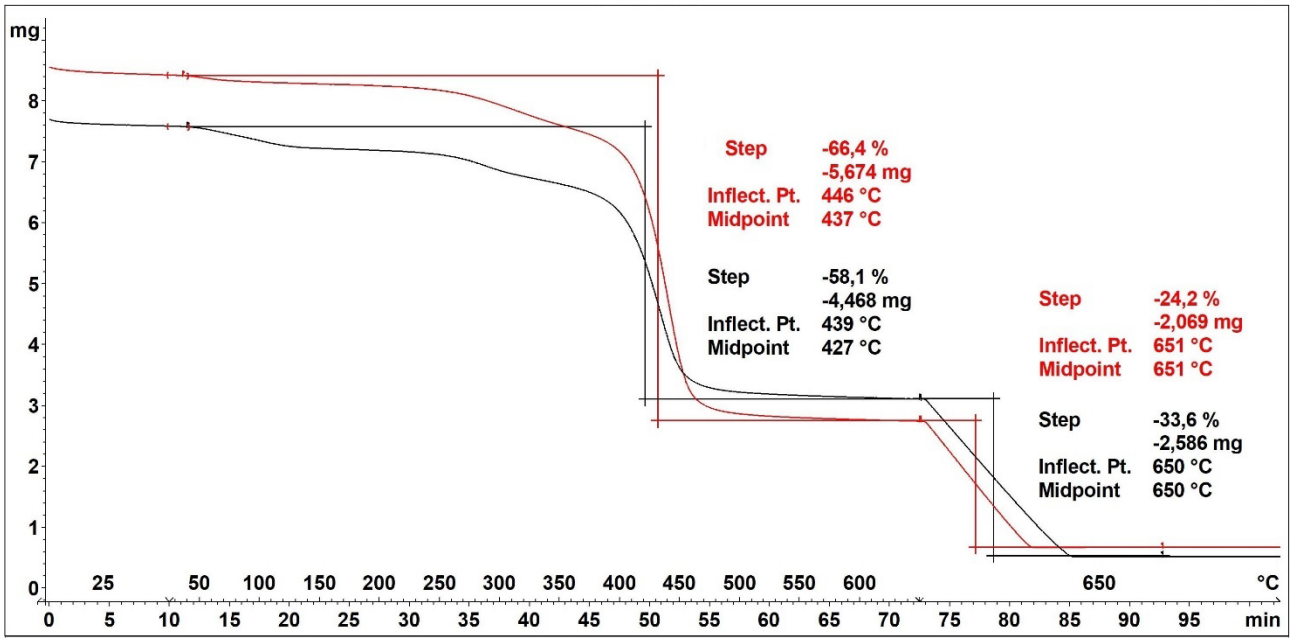

Decomposition graph. The experiment was conducted under He then air (after 650 °C). The black curve is the result from run 1, while the red curve is for run 2.

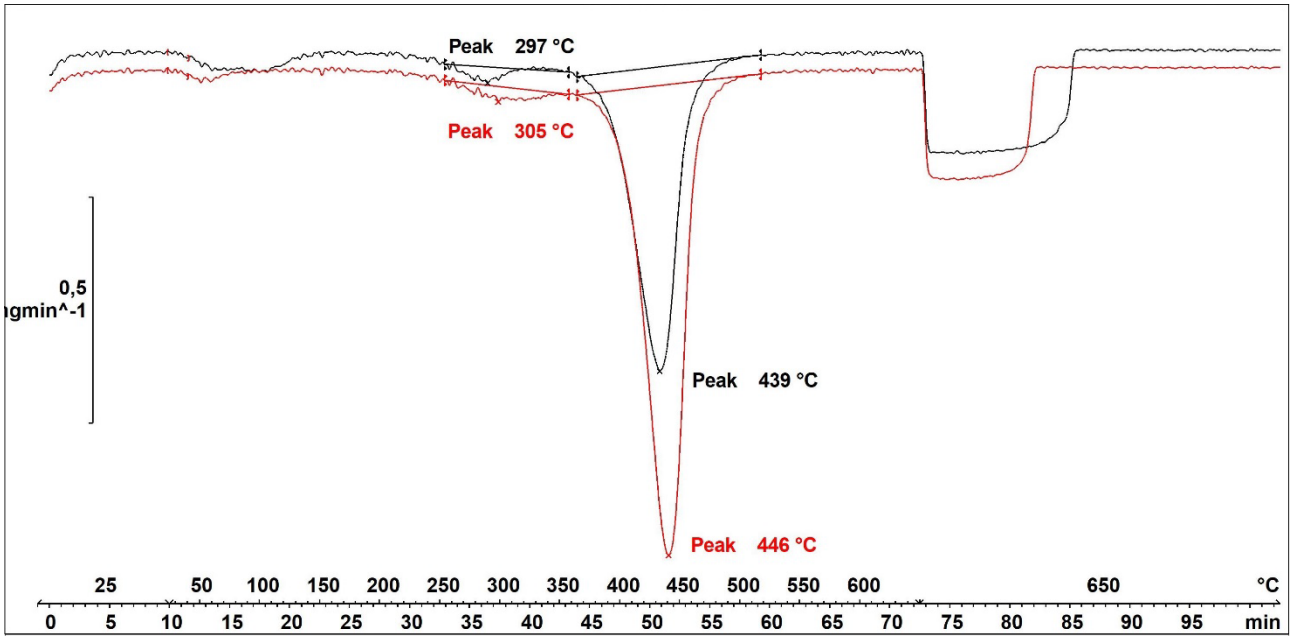

1st derivative of decomposition graph. The experiment was conducted under He then air (after 650 °C). The black curve is the result from run 1, while the red curve is for run 2.

Decomposition temperature (T_d) = 439–446 °C.

CO_2-adsorption analysis by thermogravimetric analysis

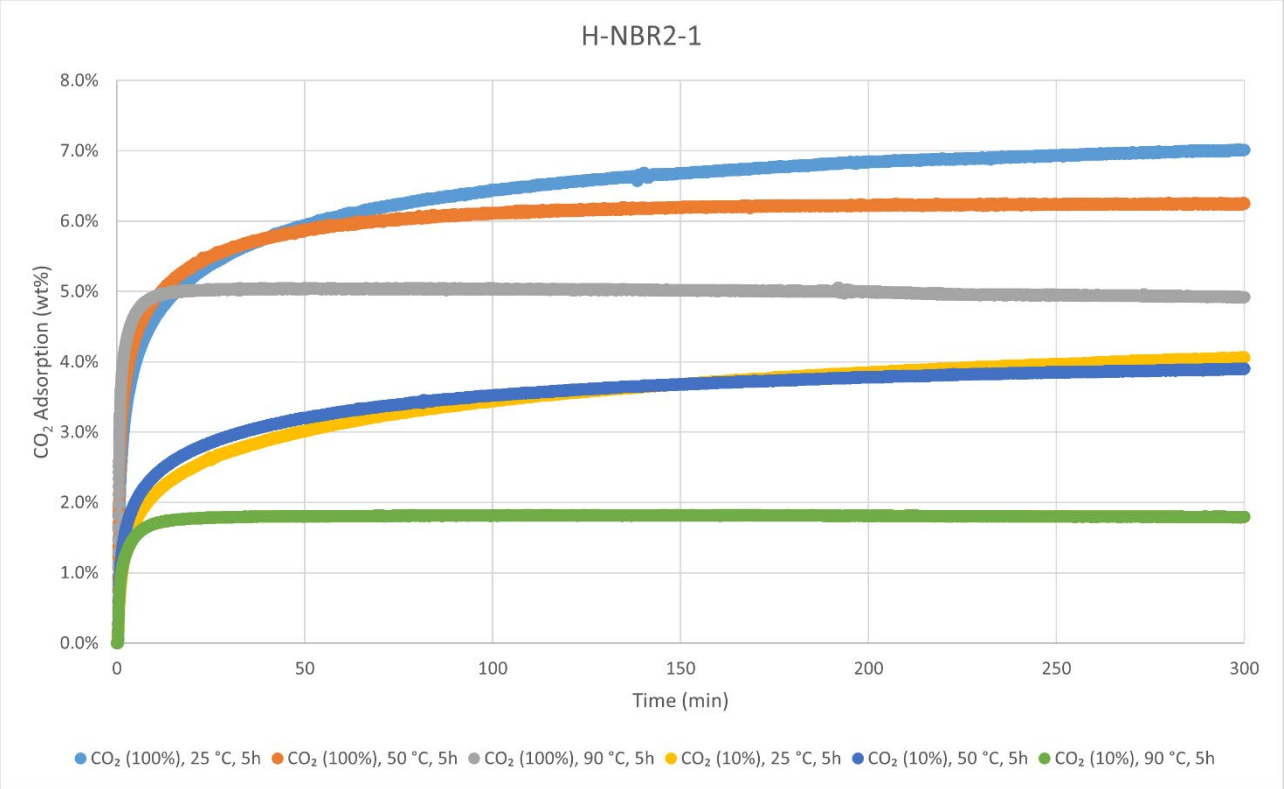

CO_2 adsorption using **TGA method 2** (measurement of product batch from run 1: H-NBR2-1).

HNBR2-1	wt%	mmol/g
CO_2 (100%), 25 °C, 5h	7.0%	1.59
CO_2 (100%), 50 °C, 5h	6.3%	1.42
CO_2 (100%), 90 °C, 5h	4.9%	1.12
CO2 (10%), 25 °C, 5h	4.1%	0.92
CO2 (10%), 50 °C, 5h	3.9%	0.89
CO2 (10%), 90 °C, 5h	1.8%	0.41

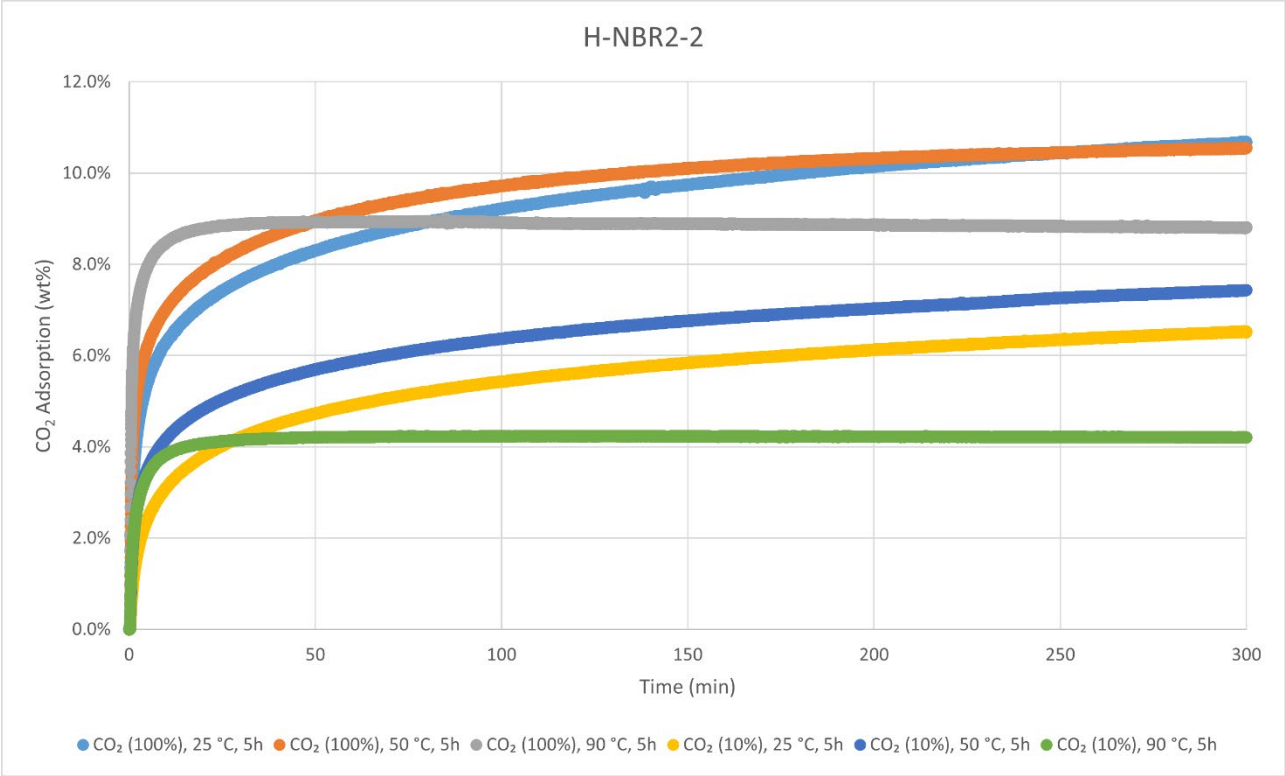

CO_2 adsorption using **TGA method 2** (measurement of product batch from run 2: H-NBR2-2).

HNBR2-2	wt%	mmol/g
CO2 (100%), 25 °C, 5h	10.7%	2.43
CO2 (100%), 50 °C, 5h	10.6%	2.40
CO2 (100%), 90 °C, 5h	8.8%	2.00
CO2 (10%), 25 °C, 5h	6.5%	1.48
CO2 (10%), 50 °C, 5h	7.4%	1.69
CO2 (10%), 90 °C, 5h	4.2%	0.96

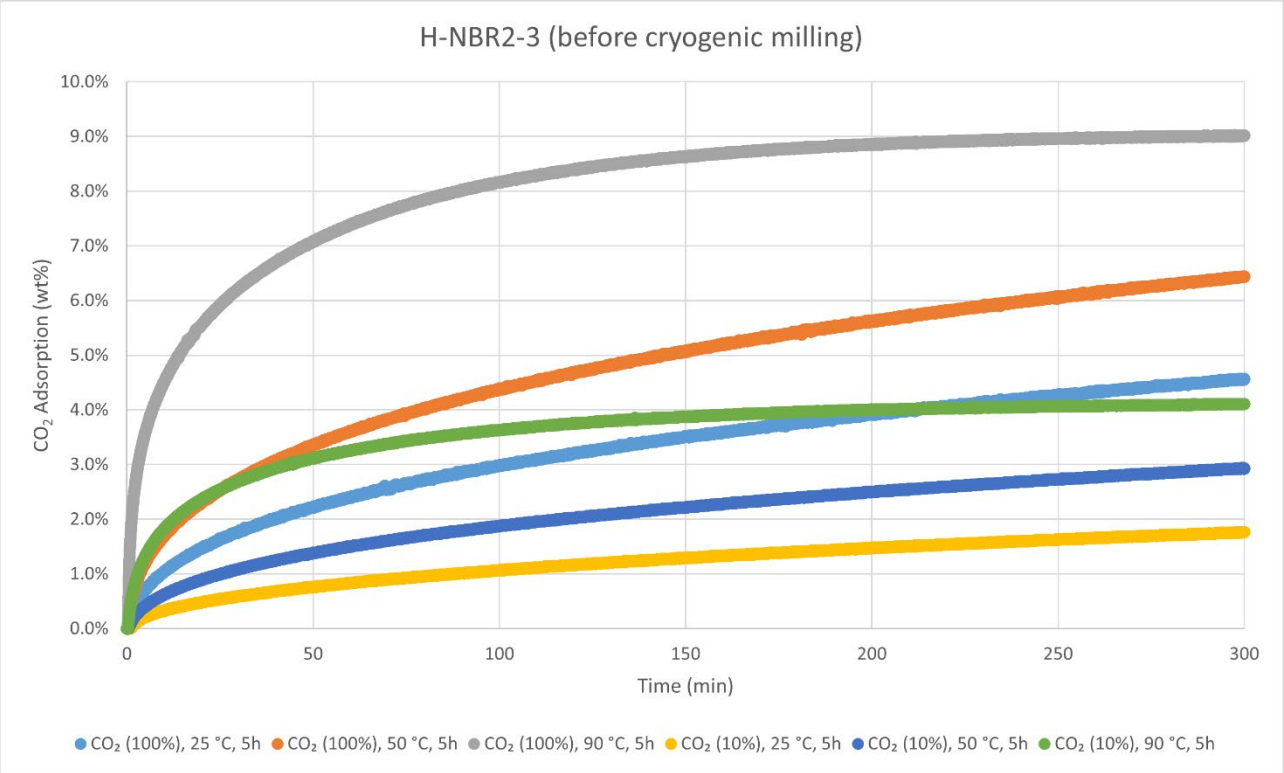

CO_2 adsorption using **TGA method 2** (measurement of product batch from run 3: H-NBR2-3). This sample was only cryogenically milled prior to the reaction and not after.

HNBR2-3 (before cryogenic milling)	wt%	mmol/g
CO_2 (100%), 25 °C, 5h	4.6%	1.04
CO_2 (100%), 50 °C, 5h	6.4%	1.46
CO_2 (100%), 90 °C, 5h	9.0%	2.05
CO_2 (10%), 25 °C, 5h	1.8%	0.40
CO_2 (10%), 50 °C, 5h	2.9%	0.67
CO_2 (10%), 90 °C, 5h	4.1%	0.93

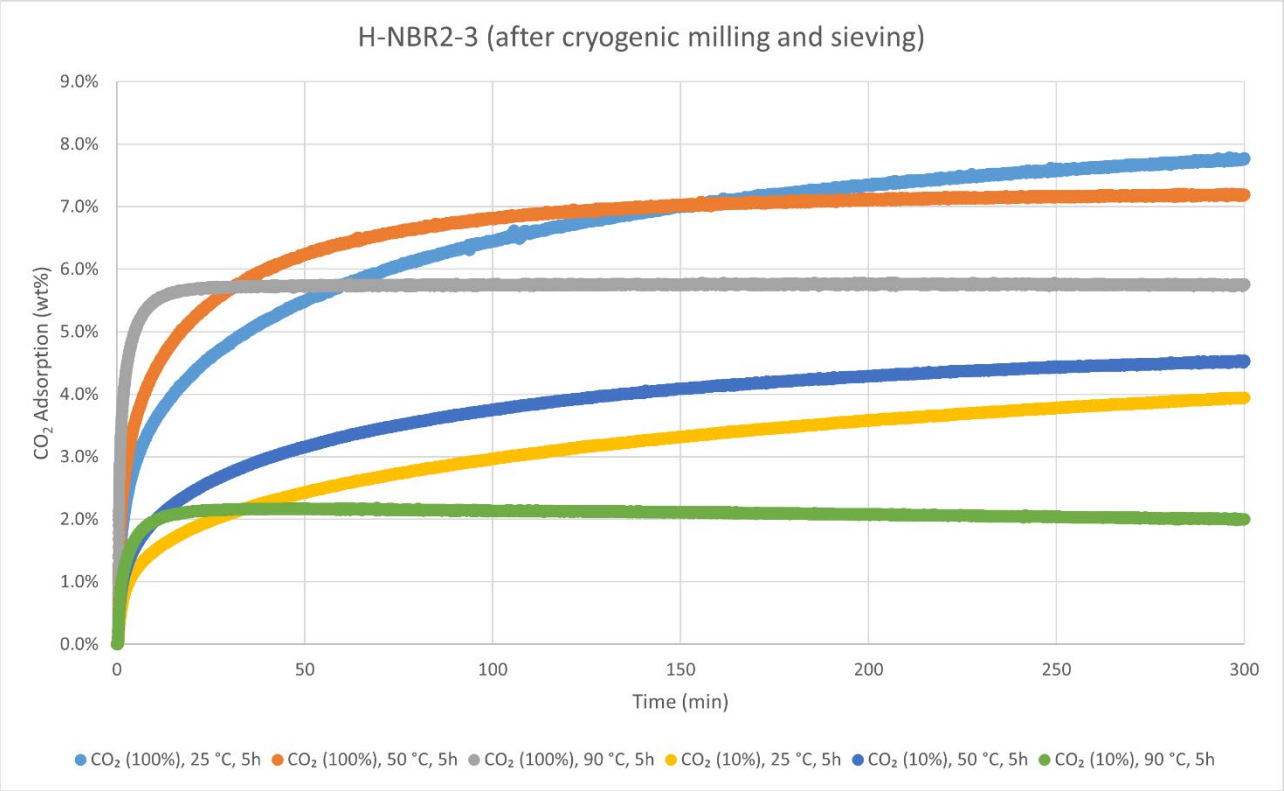

CO_2 adsorption using **TGA method 2** (measurement of product batch from run 3: H-NBR2-3). This sample was cryogenically milled and sieved to a particle size range of -140 +500 mesh after the reaction.

HNBR2-3 (after cryogenic milling and sieving)	wt%	mmol/g
CO_2 (100%), 25 °C, 5h	7.8%	1.77
CO_2 (100%), 50 °C, 5h	7.2%	1.63
CO_2 (100%), 90 °C, 5h	5.8%	1.31
CO_2 (10%), 25 °C, 5h	3.9%	0.90
CO_2 (10%), 50 °C, 5h	4.5%	1.03
CO_2 (10%), 90 °C, 5h	2.0%	0.45

Discussion on the variation of CO_2-capacities for H-NBR2 products:

H-NBR2 products were found to give higher variation in CO_2-capacity compared to most other products of this work, only apart from H-NBR1, which as another nitrile butadiene rubber behaves similarly. Besides a lower N-content for H-NBR2-1 that could explain a lower CO_2-capacity for that batch, we hypothesise that different particle size distributions could be the cause for different CO_2-capacities. Comparing the H-NBR2-2 batch with the non-cryogenically milled H-NBR2-3 sample (see above), one will find highly different capacities at 25 °C with 100% CO_2 (10.7 wt% and 4.6 wt%, respectively). However, measuring adsorption at 90 °C will show almost equal capacities for these two materials (8.8 wt% and 9.0 wt%, respectively). We hypothesise that these materials become more permeable at higher temperatures, thus giving more equal capacities even with different particle size distributions. This permeability effect was observed for nitrile rubber hydrogenation products (H-NBR1, H-NBR2, and HCN*-NBR2), and is also likely the reason for the faster rate of adsorption for these materials at 90 °C.

To further probe the reproducibility of CO_2-adsorption for H-NBR2, due to the variation between e.g. H-NBR2-1 and H-NBR2-2, a further two batches (run 4 and 5) were prepared and their CO_2-adsorption capacities were

measured. Run 4 was conducted using nitrile glove pieces of similar size to run 1 and run 2, while run 5 was conducted with cryogenically milled starting material. As can be seen from the adsorption TGA profiles, the materials show only minor adsorption capacity differences. Run 5 measured the highest capacity at 25 °C, which is likely due to a smaller particle size distribution because it was cryogenically milled before and after the reaction. Run 4, on the other hand, was only cryogenically milled after the reaction, so the particles are comparatively larger and thus higher temperature is needed to obtain higher permeability and thus higher CO_2-capacity of the material (in these example 25−50 °C yields the highest adsorption capacity after 5 hours, although the rate of adsorption is fastest with 90 °C).

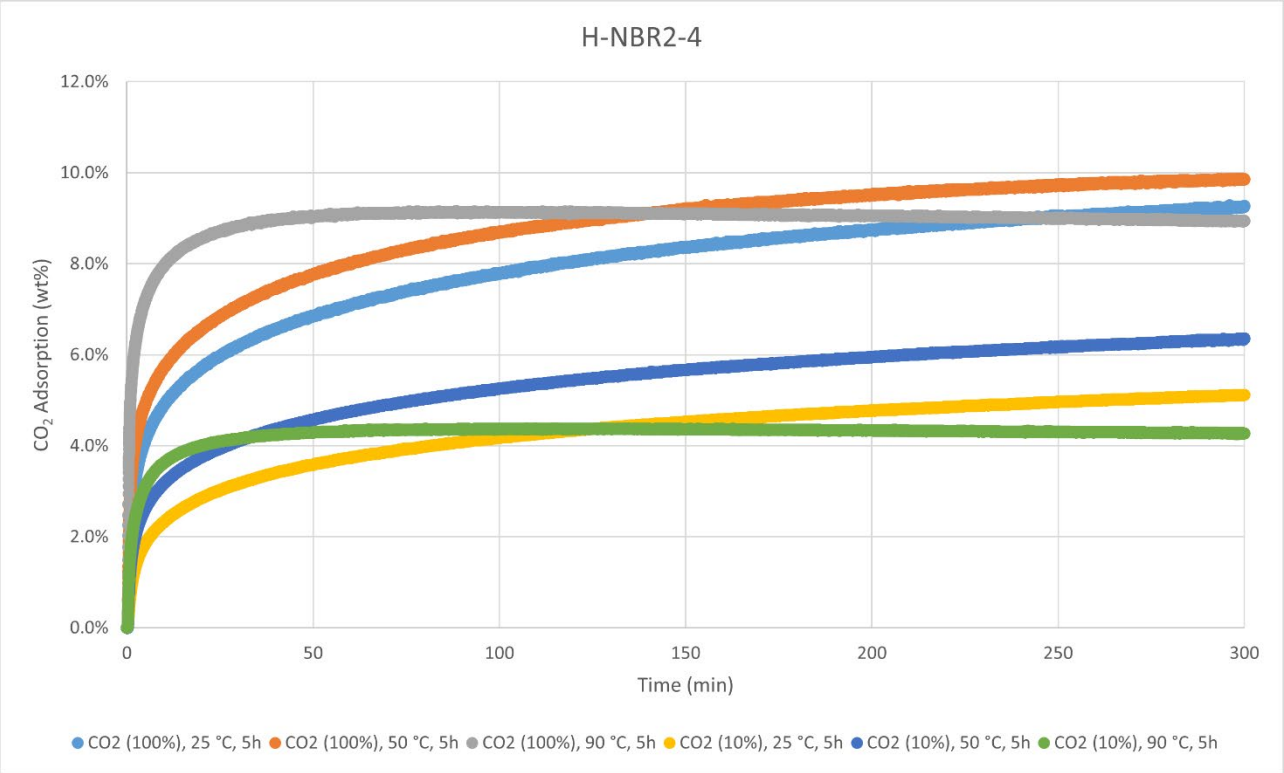

CO_2 adsorption using **TGA method 2** (measurement of product batch from run 4: H-NBR2-4).

HNBR2-4	wt%	mmol/g
CO2 (100%), 25 °C, 5h	9.3%	2.11
CO2 (100%), 50 °C, 5h	9.9%	2.24
CO2 (100%), 90 °C, 5h	8.9%	2.03
CO2 (10%), 25 °C, 5h	5.1%	1.16
CO2 (10%), 50 °C, 5h	6.4%	1.44
CO2 (10%), 90 °C, 5h	4.3%	0.97

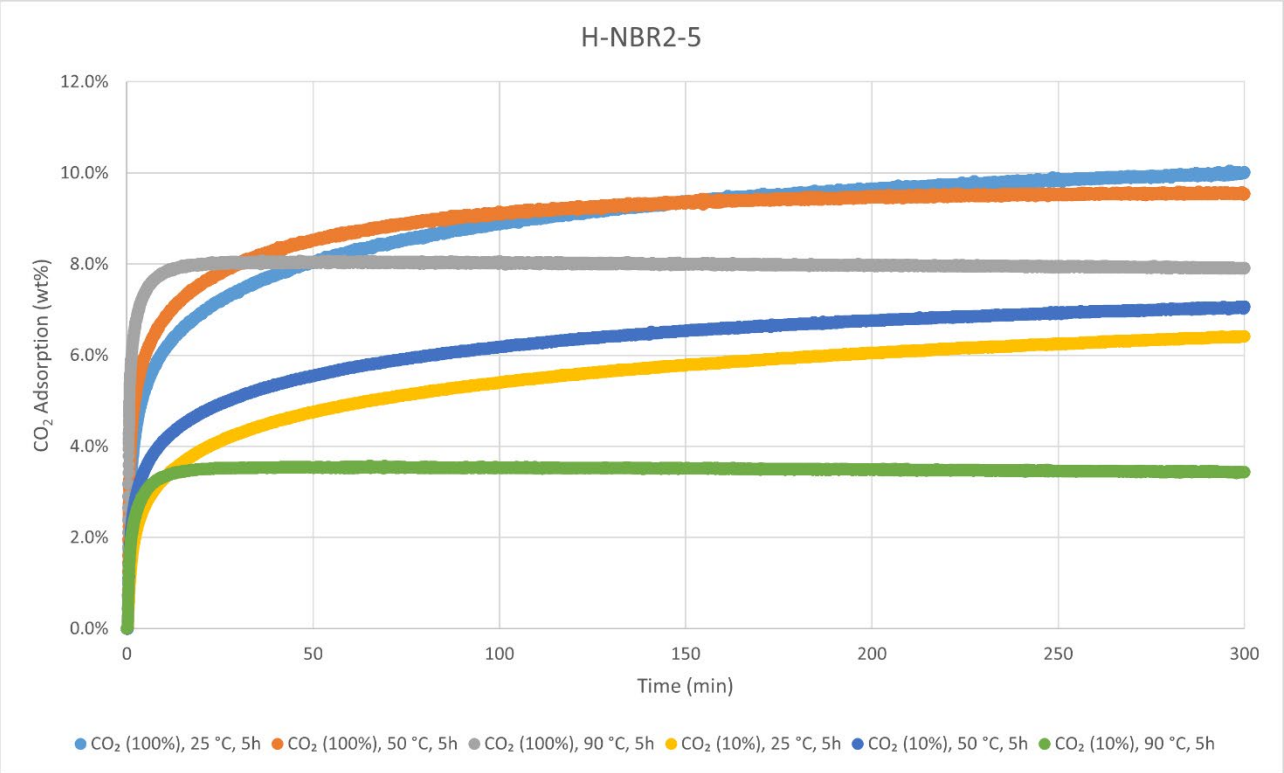

CO_2 adsorption using **TGA method 2** (measurement of product batch from run 5: H-NBR2-5).

HNBR2-5	wt%	mmol/g
CO_2 (100%), 25 °C, 5h	10.0%	2.28
CO_2 (100%), 50 °C, 5h	9.5%	2.17
CO_2 (100%), 90 °C, 5h	7.9%	1.80
CO_2 (10%), 25 °C, 5h	6.4%	1.46
CO_2 (10%), 50 °C, 5h	7.1%	1.60
CO_2 (10%), 90 °C, 5h	3.4%	0.78

Elemental Analysis (EA)

	N [%]	C [%]	H [%]	S [%]	mmol N/g	C/N ratio	C/H ratio
run 1	**6.98**	**70.23**	**9.27**	**Detected**	**4.98**	**11.73**	**0.64**
run 2	**7.45**	**71.23**	**9.62**	**Detected**	**5.32**	**11.15**	**0.62**
run 3	**7.50**	**73.30**	**9.98**	**Detected**	**5.36**	**11.40**	**0.62**
run 4	**7.56**	**72.17**	**10.06**	**Detected**	**5.40**	**11.13**	**0.60**
run 5	**7.34**	**71.87**	**9.97**	**Detected**	**5.24**	**11.43**	**0.61**

Hydrogenated Acrylonitrile Butadiene Styrene 1 (H-ABS1) was synthesised according to the General Procedure B from substrate **ABS1** (Lego® bricks) and was obtained in weight yields of 850 mg, 85 wt% and 669 mg, 67 wt%, respectively, from two independent runs (76 wt% on average). **H-ABS1** was also prepared from **ABS1** with the large-scale General Procedure B2, rendering the product in a weight yield of 6.67 g (67 wt%). For simplicity, only the full characterisation of two runs is reported. The polymer was analysed with solid-state ^{13}C CP/MAS NMR, IR-, TGA-, DSC-, and elemental analysis. Solubility tests were also conducted with several solvents. No thermal events besides decomposition were observed with DSC.

Particle size after cryogenic milling used for CO_2 adsorption-desorption experiments

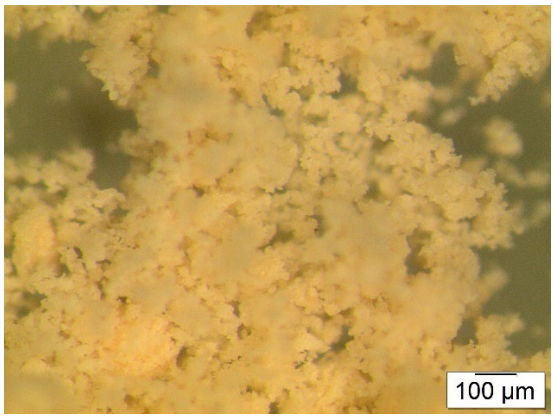

Solubility chart

Soluble **Swells** **Not soluble**

$CHCl_3$	Acetone	*i*-PrOH	DMF	DMSO	THF	PhMe	H_2O	MeOH	MeCN

^{13}C CP/MAS NMR (solid-state)

*Solid-state ^{13}C–NMR of **H-ABS1** (run 1):*

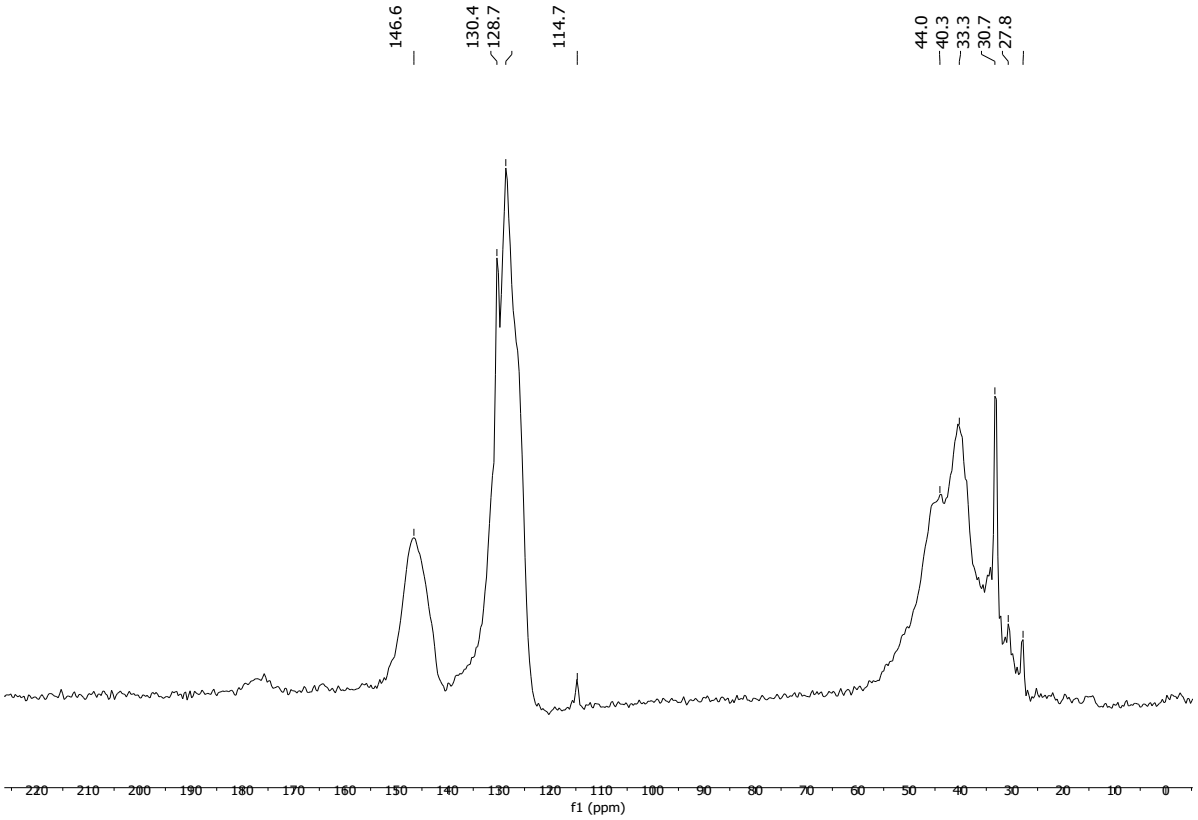

*Solid-state ^{13}C–NMR of **H-ABS1** (run 2):*

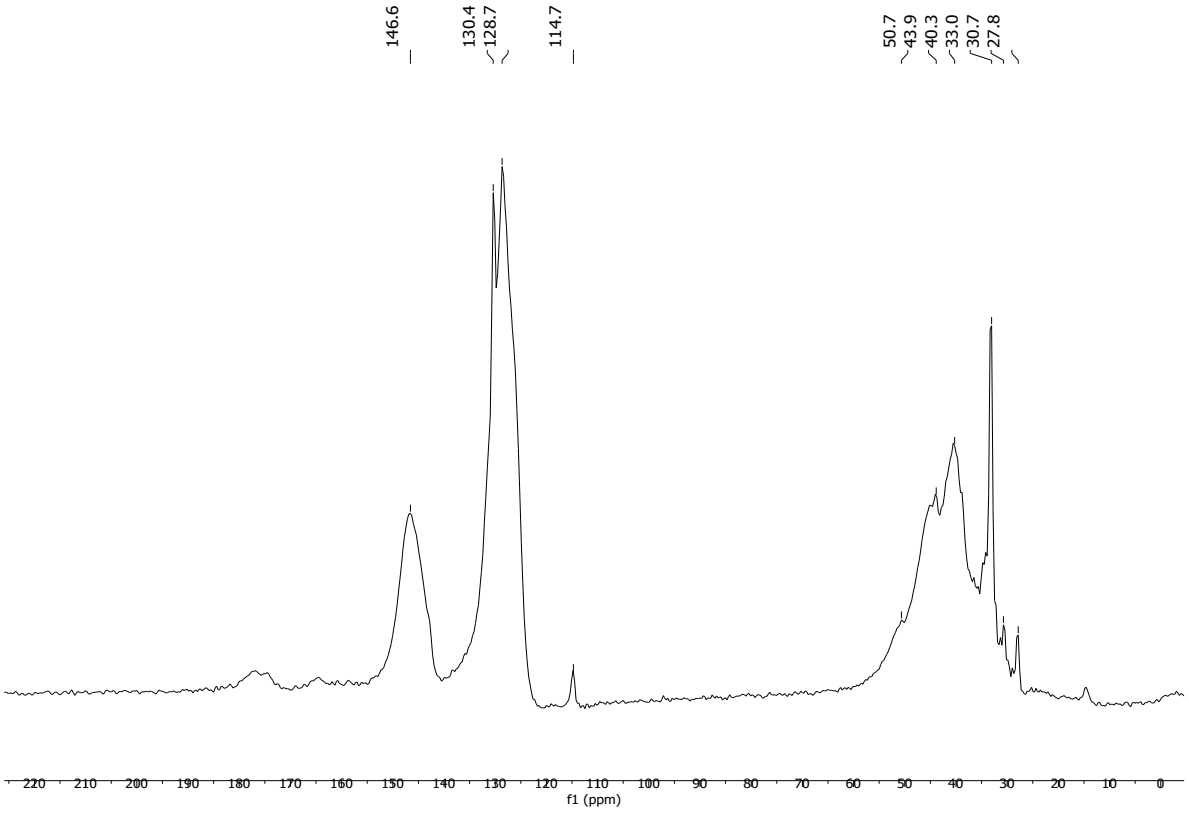

*Solid-state ^{13}C–NMR stacked spectra of **H-ABS1** (run 1, **brown**) and **ABS1** (substrate, **light blue**):*

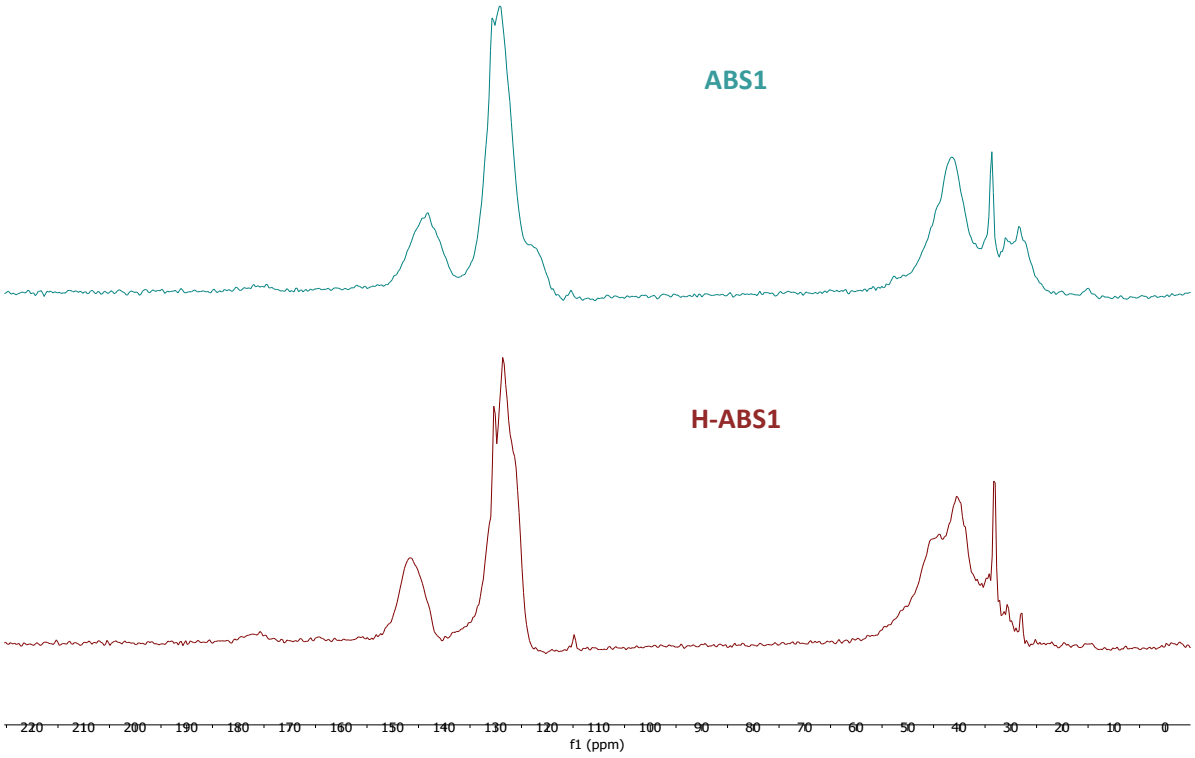

Infrared (IR) Spectroscopic Analysis

*IR-spectrum of **H-ABS1** (run 1):*

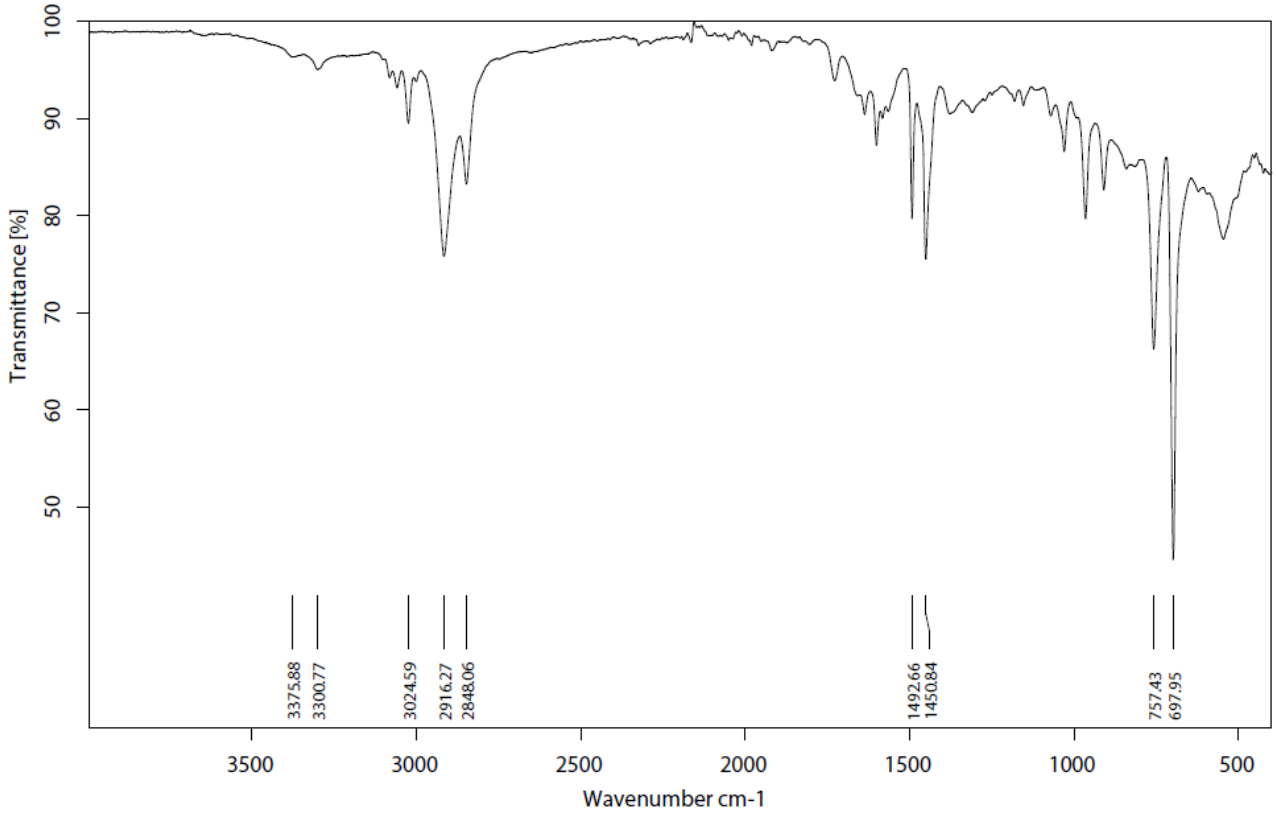

*IR-spectrum of **H-ABS1** (run 2):*

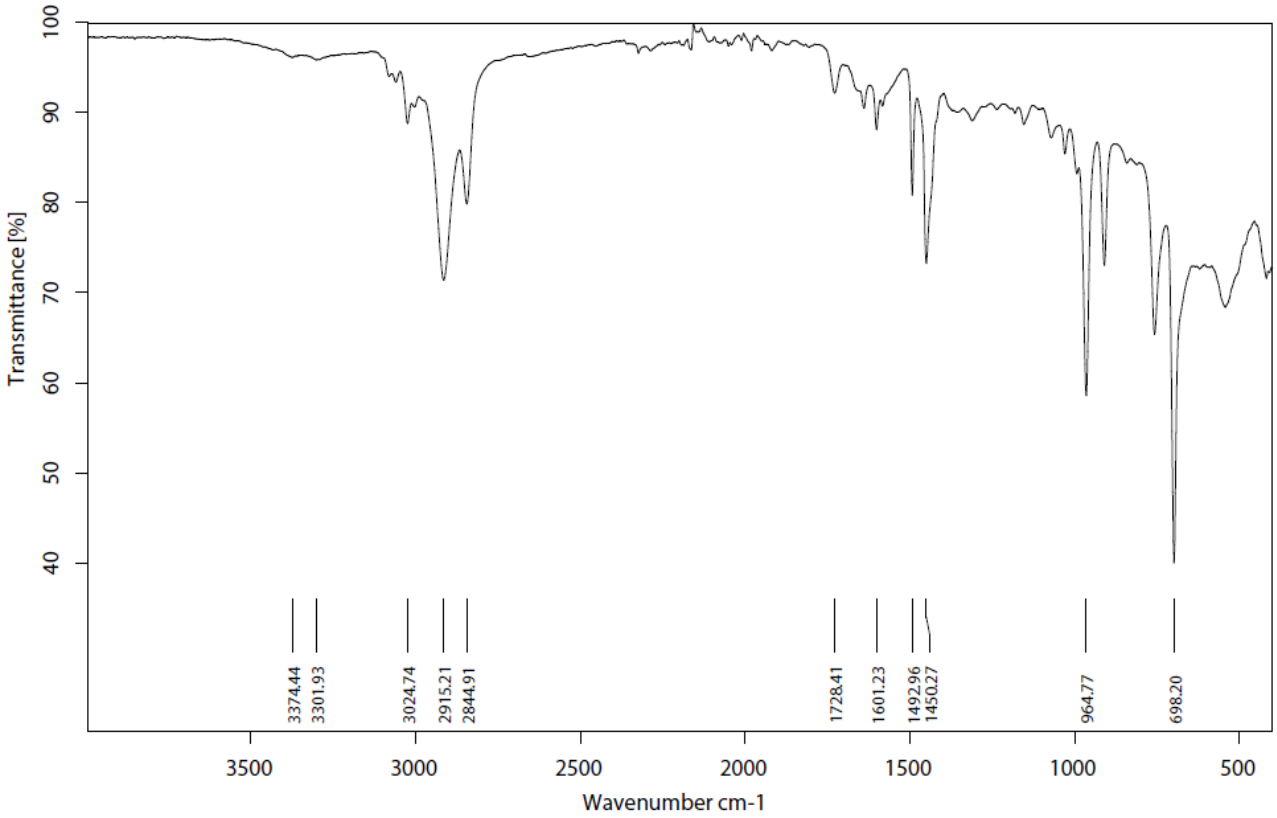

*IR-spectrum overlay of **H-ABS1** (run 1, **black**) and **ABS1** (substrate, **red**):*

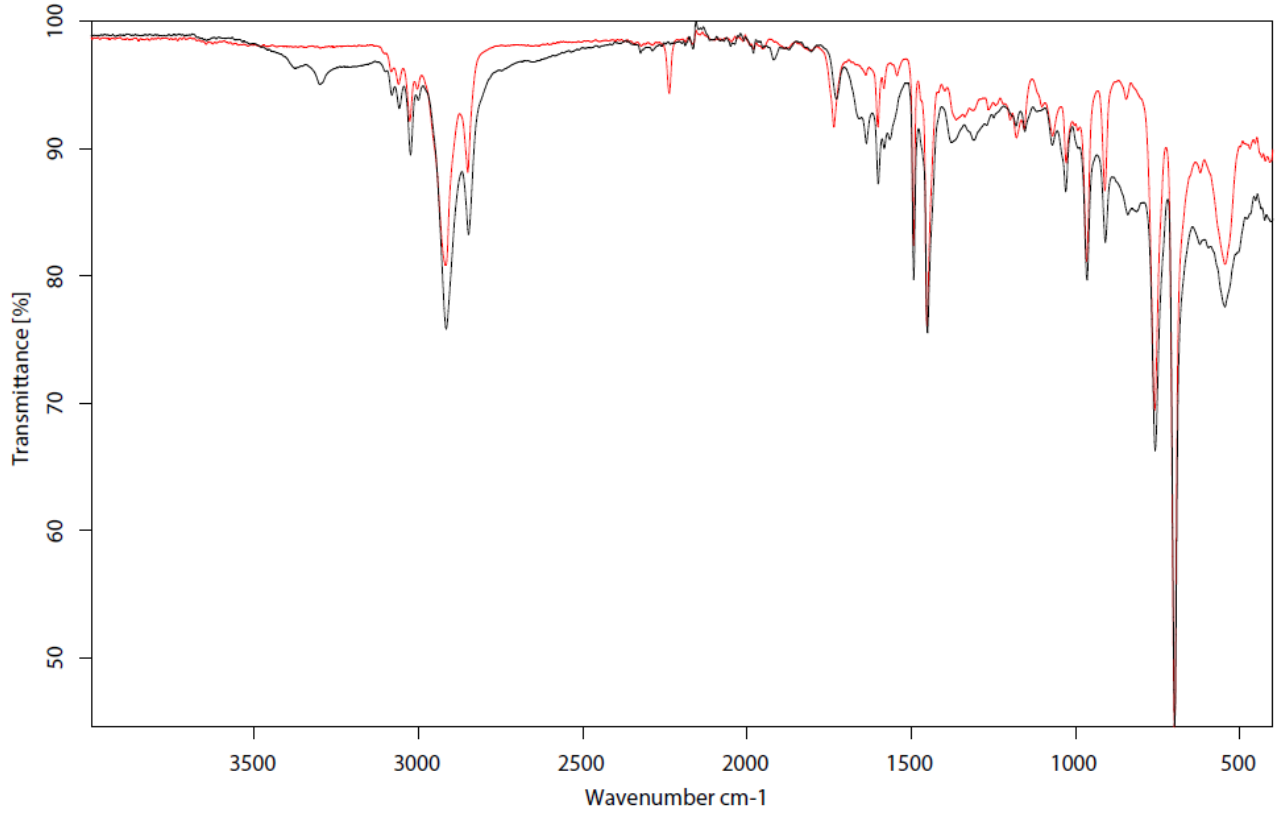

Thermogravimetric Analysis (TGA)

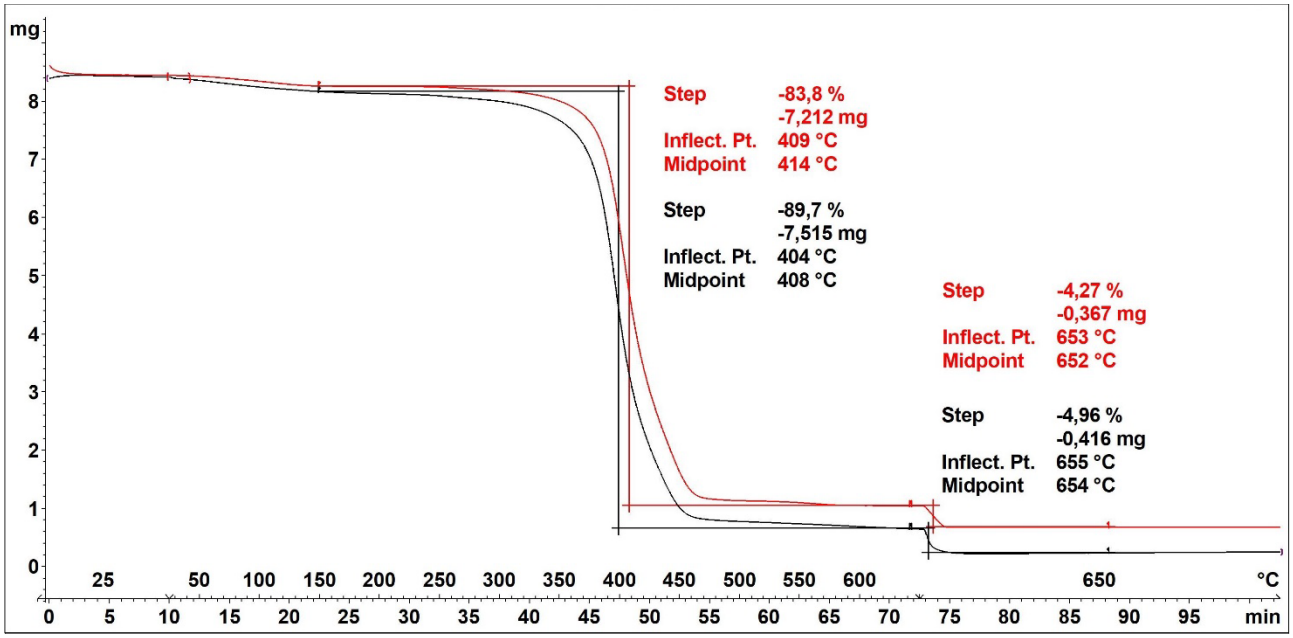

Decomposition graph. The experiment was conducted under He then air (after 650 °C). The black curve is the result from run 1, while the red curve is for run 2.

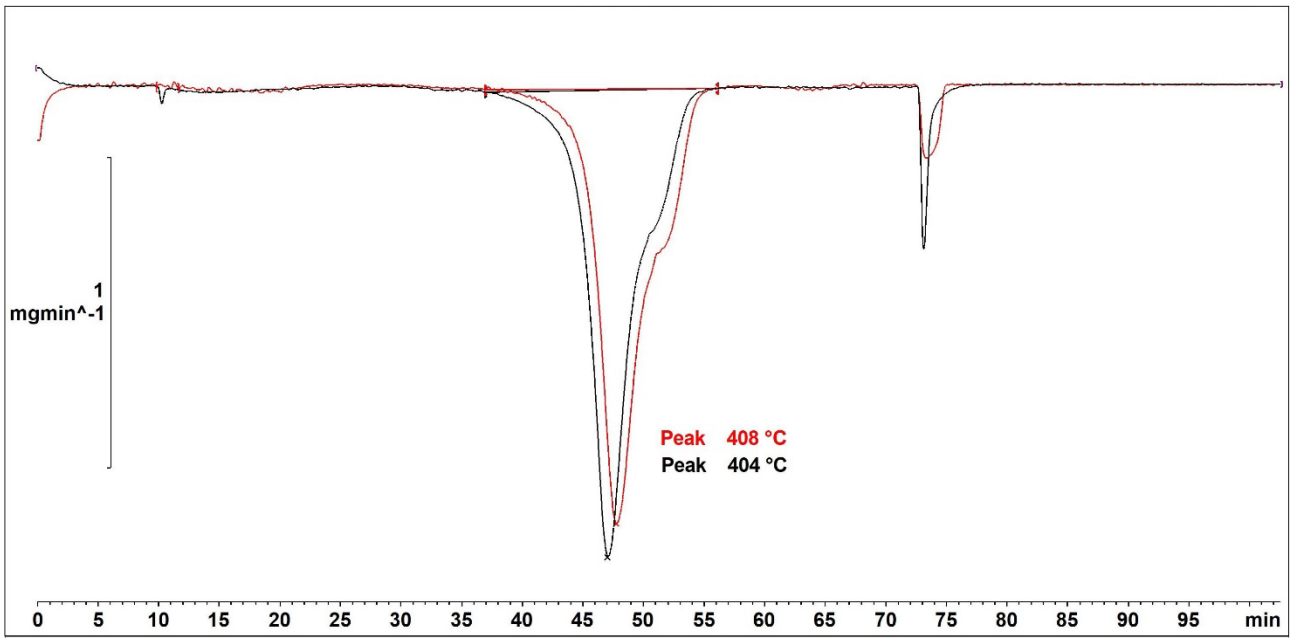

1st derivative of decomposition graph. The experiment was conducted under He then air (after 650 °C). The black curve is the result from run 1, while the red curve is for run 2.

Decomposition temperature (T_d) = 404–408 °C.

CO_2-adsorption analysis by thermogravimetric analysis

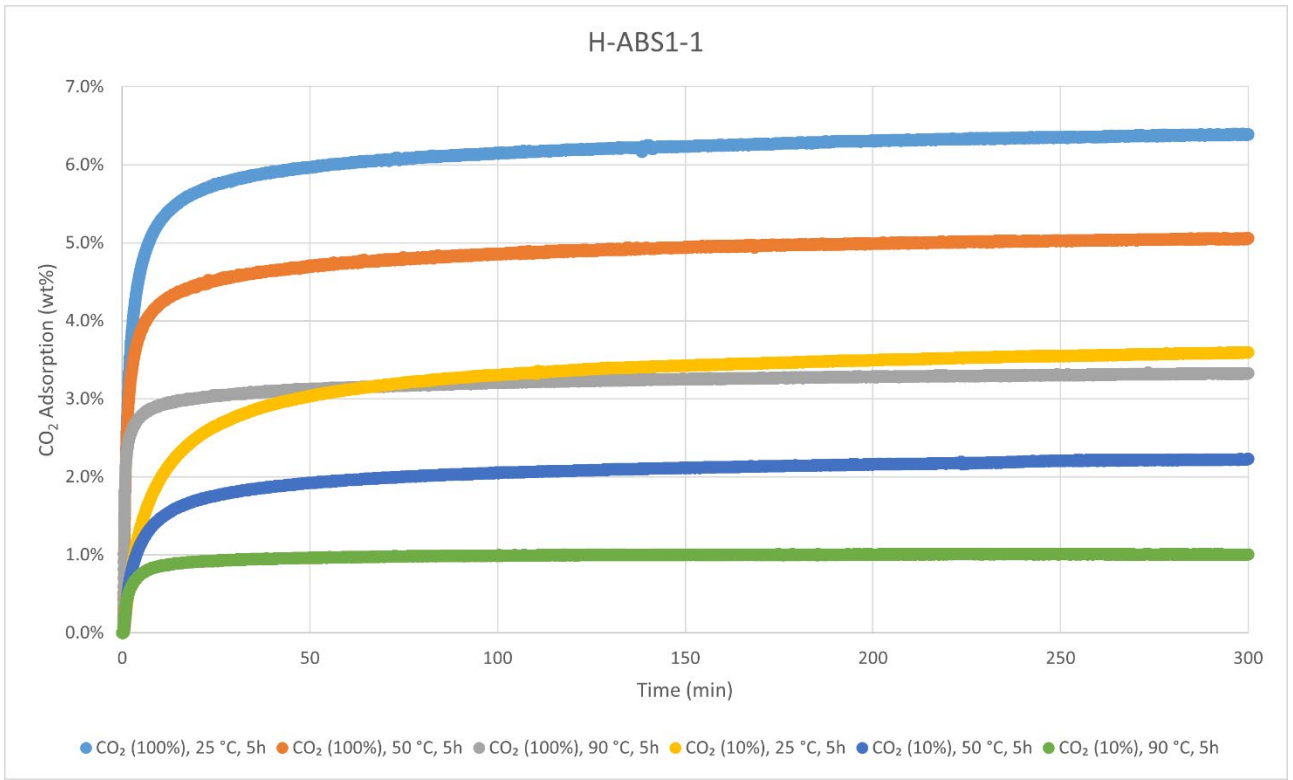

CO_2 adsorption using **TGA method 2** (measurement of product batch from run 1: H-ABS1-1).

H-ABS1-1	wt%	mmol/g
CO_2 (100%), 25 °C, 5h	6.4%	1.45
CO_2 (100%), 50 °C, 5h	5.1%	1.15
CO_2 (100%), 90 °C, 5h	3.3%	0.76
CO_2 (10%), 25 °C, 5h	3.6%	0.82
CO_2 (10%), 50 °C, 5h	2.2%	0.51
CO_2 (10%), 90 °C, 5h	1.0%	0.23

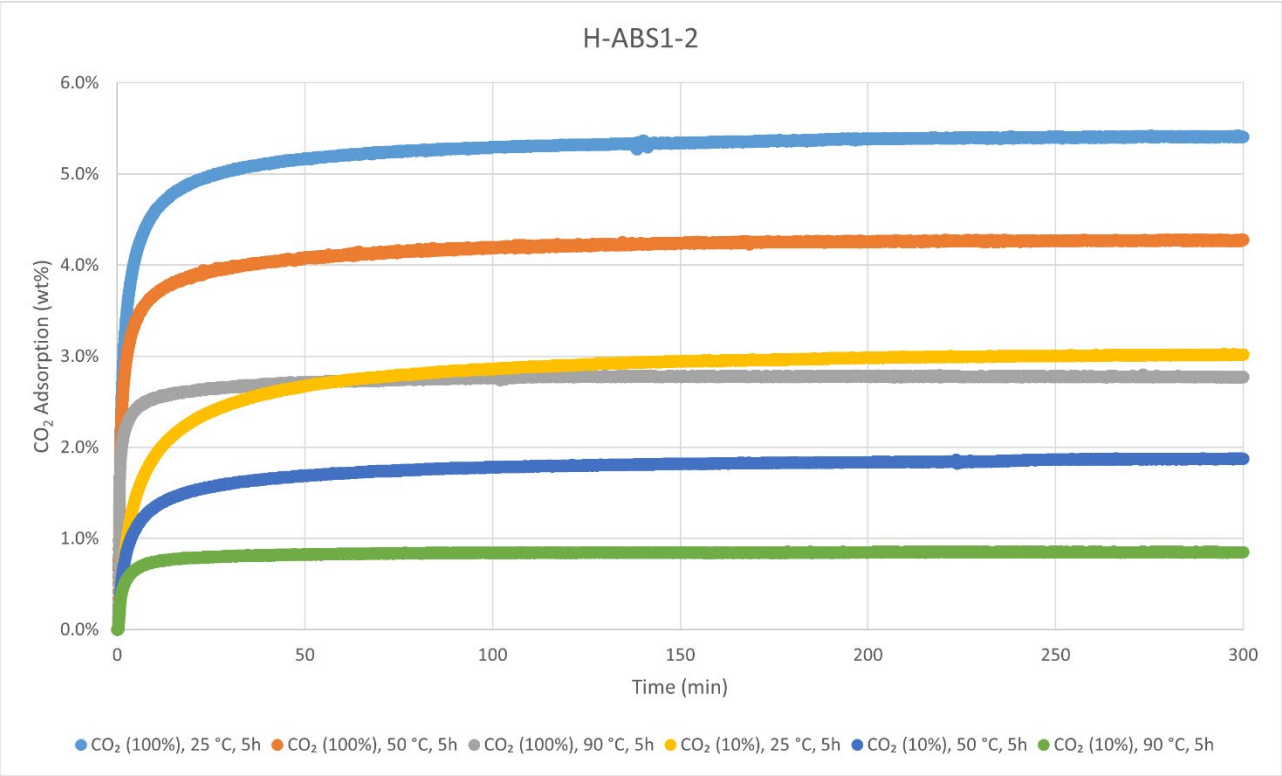

CO_2 adsorption using **TGA method 2** (measurement of product batch from run 2: H-ABS1-2).

H-ABS1-2	wt%	mmol/g
CO_2 (100%), 25 °C, 5h	5.4%	1.23
CO_2 (100%), 50 °C, 5h	4.3%	0.97
CO_2 (100%), 90 °C, 5h	2.8%	0.63
CO_2 (10%), 25 °C, 5h	3.0%	0.69
CO_2 (10%), 50 °C, 5h	1.9%	0.43
CO_2 (10%), 90 °C, 5h	0.8%	0.19

Elemental Analysis (EA)

	N [%]	C [%]	H [%]	S [%]	mmol N/g	C/N ratio	C/H ratio
run 1	**4.42**	**81.71**	**9.11**	**Not detected**	**3.16**	**21.56**	**0.75**
run 2	**3.73**	**75.29**	**8.46**		**2.67**	**23.52**	**0.75**

Hydrogenated Acrylonitrile Butadiene Styrene 2 (H-ABS2) was synthesised according to the General Procedure B from substrate **ABS2** (Fujitsu® keyboard) and was obtained in weight yields of 894 mg, 89 wt% and 971 mg, 97 wt%, respectively, from two independent runs (93 wt% on average). The polymer was analysed with solid-state ^{13}C CP/MAS NMR, IR-, TGA-, DSC-, and Elemental Analysis. Solubility tests were also conducted with several solvents. No thermal events besides decomposition were observed with DSC.

Particle size after cryogenic milling used for CO_2 adsorption-desorption experiments

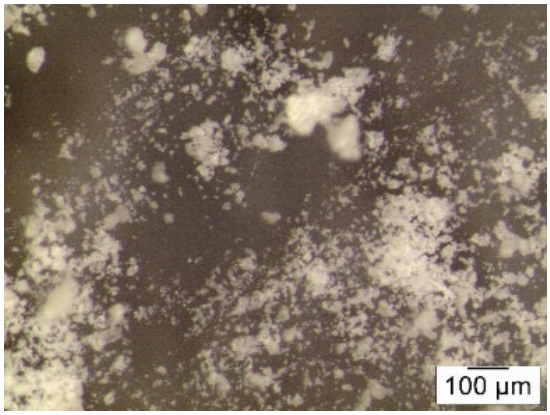

Solubility chart

Soluble **Swells** **Not soluble**

$CHCl_3$	Acetone	*i*-PrOH	DMF	DMSO	THF	PhMe	H_2O	MeOH	MeCN

^{13}C CP/MAS NMR (solid-state)

*Solid-state ^{13}C–NMR of **H-ABS2** (run 1):*

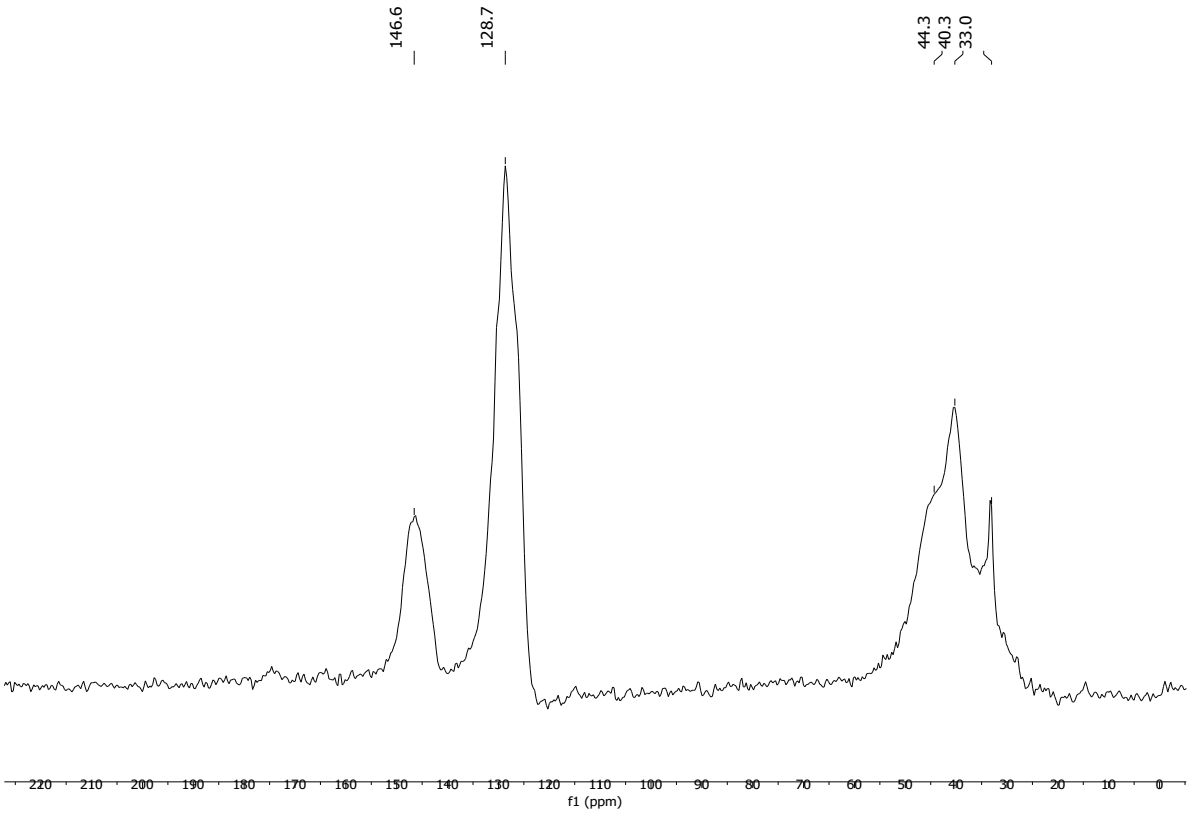

*Solid-state ^{13}C–NMR of **H-ABS2** (run 2):*

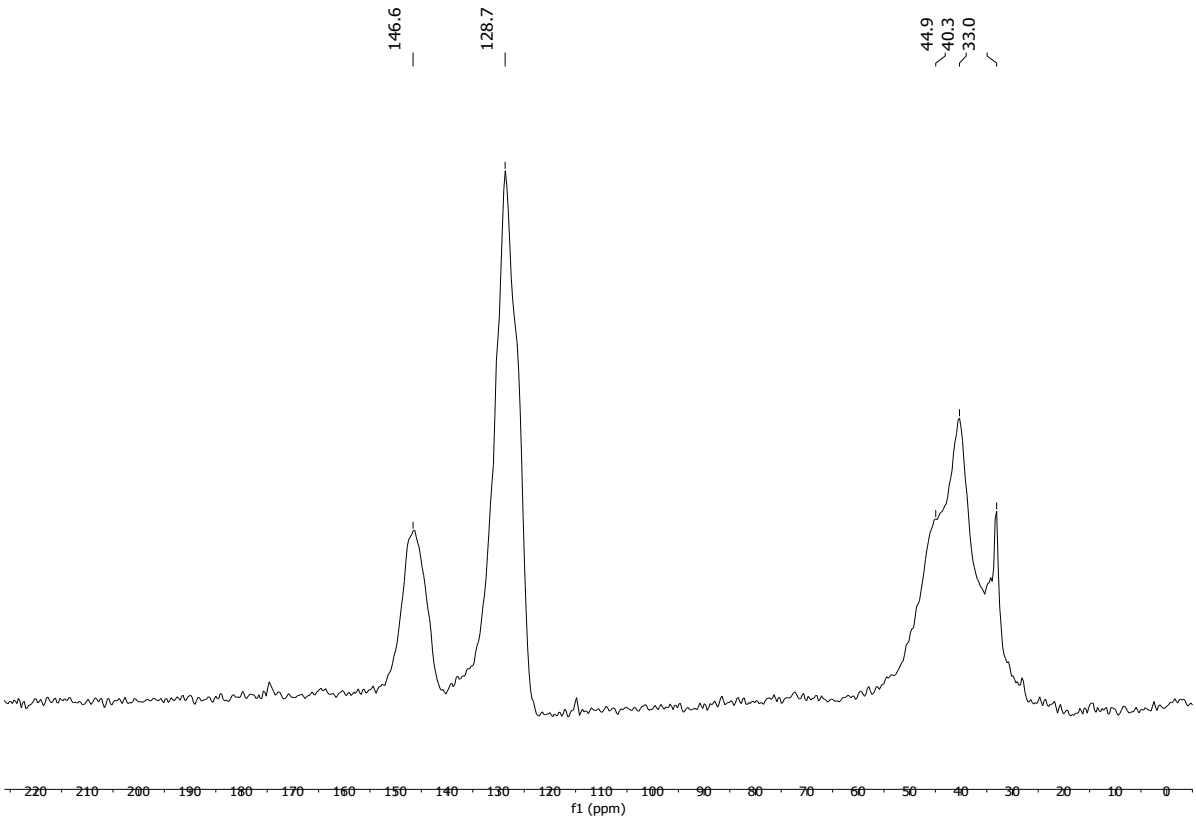

*Solid-state ^{13}C–NMR stacked spectra of **H-ABS2** (run 1, **brown**) and **ABS2** (substrate, **light blue**):*

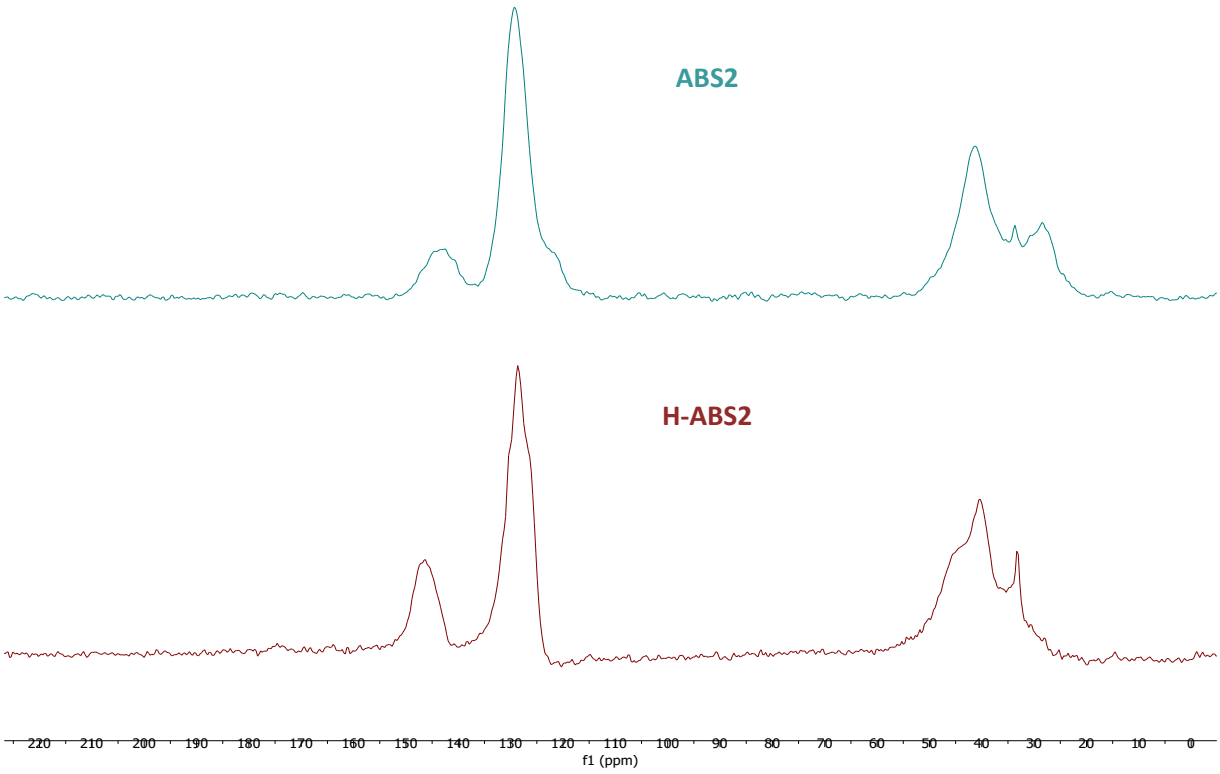

Infrared (IR) Spectroscopic Analysis

*IR-spectrum of **H-ABS2** (run 1):*

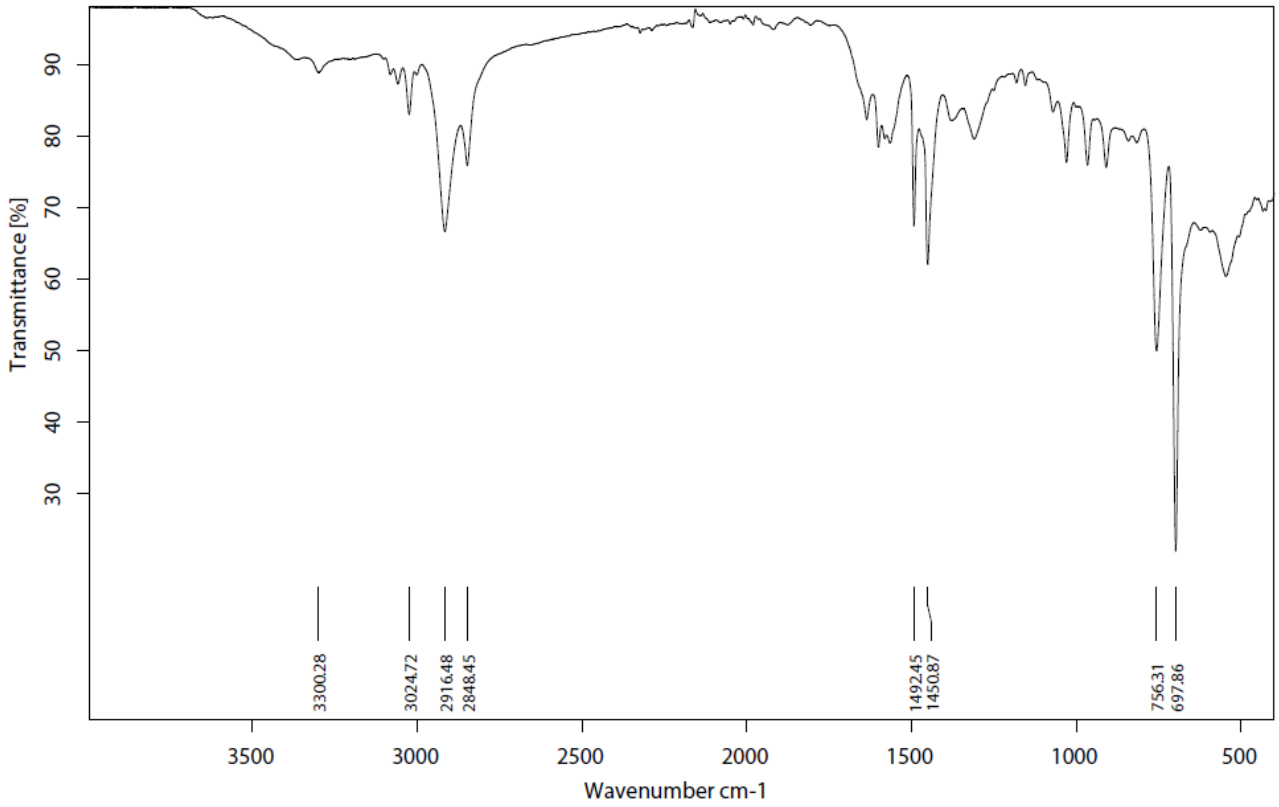

*IR-spectrum of **H-ABS2** (run 2):*

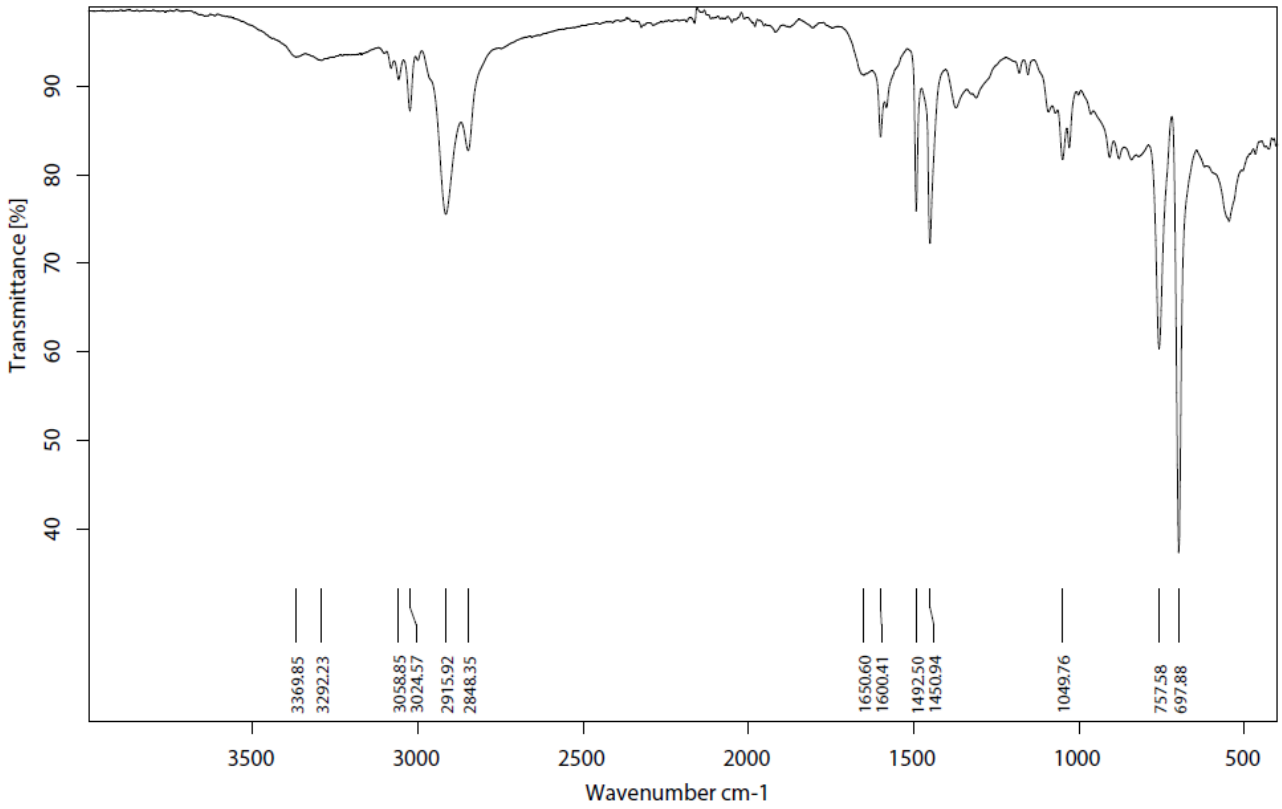

*IR-spectrum overlay of **H-ABS2** (run 1, **black**) and **ABS2** (substrate, **red**):*

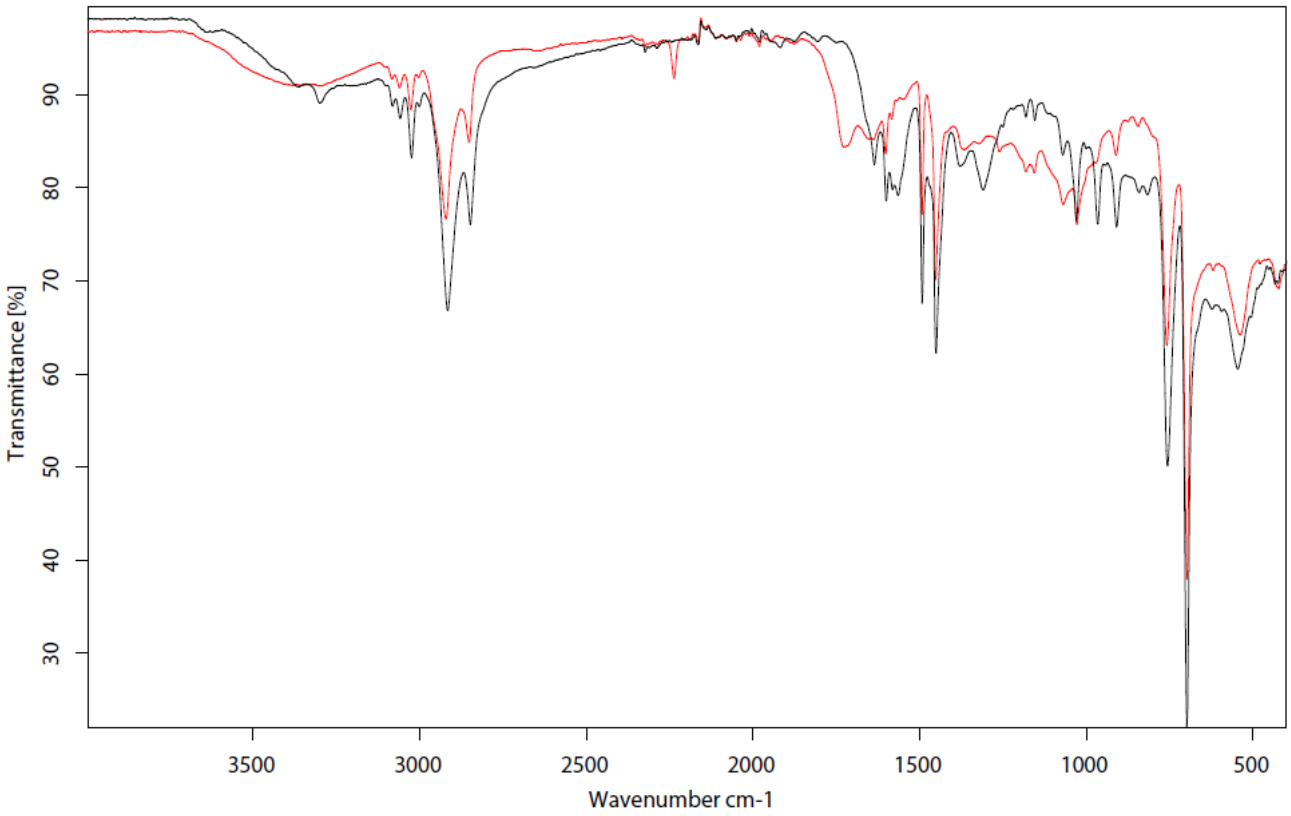

Thermogravimetric Analysis (TGA)

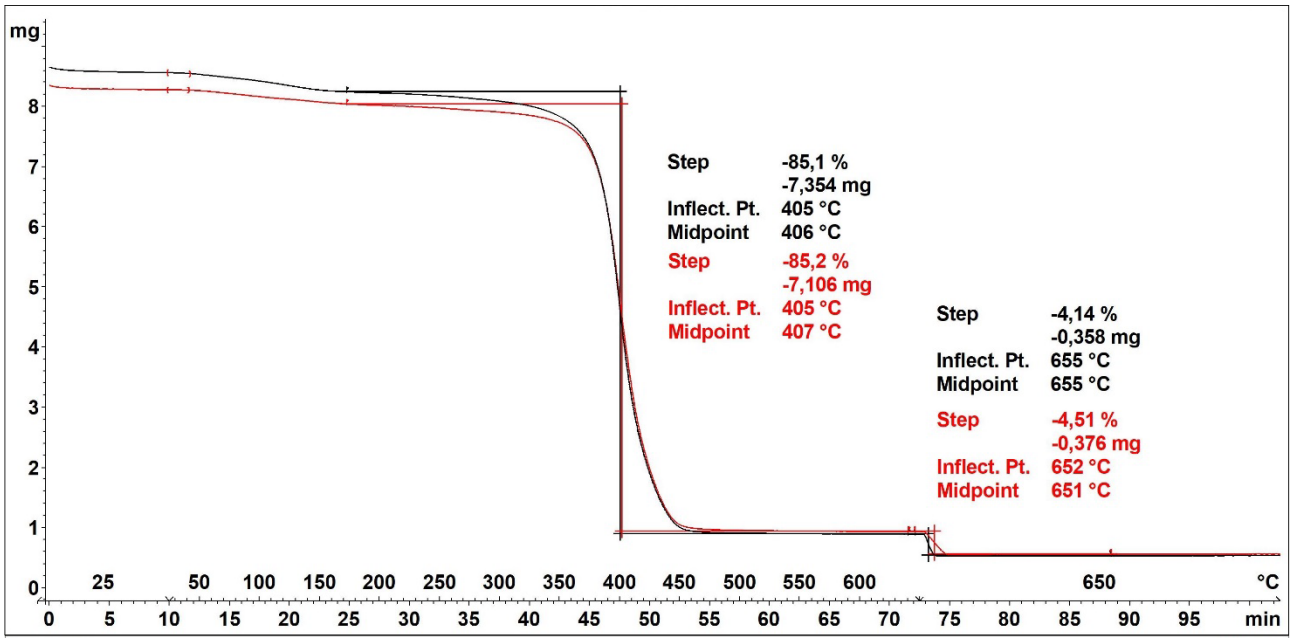

Decomposition graph. The experiment was conducted under He then air (after 650 °C). The black curve is the result from run 1, while the red curve is for run 2.

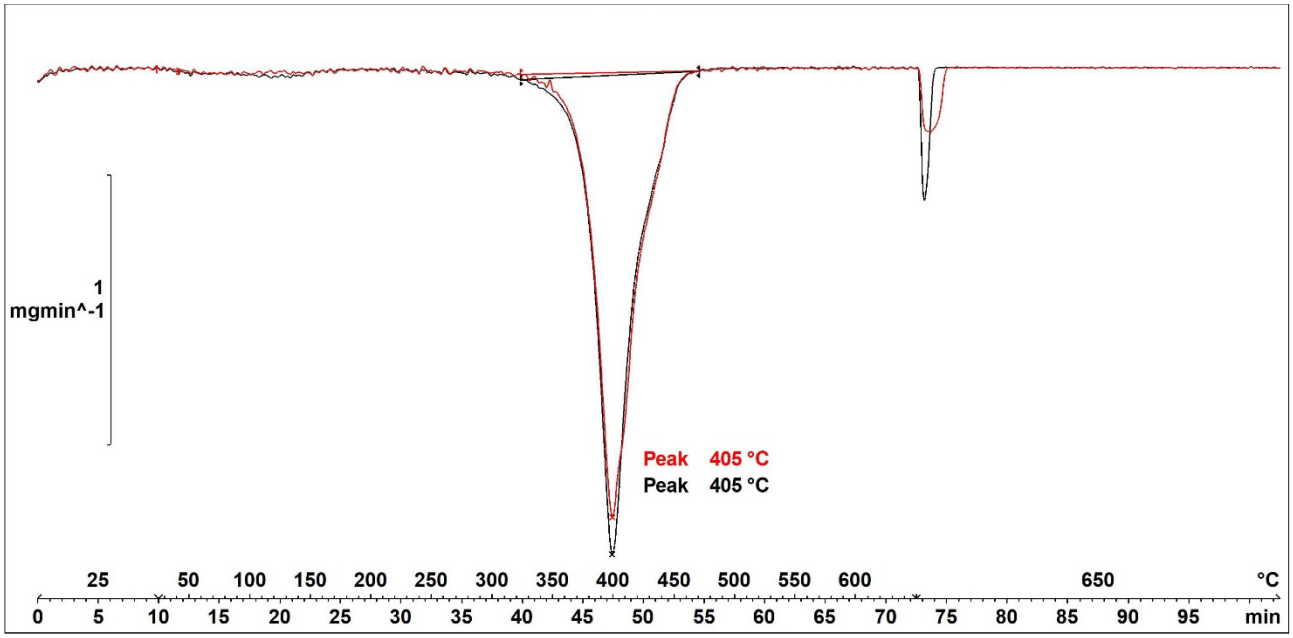

1st derivative of decomposition graph. The experiment was conducted under He then air (after 650 °C). The black curve is the result from run 1, while the red curve is for run 2.

Decomposition temperature (T_d) = 405 °C.

CO_2-adsorption analysis by thermogravimetric analysis

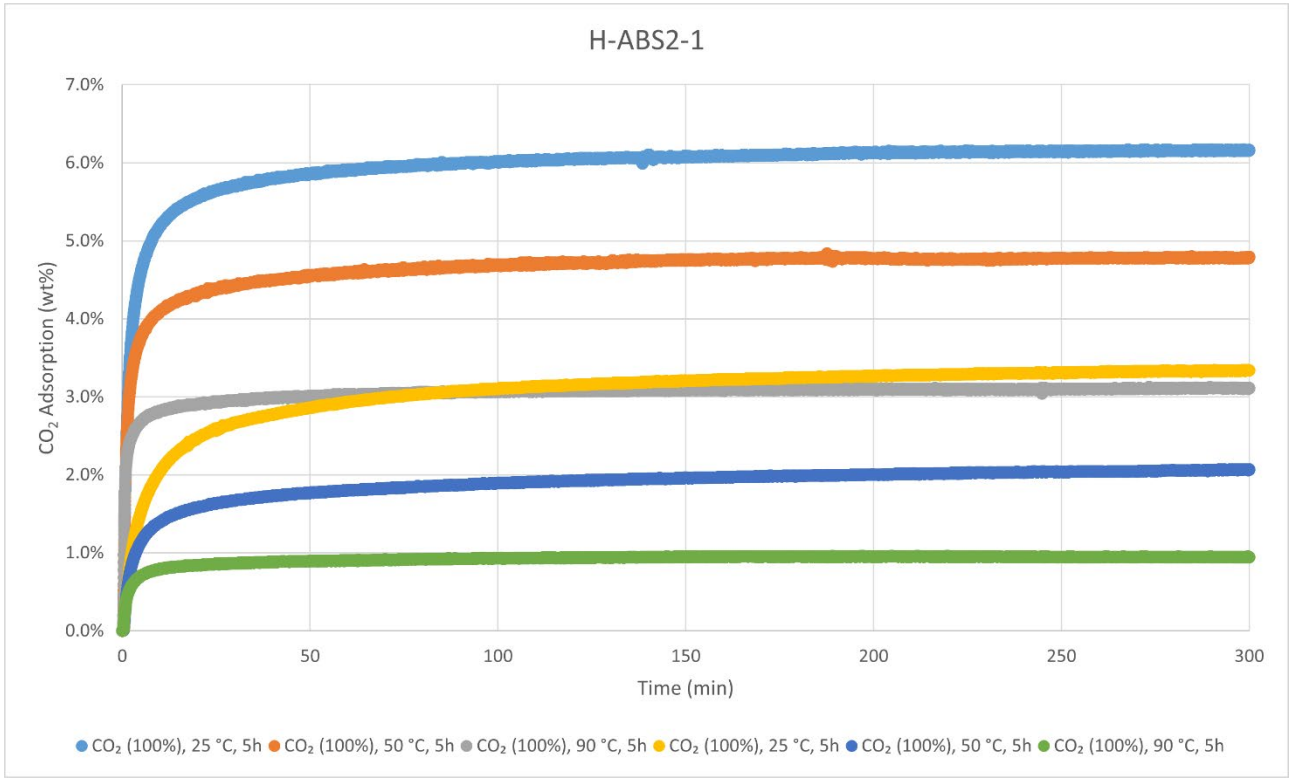

CO_2 adsorption using **TGA method 2** (measurement of product batch from run 1: H-ABS2-1).

H-ABS2-1	wt%	mmol/g
CO_2 (100%), 25 °C, 5h	6.2%	1.40
CO_2 (100%), 50 °C, 5h	4.8%	1.09
CO_2 (100%), 90 °C, 5h	3.1%	0.71
CO_2 (100%), 25 °C, 5h	3.3%	0.76
CO_2 (100%), 50 °C, 5h	2.1%	0.47
CO_2 (100%), 90 °C, 5h	0.9%	0.21

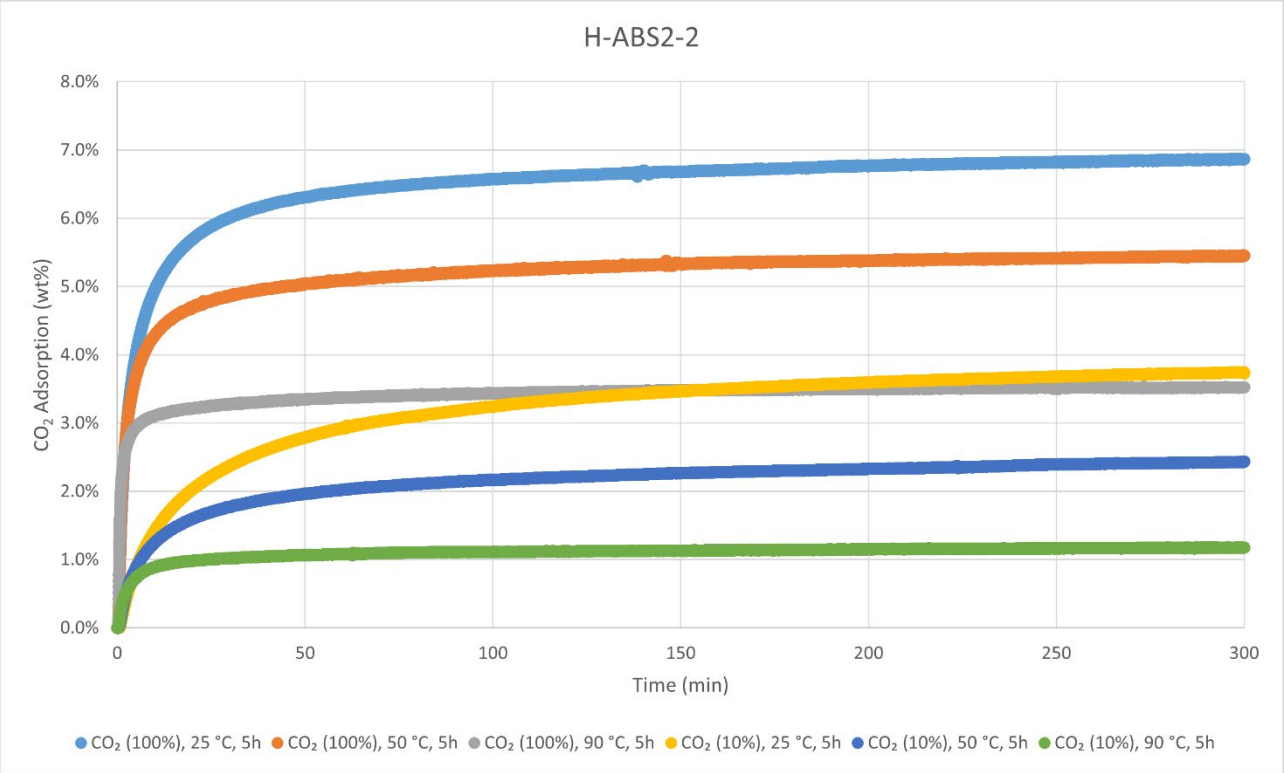

CO_2 adsorption using **TGA method 2** (measurement of product batch from run 2: H-ABS2-2).

H-ABS2-2	wt%	mmol/g
CO_2 (100%), 25 °C, 5h	6.9%	1.56
CO_2 (100%), 50 °C, 5h	5.5%	1.24
CO_2 (100%), 90 °C, 5h	3.5%	0.80
CO_2 (10%), 25 °C, 5h	3.7%	0.85
CO_2 (10%), 50 °C, 5h	2.4%	0.55
CO_2 (10%), 90 °C, 5h	1.2%	0.27

Elemental Analysis (EA)

	N [%]	C [%]	H [%]	S [%]	mmol N/g	C/N ratio	C/H ratio
run 1	**4.73**	**79.59**	**8.83**	**Not detected**	**3.38**	**19.63**	**0.76**
run 2	**4.86**	**80.14**	**8.91**		**3.47**	**19.22**	**0.76**

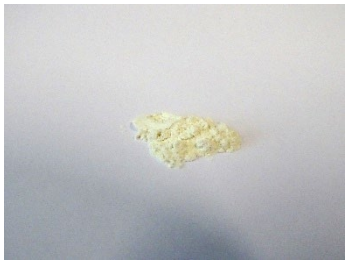

Hydrogenated Styrene Acrylonitrile 1 (H-SAN1) was synthesised according to the General Procedure B from substrate **SAN1** (Beaker) and was obtained in weight yields of 766 mg, 77 wt%, 604 mg, 60 wt%, and 582 mg, 58 wt%, respectively, from three independent runs (65 wt% on average). For simplicity, only the full characterisation of two runs is reported. The polymer was analysed with solid-state ^{13}C CP/MAS NMR, IR-, TGA-, DSC-, and Elemental Analysis. Solubility tests were also conducted with several solvents. No thermal events besides decomposition were observed with DSC.

Particle size after cryogenic milling used for CO_2 adsorption-desorption experiments

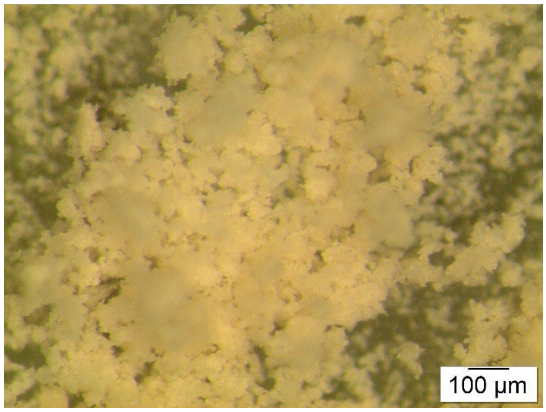

Solubility chart

Soluble **Swells** **Not soluble**

$CHCl_3$	Acetone	*i*-PrOH	DMF	DMSO	THF	PhMe	H_2O	MeOH	MeCN

^{13}C CP/MAS NMR (solid-state) *(run 1):*

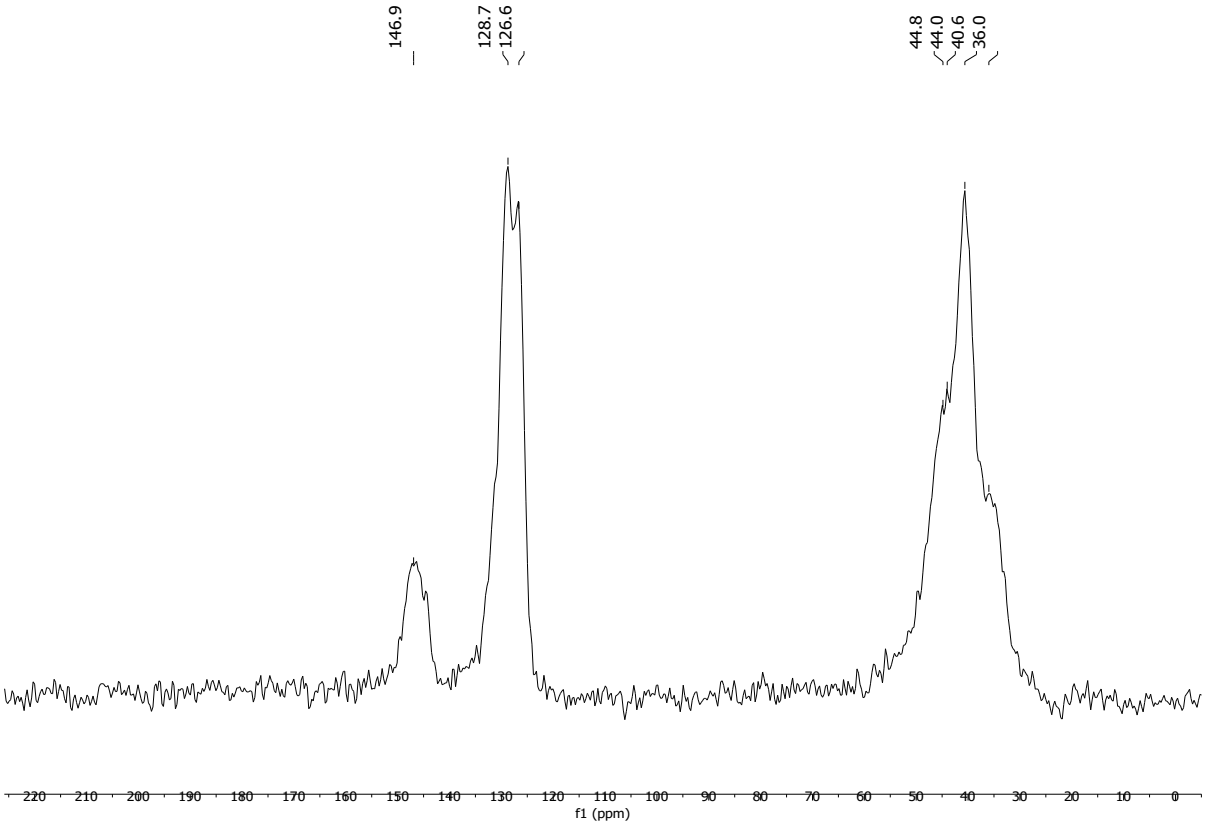

^{13}C CP/MAS NMR (solid-state) *(run 2):*

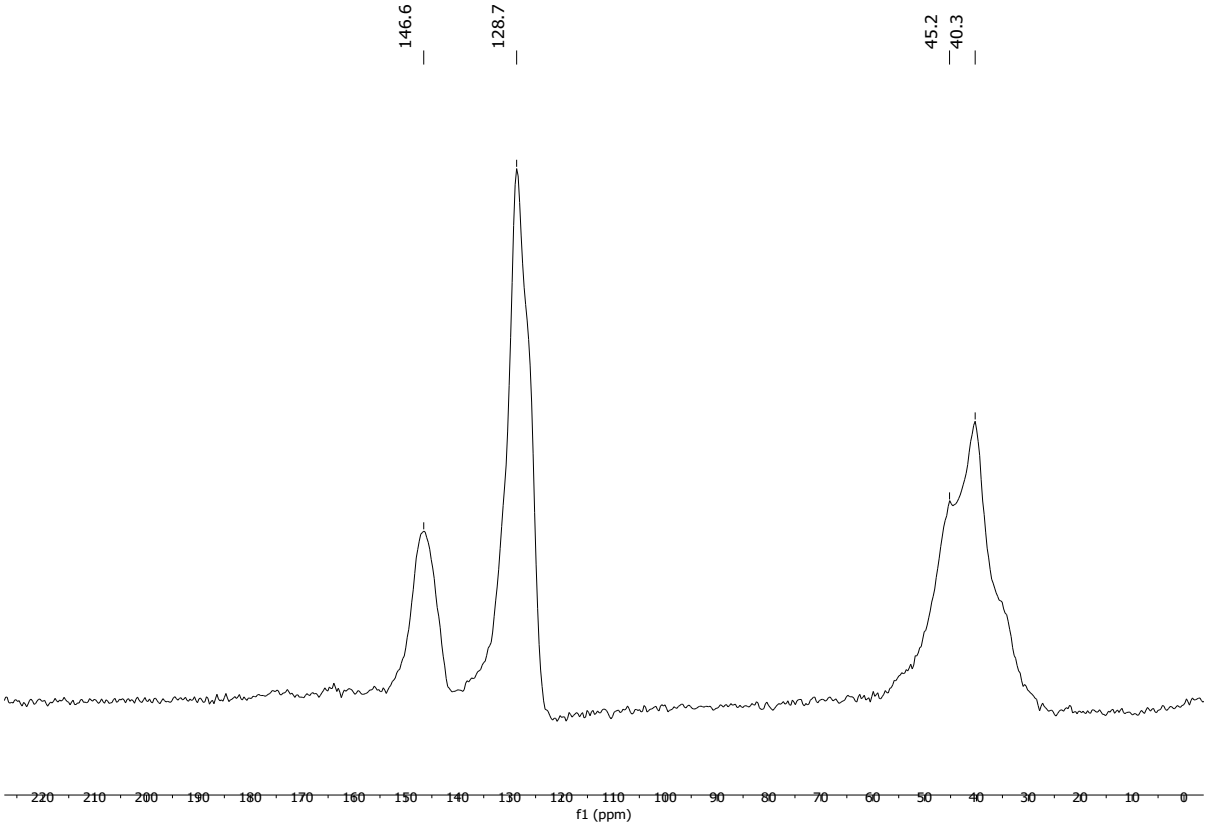

Stacked ^{13}C CP/MAS NMR spectra of H-SAN1 *(run 2,* ***brown****)* ***with substrate SAN1*** *(****light blue****)*:

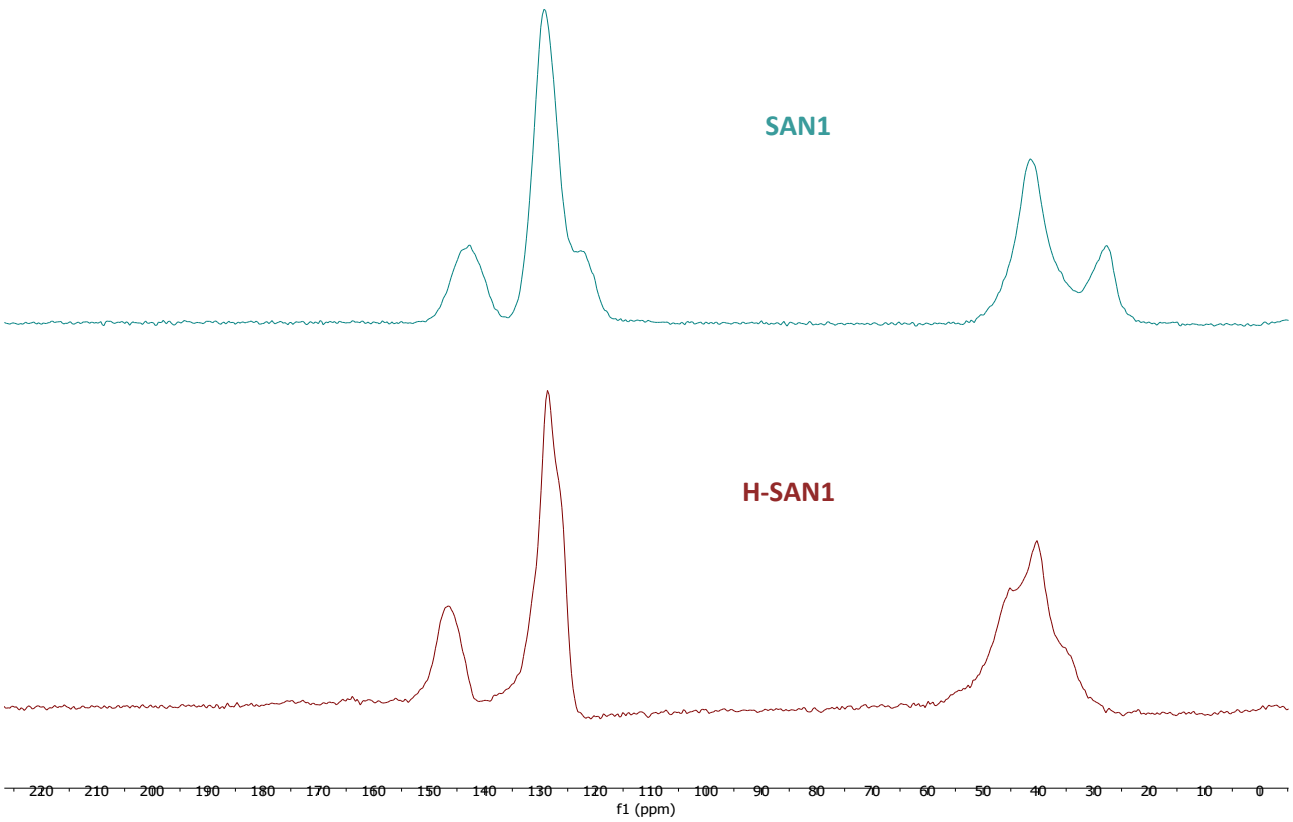

Infrared (IR) Spectroscopic Analysis

*IR-spectrum of **H-SAN1** (run 1):*

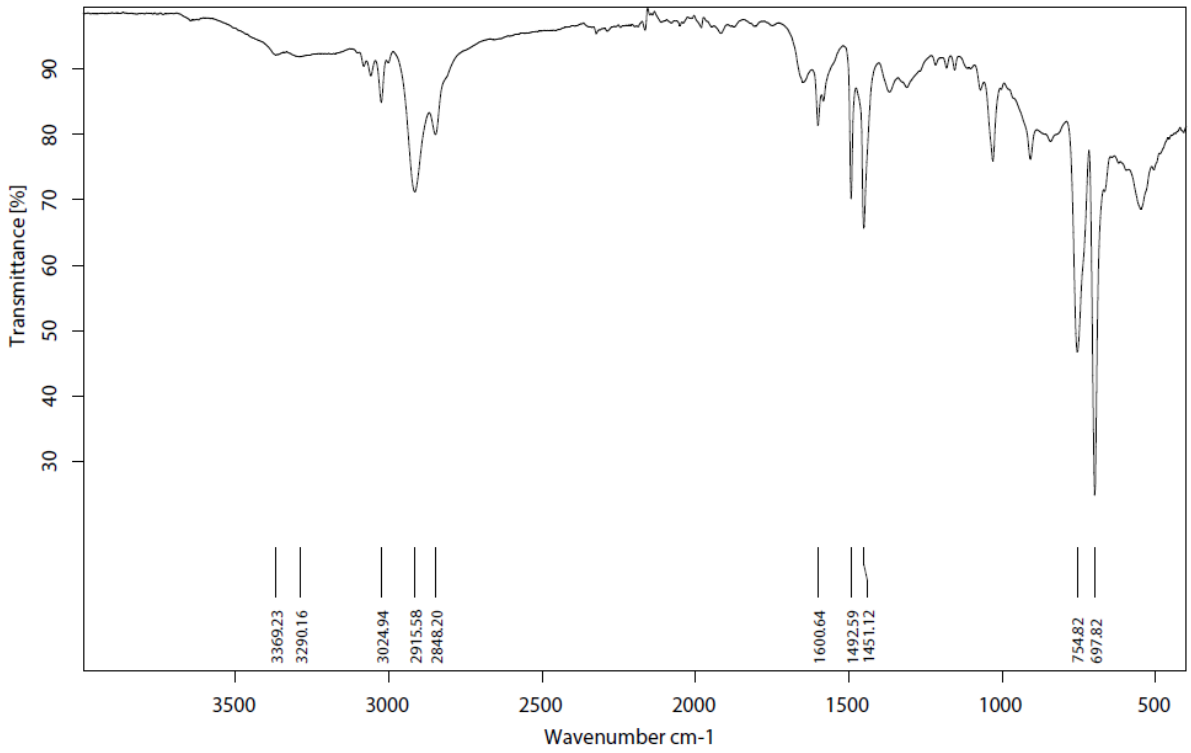

*IR-spectrum of **H-SAN1** (run 2):*

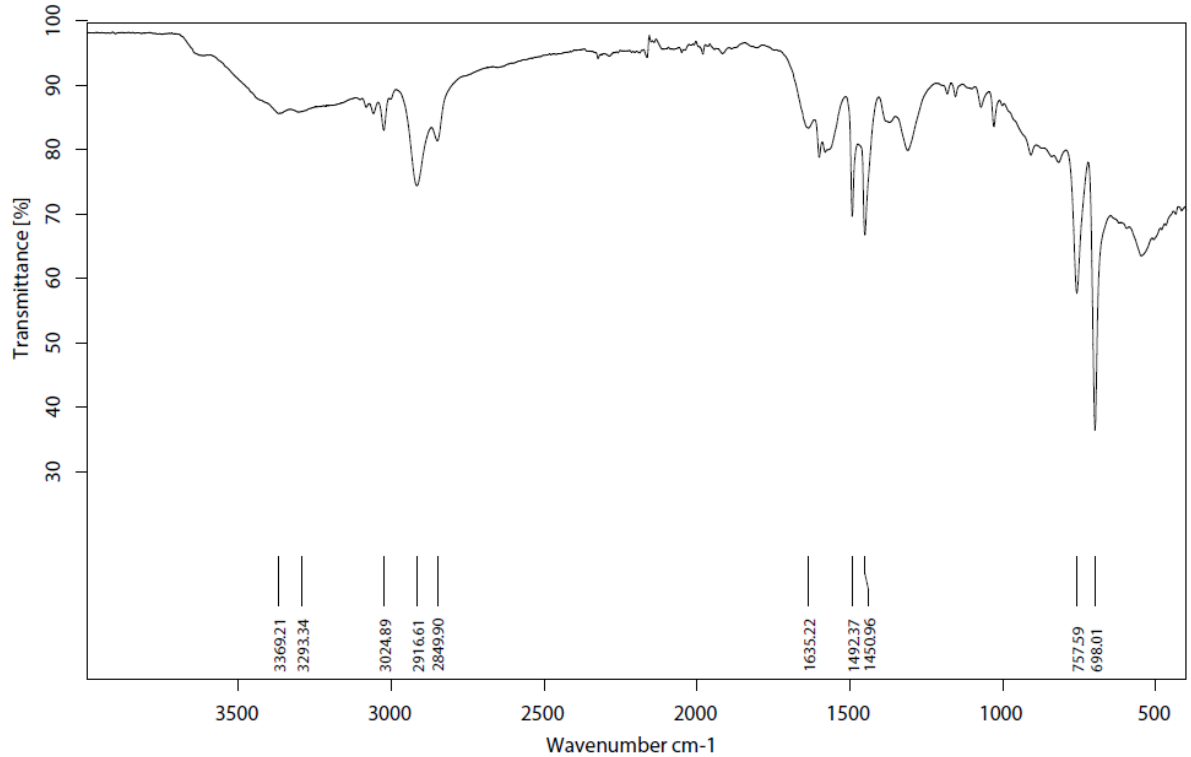

*IR-spectrum overlay of **H-SAN1** (run 1, **black**) and **SAN1** (substrate, **red**):*

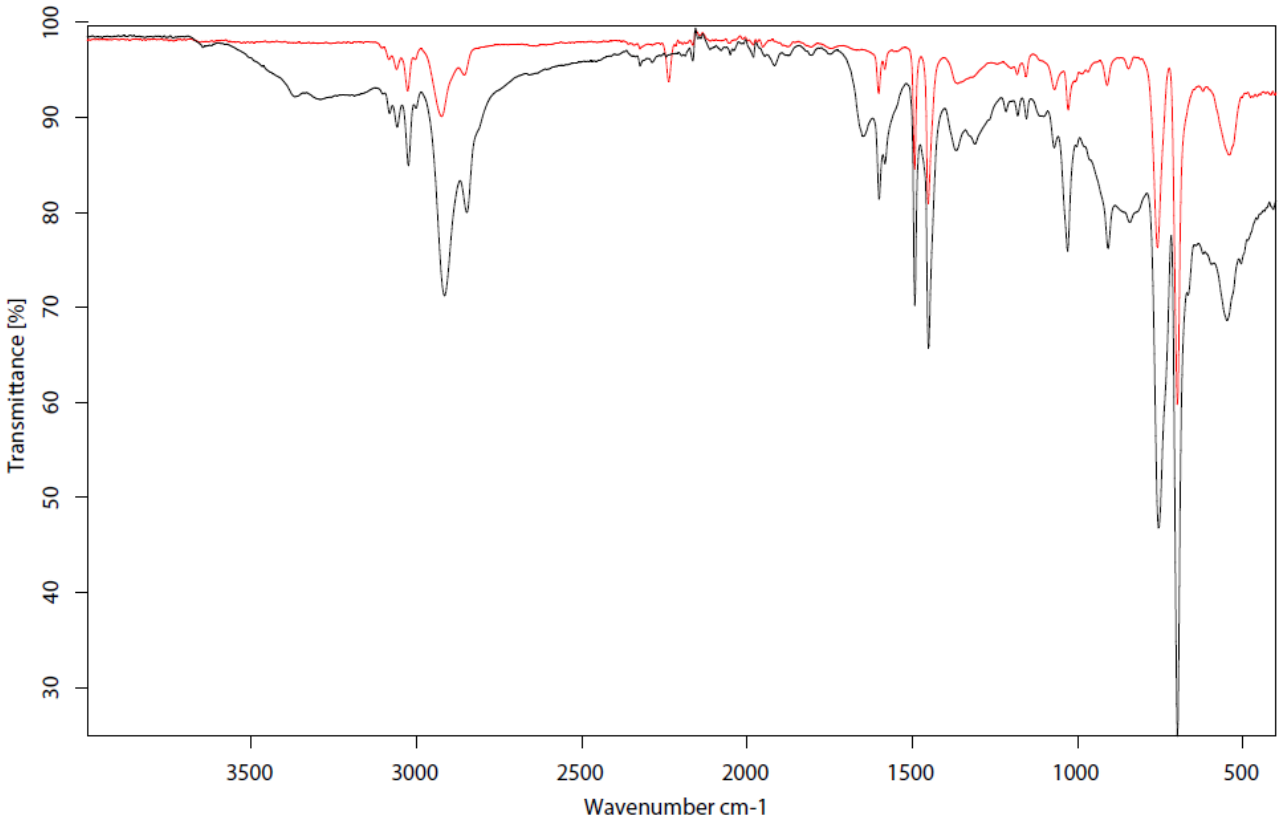

Thermogravimetric Analysis (TGA)

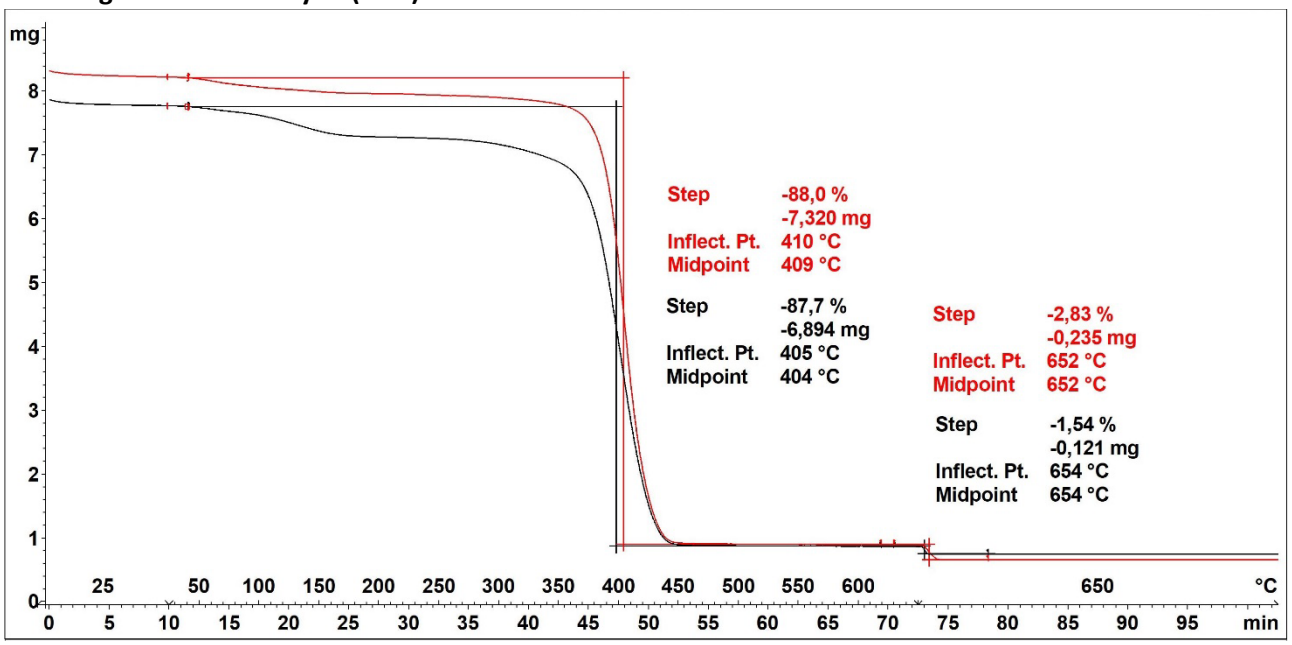

Decomposition graph. The experiment was conducted under He then air (after 650 °C). The black curve is the result from run 1, while the red curve is for run 2.

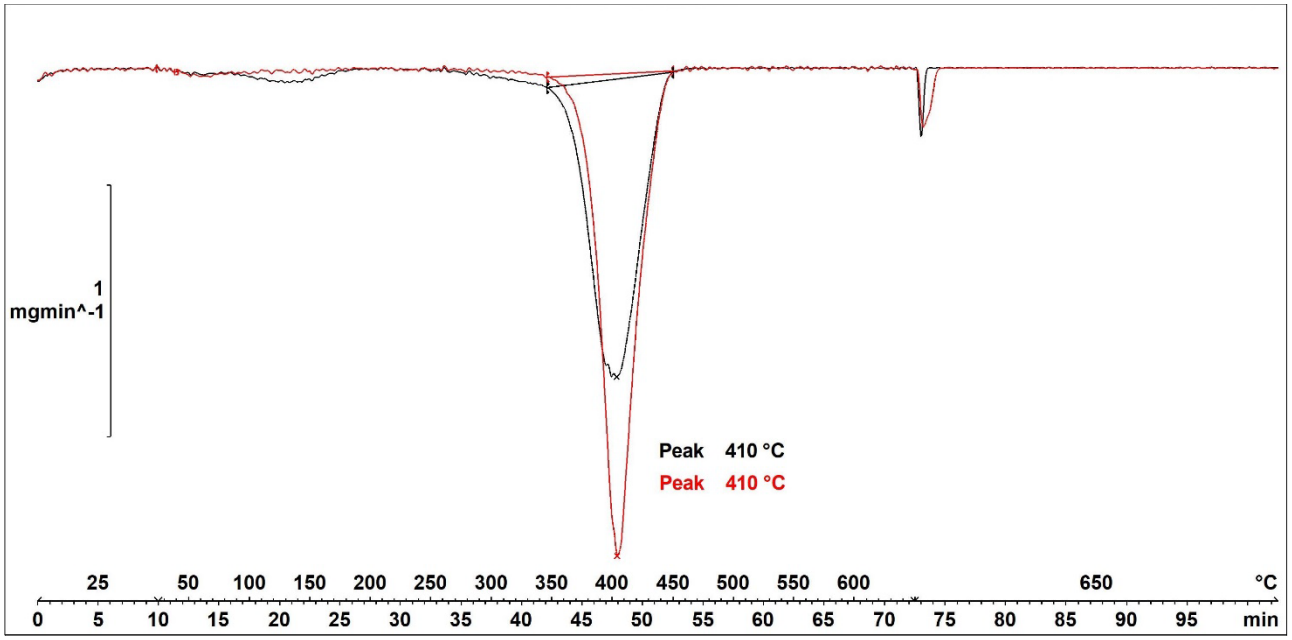

1st derivative of decomposition graph. The experiment was conducted under He then air (after 650 °C). The black curve is the result from run 1, while the red curve is for run 2.

Decomposition temperature (T_d) = 410 ℃.

CO_2-adsorption analysis by thermogravimetric analysis

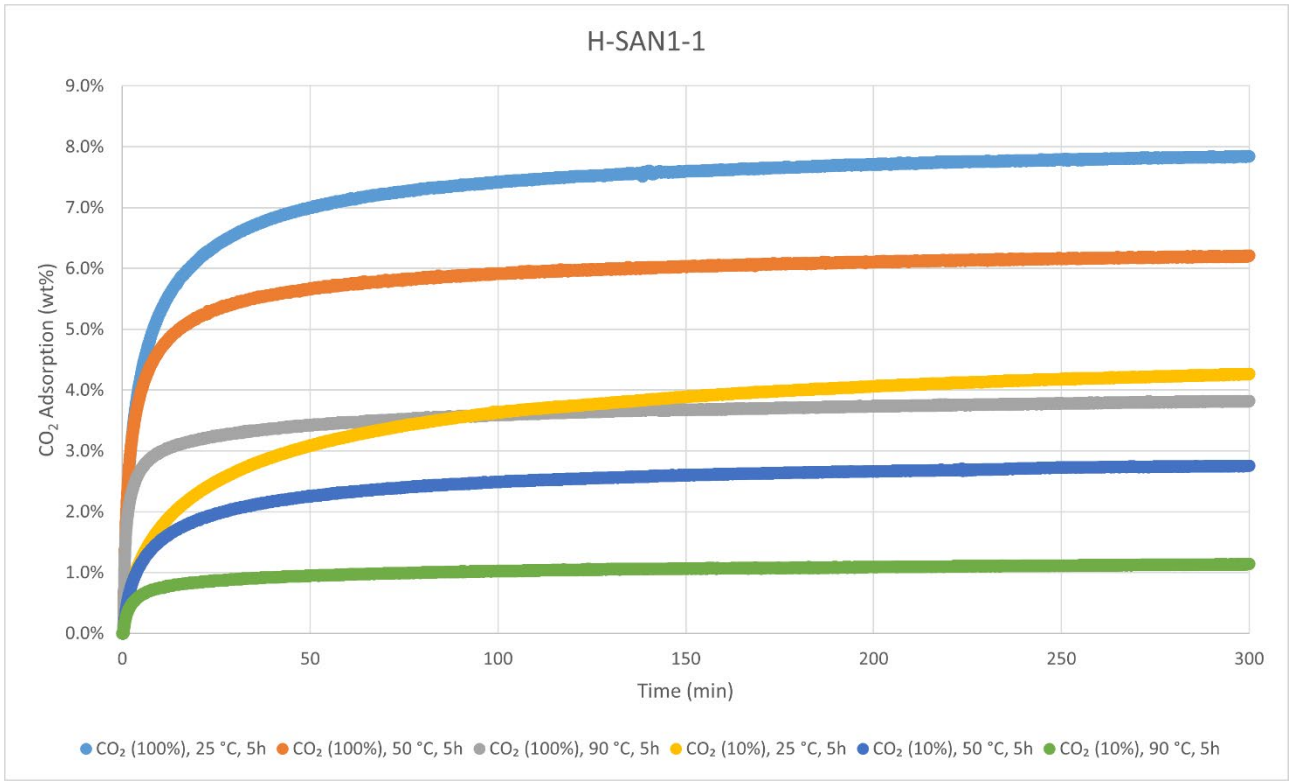

CO_2 adsorption using **TGA method 2** (measurement of product batch from run 1: H-SAN1-1).

H-SAN1-1	wt%	mmol/g
CO_2 (100%), 25 °C, 5h	7.8%	1.78
CO_2 (100%), 50 °C, 5h	6.2%	1.41
CO_2 (100%), 90 °C, 5h	3.8%	0.87
CO_2 (10%), 25 °C, 5h	4.3%	0.97
CO_2 (10%), 50 °C, 5h	2.8%	0.63
CO_2 (10%), 90 °C, 5h	1.1%	0.26

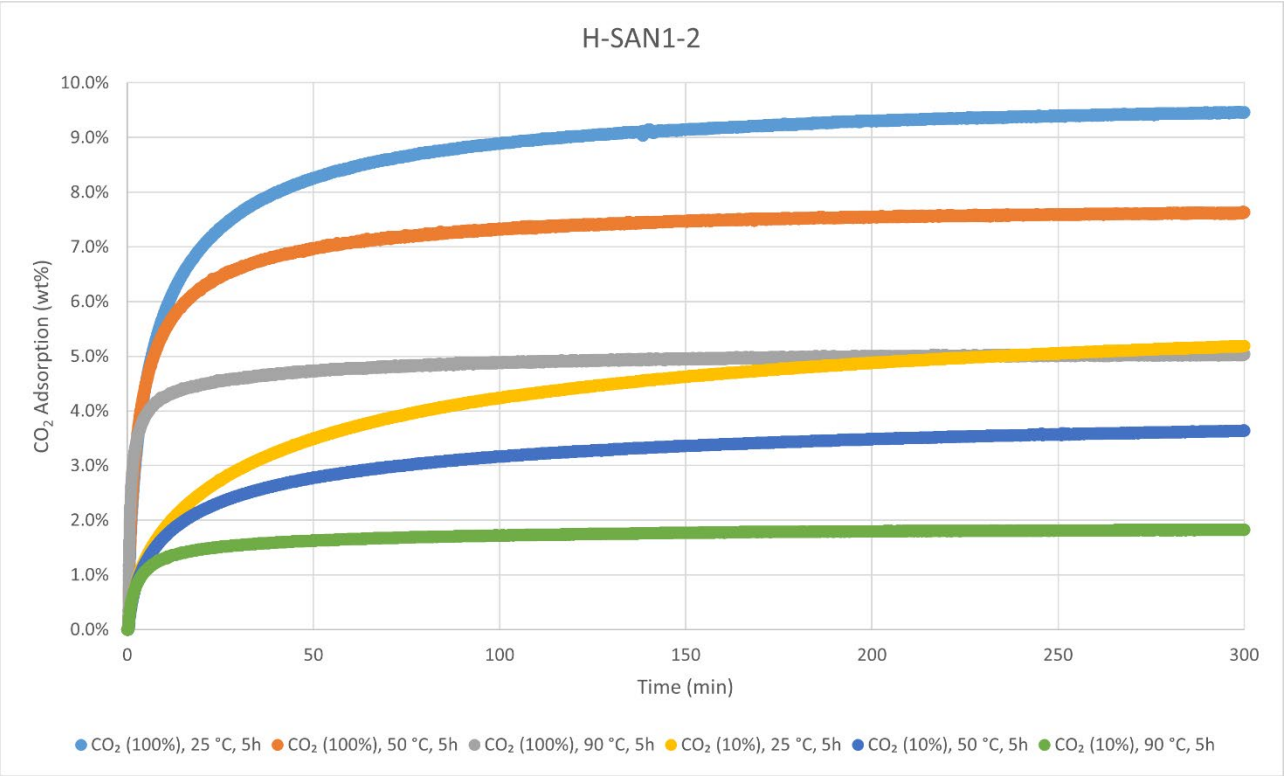

CO_2 adsorption using **TGA method 2** (measurement of product batch from run 2: H-SAN1-2).

H-SAN1-2	wt%	mmol/g
CO_2 (100%), 25 °C, 5h	9.5%	2.15
CO_2 (100%), 50 °C, 5h	7.6%	1.74
CO_2 (100%), 90 °C, 5h	5.0%	1.14
CO_2 (10%), 25 °C, 5h	5.2%	1.18
CO_2 (10%), 50 °C, 5h	3.6%	0.83
CO_2 (10%), 90 °C, 5h	1.8%	0.42

Elemental Analysis (EA)

	N [%]	C [%]	H [%]	S [%]	mmol N/g	C/N ratio	C/H ratio
run 1	**5.84**	**79.42**	**8.70**	**Not detected**	**4.17**	**15.87**	**0.77**
run 2	**6.01**	**81.28**	**8.90**		**4.29**	**15.76**	**0.77**

Hydrogenated Styrene Acrylonitrile 2 (H-SAN2) was synthesised according to the General Procedure B from substrate **SAN2** (Tandex® toothbrush) and was obtained in weight yields of 977 mg, 98 wt% and 989 mg, 99 wt%, respectively, from two independent runs (98 wt% on average). The polymer was analysed with solid-state ^{13}C CP/MAS NMR, IR-, TGA-, DSC-, and Elemental Analysis. Solubility tests were also conducted with several solvents. No thermal events besides decomposition were observed with DSC.

Particle size after cryogenic milling used for CO_2 adsorption-desorption experiments

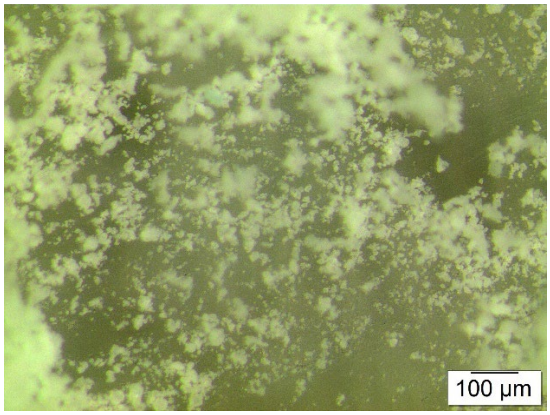

Solubility chart

Soluble **Swells** **Not soluble**

$CHCl_3$	Acetone	*i*-PrOH	DMF	DMSO	THF	PhMe	H_2O	MeOH	MeCN

^{13}C CP/MAS NMR (solid-state)

*Solid-state ^{13}C–NMR of **H-SAN2** (run 1):*

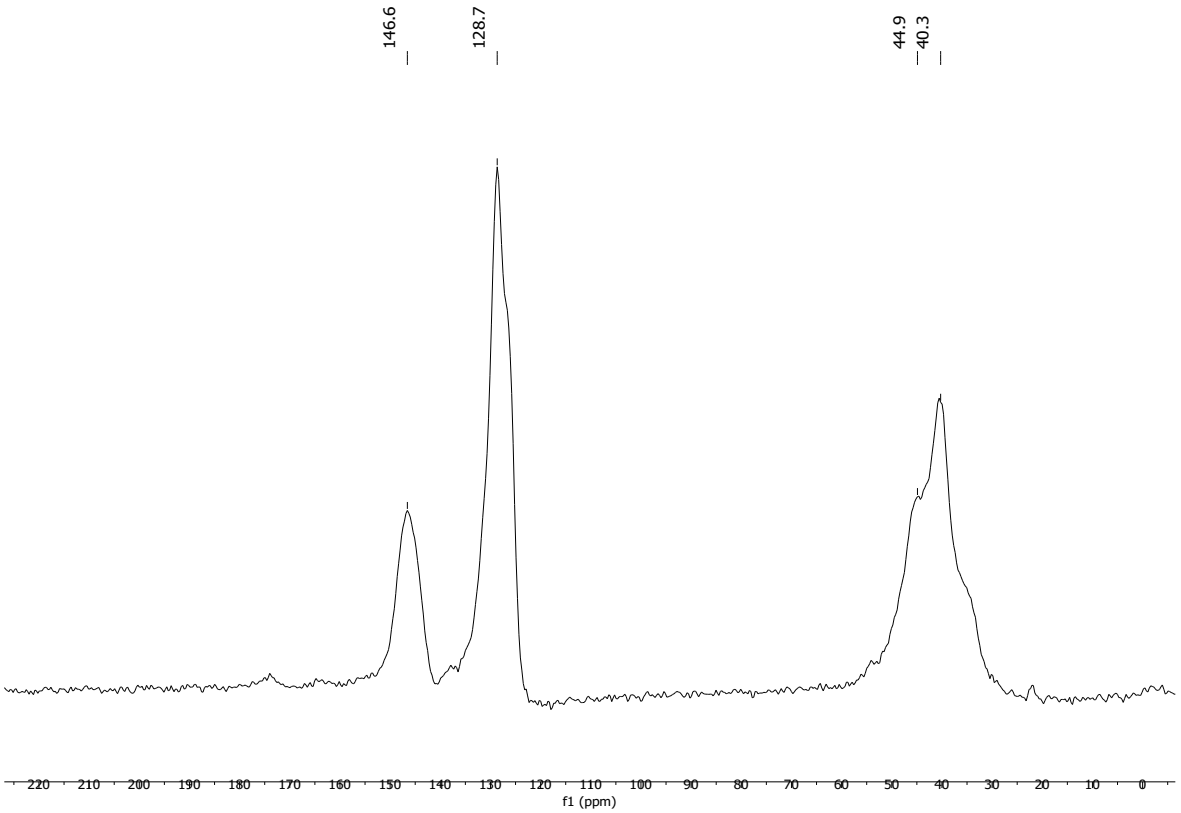

*Solid-state ^{13}C–NMR of **H-SAN2** (run 2):*

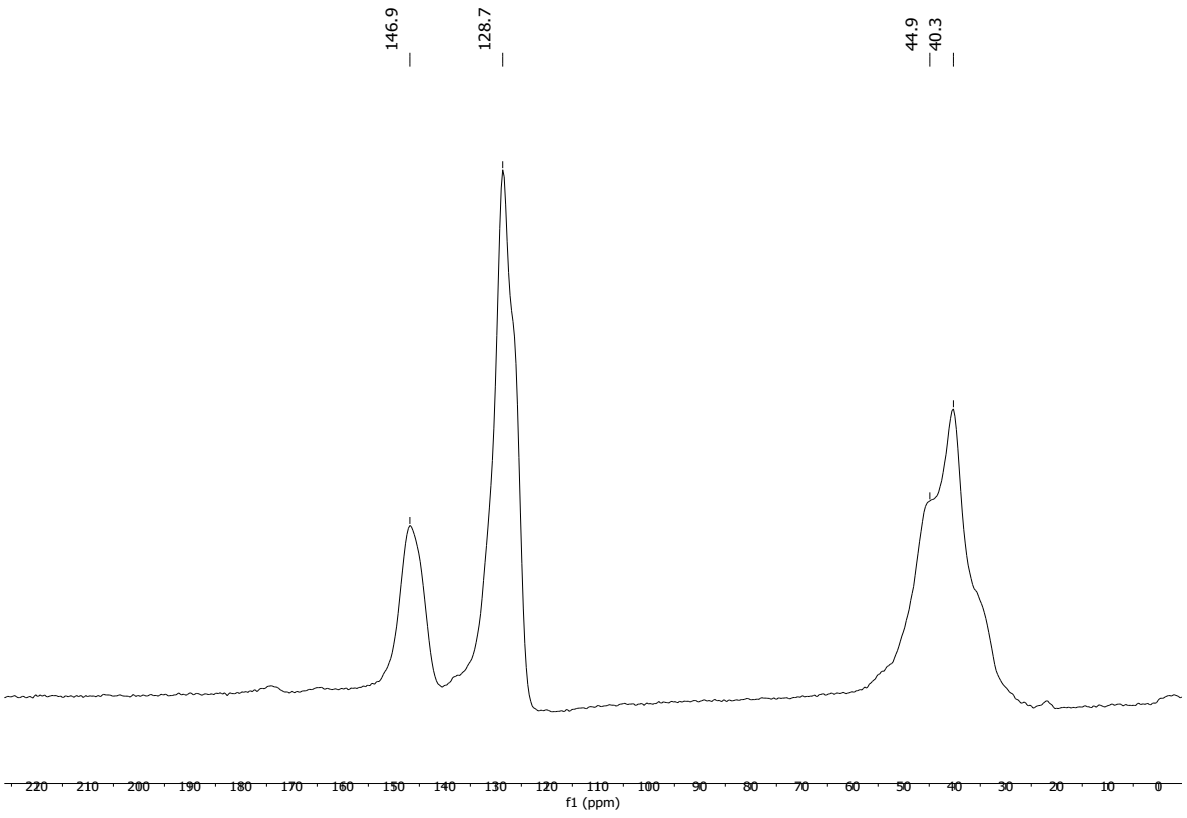

*Solid-state ^{13}C–NMR stacked spectra of **H-SAN2** (run 1, **brown**) and **SAN2** (substrate, **light blue**):*

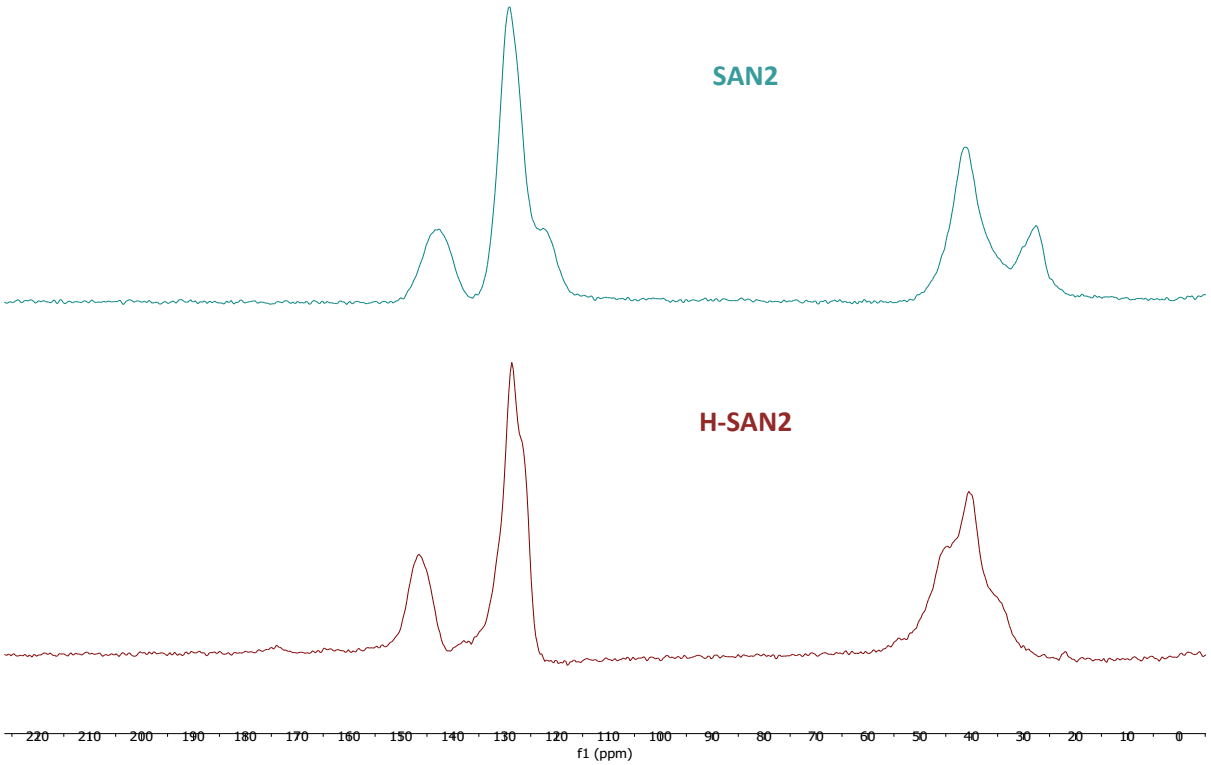

Infrared (IR) Spectroscopic Analysis

*IR-spectrum of **H-SAN2** (run 1):*

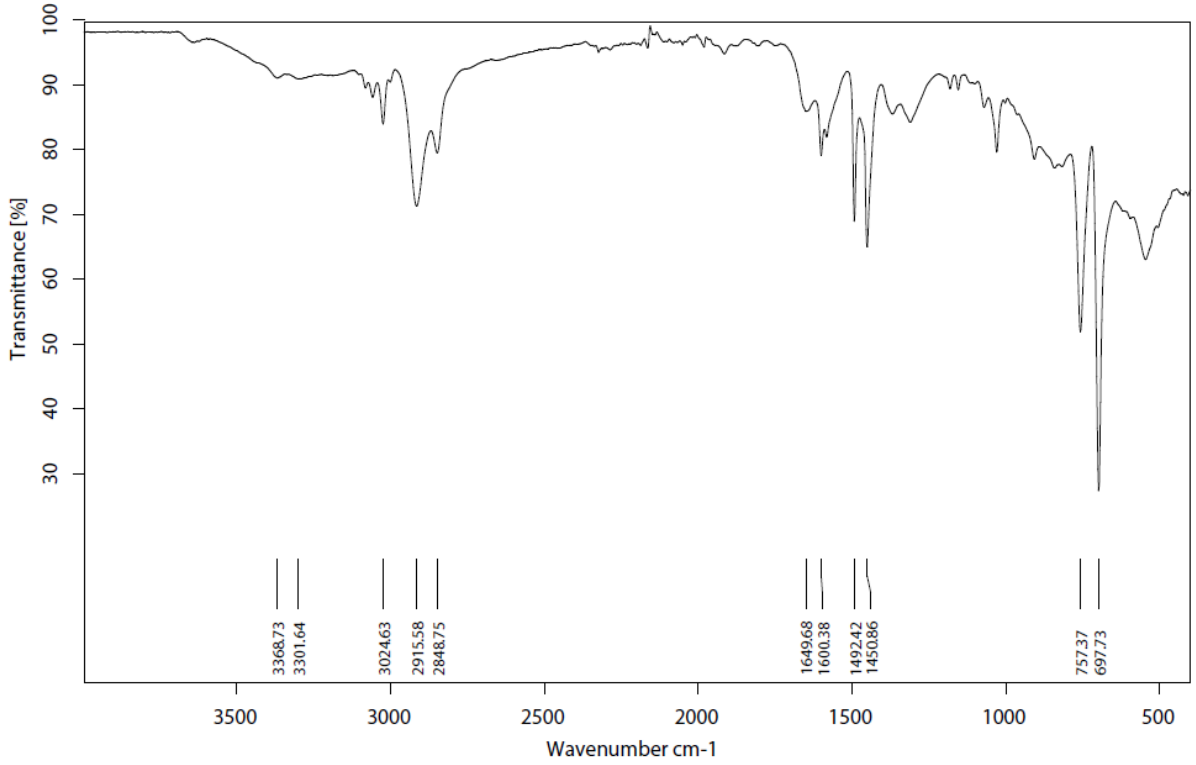

*IR-spectrum of **H-SAN2** (run 2):*

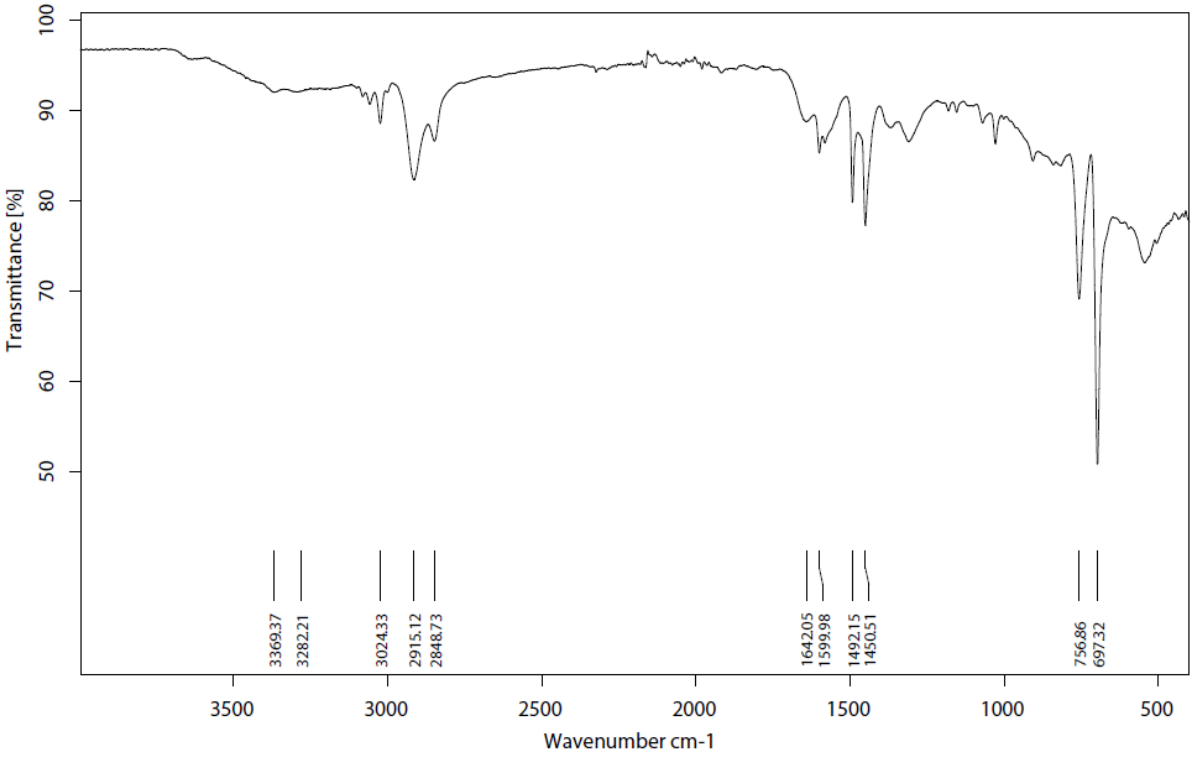

*IR-spectrum overlay of **H-SAN2** (run 1, **black**) and **SAN2** (substrate, **red**):*

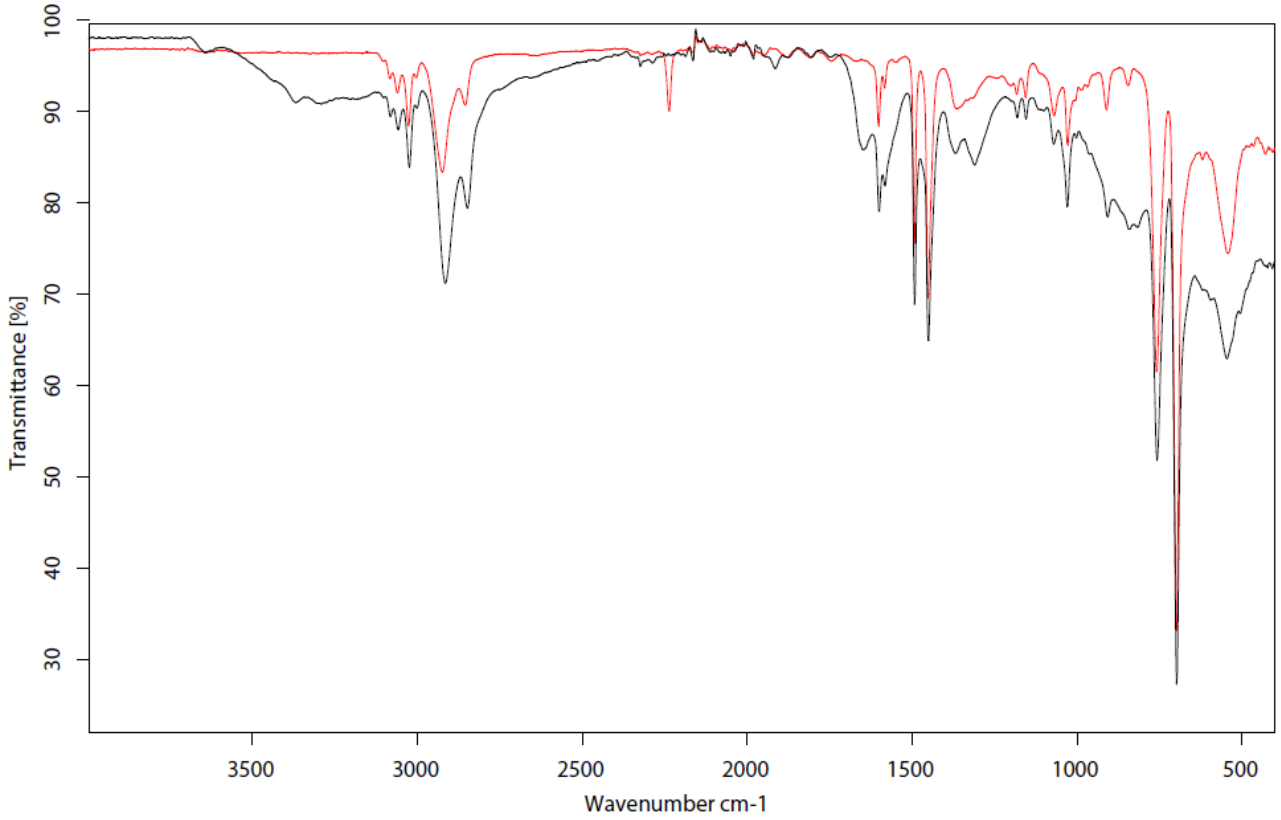

Thermogravimetric Analysis (TGA)

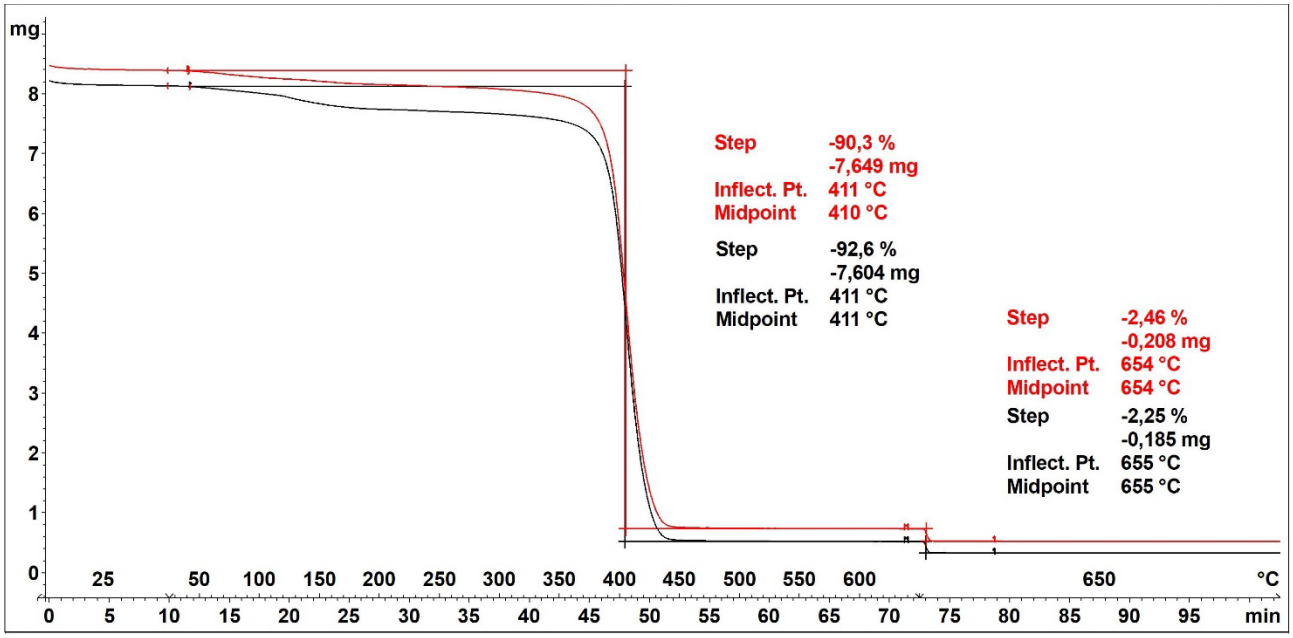

Decomposition graph. The experiment was conducted under He then air (after 650 °C). The black curve is the result from run 1, while the red curve is for run 2.

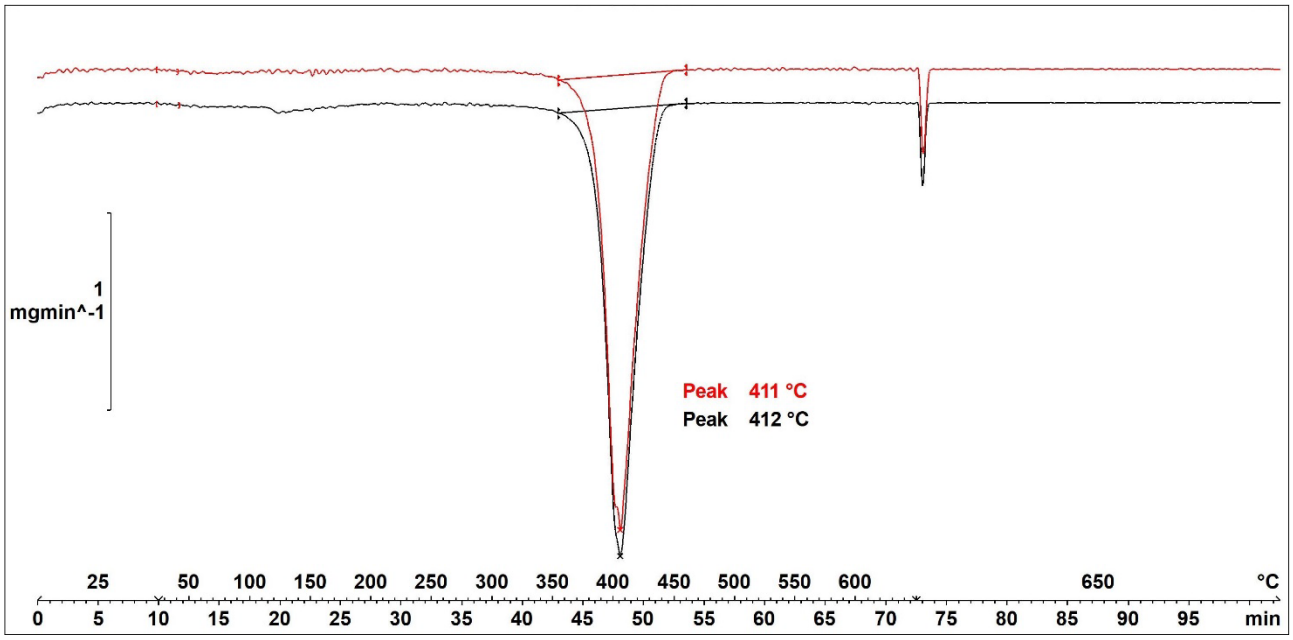

1st derivative of decomposition graph. The experiment was conducted under He then air (after 650 °C). The black curve is the result from run 1, while the red curve is for run 2.

Decomposition temperature (T_d) = 411−412 ℃.

CO_2-adsorption analysis by thermogravimetric analysis

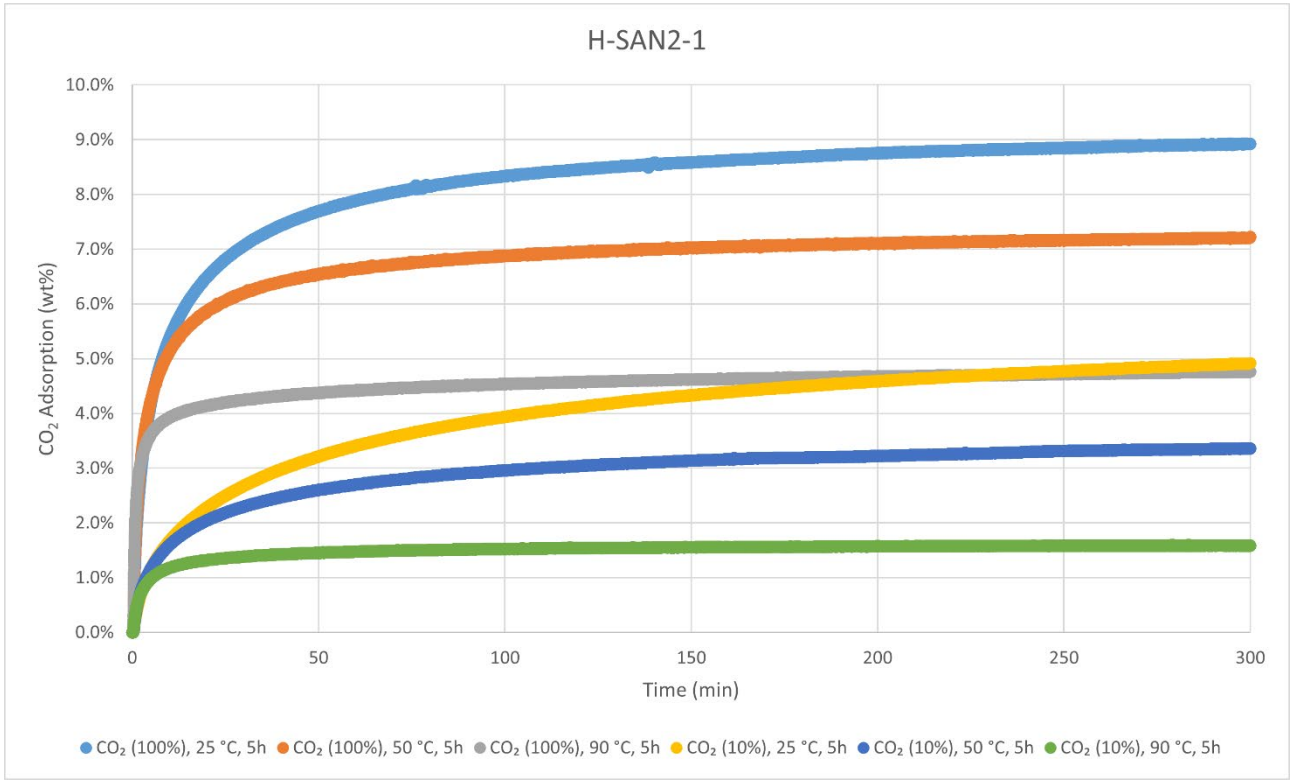

CO_2 adsorption using **TGA method 2** (measurement of product batch from run 1: H-SAN2-1).

H-SAN2-1	wt%	mmol/g
CO_2 (100%), 25 °C, 5h	8.9%	2.03
CO_2 (100%), 50 °C, 5h	7.2%	1.64
CO_2 (100%), 90 °C, 5h	4.8%	1.08
CO_2 (10%), 25 °C, 5h	4.9%	1.12
CO_2 (10%), 50 °C, 5h	3.4%	0.76
CO_2 (10%), 90 °C, 5h	1.6%	0.36

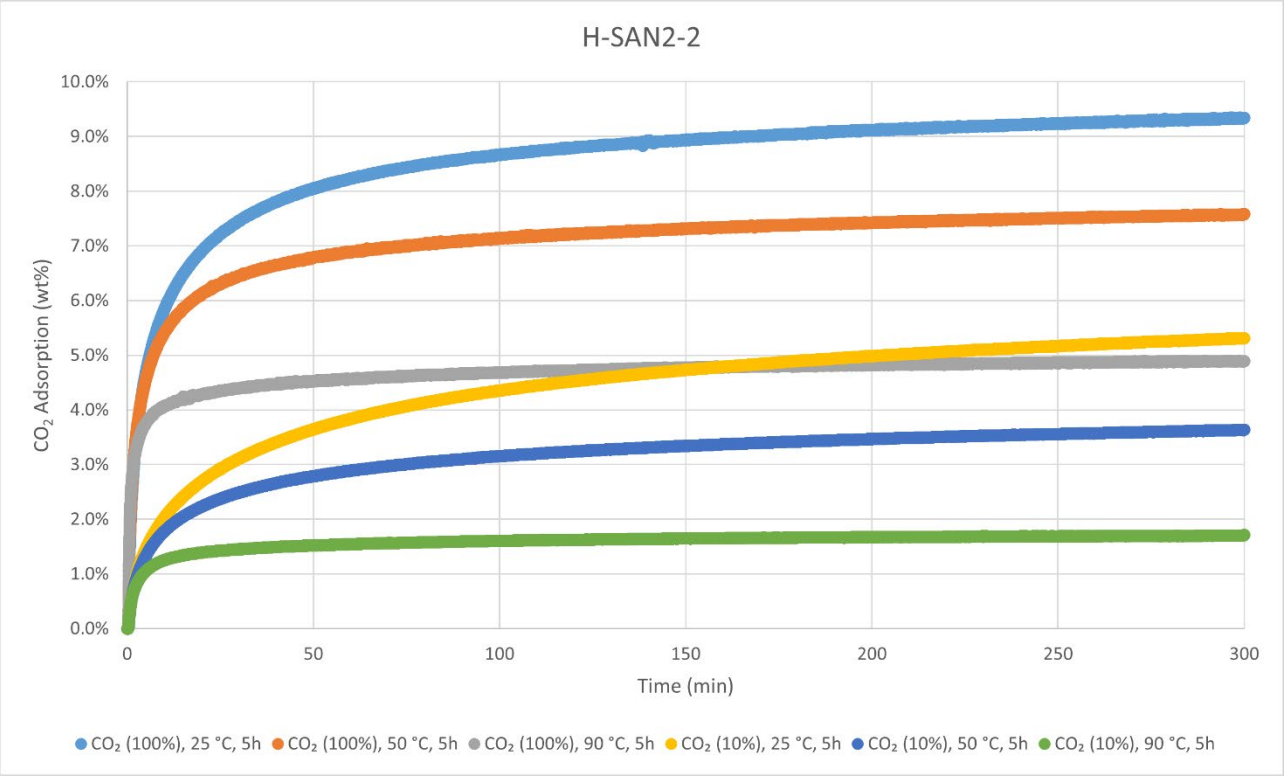

CO_2 adsorption using **TGA method 2** (measurement of product batch from run 2: H-SAN2-2).

H-SAN2-2	wt%	mmol/g
CO_2 (100%), 25 °C, 5h	9.3%	2.12
CO_2 (100%), 50 °C, 5h	7.6%	1.72
CO_2 (100%), 90 °C, 5h	4.9%	1.11
CO_2 (10%), 25 °C, 5h	5.3%	1.21
CO_2 (10%), 50 °C, 5h	3.6%	0.83
CO_2 (10%), 90 °C, 5h	1.7%	0.39

Elemental Analysis (EA)

	N [%]	C [%]	H [%]	S [%]	mmol N/g	C/N ratio	C/H ratio
run 1	**5.82**	**79.71**	**8.67**	**Not detected**	**4.16**	**15.97**	**0.77**
run 2	**5.93**	**80.59**	**8.89**		**4.24**	**15.84**	**0.76**

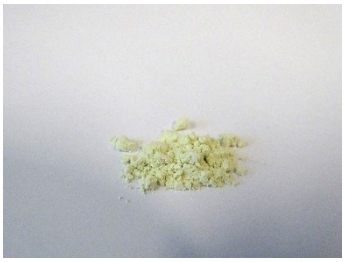

Hydrogenated Mixture of ABS and SAN (H-MIX1) was synthesised according to the General Procedure B from a 1 g mixture of **ABS1** (LEGO® bricks), **ABS2** (Fujitsu® keyboard tabs), **SAN1** (plastic beaker), and **SAN2** (Tandex® toothbrush) (250 mg of each). The polymer product was obtained in weight yields of 518 mg, 52 wt% and 668 mg, 67 wt%, respectively, from two independent runs (59 wt% on average). The polymer was analysed with solid-state ^{13}C CP/MAS NMR, IR-, TGA-, DSC-, and Elemental Analysis. Solubility tests were also conducted with several solvents. No thermal events besides decomposition were observed with DSC.

Particle size after cryogenic milling used for CO_2 adsorption-desorption experiments

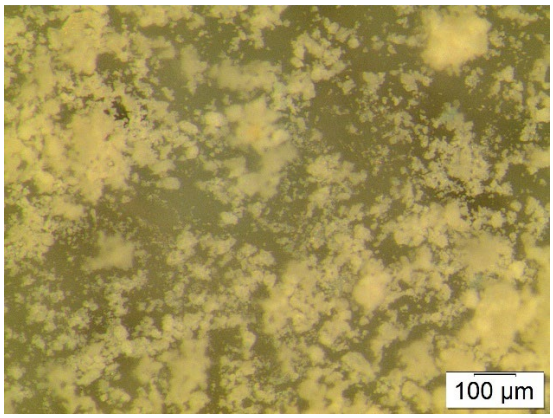

Solubility chart

Soluble **Swells** **Not soluble**

$CHCl_3$	Acetone	*i*-PrOH	DMF	DMSO	THF	PhMe	H_2O	MeOH	MeCN

^{13}C CP/MAS NMR (solid-state)

*Solid-state ^{13}C–NMR of **H-MIX1** (run 1):*

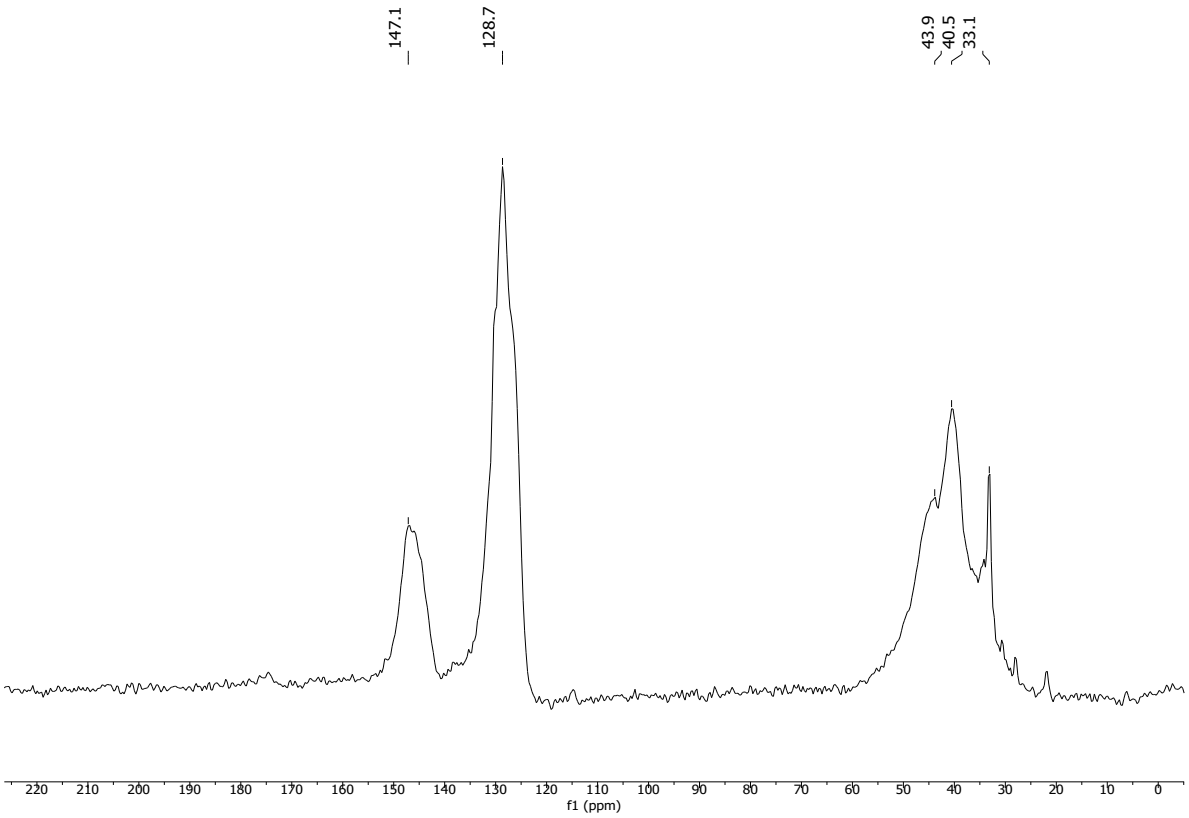

*Solid-state ^{13}C–NMR of **H-MIX1** (run 2):*

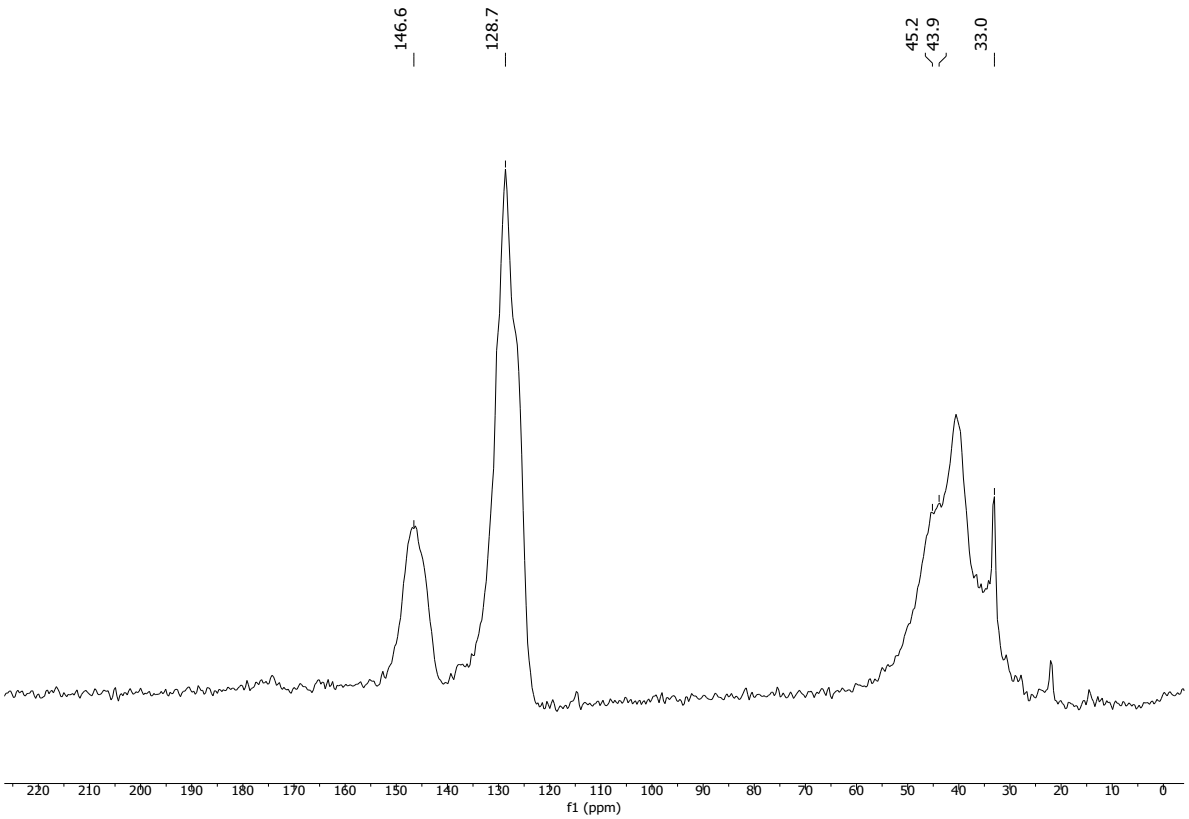

*Solid-state ^{13}C–NMR stacked spectra of **H-MIX1** (run 1, **brown**) and **ABS1** (**olive**), **ABS2** (**emerald**), **SAN1** (**blue**), and **SAN2** (**purple**):*

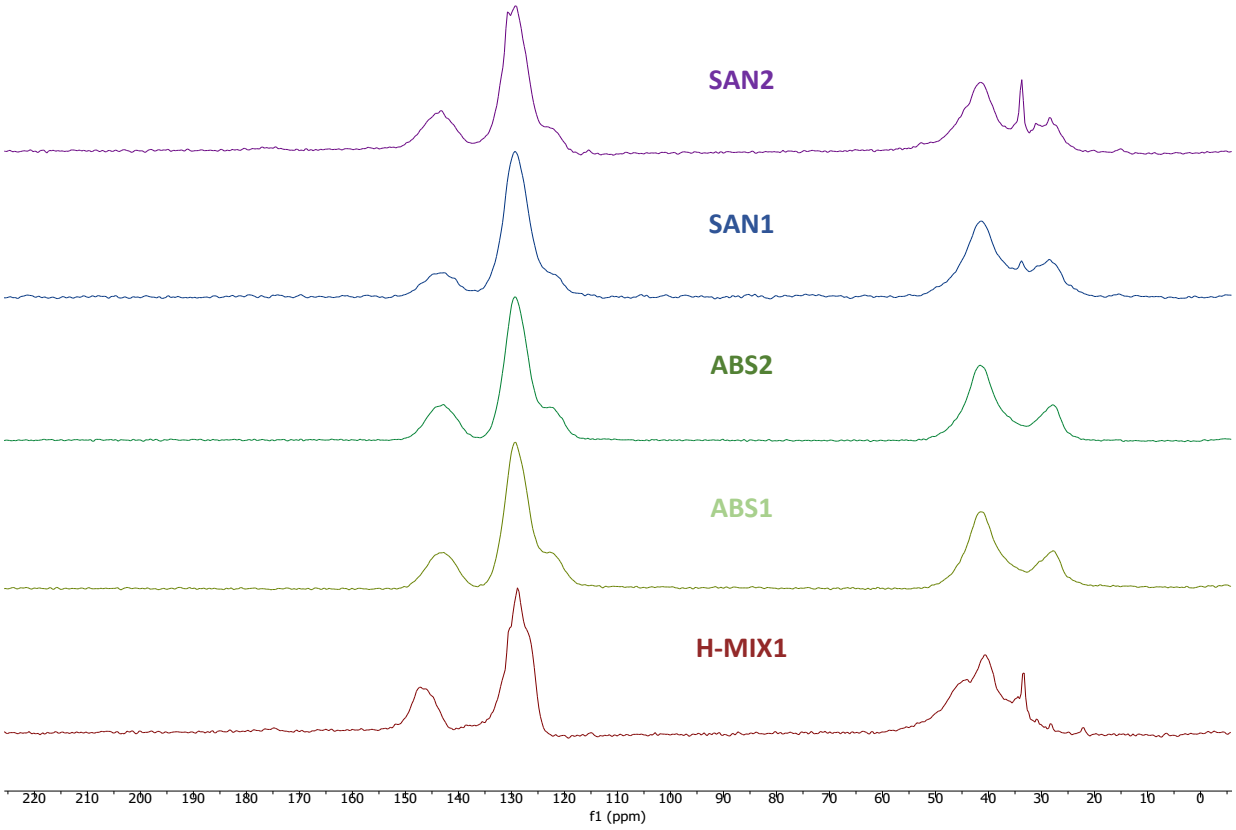

Infrared (IR) Spectroscopic Analysis

*IR-spectrum of **H-MIX1** (run 1):*

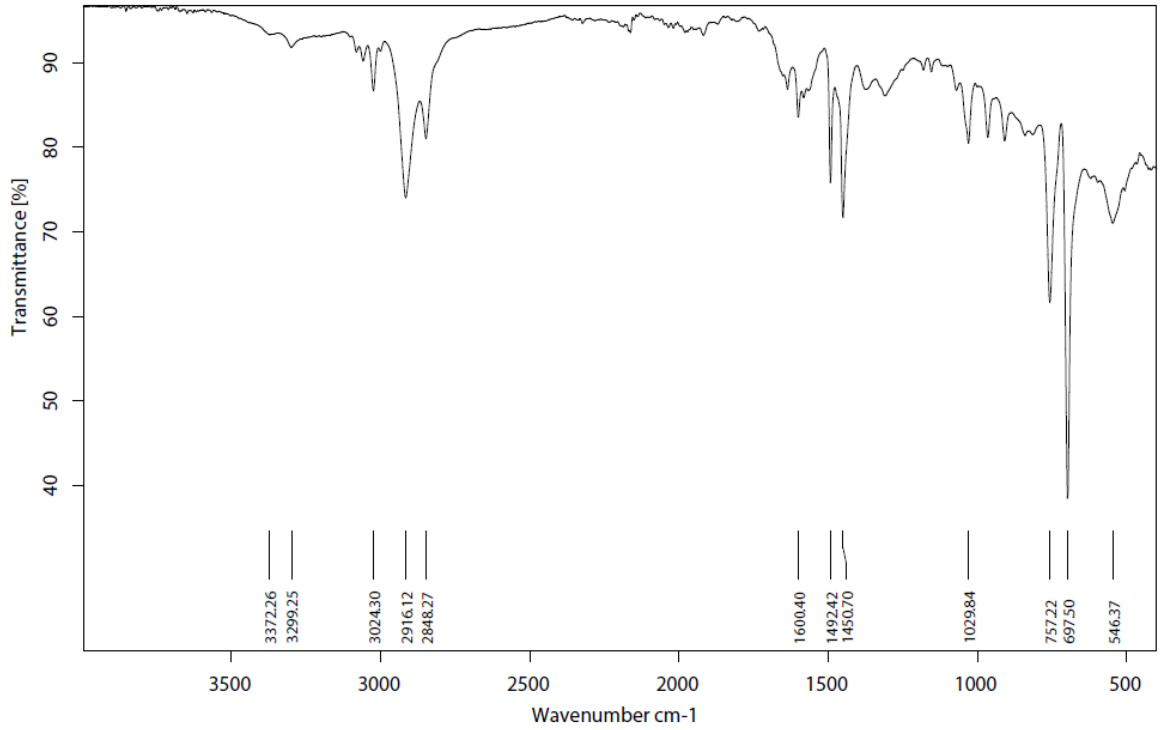

*IR-spectrum of **H-MIX2** (run 2):*

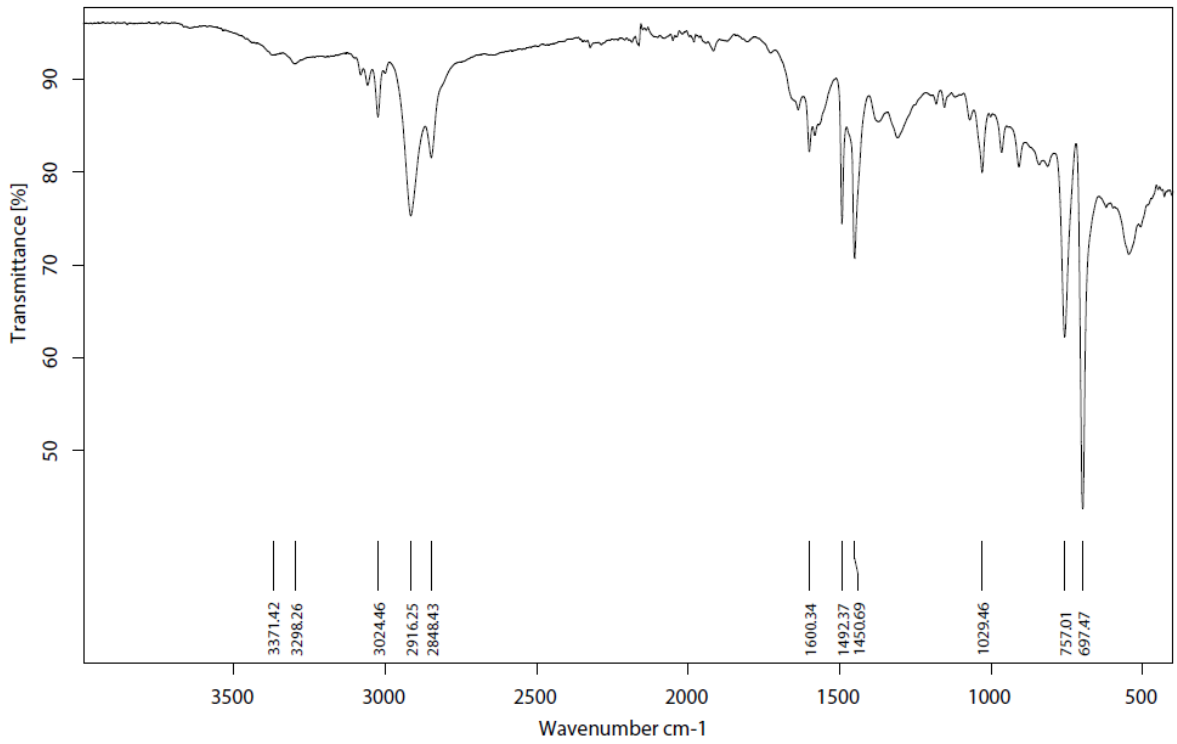

*IR-spectrum overlay of **H-MIX1** (run 1, **black**) and **ABS1** (**red**), **ABS2** (**blue**), **SAN1** (**brown**), and **SAN2** (**purple**):*

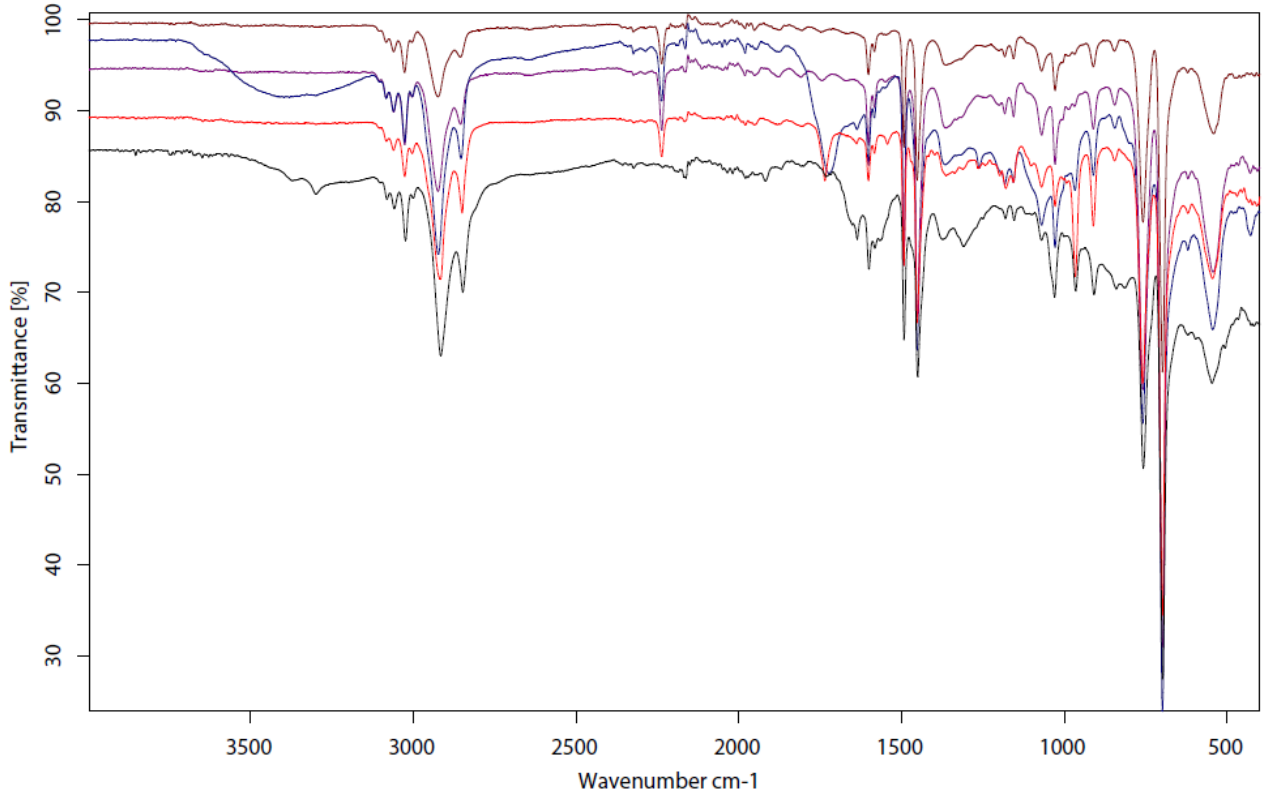

Thermogravimetric Analysis (TGA)

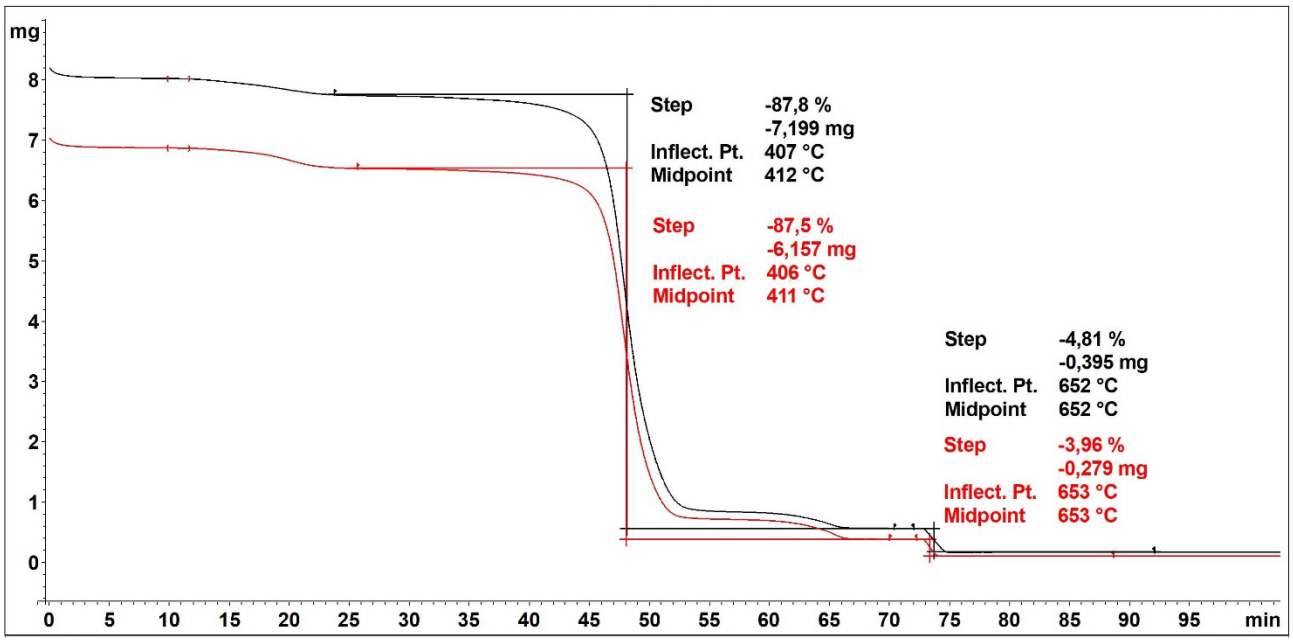

Decomposition graph. The experiment was conducted under He then air (after 650 °C). The black curve is the result from run 1, while the red curve is for run 2.

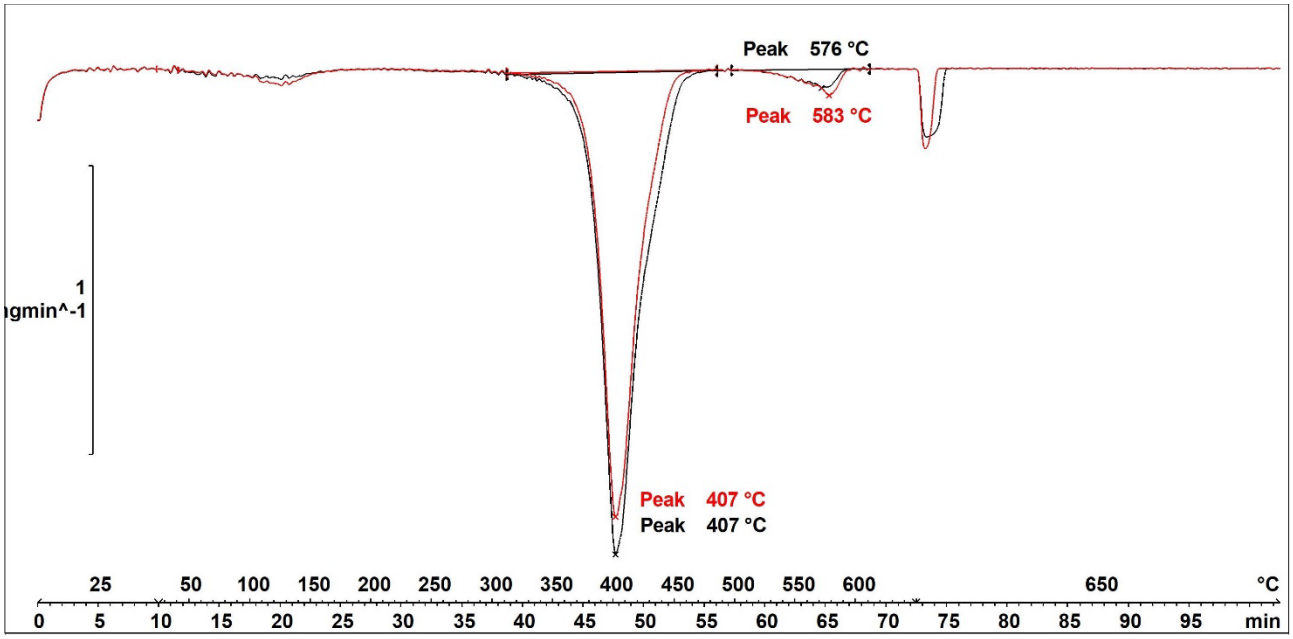

1st derivative of decomposition graph. The experiment was conducted under He then air (after 650 °C). The black curve is the result from run 1, while the red curve is for run 2.

Decomposition temperature (T_d) = 407 ℃.

CO_2-adsorption analysis by thermogravimetric analysis

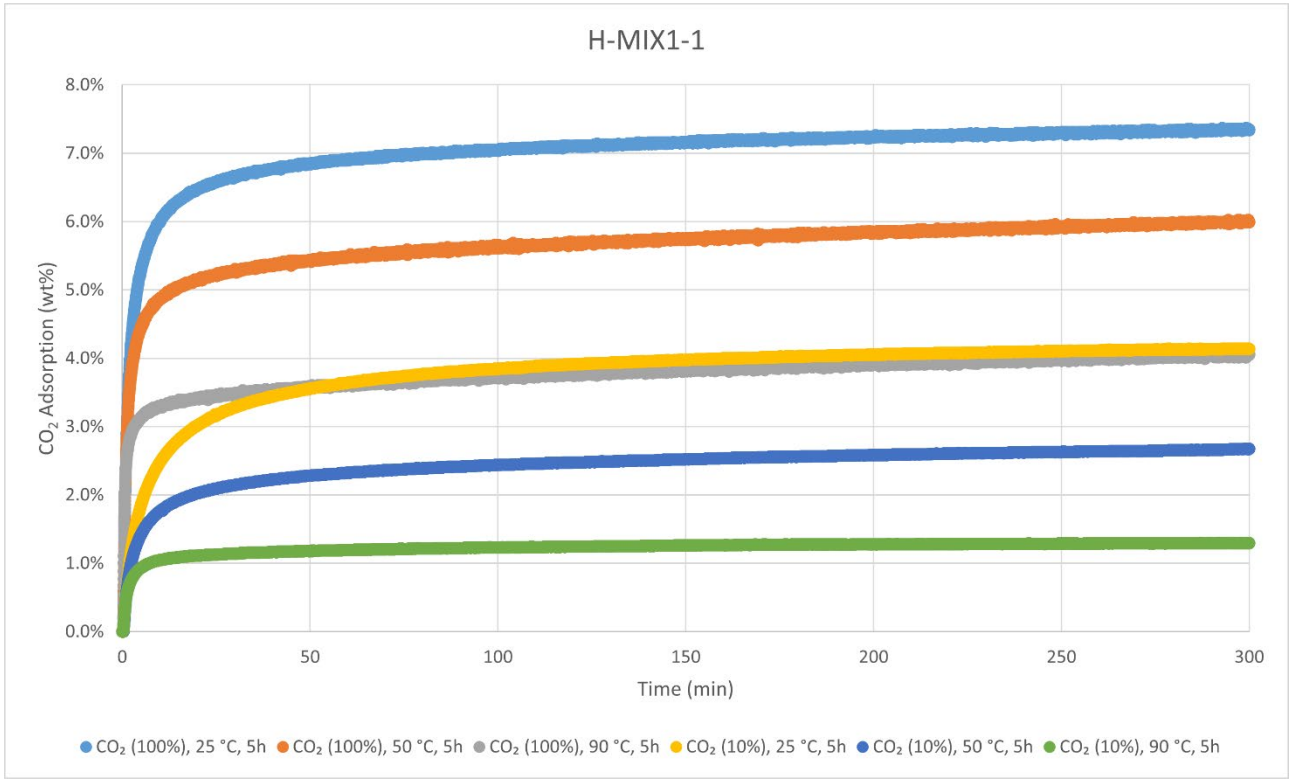

CO_2 adsorption using **TGA method 2** (measurement of product batch from run 1: H-MIX1-1).

H-MIX1-1	wt%	mmol/g
CO_2 (100%), 25 °C, 5h	7.3%	1.67
CO_2 (100%), 50 °C, 5h	6.0%	1.36
CO_2 (100%), 90 °C, 5h	4.1%	0.92
CO_2 (10%), 25 °C, 5h	4.1%	0.94
CO_2 (10%), 50 °C, 5h	2.7%	0.61
CO_2 (10%), 90 °C, 5h	1.3%	0.29

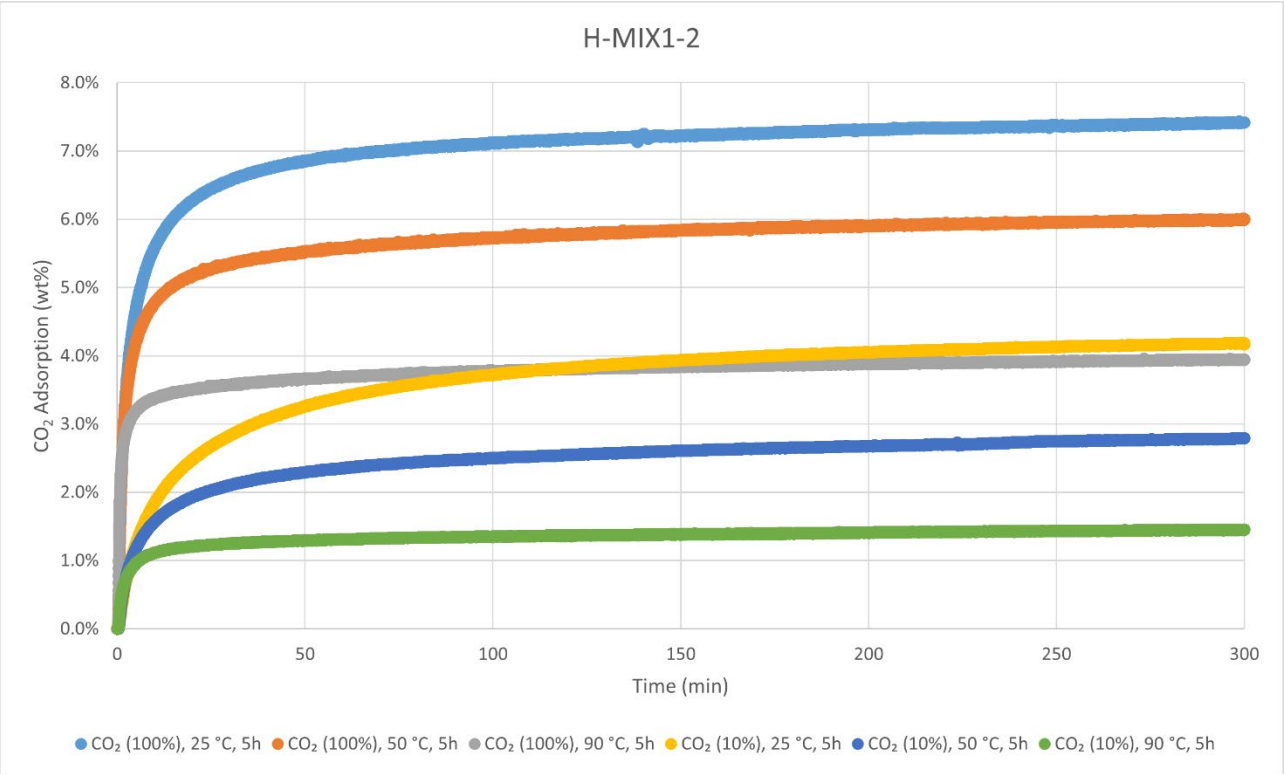

CO_2 adsorption using **TGA method 2** (measurement of product batch from run 2: H-MIX1-2).

H-MIX1-2	wt%	mmol/g
CO_2 (100%), 25 °C, 5h	7.4%	1.69
CO_2 (100%), 50 °C, 5h	6.0%	1.36
CO_2 (100%), 90 °C, 5h	3.9%	0.90
CO_2 (10%), 25 °C, 5h	4.2%	0.95
CO_2 (10%), 50 °C, 5h	2.8%	0.63
CO_2 (10%), 90 °C, 5h	1.5%	0.33

Elemental Analysis (EA)

	N [%]	C [%]	H [%]	S [%]	mmol N/g	C/N ratio	C/H ratio
run 1	**4.95**	**78.56**	**8.62**	**Not detected**	**3.54**	**18.49**	**0.77**
run 2	**4.89**	**78.42**	**8.62**		**3.49**	**18.69**	**0.76**

Polymer Products from Hydrogenation of Acrylic Textiles

Hydrogenated Acrylic yarn (H-TEX1) was synthesised according to the General Procedure C from substrate **TEX1** (White yarn) and was obtained in weight yields of 39.8 mg, 80 wt% and 32.4 mg, 65 wt%, respectively, from two independent runs (72 wt% on average). The polymer was analysed with solid-state ^{13}C CP/MAS NMR, IR-, TGA-, DSC-, and Elemental Analysis. Solubility tests were also conducted with several solvents. No thermal events besides decomposition were observed with DSC. As indicated from ^{13}C CP/MAS NMR spectroscopic analysis before/after the reaction, the material is only partly hydrogenated likely due to low/no solubility or swelling in the reaction medium.

Particle size after cryogenic milling used for CO_2 adsorption-desorption experiments

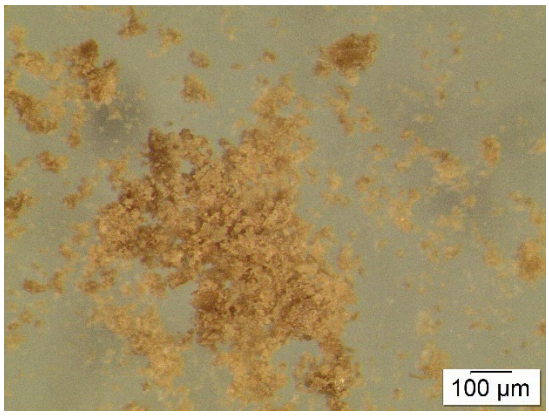

Solubility chart

Soluble **Swells** **Not soluble**

$CHCl_3$	Acetone	*i*-PrOH	DMF	DMSO	THF	PhMe	H_2O	MeOH	MeCN

^{13}C CP/MAS NMR (solid-state)

*Solid-state ^{13}C–NMR of **H-TEX1** (run 1):*

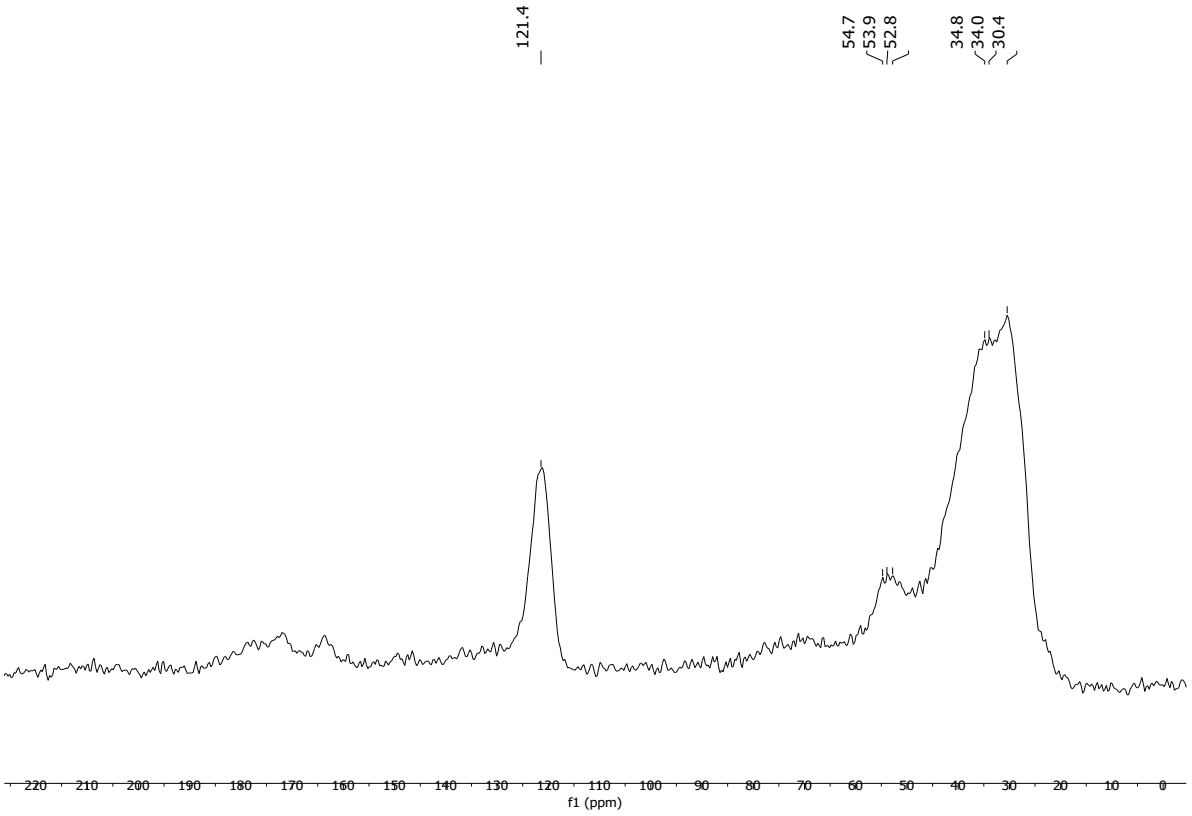

*Solid-state ^{13}C–NMR stacked spectra of **H-TEX1** (run 1, **brown**) and **TEX1** (**light blue**):*

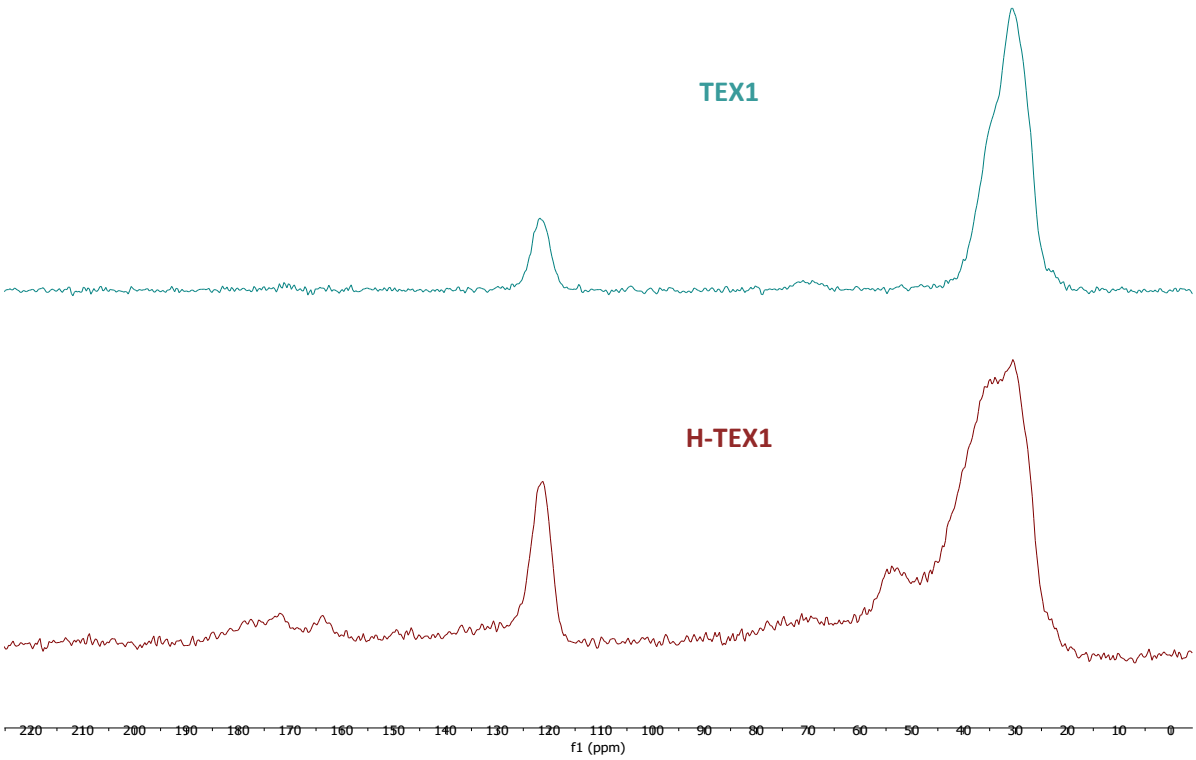

Infrared (IR) Spectroscopic Analysis

*IR-spectrum of **H-TEX1** (run 1):*

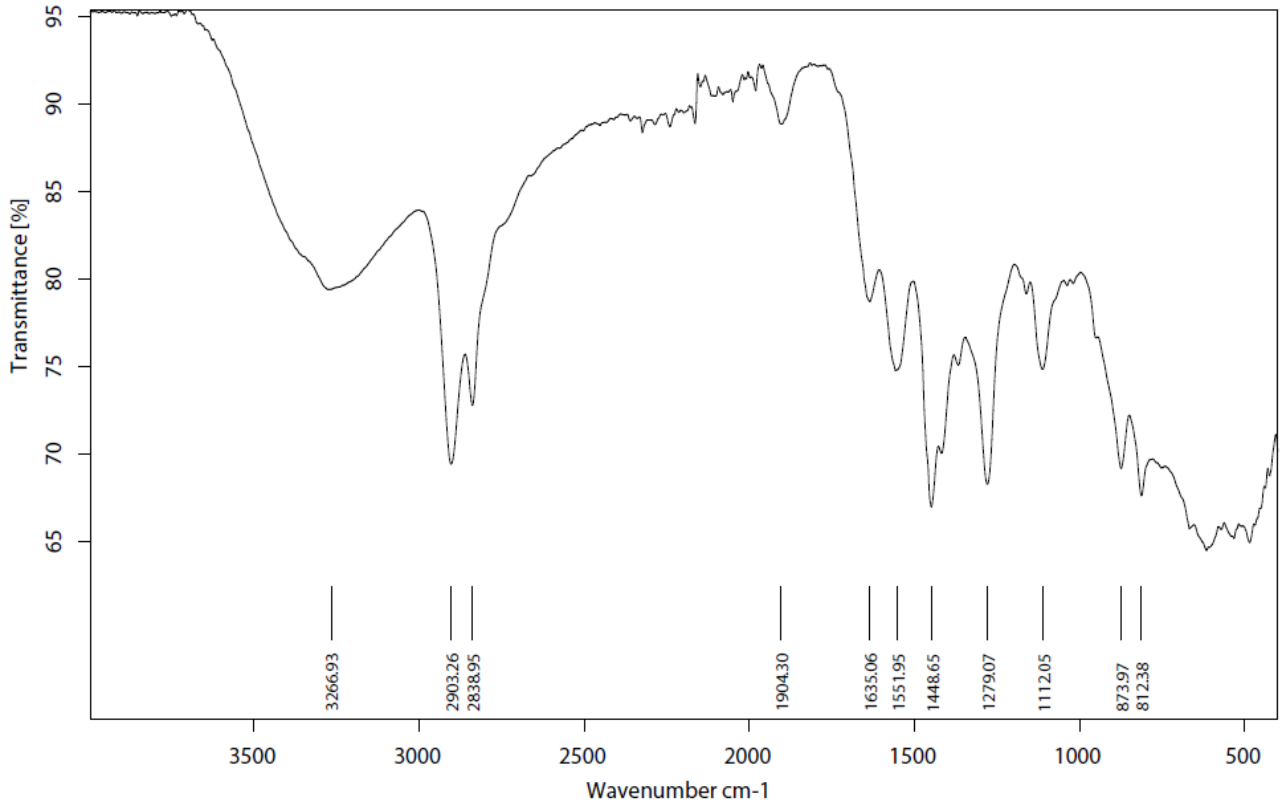

*IR-spectrum of **H-TEX1** (run 2):*

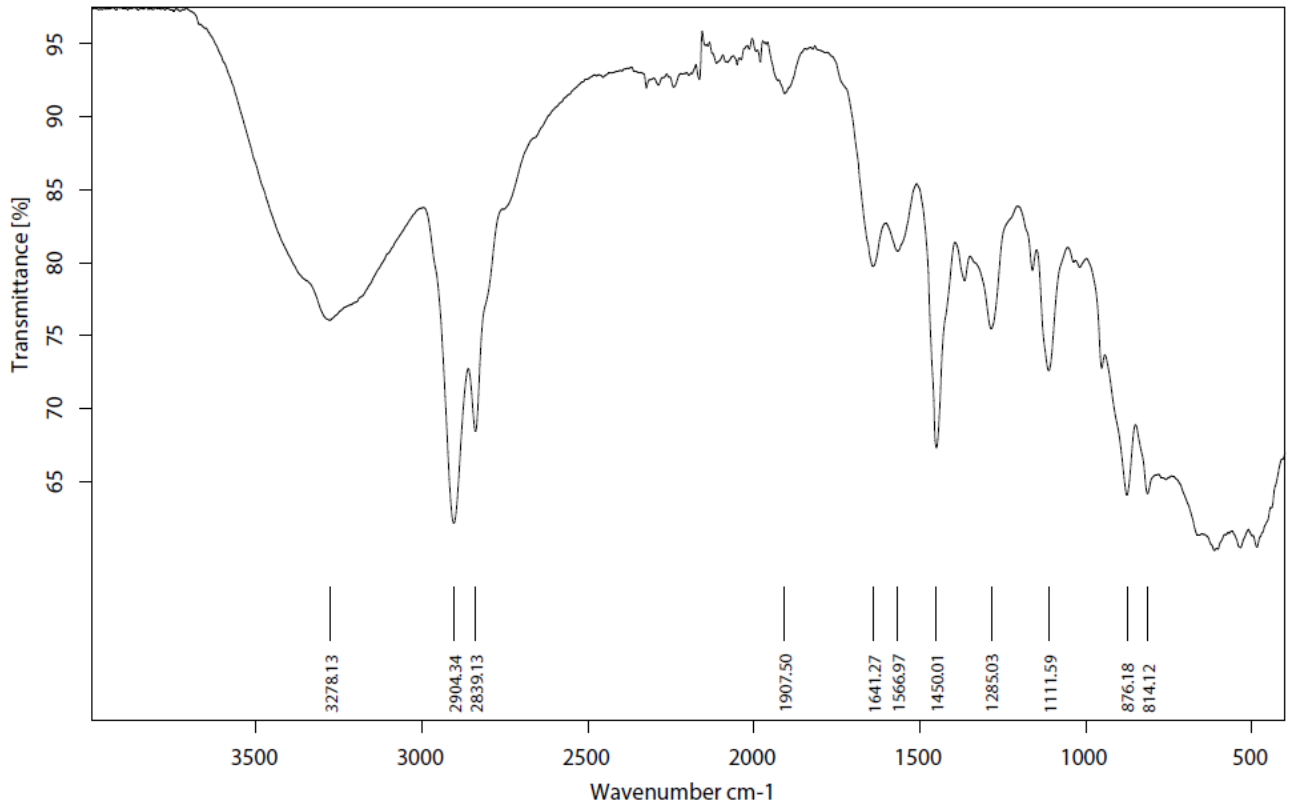

*IR-spectrum overlay of **H-TEX1** (run 1, **black**) and **TEX1** (substrate, **red**):*

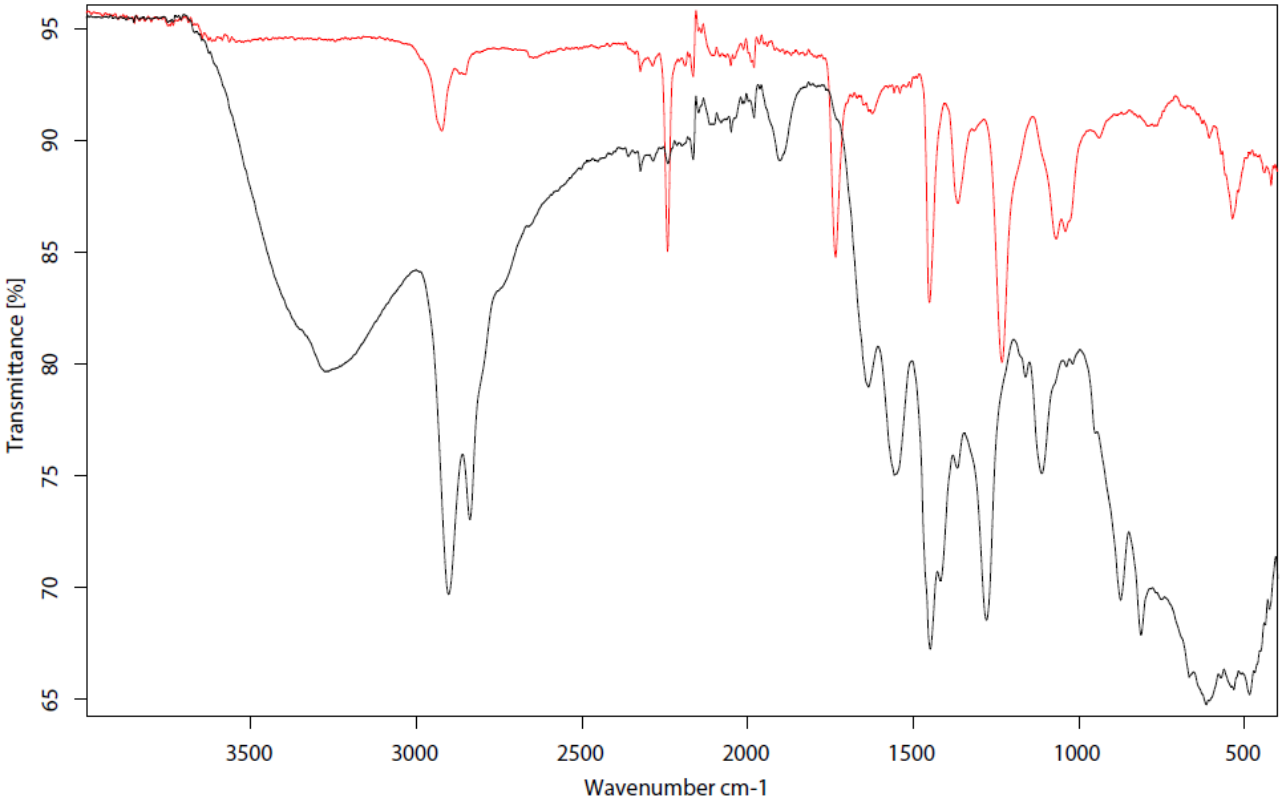

Thermogravimetric Analysis (TGA)

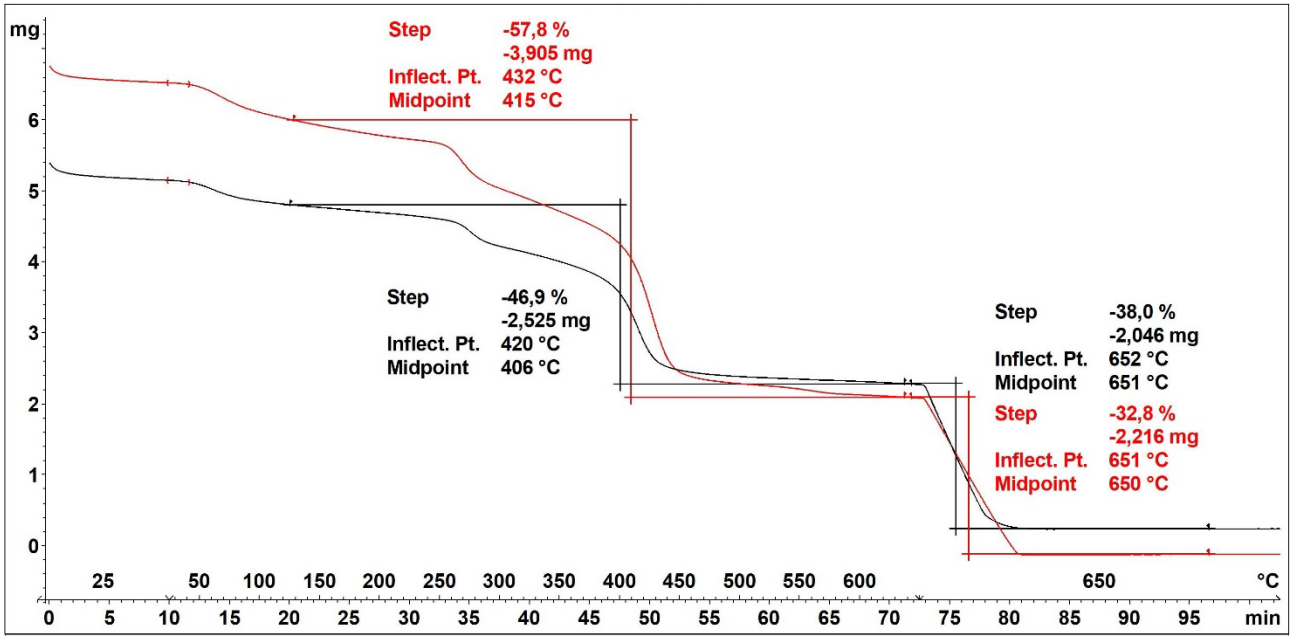

Decomposition graph. The experiment was conducted under He then air (after 650 °C). The black curve is the result from run 1, while the red curve is for run 2.

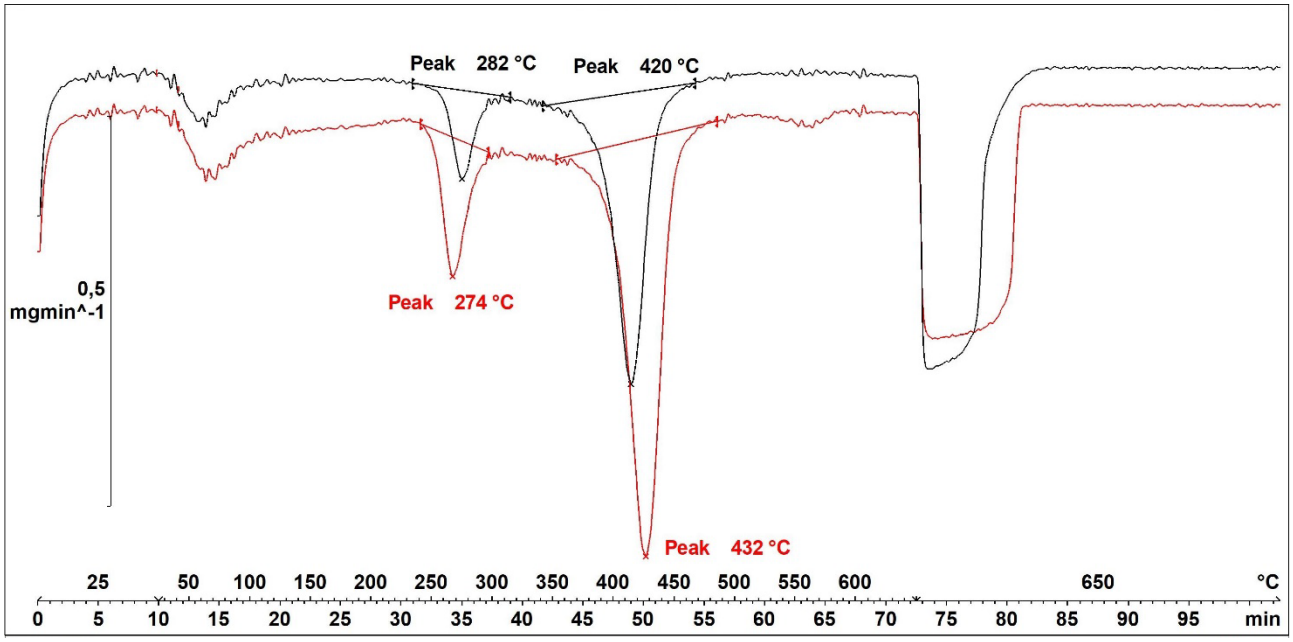

1st derivative of decomposition graph. The experiment was conducted under He then air (after 650 °C). The black curve is the result from run 1, while the red curve is for run 2. The peak at ~ 70 °C corresponds to residual MeOH.

Decomposition temperature (T_d) = 274−282 °C and 420−432 °C (two decomposition steps).

CO_2-adsorption analysis by thermogravimetric analysis

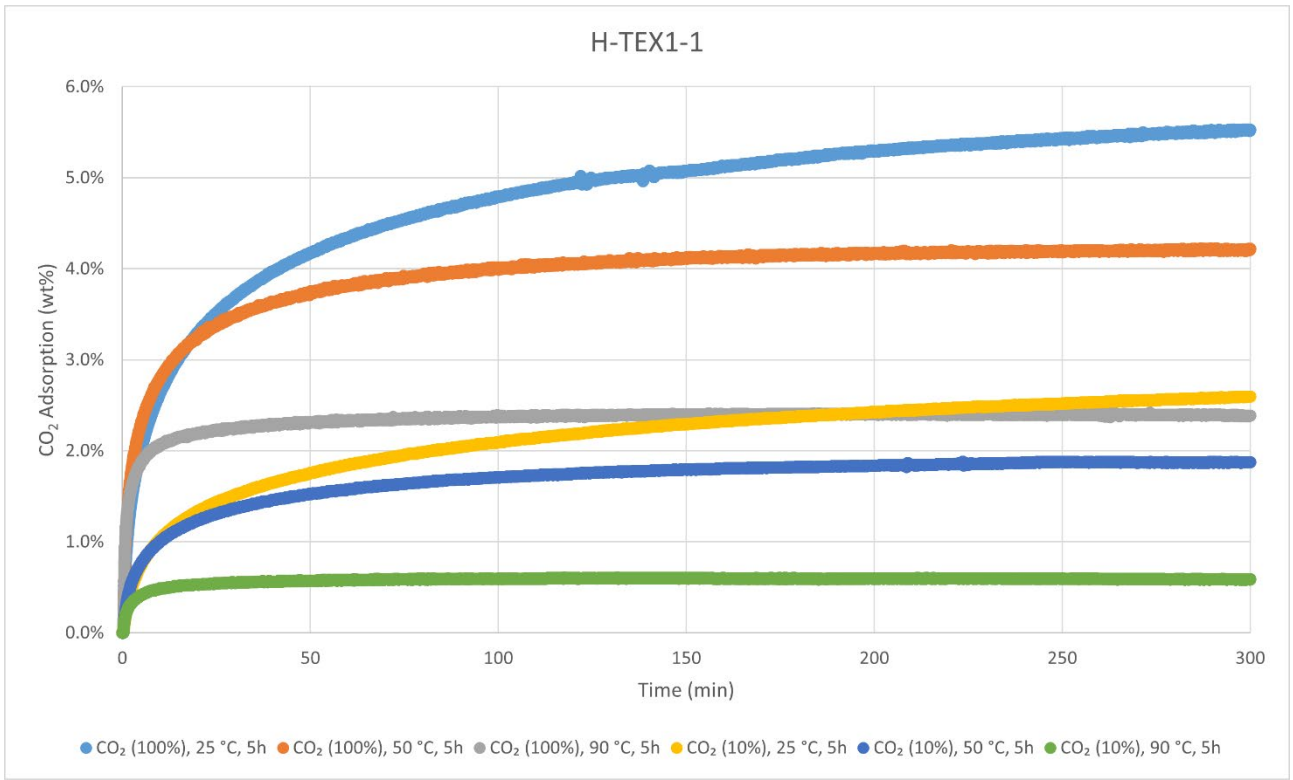

CO_2 adsorption using **TGA method 2** (measurement of product batch from run 1: H-TEX1-1).

H-TEX1-1	wt%	mmol/g
CO_2 (100%), 25 °C, 5h	5.5%	1.26
CO_2 (100%), 50 °C, 5h	4.2%	0.96
CO_2 (100%), 90 °C, 5h	2.4%	0.54
CO_2 (10%), 25 °C, 5h	2.6%	0.59
CO_2 (10%), 50 °C, 5h	1.9%	0.43
CO_2 (10%), 90 °C, 5h	0.6%	0.13

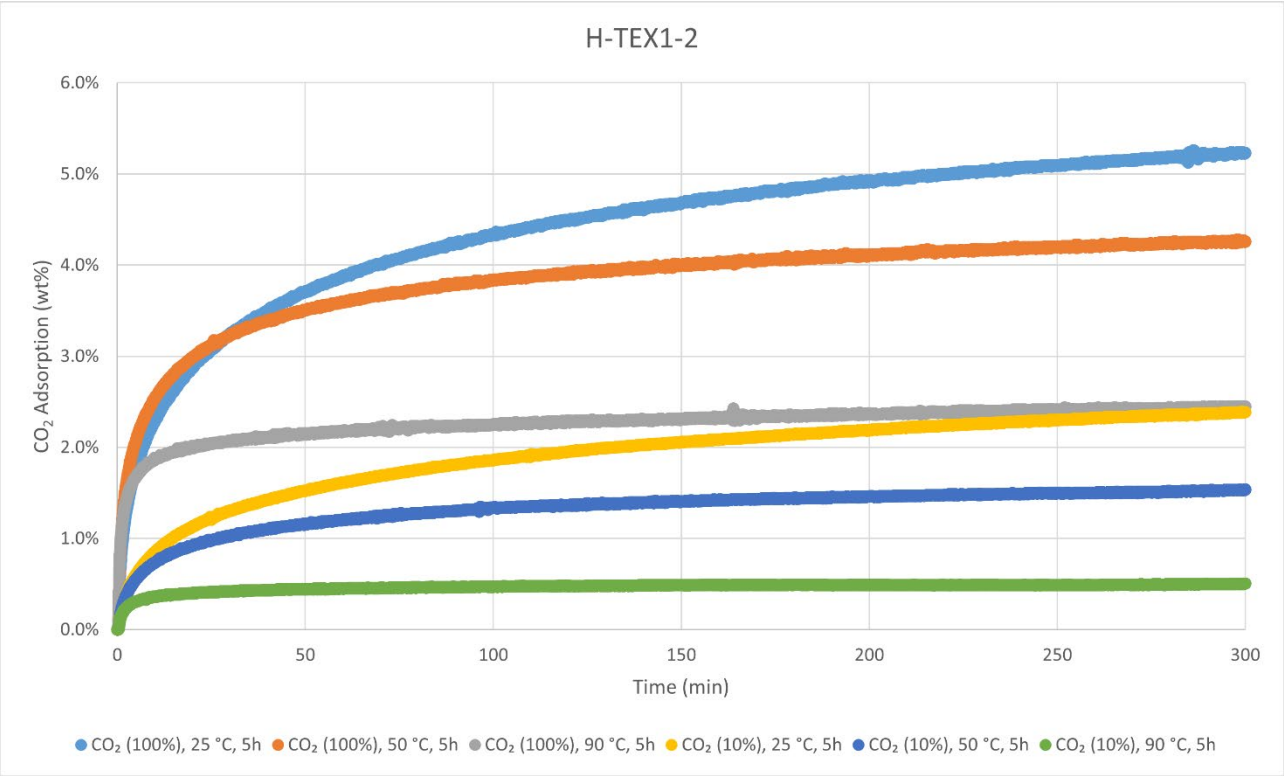

CO_2 adsorption using **TGA method 2** (measurement of product batch from run 2: H-TEX1-2).

H-TEX1-2	wt%	mmol/g
CO_2 (100%), 25 °C, 5h	5.2%	1.19
CO_2 (100%), 50 °C, 5h	4.3%	0.97
CO_2 (100%), 90 °C, 5h	2.4%	0.56
CO_2 (10%), 25 °C, 5h	2.4%	0.54
CO_2 (10%), 50 °C, 5h	1.5%	0.35
CO_2 (10%), 90 °C, 5h	0.5%	0.11

Elemental Analysis (EA)

	N [%]	C [%]	H [%]	S [%]	mmol N/g	C/N ratio	C/H ratio
run 1	**16.04**	**60.38**	**7.55**	**Not detected**	**11.45**	**4.39**	**0.67**
run 2	**14.78**	**59.53**	**7.92**		**10.55**	**4.70**	**0.63**

Hydrogenated Acrylic yarn with poly(amide) (H-TEX2) was synthesised according to the General Procedure C from substrate **TEX2** (Puffy yarn) and was obtained in weight yields of 45.0 mg, 90 wt% and 35.2 mg, 70 wt%, respectively, from two independent runs (80 wt% on average). The polymer was analysed with solid-state ^{13}C CP/MAS NMR, IR-, TGA-, DSC-, and Elemental Analysis. Solubility tests were also conducted with several solvents. As indicated from ^{13}C CP/MAS NMR spectroscopic analysis before/after the reaction, the material is only partly hydrogenated likely due to low/no solubility or swelling in the reaction medium.

Particle size after cryogenic milling used for CO_2 adsorption-desorption experiments

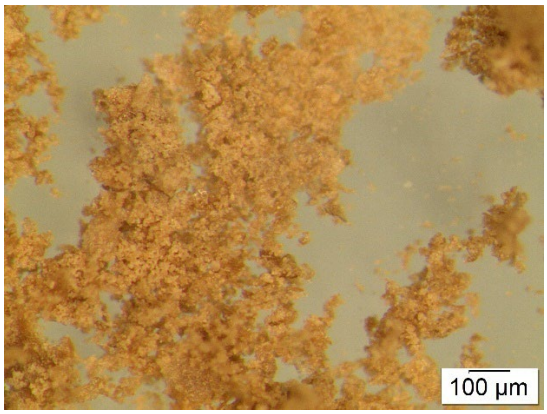

Solubility chart

Soluble **Swells** **Not soluble**

$CHCl_3$	Acetone	*i*-PrOH	DMF	DMSO	THF	PhMe	H_2O	MeOH	MeCN

^{13}C CP/MAS NMR (solid-state)

*Solid-state ^{13}C–NMR of **H-TEX2** (run 1):*

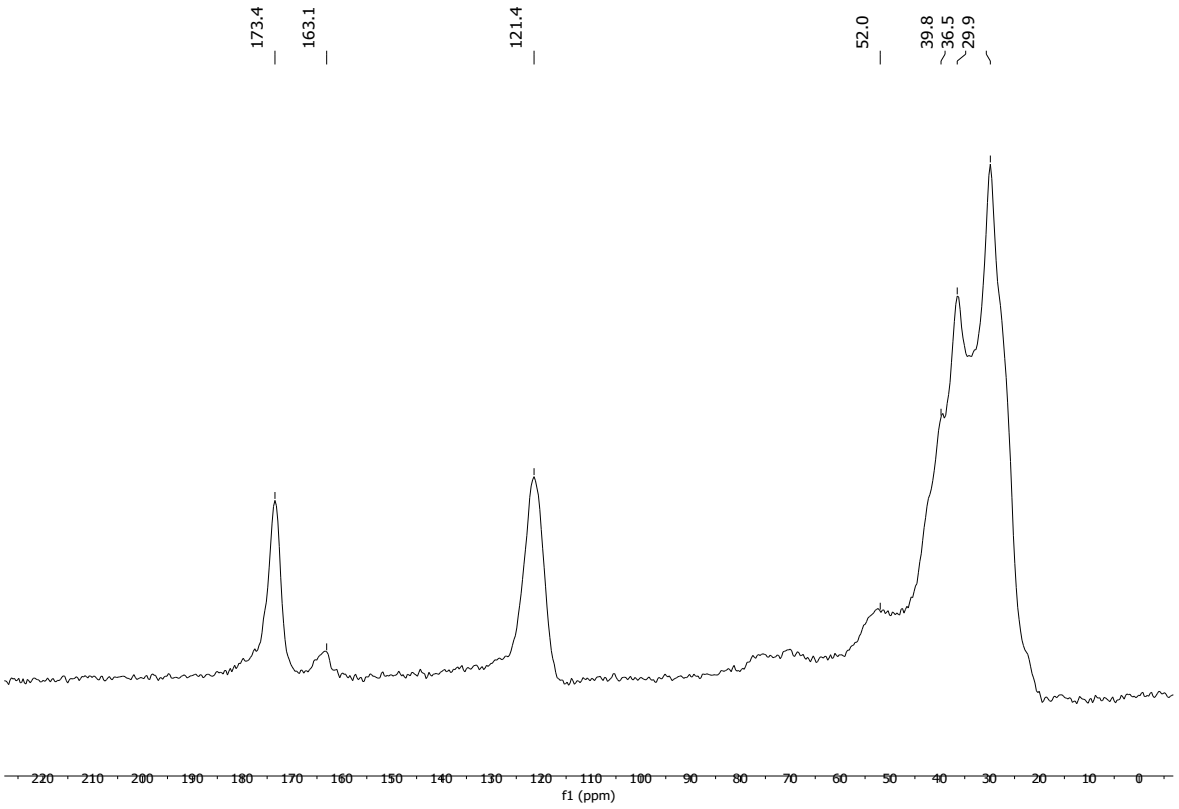

*Solid-state ^{13}C–NMR stacked spectra of **H-TEX2** (run 1, **red**) and **TEX2** (**black**):*

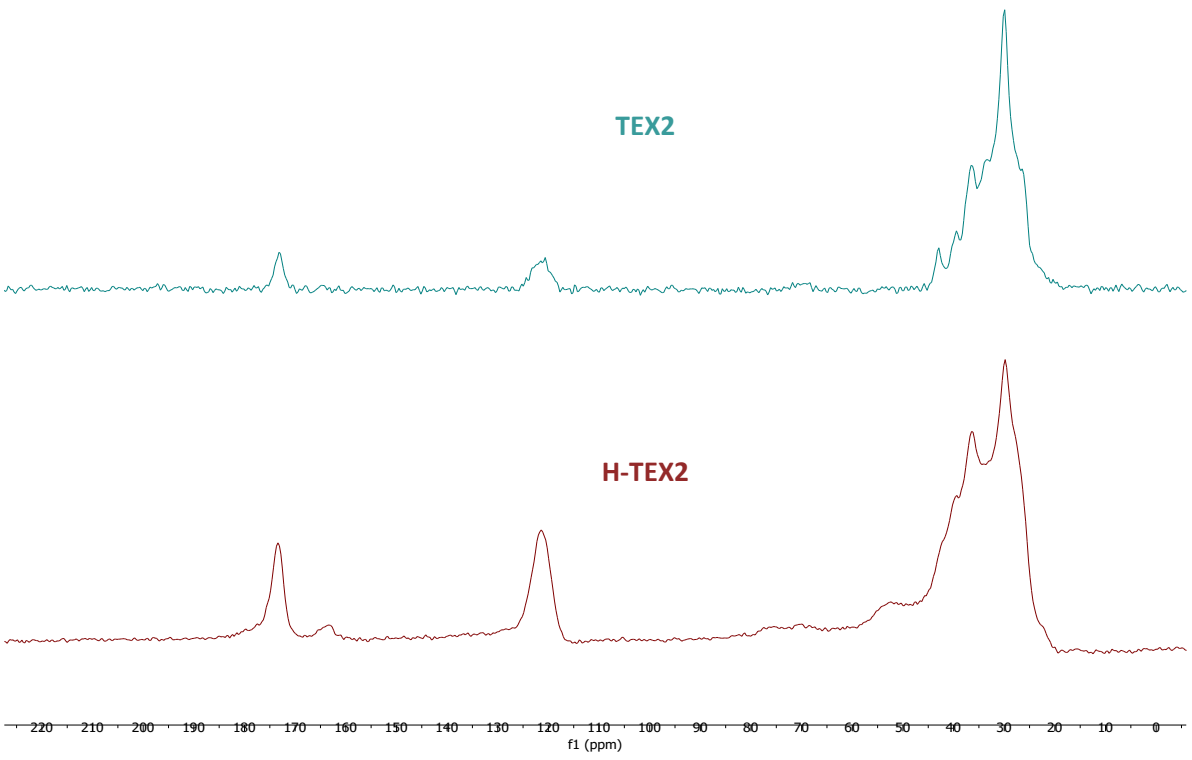

Infrared (IR) Spectroscopic Analysis

*IR-spectrum of **H-TEX2** (run 1):*

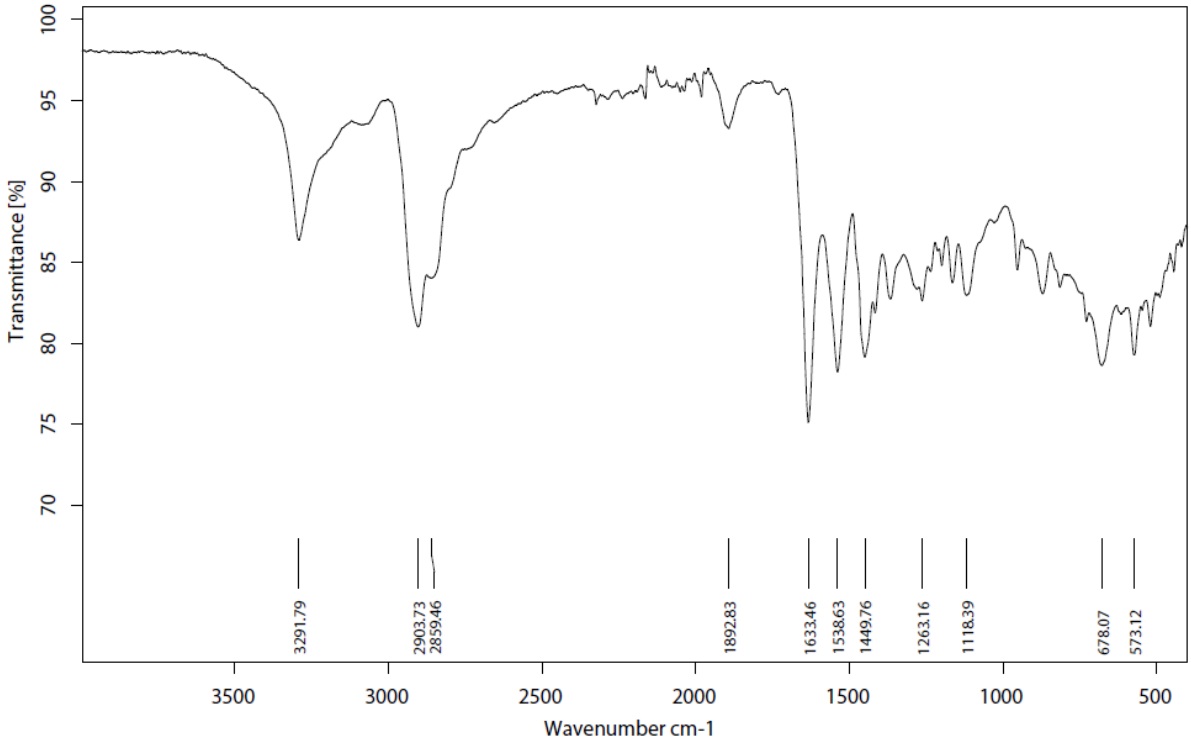

*IR-spectrum of **H-TEX2** (run 2):*

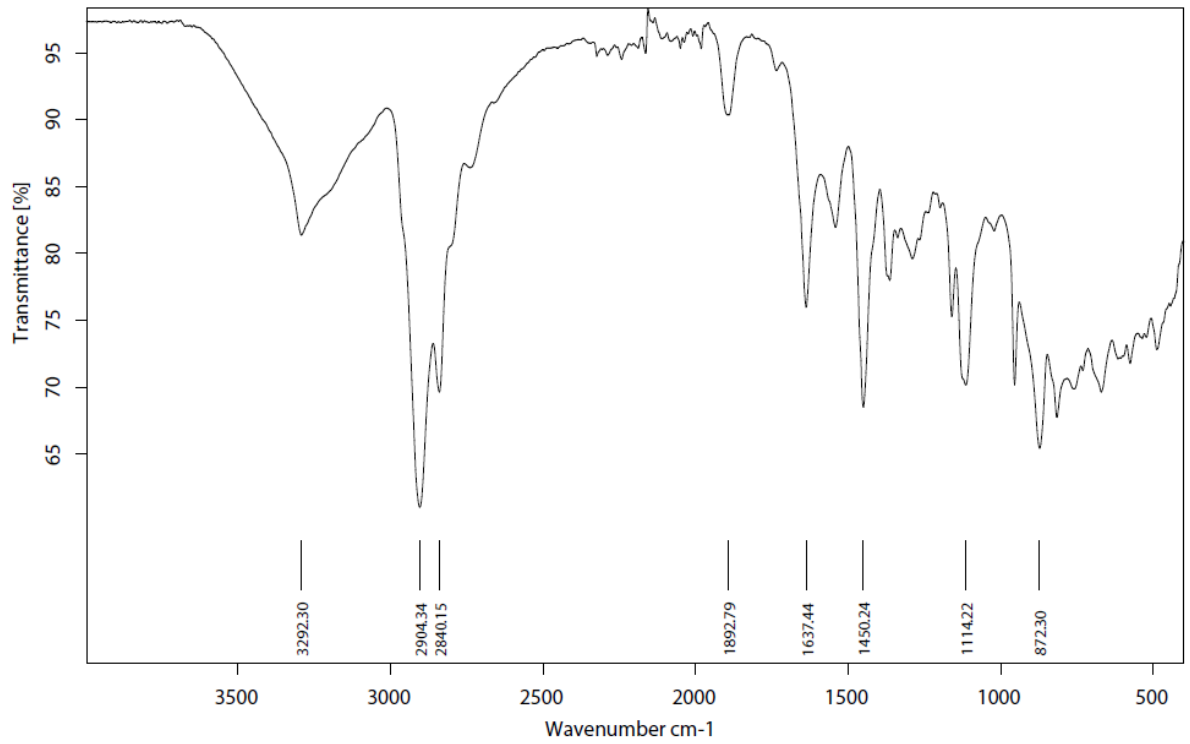

*IR-spectrum overlay of **H-TEX2** (run 1, **black**) and **TEX2** (substrate, **red**):*

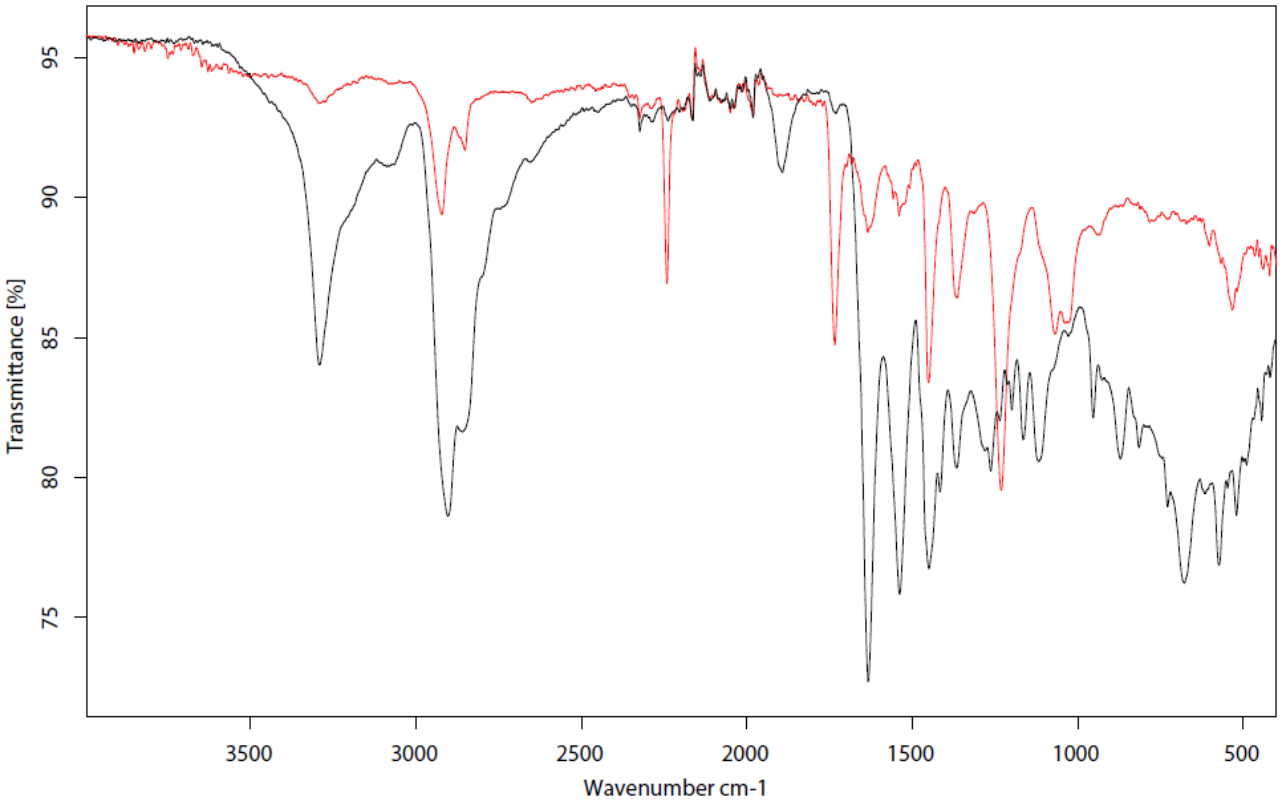

Thermogravimetric Analysis (TGA)

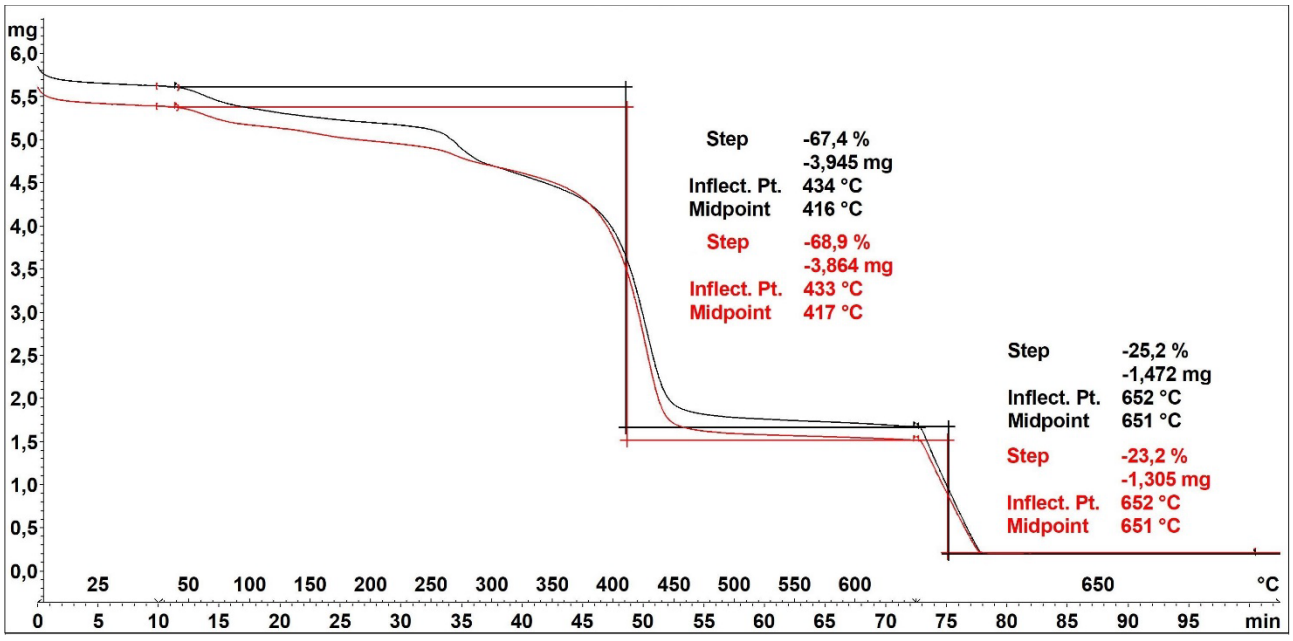

Decomposition graph. The experiment was conducted under He then air (after 650 °C). The black curve is the result from run 1, while the red curve is for run 2.

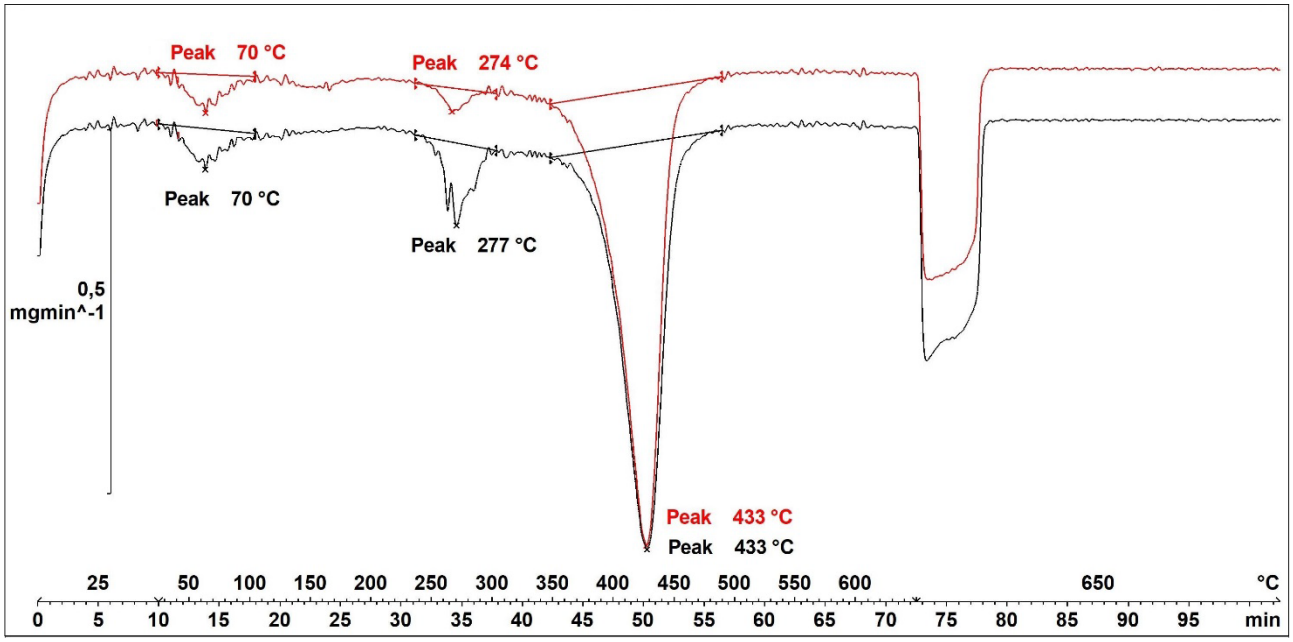

1st derivative of decomposition graph. The experiment was conducted under He then air (after 650 °C). The black curve is the result from run 1, while the red curve is for run 2. The peak at ~ 70 °C corresponds to residual MeOH.

Decomposition temperature (T_d) = 274–277 °C and 433 °C (two decomposition steps).

CO_2-adsorption analysis by thermogravimetric analysis

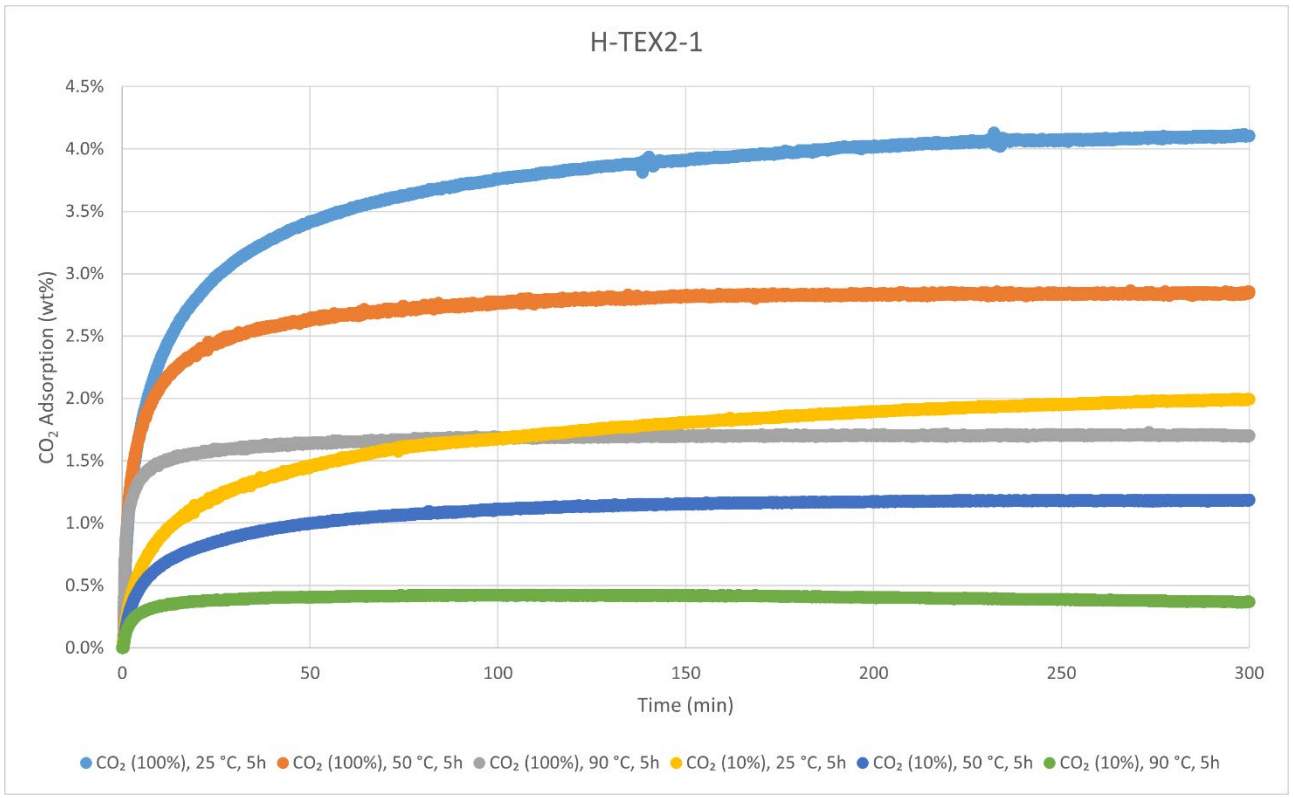

CO_2 adsorption using **TGA method 2** (measurement of product batch from run 1: H-TEX2-1).

H-TEX2-1	wt%	mmol/g
CO_2 (100%), 25 °C, 5h	4.1%	0.93
CO_2 (100%), 50 °C, 5h	2.9%	0.65
CO_2 (100%), 90 °C, 5h	1.7%	0.39
CO_2 (10%), 25 °C, 5h	2.0%	0.45
CO_2 (10%), 50 °C, 5h	1.2%	0.27
CO_2 (10%), 90 °C, 5h	0.4%	0.08

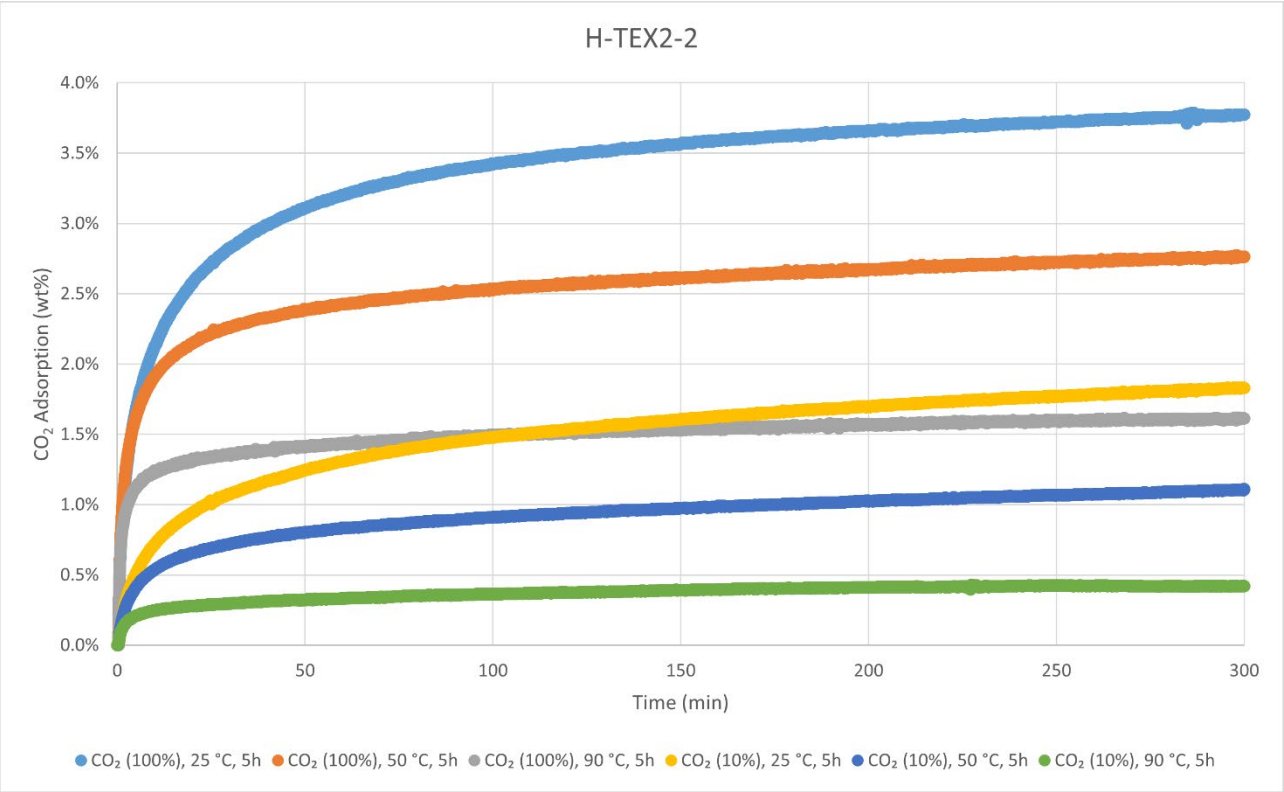

CO_2 adsorption using **TGA method 2** (measurement of product batch from run 2: H-TEX2-2).

H-TEX2-2	wt%	mmol/g
CO_2 (100%), 25 °C, 5h	3.8%	0.86
CO_2 (100%), 50 °C, 5h	2.8%	0.63
CO_2 (100%), 90 °C, 5h	1.6%	0.37
CO_2 (10%), 25 °C, 5h	1.8%	0.42
CO_2 (10%), 50 °C, 5h	1.1%	0.25
CO_2 (10%), 90 °C, 5h	0.4%	0.10

Differential Scanning Calorimetry (DSC) Analysis

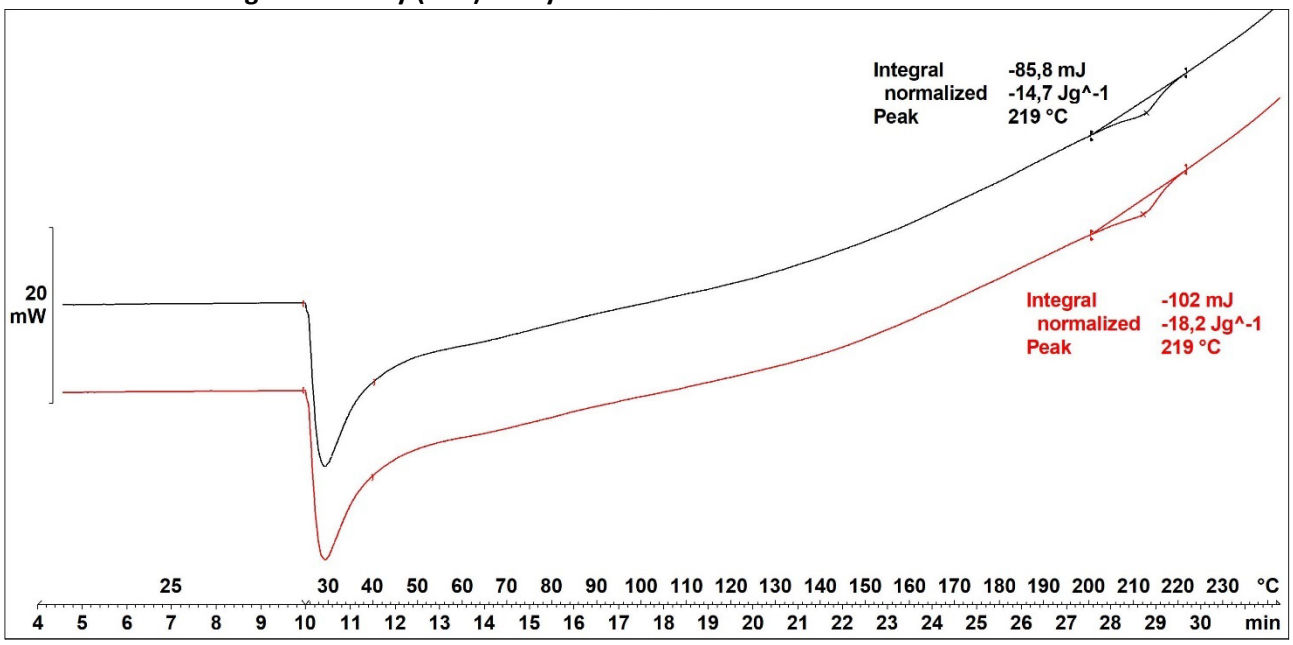

For both runs, the melting point of PA-6 is still visible in the hydrogenated material, suggesting that this co-polymer is inert to the hydrogenation reaction.

Elemental Analysis (EA)

	N [%]	C [%]	H [%]	S [%]	mmol N/g	C/N ratio	C/H ratio
run 1	15.09	58.00	8.05	Not detected	10.78	4.48	0.60
run 2	13.43	60.05	9.05		9.59	5.21	0.56

Hydrogenated GVL-extracted acrylic polymer from mixed texiles (H-MIX2) was synthesised according to the General Procedure C from substrate **MIX2** (GVL-extracted acrylic polymer, see p. S63) and was obtained in weight yields of 30.4 mg, 61 wt%, 26.6 mg, 53 wt%, 35.0 mg, 70 wt%, and 42.5 mg, 82 wt% respectively, from four independent runs (67 wt% on average). For these reactions, 54 mg of the **MIX2** powder was used in order to take into account the residual 8.2 wt% GVL. For simplicity, only the characterisation of two runs is reported and three runs were analysed by TGA for CO_2-adsorption. The polymer was analysed with solid-state ^{13}C CP/MAS NMR, IR-, TGA-, DSC-, and Elemental Analysis. Solubility tests were also conducted with several solvents. No thermal events besides decomposition were observed with DSC. Although challenging to observe for **H-MIX2** specifically, the material is likely only partly hydrogenated likely due to low/no solubility or swelling in the reaction medium as indicated from ^{13}C CP/MAS NMR spectroscopic analysis of like materials: **H-TEX1** and **H-TEX2**.

Particle size after cryogenic milling used for CO_2 adsorption-desorption experiments

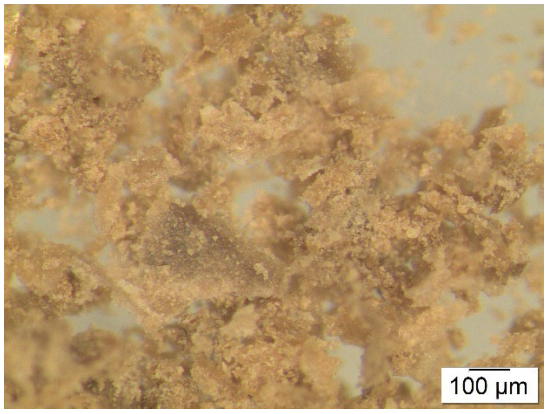

Solubility chart

Soluble **Swells** **Not soluble**

$CHCl_3$	Acetone	*i*-PrOH	DMF	DMSO	THF	PhMe	H_2O	MeOH	MeCN

^{13}C CP/MAS NMR (solid-state)

*Solid-state ^{13}C–NMR of **H-MIX2** (run 2):*

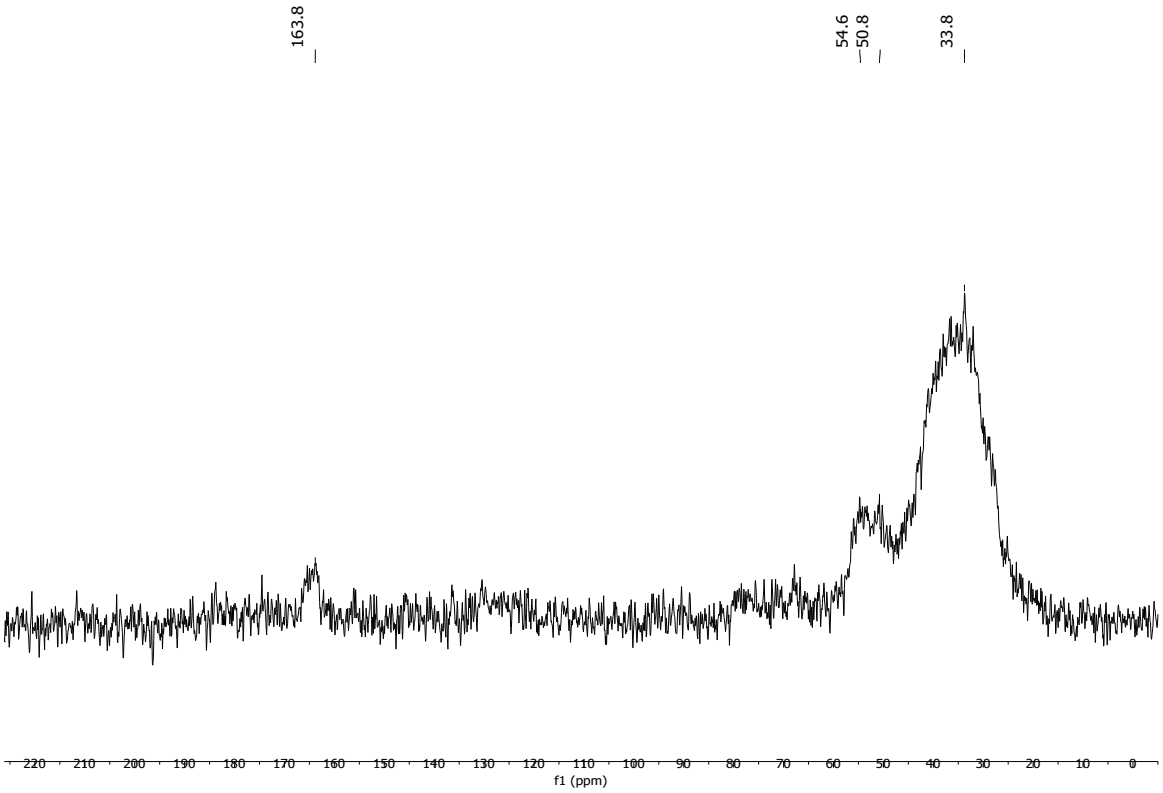

*Solid-state ^{13}C–NMR stacked spectra of **H-MIX2** (run 2, **brown**) and **MIX2** (**light blue**):*

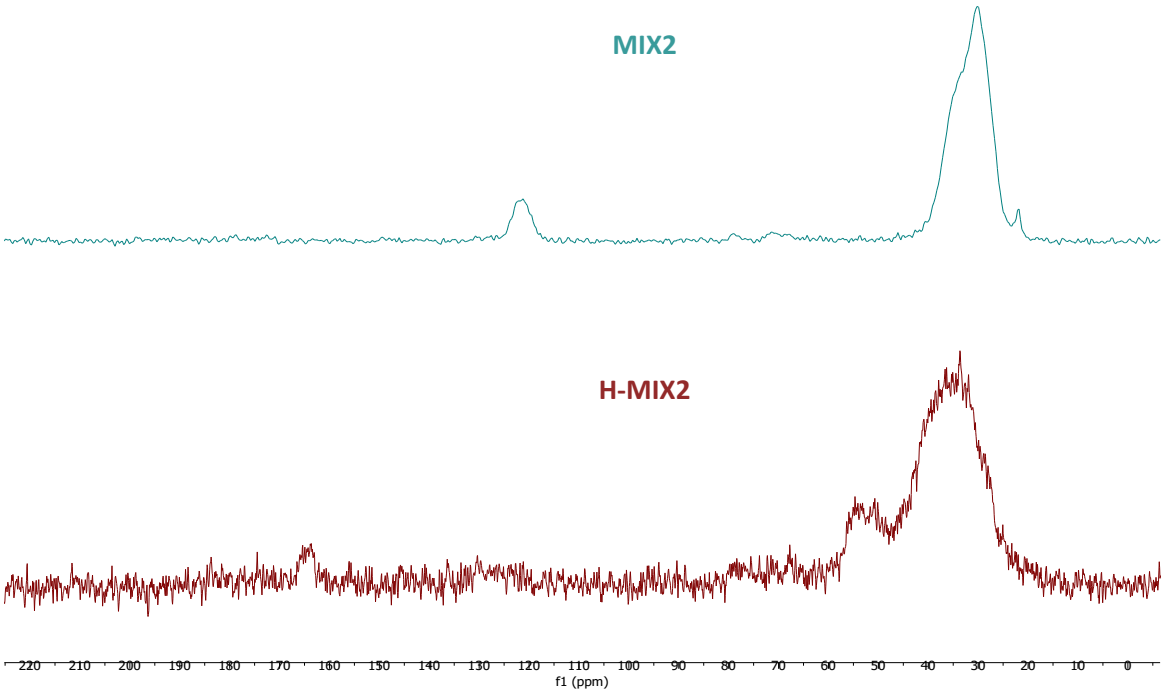

Infrared (IR) Spectroscopic Analysis

*IR-spectrum of **H-MIX2** (run 1):*

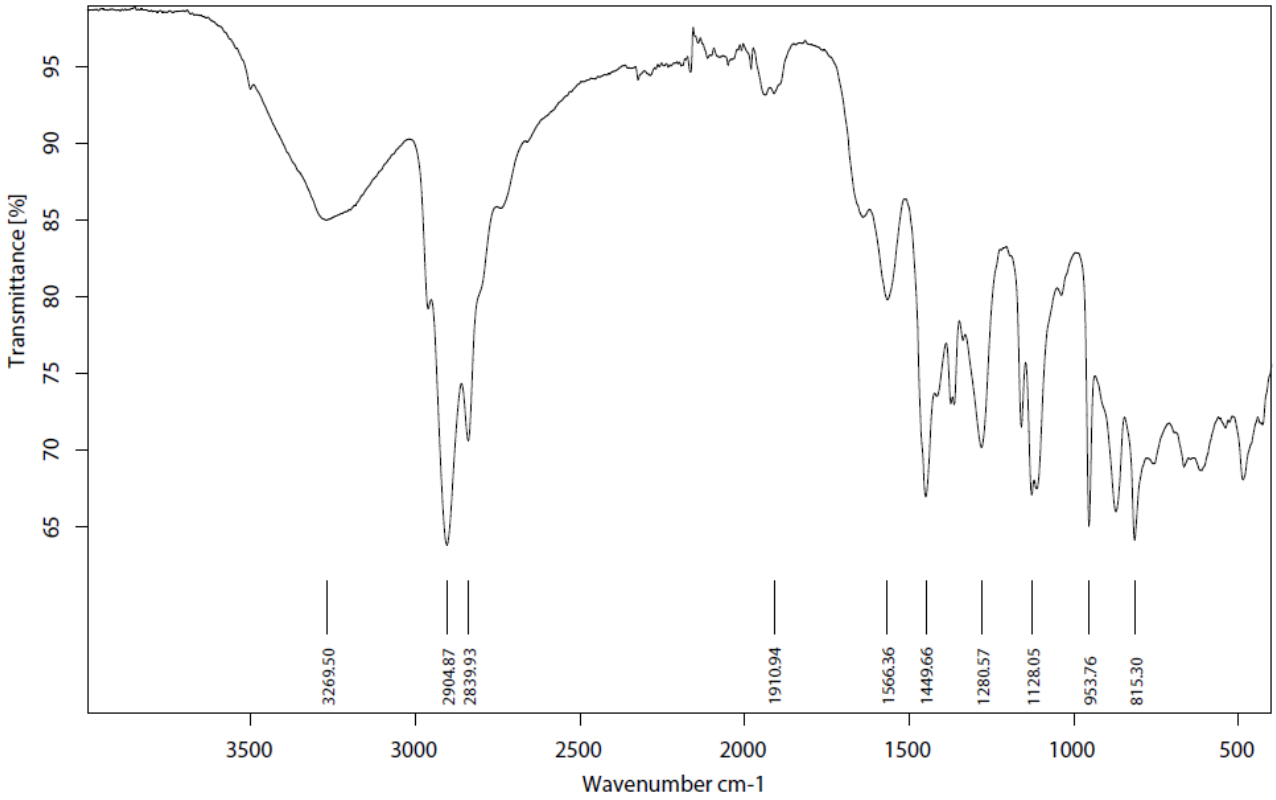

*IR-spectrum of **H-MIX2** (run 2):*

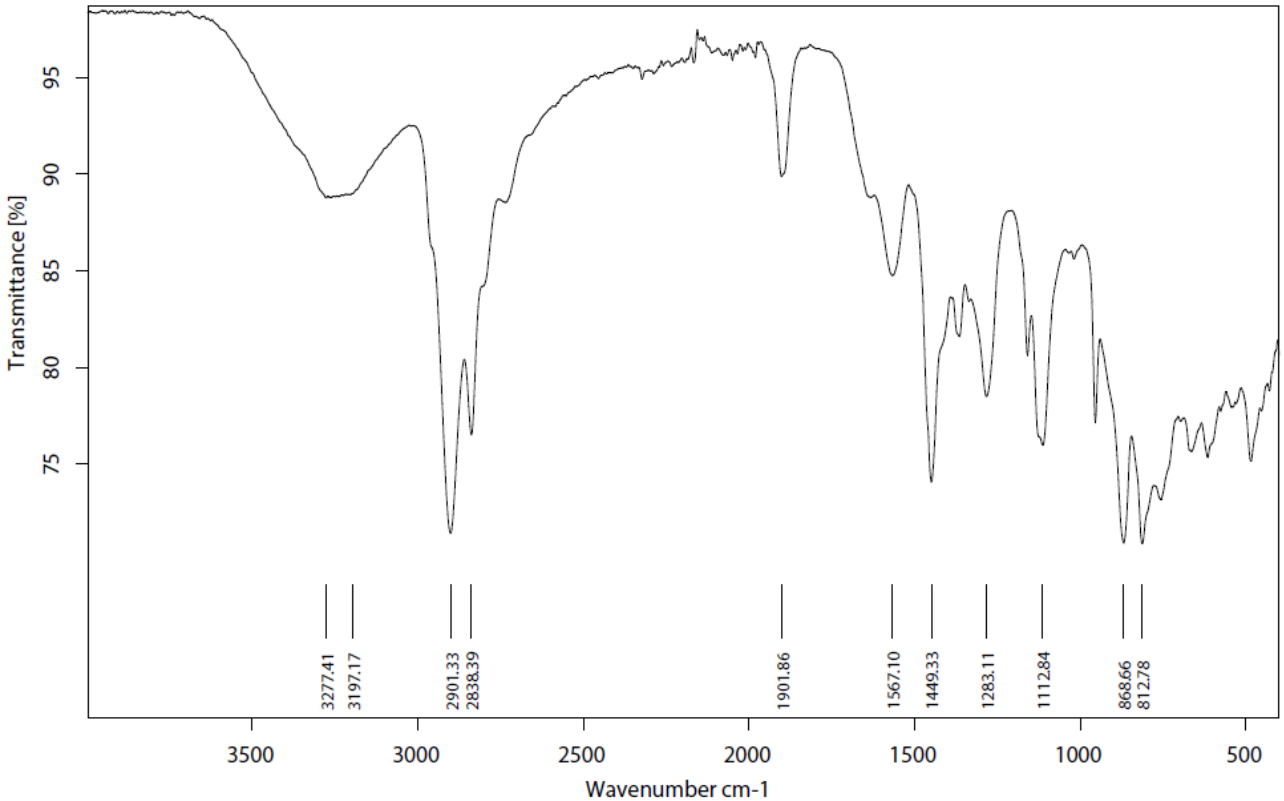

*IR-spectrum overlay of **H-MIX2** (run 1, **black**) and **MIX2** (substrate, **red**):*

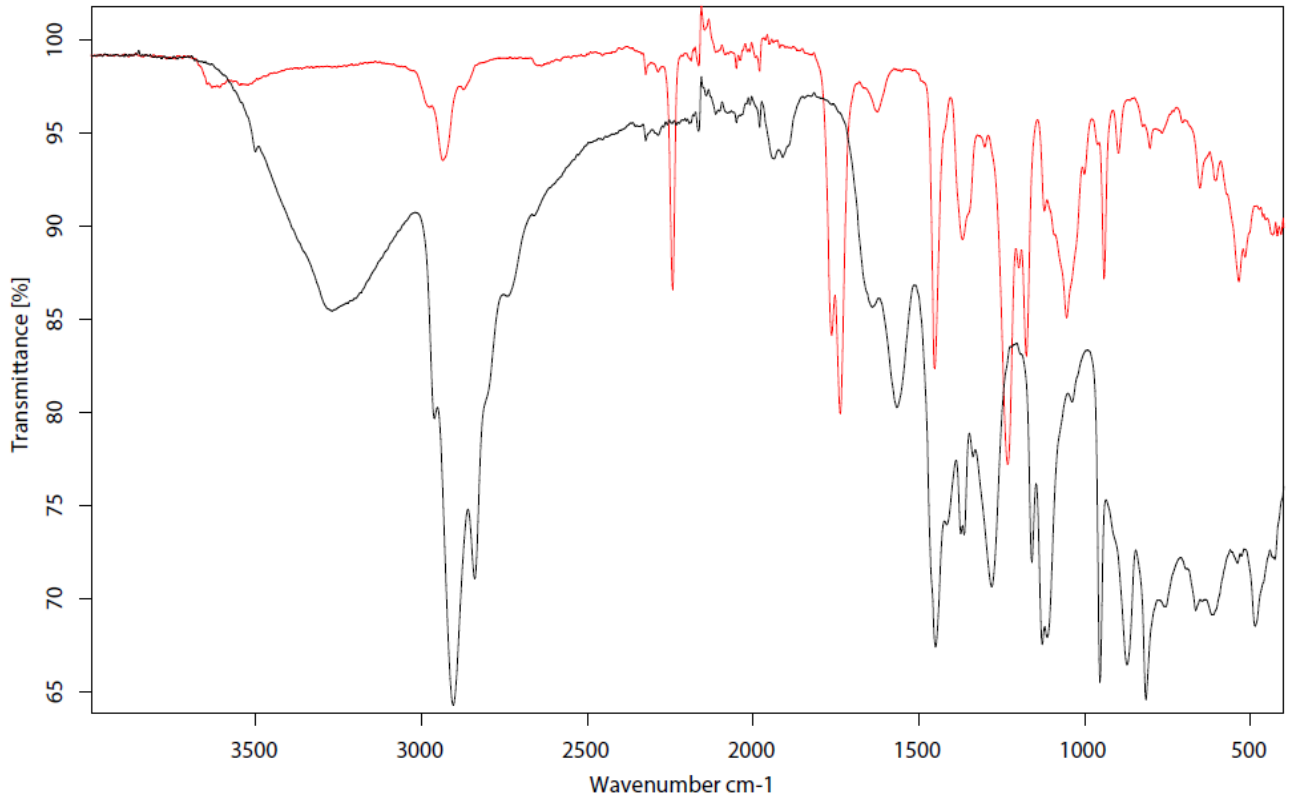

Thermogravimetric Analysis (TGA)

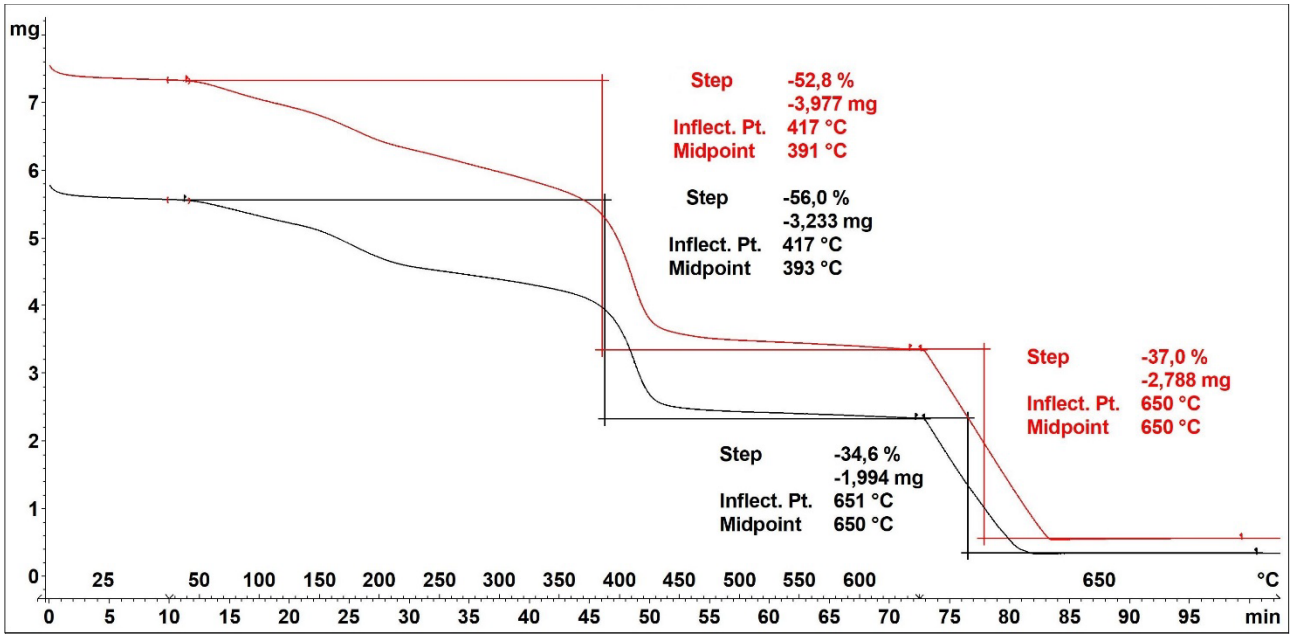

Decomposition graph. The experiment was conducted under He then air (after 650 °C). The black curve is the result from run 1, while the red curve is for run 2.

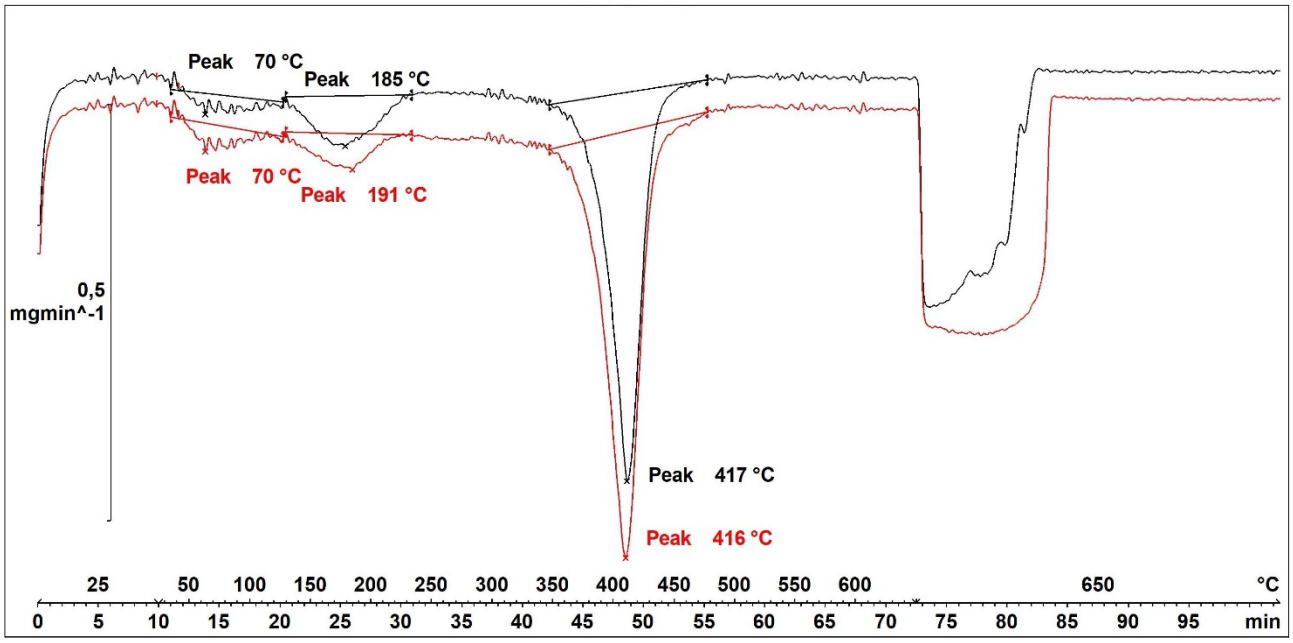

1st derivative of decomposition graph. The experiment was conducted under He then air (after 650 °C). The black curve is the result from run 1, while the red curve is for run 2. The peak at ~ 70 °C corresponds to residual MeOH and the 185-191 °C to residual GVL.

Decomposition temperature (T_d) = 416−417 °C.

CO_2-adsorption analysis by thermogravimetric analysis

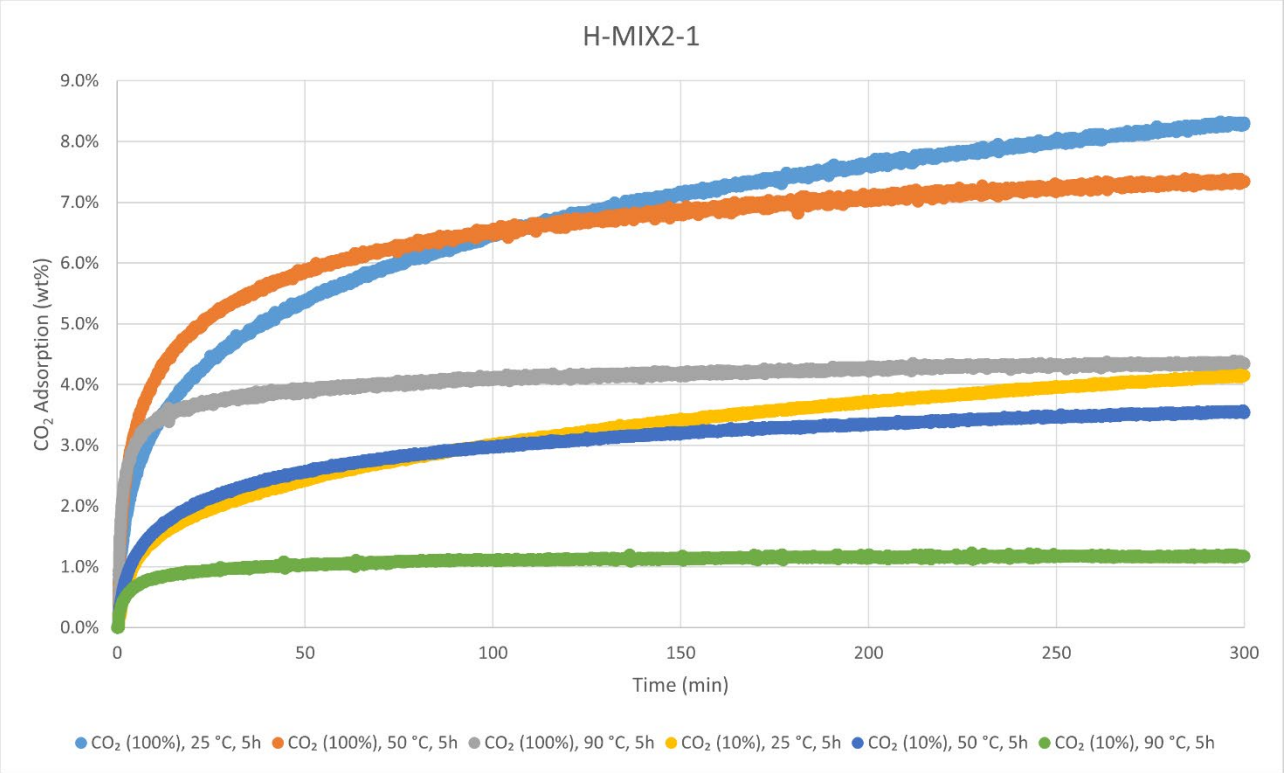

CO_2 adsorption using **TGA method 2** (measurement of product batch from run 1: H-MIX2-1).

H-MIX2-1	wt%	mmol/g
CO_2 (100%), 25 °C, 5h	8.3%	1.89
CO_2 (100%), 50 °C, 5h	7.3%	1.67
CO_2 (100%), 90 °C, 5h	4.3%	0.99
CO_2 (10%), 25 °C, 5h	4.2%	0.94
CO_2 (10%), 50 °C, 5h	3.5%	0.81
CO_2 (10%), 90 °C, 5h	1.2%	0.27

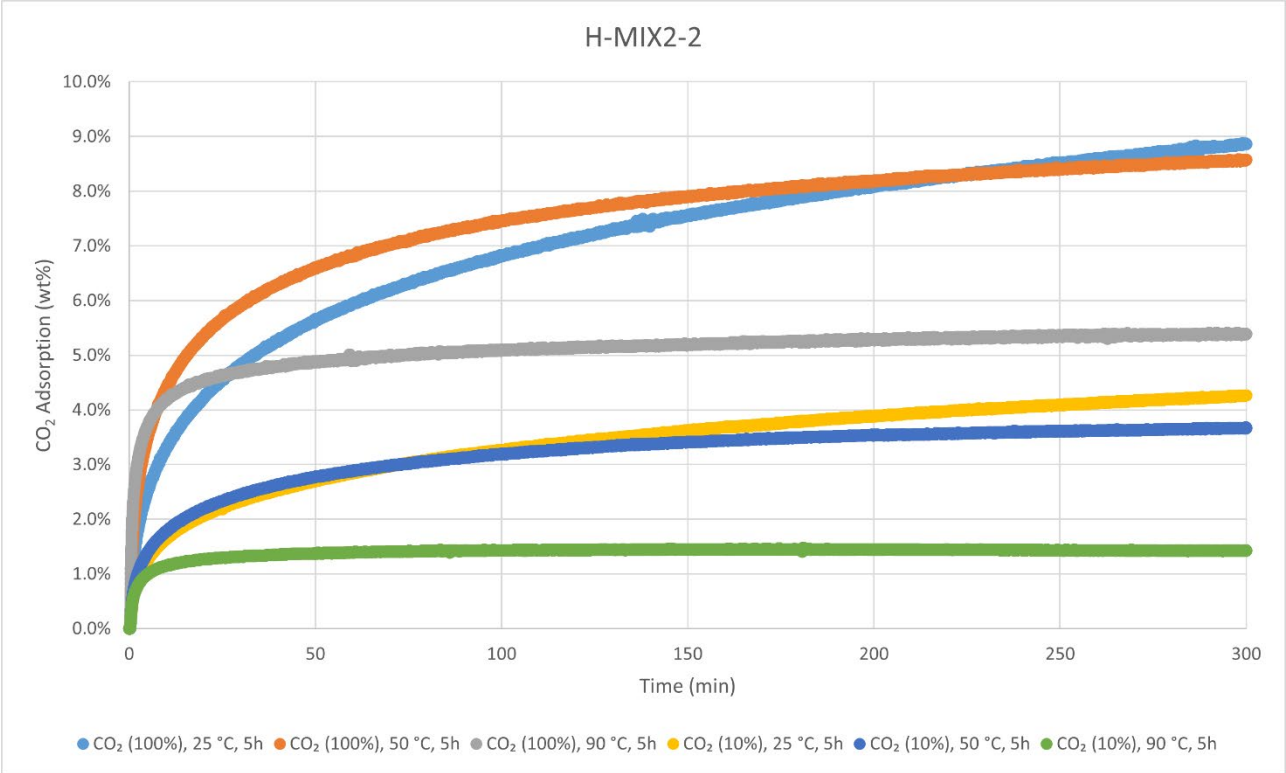

CO_2 adsorption using **TGA method 2** (measurement of product batch from run 2: H-MIX2-2).

H-MIX2-2	wt%	mmol/g
CO_2 (100%), 25 °C, 5h	8.9%	2.01
CO_2 (100%), 50 °C, 5h	8.6%	1.95
CO_2 (100%), 90 °C, 5h	5.4%	1.22
CO_2 (10%), 25 °C, 5h	4.3%	0.97
CO_2 (10%), 50 °C, 5h	3.7%	0.83
CO_2 (10%), 90 °C, 5h	1.4%	0.32

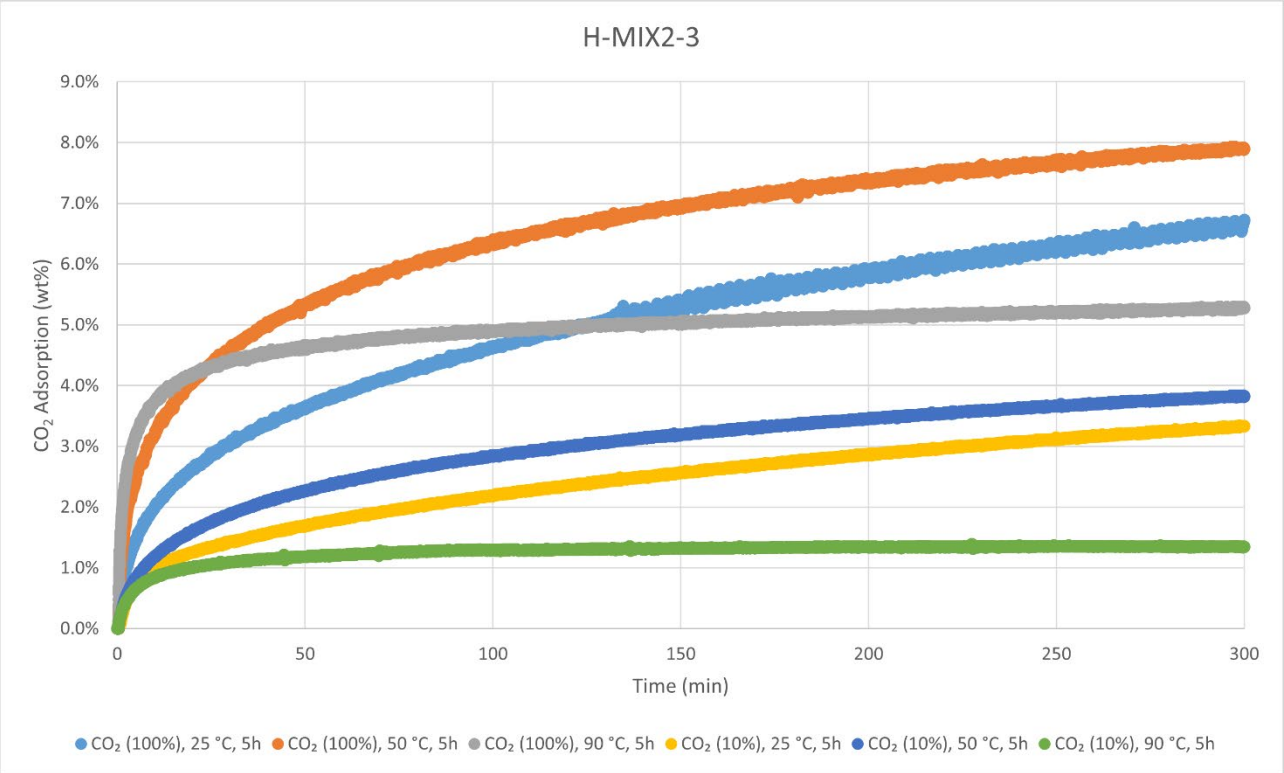

CO_2 adsorption using **TGA method 2** (measurement of product batch from run 3: H-MIX2-3).

H-MIX2-3	wt%	mmol/g
CO_2 (100%), 25 °C, 5h	6.7%	1.53
CO_2 (100%), 50 °C, 5h	7.9%	1.80
CO_2 (100%), 90 °C, 5h	5.3%	1.20
CO_2 (10%), 25 °C, 5h	3.3%	0.76
CO_2 (10%), 50 °C, 5h	3.8%	0.87
CO_2 (10%), 90 °C, 5h	1.3%	0.31

Elemental Analysis (EA)

	N [%]	C [%]	H [%]	S [%]	mmol N/g	C/N ratio	C/H ratio
Average of runs 1-4	**12.87 ± 1.51**	**57.36 ± 1.84**	**9.11 ± 0.26**	**Not detected**	**9.19**	**5.20**	**0.53**

Polymer Products from the Hydrocyanation-Hydrogenation of Poly(butadiene) Polymers

Hydrocyanated Styrene Butadiene Rubber 1 (HCN-SBR1) was synthesised according to the General Procedure E (run 1) or the General Procedure F (run 2) from substrate **SBR1** (SBR block co-polymer pellets). Work-up was performed by washing the polymer solution in chamber A with aq. NaOH (2 M, 3 x 10 mL) and H_2O (3 x 10 mL). The washed reaction mixture was then added dropwise into a brown flask (50 mL total volume containing MeOH (30 mL)) with stirring to precipitate the polymer. The liquid phase was removed by decantation, and the polymer was dried *in vacuo*, then cut to smaller pieces with scissors and then dried *in vacuo* again. The polymer product was obtained in weight yields of 269 mg (108 wt%), 257 mg (103 wt%), 246 (98 wt%) and 281 mg (113 wt%), respectively, from four independent runs (106 wt% on average). All yields are corrected for volatiles that were trapped within the polymer after drying under high vacuum for 2 days (volatile content percentages were determined by TGA). The fourth run (General Procedure F) used a mixture of $K^{12}CN$ and $K^{13}CN$ in a 4:1 ratio to generate a 20% ^{13}C-labelled polymer product, which facilitates characterisation by ^{13}C–NMR spectroscopic analysis. The polymers were reacted in the subsequent hydrogenation step without further purification. For analytical purposes, the polymers were suspended in $CHCl_3$ and then dried (repeated twice) to obtain pure NMR spectra free from other solvents. Obtaining a useful solution-state ^{13}C-NMR spectrum was not possible due to a very low solubility in deuterated NMR solvent. For simplicity, only the characterisation of two product batches is reported.

Particle size obtained from cryogenic milling used for ensuing hydrogenation reactions

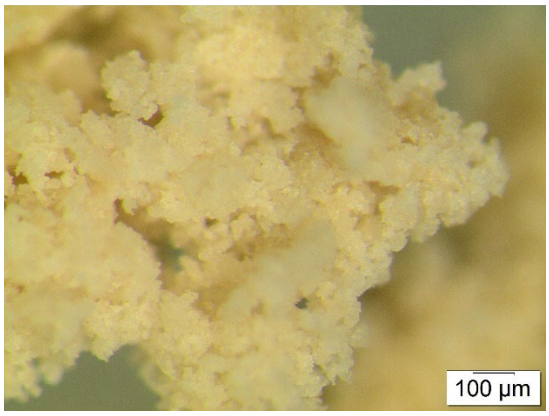

^{1}H–NMR ($CDCl_3$)

*^{1}H–NMR of **HCN-SBR1** (run 1):*

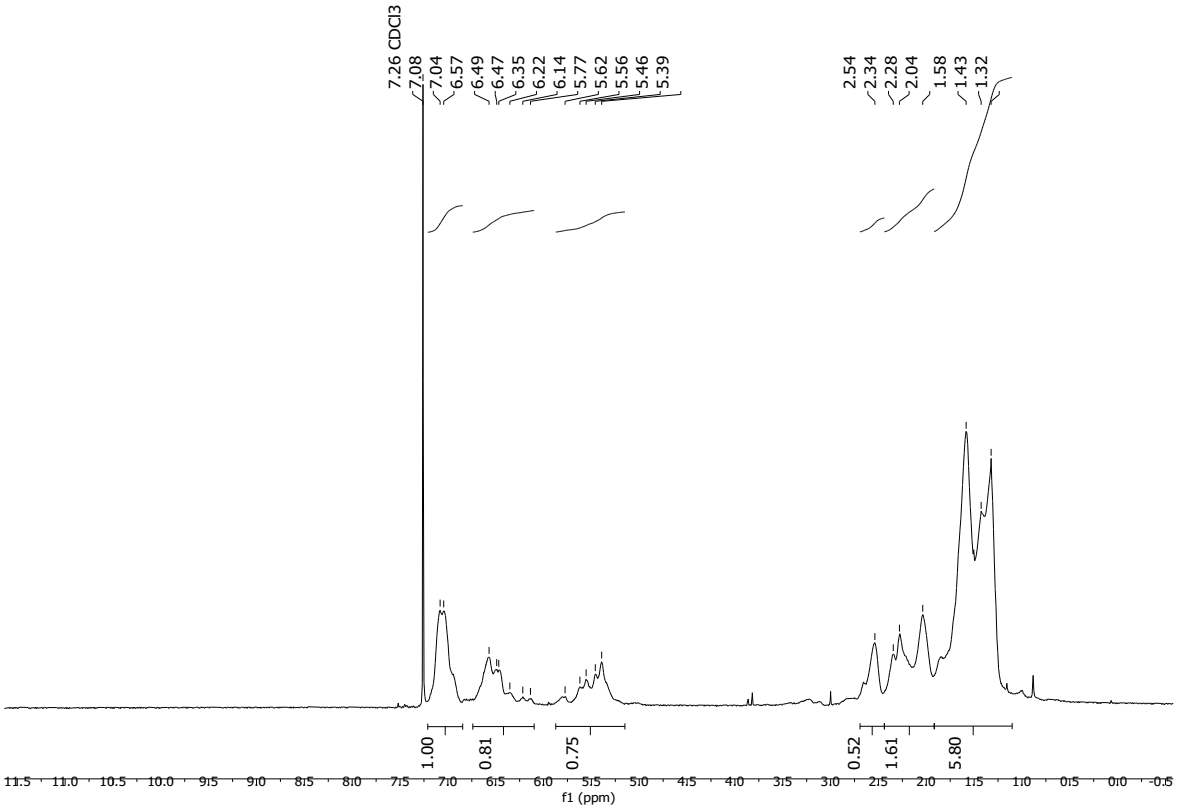

*^{1}H–NMR of **H$^{12/13}$CN-SBR1** (run 4):*

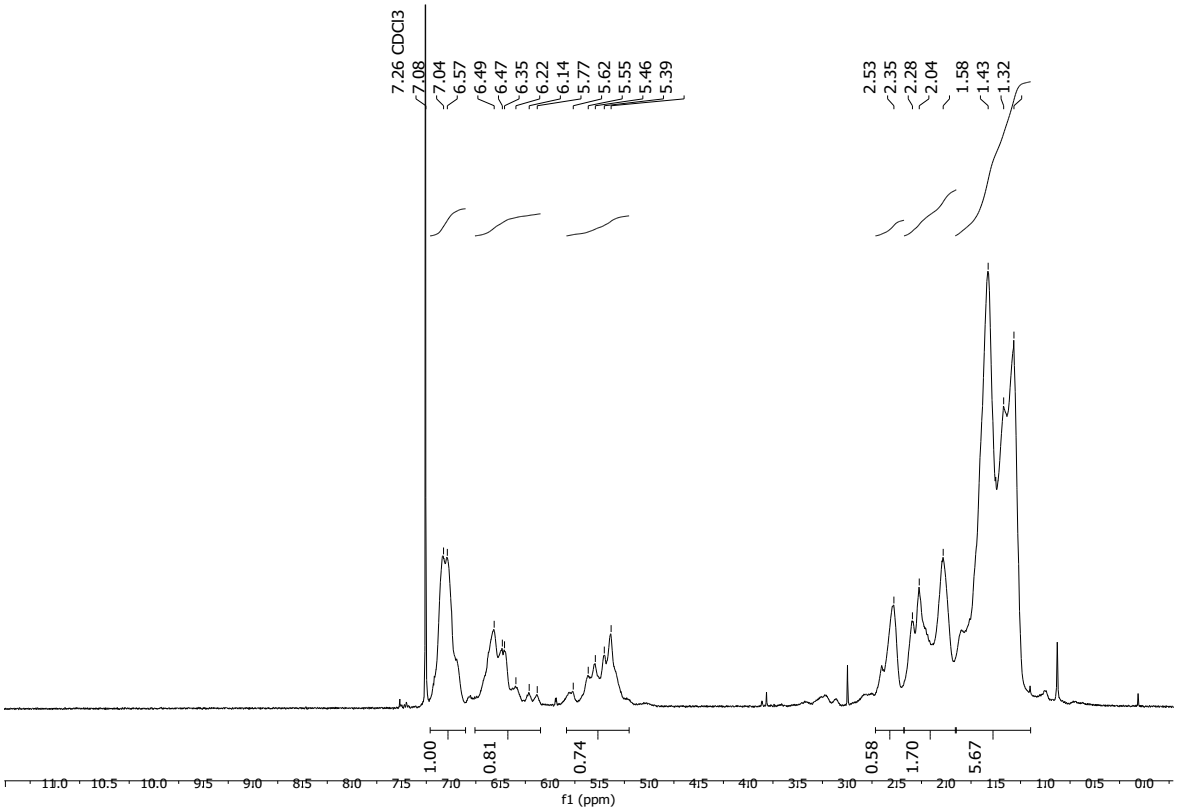

*^{1}H–NMR spectrum overlay of **HCN-SBR1** (run 1, **black**) and **SBR1** (substrate, **grey**):*

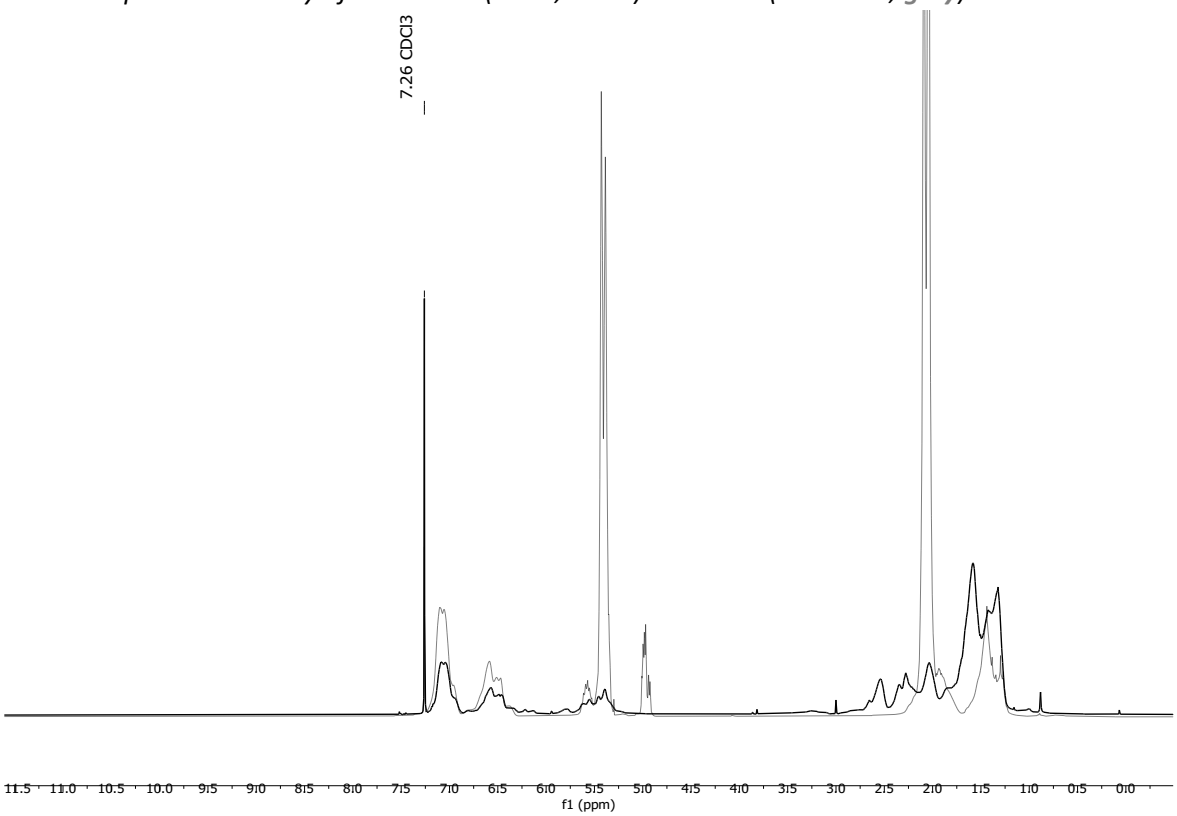

^{13}C CP/MAS NMR (solid-state)

*Solid-state ^{13}C–NMR of **HCN-SBR1** (run 1):*

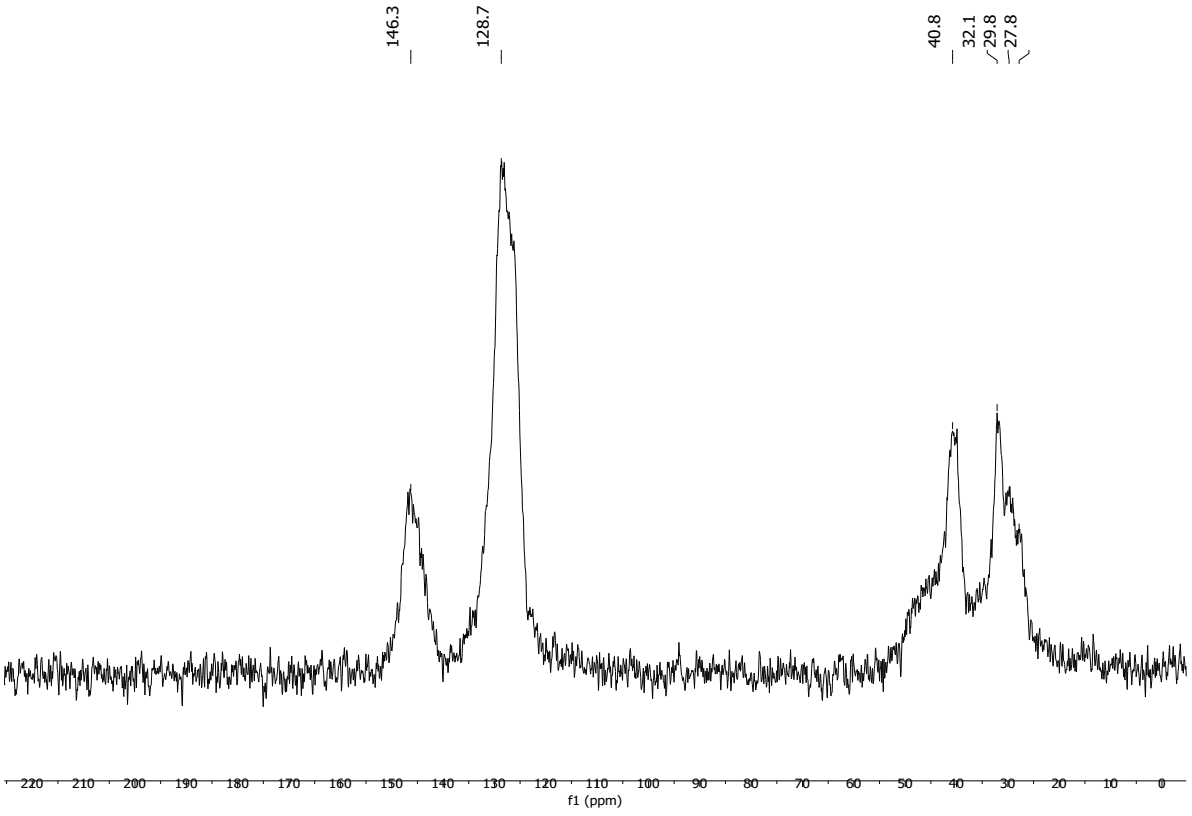

*Solid-state ^{13}C–NMR of **H$^{12/13}$CN-SBR1** (run 4): The ^{13}C-enriched nitrile peak is visible at δ_C : 122.4 ppm.*

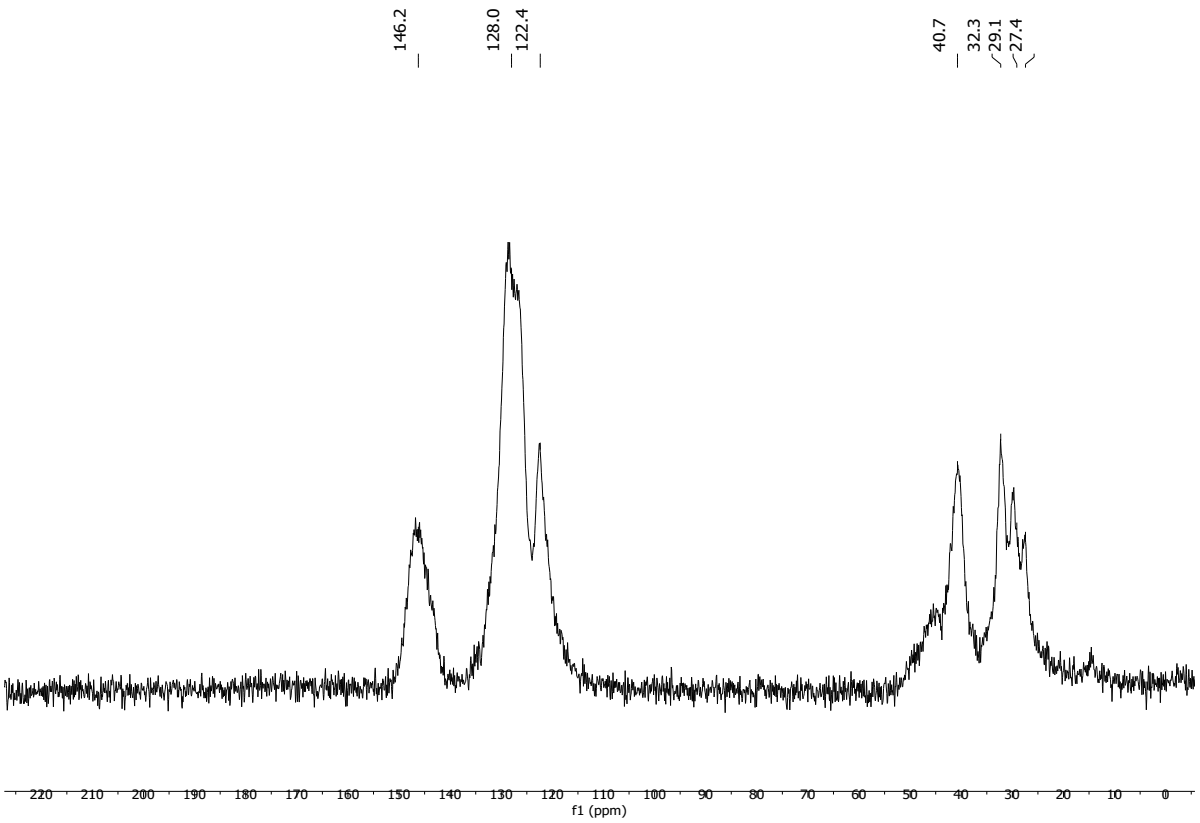

*Solid-state ^{13}C–NMR stacked spectra of **SBR1** (substrate, **light blue**) and **H$^{12/13}$CN-SBR1** (run 4, **brown**):*

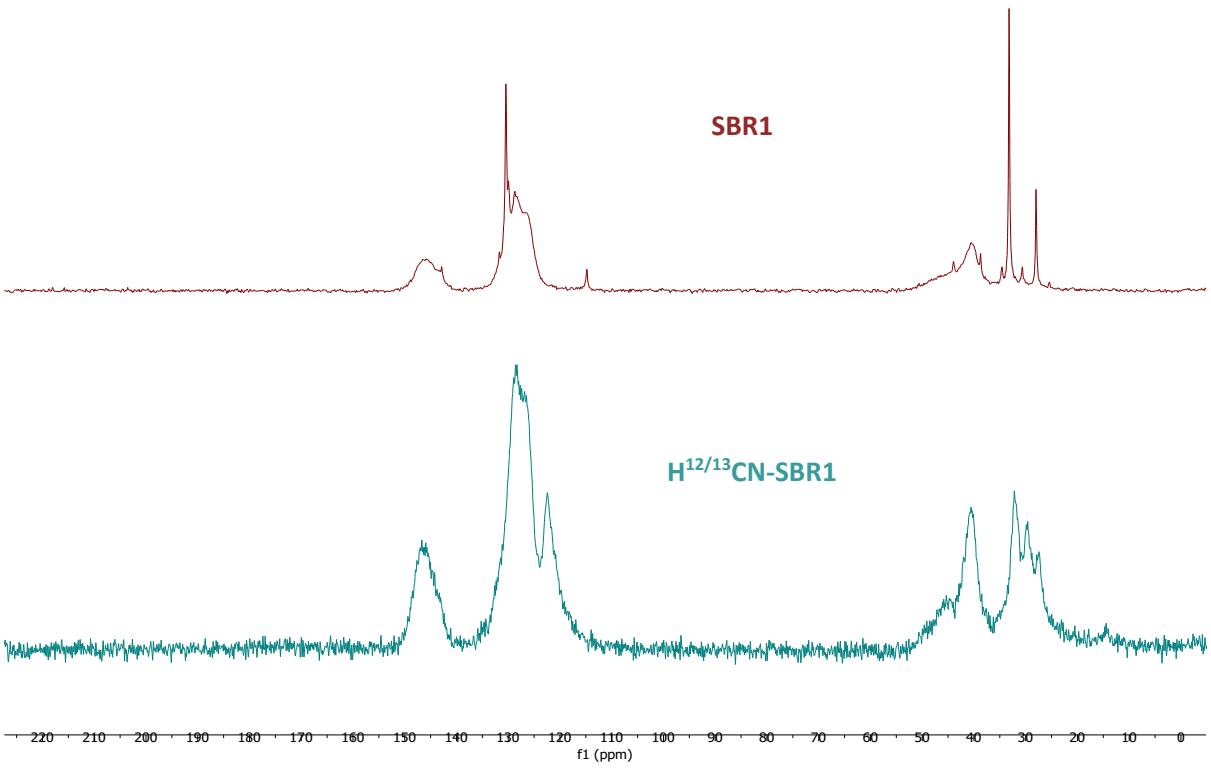

*Solid-state ^{13}C–NMR stacked spectra of **HCN-SBR1** (run 1, **light blue**) and **H$^{12/13}$CN-SBR1** (run 4, **brown**):*

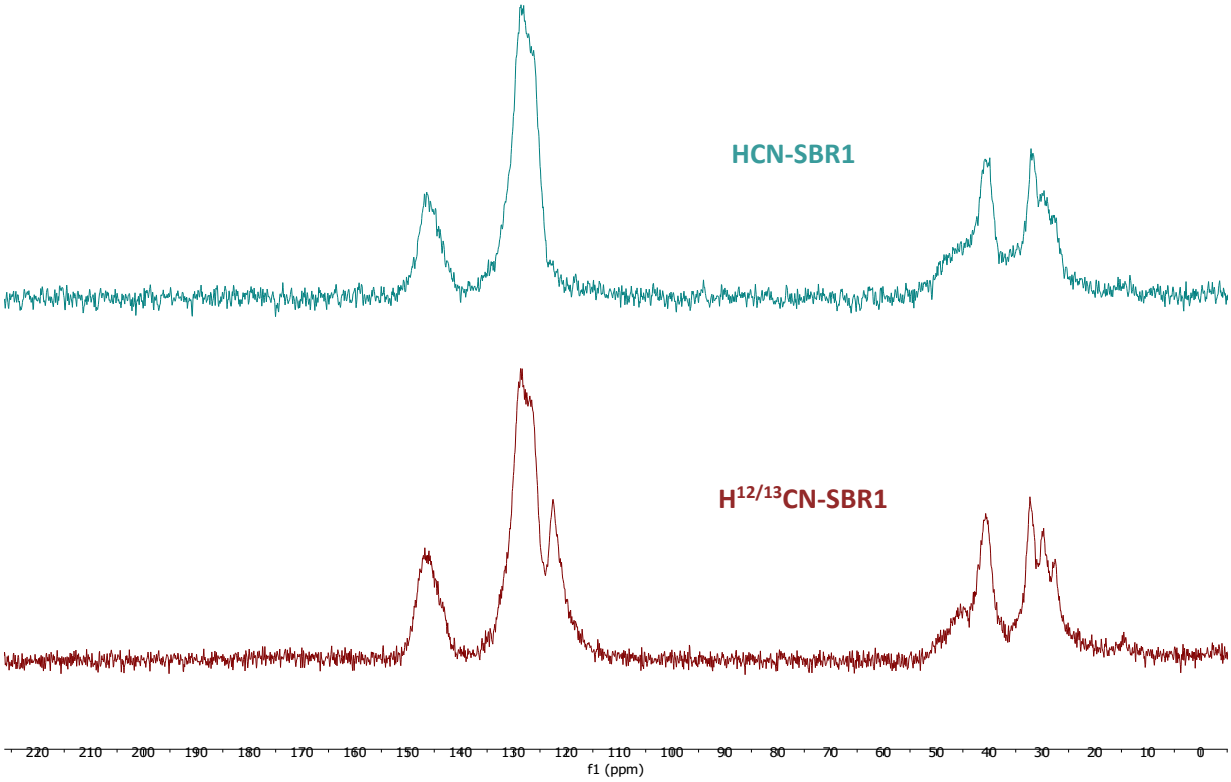

The ^{13}C-enriched signal is the major difference between the two spectra (at δ_C : 122.4 ppm).

Infrared (IR) Spectroscopic Analysis

*IR-spectrum of **HCN-SBR1** (run 1):*

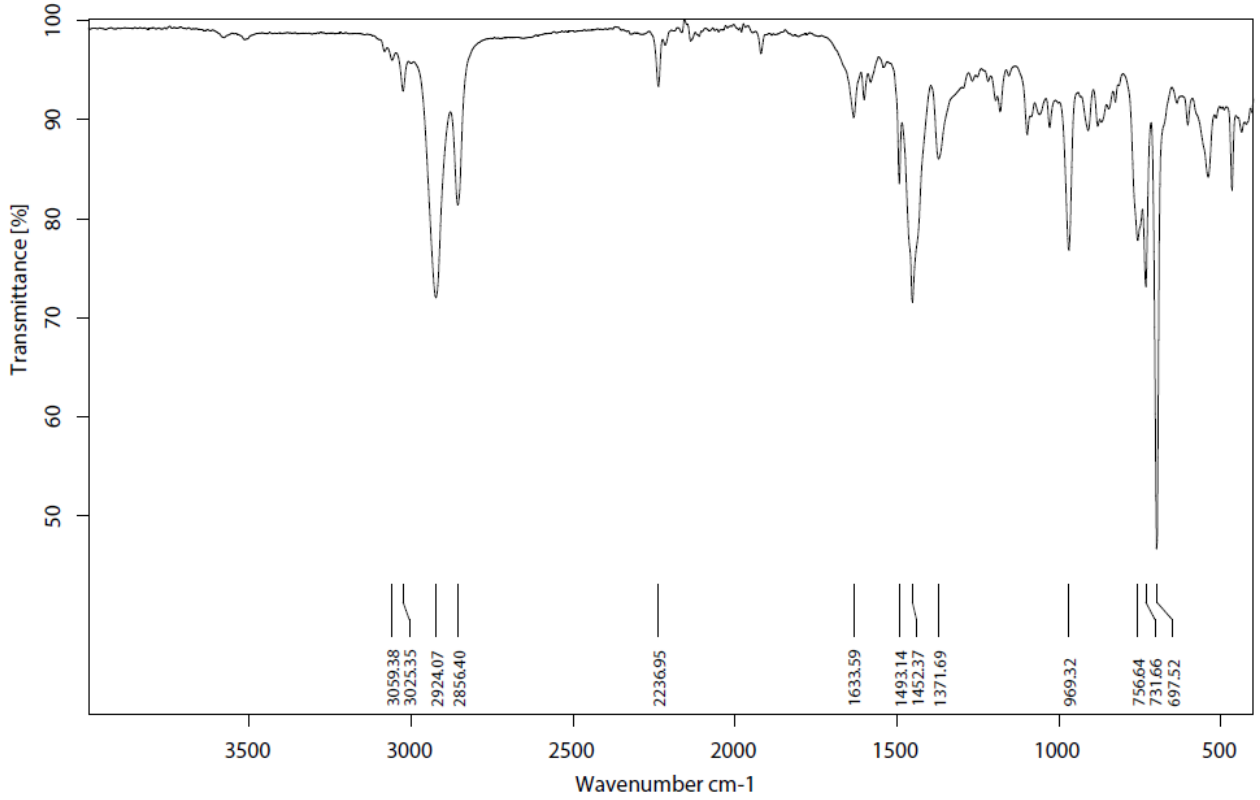

*IR-spectrum of **H$^{12/13}$CN-SBR1** (run 4): The ^{13}C-enriched nitrile C≡N band is visible at 2129.3 cm^{-1}.*

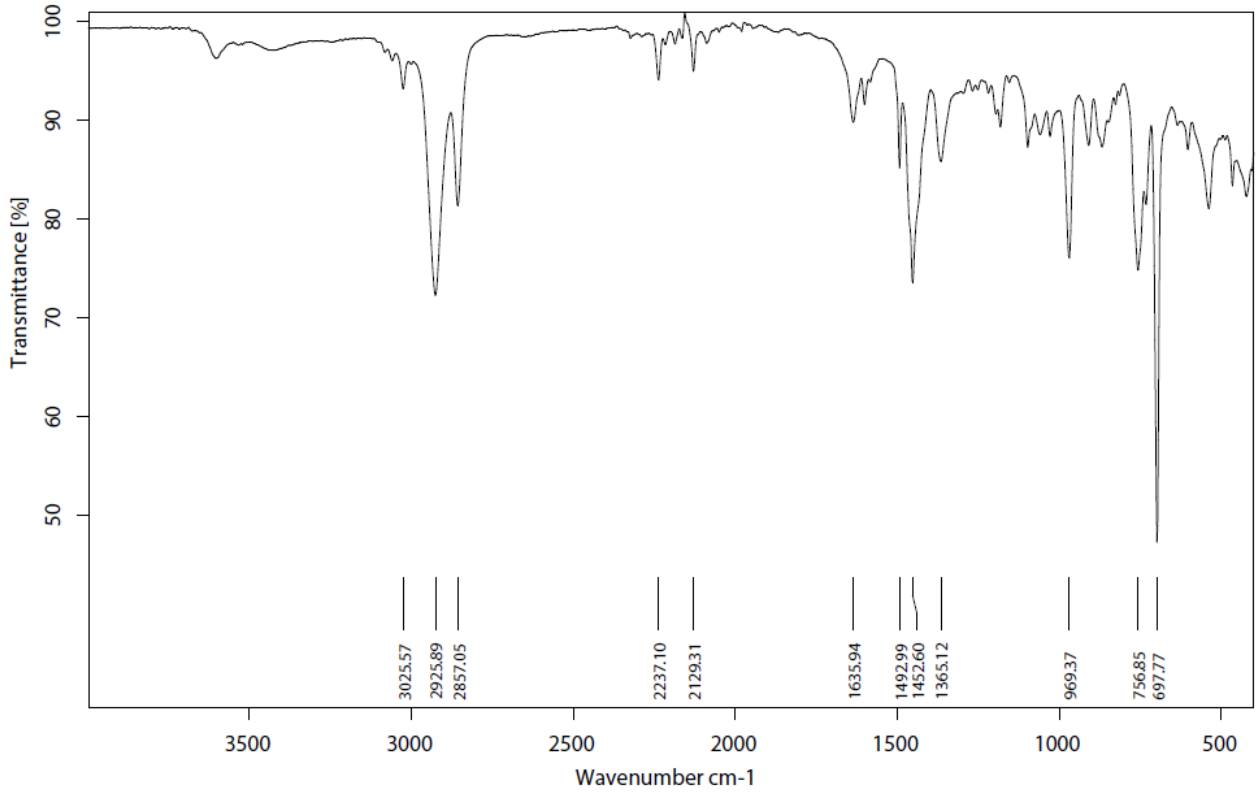

*IR-spectrum overlay of **HCN-SBR1** (run 1, **black**) and **SBR1** (substrate, **red**):*

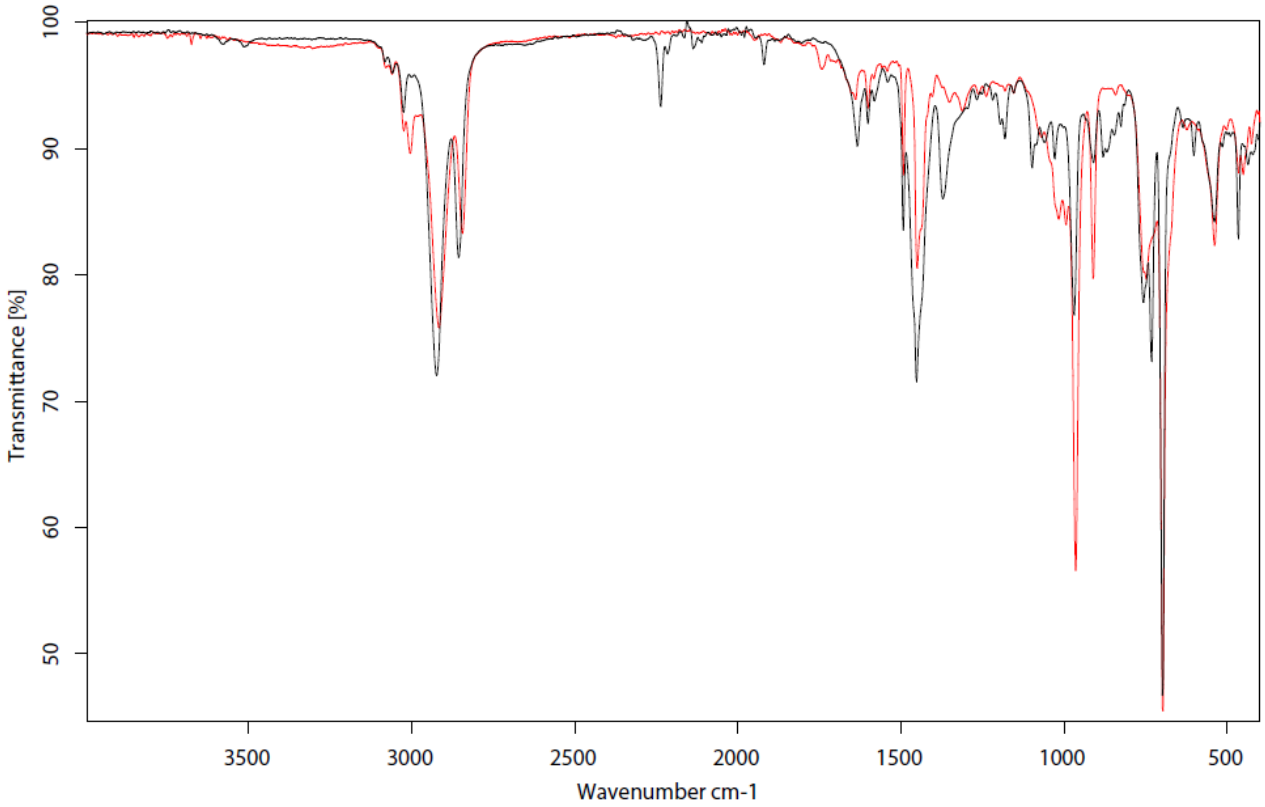

Elemental Analysis (EA)

	N [%]	C [%]	H [%]	S [%]	mmol N/g	C/N ratio	C/H ratio
run 3	**8.05**	**78.07**	**8.80**	**Not detected**	**5.75**	**11.31**	**0.74**
run 4	**7.86**	**76.28**	**8.56**		**5.61**	**11.31**	**0.75**

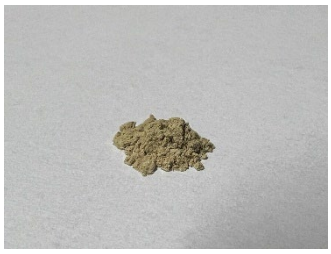

Hydrogenated hydrocyanated Styrene Butadiene Rubber 1 (HCN*-SBR1) was synthesised according to the General Procedure G from substrate **HCN-SBR1** or **H$^{12/13}$CN-SBR1** (max. 20% ^{13}C) and was obtained in weight yields of 86.9 mg (87 wt%), 75.1 mg, (75 wt%), and 91.5 mg (92 wt%) respectively, from two independent runs (85 wt% on average). Run 1 and 3 were conducted with the General Procedure G, while run 2 ($^{12/13}$C-labelled substrate) was the result of two hydrogenation reactions, since the first did not achieve a full reduction of nitrile. More specifically, run 2 was carried out according to the General Procedure G, but with RuMACHO (5 wt%), and KOtBu (4 wt%), followed by a second hydrogenation reaction with the exact conditions of the General Procedure G. For simplicity, only the characterisation of two product batches is reported. The products were analysed with solid-state ^{13}C CP/MAS NMR, IR-, TGA-, and Elemental Analysis.

Particle size after cryogenic milling used for CO_2 adsorption-desorption experiments

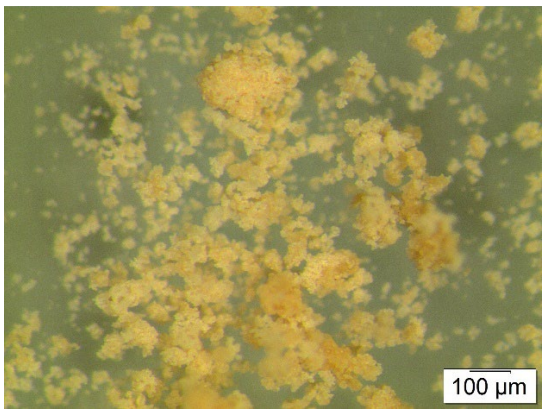

Solubility chart (HCN*-SBR1)

Soluble **Swells** **Not soluble**

$CHCl_3$	Acetone	*i*-PrOH	DMF	DMSO	THF	PhMe	H_2O	MeOH	MeCN

^{13}C CP/MAS NMR (solid-state)

*Solid-state ^{13}C–NMR of **HCN*-SBR1** (run 1):*

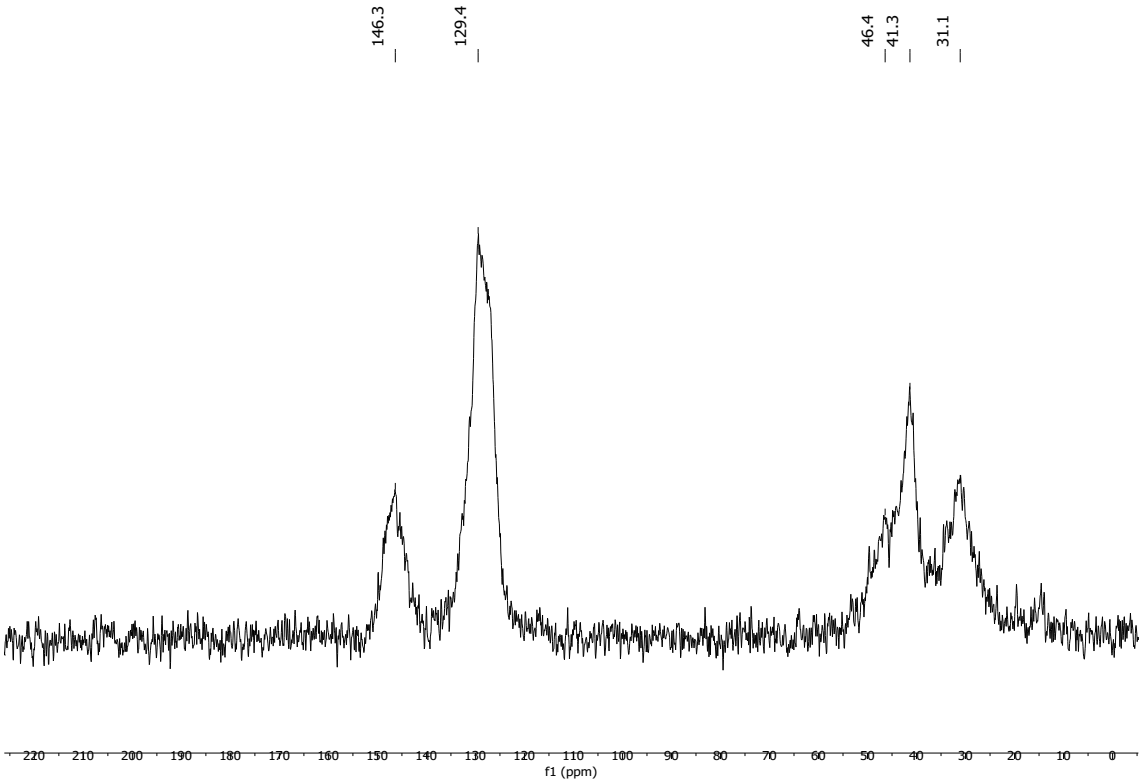

*Solid-state ^{13}C–NMR of **H$^{12/13}$CN*-SBR1** (run 2): The ^{13}C-enriched signal at 46.7 ppm corresponds to the α-carbon of the NH_2 group.*

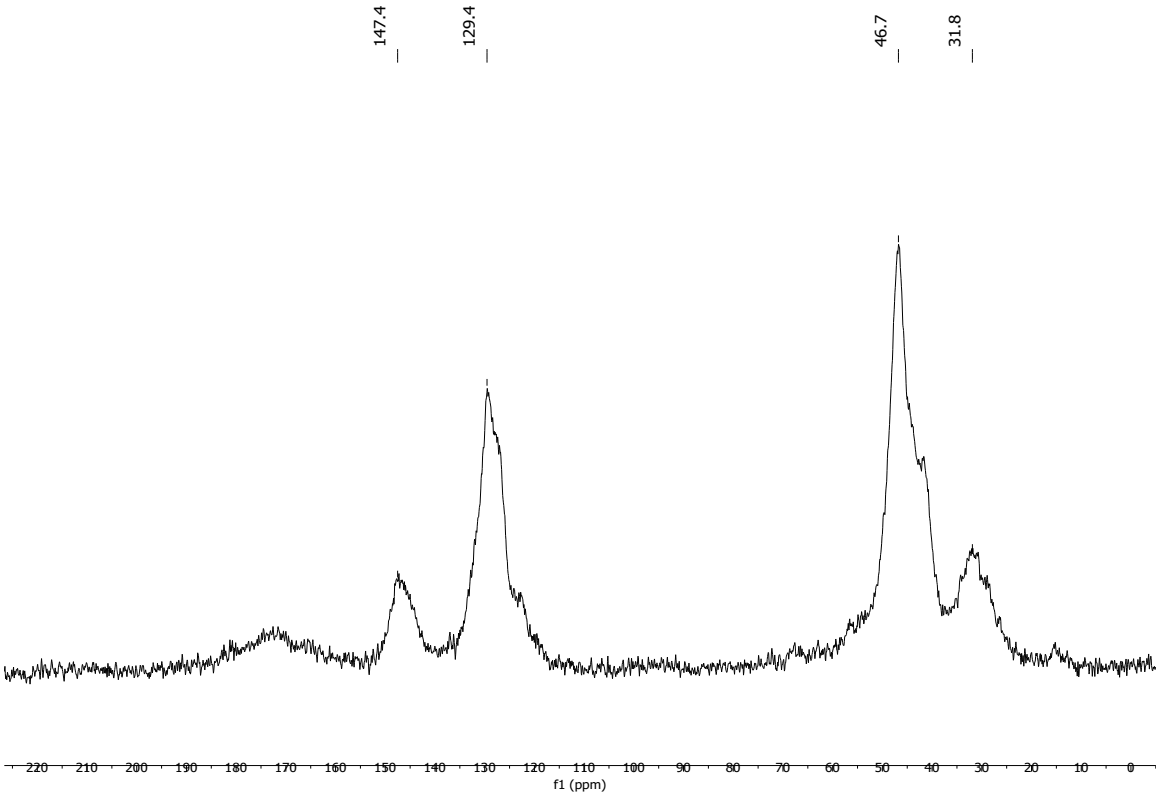

*Solid-state ^{13}C–NMR spectrum overlay of **HCN*-SBR1** (run 1, **brown**) and **HCN-SBR1** (substrate, **light blue**):*

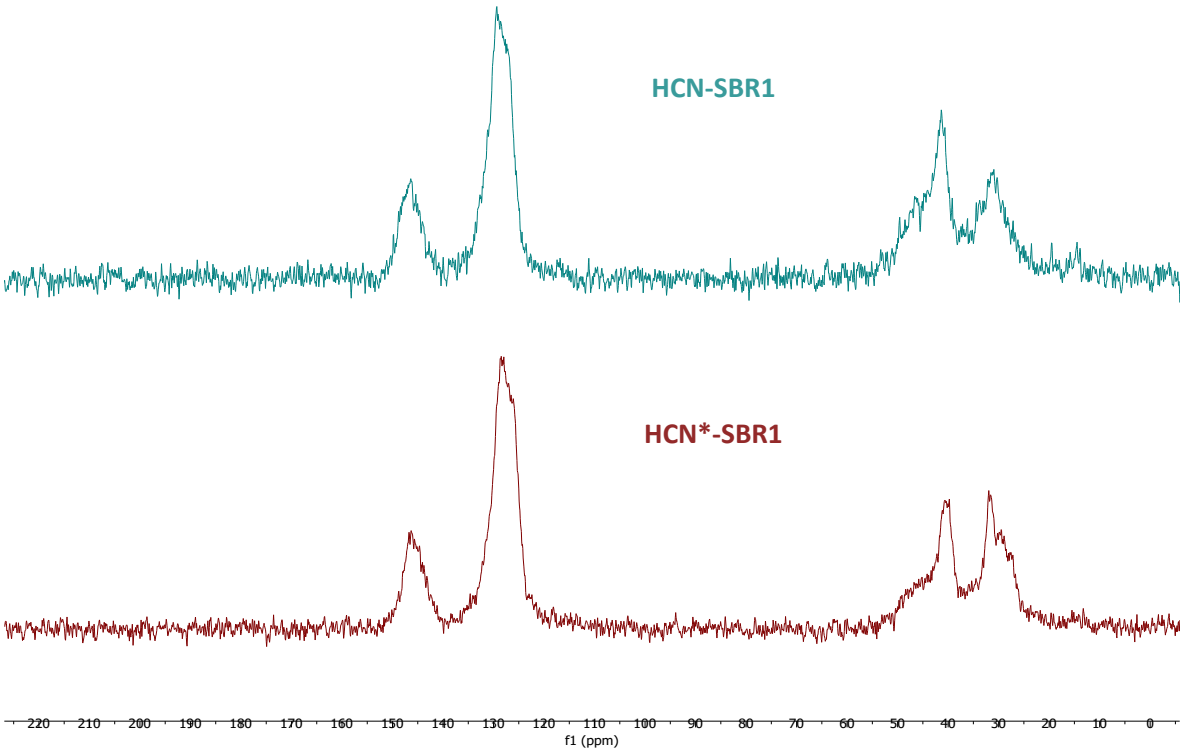

*Solid-state ^{13}C–NMR spectrum overlay of **H$^{12/13}$CN-SBR1** (run 4, **light blue**) and **H$^{12/13}$CN*-SBR1** (run 2, **brown**):*

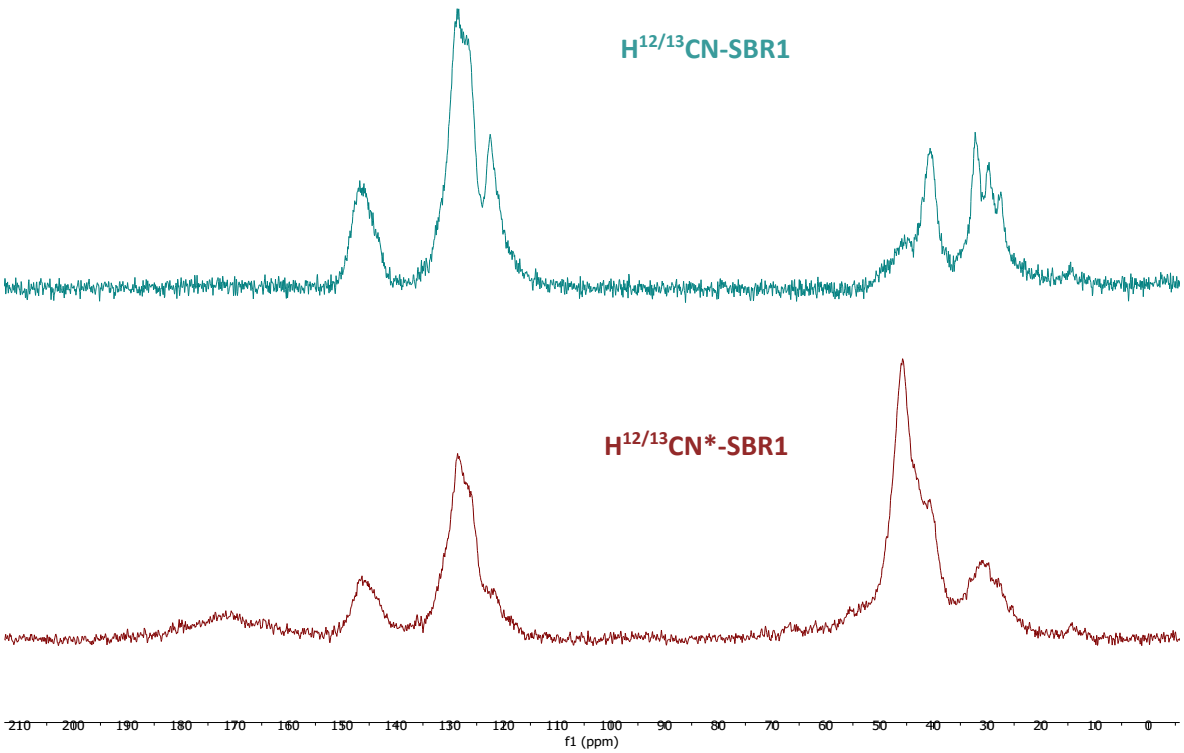

The ^{13}C-enriched nitrile peak at 122.4 ppm (top spectrum) is converted into the ^{13}C-enriched peak at 46.7 ppm after the hydrogenation reaction indicating primary amine formation.

Infrared (IR) Spectroscopic Analysis

*IR-spectrum of **HCN*-SBR1** (run 1):*

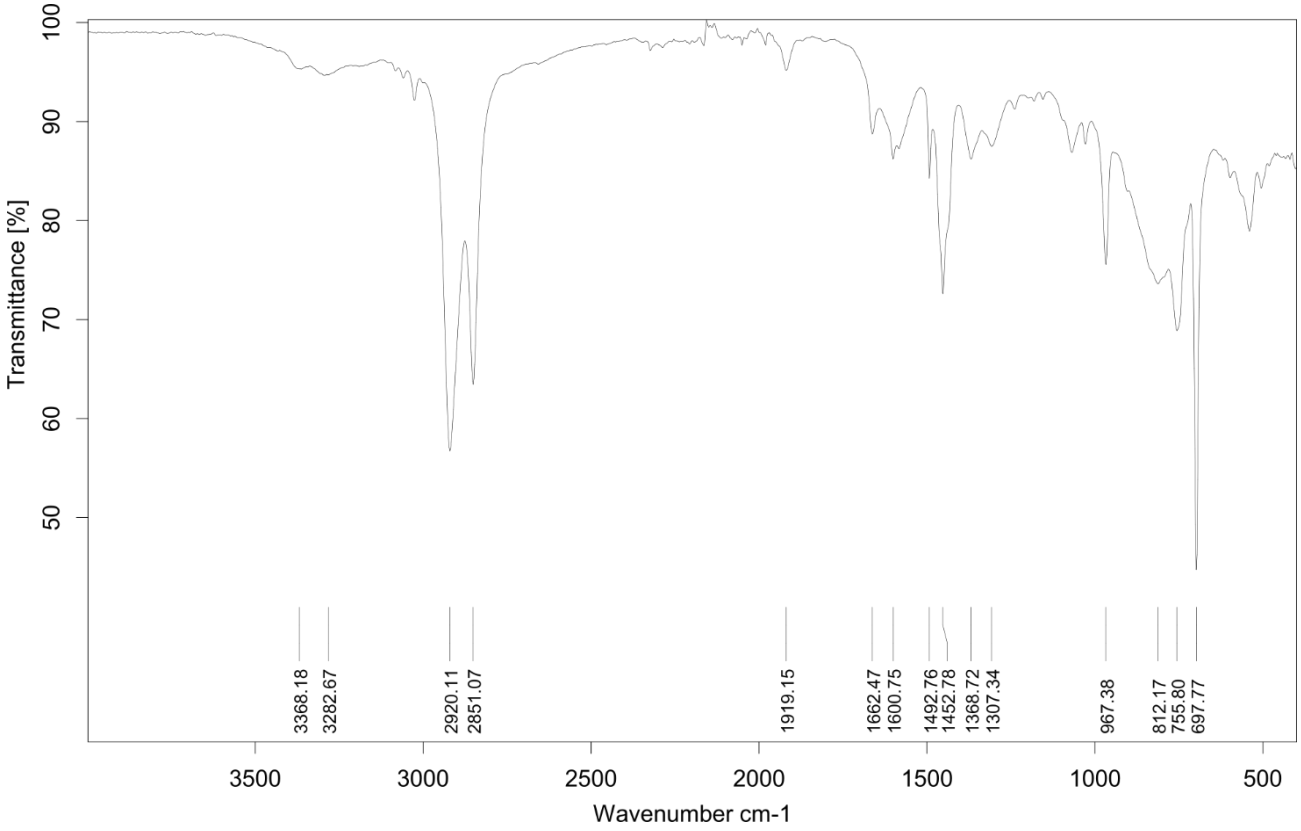

*IR-spectrum of **H$^{12/13}$CN*-SBR1** (run 2):*

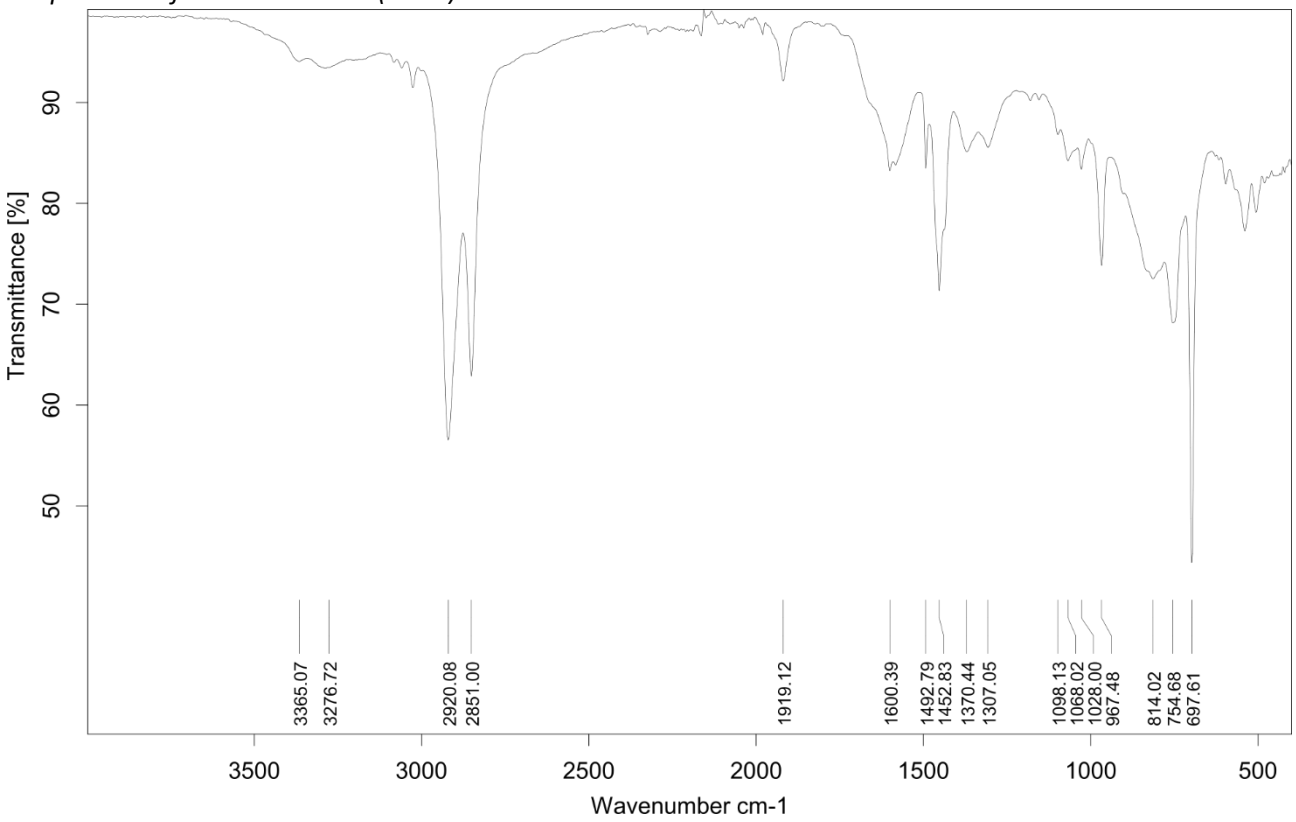

*IR-spectrum overlay of **HCN*-SBR1** (run 1, **black**) and **HCN-SBR1** (substrate, **red**):*

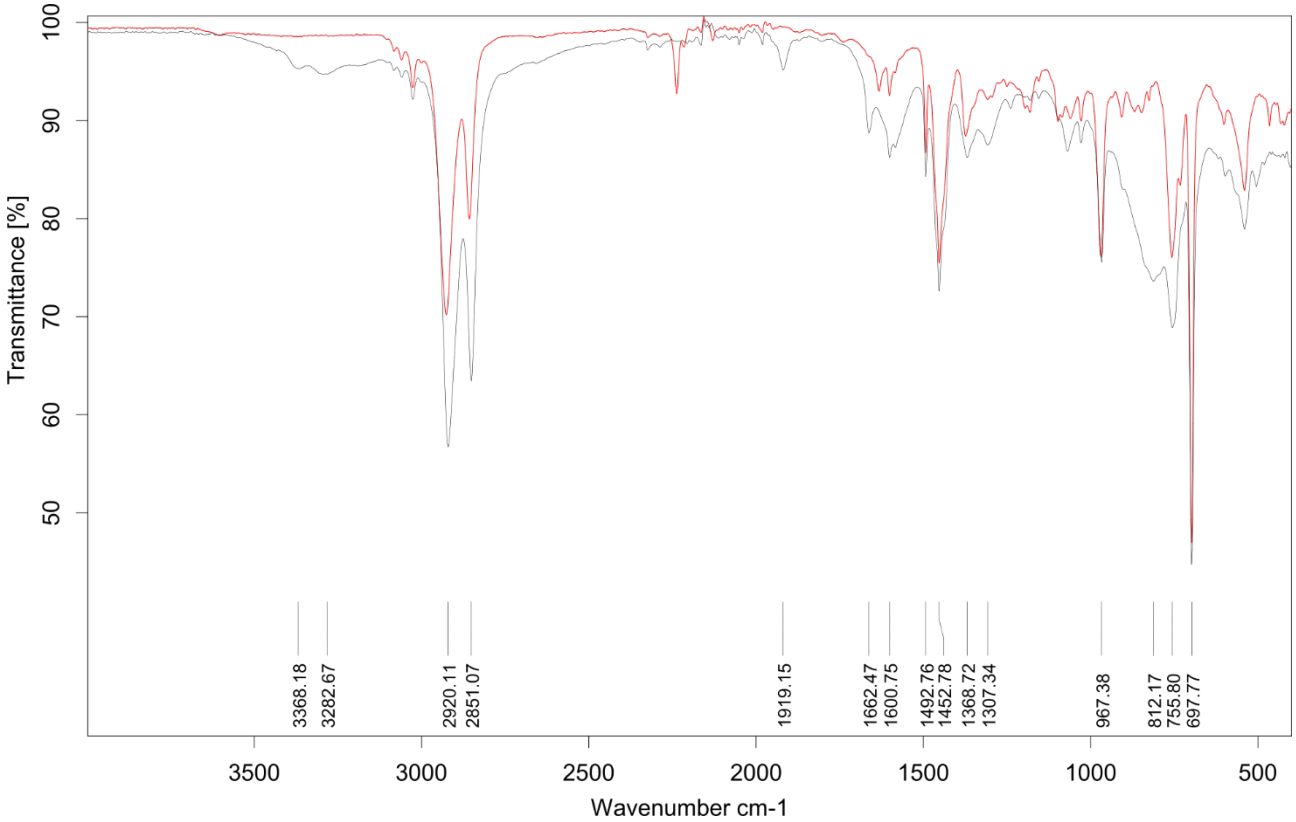

Thermogravimetric Analysis (TGA)

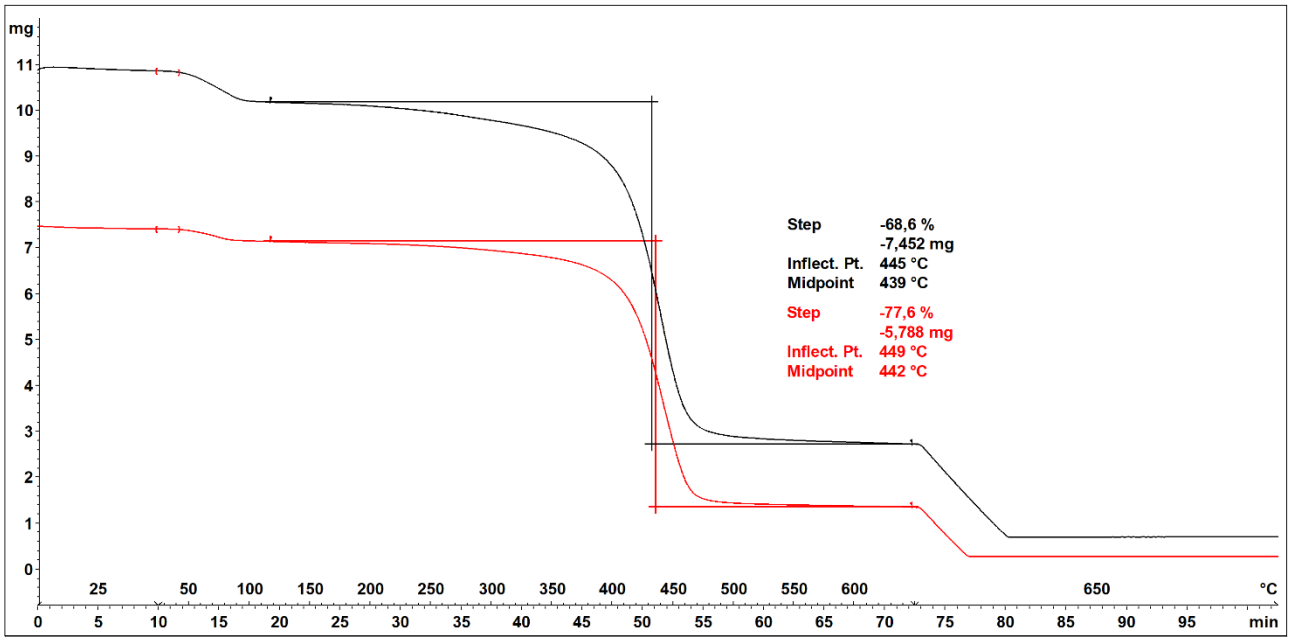

Decomposition graph. The experiment was conducted under He then air (after 650 °C). The black curve is the result from run 1, while the red curve is for run 2.

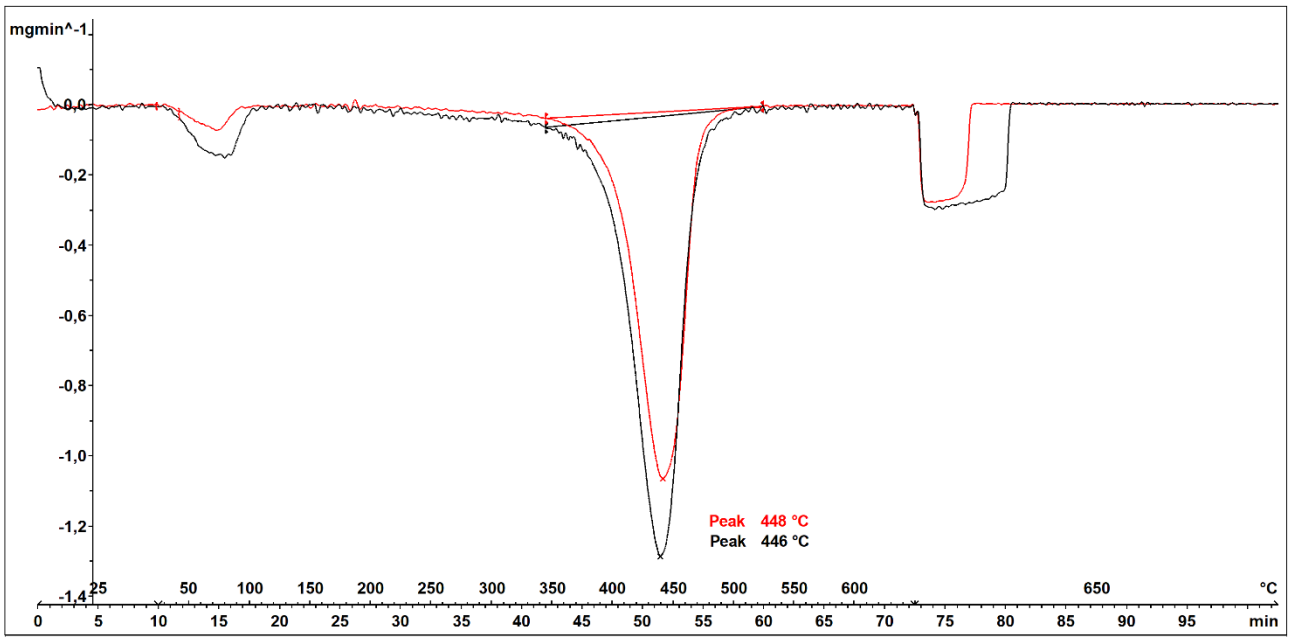

1st derivative of decomposition graph. The experiment was conducted under He then air (after 650 °C). The black curve is the result from run 1, while the red curve is for run 2.

Decomposition temperature (T_d) = 446−448 ℃.

CO_2-adsorption analysis by thermogravimetric analysis

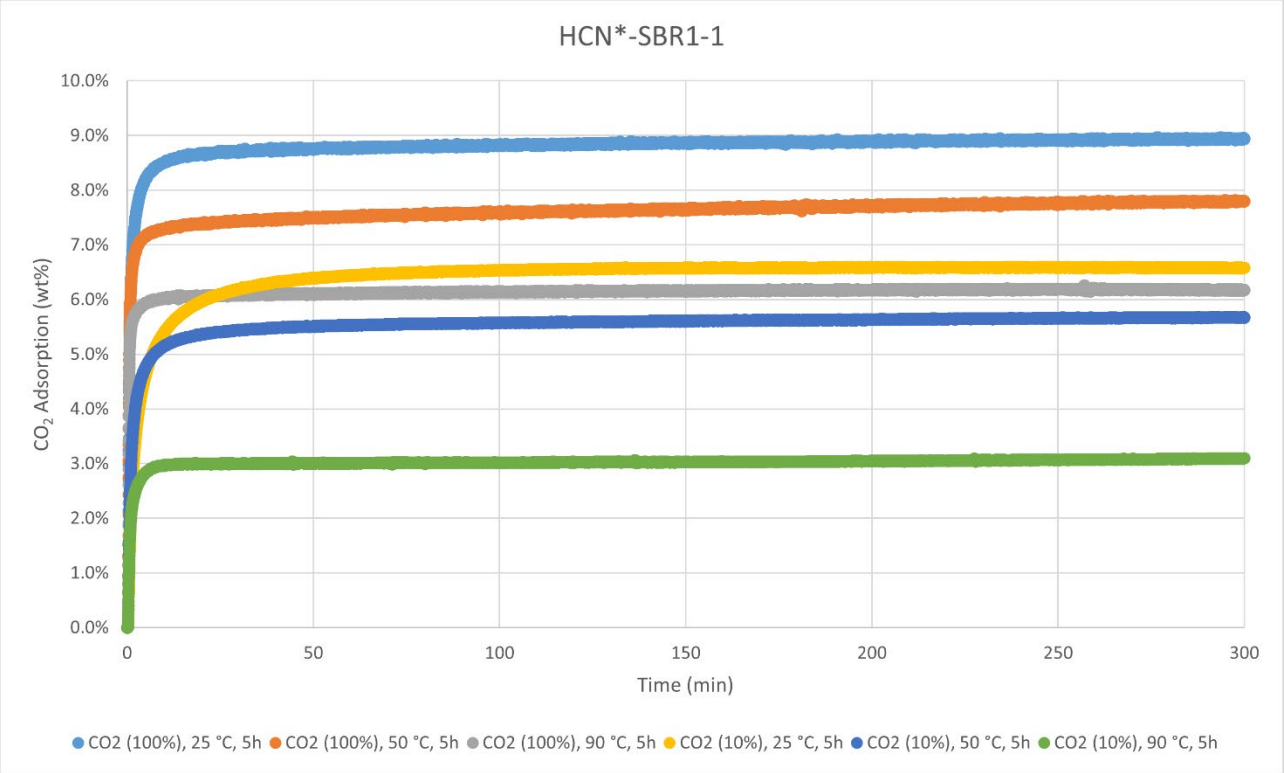

CO_2 adsorption using **TGA method 2** (measurement of product batch from run 1: HCN*-SBR1-1).

HCN*-SBR1-1	wt%	mmol/g
CO2 (100%), 25 °C, 5h	8.9%	2.03
CO2 (100%), 50 °C, 5h	7.8%	1.77
CO2 (100%), 90 °C, 5h	6.2%	1.40
CO2 (10%), 25 °C, 5h	6.6%	1.50
CO2 (10%), 50 °C, 5h	5.7%	1.29
CO2 (10%), 90 °C, 5h	3.1%	0.70

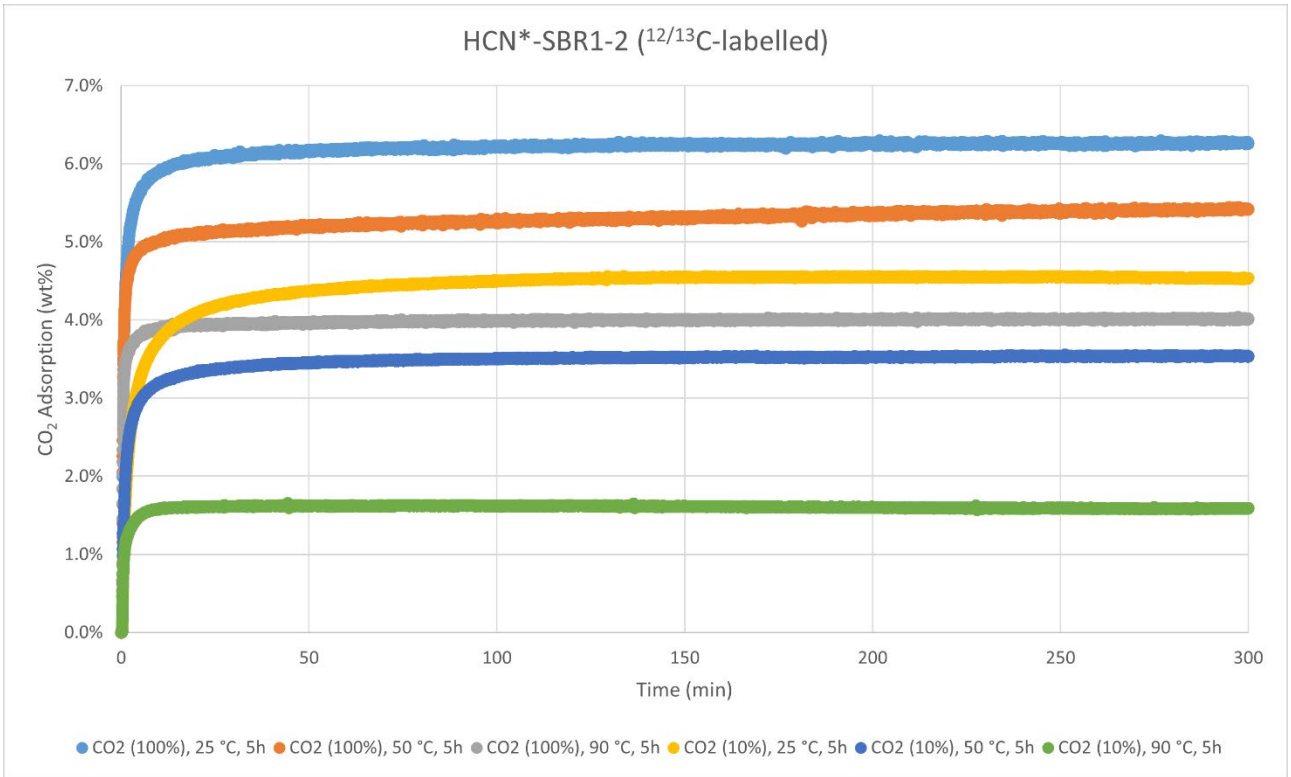

CO_2 adsorption using **TGA method 2** (measurement of product batch from run 2: HCN*-SBR1-2).

HCN*-SBR1-2 ($^{12/13}$C-labelled)	wt%	mmol/g
CO2 (100%), 25 °C, 5h	6.3%	1.42
CO2 (100%), 50 °C, 5h	5.4%	1.23
CO2 (100%), 90 °C, 5h	4.0%	0.91
CO2 (10%), 25 °C, 5h	4.5%	1.03
CO2 (10%), 50 °C, 5h	3.5%	0.80
CO2 (10%), 90 °C, 5h	1.6%	0.36

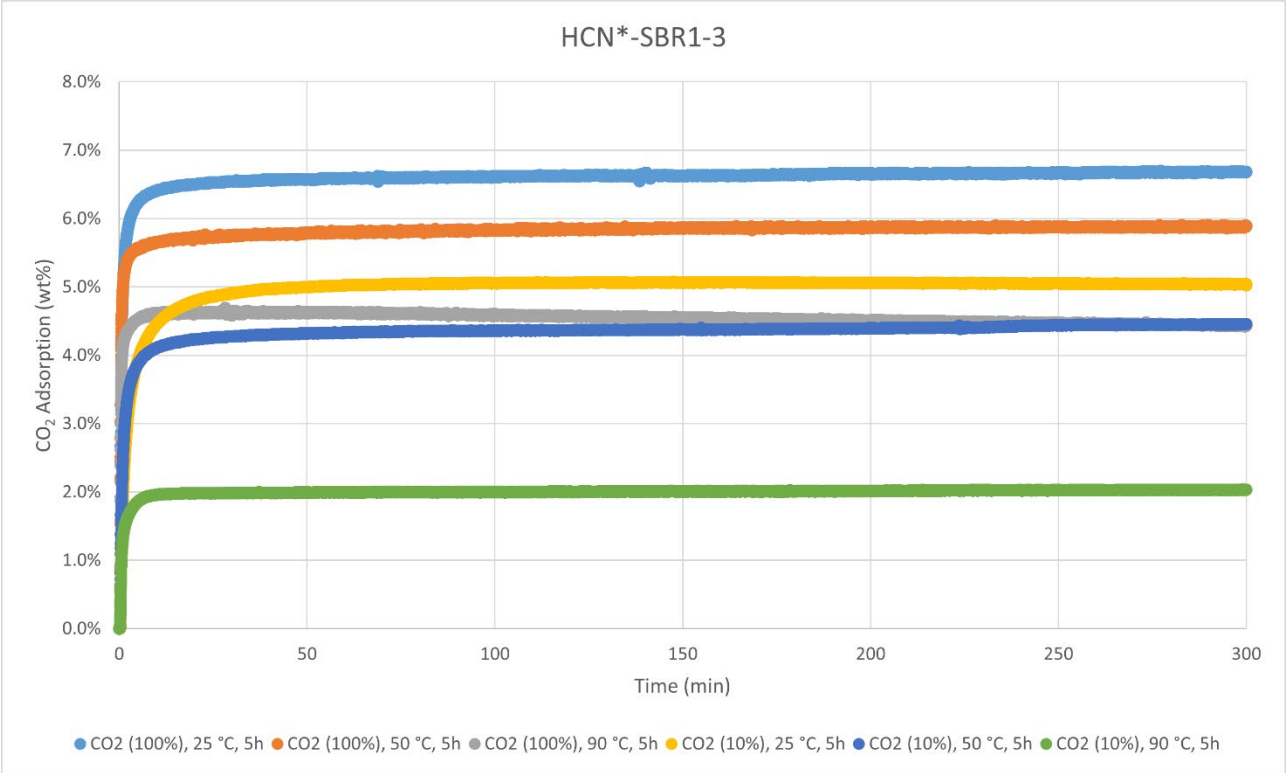

CO_2 adsorption using **TGA method 2** (measurement of product batch from run 3: HCN*-SBR1-3).

HCN*-SBR1-3	wt%	mmol/g
CO2 (100%), 25 °C, 5h	6.7%	1.52
CO2 (100%), 50 °C, 5h	5.9%	1.34
CO2 (100%), 90 °C, 5h	4.4%	1.01
CO2 (10%), 25 °C, 5h	5.0%	1.15
CO2 (10%), 50 °C, 5h	4.5%	1.01
CO2 (10%), 90 °C, 5h	2.0%	0.46

Elemental Analysis

	N [%]	C [%]	H [%]	S [%]	mmol N/g	C/N ratio	C/H ratio
Run 1	**6.97**	**73.28**	**10.30**	**Not detected**	**4.97**	**12.27**	**0.60**
Run 2	**7.22**	**75.78**	**9.07**	**Not detected**	**5.15**	**12.25**	**0.70**
Run 3	**6.98**	**75.67**	**10.16**	**Not detected**	**4.98**	**12.64**	**0.63**

Hydrocyanated Styrene Butadiene Rubber 2 (HCN-SBR2) was synthesised according to the General Procedure E from substrate **SBR2** (shoe sole). Workup was performed by washing the suspension in chamber A, containing dissolved polymer and carbon black, with 3 x 10 mL aq. 2 M NaOH and 3 x 10 mL water. The washed suspension was then filtered through a short plug of celite into 30 mL well-stirred MeOH. The plug was additionally rinsed with PhMe (5 mL). After ensuring full precipitation of the product polymer by diluting with another 100 mL MeOH, it was separated by decantation and dried in high vacuum overnight. The product was obtained in weight yields of 164 mg (66 wt%), 162 mg (65 wt%), 125 mg (50 wt%), and 137 mg (55 wt%), respectively, from four independent runs (59 wt% on average). The lower yield of this polymer can be partly explained by the presence of carbon black, which is filtered off before precipitation of the **HCN-SBR2** product, thus losing some mass. The polymers were reacted in the subsequent hydrogenation step without further purification. For analytical purposes, the polymers were suspended in $CHCl_3$ and then dried (repeated twice) to obtain pure NMR spectra free from other solvents. Due to a low solubility of the polymer, only enough polymer could be dissolved for obtaining ^{1}H-NMR spectra, while too little for ^{13}C-NMR spectra. For simplicity, only the characterisation of two product batches is reported.

Particle size used for ensuing hydrogenation reactions

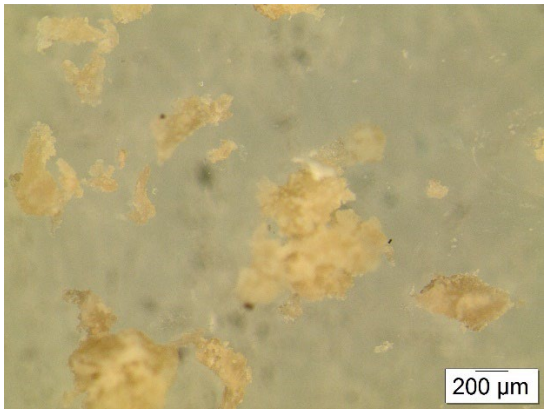

^{1}H–NMR ($CDCl_3$) (The polymer is only minimally soluble in $CDCl_3$)

*^{1}H–NMR of **HCN-SBR2** (run 1):*

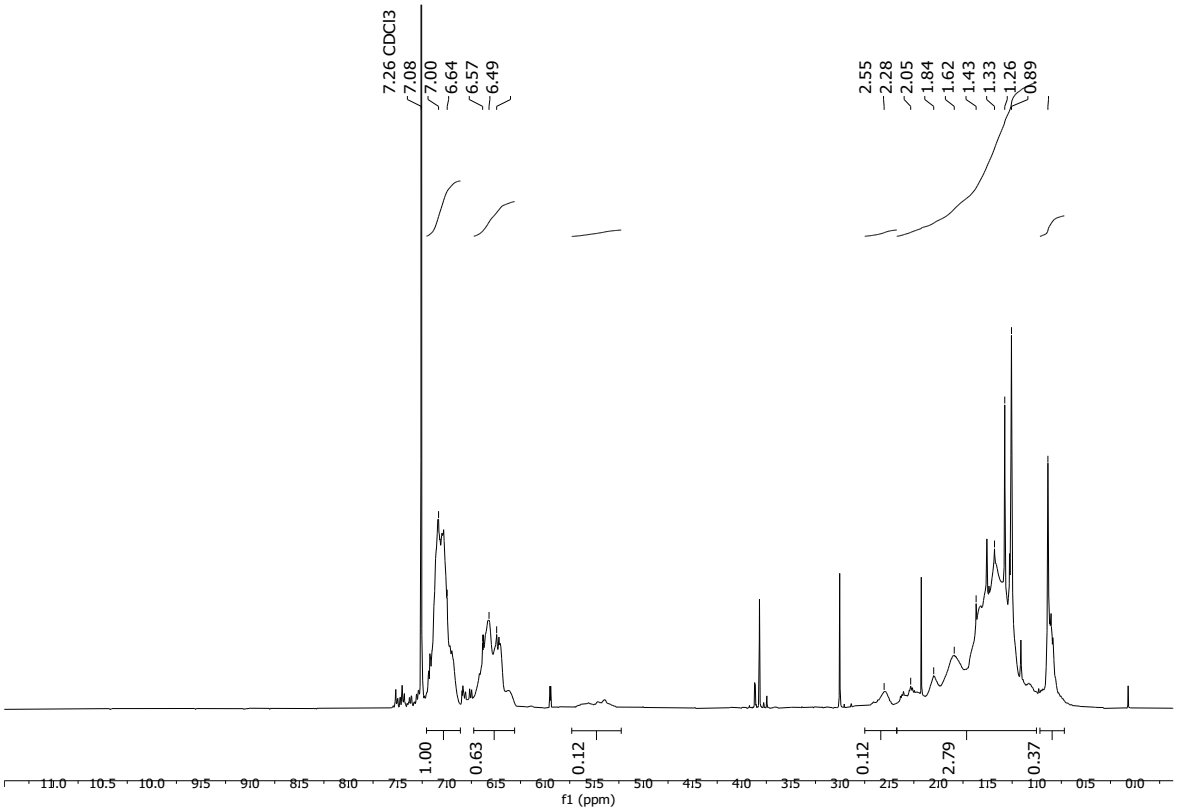

*^{1}H–NMR of **HCN-SBR2** (run 2):*

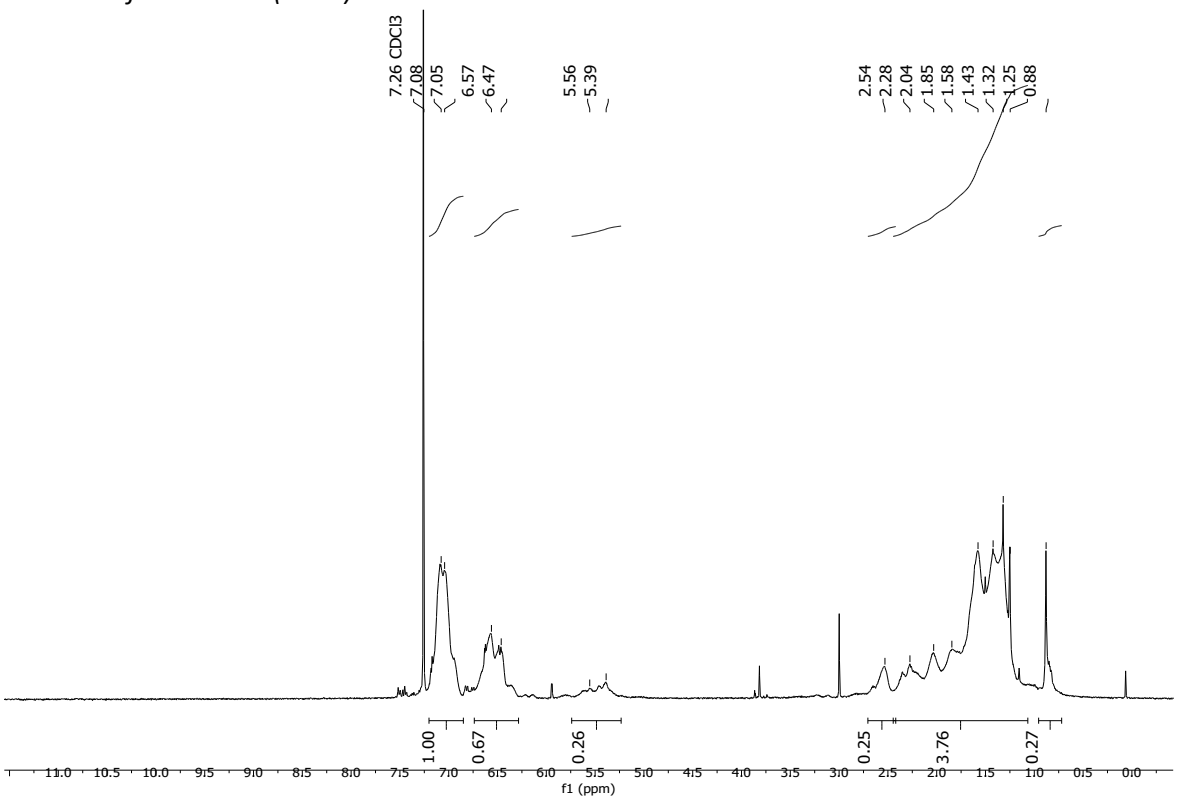

*^{1}H–NMR spectrum overlay of **HCN-SBR2** (run 2, **black**) and **SBR2** (substrate, **grey**):*

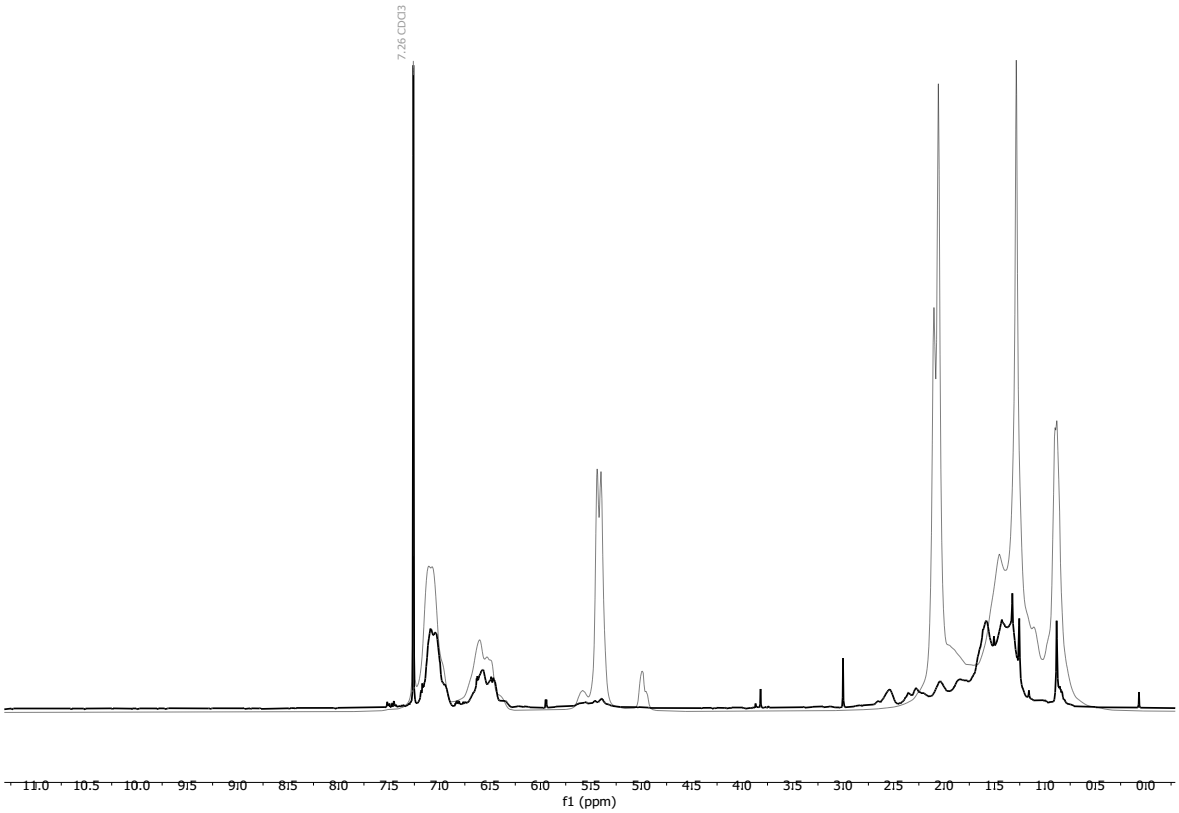

^{13}C CP/MAS NMR (solid-state)

*Solid-state ^{13}C–NMR of **HCN-SBR2** (runs 1 and 2 in a combined sample):*

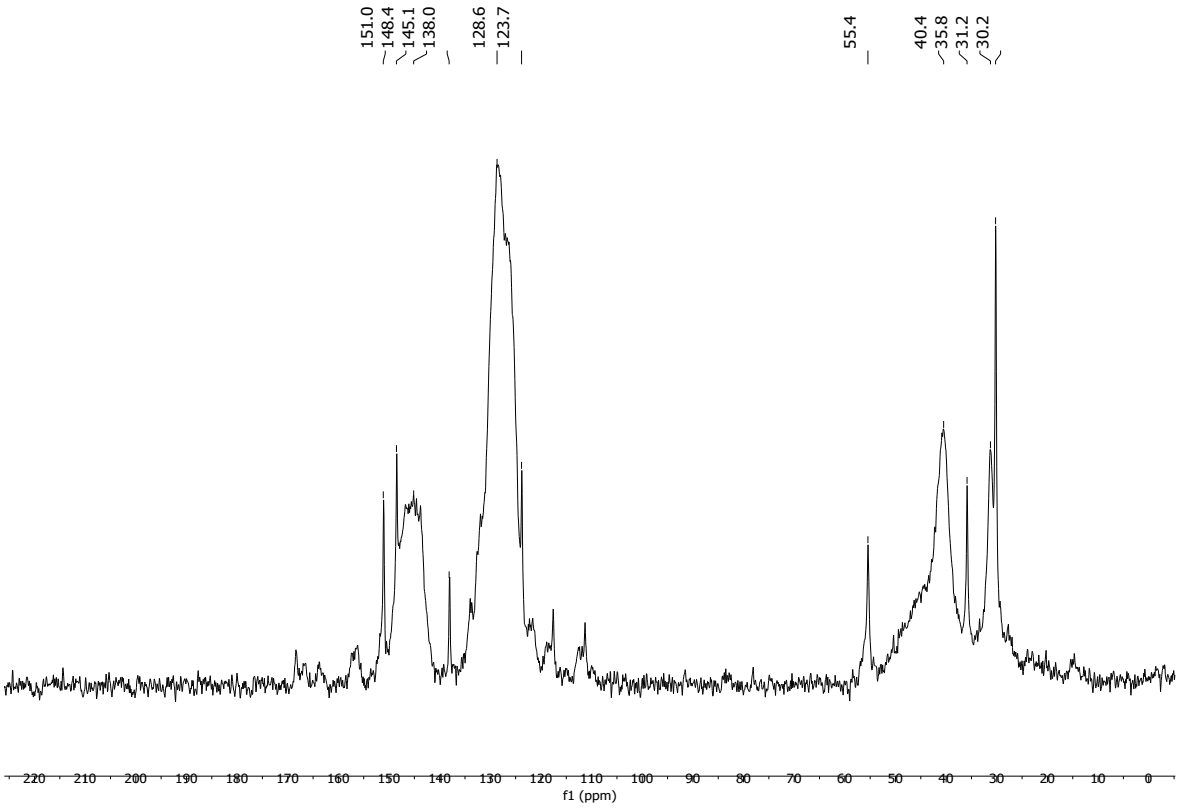

*Solid-state ^{13}C–NMR spectrum overlay of **HCN-SBR2** (runs 1 and 2, **brown**) and **SBR2** (substrate, **light blue**):*

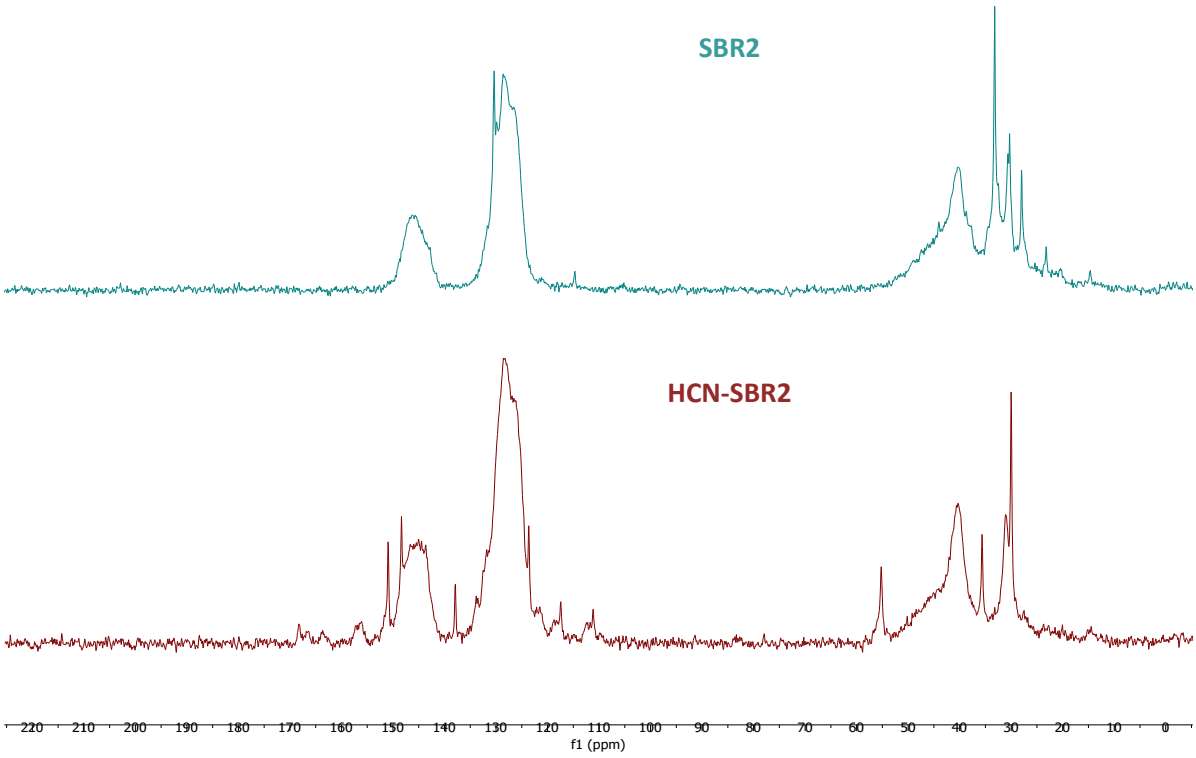

Infrared (IR) Spectroscopic Analysis

*IR-spectrum of **HCN-SBR2** (run 1):*

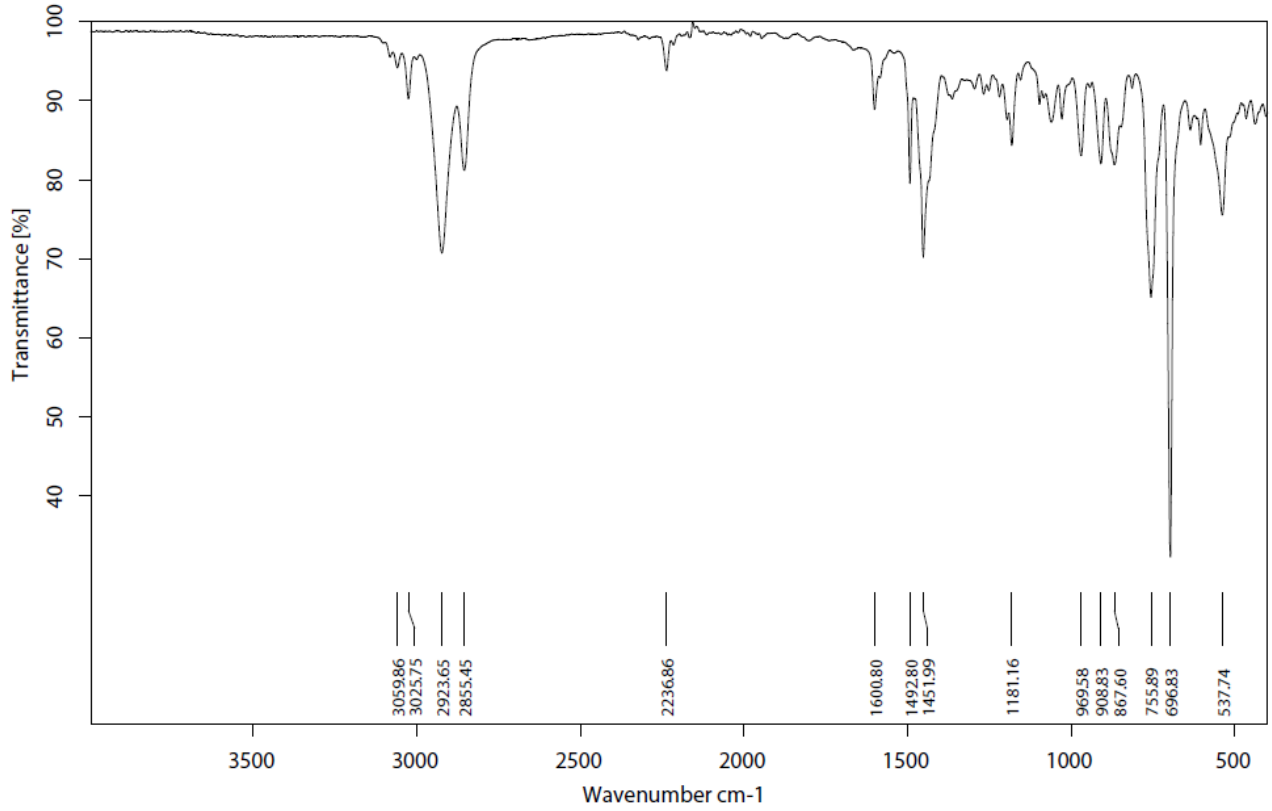

*IR-spectrum of **HCN-SBR2** (run 2):*

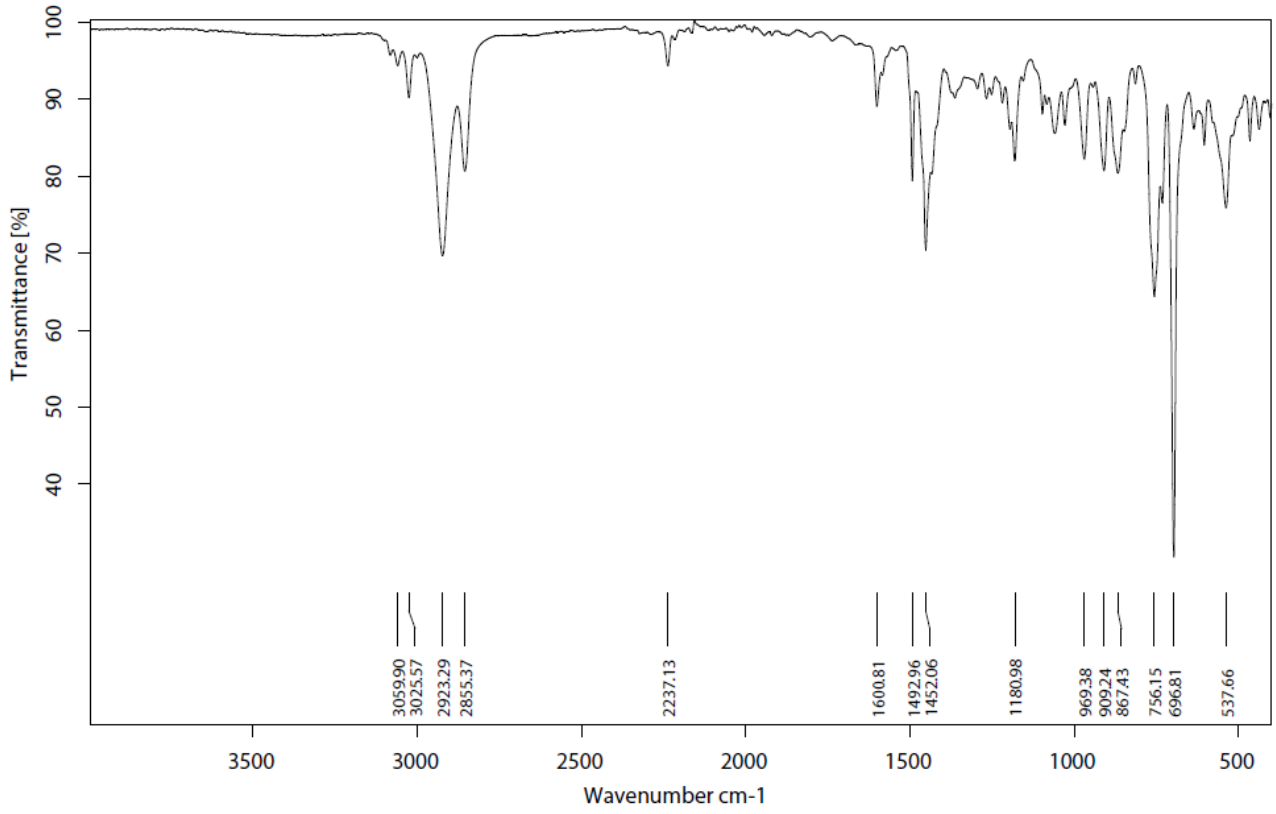

*IR-spectrum overlay of **HCN-SBR2** (run 1, **black**) and **SBR2** (substrate, **red**):*

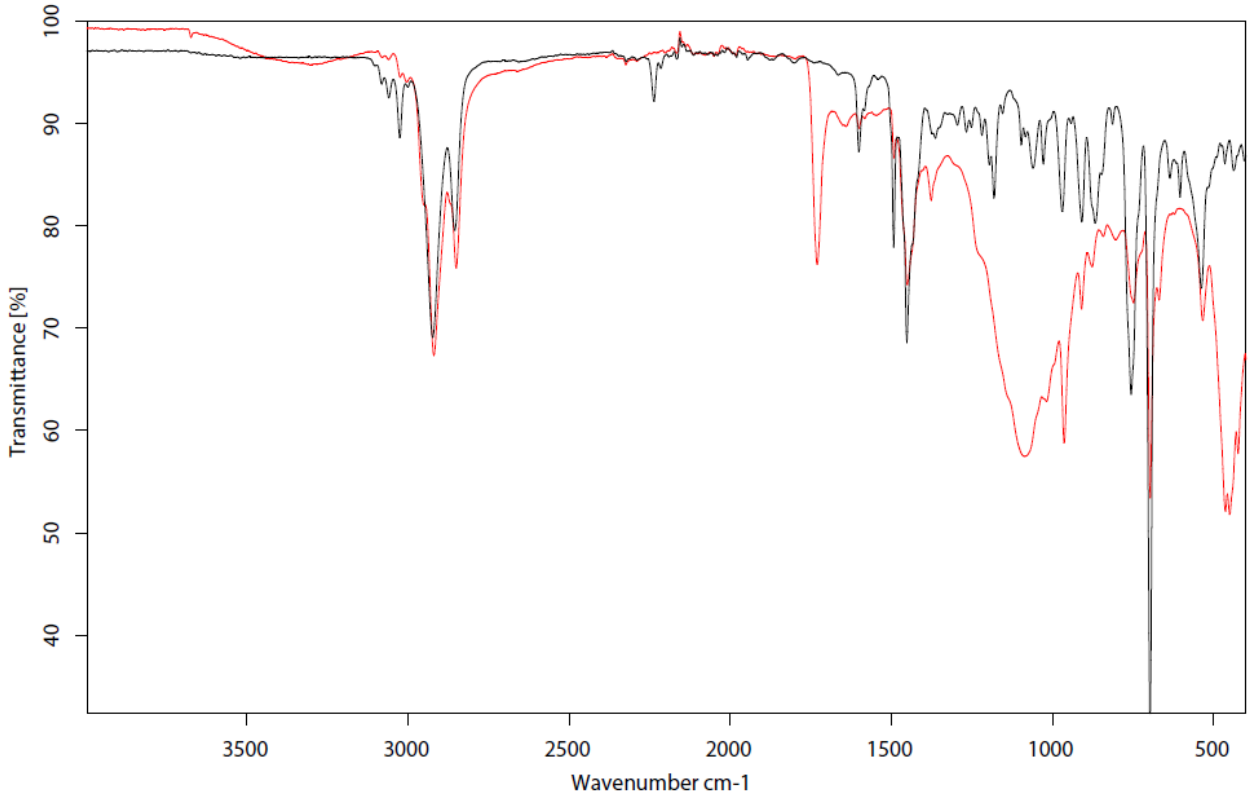

Elemental Analysis (EA)

	N [%]	C [%]	H [%]	S [%]	mmol N/g	C/N ratio	C/H ratio
Combined runs 1 & 2	**4.24**	**78.01**	**9.27**	**Not detected**	**3.03**	**21.45**	**0.71**

Hydrogenated hydrocyanated Styrene Butadiene Rubber 1 (HCN*-SBR2) was synthesised according to the General Procedure G from substrate **HCN-SBR2** and was obtained in weight yields of 76.7 mg, 77 wt% and 56.3 mg, 56 wt%, respectively, from two independent runs (67 wt% on average). The polymer was analysed with solid-state ^{13}C CP/MAS NMR, IR-, TGA-, and elemental analysis.

Particle size after cryogenic milling used for CO_2 adsorption-desorption experiments

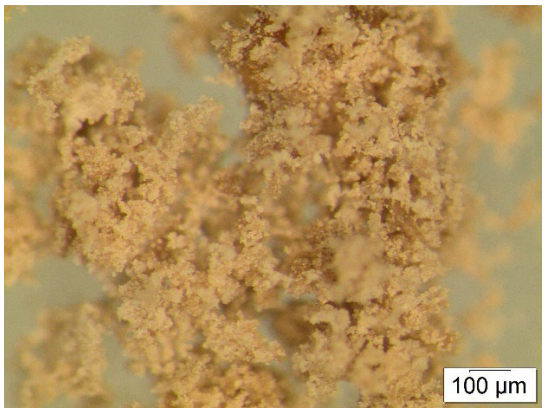

Solubility chart

Soluble **Swells** **Not soluble**

$CHCl_3$	Acetone	*i*-PrOH	DMF	DMSO	THF	PhMe	H_2O	MeOH	MeCN

^{13}C CP/MAS NMR (solid-state)

*Solid-state ^{13}C–NMR of **HCN*-SBR2** (run 1 and run 2 combined):*

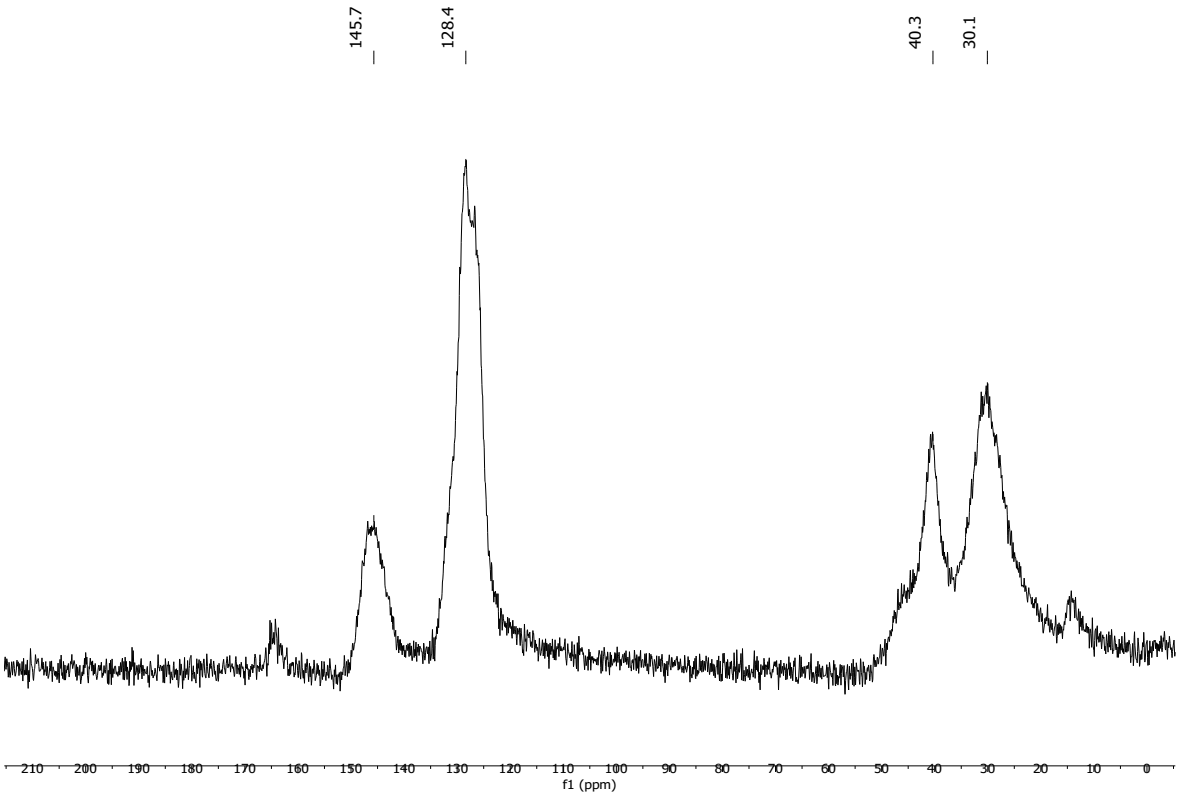

*Solid-state ^{13}C–NMR spectrum overlay of **HCN-SBR2** (run 1+2 combined, **light blue**) and **HCN*-SBR2** (run 1+2 combined, **brown**):*

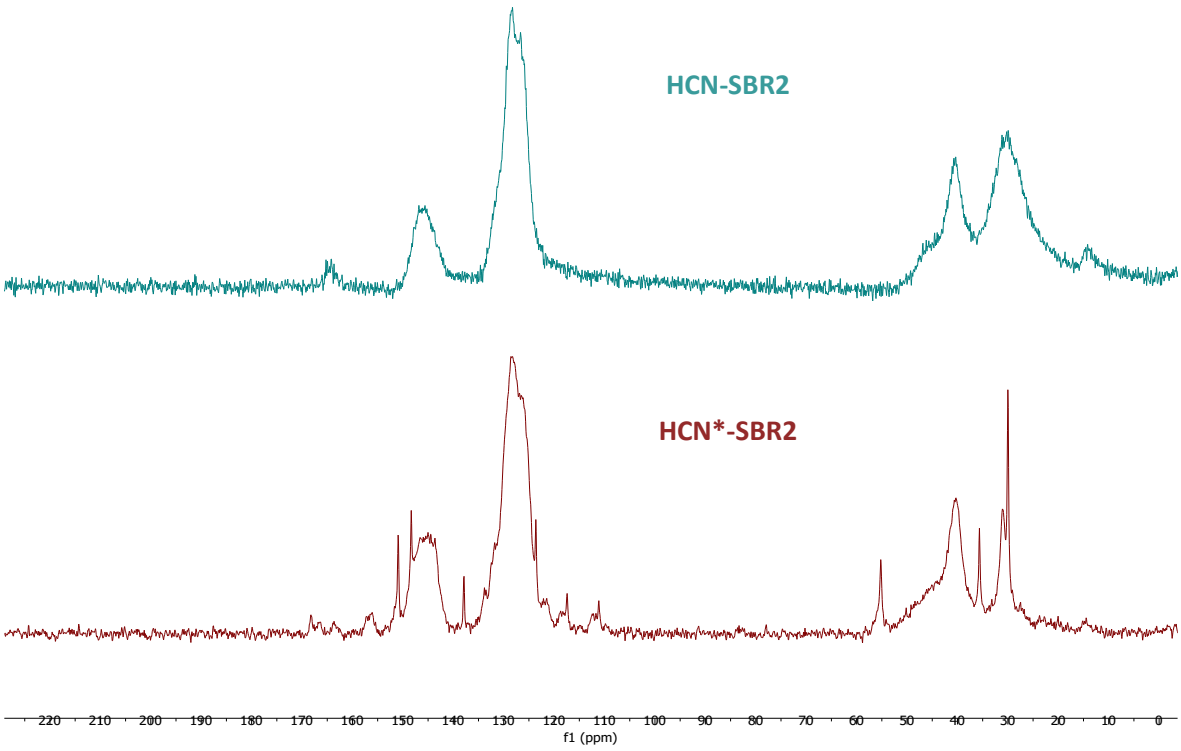

Infrared (IR) Spectroscopic Analysis

*IR-spectrum of **HCN*-SBR2** (run 1):*

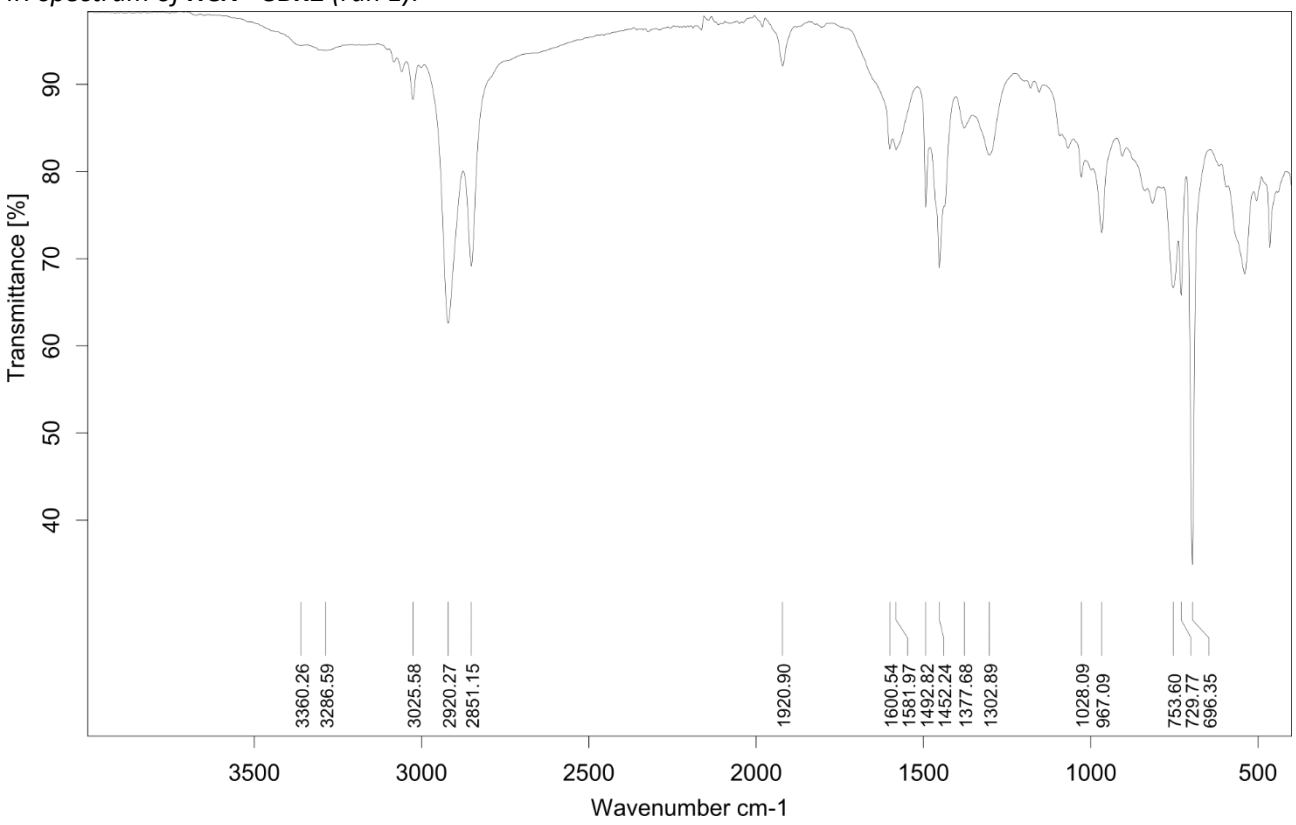

*IR-spectrum of **HCN*-SBR2** (run 2):*

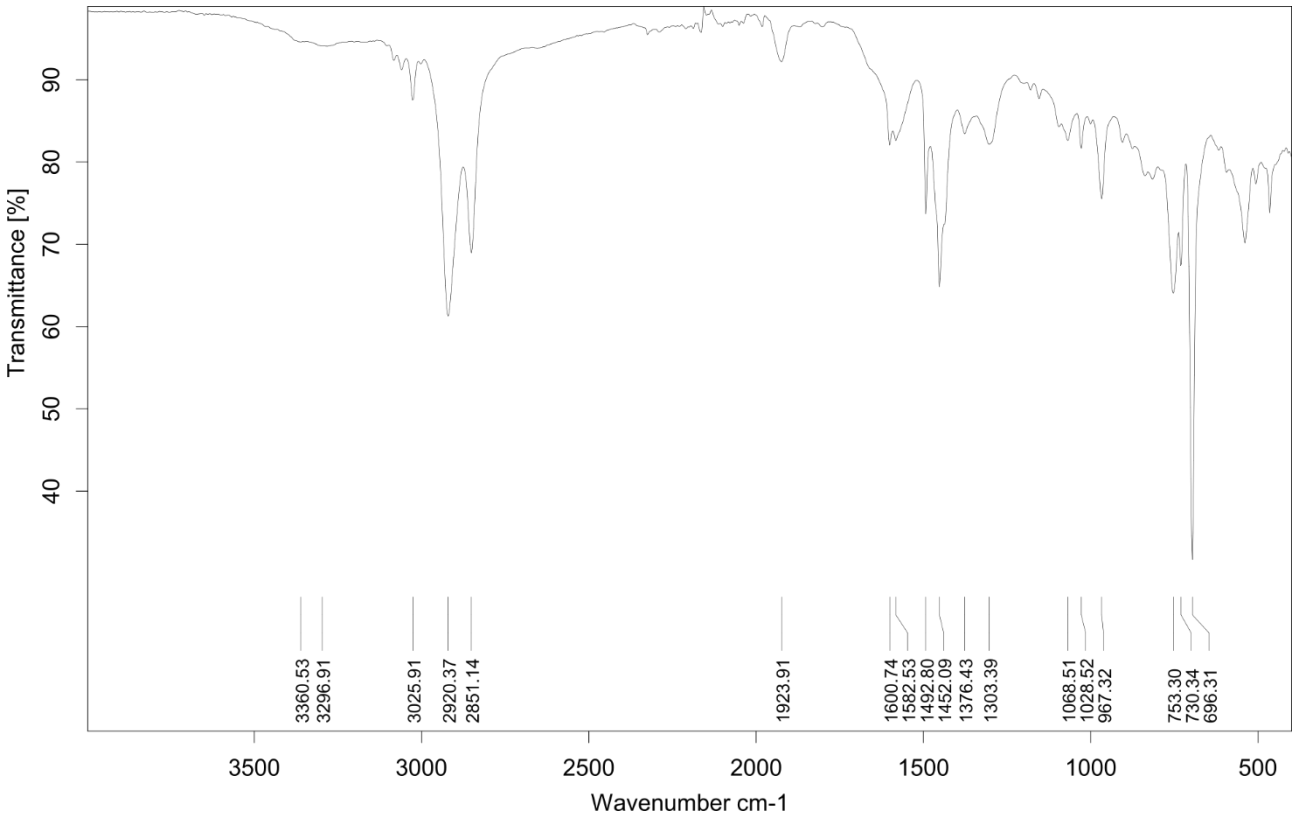

*IR-spectrum overlay of **HCN*-SBR2** (run 1, **black**) and **HCN-SBR2** (substrate, **red**):*

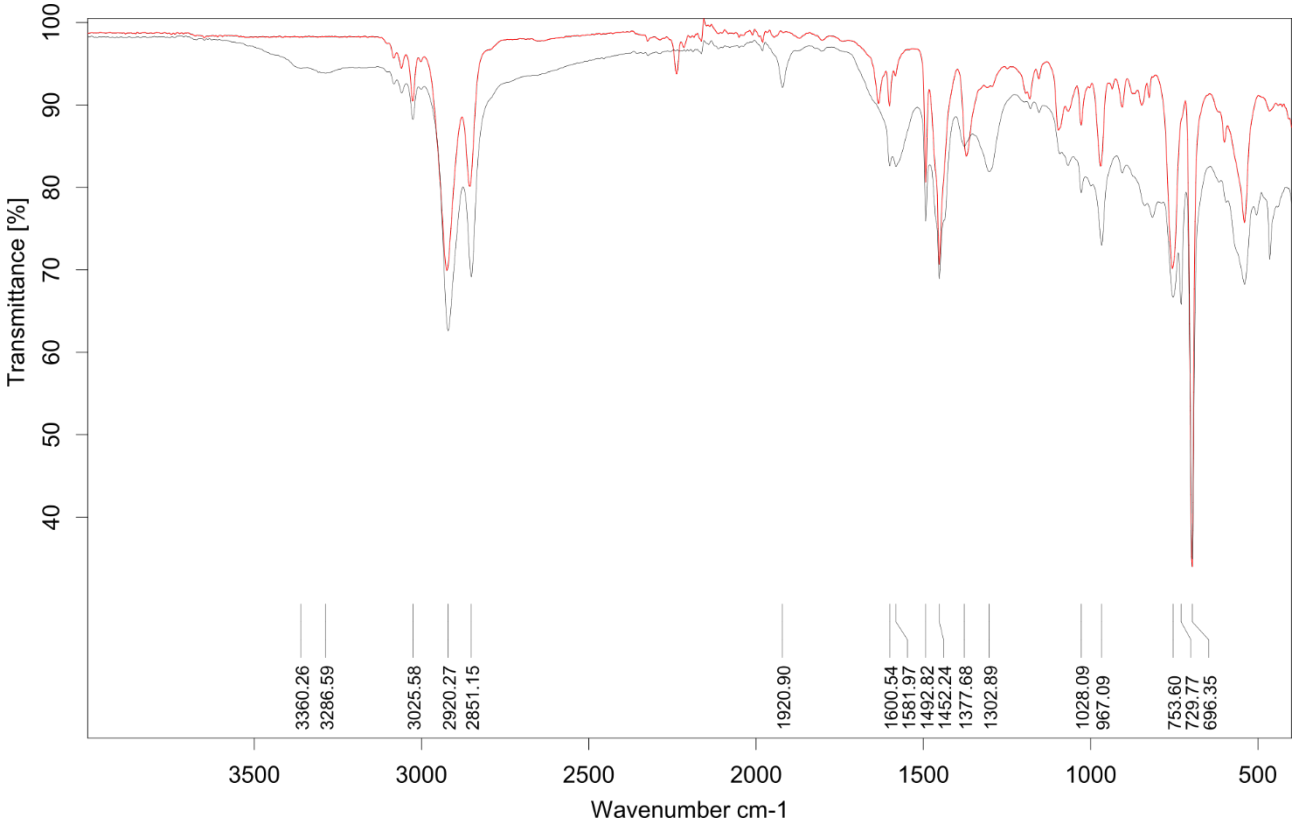

Thermogravimetric Analysis (TGA)

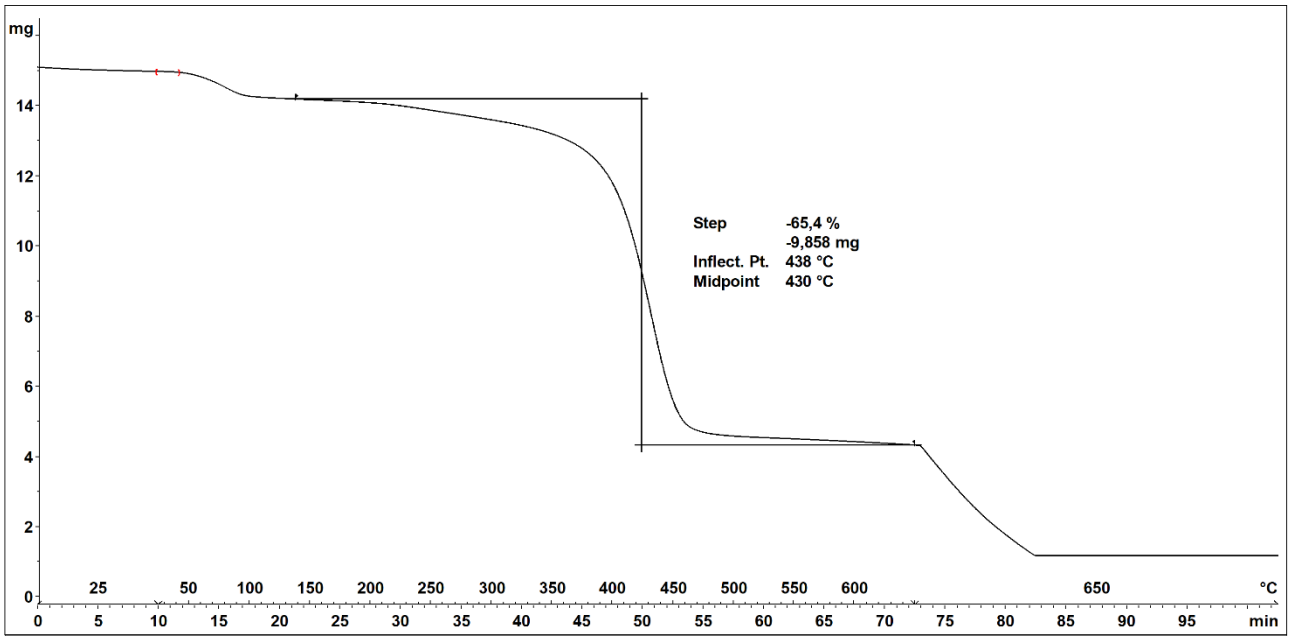

Decomposition graph. The experiment was conducted under He then air (after 650 °C). A combined sample of HCN-SBR2 run 1 and run 2 was used for this analysis.*

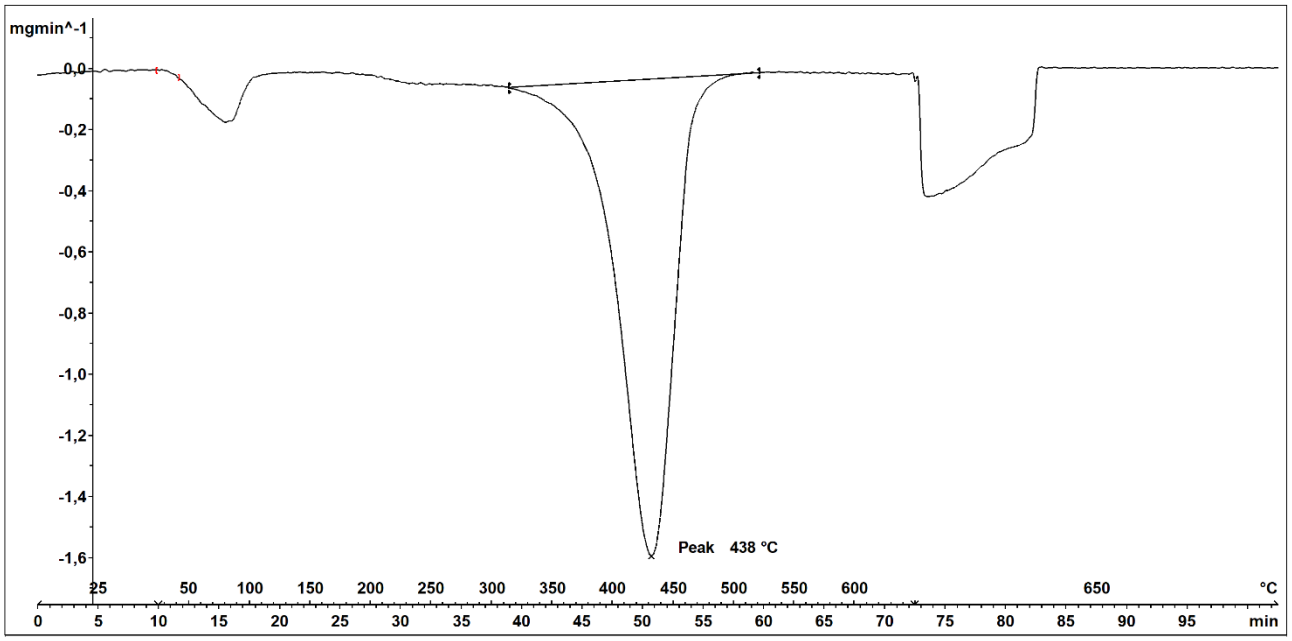

1st derivative of decomposition graph. The experiment was conducted under He then air (after 650 °C). A combined sample of HCN-SBR2 run 1 and run 2 was used for this analysis.*

Decomposition temperature (T_d) = 438 ℃.

CO_2-adsorption analysis by thermogravimetric analysis

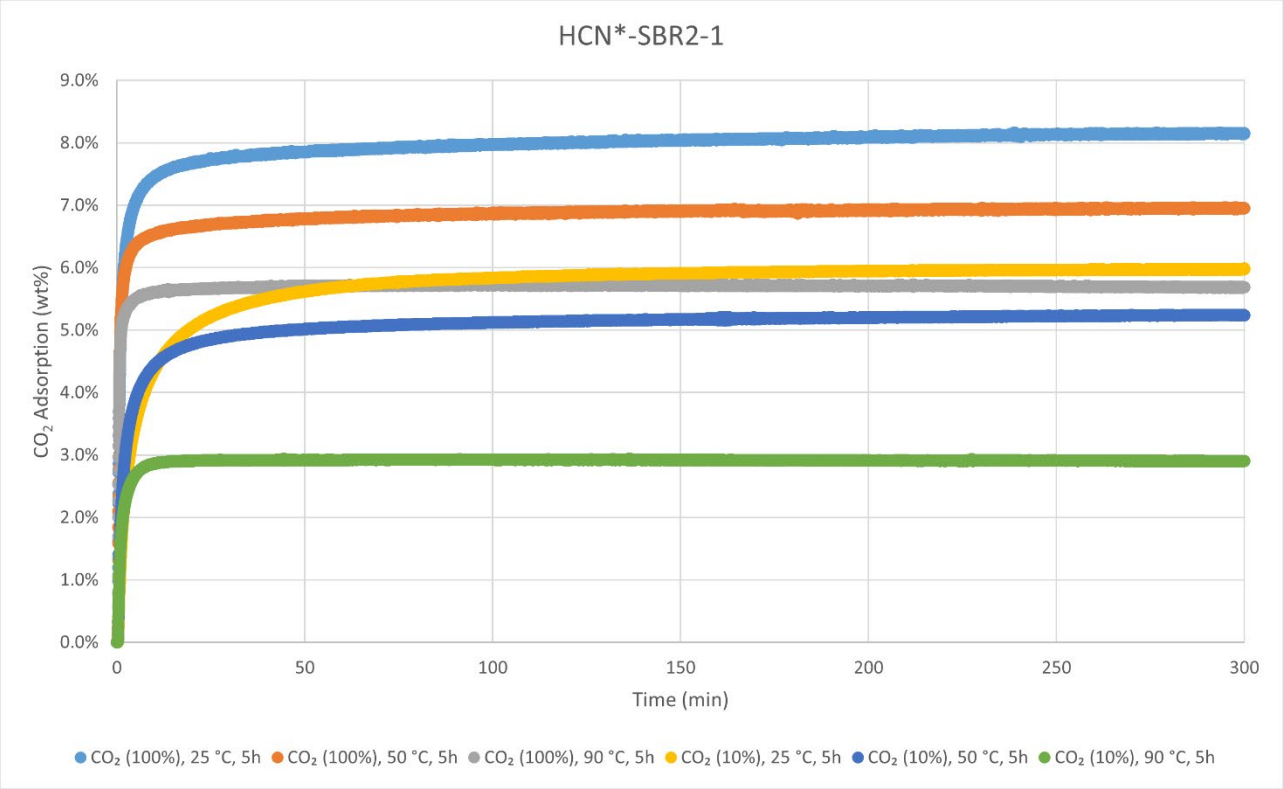

CO_2 adsorption using **TGA method 2** (measurement of product batch from run 1: HCN*-SBR2-1).

HCN*-SBR2-1	wt%	mmol/g
CO_2 (100%), 25 °C, 5h	8.2%	1.85
CO_2 (100%), 50 °C, 5h	7.0%	1.58
CO_2 (100%), 90 °C, 5h	5.7%	1.29
CO_2 (10%), 25 °C, 5h	6.0%	1.36
CO_2 (10%), 50 °C, 5h	5.2%	1.19
CO_2 (10%), 90 °C, 5h	2.9%	0.66

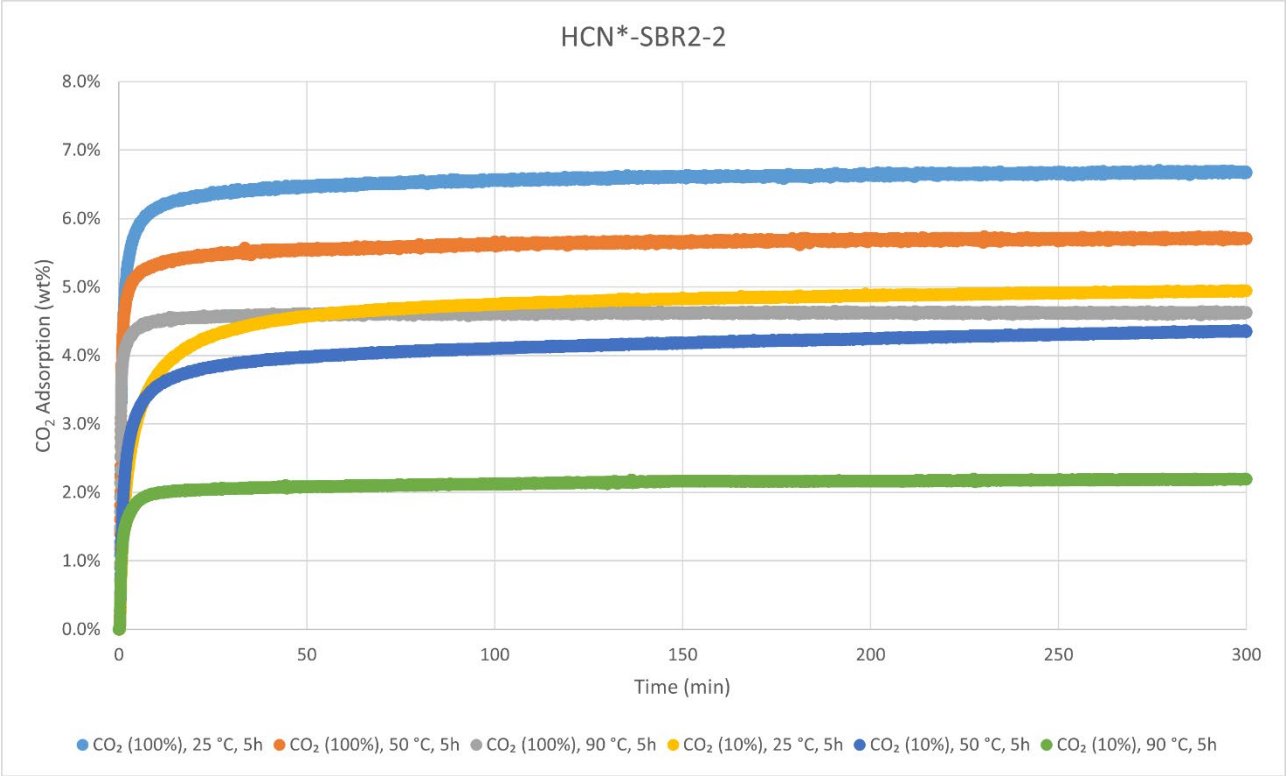

CO_2 adsorption using **TGA method 2** (measurement of product batch from run 2: HCN*-SBR2-2).

HCN*-SBR2-2	wt%	mmol/g
CO_2 (100%), 25 °C, 5h	6.7%	1.52
CO_2 (100%), 50 °C, 5h	5.7%	1.30
CO_2 (100%), 90 °C, 5h	4.6%	1.05
CO_2 (10%), 25 °C, 5h	4.9%	1.12
CO_2 (10%), 50 °C, 5h	4.4%	0.99
CO_2 (10%), 90 °C, 5h	2.2%	0.50

Elemental Analysis

	N [%]	C [%]	H [%]	S [%]	mmol N/g	C/N ratio	C/H ratio
run 1	**5.39**	**73.34**	**9.67**	**Not detected**	**3.84**	**15.88**	**0.64**
run 2	**5.37**	**74.67**	**9.68**		**3.83**	**16.22**	**0.65**

Hydrocyanated Nitrile Butadiene Rubber 2 (HCN-NBR2) was synthesised according to the General Procedure E from cryogenically milled substrate **NBR2** (Nitrile glove). Workup was initiated by filtering the reaction mixture through an empty Puriflash column using compressed air. The product was then first washed in small portions with PhMe (90 mL). Washing of the polymer in the column with aq. NaOH (2 M, 150 mL) was aided by ultrasonication (1 h in an 8 mL vial) after approx. half the volume. The last washing/ultrasonication combination was repeated with 90 mL water. Finally, the product was washed with 90 mL acetone and dried in high vacuum overnight. It was obtained in weight yields of 211.9 mg, 85 wt% and 224.3 mg, 90 wt%, respectively, from two independent runs (87 wt% on average). The polymer was analysed with IR-, TGA-, DSC-, and Elemental Analysis. Solubility tests were also conducted with several solvents. Attempts to analyse by ^{13}C CP/MAS NMR failed due to a high level of noise in the spectra, potentially due to paramagnetic nickel residues.

Solubility chart

Soluble **Swells** **Not soluble**

$CHCl_3$	Acetone	*i*-PrOH	DMF	DMSO	THF	PhMe	H_2O	MeOH	MeCN

Infrared (IR) Spectroscopic Analysis

*IR-spectrum of **HCN-NBR2** (run 1):*

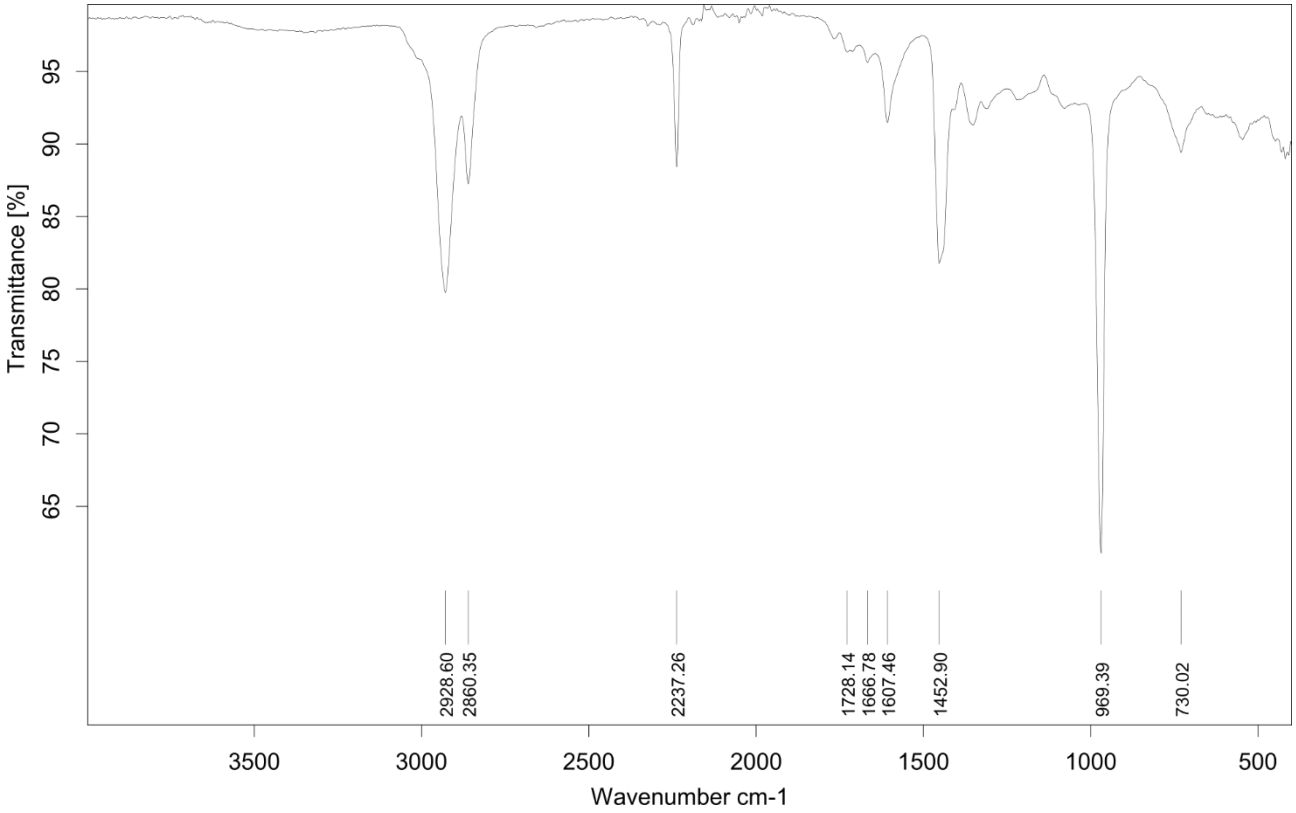

*IR-spectrum of **HCN-NBR2** (run 2):*

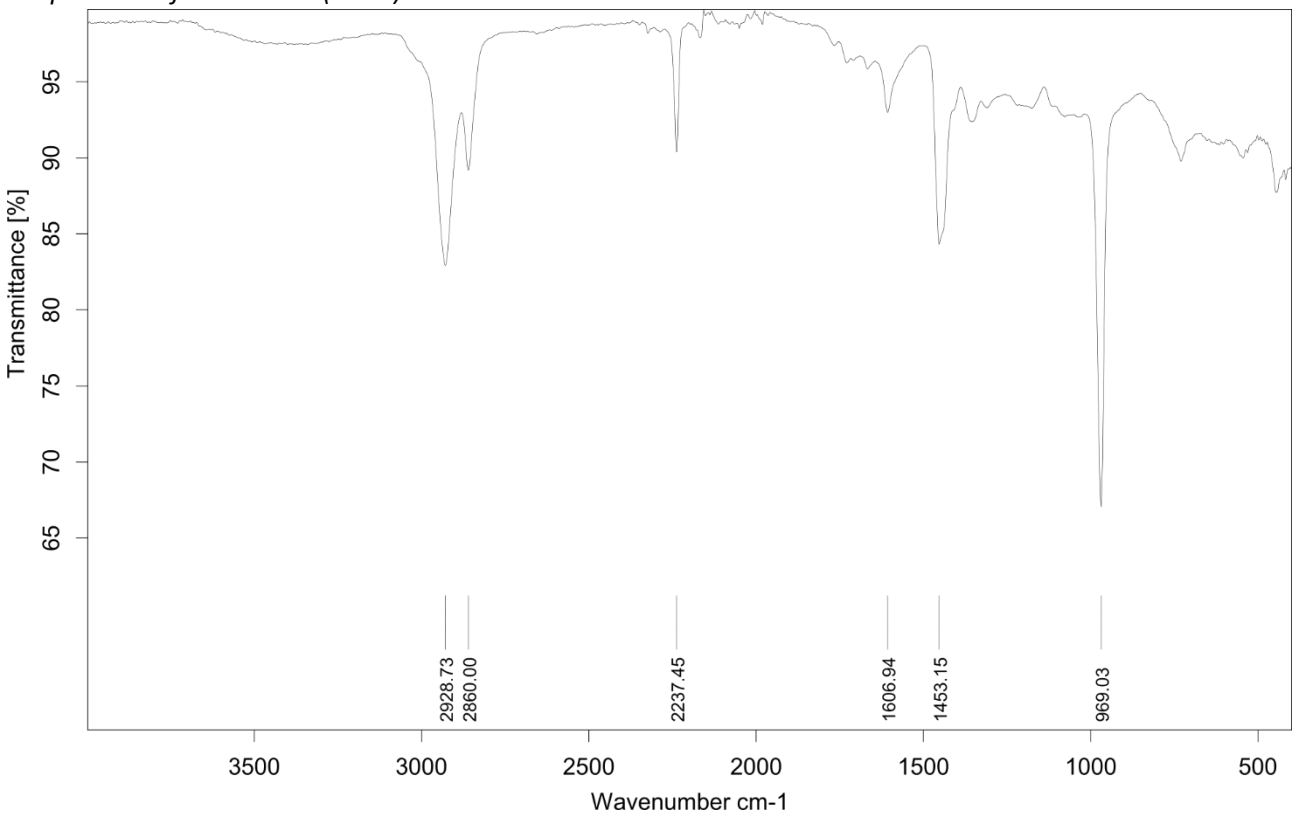

*IR-spectrum overlay of **HCN-NBR2** (run 1, **black**) and **NBR2** (substrate, **red**):*

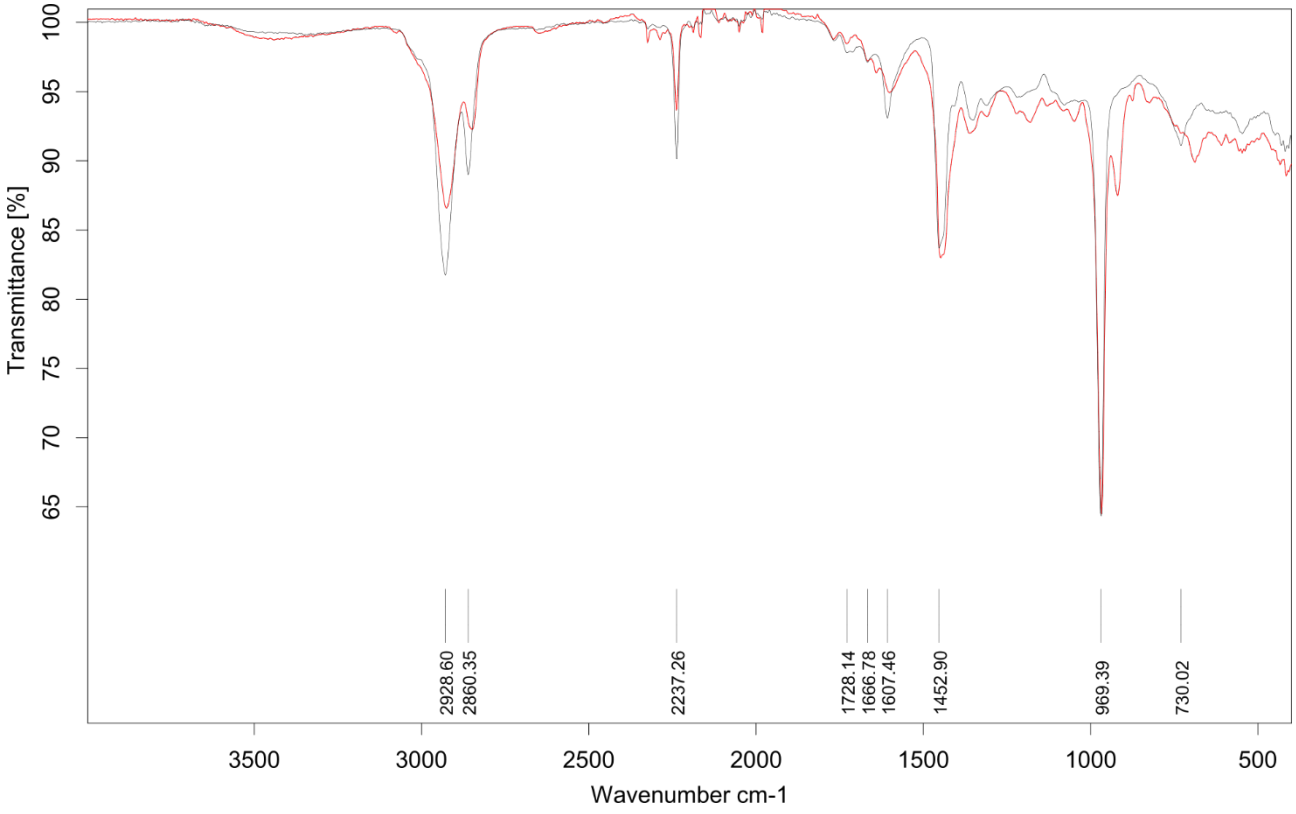

Elemental Analysis (EA)

	N [%]	C [%]	H [%]	S [%]	mmol N/g	C/N ratio	C/H ratio
run 1	**12.55**	**70.39**	**7.66**	**traces**	**8.96**	**6.54**	**0.77**
run 2	**12.10**	**69.00**	**7.52**	**traces**	**8.64**	**6.65**	**0.77**

The incorporation of nitrile through hydrocyanation is evident from the increase in N%, as the substrate **NBR2** contained 8.84% nitrogen.

Hydrogenated hydrocyanated Styrene Butadiene Rubber 1 (HCN*-NBR2) was synthesised according to the General Procedure H from substrate **HCN-NBR2** and was obtained in weight yields of 40.8 mg (82 wt%), 51.7 (103 wt%), and 51.5 mg (103 wt%), respectively, from three independent runs (96 wt% on average). The polymer was analysed with IR-, TGA-, and Elemental Analysis. Attempts to analyse by ^{13}C CP/MAS NMR failed due to a high level of noise in the spectra, potentially due to paramagnetic nickel residues. For simplicity, only the characterisation of two product batches is reported.

Particle size after cryogenic milling used for CO_2 adsorption-desorption experiments

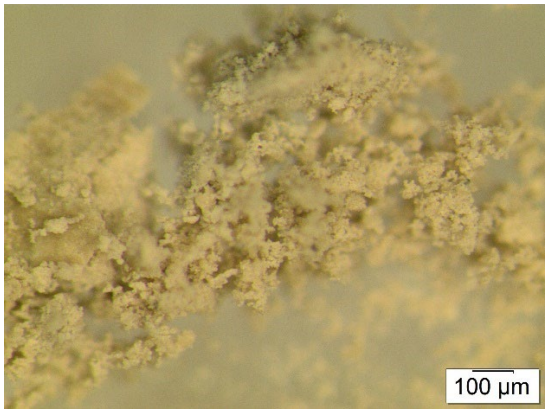

Solubility chart

Soluble **Swells** **Not soluble**

$CHCl_3$	Acetone	*i*-PrOH	DMF	DMSO	THF	PhMe	H_2O	MeOH	MeCN

Infrared (IR) Spectroscopic Analysis

*IR-spectrum of **HCN*-NBR2** (run 1):*

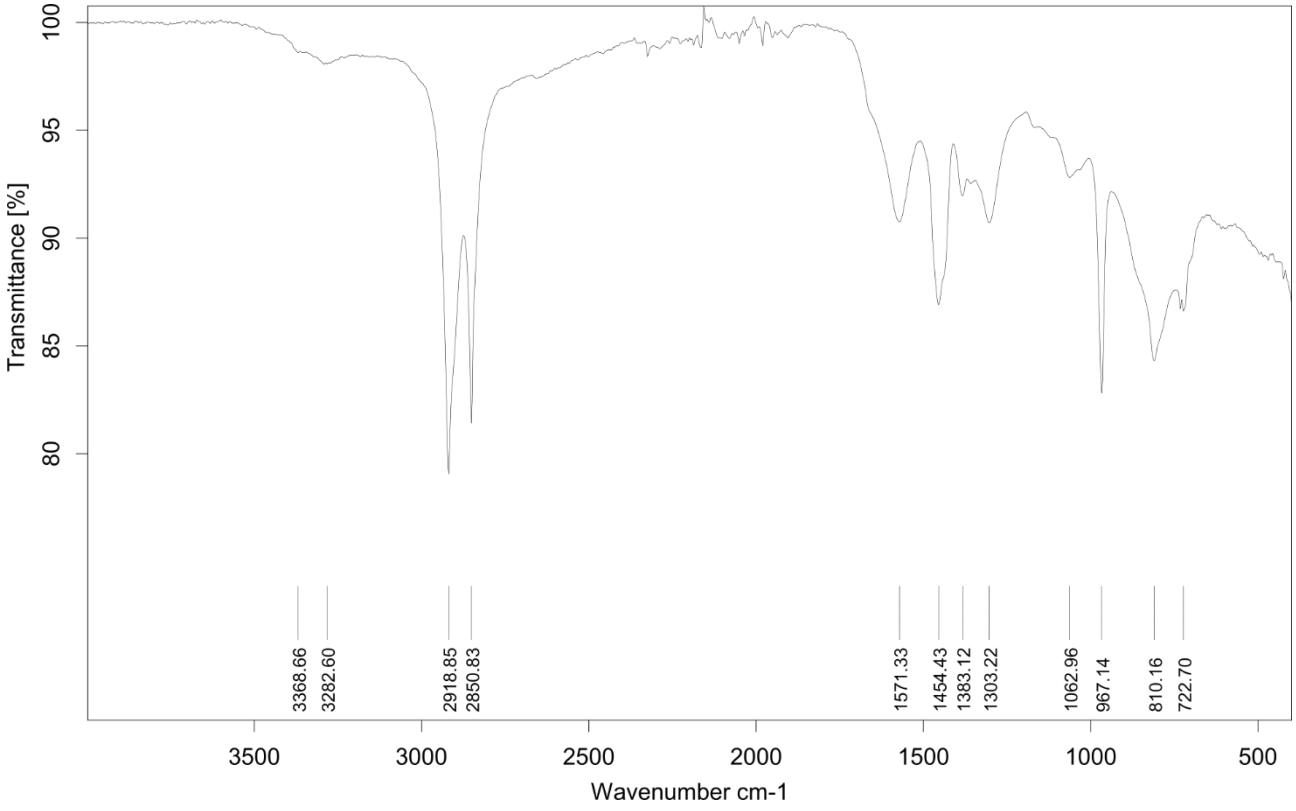

*IR-spectrum of **HCN*-NBR2** (run 2):*

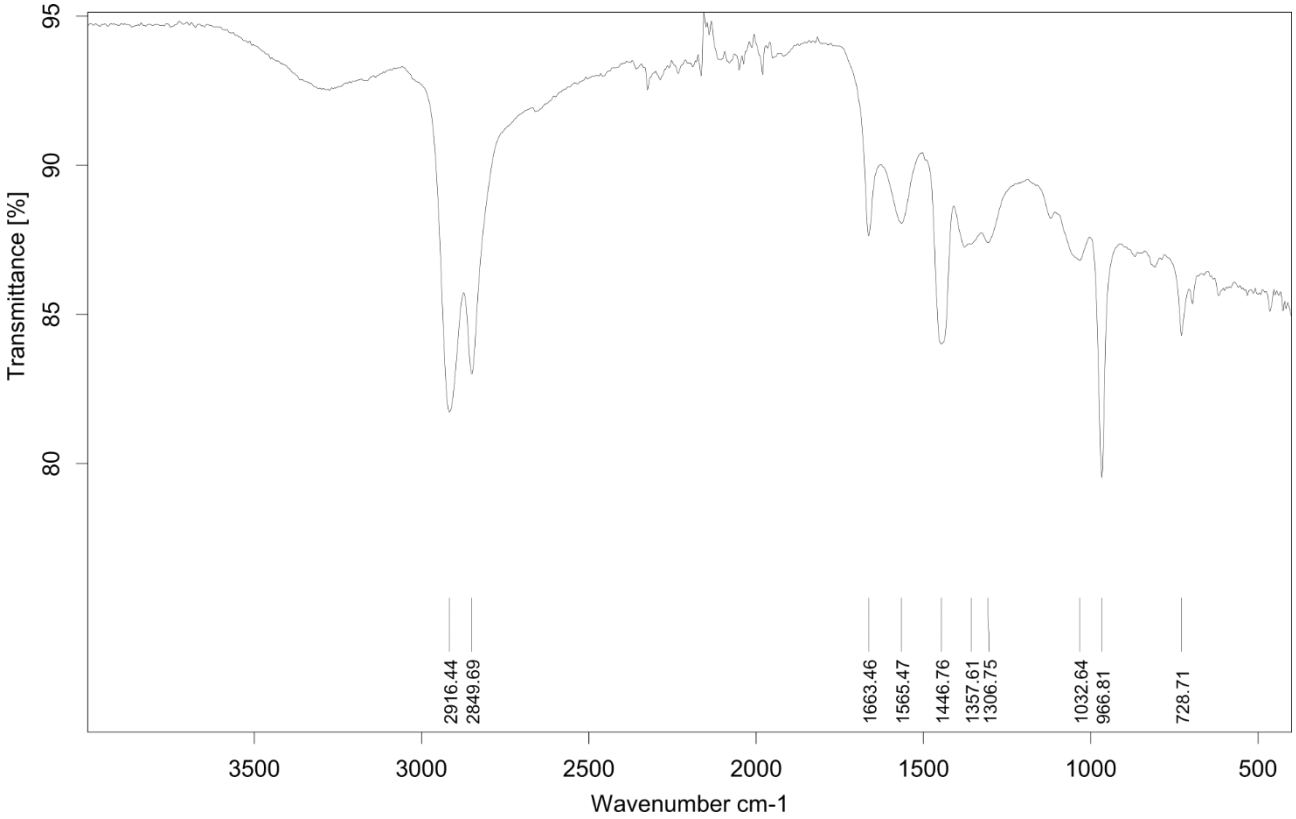

*IR-spectrum overlay of **HCN*-NBR2** (run 1, **black**) and **HCN-NBR2** (substrate, **red**):*

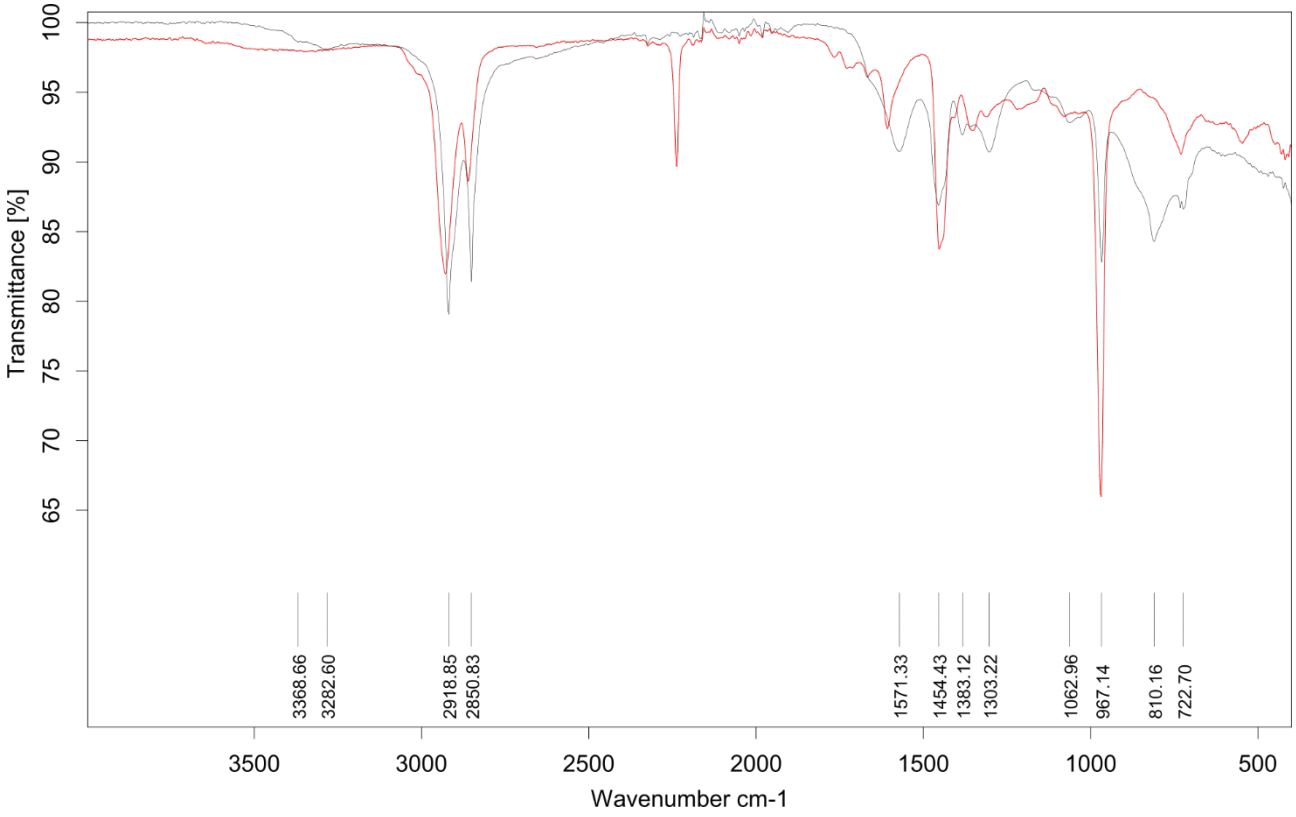

Thermogravimetric Analysis (TGA)

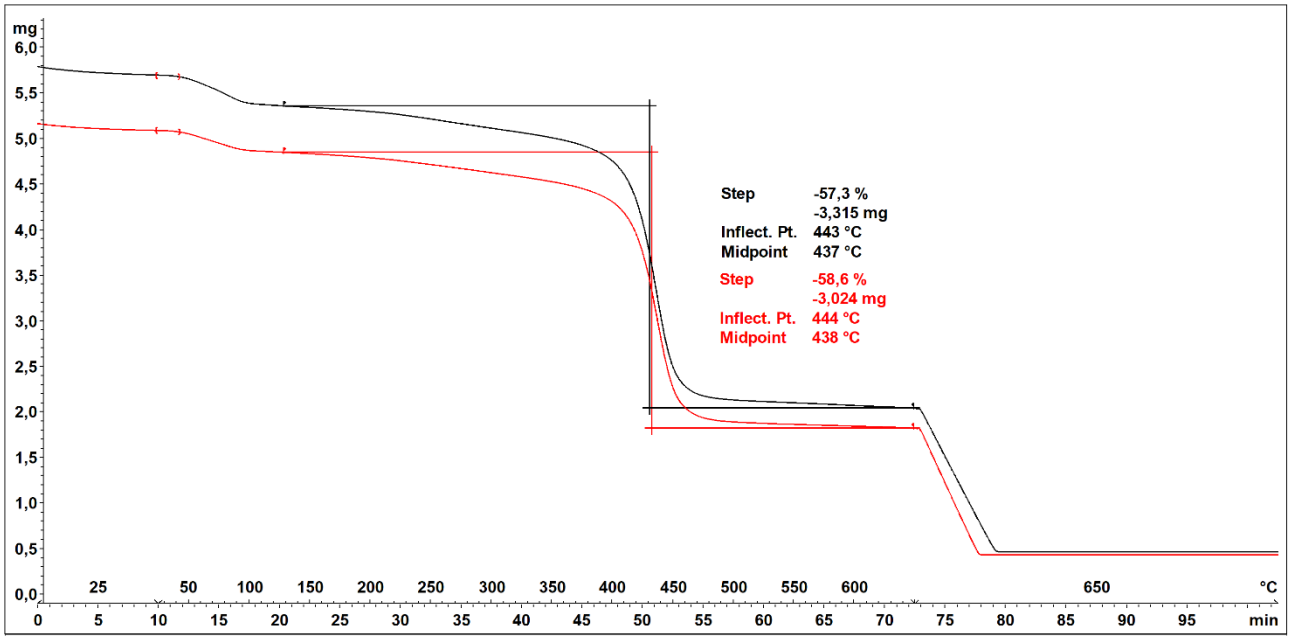

Decomposition graph. The experiment was conducted under He then air (after 650 °C). The black curve is the result from run 1, while the red curve is for run 2.

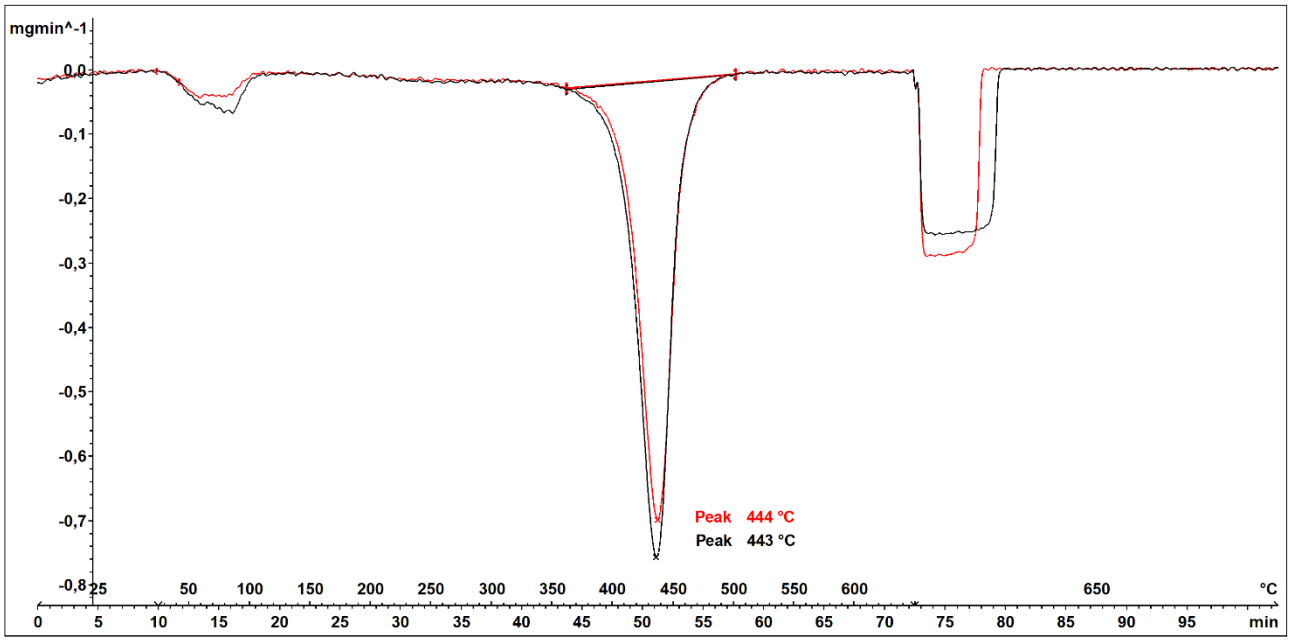

1st derivative of decomposition graph. The experiment was conducted under He then air (after 650 °C). The black curve is the result from run 1, while the red curve is for run 2.

Decomposition temperature (T_d) = 443−444 °C.

CO_2-adsorption analysis by thermogravimetric analysis

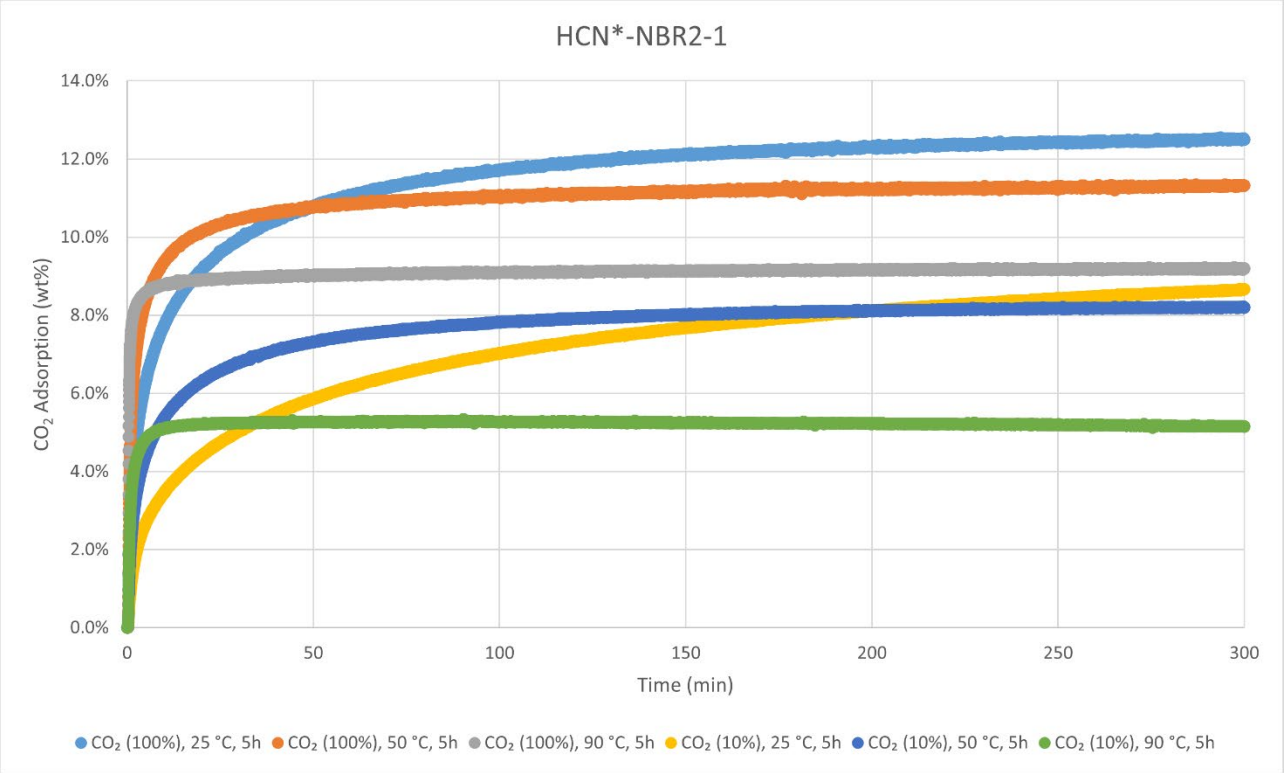

CO_2 adsorption using **TGA method 2** (measurement of product batch from run 1: HCN*-NBR2-1).

HCN*-NBR2-1	wt%	mmol/g
CO_2 (100%), 25 °C, 5h	12.5%	2.84
CO_2 (100%), 50 °C, 5h	11.3%	2.57
CO_2 (100%), 90 °C, 5h	9.2%	2.09
CO_2 (10%), 25 °C, 5h	8.7%	1.97
CO_2 (10%), 50 °C, 5h	8.2%	1.86
CO_2 (10%), 90 °C, 5h	5.1%	1.17

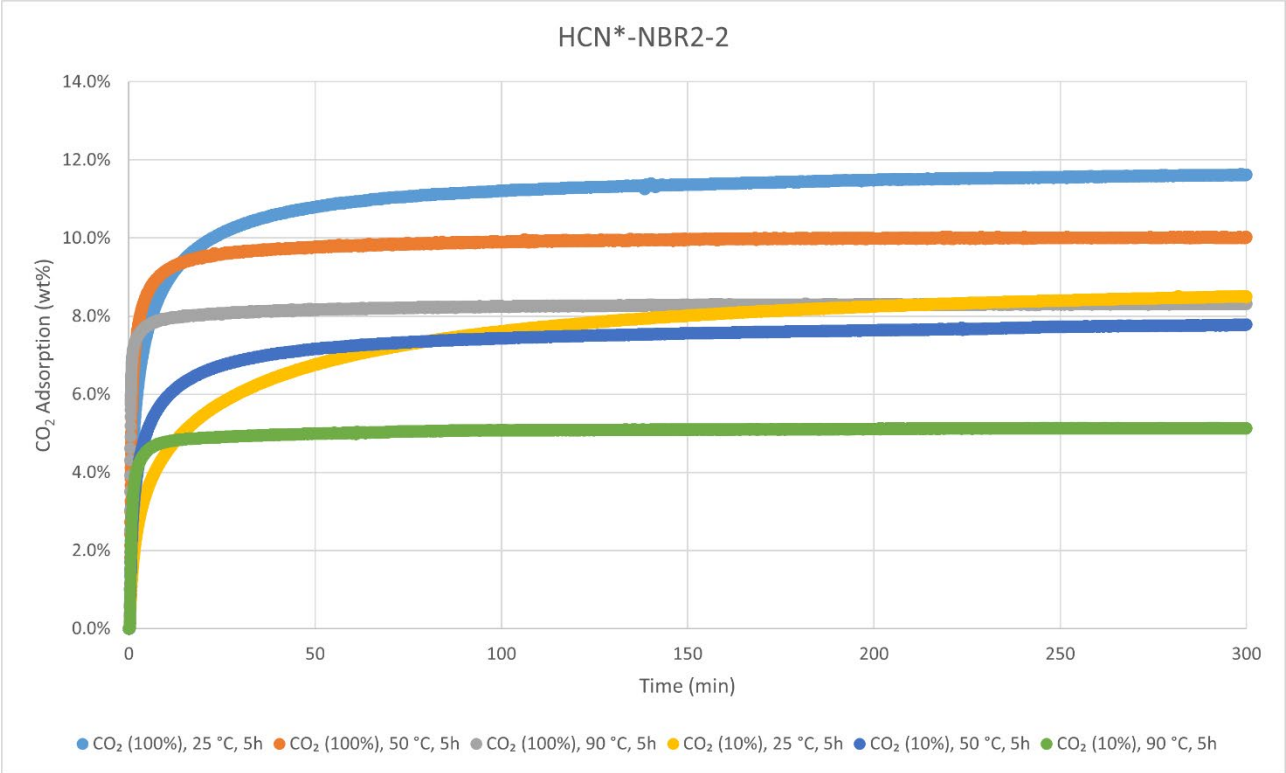

CO_2 adsorption using **TGA method 2** (measurement of product batch from run 2: HCN*-NBR2-2).

HCN*-NBR2-2	wt%	mmol/g
CO_2 (100%), 25 °C, 5h	11.6%	2.64
CO_2 (100%), 50 °C, 5h	10.0%	2.28
CO_2 (100%), 90 °C, 5h	8.3%	1.89
CO_2 (10%), 25 °C, 5h	8.5%	1.93
CO_2 (10%), 50 °C, 5h	7.8%	1.77
CO_2 (10%), 90 °C, 5h	5.1%	1.17

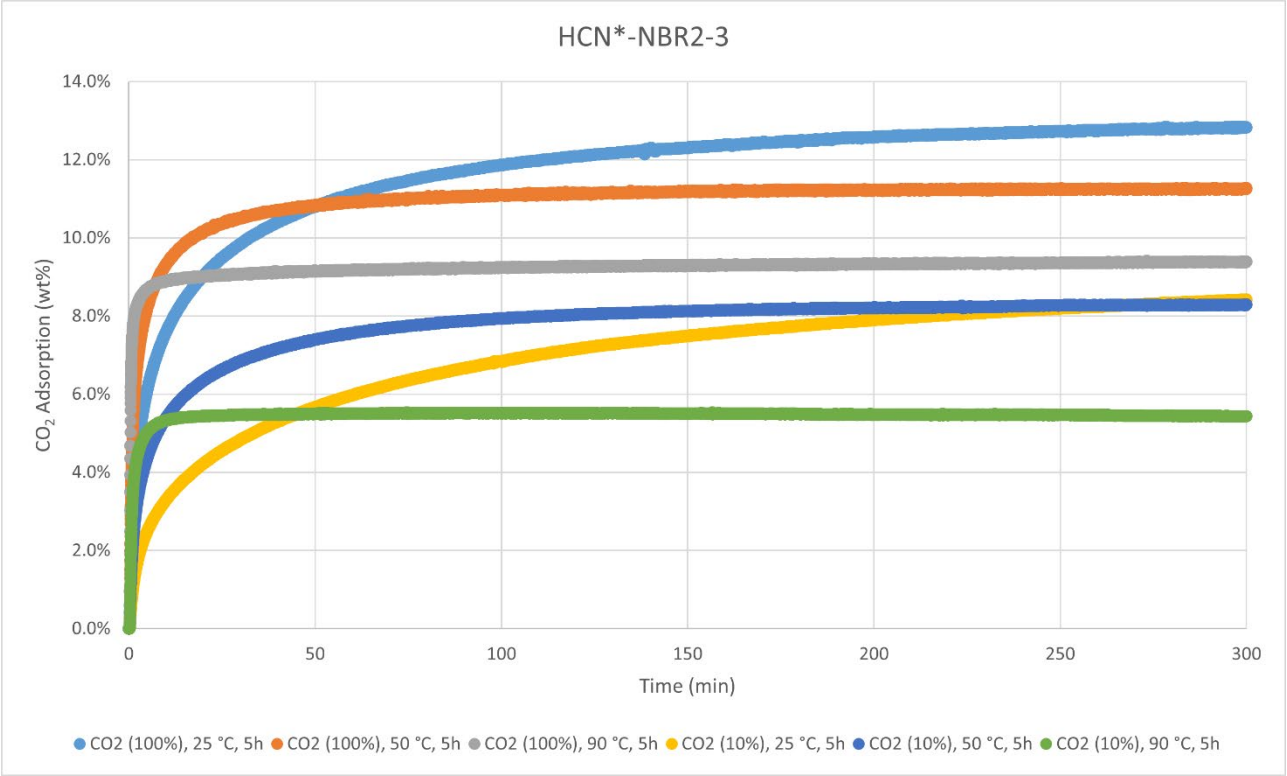

CO_2 adsorption using **TGA method 2** (measurement of product batch from run 3: HCN*-NBR2-3).

HCN*-NBR2-3	wt%	mmol/g
CO2 (100%), 25 °C, 5h	12.8%	2.92
CO2 (100%), 50 °C, 5h	11.3%	2.56
CO2 (100%), 90 °C, 5h	9.4%	2.13
CO2 (10%), 25 °C, 5h	8.4%	1.91
CO2 (10%), 50 °C, 5h	8.3%	1.89
CO2 (10%), 90 °C, 5h	5.4%	1.23

Elemental Analysis

	N [%]	C [%]	H [%]	S [%]	mmol N/g	C/N ratio	C/H ratio
Run 1	**9.37**	**67.43**	**10.79**	**traces**	**6.69**	**8.39**	**0.52**
Run 2	**8.83**	**65.93**	**9.54**	**traces**	**6.30**	**8.71**	**0.58**
Run 3	**8.91**	**64.69**	**9.96**	**traces**	**6.36**	**8.47**	**0.55**

Hydrocyanated Acrylonitrile Butadiene Styrene 1 (HCN-ABS1) was synthesised according to the General Procedure E from cryogenically milled substrate **ABS1** (LEGO® bricks). The semi-soluble product was worked up by first precipitating it through dropwise addition into 50−100 mL vigorously stirred MeOH. It was decanted and then ultrasonicated for 1 h in aq. NaOH (2 M, 8 mL), followed by washing with another aq. NaOH (2 M, 60 mL). This sequence was repeated with water, and after washing with acetone (90 mL), the polymer was dried in high vacuum overnight. Leftover residual free cyanide as discerned by IR required further purification by dissolving in $CHCl_3$ (8 mL) at 55 °C under ultrasonication and dropwise addition of the resulting solution into 75 mL 2 M methanolic NaOH (well stirred). The polymer was filtered off and washed with 70−100 mL until neutral. Finally, washing with MeOH (20 mL) and drying in high vacuum overnight again afforded the product in weight yields of 122.5 mg, 49 wt% and 101.6 mg, 41 wt%, respectively, from two independent runs (45 wt% on average). The polymer was analysed with IR-, TGA-, DSC-, and elemental analysis. Attempts to analyse by ^{13}C CP/MAS NMR failed due to a high level of noise in the spectra, potentially due to paramagnetic nickel residues.

Solubility chart

Soluble **Swells** **Not soluble**

$CHCl_3$	Acetone	*i*-PrOH	DMF	DMSO	THF	PhMe	H_2O	MeOH	MeCN

Infrared (IR) Spectroscopic Analysis

*IR-spectrum of **HCN-ABS1** (run 1):*

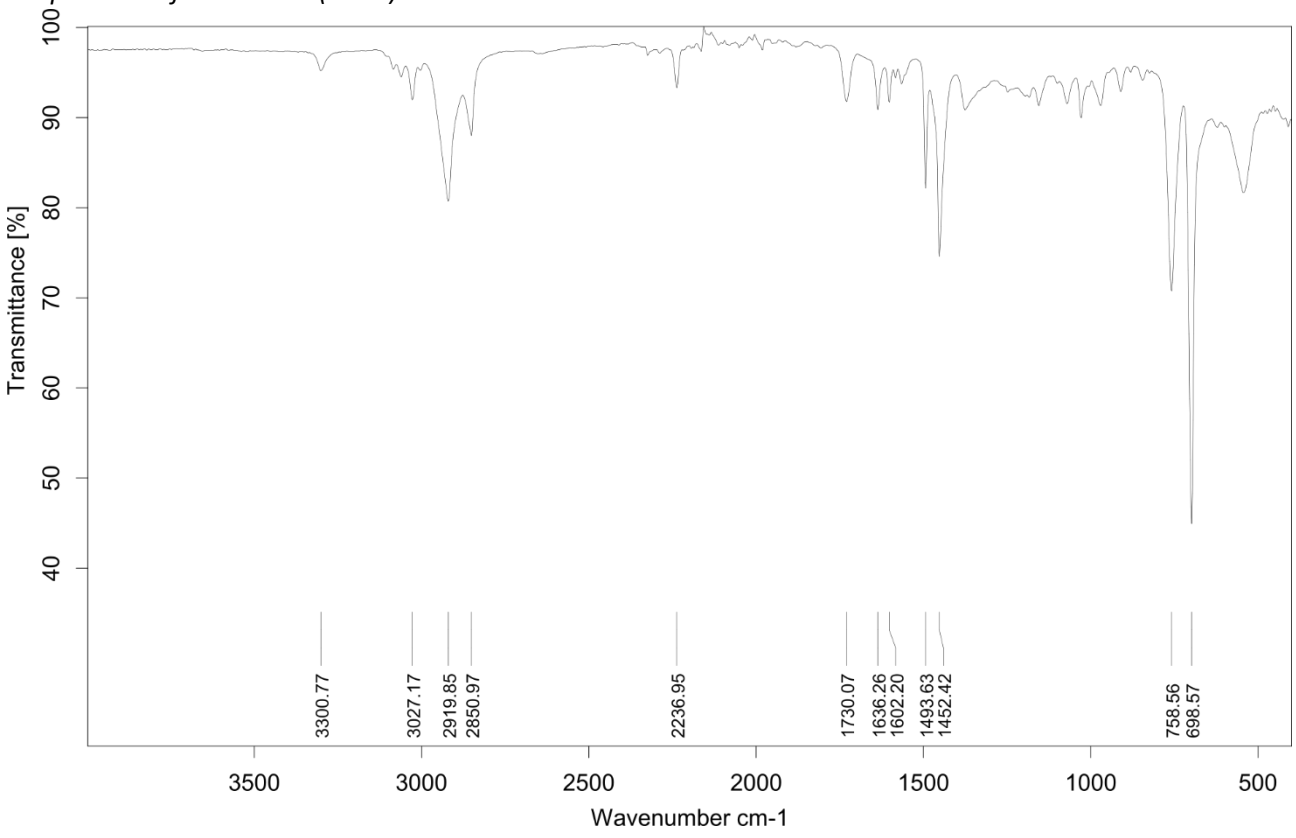

*IR-spectrum of **HCN-ABS1** (run 2):*

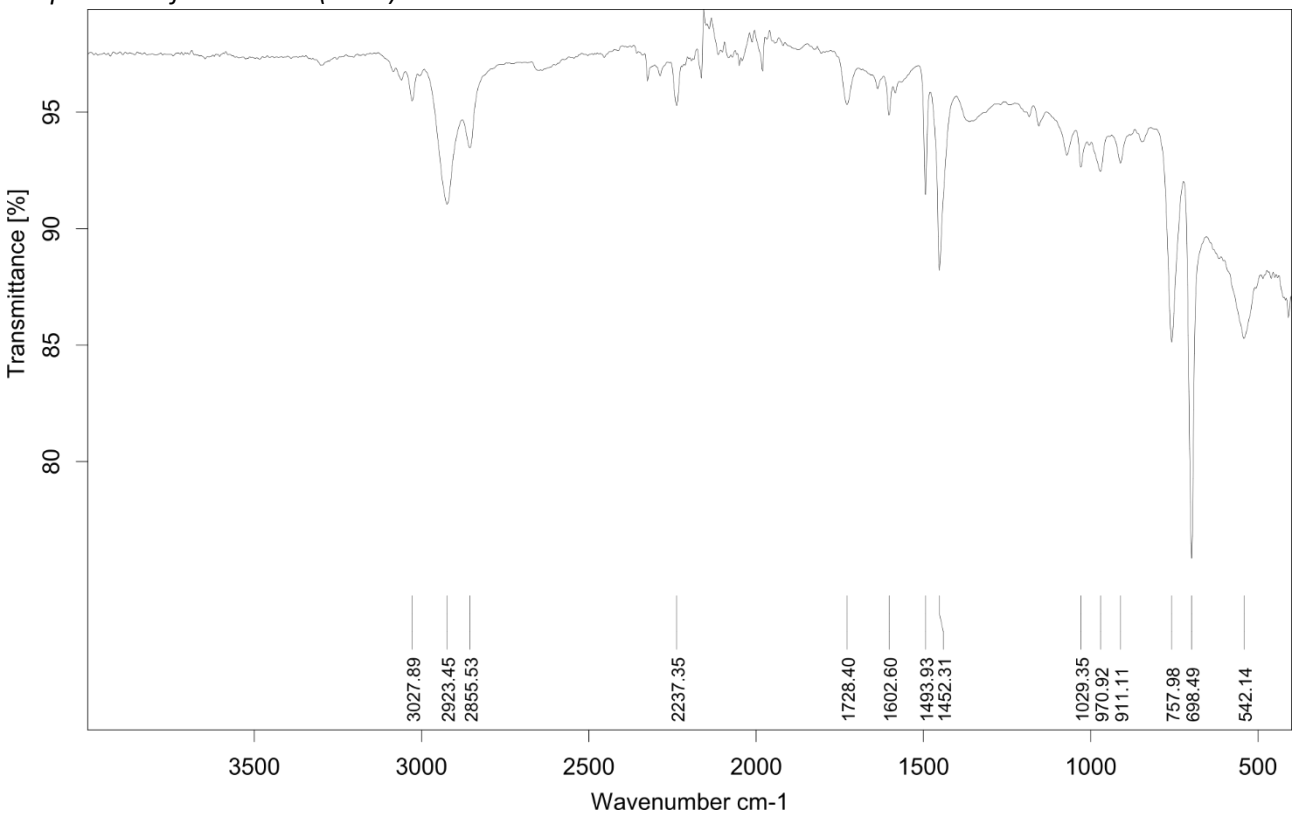

*IR-spectrum overlay of **HCN-ABS1** (run 1, **grey**) and **ABS1** (substrate, **red**):*

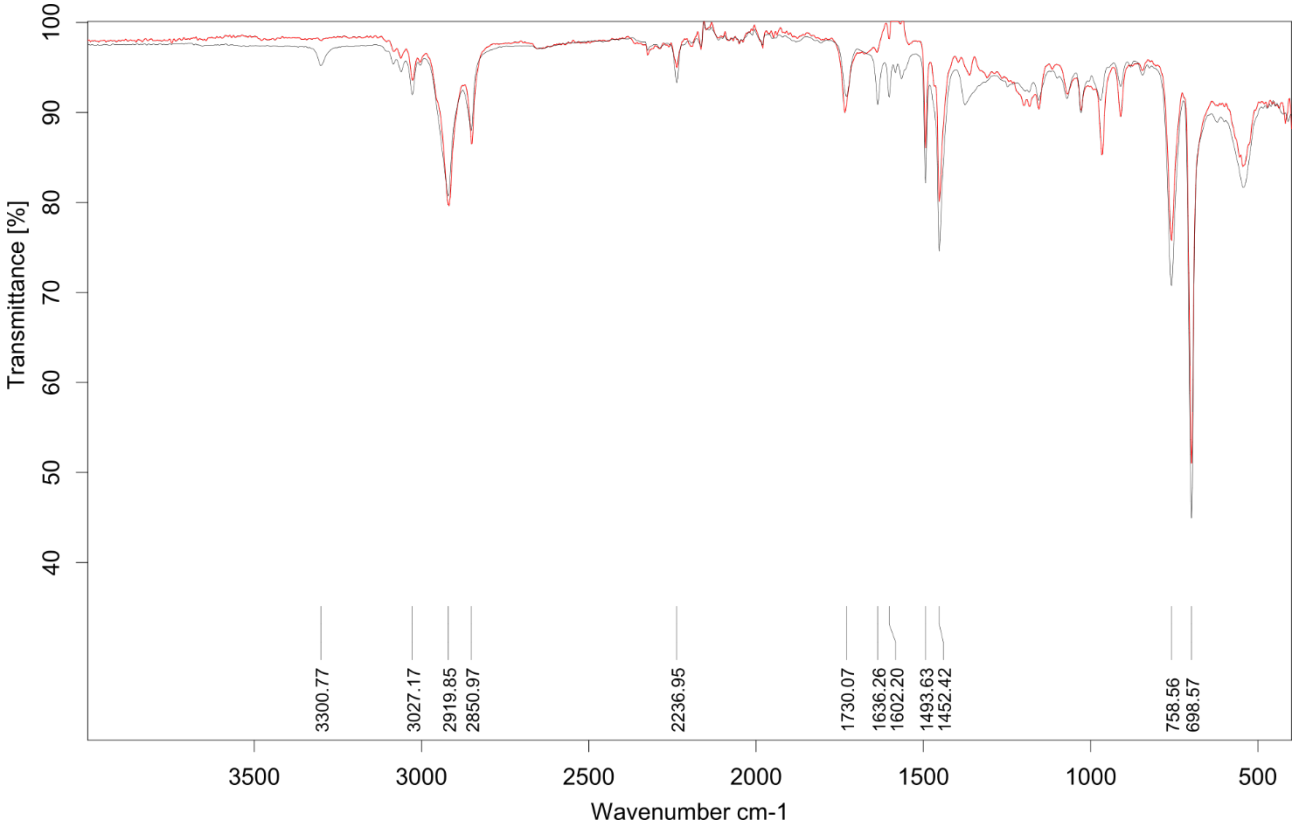

Elemental Analysis (EA)

	N [%]	C [%]	H [%]	S [%]	mmol N/g	C/N ratio	C/H ratio
run 1	**6.51**	**78.56**	**7.74**	**Not detected**	**4.65**	**14.08**	**0.85**
run 2	**6.71**	**77.70**	**7.68**		**4.79**	**13.51**	**0.85**

The incorporation of nitrile through hydrocyanation is evident from the increase in N%, as the substrate **ABS1** contained 5.33% nitrogen.

Hydrogenated hydrocyanated Acrylonitrile Butadiene Styrene 1 (HCN*-ABS1) was synthesised according to a modified General Procedure G (50 mg scale, precipitated the crude polymer into water (10 mL) before filtering and washing) from substrate **HCN-ABS1** and was obtained in weight yields of 34.7 mg, 69 wt% and 44.3 mg, 89 wt%, respectively, from two independent runs (79 wt% on average). The polymer was analysed with IR-, TGA-, and elemental analysis. Solubility tests were also conducted with several solvents. Attempts to analyse by ^{13}C CP/MAS NMR failed due to a high level of noise in the spectra, potentially due to paramagnetic nickel residues.

Particle size after cryogenic milling used for CO_2 adsorption-desorption experiments

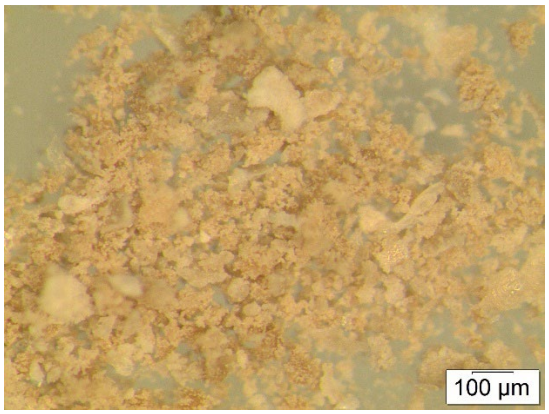

Solubility chart

Soluble **Swells** **Not soluble**

$CHCl_3$	Acetone	*i*-PrOH	DMF	DMSO	THF	PhMe	H_2O

Infrared (IR) Spectroscopic Analysis

*IR-spectrum of **HCN*-ABS1** (run 1):*

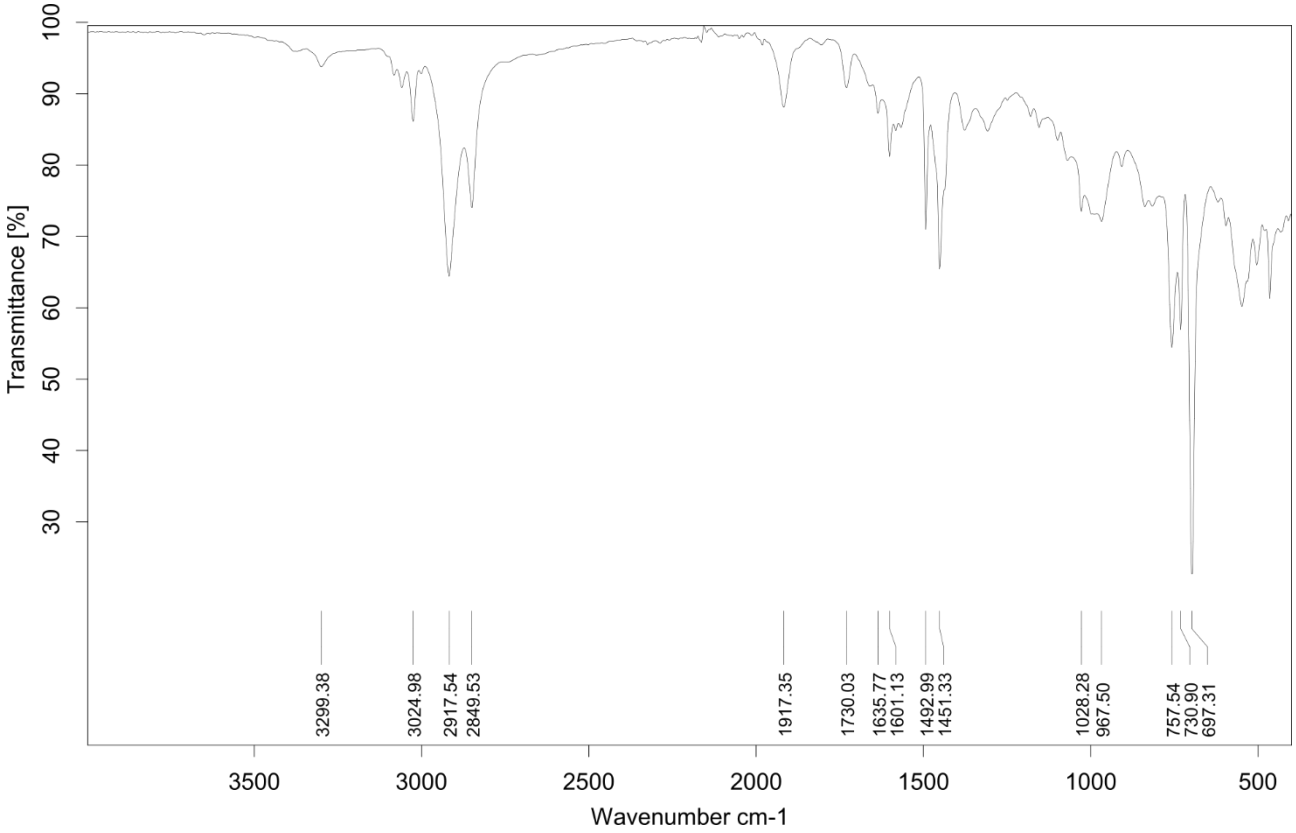

*IR-spectrum of **HCN*-ABS1** (run 2):*

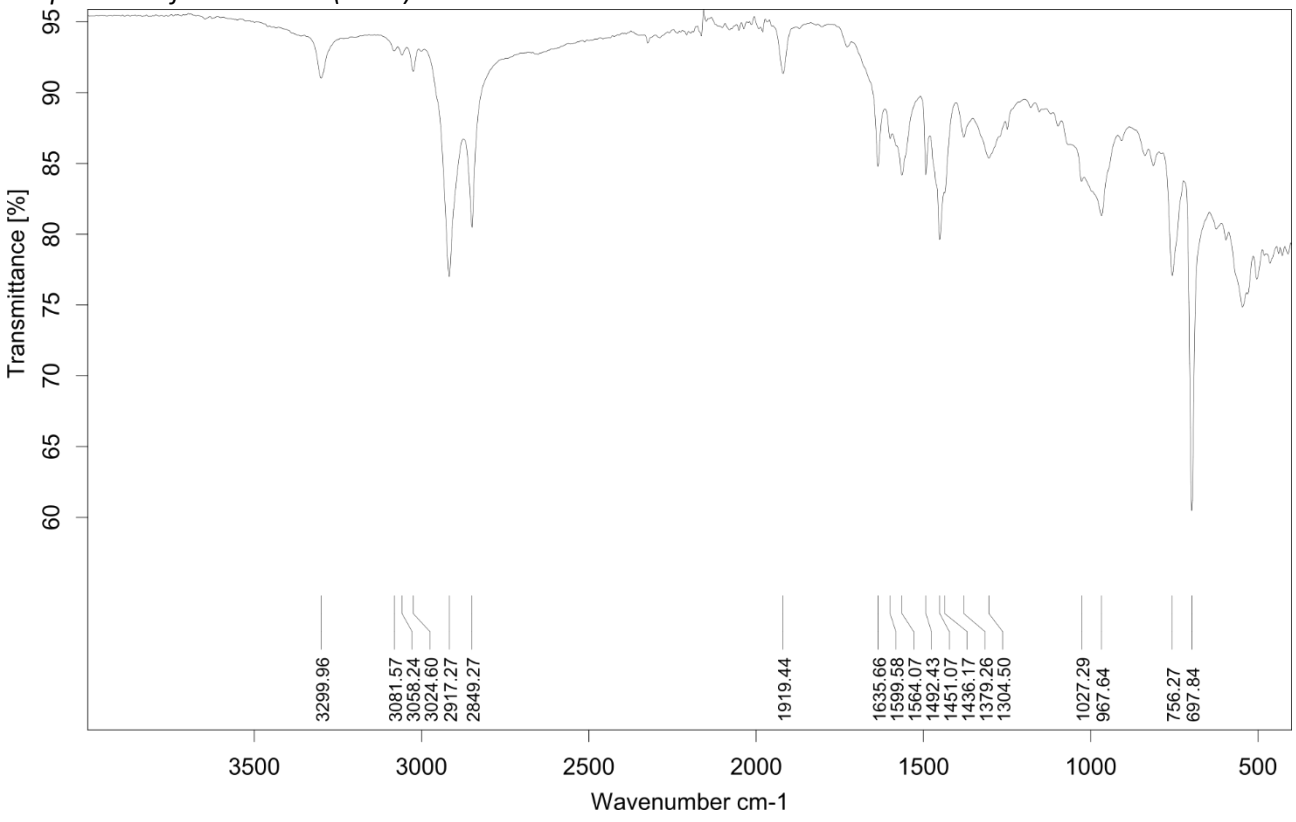

*IR-spectrum overlay of **HCN*-ABS1** (run 1, **grey**) and **HCN-ABS1** (substrate, **red**):*

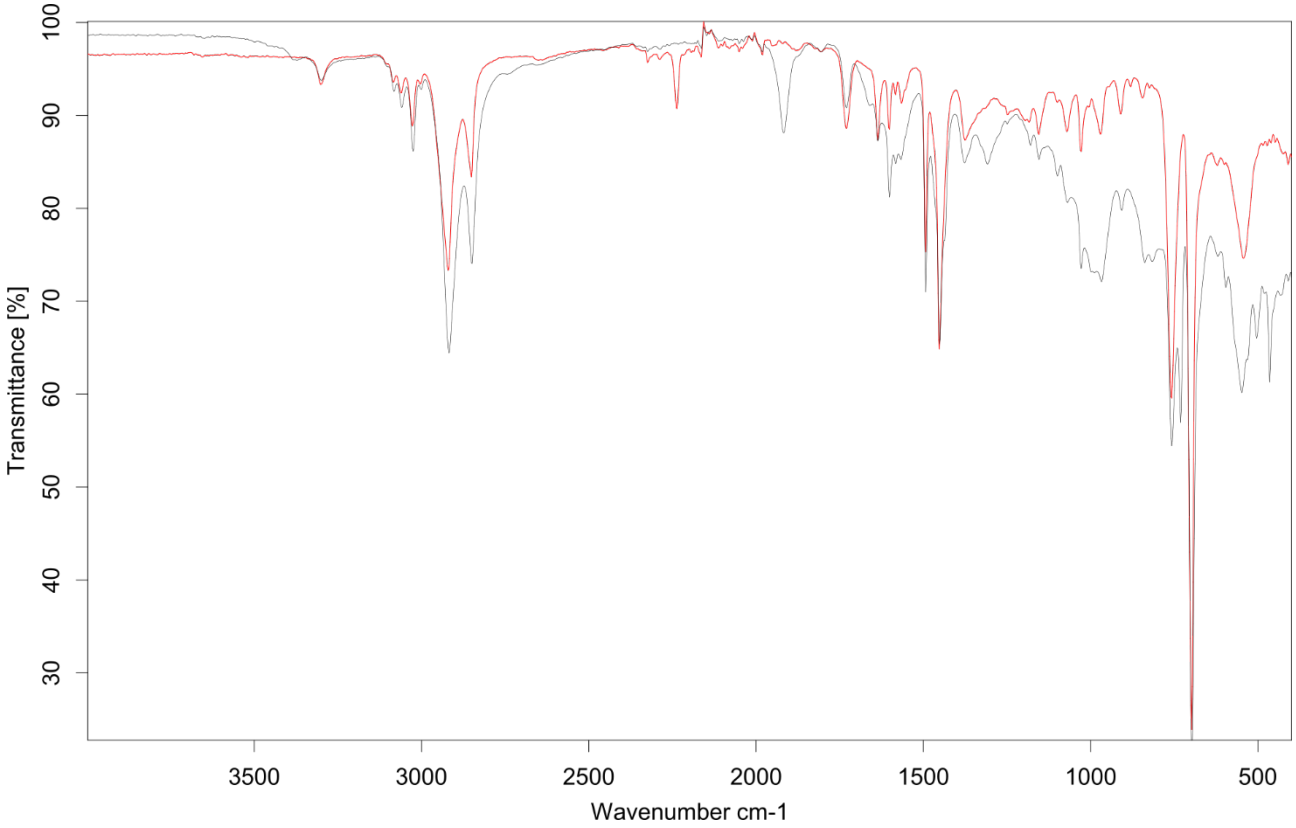

Thermogravimetric Analysis (TGA)

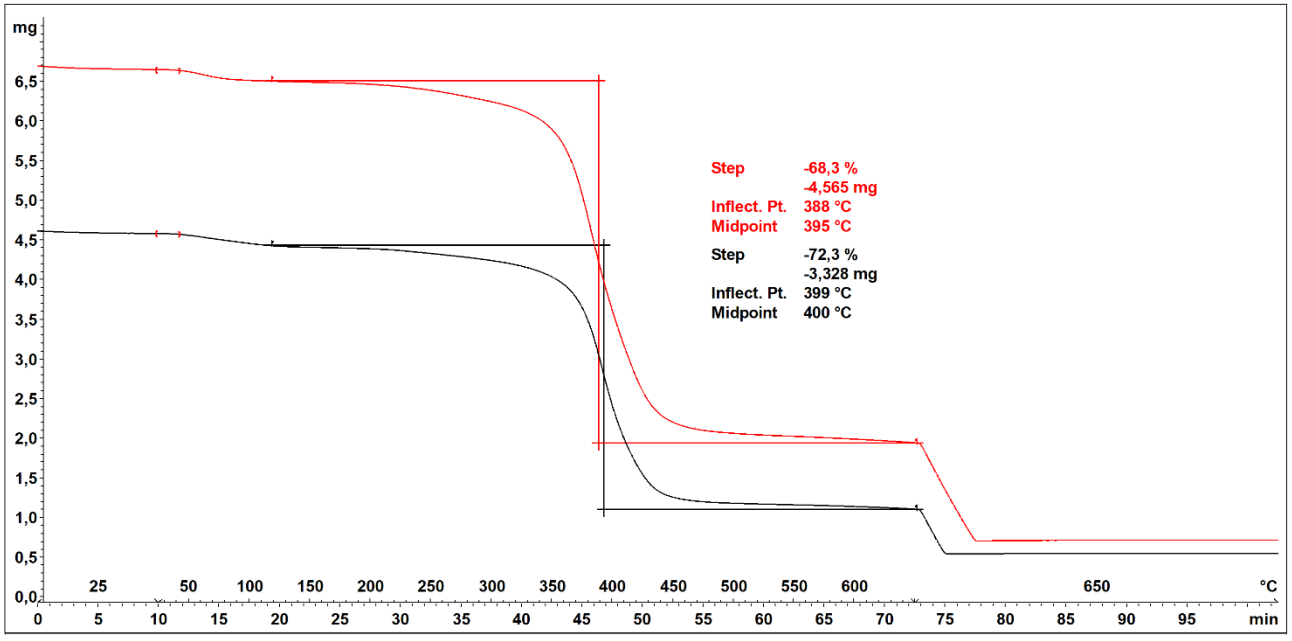

Decomposition graph. The experiment was conducted under He then air (after 650 °C). The black curve is the result from run 1, while the red curve is for run 2.

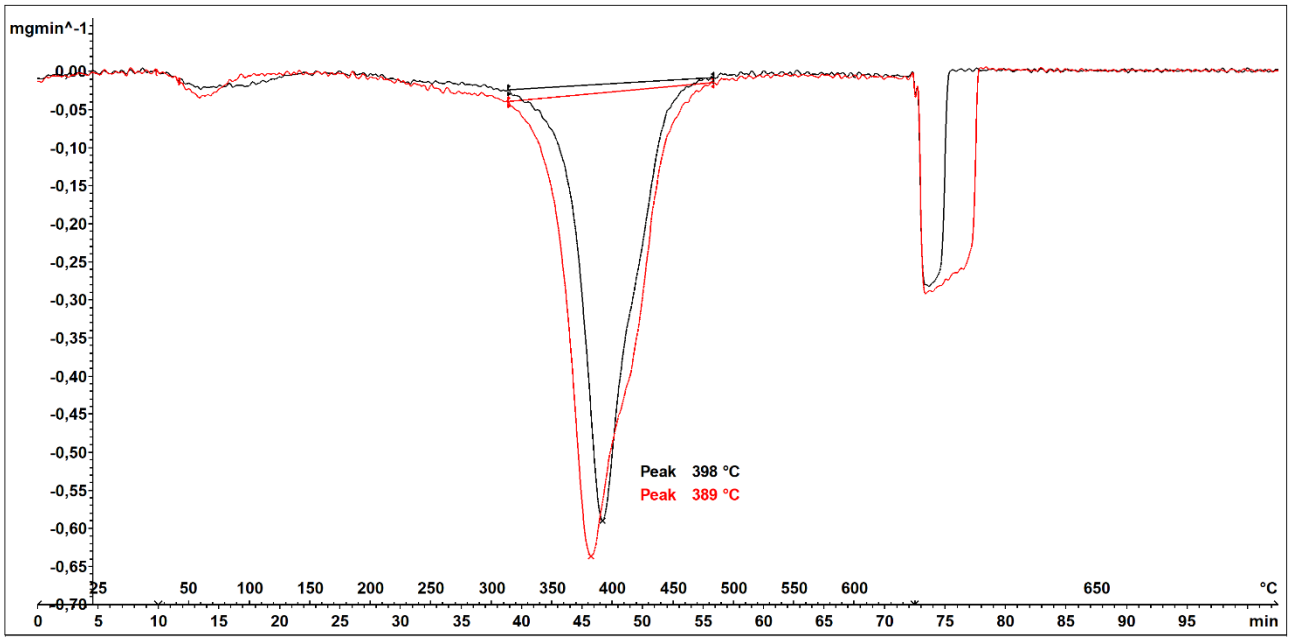

1st derivative of decomposition graph. The experiment was conducted under He then air (after 650 °C). The black curve is the result from run 1, while the red curve is for run 2.

Decomposition temperature (T_d) = 389−398 °C.

CO_2-adsorption analysis by thermogravimetric analysis

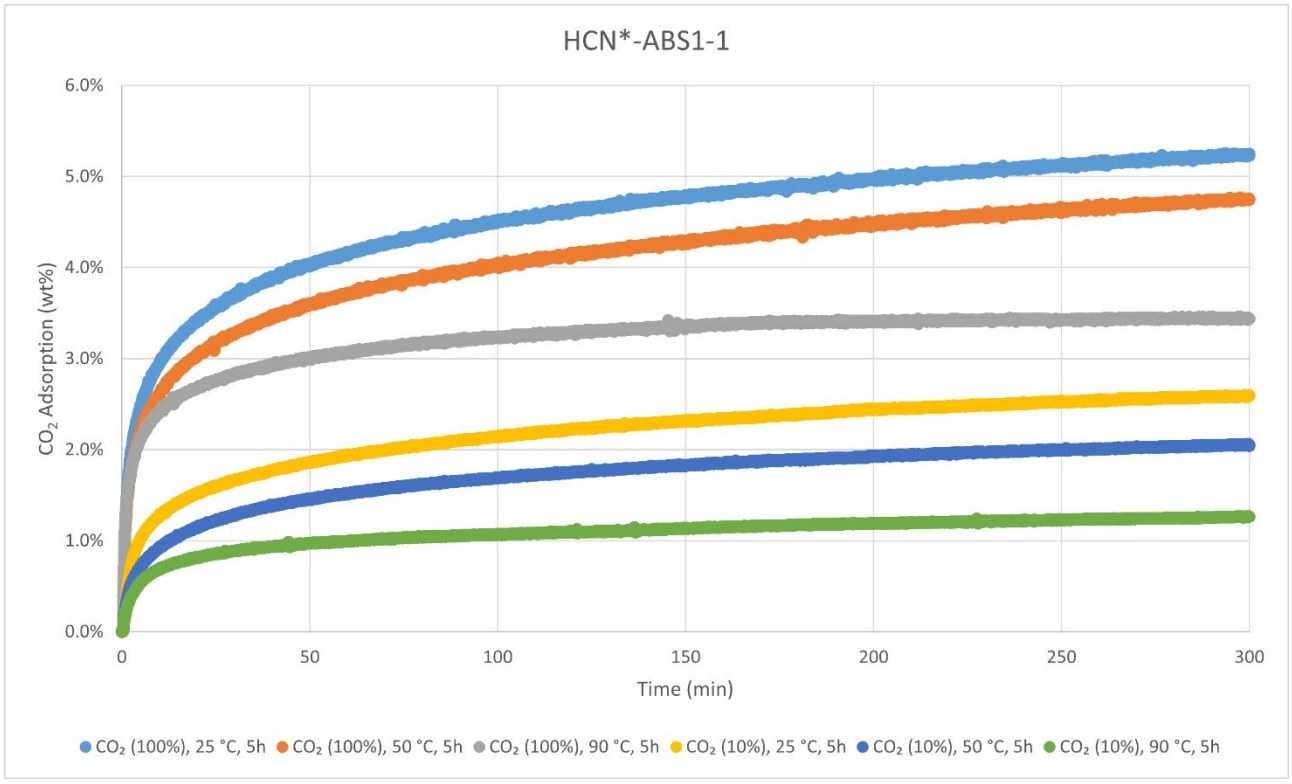

CO_2 adsorption using **TGA method 2** (measurement of product batch from run 1: HCN*-ABS1-1).

HCN*-ABS1-1	wt%	mmol/g
CO_2 (100%), 25 °C, 5h	5.2%	1.19
CO_2 (100%), 50 °C, 5h	4.8%	1.08
CO_2 (100%), 90 °C, 5h	3.4%	0.78
CO_2 (10%), 25 °C, 5h	2.6%	0.59
CO_2 (10%), 50 °C, 5h	2.1%	0.47
CO_2 (10%), 90 °C, 5h	1.3%	0.29

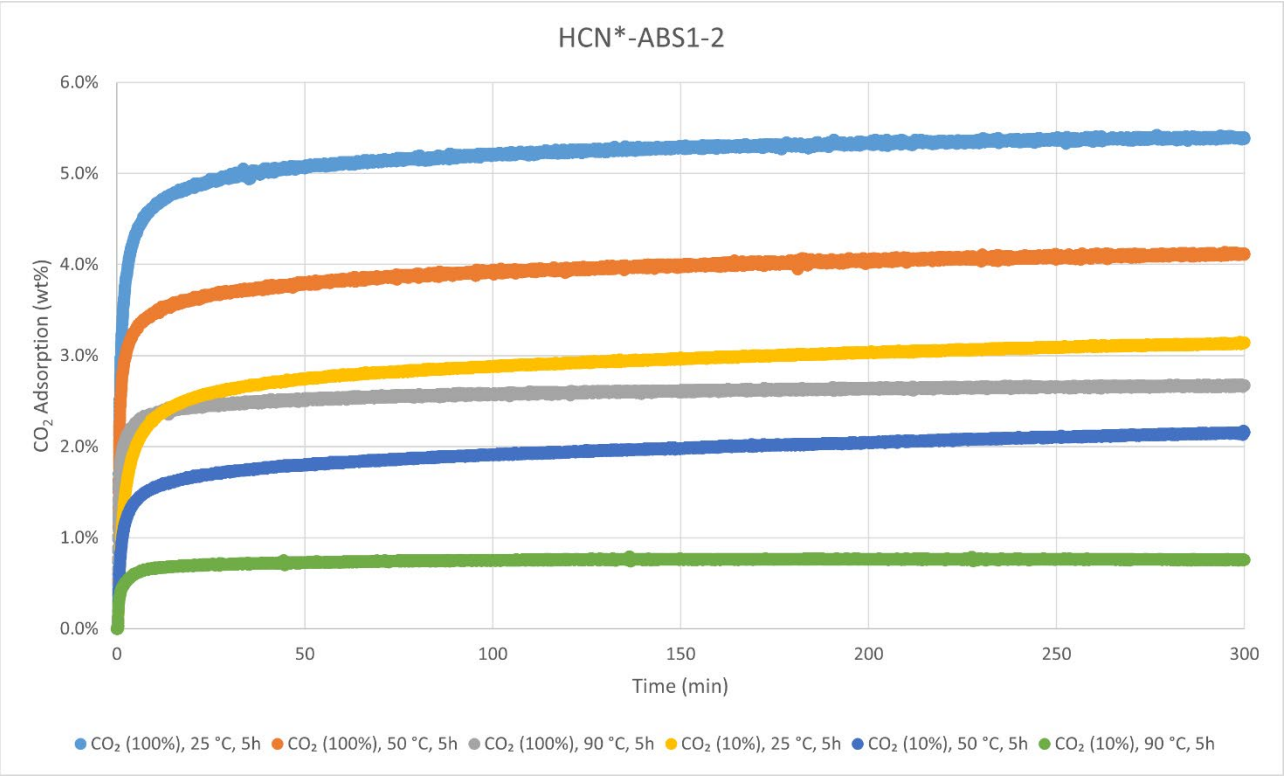

CO_2 adsorption using **TGA method 2** (measurement of product batch from run 2: HCN*-ABS1-2).

HCN*-ABS1-2	wt%	mmol/g
CO_2 (100%), 25 °C, 5h	5.4%	1.23
CO_2 (100%), 50 °C, 5h	4.1%	0.94
CO_2 (100%), 90 °C, 5h	2.7%	0.61
CO_2 (10%), 25 °C, 5h	3.1%	0.71
CO_2 (10%), 50 °C, 5h	2.2%	0.49
CO_2 (10%), 90 °C, 5h	0.8%	0.17

Elemental Analysis

	N [%]	C [%]	H [%]	S [%]	mmol N/g	C/N ratio	C/H ratio
run 1	**5.13**	**70.20**	**8.07**	**Not detected**	**3.66**	**15.96**	**0.73**
run 2	**5.25**	**69.76**	**8.25**		**3.74**	**15.51**	**0.71**

Polymer Products from the Post-Modification of Amine Polymers with Boc-Aziridine

Aziridine-extended H-NBR2 (Az-HNBR2) was synthesised according to the General Procedure I from substrate **H-NBR2** (hydrogenated nitrile glove) and was obtained in weight yields of 96.8 mg, 97 wt% and 111.7 mg, 112 wt%, respectively, from two independent runs over two steps (105 wt% on average). The polymer was analysed with solid-state ^{13}C CP/MAS NMR, IR-, TGA-, DSC-, and elemental analysis. Solubility tests were also conducted with several solvents. No thermal events besides decomposition were observed with DSC.

Particle size after cryogenic milling used for CO_2 adsorption-desorption experiments

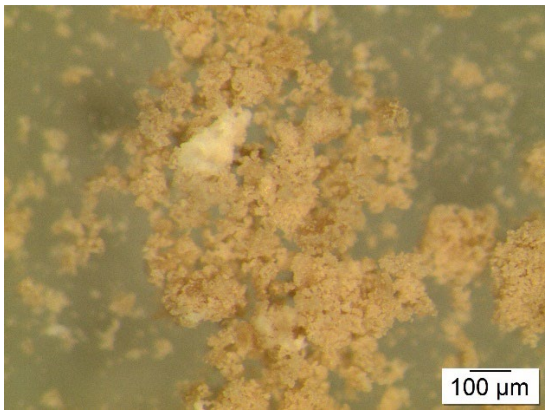

Solubility chart

Soluble **Swells** **Not soluble**

$CHCl_3$	Acetone	*i*-PrOH	DMF	DMSO	THF	PhMe	H_2O	MeOH	MeCN

^{13}C CP/MAS NMR (solid-state)

Solid-state ^{13}C–NMR of **Az-HNBR2** *(run 2):*

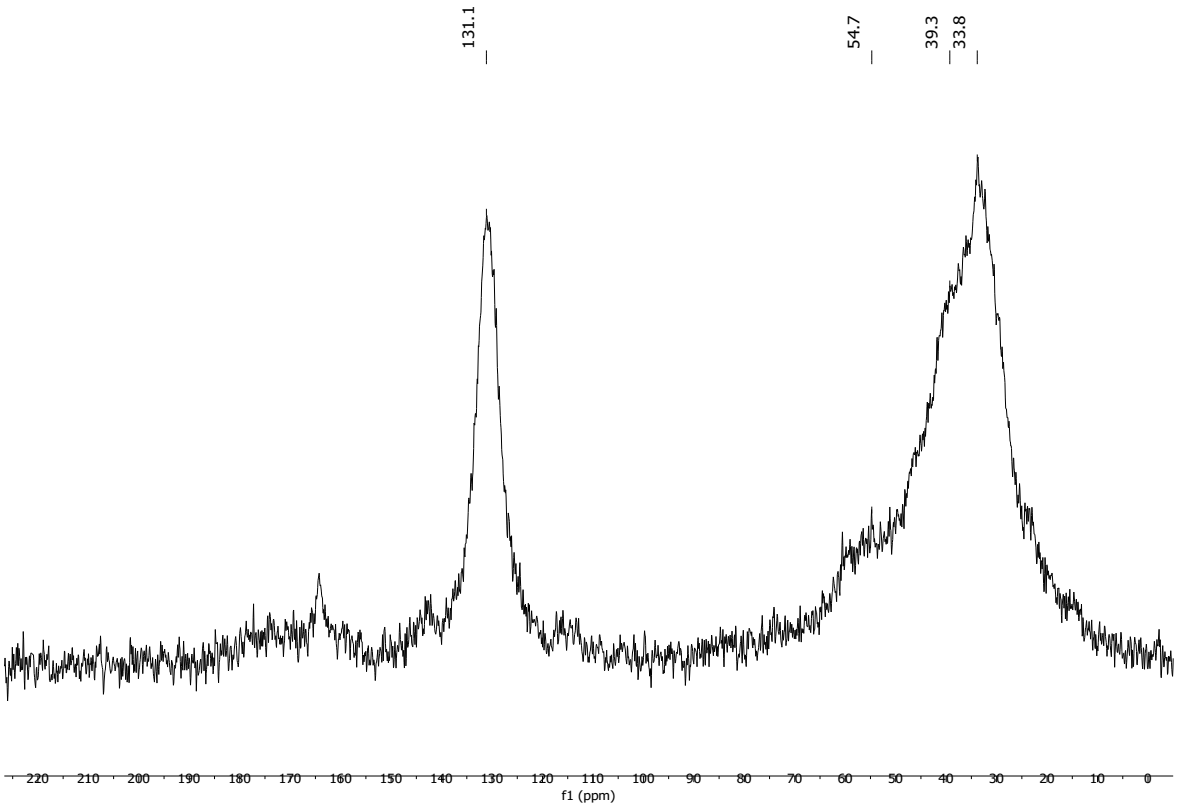

Solid-state ^{13}C–NMR stacked spectra of **Az-HNBR2** *(run 2,* ***brown****) and* ***H-NBR2*** *(run 2, substrate,* ***light blue****):*

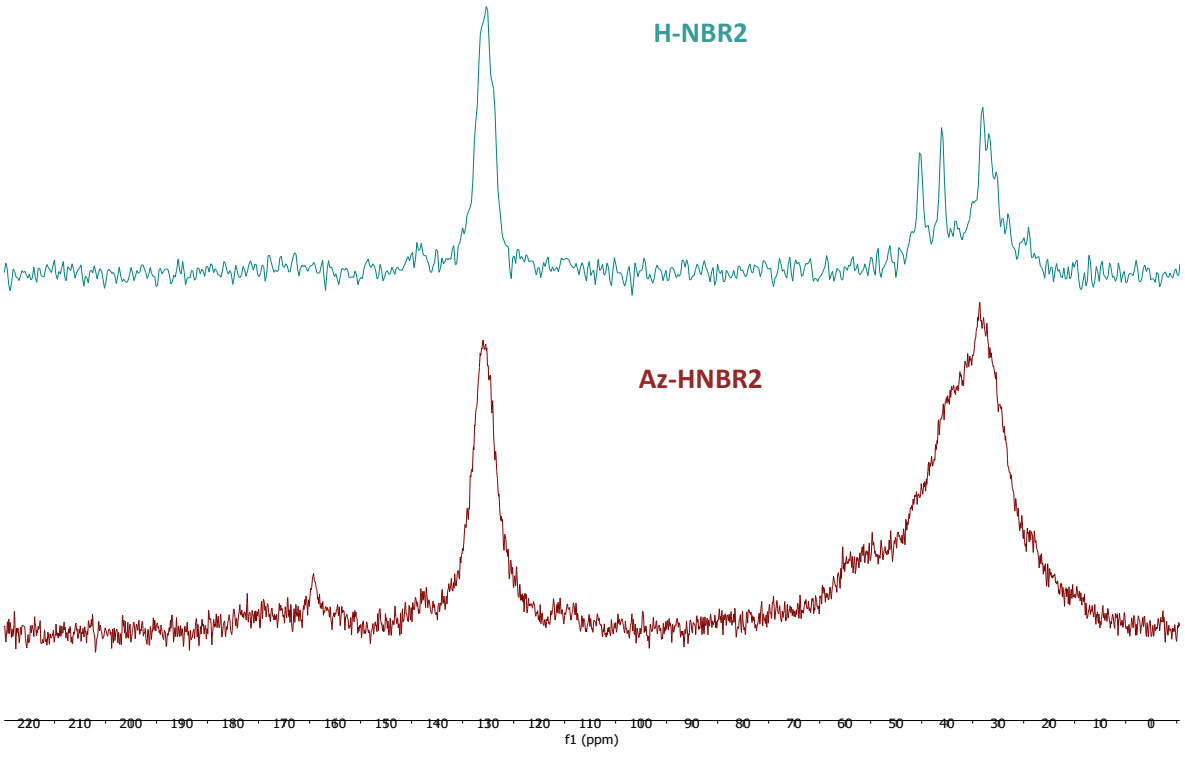

Infrared (IR) Spectroscopic Analysis

IR-spectrum of **Az-HNBR2** *(run 1):*

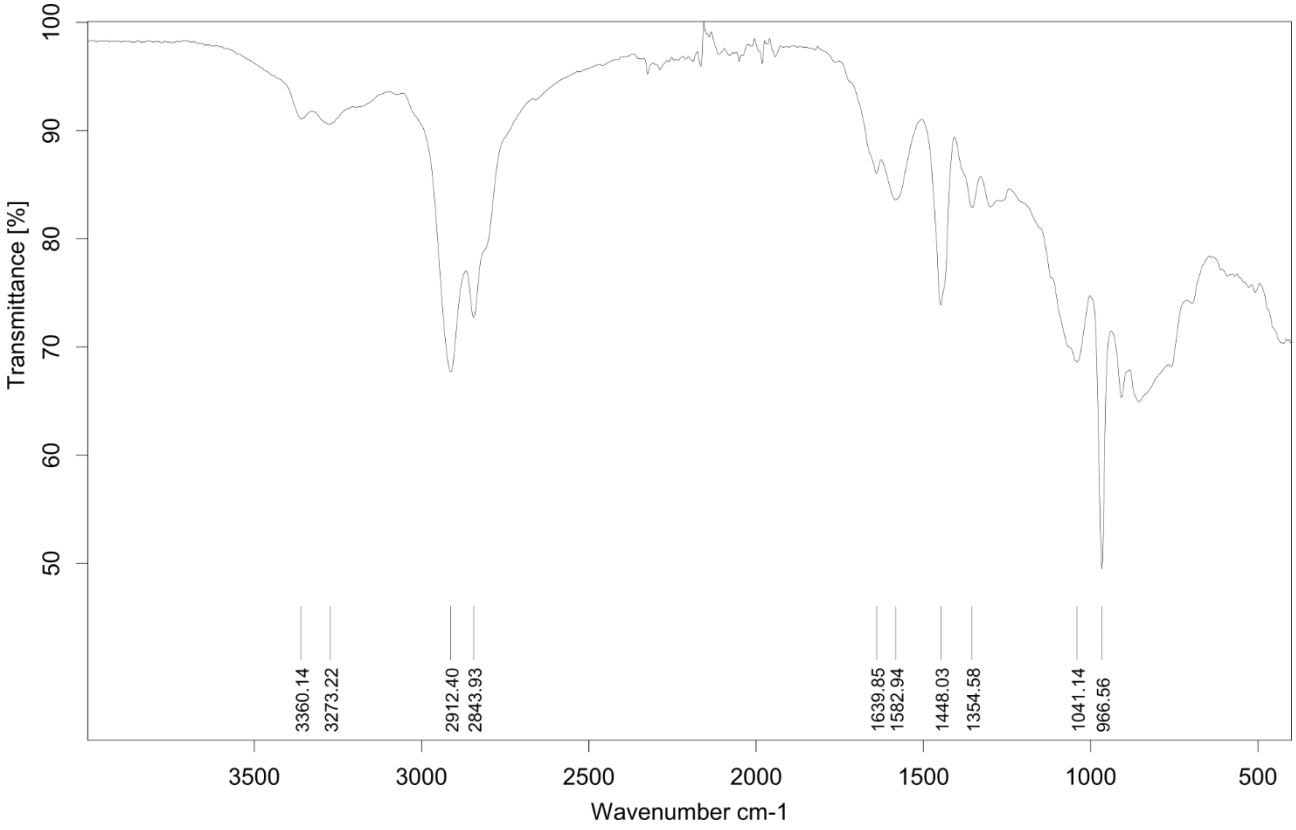

IR-spectrum of **Az-HNBR2** *(run 2):*

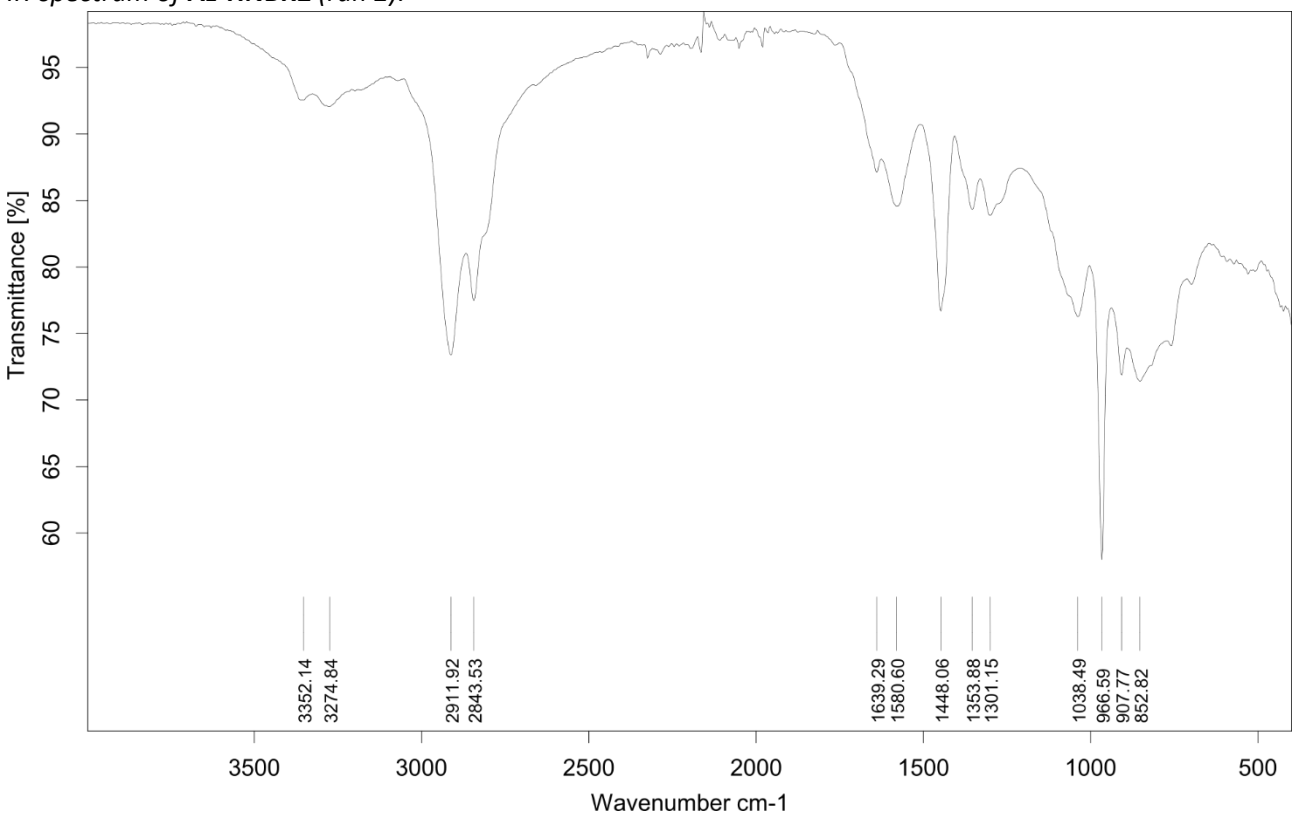

IR-spectrum overlay of **Az-HNBR2** *(run 1,* ***black****) and* ***H-NBR2*** *(substrate,* ***red****):*

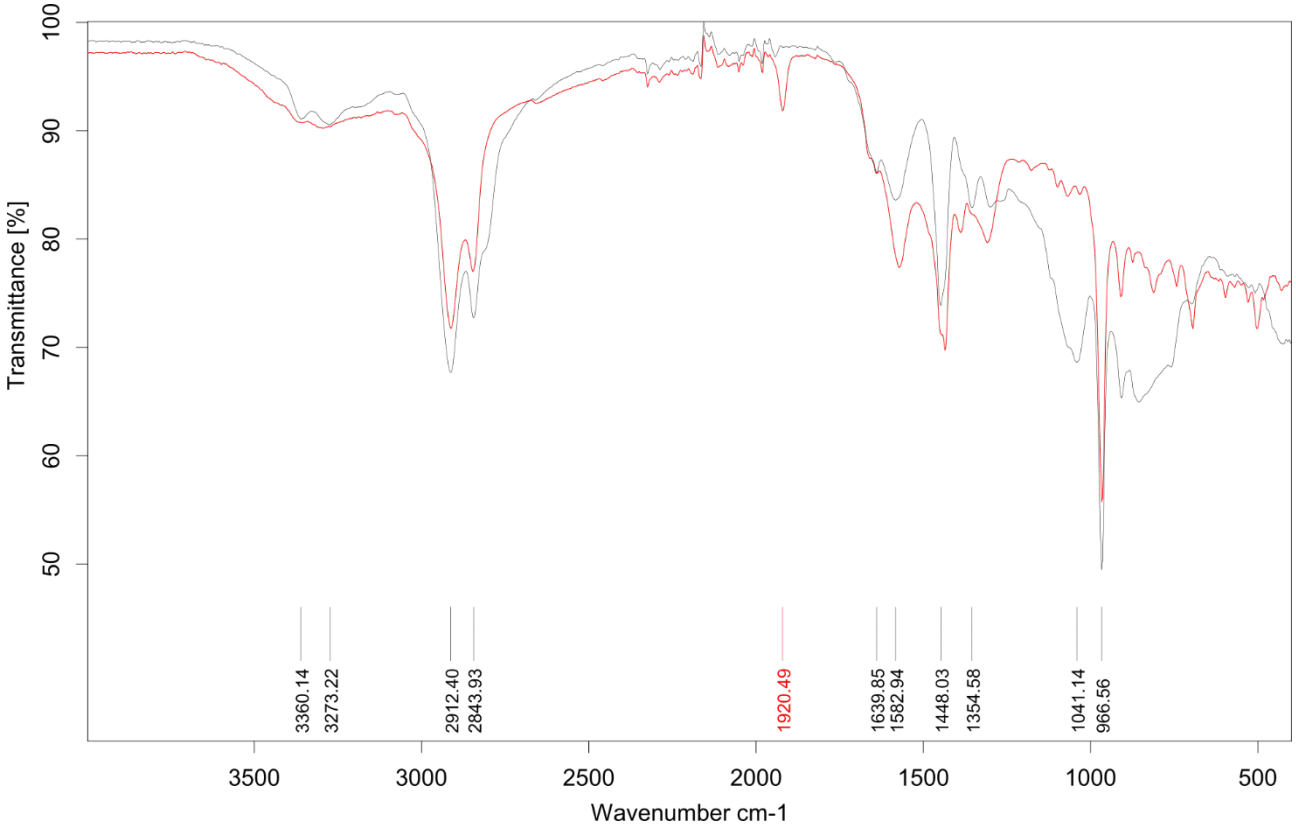

IR-spectrum of protected **Boc-Az-HNBR2** *(run 1):*

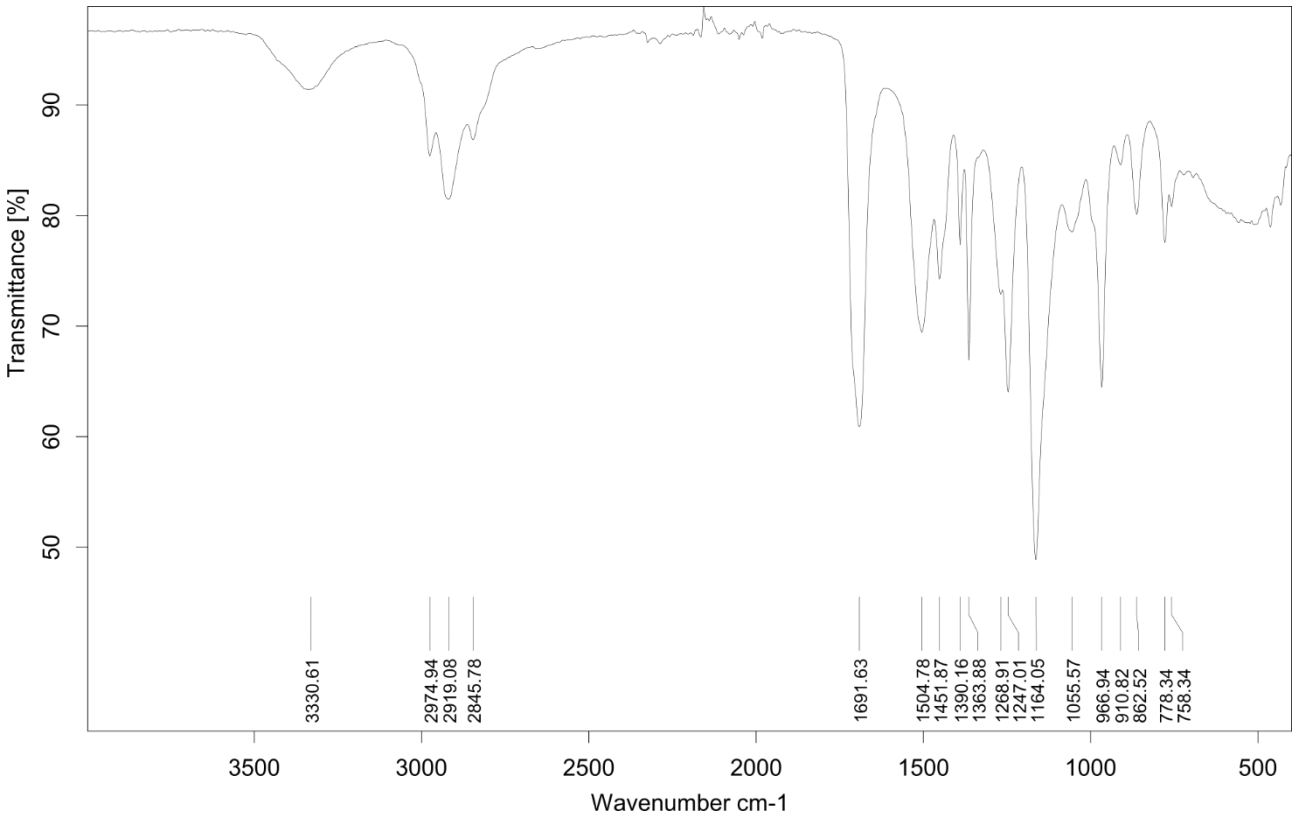

IR-spectrum of protected **Boc-Az-HNBR2** *(run 2):*

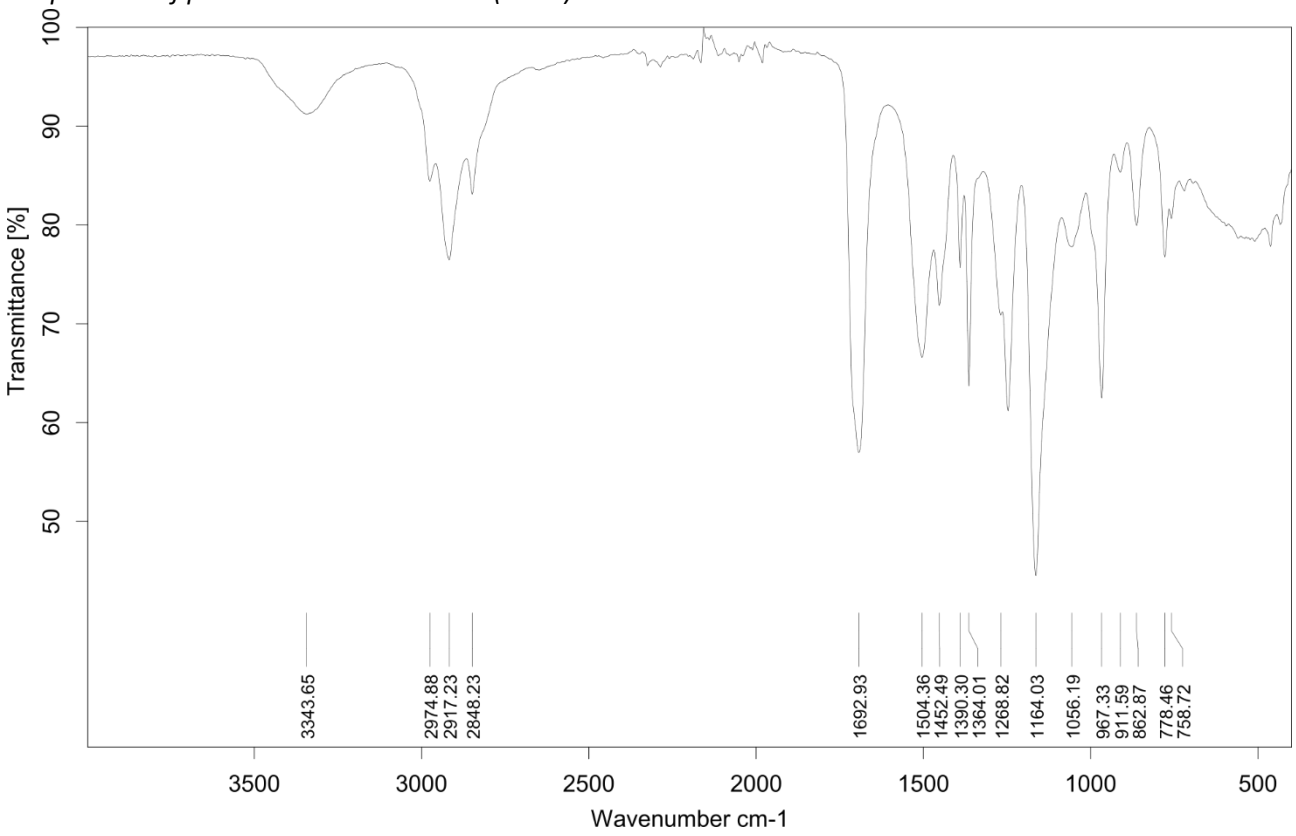

IR-spectrum overlay of protected **Boc-Az-HNBR2** *(run 1,* ***black****) and* ***H-NBR2*** *(substrate,* ***red****):*

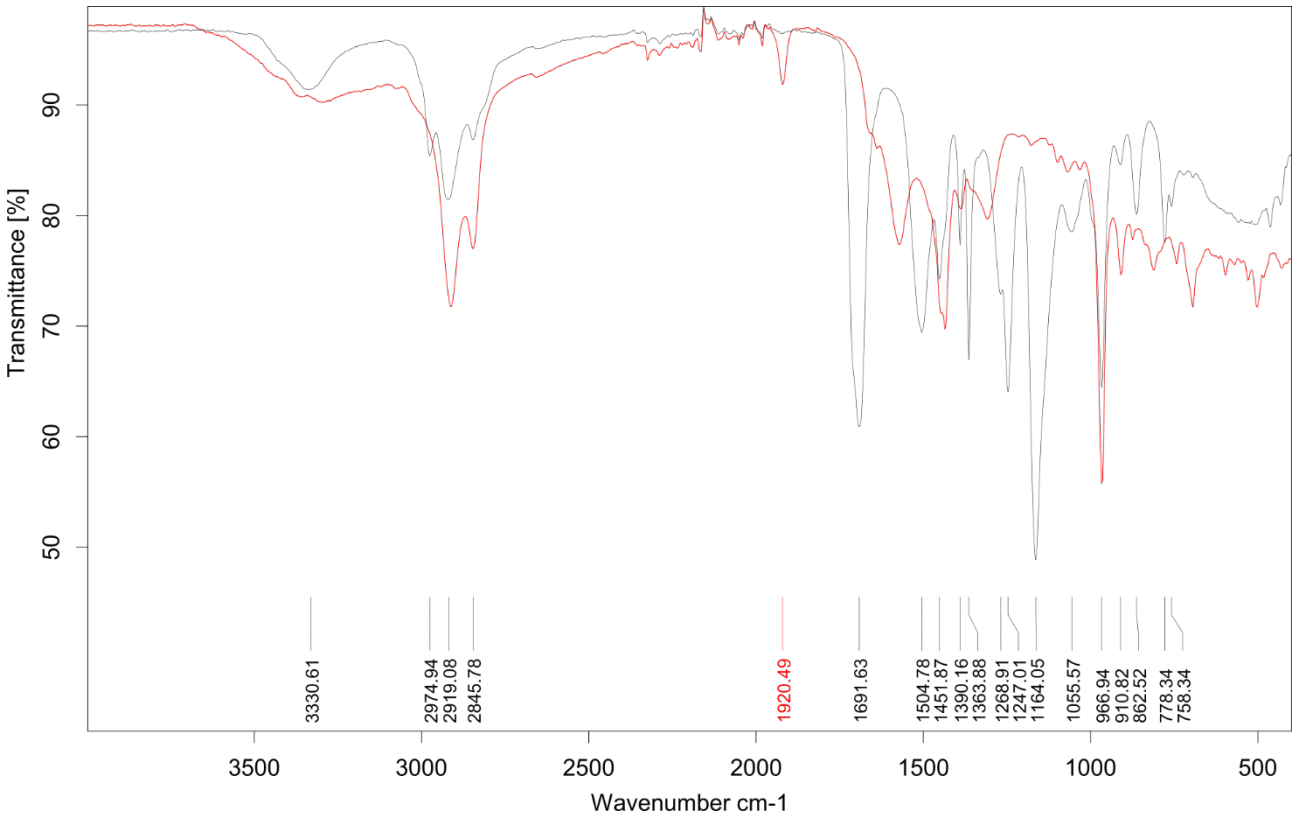

Thermogravimetric Analysis (TGA)

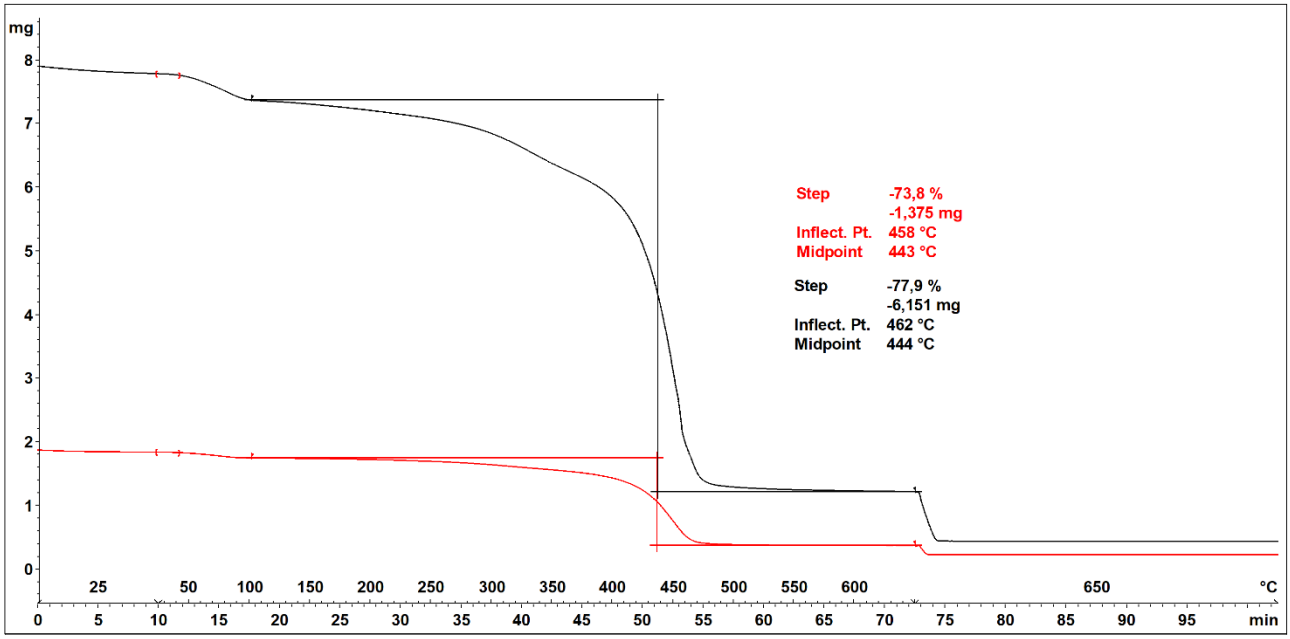

*Decomposition graph for **Az-HNBR2**. The experiment was conducted under He then air (after 650 °C). The black curve is the result from run 1, while the red curve is for run 2. Only ~ 2 mg was analysed for run 2 due to a shortage of material.*

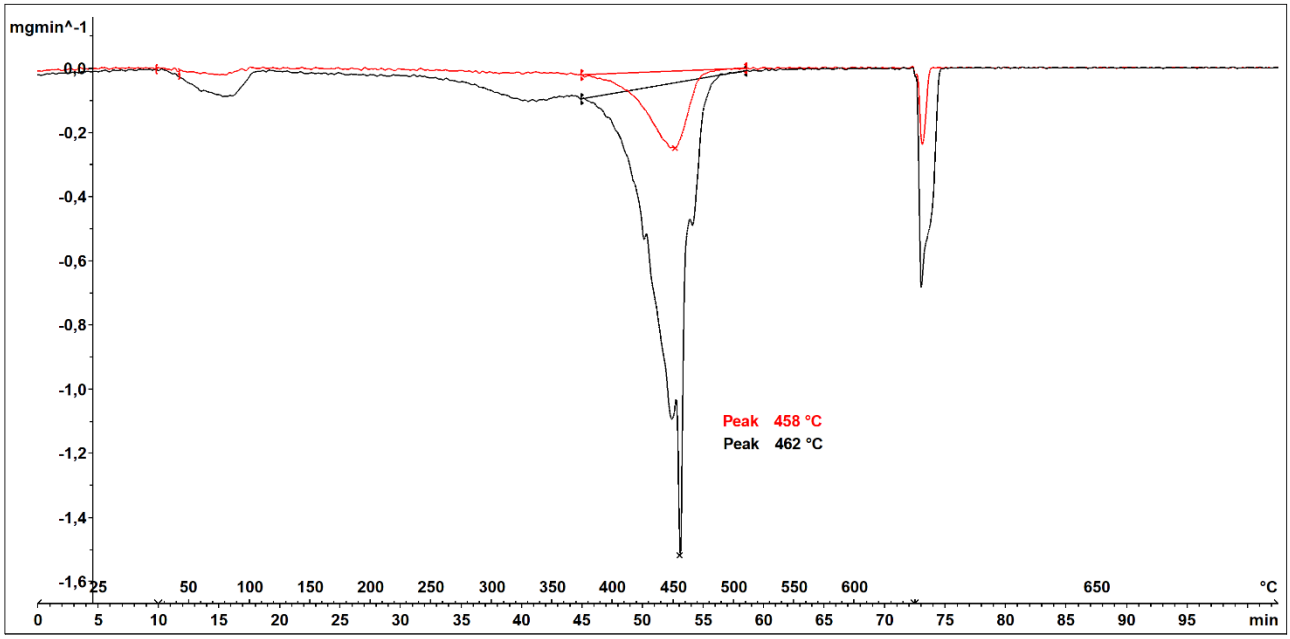

*1st derivative of decomposition graph for **Az-HNBR2**. The experiment was conducted under He then air (after 650 °C). The black curve is the result from run 1, while the red curve is for run 2. Only ~ 2 mg was analysed for run 2 due to a shortage of material.*

Decomposition temperature (T_d) = 458−462 ℃.

CO_2-adsorption analysis by thermogravimetric analysis

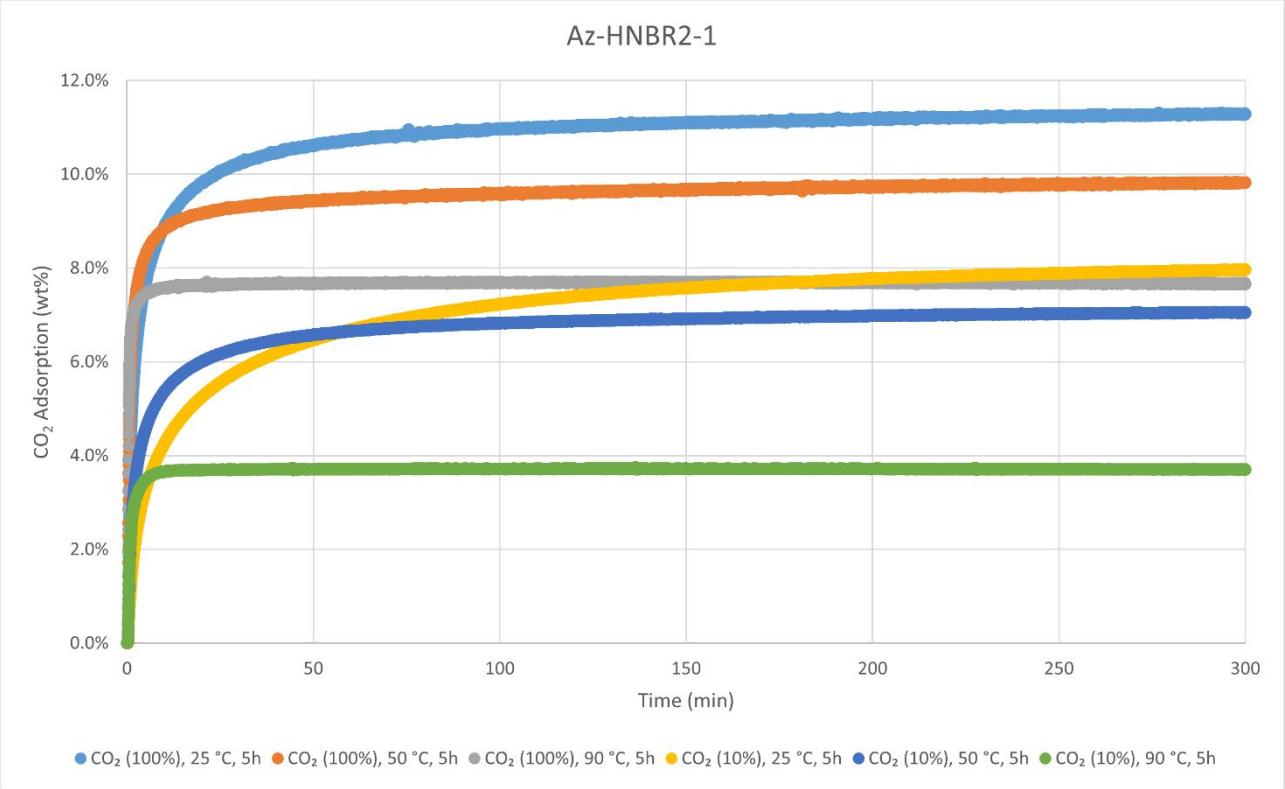

CO_2 adsorption using **TGA method 2** (measurement of product batch from run 1: Az-HNBR2-1).

Az-HNBR2-1	wt%	mmol/g
CO_2 (100%), 25 °C, 5h	11.3%	2.57
CO_2 (100%), 50 °C, 5h	9.8%	2.23
CO_2 (100%), 90 °C, 5h	7.7%	1.74
CO_2 (10%), 25 °C, 5h	8.0%	1.81
CO_2 (10%), 50 °C, 5h	7.1%	1.60
CO_2 (10%), 90 °C, 5h	3.7%	0.84

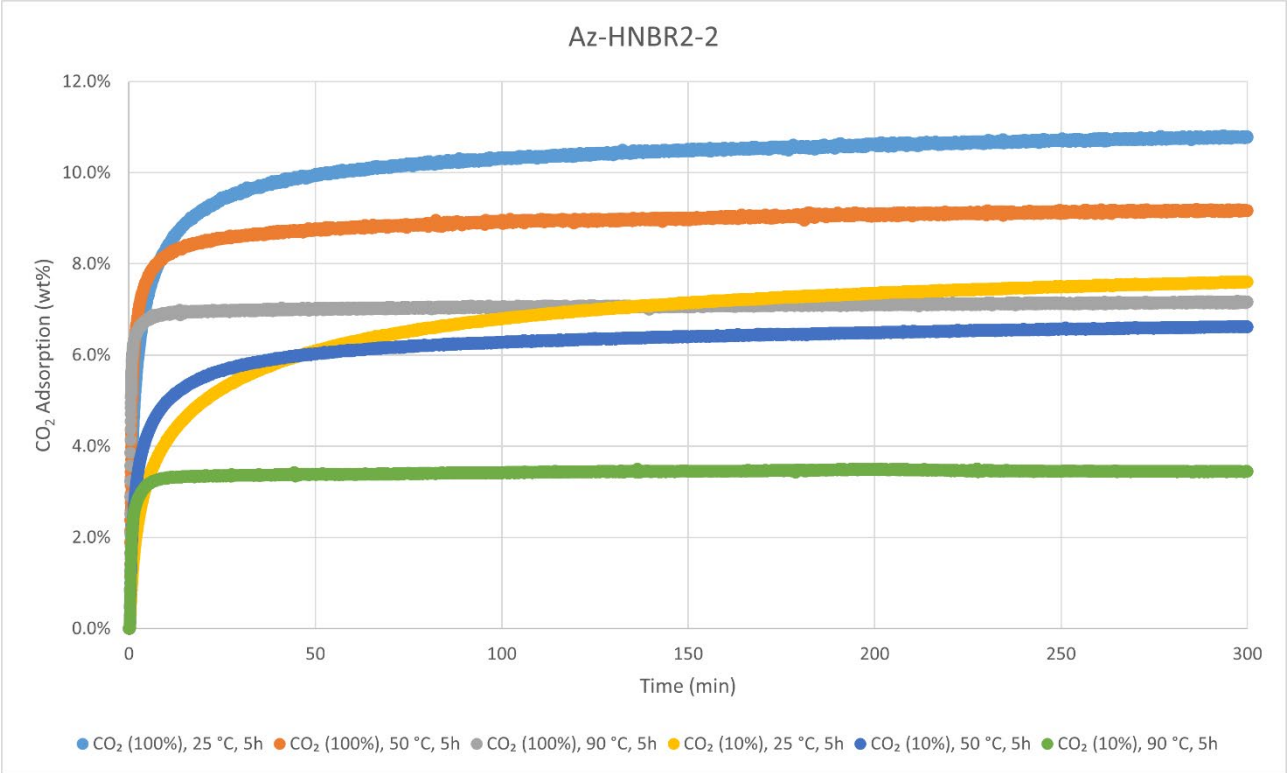

CO_2 adsorption using **TGA method 2** (measurement of product batch from run 2: Az-HNBR2-2).

Az-HNBR2-2	wt%	mmol/g
CO_2 (100%), 25 °C, 5h	10.8%	2.45
CO_2 (100%), 50 °C, 5h	9.2%	2.08
CO_2 (100%), 90 °C, 5h	7.2%	1.63
CO_2 (10%), 25 °C, 5h	7.6%	1.73
CO_2 (10%), 50 °C, 5h	6.6%	1.50
CO_2 (10%), 90 °C, 5h	3.4%	0.78

Elemental Analysis (EA)

Az-HNBR2	N [%]	C [%]	H [%]	S [%]	mmol N/g	C/N ratio	C/H ratio
run 1	**11.63**	**63.44**	**9.89**	**Not detected**	**8.30**	**6.36**	**0.54**
run 2	**11.35**	**63.43**	**9.62**		**8.10**	**6.52**	**0.55**

Aziridine-extended H-ABS2 (Az-HABS2) was synthesised according to the General Procedure I from substrate **H-ABS2** (hydrogenated keyboard) and was obtained in weight yields of 93.9 mg, 94 wt% and 91.5 mg, 92 wt%, respectively, from two independent runs over two steps (93 wt% on average). The polymer was analysed with solid-state ^{13}C CP/MAS NMR, IR-, TGA-, DSC-, and elemental analysis. Solubility tests were also conducted with several solvents. No thermal events besides decomposition were observed with DSC.

Particle size after cryogenic milling used for CO_2 adsorption-desorption experiments

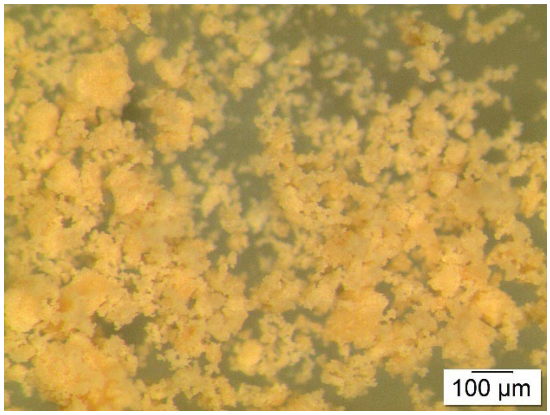

Solubility chart

Soluble **Swells** **Not soluble**

$CHCl_3$	Acetone	*i*-PrOH	DMF	DMSO	THF	PhMe	H_2O	MeOH	MeCN

^{13}C CP/MAS NMR (solid-state)

*Solid-state ^{13}C–NMR of **Az-HABS2** (run 1):*

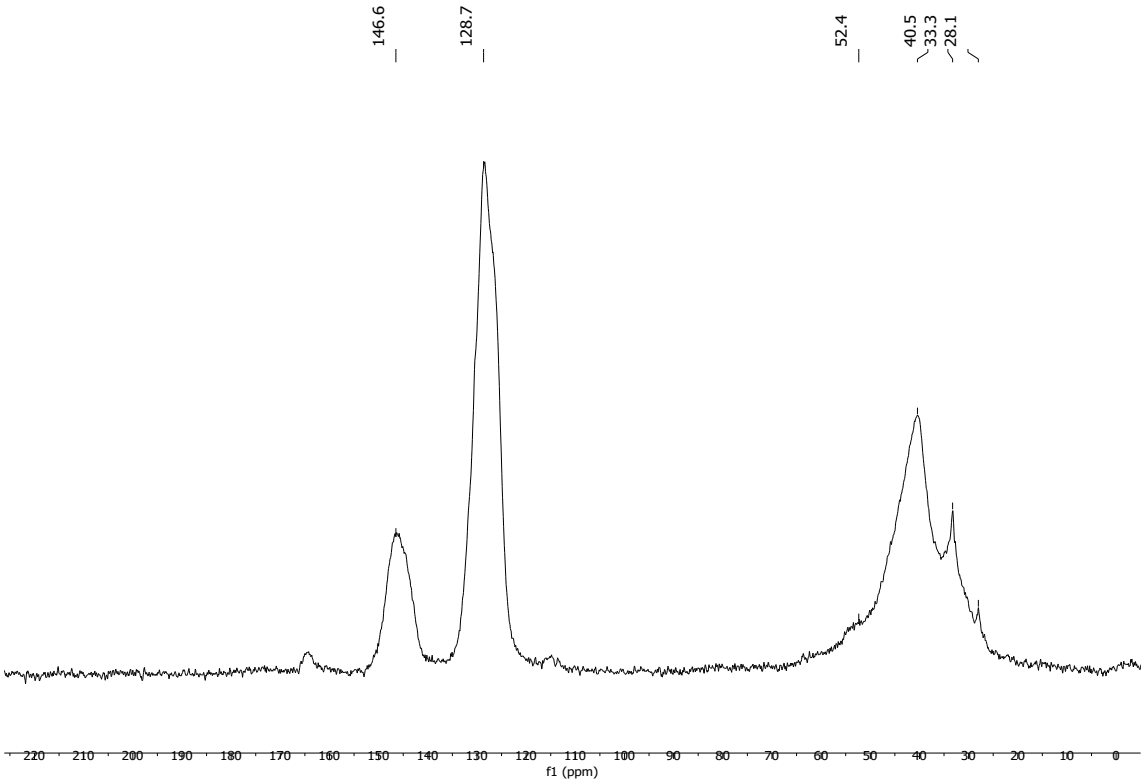

*Solid-state ^{13}C–NMR stacked spectra of **Az-HABS2** (run 1, **brown**) and **H-ABS2** (substrate, run 2, **light blue**):*

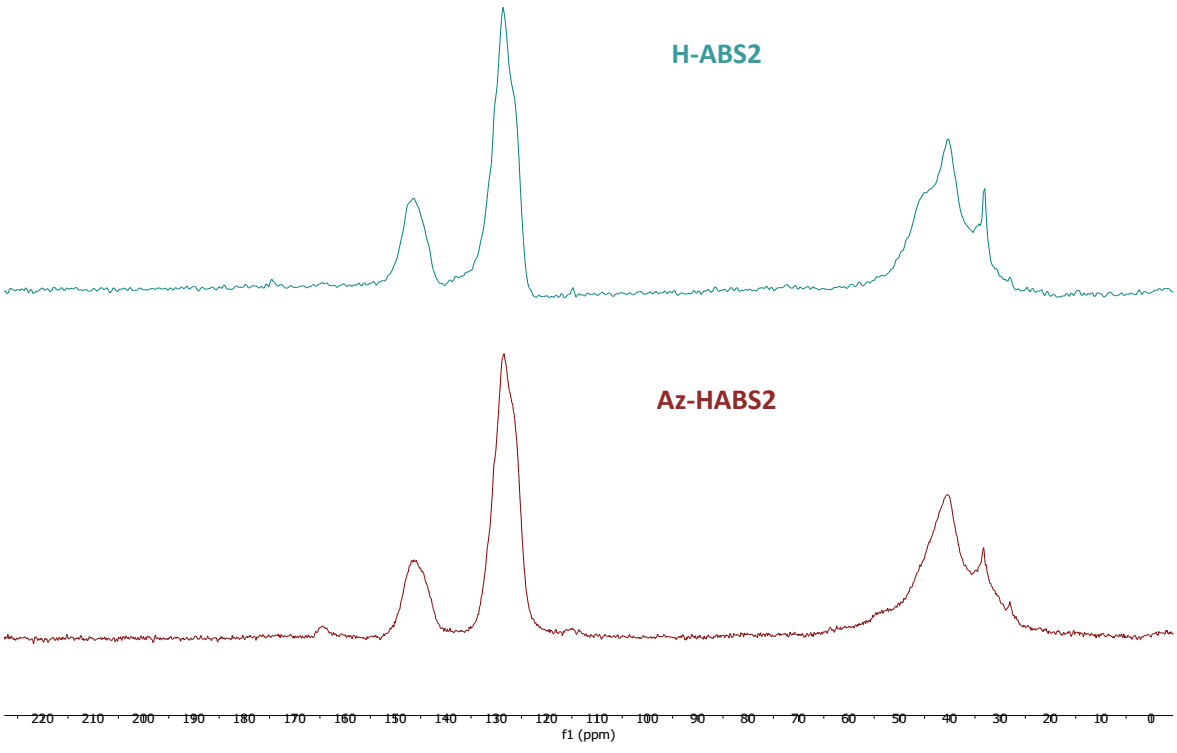

Infrared (IR) Spectroscopic Analysis

*IR-spectrum of **Az-HABS2** (run 1):*

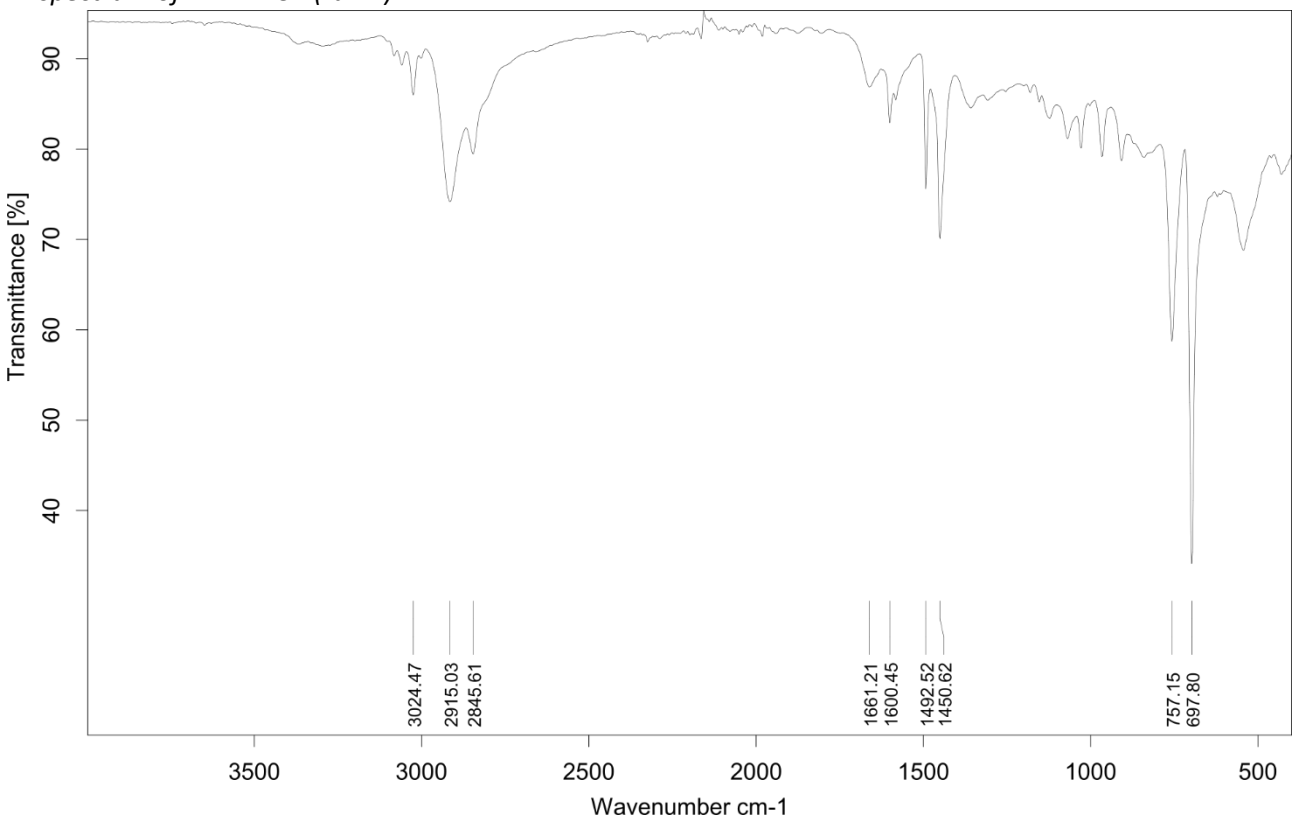

*IR-spectrum of **Az-HABS2** (run 2):*

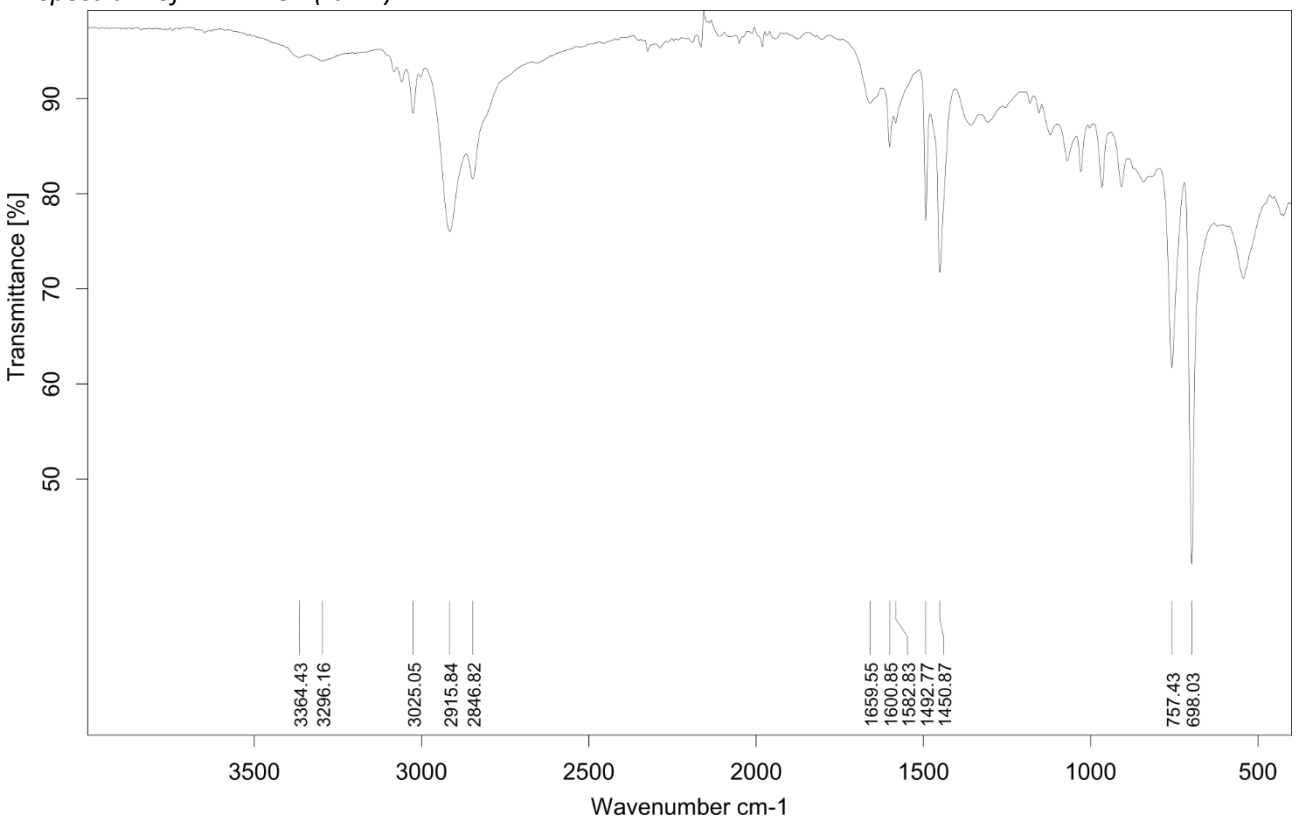

*IR-spectrum overlay of **Az-HABS2** (run 1, **black**) and **H-ABS2** (substrate, **red**):*

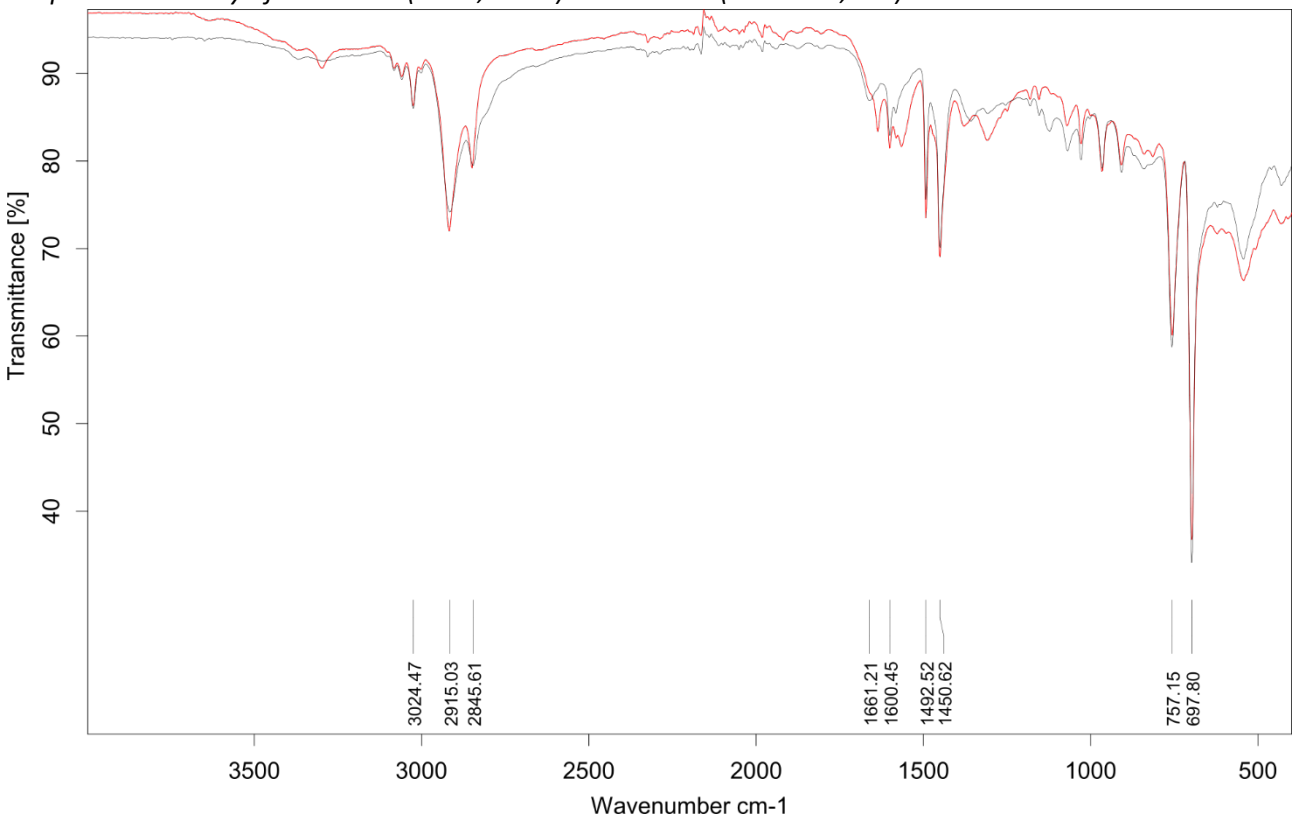

*IR-spectrum of protected **Boc-Az-HABS2** (run 1):*

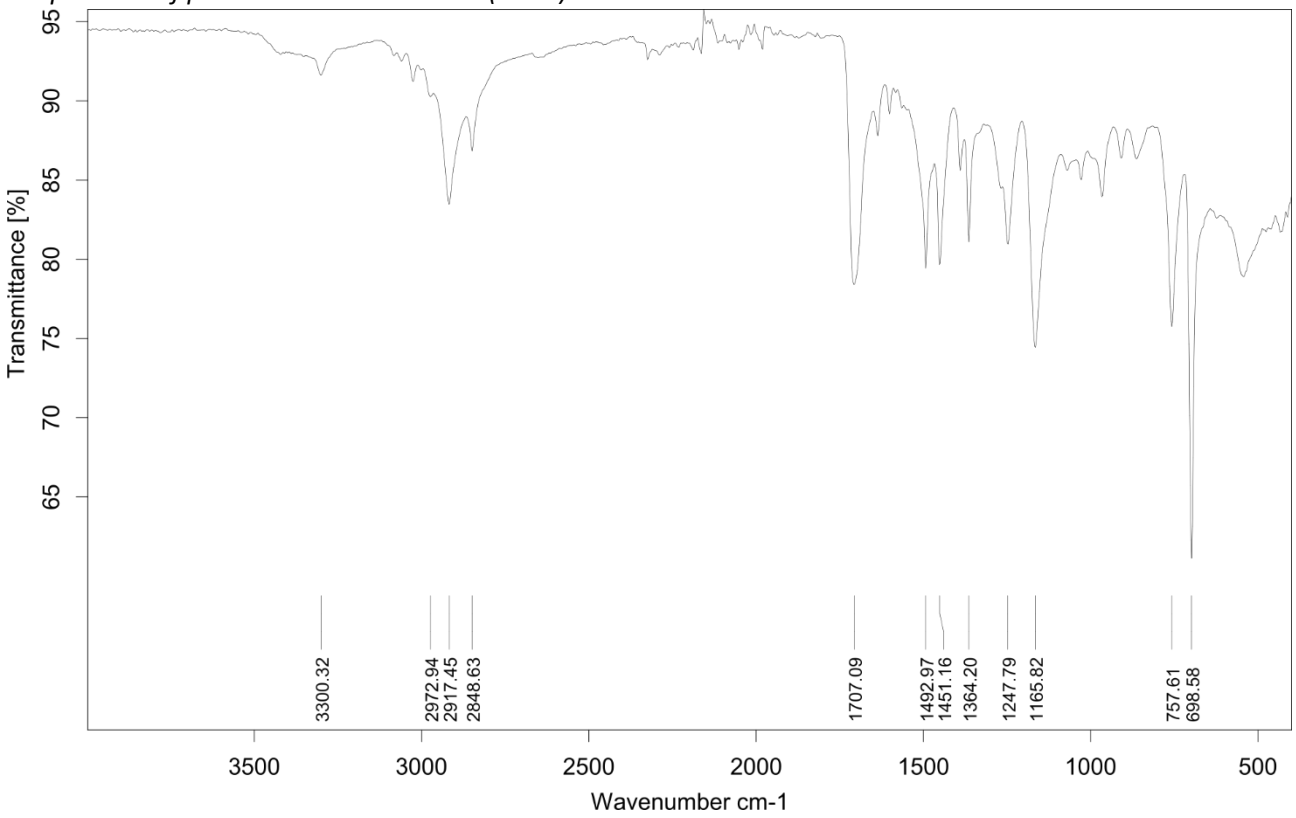

*IR-spectrum of protected **Boc-Az-HABS2** (run 2):*

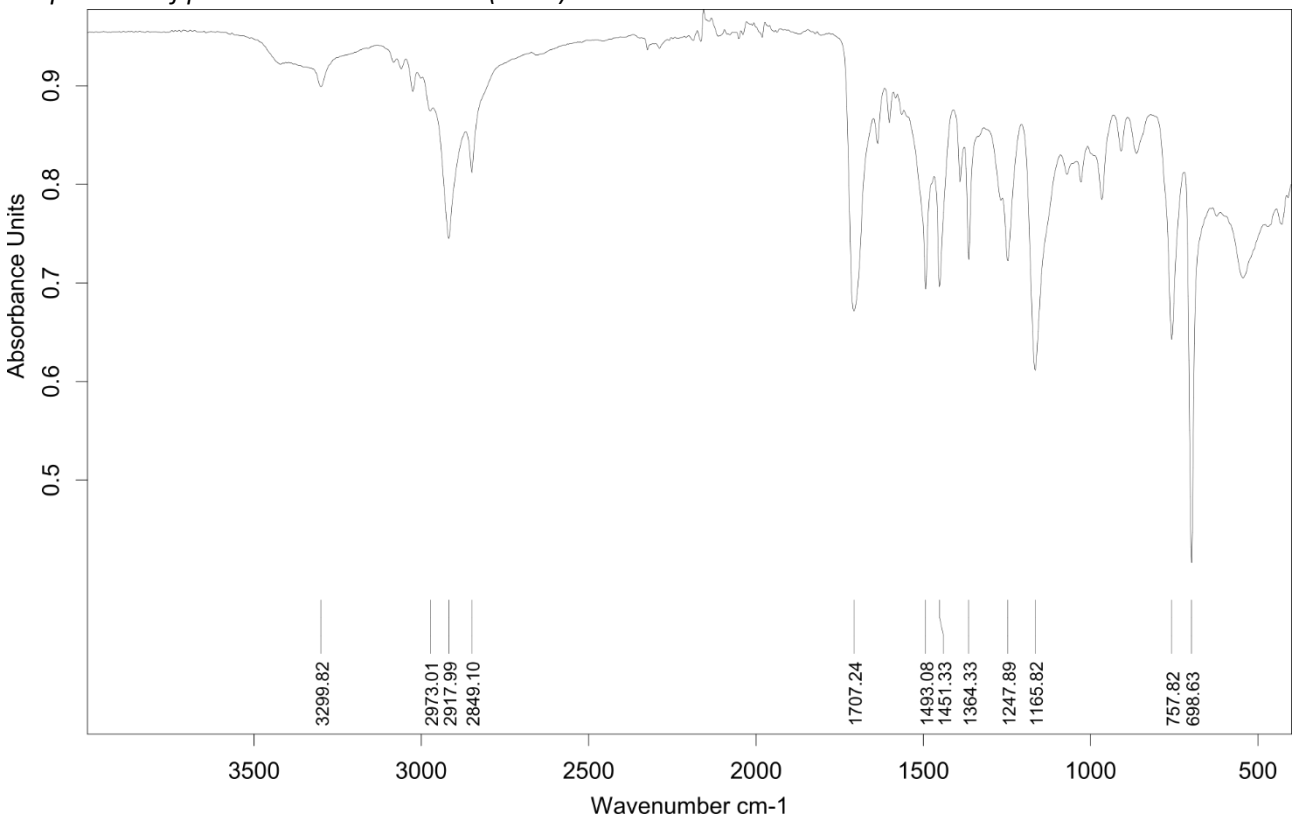

*IR-spectrum overlay of protected **Boc-Az-HABS2** (run 1, **black**) and **H-ABS2** (substrate, **red**):*

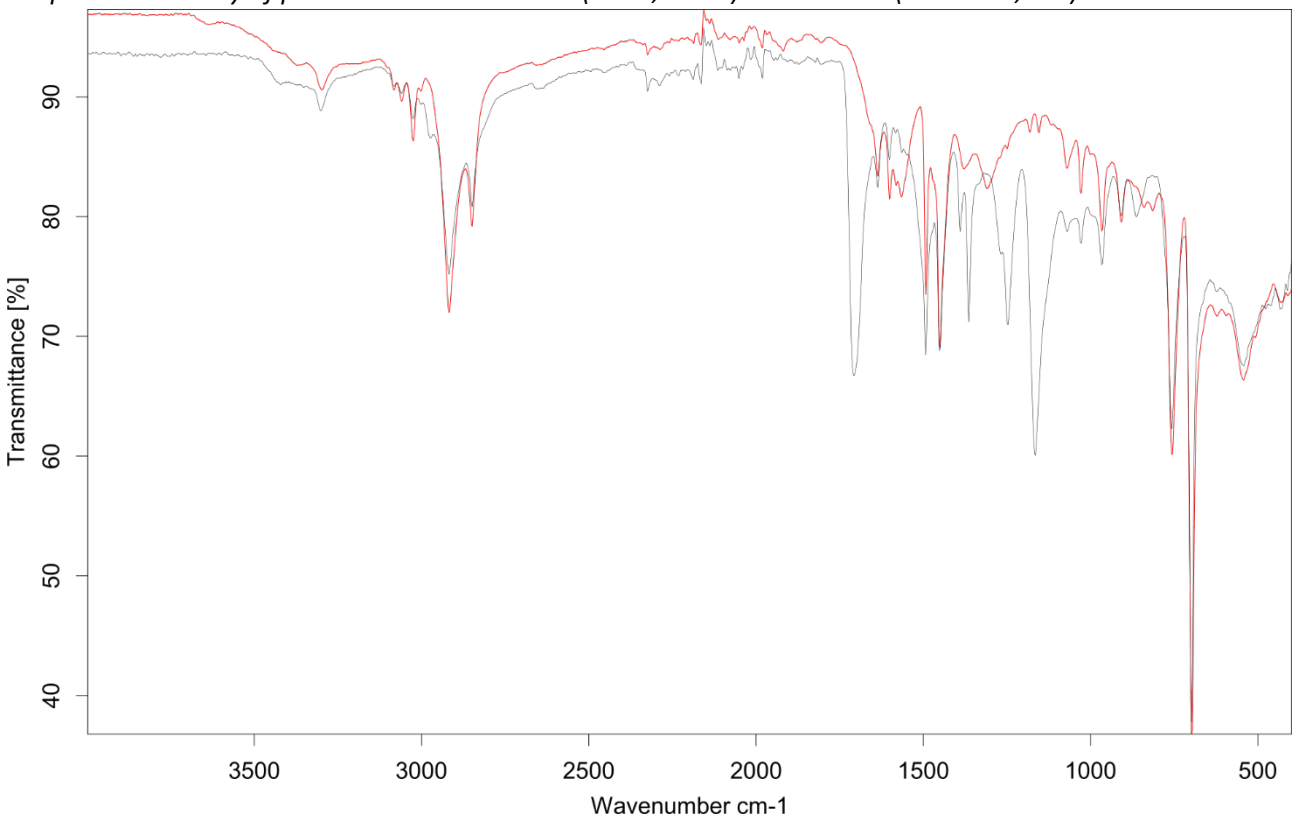

Thermogravimetric Analysis (TGA)

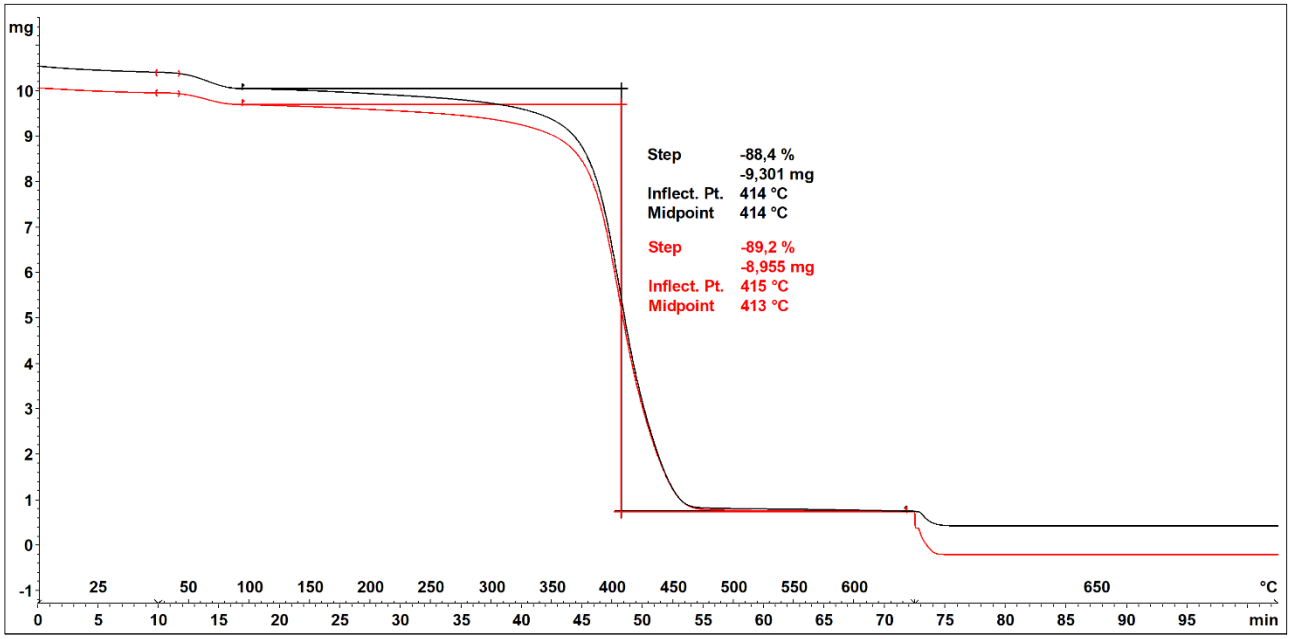

*Decomposition graph for **Az-HABS2**. The experiment was conducted under He then air (after 650 °C). The black curve is the result from run 1, while the red curve is for run 2.*

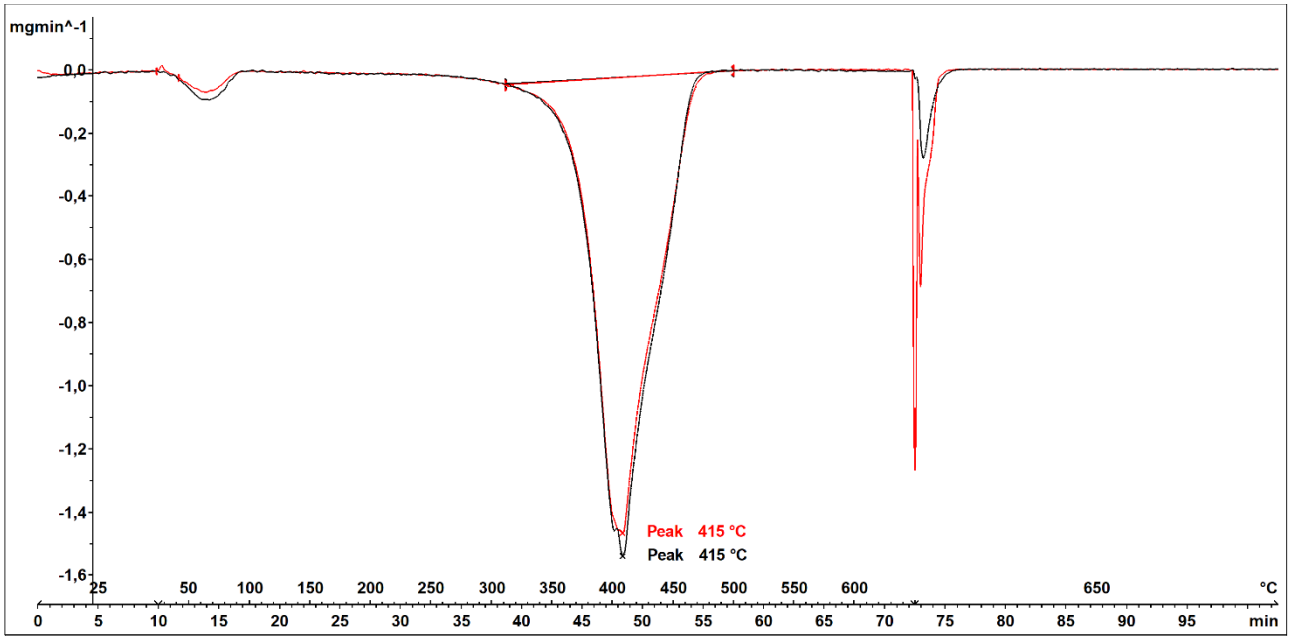

*1st derivative of decomposition graph for **Az-HABS2**. The experiment was conducted under He then air (after 650 °C). The black curve is the result from run 1, while the red curve is for run 2.*

Decomposition temperature (T_d) = 415 °C.

CO_2-adsorption analysis by thermogravimetric analysis

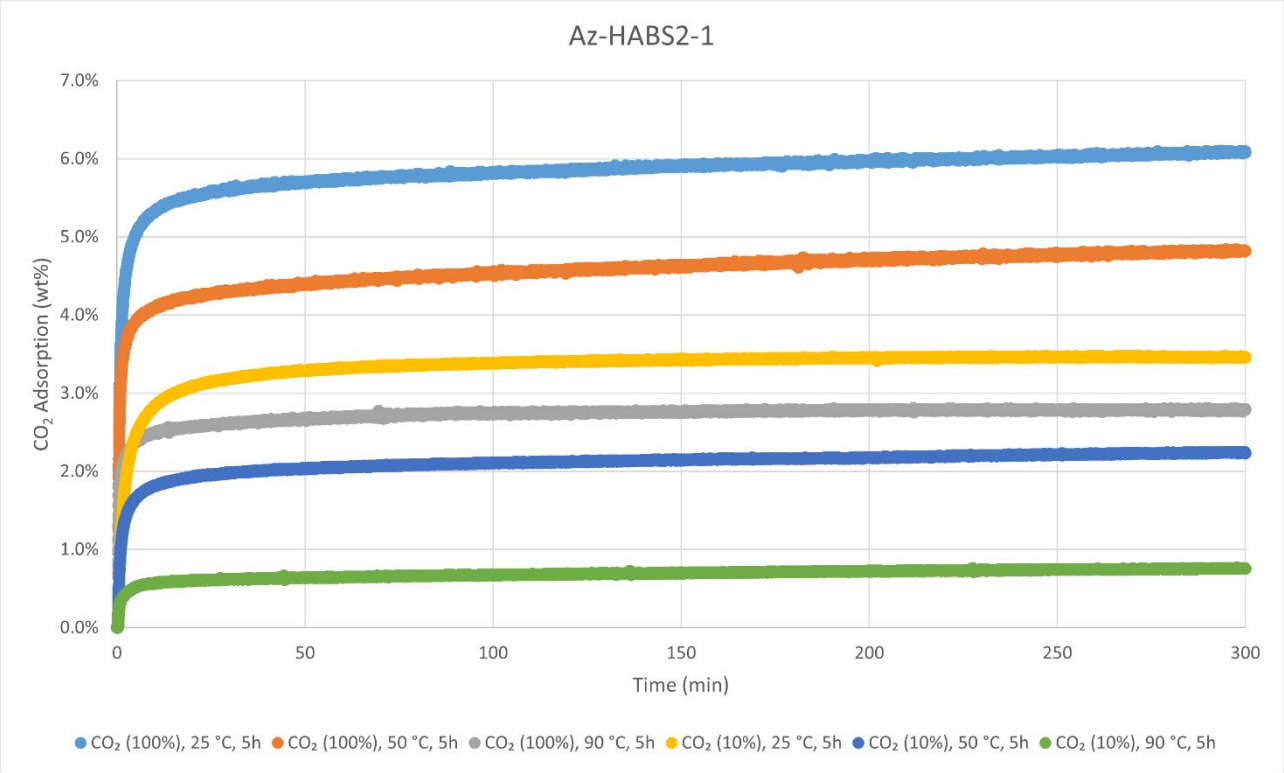

CO_2 adsorption using **TGA method 2** (measurement of product batch from run 1: Az-HABS2-1).

Az-HABS2-1	wt%	mmol/g
CO_2 (100%), 25 °C, 5h	6.1%	1.38
CO_2 (100%), 50 °C, 5h	4.8%	1.10
CO_2 (100%), 90 °C, 5h	2.8%	0.63
CO_2 (10%), 25 °C, 5h	3.5%	0.79
CO_2 (10%), 50 °C, 5h	2.2%	0.51
CO_2 (10%), 90 °C, 5h	0.8%	0.17

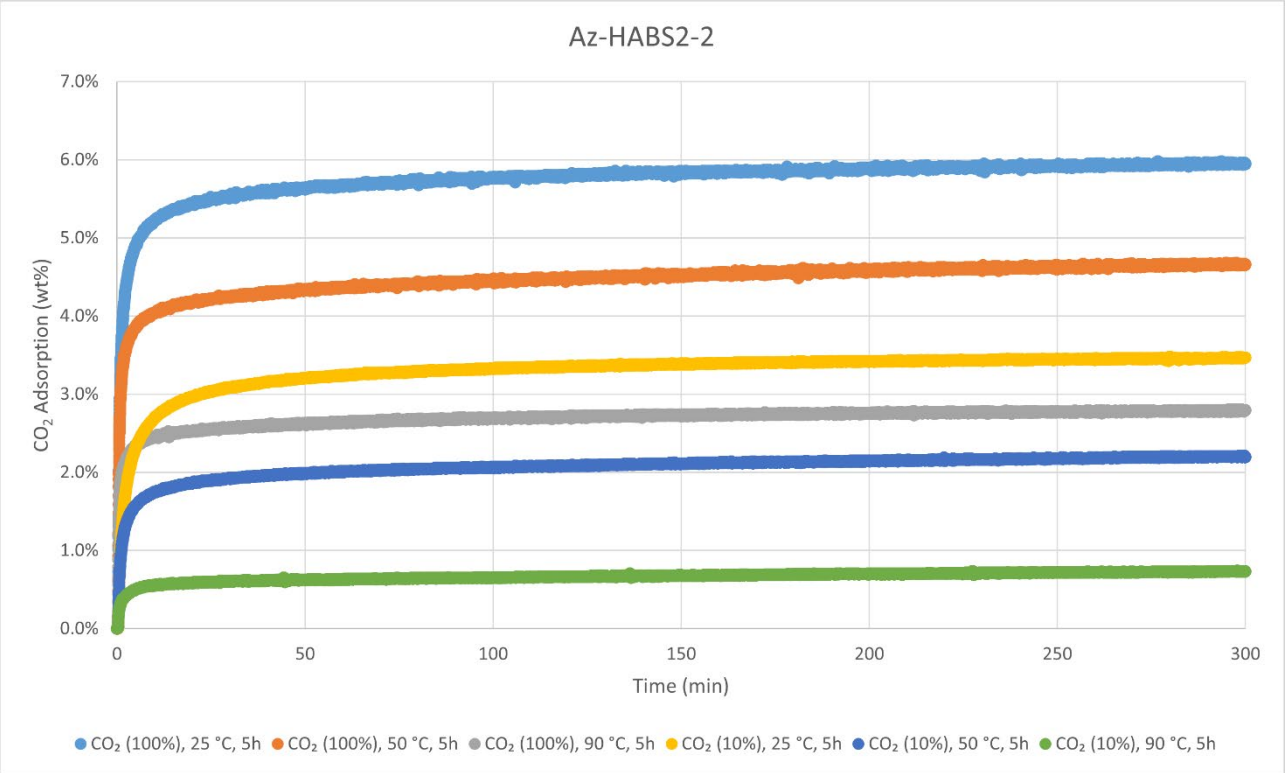

CO_2 adsorption using **TGA method 2** (measurement of product batch from run 2: Az-HABS2-2).

Az-HABS2-2	wt%	mmol/g
CO_2 (100%), 25 °C, 5h	6.0%	1.35
CO_2 (100%), 50 °C, 5h	4.7%	1.06
CO_2 (100%), 90 °C, 5h	2.8%	0.63
CO_2 (10%), 25 °C, 5h	3.5%	0.79
CO_2 (10%), 50 °C, 5h	2.2%	0.50
CO_2 (10%), 90 °C, 5h	0.7%	0.17

Elemental Analysis (EA)

Az-HABS2	N [%]	C [%]	H [%]	S [%]	mmol N/g	C/N ratio	C/H ratio
run 1	6.61	74.97	8.58	Not detected	4.72	13.22	0.73
run 2	6.76	76.57	8.87		4.83	13.21	0.72

Aziridine-extended H-SAN2 (Az-HSAN2) was synthesised according to the General Procedure I from substrate **H-SAN2** (hydrogenated toothbrush handle) and was obtained in weight yields of 59.6 mg, 60 wt% and 75.3 mg, 64 wt%, respectively, from two independent runs over two steps (62 wt% on average). The polymer was analysed with solid-state ^{13}C CP/MAS NMR, IR-, TGA-, DSC-, and elemental analysis. Solubility tests were also conducted with several solvents. No thermal events besides decomposition were observed with DSC.

Particle size after cryogenic milling used for CO_2 adsorption-desorption experiments

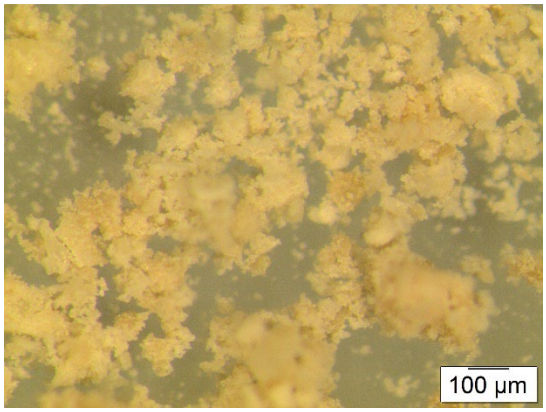

Solubility chart

Soluble **Swells** **Not soluble**

$CHCl_3$	Acetone	*i*-PrOH	DMF	DMSO	THF	PhMe	H_2O	MeOH	MeCN

^{13}C CP/MAS NMR (solid-state)

*Solid-state ^{13}C–NMR of **Az-HSAN2** (run 1):*

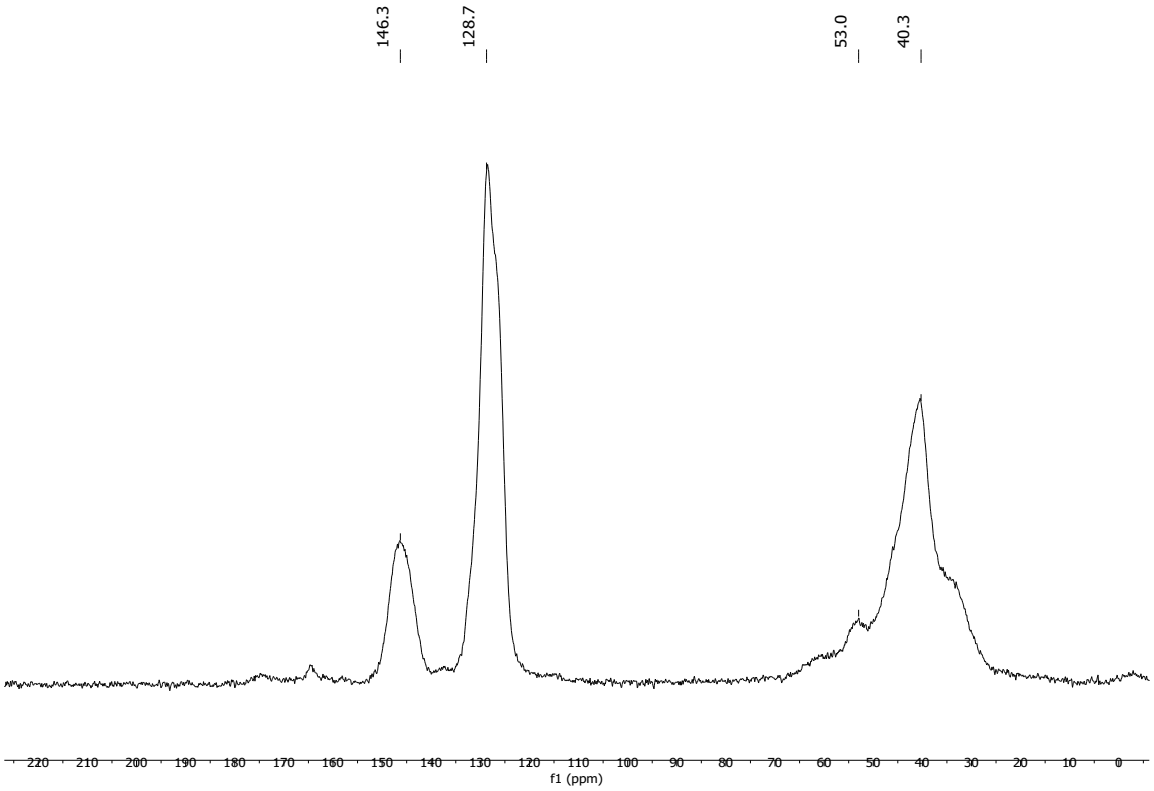

*Solid-state ^{13}C–NMR stacked spectra of **Az-HSAN2** (run 1, **brown**) and **H-SAN2** (substrate, **light blue**):*

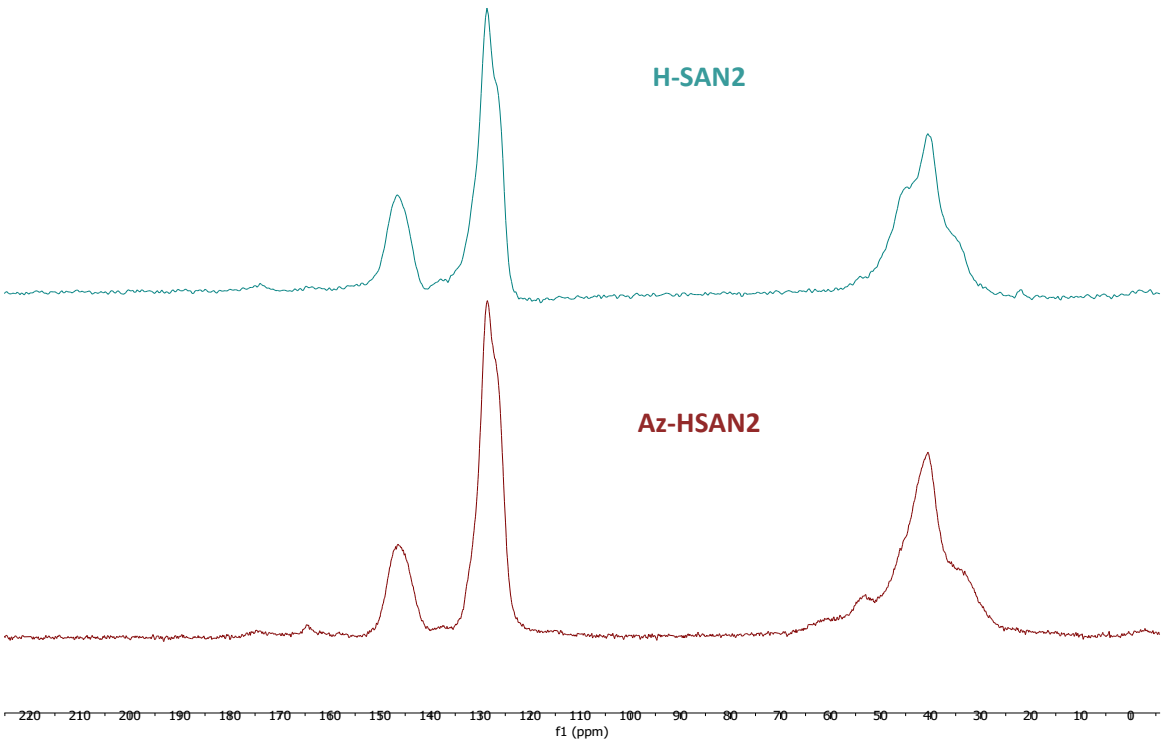

Infrared (IR) Spectroscopic Analysis

*IR-spectrum of **Az-HSAN2** (run 1):*

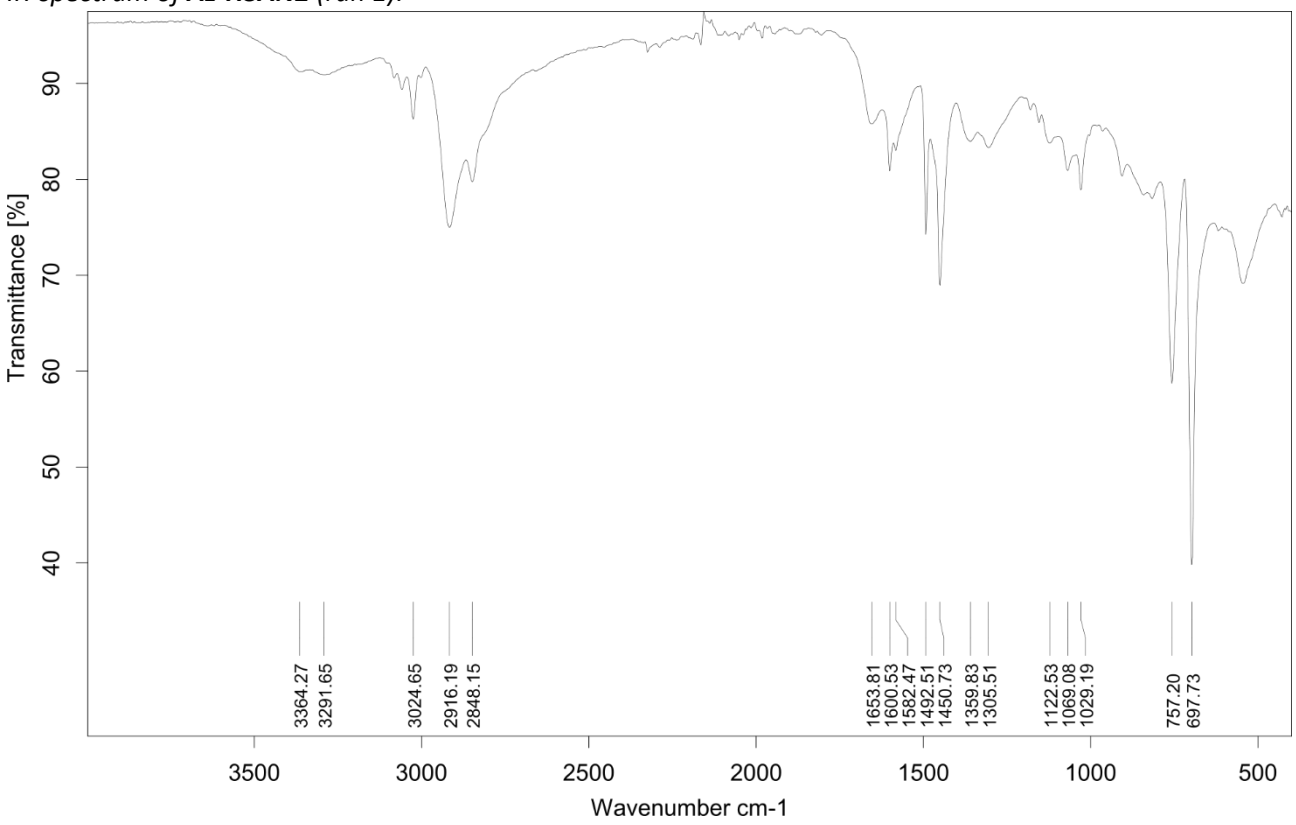

*IR-spectrum of **Az-HSAN2** (run 2):*

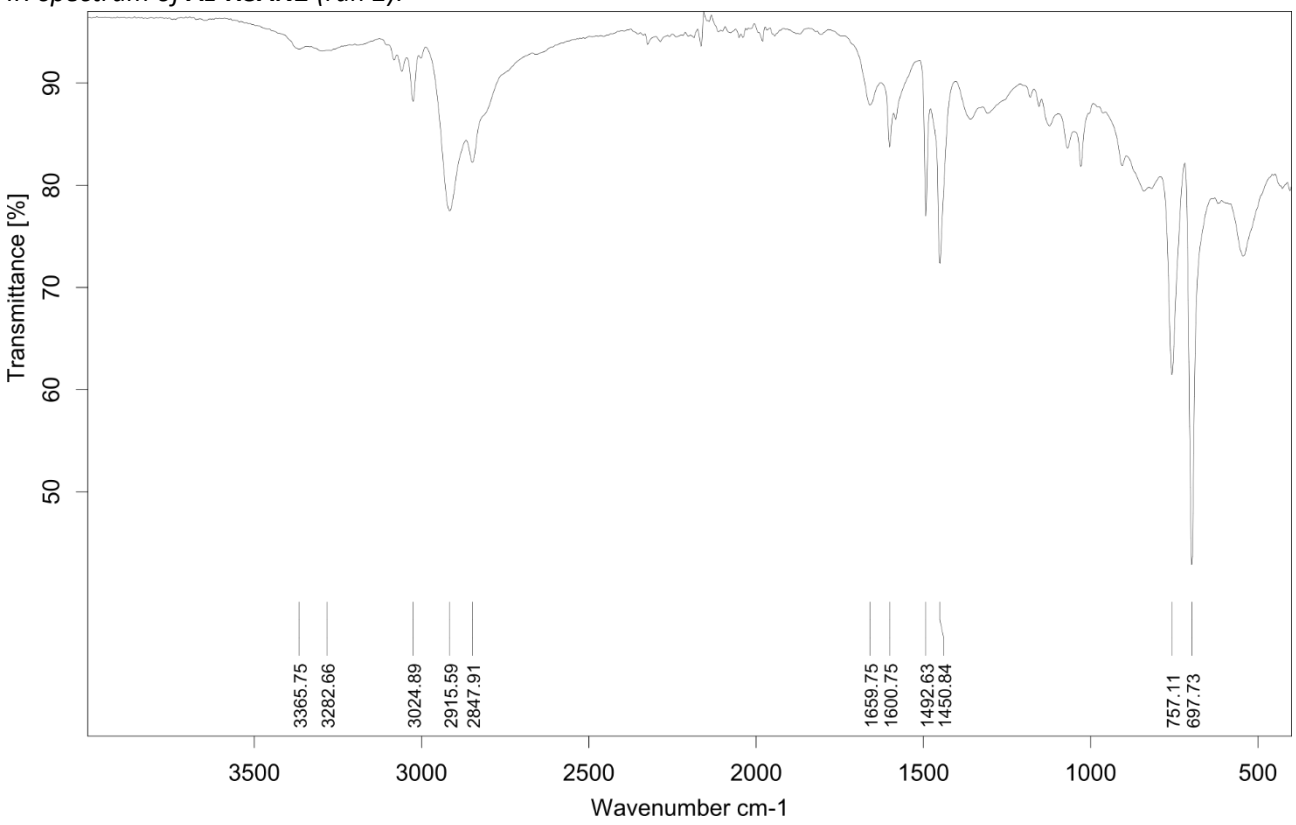

*IR-spectrum overlay of **Az-HSAN2** (run 1, **black**) and **H-SAN2** (substrate, **red**):*

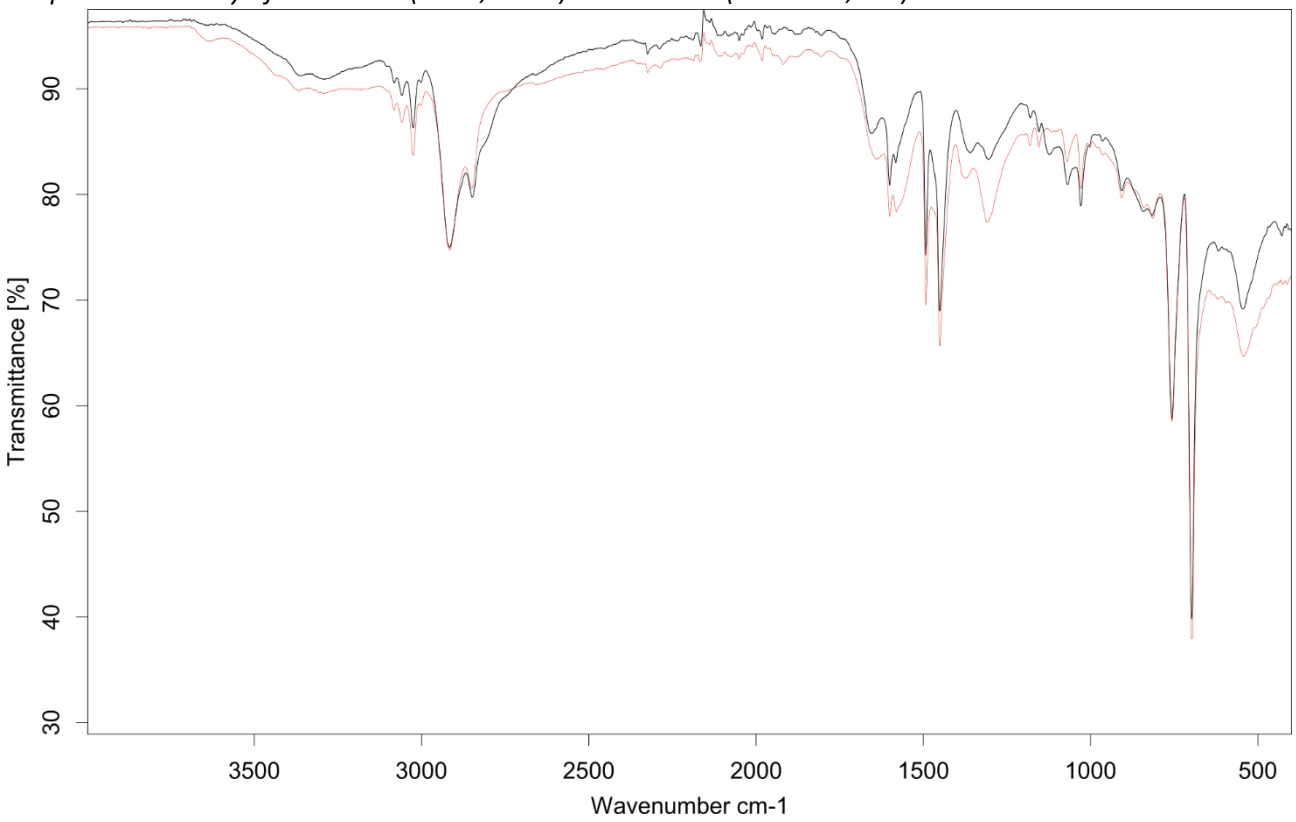

*IR-spectrum of protected **Boc-Az-HSAN2** (run 1):*

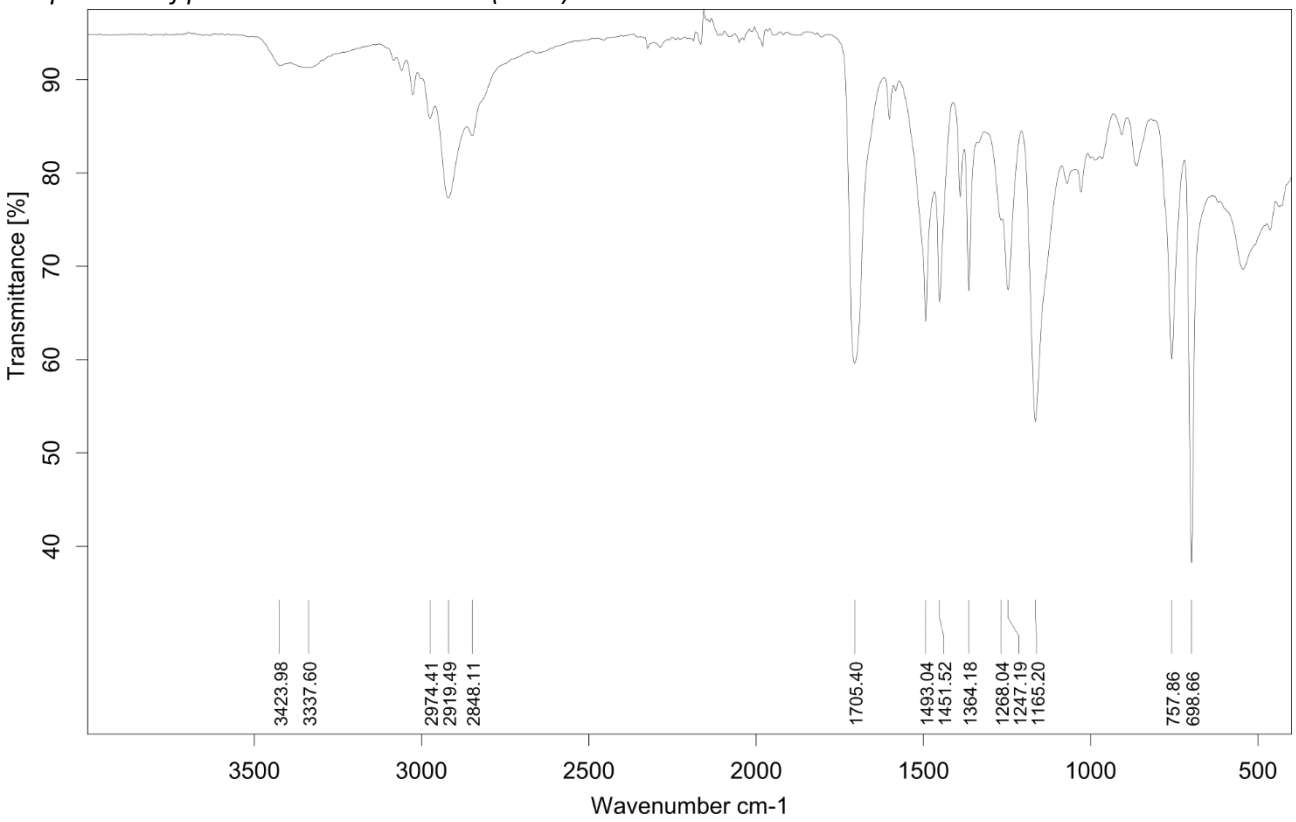

*IR-spectrum of protected **Boc-Az-HSAN2** (run 2):*

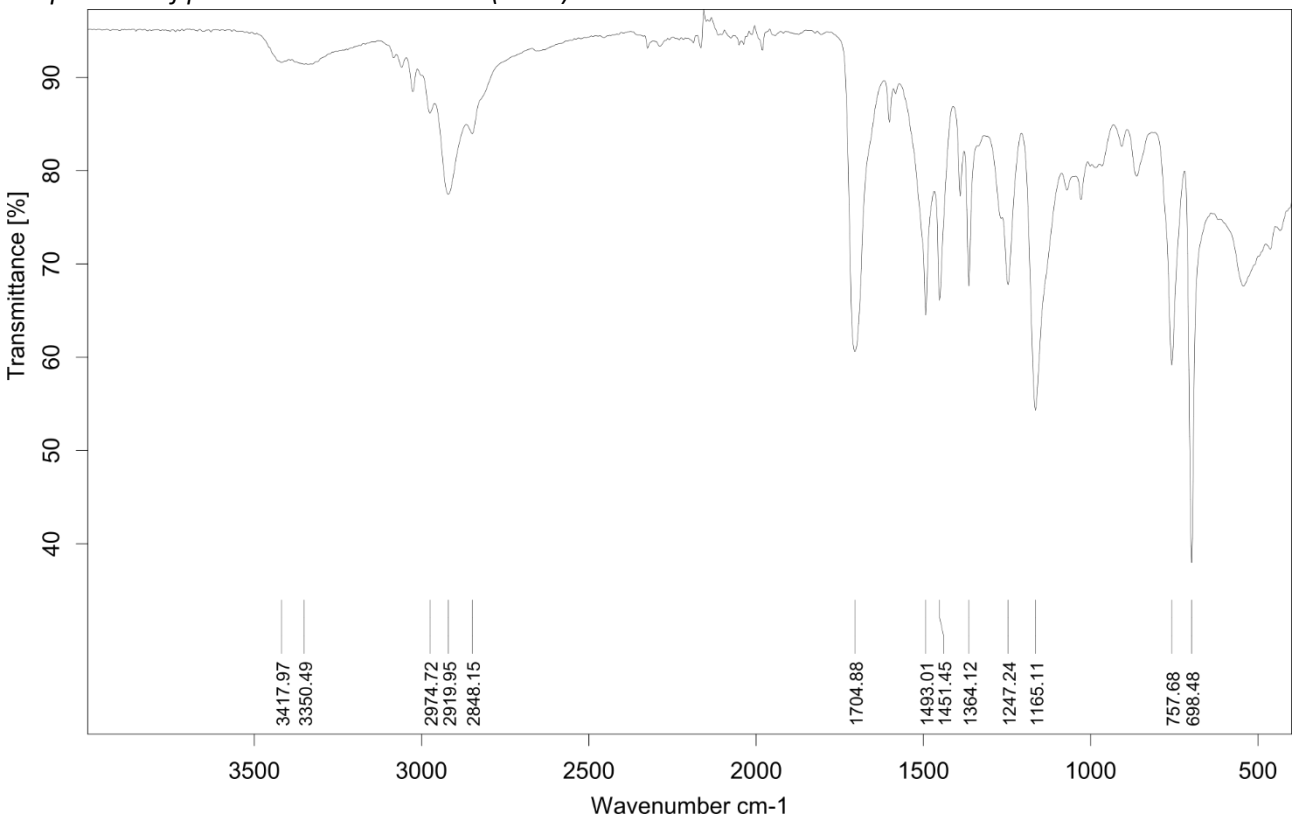

*IR-spectrum overlay of protected **Boc-Az-HSAN2** (run 1, **black**) and **H-SAN2** (substrate, **red**):*

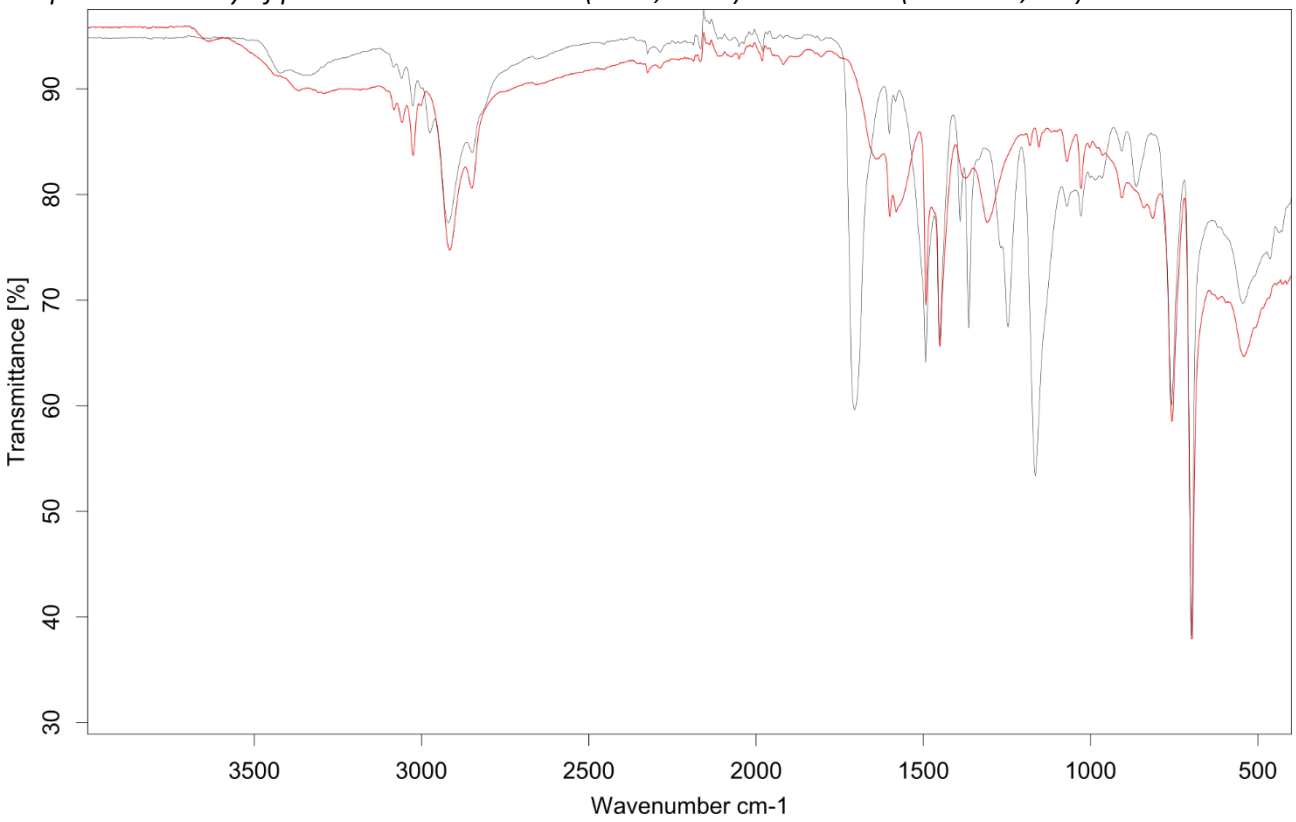

Thermogravimetric Analysis (TGA)

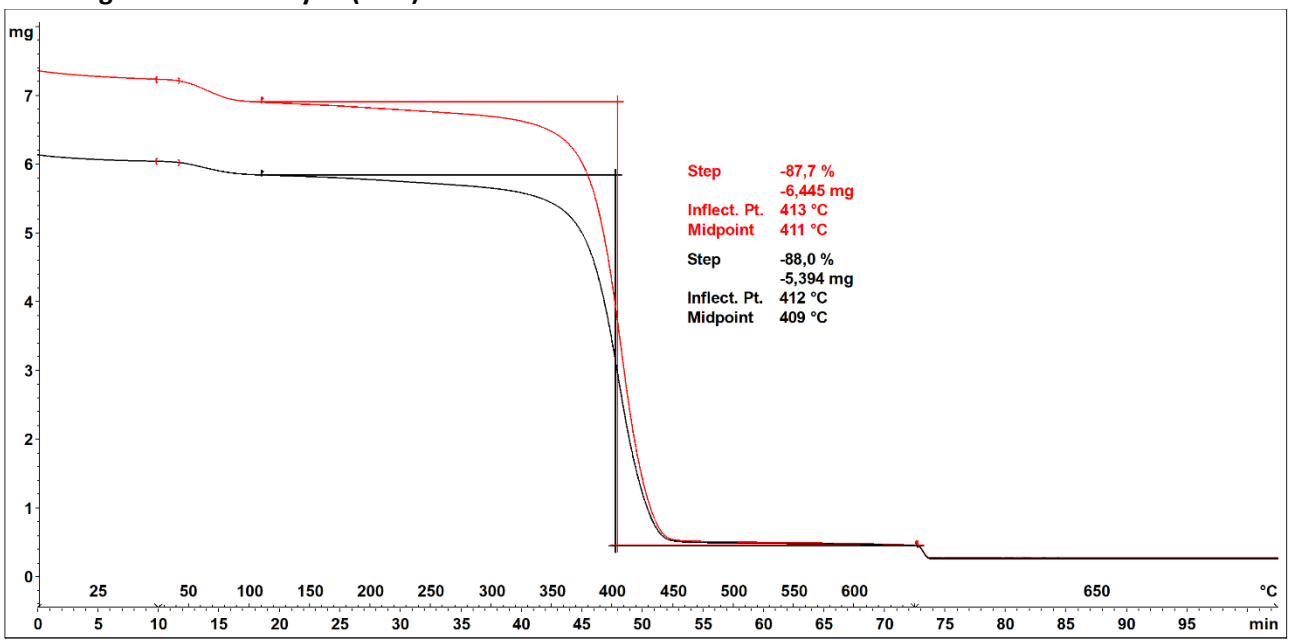

*Decomposition graph for **Az-HSAN2**. The experiment was conducted under He then air (after 650 °C). The black curve is the result from run 1, while the red curve is for run 2.*

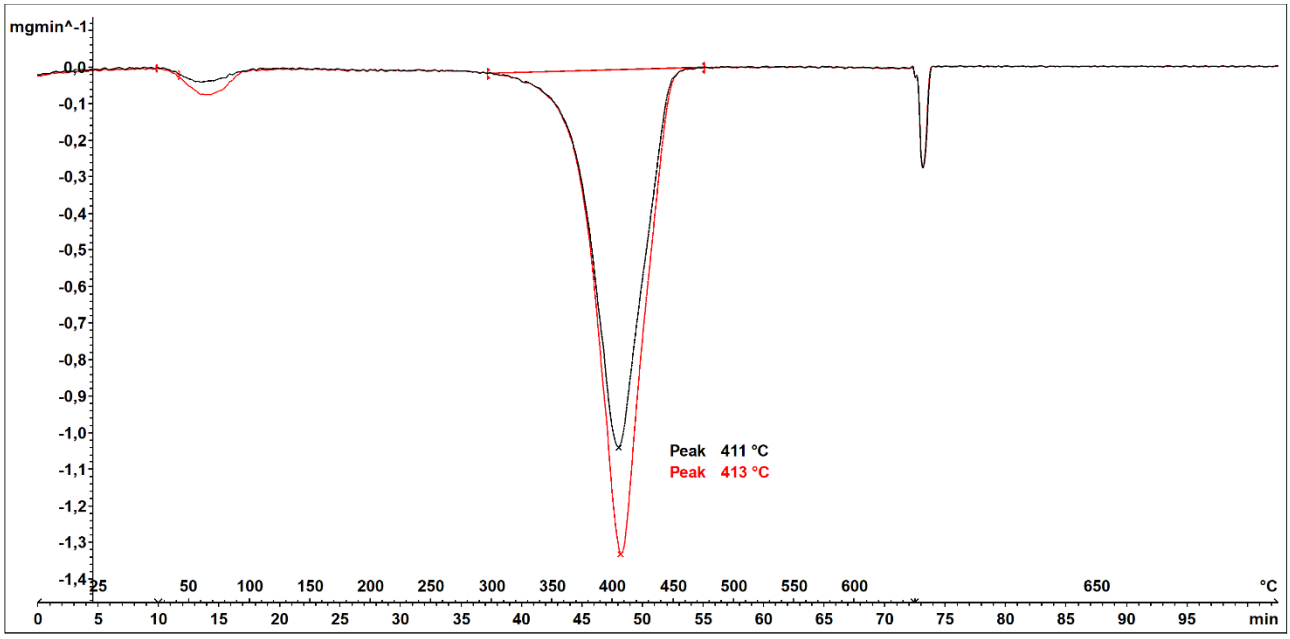

*1st derivative of decomposition graph for **Az-HSAN2**. The experiment was conducted under He then air (after 650 °C). The black curve is the result from run 1, while the red curve is for run 2.*

Decomposition temperature (T_d) = 411−413 °C.

CO_2-adsorption analysis by thermogravimetric analysis

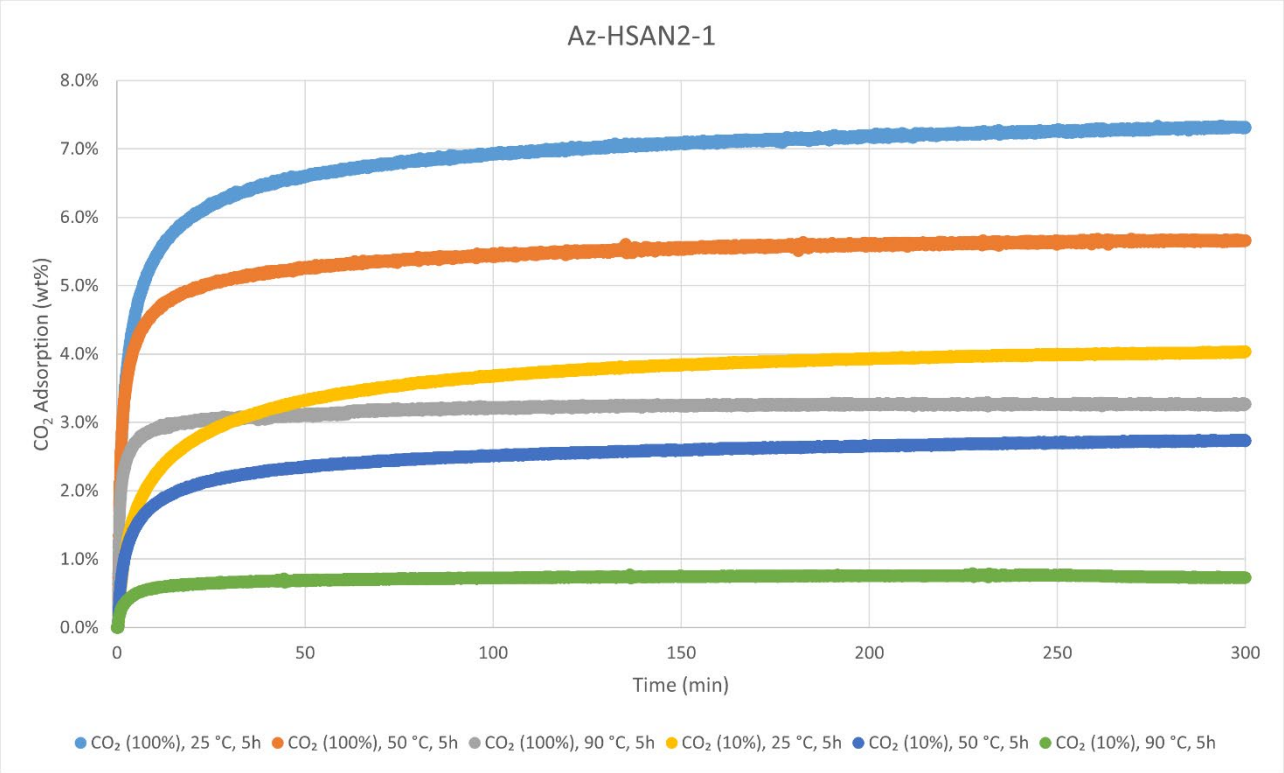

CO_2 adsorption using **TGA method 2** (measurement of product batch from run 1: Az-HSAN2-1).

Az-HSAN2-1	wt%	mmol/g
CO_2 (100%), 25 °C, 5h	7.3%	1.66
CO_2 (100%), 50 °C, 5h	5.7%	1.29
CO_2 (100%), 90 °C, 5h	3.3%	0.74
CO_2 (10%), 25 °C, 5h	4.0%	0.92
CO_2 (10%), 50 °C, 5h	2.7%	0.62
CO_2 (10%), 90 °C, 5h	0.7%	0.17

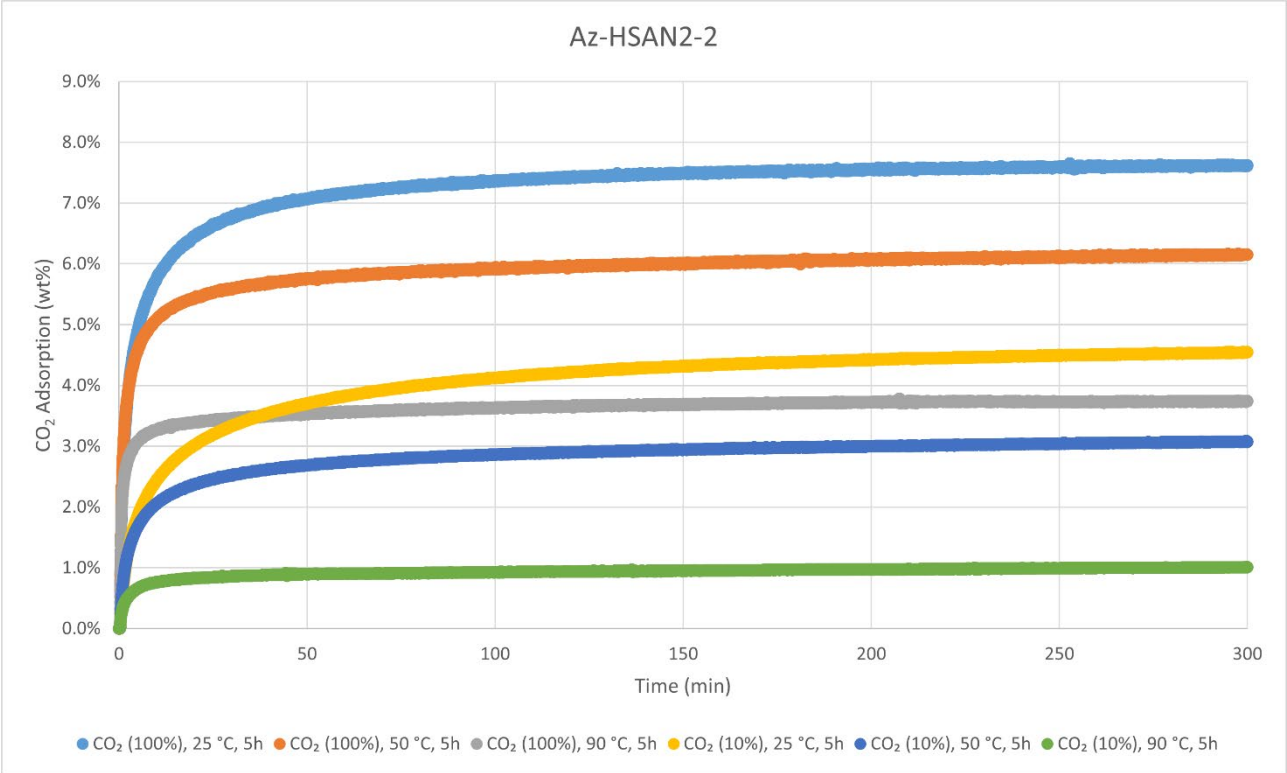

CO_2 adsorption using **TGA method 2** (measurement of product batch from run 2: Az-HSAN2-2).

Az-HSAN2-2	wt%	mmol/g
CO_2 (100%), 25 °C, 5h	7.6%	1.73
CO_2 (100%), 50 °C, 5h	6.2%	1.40
CO_2 (100%), 90 °C, 5h	3.7%	0.85
CO_2 (10%), 25 °C, 5h	4.6%	1.03
CO_2 (10%), 50 °C, 5h	3.1%	0.70
CO_2 (10%), 90 °C, 5h	1.0%	0.23

Elemental Analysis (EA)

Az-HSAN2	N [%]	C [%]	H [%]	S [%]	mmol N/g	C/N ratio	C/H ratio
run 1	8.06	75.61	8.74	Not detected	5.75	10.94	0.73
run 2	7.97	74.71	8.66		5.69	10.94	0.72

CO_2-Adsorption Analysis Data

CO_2-capacities, amine efficiencies, desorption, and working capacities for all amine polymer products. The data were obtained with **TGA method 2**, which measures CO_2 adsorbed over 5 hours at 25 °C, 50 °C, 90 °C with a CO_2-concentration of 100% or 10% in N_2. Pre-conditioning and desorption stages are conducted under helium at 130 °C.

CO_2-adsorption (100 % CO_2, 25 °C, 5 h)	CO_2-capacity wt(%)	CO_2-capacity (mmol/g)	N-efficiency (CO_2/amine)[a]
H-NBR1	7.6	1.73	0.26
H-NBR2[b]	9.0	2.03	0.39
H-ABS1	5.9	1.34	0.46
H-ABS2	6.5	1.48	0.43
H-SAN1	8.7	1.97	0.46
H-SAN2	9.1	2.08	0.49
H-TEX1	5.4	1.22	0.11
H-TEX2	3.9	0.90	0.09
H-MIX1	7.4	1.68	0.48
H-MIX2	8.0	1.81	0.14
HCN*-SBR1	7.3	1.66	0.33
HCN*-SBR2	7.4	1.68	0.44
HCN*-NBR2	12	2.80	0.43
HCN*-ABS1	5.3	1.21	0.33
Az-HNBR2	11	2.51	0.31
Az-HABS2	6.0	1.37	0.29
Az-HSAN2	7.5	1.70	0.30

Table S5. CO_2 adsorption with 100% CO_2 at 25 °C for 5 h. The values are given as averages of the results from two or more polymer product batches of the same type. [a]Was calculated from average amine contents of the polymer products as determined by elemental analysis. [b]The average H-NBR2 CO_2-adsorption capacity was calculated from the average of product batches 1−5, of which only the values for cryogenically milled H-NBR2-3 was used, since all other batches were also cryogenically milled.

CO_2-adsorption (100 % CO_2, 50 °C, 5 h)	CO_2-capacity wt(%)	CO_2-capacity (mmol/g)	N-efficiency (CO_2/amine)[a]
H-NBR1	10	2.28	0.34
H-NBR2	8.7	1.97	0.38
H-ABS1	4.7	1.06	0.36
H-ABS2	5.1	1.16	0.34
H-SAN1	6.9	1.57	0.37
H-SAN2	7.4	1.68	0.40
H-TEX1	4.2	0.96	0.09
H-TEX2	2.8	0.64	0.06
H-MIX1	6.0	1.36	0.39
H-MIX2	7.9	1.80	0.14
HCN*-SBR1	6.4	1.45	0.29
HCN*-SBR2	6.3	1.44	0.38
HCN*-NBR2	11	2.47	0.38
HCN*-ABS1	4.4	1.01	0.27
Az-HNBR2	9.5	2.16	0.26
Az-HABS2	4.7	1.08	0.23
Az-HSAN2	5.9	1.34	0.23

Table S6. CO_2 adsorption with 100% CO_2 at 50 °C for 5 h. The values are given as averages of the results from two or more polymer product batches of the same type. [a]Was calculated from average amine contents of the polymer products as determined by elemental analysis. [b]The average H-NBR2 CO_2-adsorption capacity was calculated from the average of product batches 1−5, of which only the values for cryogenically milled H-NBR2-3 was used, since all other batches were also cryogenically milled.

CO_2-adsorption (100 % CO_2, 90 °C, 5 h)	CO_2-capacity wt(%)	CO_2-capacity (mmol/g)	N-efficiency (CO_2/amine)[a]
H-NBR1	13	2.98	0.44
H-NBR2	7.3	1.65	0.31
H-ABS1	3.1	0.69	0.24
H-ABS2	3.3	0.75	0.22
H-SAN1	4.4	1.01	0.24
H-SAN2	4.8	1.10	0.26
H-TEX1	2.4	0.55	0.05
H-TEX2	1.7	0.38	0.04
H-MIX1	4.0	0.91	0.26
H-MIX2	5.0	1.14	0.09
HCN*-SBR1	4.9	1.11	0.22
HCN*-SBR2	5.2	1.17	0.31
HCN*-NBR2	9.0	2.04	0.32
HCN*-ABS1	3.1	0.69	0.19
Az-HNBR2	7.4	1.68	0.21
Az-HABS2	2.8	0.63	0.13
Az-HSAN2	3.5	0.80	0.14

Table S7. CO_2 adsorption with 100% CO_2 at 90 °C for 5 h. The values are given as averages of the results from two or more polymer product batches of the same type. [a]Was calculated from average amine contents of the

polymer products as determined by elemental analysis. [b]The average H-NBR2 CO_2-adsorption capacity was calculated from the average of product batches 1−5, of which only the values for cryogenically milled H-NBR2-3 was used, since all other batches were also cryogenically milled.

CO_2-adsorption (10 % CO_2, 25 °C, 5 h)	CO_2-capacity wt(%)	CO_2-capacity (mmol/g)	N-efficiency (CO_2/amine)[a]
H-NBR1	3.6	0.81	0.12
H-NBR2	5.2	1.18	0.23
H-ABS1	3.3	0.75	0.26
H-ABS2	3.5	0.80	0.23
H-SAN1	4.7	1.07	0.25
H-SAN2	5.1	1.16	0.28
H-TEX1	2.5	0.57	0.05
H-TEX2	1.9	0.43	0.04
H-MIX1	4.2	0.95	0.27
H-MIX2	3.9	0.89	0.07
HCN*-SBR1	5.4	1.22	0.24
HCN*-SBR2	5.5	1.24	0.32
HCN*-NBR2	8.5	1.94	0.30
HCN*-ABS1	2.9	0.65	0.18
Az-HNBR2	7.8	1.77	0.22
Az-HABS2	3.5	0.79	0.16
Az-HSAN2	4.3	0.98	0.17

Table S8. CO_2 adsorption with 10% CO_2 at 25 °C for 5 h. The values are given as averages of the results from two or more polymer product batches of the same type. [a]Was calculated from average amine contents of the polymer products as determined by elemental analysis. [b]The average H-NBR2 CO_2-adsorption capacity was calculated from the average of product batches 1−5, of which only the values for cryogenically milled H-NBR2-3 was used, since all other batches were also cryogenically milled.

CO_2-adsorption (10 % CO_2, 50 °C, 5 h)	CO_2-capacity wt(%)	CO_2-capacity (mmol/g)	N-efficiency (CO_2/amine)[a]
H-NBR1	6.1	1.38	0.20
H-NBR2	5.9	1.33	0.25
H-ABS1	2.1	0.47	0.16
H-ABS2	2.3	0.51	0.15
H-SAN1	3.2	0.73	0.17
H-SAN2	3.5	0.80	0.19
H-TEX1	1.7	0.39	0.04
H-TEX2	1.2	0.26	0.03
H-MIX1	2.7	0.62	0.18
H-MIX2	3.7	0.84	0.06
HCN*-SBR1	4.6	1.04	0.21
HCN*-SBR2	4.8	1.09	0.28
HCN*-NBR2	8.1	1.84	0.29
HCN*-ABS1	2.1	0.48	0.13
Az-HNBR2	6.8	1.55	0.19
Az-HABS2	2.2	0.50	0.11
Az-HSAN2	2.9	0.66	0.12

Table S9. CO_2 adsorption with 10% CO_2 at 50 °C for 5 h. The values are given as averages of the results from two or more polymer product batches of the same type. [a]Was calculated from average amine contents of the polymer products as determined by elemental analysis. [b]The average H-NBR2 CO_2-adsorption capacity was calculated from the average of product batches 1−5, of which only the values for cryogenically milled H-NBR2-3 was used, since all other batches were also cryogenically milled.

CO_2-adsorption (10 % CO_2, 90 °C, 5 h)	CO_2-capacity wt(%)	CO_2-capacity (mmol/g)	N-efficiency (CO_2/amine)[a]
H-NBR1	7.2	1.64	0.24
H-NBR2	3.1	0.71	0.14
H-ABS1	0.9	0.21	0.07
H-ABS2	1.1	0.24	0.07
H-SAN1	1.5	0.34	0.08
H-SAN2	1.7	0.37	0.09
H-TEX1	0.5	0.12	0.01
H-TEX2	0.4	0.09	0.01
H-MIX1	1.4	0.31	0.09
H-MIX2	1.3	0.30	0.02
HCN*-SBR1	2.2	0.51	0.10
HCN*-SBR2	2.5	0.58	0.15
HCN*-NBR2	5.2	1.19	0.18
HCN*-ABS1	1.0	0.23	0.06
Az-HNBR2	3.6	0.81	0.10
Az-HABS2	0.7	0.17	0.04
Az-HSAN2	0.9	0.20	0.03

Table S10. CO_2 adsorption with 10% CO_2 at 90 °C for 5 h. The values are given as averages of the results from two or more polymer product batches of the same type. [a]Was calculated from average amine contents of the polymer products as determined by elemental analysis. [b]The average H-NBR2 CO_2-adsorption capacity was

calculated from the average of product batches 1−5, of which only the values for cryogenically milled H-NBR2-3 was used, since all other batches were also cryogenically milled.

From evaluating the various adsorbents, we find that although some show comparable 5 h CO_2-capacities to the Lewatit benchmark, Lewatit still shows a significantly faster rate of adsorption. However, for high-temperature adsorption (90 °C), this is not the case. We see an increasing rate trend of 25 °C < 50 °C < 90 °C for all synthesised adsorbents (see Polymer Products sections, pp. S88−S237). However, the effect is most pronounced for rubber-based adsorbents, and when evaluating some of the best-performing adsorbents against the commercial Lewatit adsorbent, it is evident that for high-temperature adsorption (90 °C), our adsorbents are able to match and, in some cases, surpass the adsorption rate and capacity of Lewatit within the 5−15 minute timeframe, when using diluted CO_2 (10%) to simulate flue gas (see below).

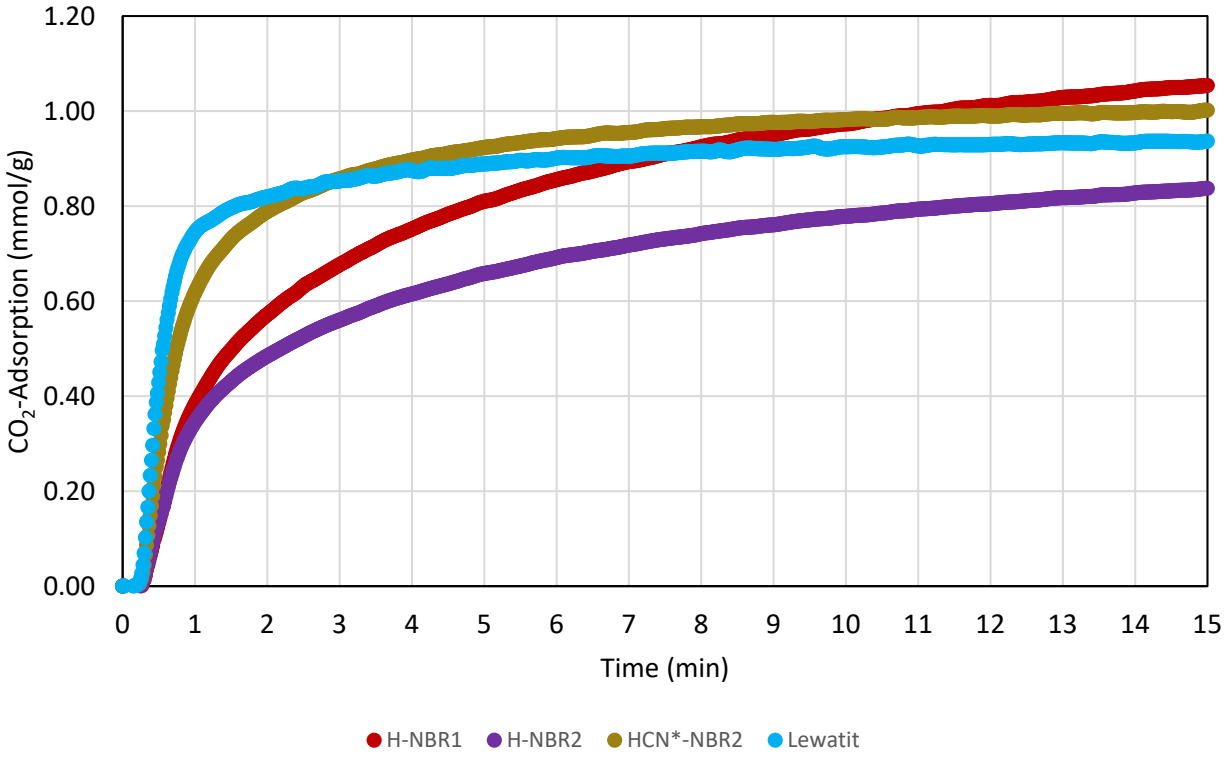

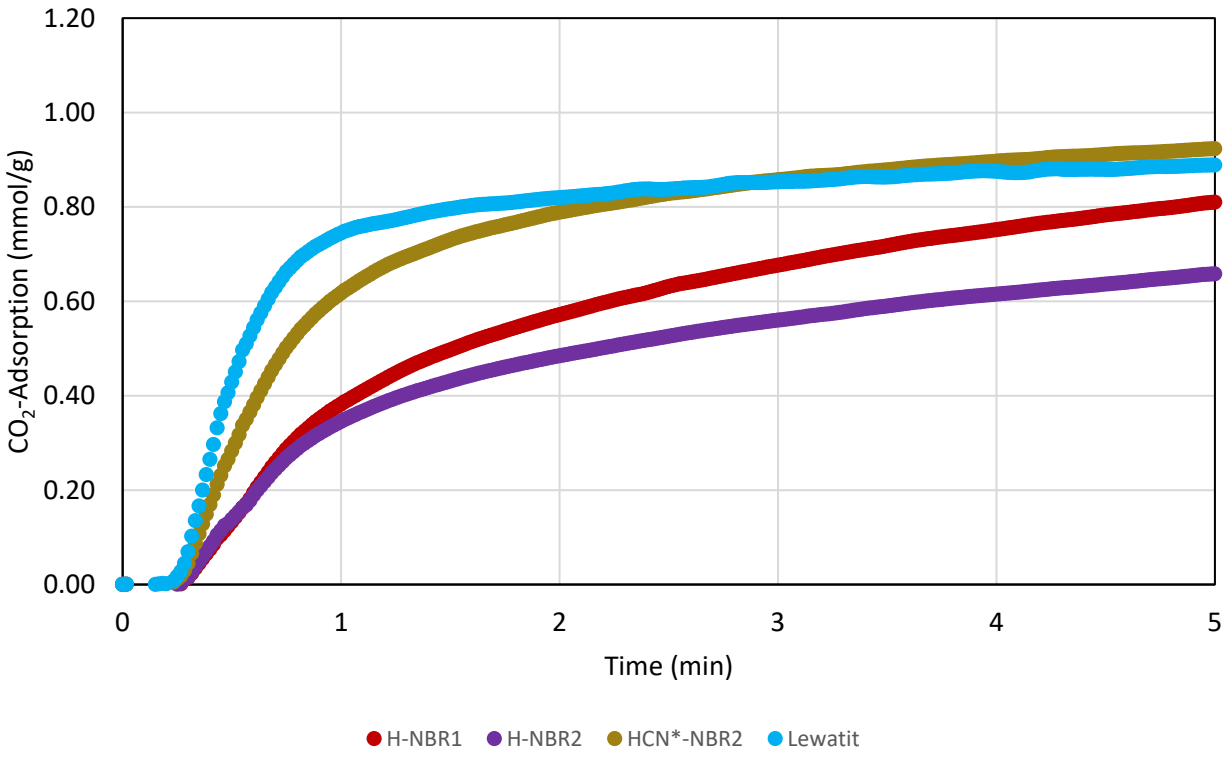

CO_2 (10% in N_2), 90 °C	CO_2-capacity (5 min, mmol/g)	CO_2-capacity (15 min, mmol/g)
H-NBR1-1	0.81	1.05
H-NBR2-4	0.66	0.84
HCN*-NBR2-4	0.92	1.00
Lewatit	0.89	0.94

Table S11. CO_2-adsorption for nitrile rubber-derived adsorbents vs. Lewatit (5 min and 15 min using 10% CO_2 at 90 °C).

40 adsorption-desorption cycles were conducted with selected best-performing adsorbents and the Lewatit benchmark to compare adsorbent effectiveness at high temperature conditions (90 °C, **TGA method 4**). Adsorption was conducted for 15 minutes under a diluted CO_2-stream (10% balanced by N_2) at 90 °C. Desorption was conducted under a pure CO_2-stream at 150 °C for 15 min. to prevent dilution of the CO_2-desorption product, as would be the case when using inert gases for desorption (He, Ar, N_2).[18] The mass difference between the mass by the end of adsorption, and the mass at the end of desorption under CO_2, was used for deriving the working capacity of each cycle. Furthermore, in between each cycle, helium purging was used to remove non-desorbed CO_2 after the hot CO_2-desorption step. The three measured adsorbents show bands between 1643−1666 cm^{-1} that could indicate urea formation, thus an explanation to the observed decrease in working capacity.[19,20]

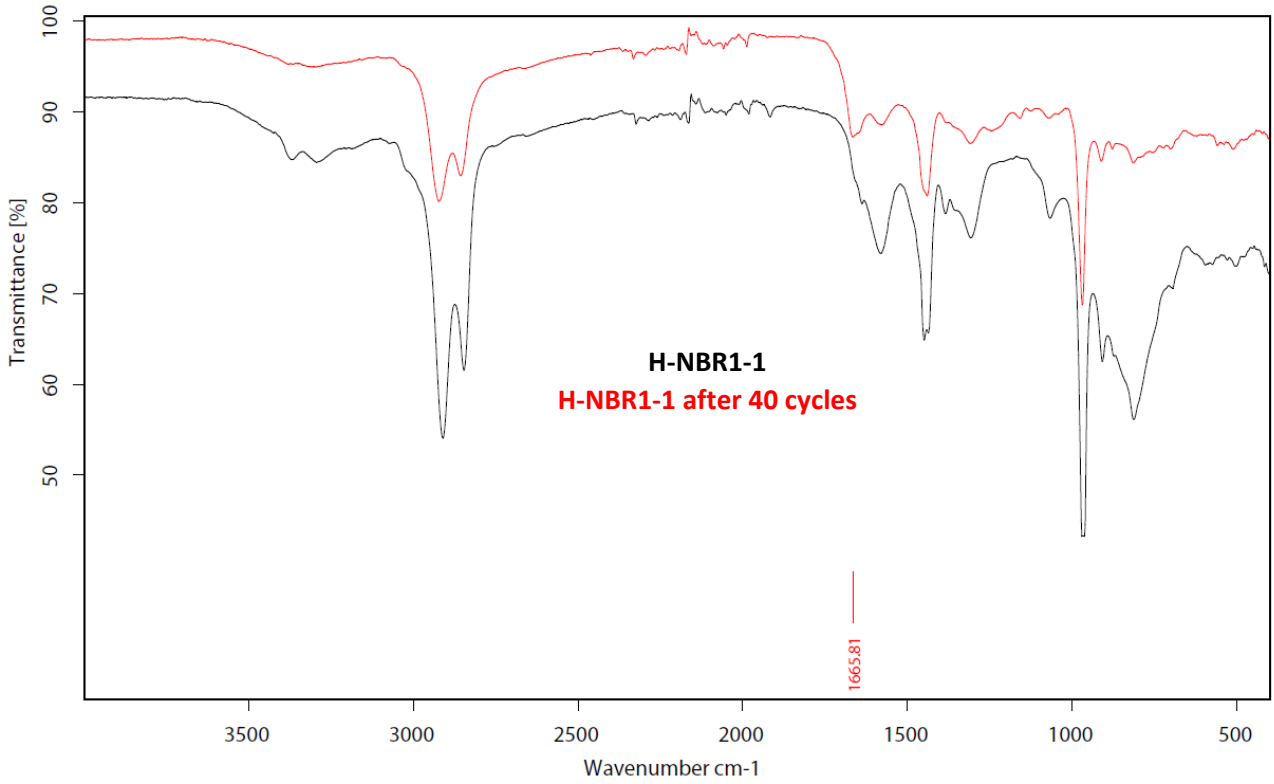
H-NBR1-1
H-NBR1-1 after 40 cycles
Transmittance [%]
100
90
80
70
60
50
1665.81
3500
3000
2500
2000
1500
1000
500
Wavenumber cm-1

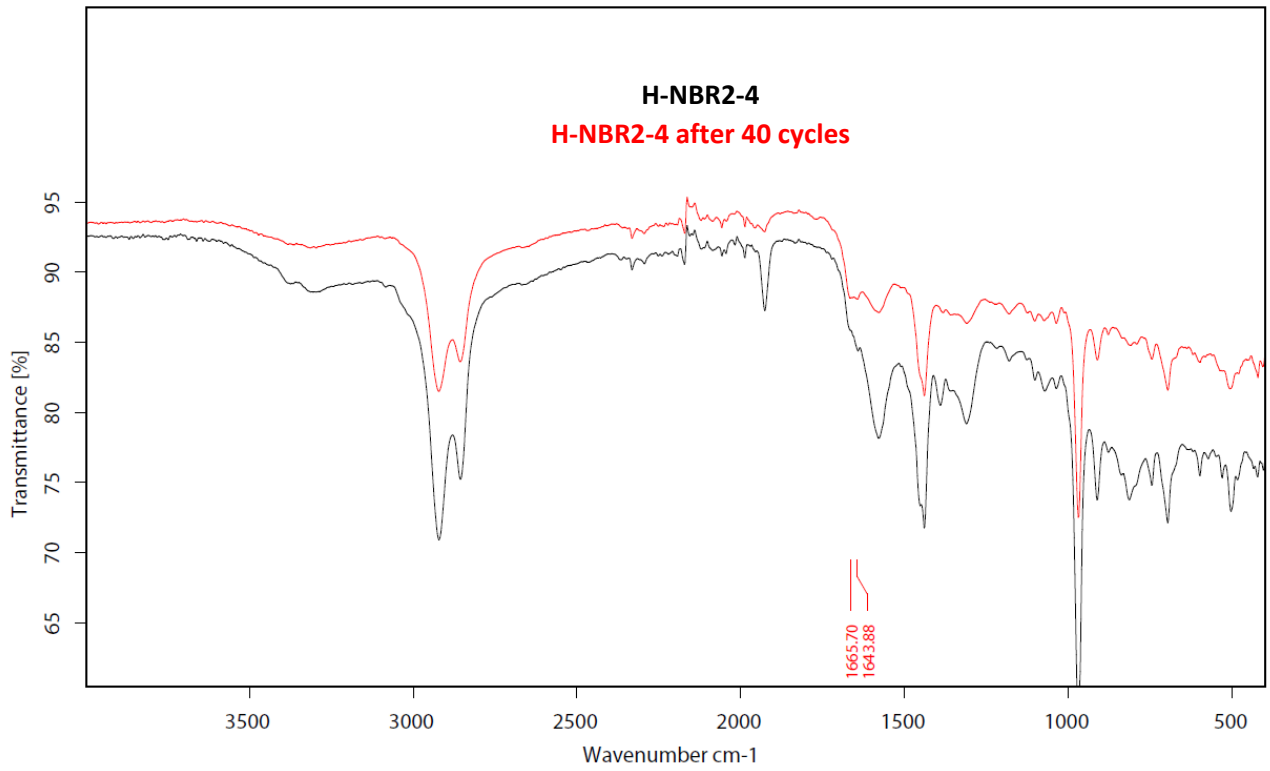
H-NBR2-4
H-NBR2-4 after 40 cycles
Transmittance [%]
95
90
85
80
75
70
65
1665.70
1643.88
3500
3000
2500
2000
1500
1000
500
Wavenumber cm-1

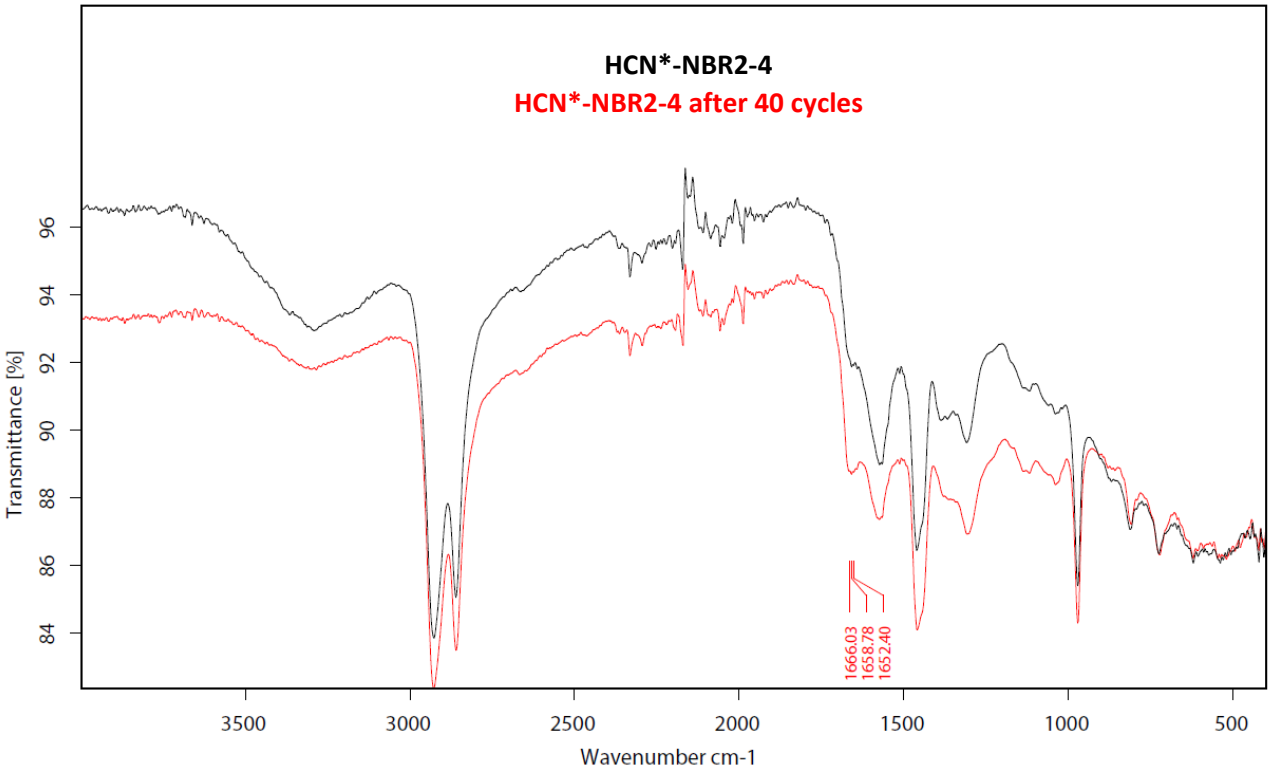
HCN*-NBR2-4
HCN*-NBR2-4 after 40 cycles
Transmittance [%]
96
94
92
90
88
86
84
1666.03
1658.78
1652.40
3500
3000
2500
2000
1500
1000
500
Wavenumber cm-1

H-NBR1-1			
Cycle number	Working capacity (wt%)	Working capacity (mmol/g)	Retention of working capacity (%)
1	4.19%	0.95	100%
2	4.02%	0.91	96%
3	3.84%	0.87	92%
4	3.74%	0.85	89%
5	3.57%	0.81	85%
6	3.39%	0.77	81%
7	3.32%	0.75	79%
8	3.19%	0.72	76%
9	3.04%	0.69	73%
10	2.94%	0.67	70%
11	2.83%	0.64	67%
12	2.72%	0.62	65%
13	2.62%	0.59	62%
14	2.52%	0.57	60%
15	2.43%	0.55	58%
16	2.36%	0.54	56%
17	2.29%	0.52	55%
18	2.21%	0.50	53%
19	2.14%	0.49	51%
20	2.07%	0.47	49%
21	2.01%	0.46	48%
22	1.95%	0.44	46%
23	1.90%	0.43	45%
24	1.88%	0.43	45%
25	1.80%	0.41	43%
26	1.77%	0.40	42%
27	1.73%	0.39	41%
28	1.66%	0.38	39%
29	1.61%	0.37	38%
30	1.59%	0.36	38%
31	1.55%	0.35	37%
32	1.47%	0.34	35%
33	1.47%	0.34	35%
34	1.44%	0.33	34%
35	1.45%	0.33	34%
36	1.36%	0.31	32%
37	1.35%	0.31	32%
38	1.33%	0.30	32%
39	1.29%	0.29	31%
40	1.25%	0.28	30%

H-NBR2-4			
Cycle number	Working capacity (wt%)	Working capacity (mmol/g)	Retention of working capacity (%)
1	2.95%	0.67	100%
2	2.88%	0.65	97%
3	2.82%	0.64	95%
4	2.81%	0.64	95%
5	2.77%	0.63	94%
6	2.67%	0.61	90%
7	2.69%	0.61	91%
8	2.64%	0.60	90%
9	2.59%	0.59	88%
10	2.54%	0.58	86%
11	2.50%	0.57	85%
12	2.43%	0.55	82%
13	2.38%	0.54	81%
14	2.32%	0.53	79%
15	2.27%	0.51	77%
16	2.21%	0.50	75%
17	2.15%	0.49	73%
18	2.09%	0.48	71%
19	2.04%	0.46	69%
20	1.98%	0.45	67%
21	1.93%	0.44	66%
22	1.89%	0.43	64%
23	1.84%	0.42	62%
24	1.78%	0.40	60%
25	1.75%	0.40	59%
26	1.70%	0.39	58%
27	1.65%	0.38	56%
28	1.61%	0.37	54%
29	1.57%	0.36	53%
30	1.53%	0.35	52%
31	1.48%	0.34	50%
32	1.41%	0.32	48%
33	1.42%	0.32	48%
34	1.37%	0.31	46%
35	1.36%	0.31	46%
36	1.28%	0.29	43%
37	1.28%	0.29	43%
38	1.24%	0.28	42%
39	1.21%	0.28	41%
40	1.18%	0.27	40%

HCN*-NBR2-4			
Cycle number	Working capacity (wt%)	Working capacity (mmol/g)	Retention of working capacity (%)
1	3.19%	0.73	100%
2	2.87%	0.65	90%
3	2.63%	0.60	82%
4	2.47%	0.56	77%
5	2.31%	0.53	72%
6	2.11%	0.48	66%
7	2.03%	0.46	63%
8	1.91%	0.43	60%
9	1.78%	0.40	56%
10	1.68%	0.38	53%
11	1.59%	0.36	50%
12	1.50%	0.34	47%
13	1.43%	0.32	45%
14	1.31%	0.30	41%
15	1.26%	0.29	39%
16	1.20%	0.27	37%
17	1.16%	0.26	36%
18	1.11%	0.25	35%
19	1.06%	0.24	33%
20	1.00%	0.23	31%
21	1.01%	0.23	32%
22	0.97%	0.22	30%
23	0.92%	0.21	29%
24	0.88%	0.20	28%
25	0.86%	0.20	27%
26	0.86%	0.19	27%
27	0.82%	0.19	26%
28	0.81%	0.18	25%
29	0.79%	0.18	25%
30	0.78%	0.18	24%
31	0.75%	0.17	24%
32	0.70%	0.16	22%
33	0.74%	0.17	23%
34	0.71%	0.16	22%
35	0.72%	0.16	23%
36	0.67%	0.15	21%
37	0.68%	0.16	21%
38	0.67%	0.15	21%
39	0.65%	0.15	20%
40	0.65%	0.15	20%

Lewatit			
Cycle number	Working capacity (wt%)	Working capacity (mmol/g)	Retention of working capacity (%)
1	2.54%	0.58	100%
2	2.48%	0.56	98%
3	2.44%	0.55	96%
4	2.44%	0.55	96%
5	2.42%	0.55	95%
6	2.33%	0.53	92%
7	2.40%	0.54	94%
8	2.39%	0.54	94%
9	2.36%	0.54	93%
10	2.34%	0.53	92%
11	2.34%	0.53	92%
12	2.32%	0.53	91%
13	2.31%	0.52	91%
14	2.30%	0.52	90%
15	2.28%	0.52	90%
16	2.27%	0.52	90%
17	2.25%	0.51	89%
18	2.26%	0.51	89%
19	2.25%	0.51	89%
20	2.24%	0.51	88%
21	2.22%	0.50	87%
22	2.22%	0.50	88%
23	2.19%	0.50	86%
24	2.19%	0.50	86%
25	2.20%	0.50	86%
26	2.18%	0.50	86%
27	2.16%	0.49	85%
28	2.16%	0.49	85%
29	2.16%	0.49	85%
30	2.11%	0.48	83%
31	2.12%	0.48	83%
32	2.05%	0.47	81%
33	2.13%	0.48	84%
34	2.09%	0.48	82%
35	2.09%	0.48	82%
36	2.07%	0.47	81%
37	2.09%	0.48	82%
38	2.05%	0.47	81%
39	2.05%	0.47	81%
40	2.05%	0.47	81%

Further Characterisation of H-NBR2, H-ABS2, and H-SAN2

Three representative product samples, namely **H-NBR2**, **H-ABS2**, and **H-SAN2** (one of each polymer type besides acrylic textiles and SBR), were evaluated with respect to parameters such as rate of adsorption and adsorbent stability, which was analysed by observing changes in CO_2-capacity after treatments with various flue gas components or certain stress tests. To signify whether the measured sample is carried out with product from run 1, 2, 3, and so on, the final number in their abbreviation will indicate this (e.g. **H-NBR2-3** is product sample from the third hydrogenation run). **Note:** Concerning **H-NBR2-3**, the material used for this section was cryogenically milled before analysis.

Rate of adsorption: Cryogenic milling of materials, as was carried out for all adsorbents in the prior section, leads to a wide particle size distribution as can be seen for the individual samples with a microscope. Particle size sieving, collecting particles of -140 +500 mesh, was carried out for selected adsorbents to evaluate the effect. We compared the rate of adsorption over 5 hours at 25 °C with sieved and non-sieved samples using 100% CO_2. The results are compiled in the following TGA-derived plots.

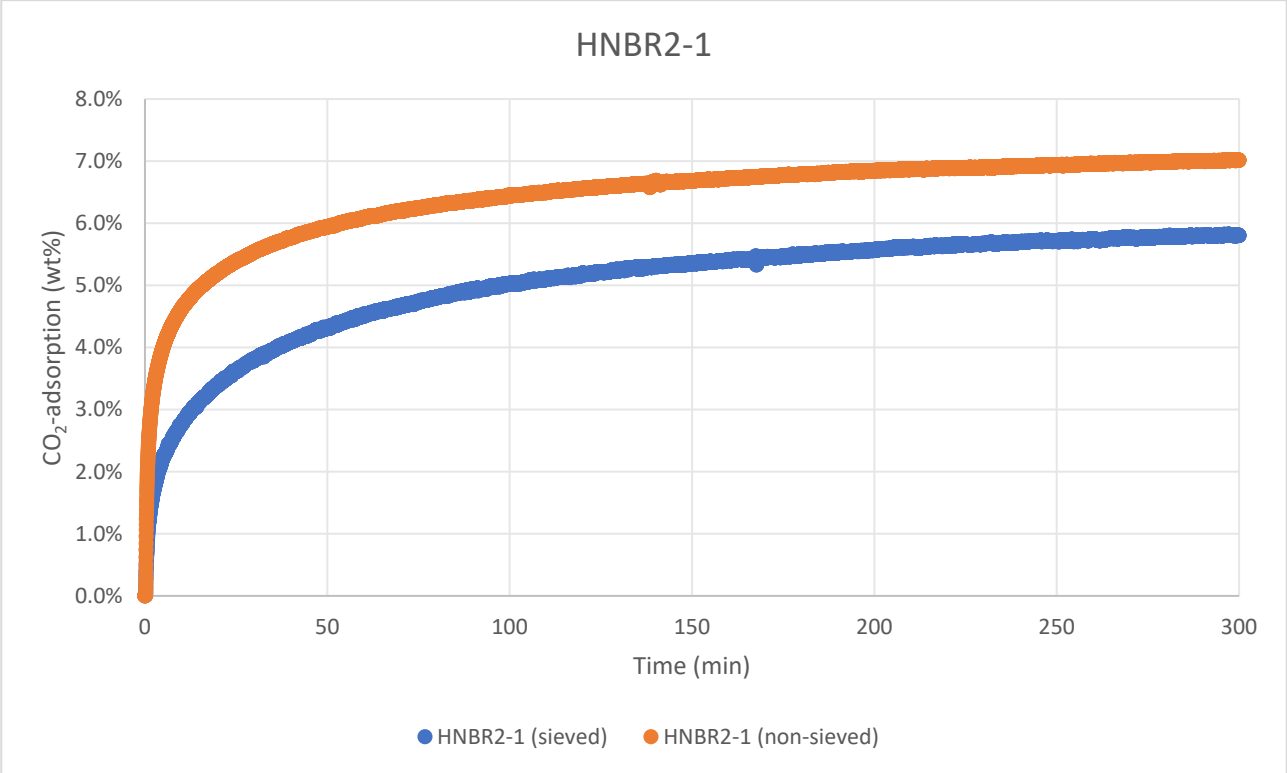

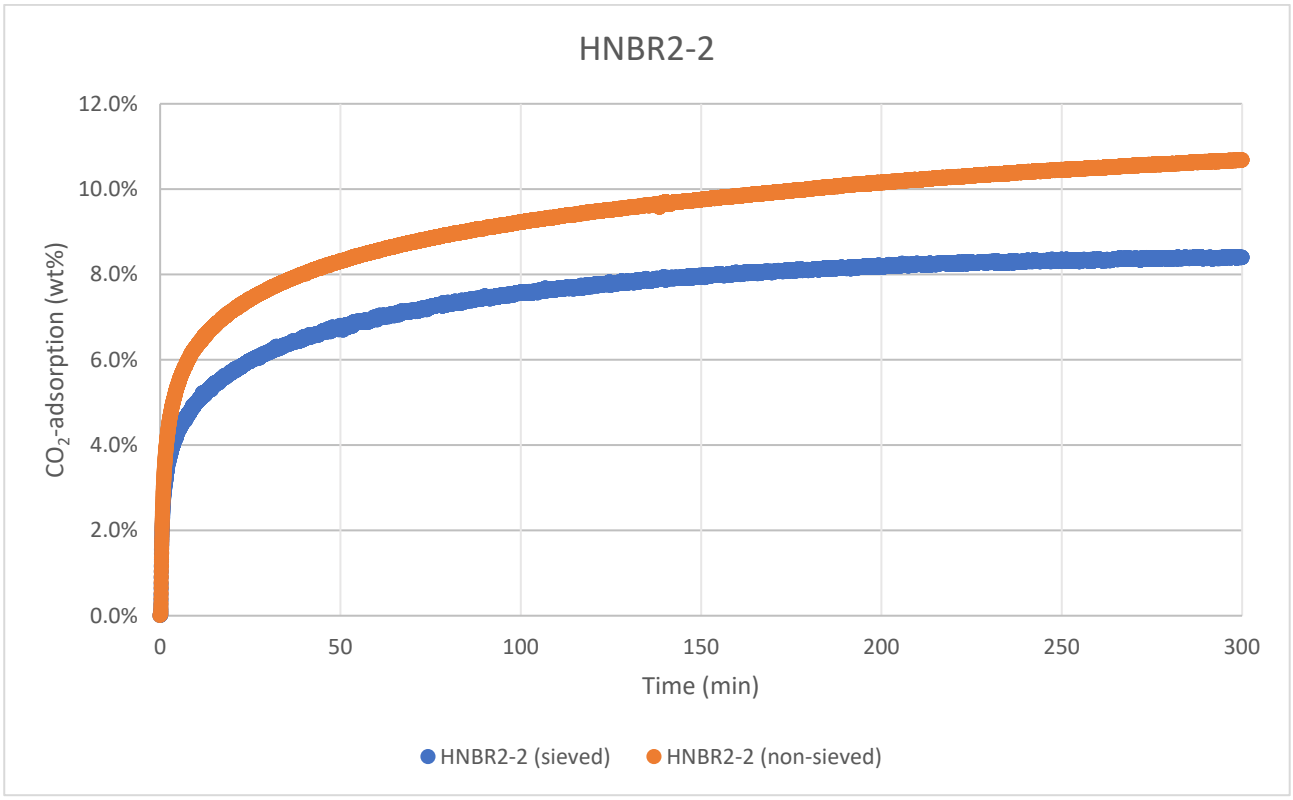
HNBR2-2
12.0%
10.0%
8.0%
6.0%
4.0%
2.0%
0.0%
CO2-adsorption (wt%)
0
50
100
150
200
250
300
Time (min)
HNBR2-2 (sieved)
HNBR2-2 (non-sieved)

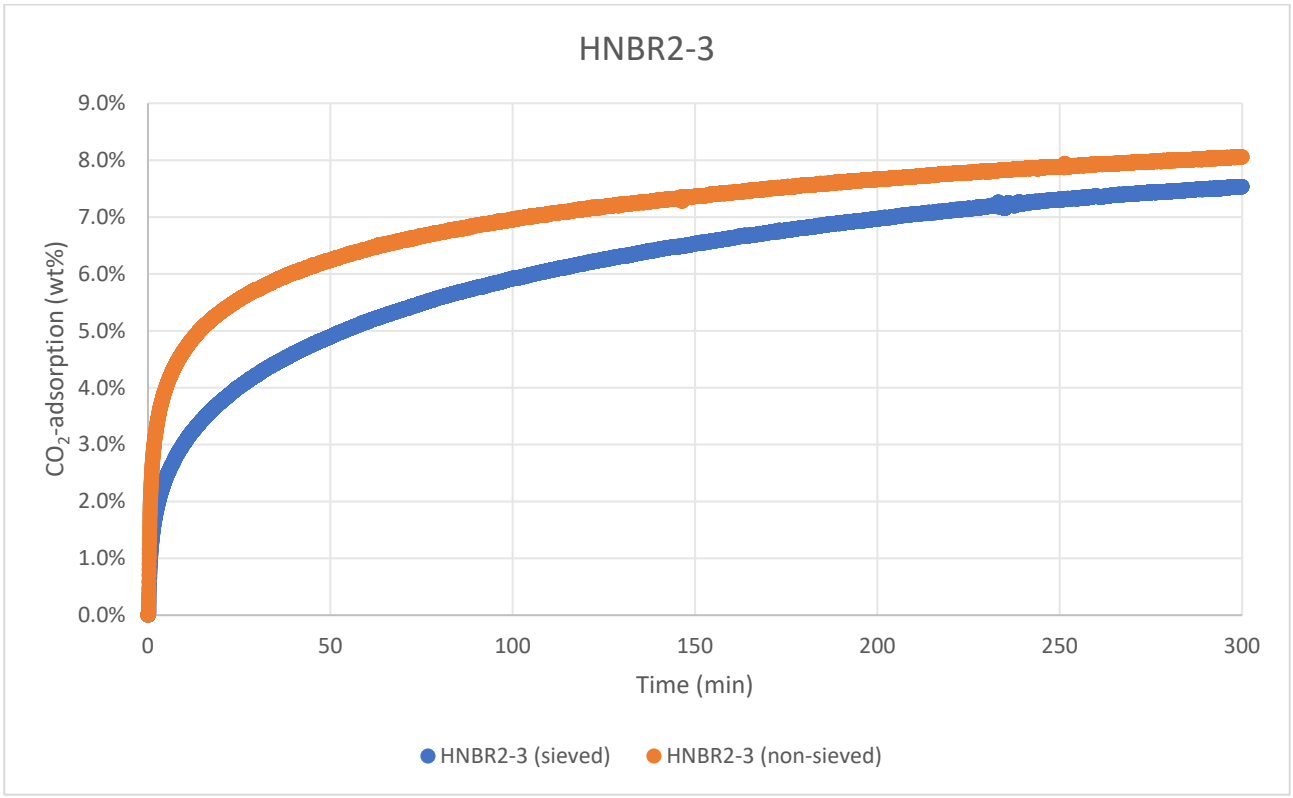
HNBR2-3
9.0%
8.0%
7.0%
6.0%
5.0%
4.0%
3.0%
2.0%
1.0%
0.0%
CO2-adsorption (wt%)
0
50
100
150
200
250
300
Time (min)
HNBR2-3 (sieved)
HNBR2-3 (non-sieved)

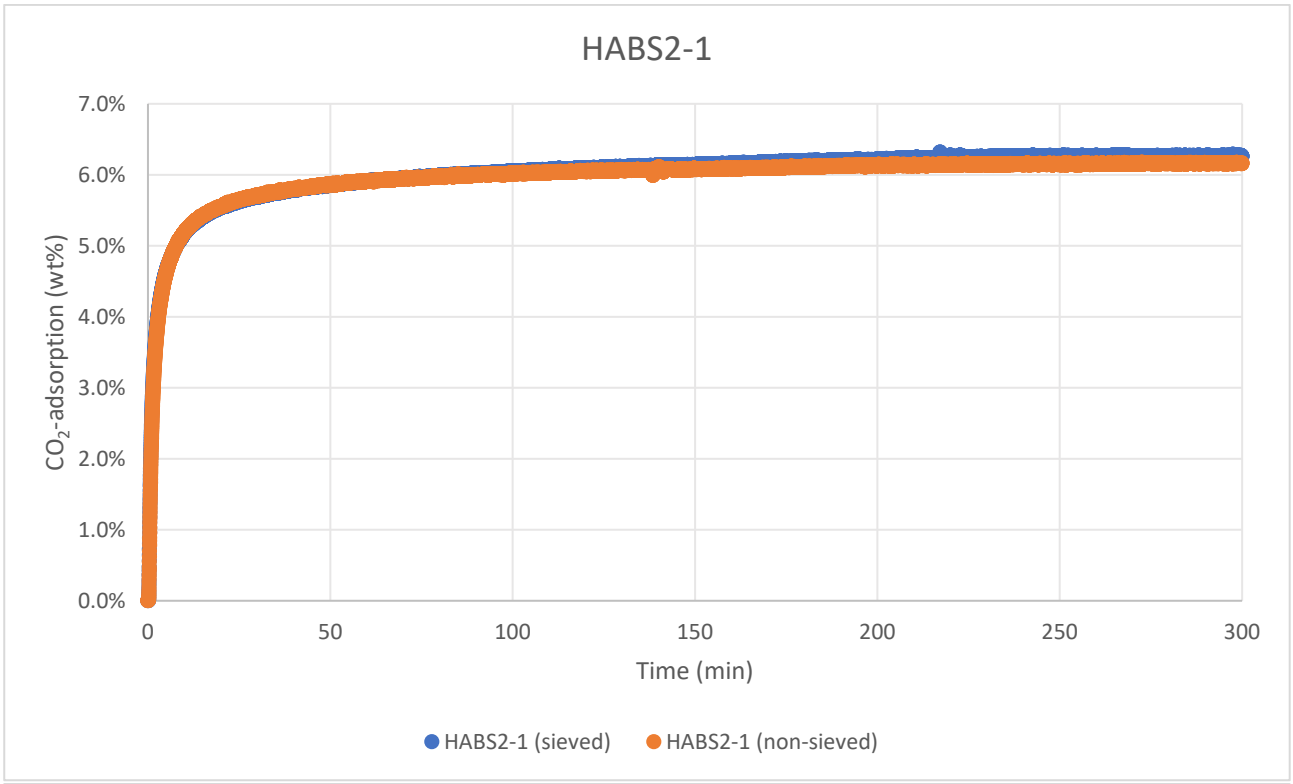
HABS2-1
7.0%
6.0%
5.0%
4.0%
3.0%
2.0%
1.0%
0.0%
CO2-adsorption (wt%)
0
50
100
150
200
250
300
Time (min)
HABS2-1 (sieved)
HABS2-1 (non-sieved)

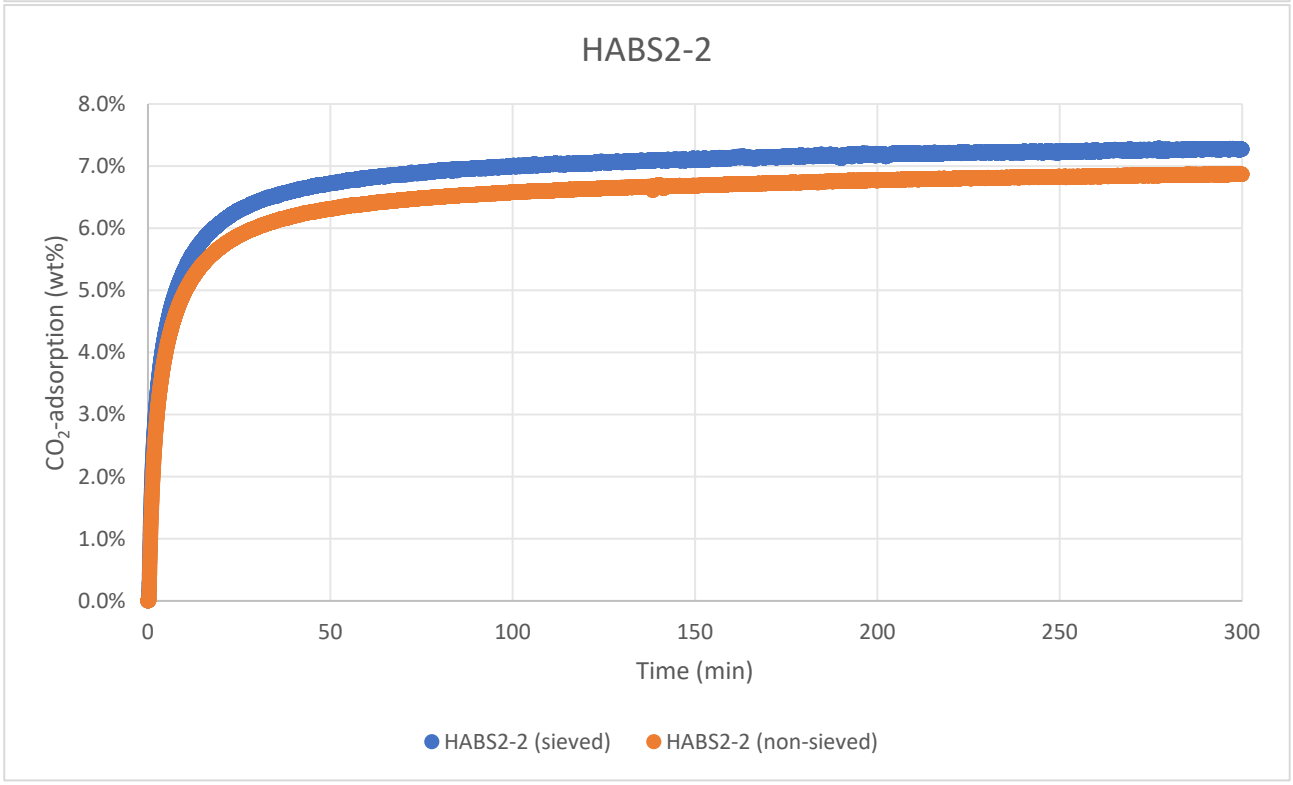
HABS2-2
8.0%
7.0%
6.0%
5.0%
4.0%
3.0%
2.0%
1.0%
0.0%
CO2-adsorption (wt%)
0
50
100
150
200
250
300
Time (min)
HABS2-2 (sieved)
HABS2-2 (non-sieved)

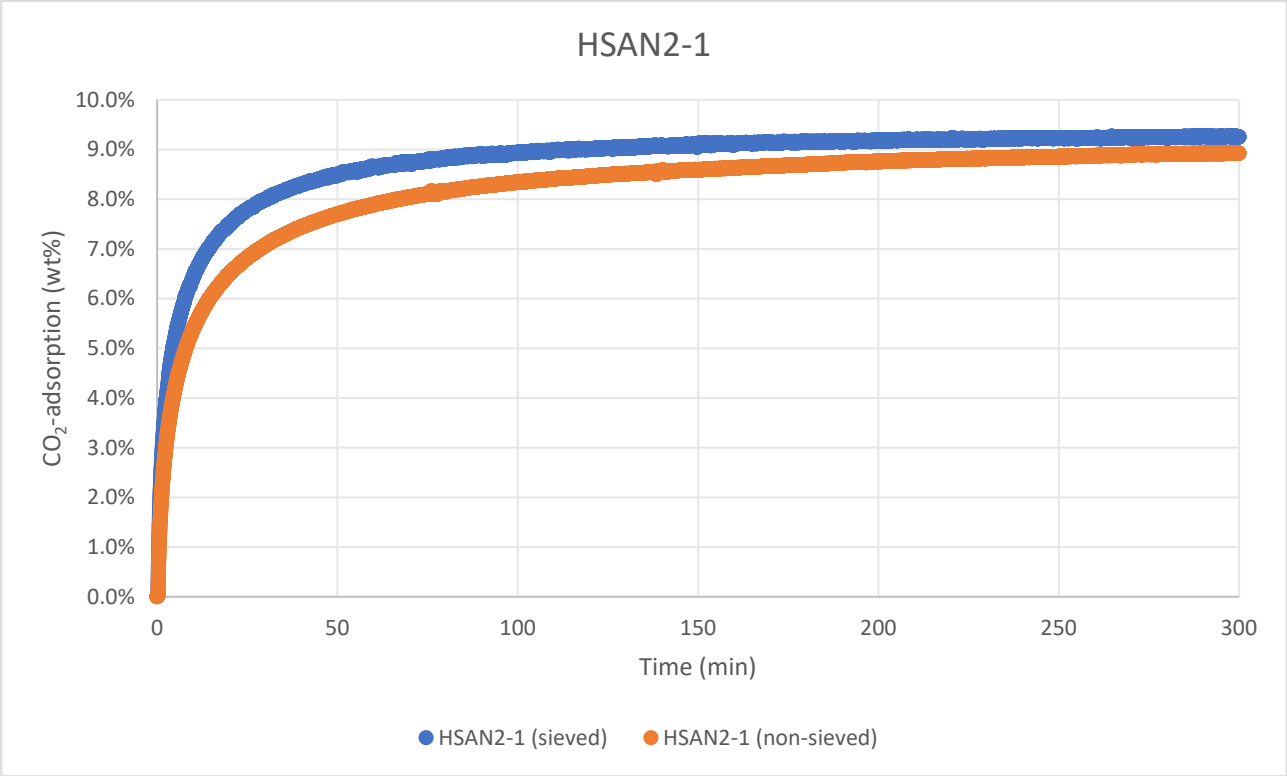

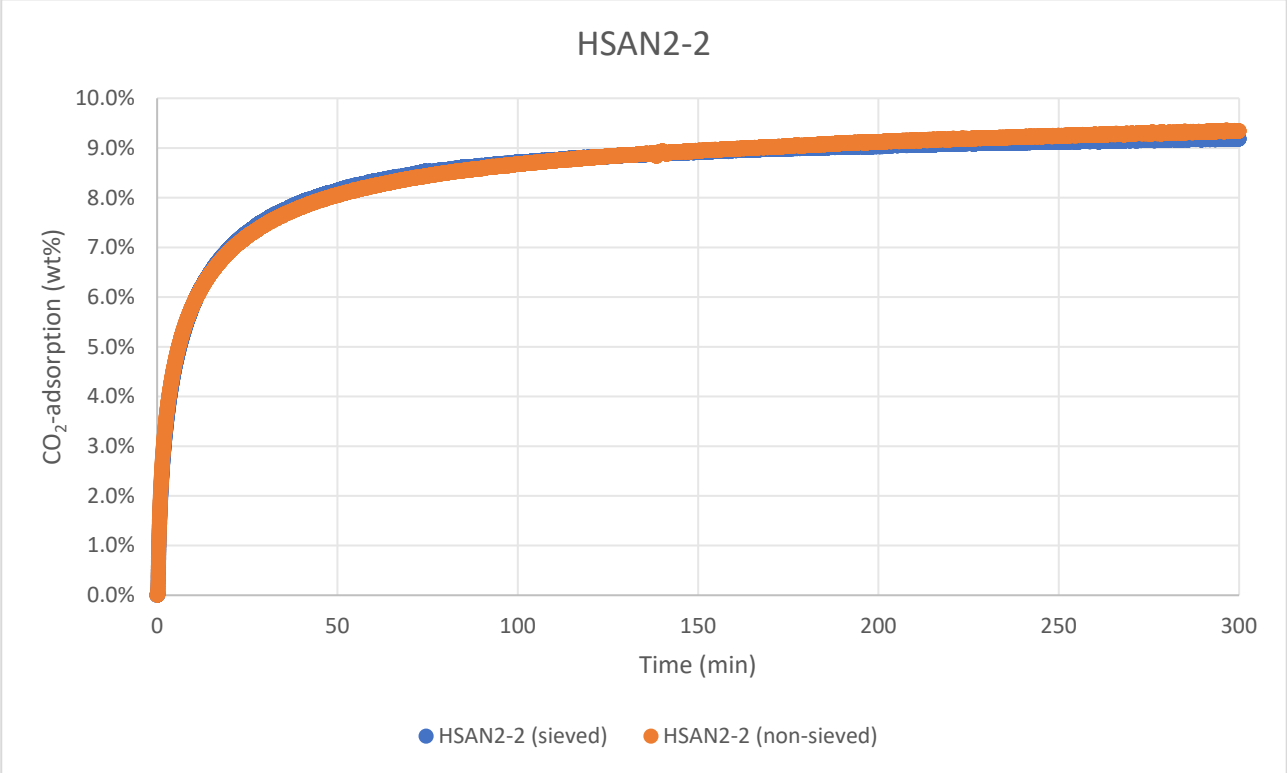

From the results shown above, we found that isolating -140 +500 mesh particles for CO_2-adsorption was slightly or not beneficial to the rate for adsorbents derived from hard plastics, namely **H-ABS2** and **H-SAN2**. This can be explained by the corresponding higher surface area of the smaller particles, thus a better adsorption. On the other hand, the hydrogenated nitrile rubber glove (**H-NBR2**) showed a worse adsorption rate after sieving. This counterintuitive finding that smaller particles, with a higher surface area, results in a

slower rate of adsorption, and lower CO_2-capacity, for **H-NBR2** samples, could be explained by a faster particle agglomeration due to a higher surface area. We found that both **H-NBR2**, **H-ABS2**, and **H-SAN2**, underwent particle agglomeration (see **Figure S12**, p. S256), but these sieved vs. non-sieved rate experiments could point towards **H-NBR2** undergoing a faster agglomeration, thereby decreasing rate of adsorption with sieved particles.

CO_2-capacity after hot helium stress test: TGA method 5 was used to measure the weight of adsorbed CO_2 before and after a 10 h flow of helium at 150 °C.

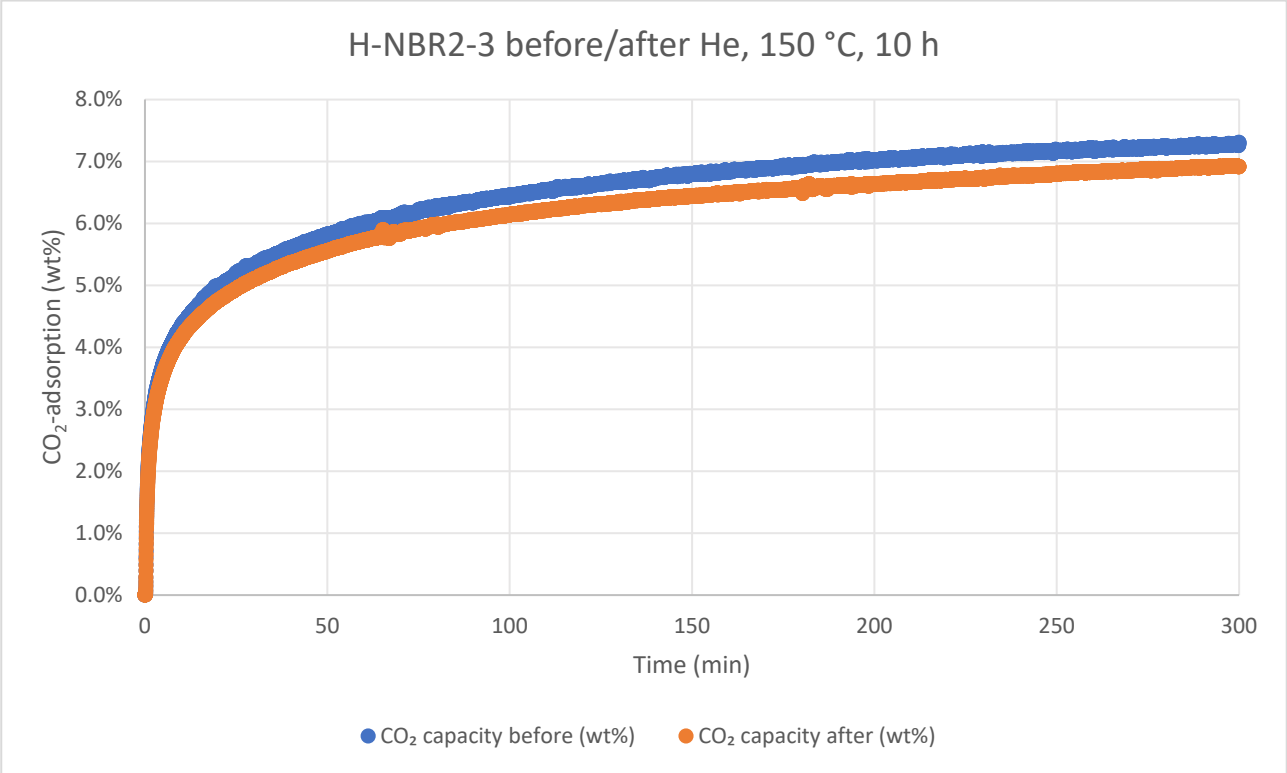

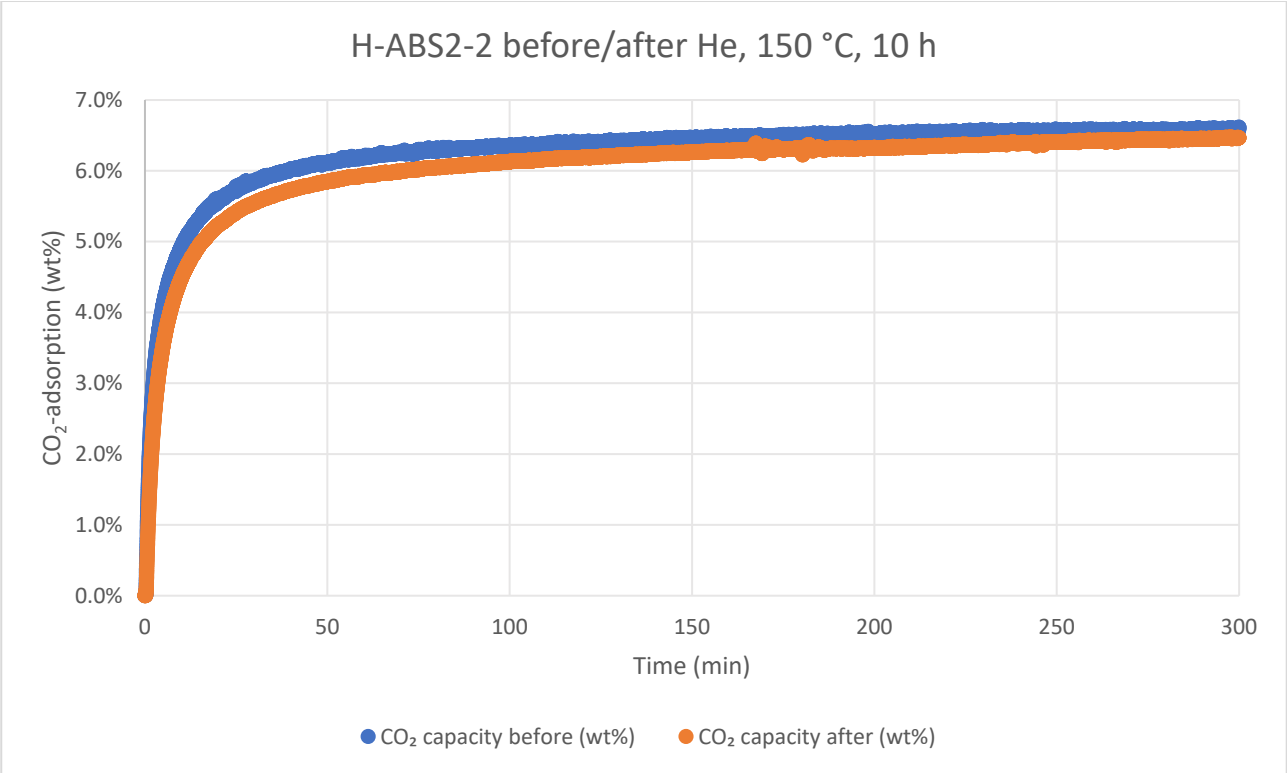

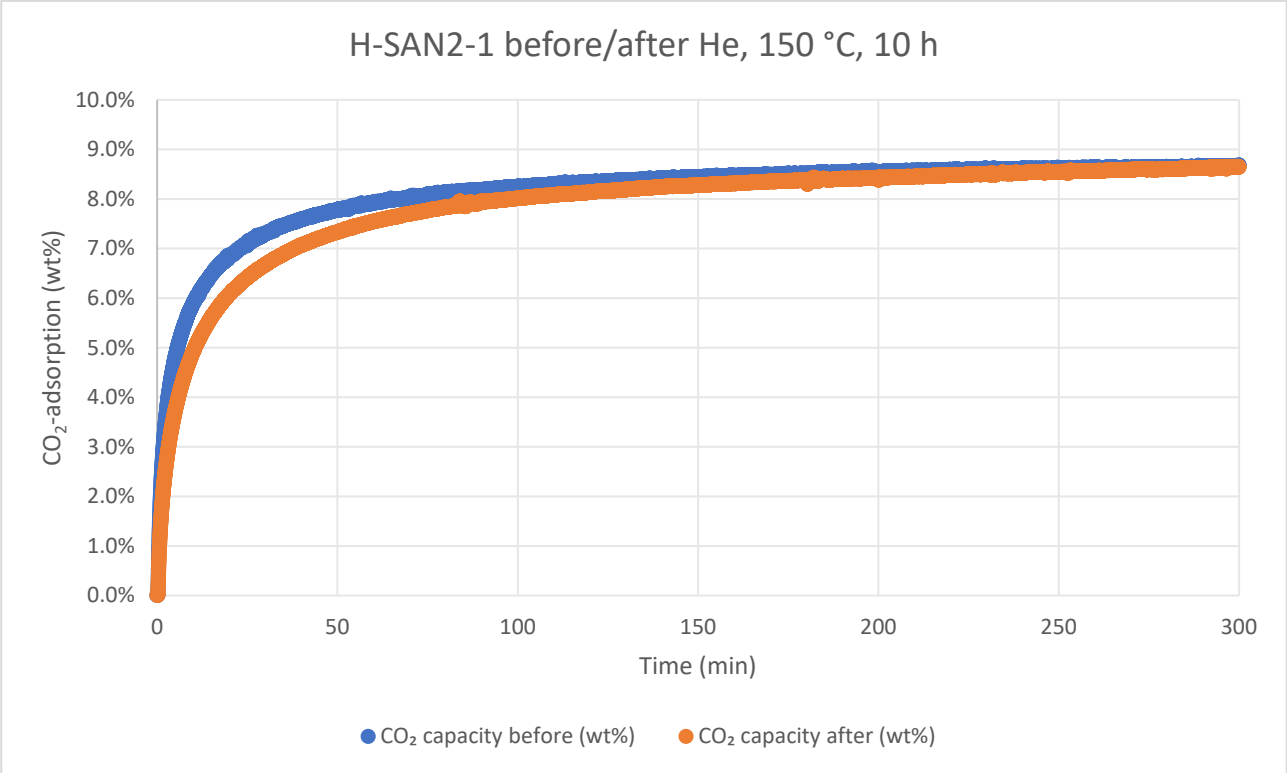

The test showed that there is a small reduction in CO_2-capacity for all three analysed adsorbents after the treatment (**Table S12**). It was found that the adsorbent powders had agglomerated into solid blocks during the experiment (**Figure S12**), which was also the case for other TGA-experiments, where heating was applied. The loss in CO_2-capacity is likely caused by a decrease in surface area due to particle agglomeration. FT-IR spectroscopic analysis showed no visible changes after the treatment of each of the three adsorbents.

He, 150 °C, 10 h Stress test	**CO_2-capacity before** (wt%)	**CO_2-capacity after** (wt%)	**Capacity retained** (%)
H-NBR2-3	7.3	6.9	95%
H-ABS2-2	6.6	6.5	98%
H-SAN2-1	8.7	8.6	100%

Table S12. CO_2-adsorption capacities at 25 °C, 5 h, before and after 10 hours of heating at 150 °C in helium. In comparison, the capacity retention of Lewatit for the same treatment was found to be 100% (see Lewatit benchmark section, p. S297).

Figure S12. From left to right: **H-NBR2-3**, **H-ABS2-2**, and **H-SAN2-1** after helium for 10 h at 150 °C. Note the agglomerated samples, such as the **H-NBR2-3** sample, which was originally a powder.

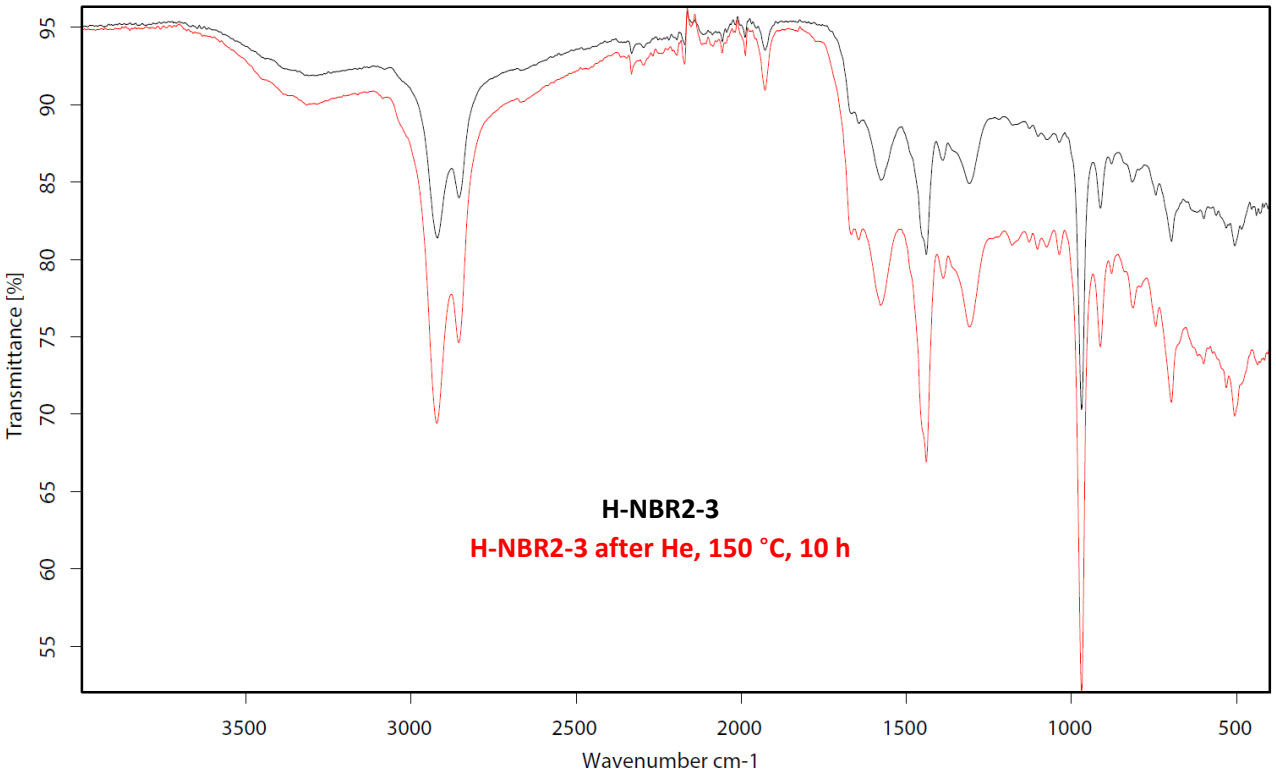

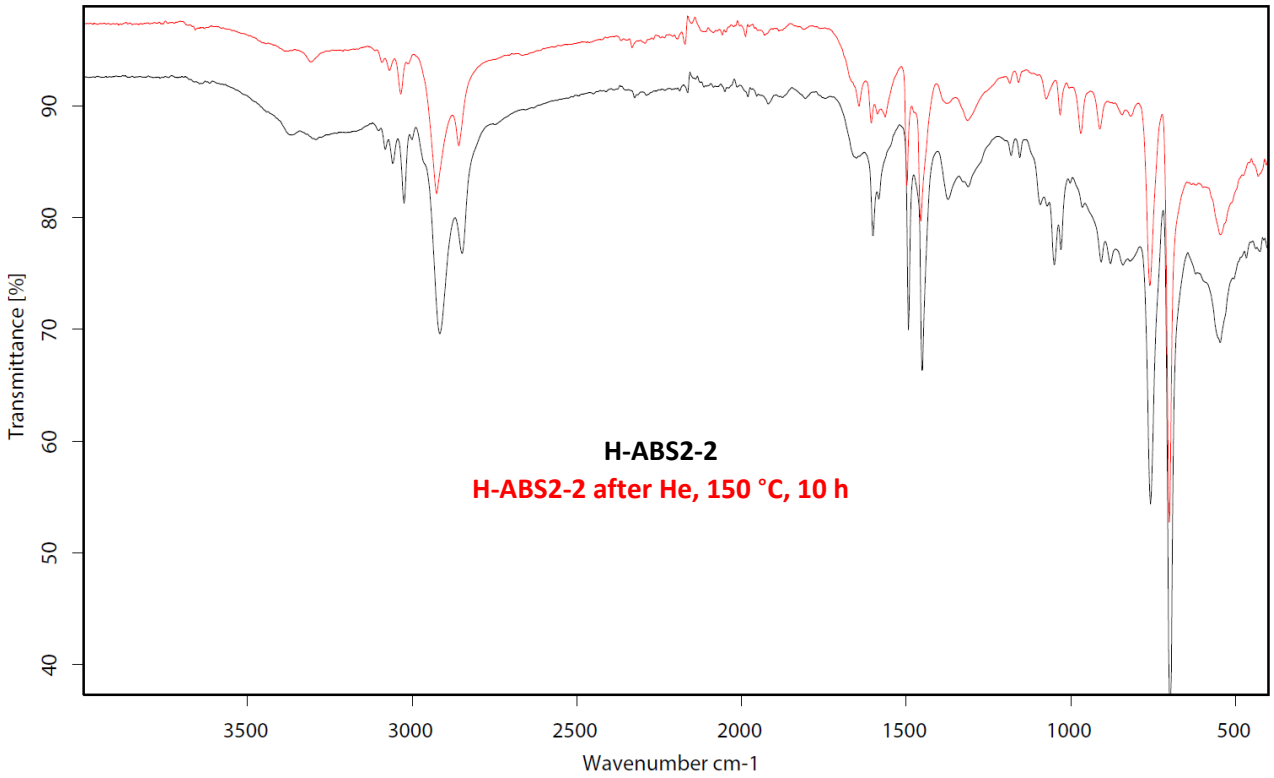
Transmittance [%]
90
80
70
60
50
40
H-ABS2-2
H-ABS2-2 after He, 150 °C, 10 h
3500
3000
2500
2000
1500
1000
500
Wavenumber cm-1

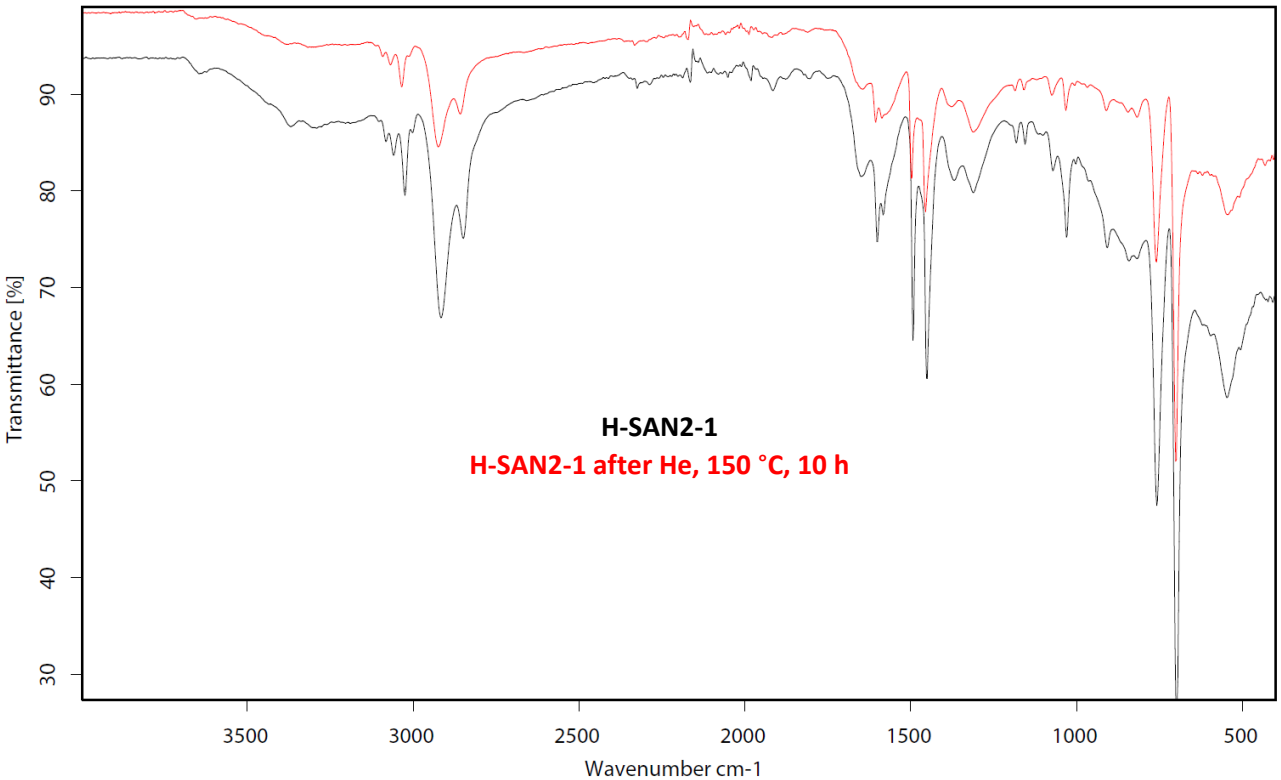
Transmittance [%]
90
80
70
60
50
40
30
H-SAN2-1
H-SAN2-1 after He, 150 °C, 10 h
3500
3000
2500
2000
1500
1000
500
Wavenumber cm-1

CO_2-capacity after oxidative stress test: TGA method 6 was used to measure the weight of adsorbed CO_2 before and after a 10 h flow of air at 150 °C.

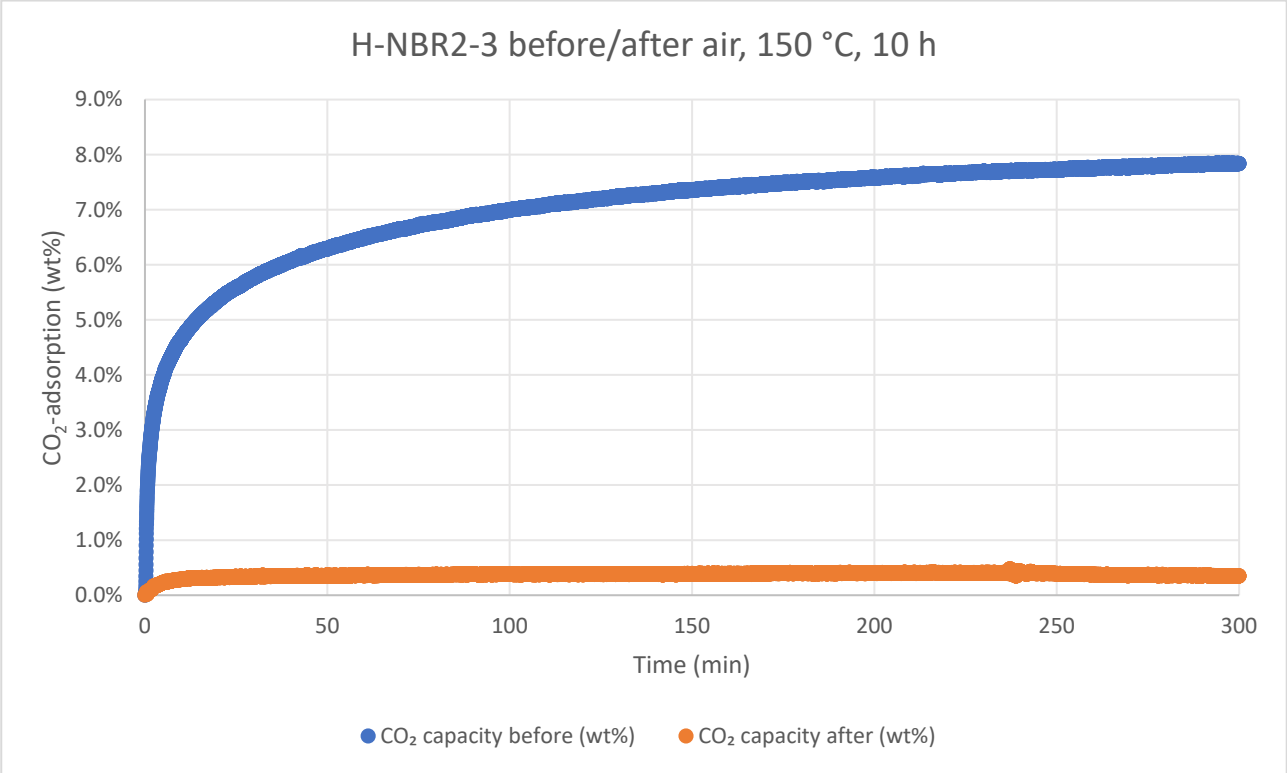

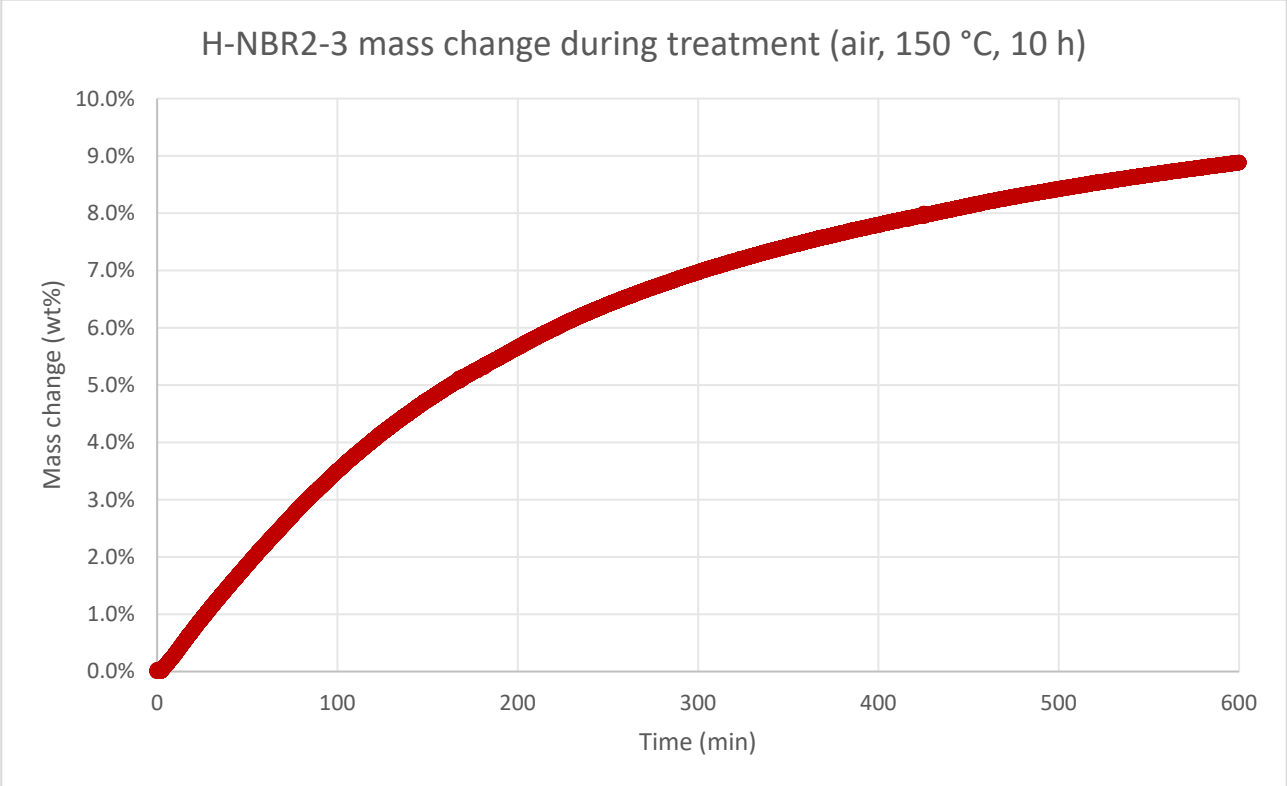

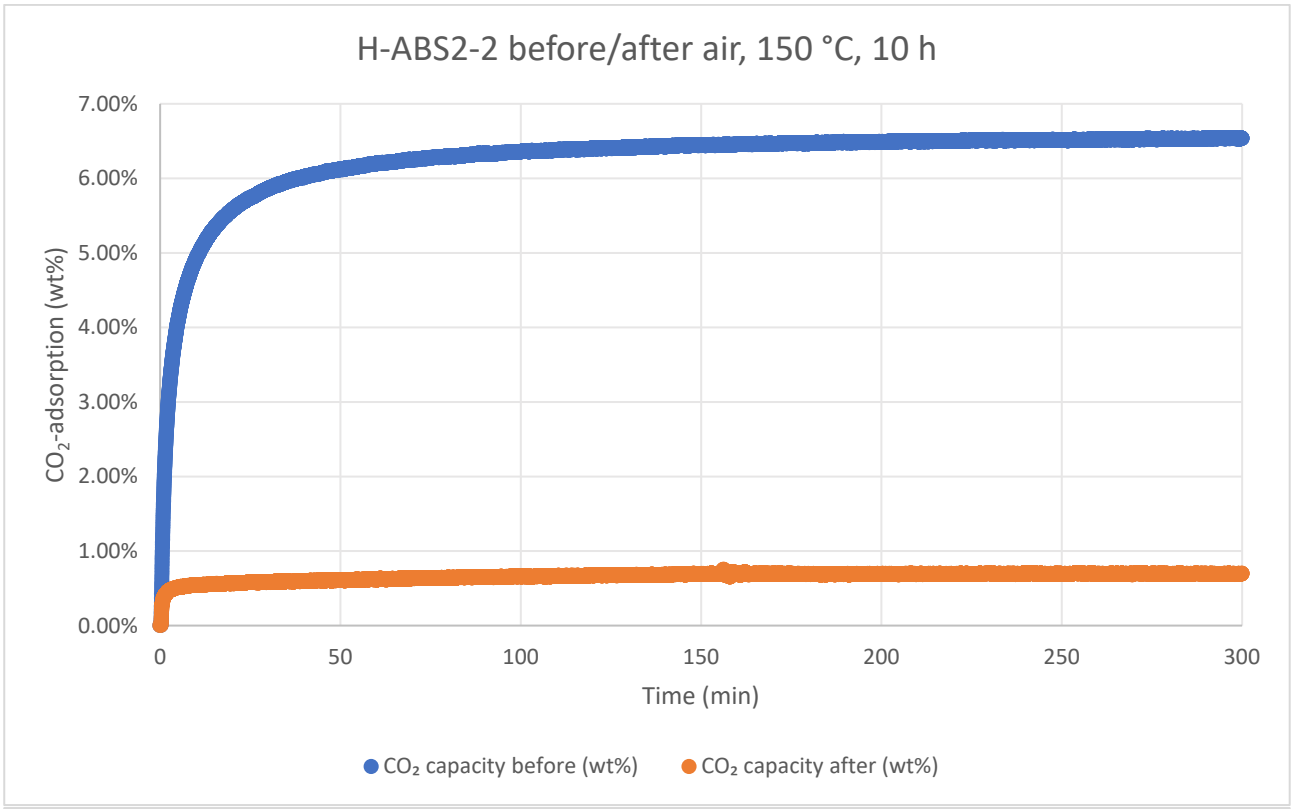
H-ABS2-2 before/after air, 150 °C, 10 h
7.00%
6.00%
5.00%
4.00%
3.00%
2.00%
1.00%
0.00%
CO2-adsorption (wt%)
0
50
100
150
200
250
300
Time (min)
CO2 capacity before (wt%)
CO2 capacity after (wt%)

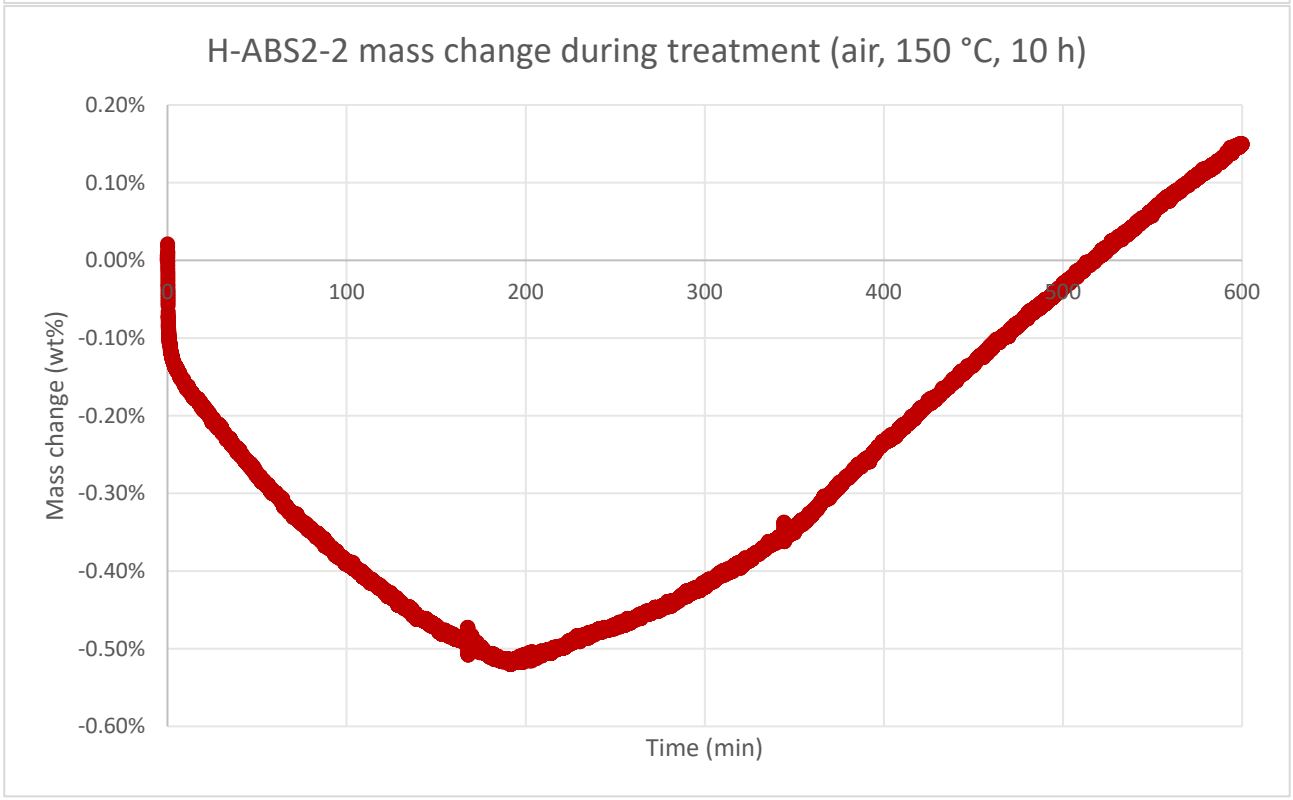
H-ABS2-2 mass change during treatment (air, 150 °C, 10 h)
0.20%
0.10%
0.00%
-0.10%
-0.20%
-0.30%
-0.40%
-0.50%
-0.60%
Mass change (wt%)
0
100
200
300
400
500
600
Time (min)

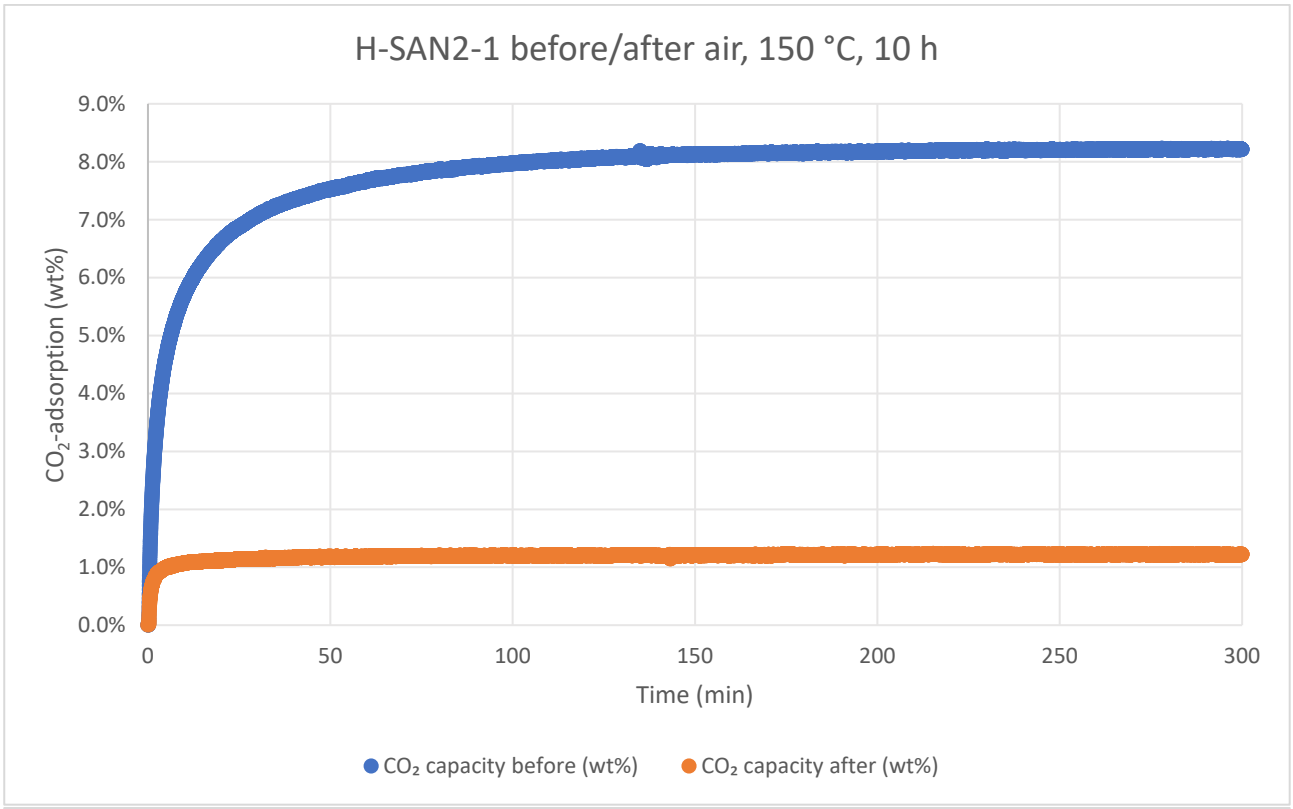
H-SAN2-1 before/after air, 150 °C, 10 h
9.0%
8.0%
7.0%
6.0%
5.0%
4.0%
3.0%
2.0%
1.0%
0.0%
CO2-adsorption (wt%)
0
50
100
150
200
250
300
Time (min)
CO2 capacity before (wt%)
CO2 capacity after (wt%)

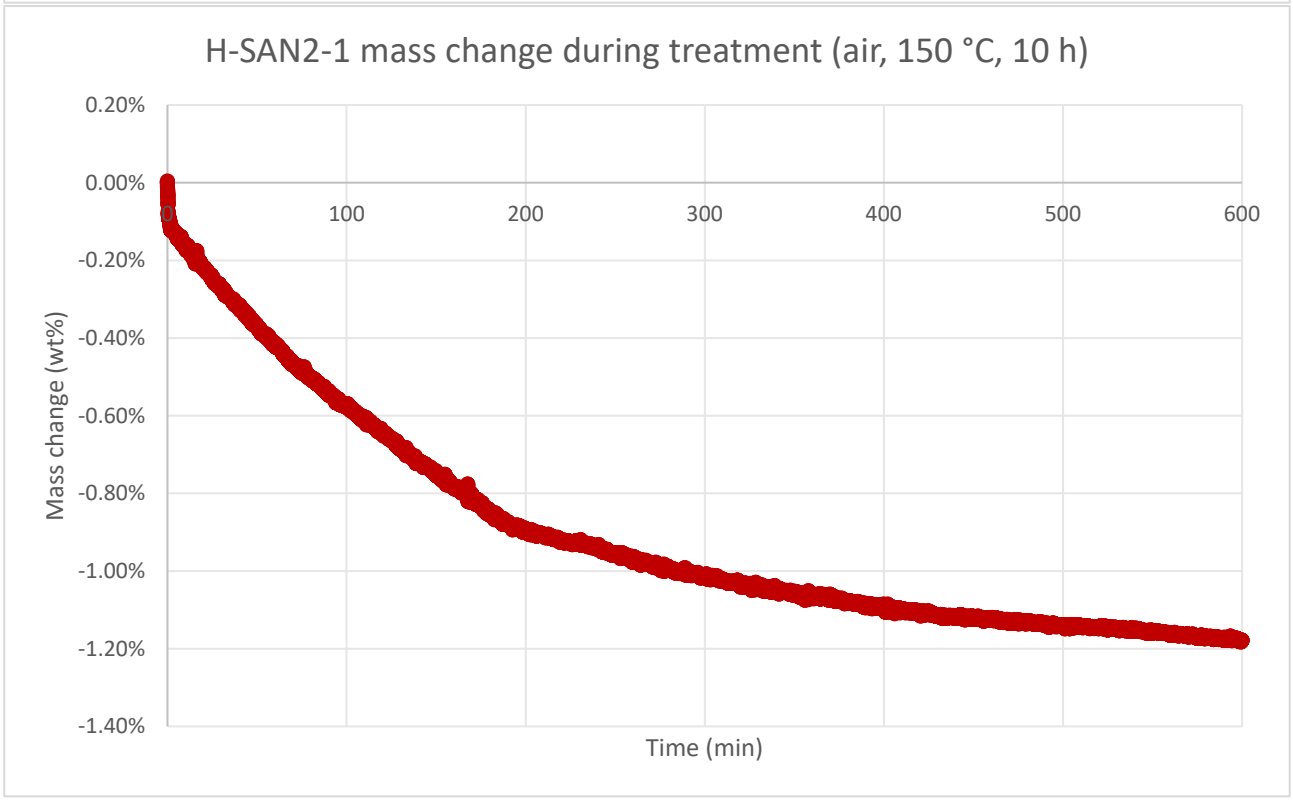
H-SAN2-1 mass change during treatment (air, 150 °C, 10 h)
0.20%
0.00%
-0.20%
-0.40%
-0.60%
-0.80%
-1.00%
-1.20%
-1.40%
Mass change (wt%)
0
100
200
300
400
500
600
Time (min)

The air stress test showed different outcomes for the three adsorbents. Firstly, **H-NBR-2-3** showed a high mass increase during the hot air segment of 8.9 wt%, indicating O-incorporation by oxidation, likely amine to amide, which is also supported by a new band in the IR-spectrum at 1644 cm^{-1}. The CO_2-capacity was significantly lowered to 0.4 wt% (4% capacity retention). For **H-ABS2-2**, the hot air segment shows first a minor decrease in mass followed by a slight mass increase, which overall yields a 0.2 wt% increase. This suggests initial minor decomposition (due to the mass loss) combined with O-incorporation similarly to with **H-NBR2-3** but at a lower degree. The CO_2-capacity was also significantly lowered to 0.7 wt% (11% capacity retention). Finally, **H-SAN2-1** shows no visible weight uptake over the 10 h hot air segment but instead a 1.2 wt% mass loss, indicating oxidative decomposition. Although the CO_2-capacity is substantially lower after the treatment (1.2 wt%), **H-SAN2-1** showed the best stability of the three adsorbents with a 15% capacity retention. In comparison, the capacity retention of Lewatit for the same treatment was found to be 41%.

Air, 150 °C, 10 h Stress test	**CO_2-capacity before** (wt%)	**CO_2-capacity after** (wt%)	**Capacity retained** (%)
H-NBR2-3	7.8	0.4	4%
H-ABS2-2	6.5	0.7	11%
H-SAN2-1	8.2	1.2	15%

Table S13. CO_2-adsorption capacities at 25 °C, 5 h, before and after 10 hours of heating at 150 °C in air. In comparison, the capacity retention of Lewatit for the same treatment was found to be 41% (see Lewatit benchmark section, p. S297).

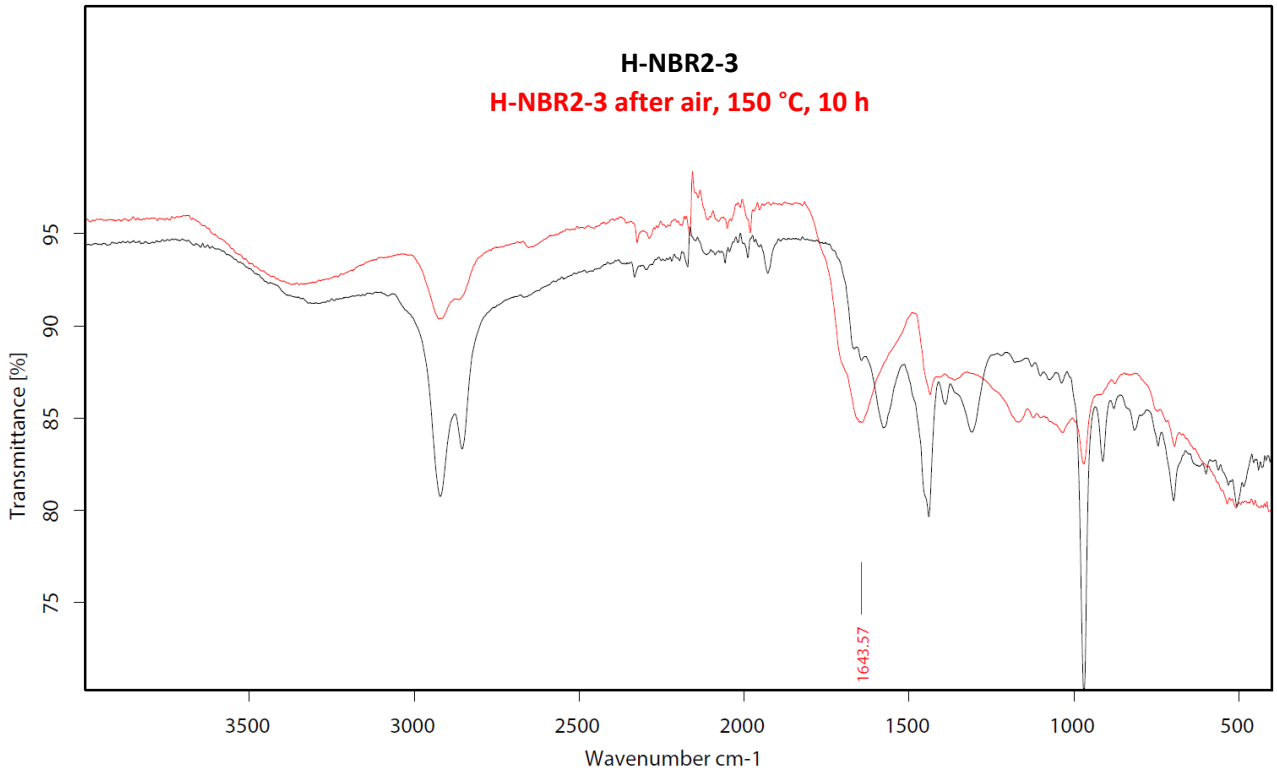

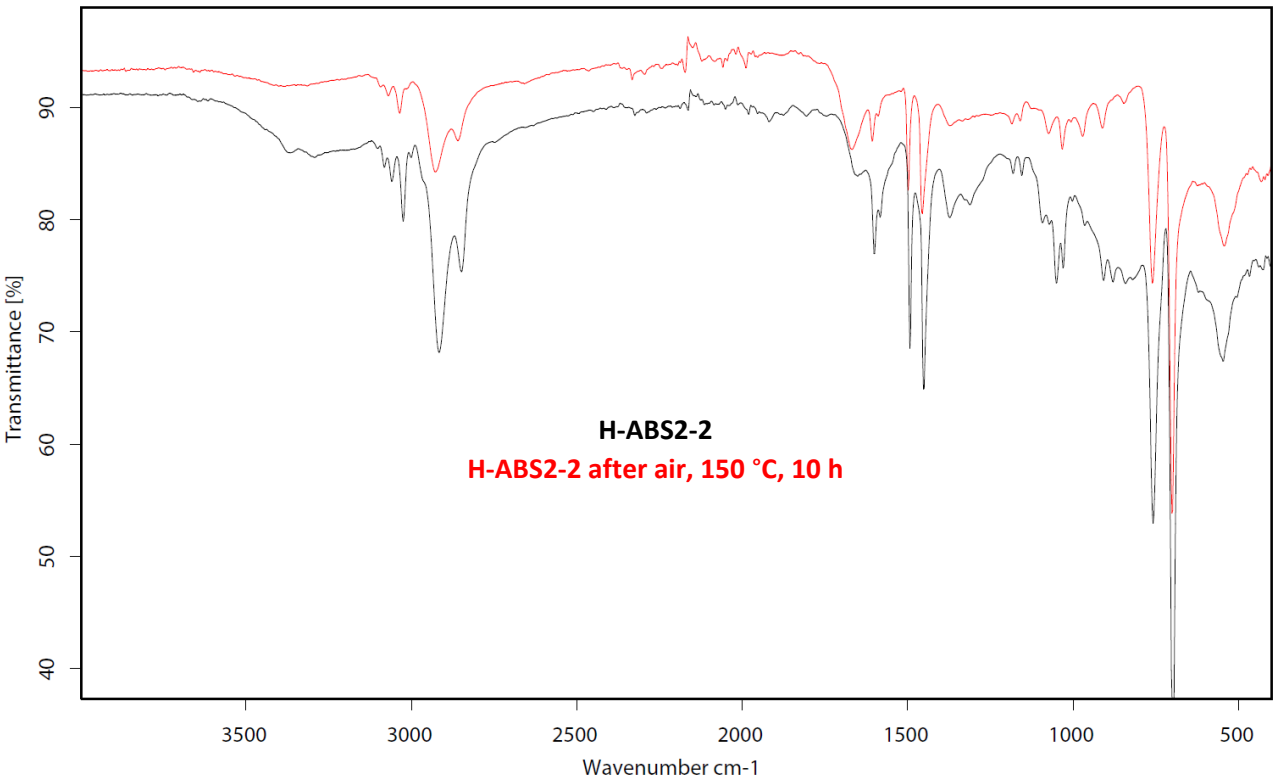
Transmittance [%]
90
80
70
60
50
40
3500
3000
2500
2000
1500
1000
500
Wavenumber cm-1
H-ABS2-2
H-ABS2-2 after air, 150 °C, 10 h

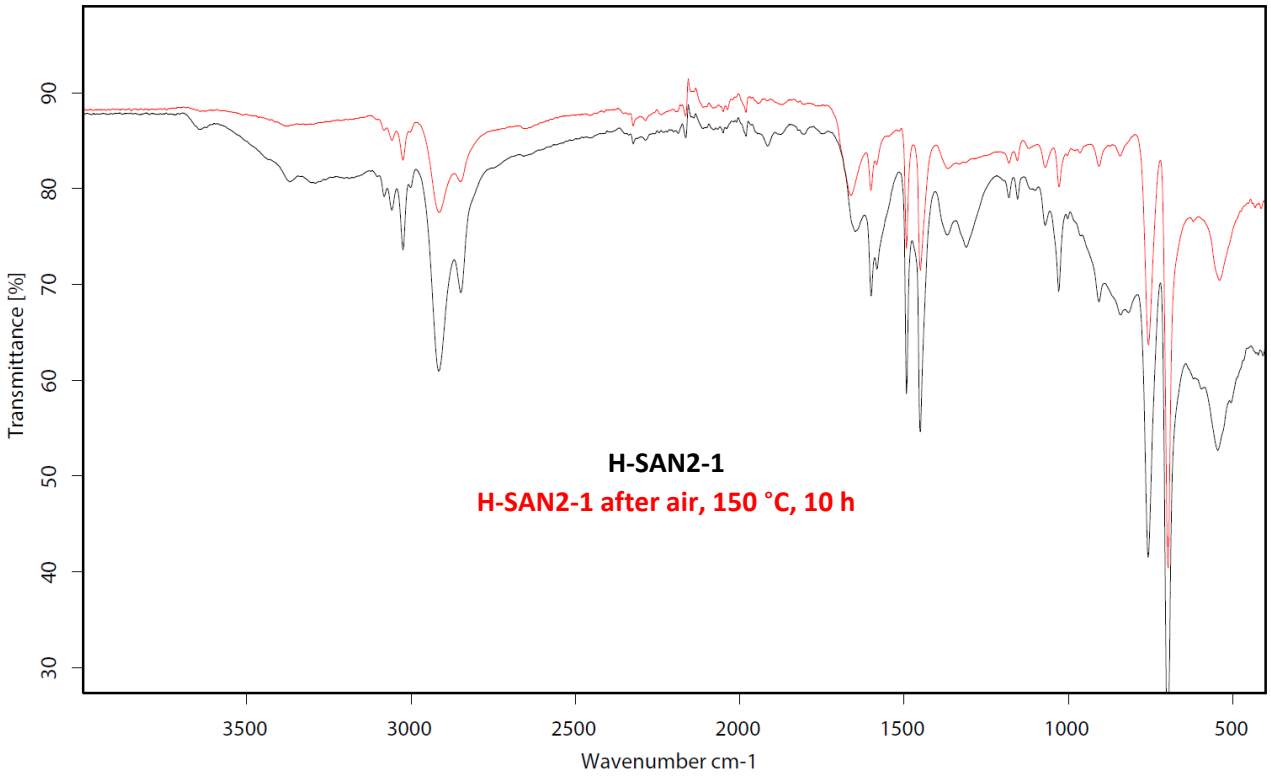
Transmittance [%]
90
80
70
60
50
40
30
3500
3000
2500
2000
1500
1000
500
Wavenumber cm-1
H-SAN2-1
H-SAN2-1 after air, 150 °C, 10 h

CO_2-capacity after hot CO_2 stress test: TGA method 7 was used to measure the weight of adsorbed CO_2 before and after a 10 h flow of CO_2 at 150 °C.

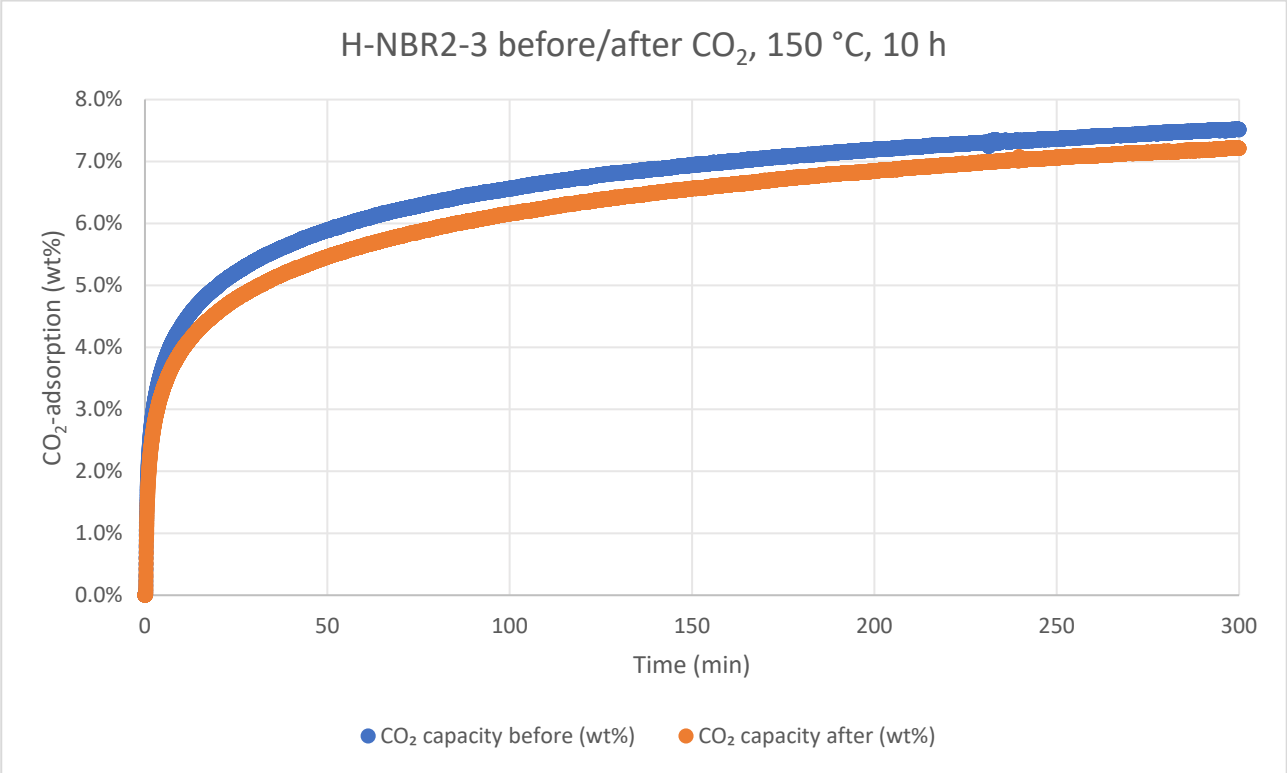

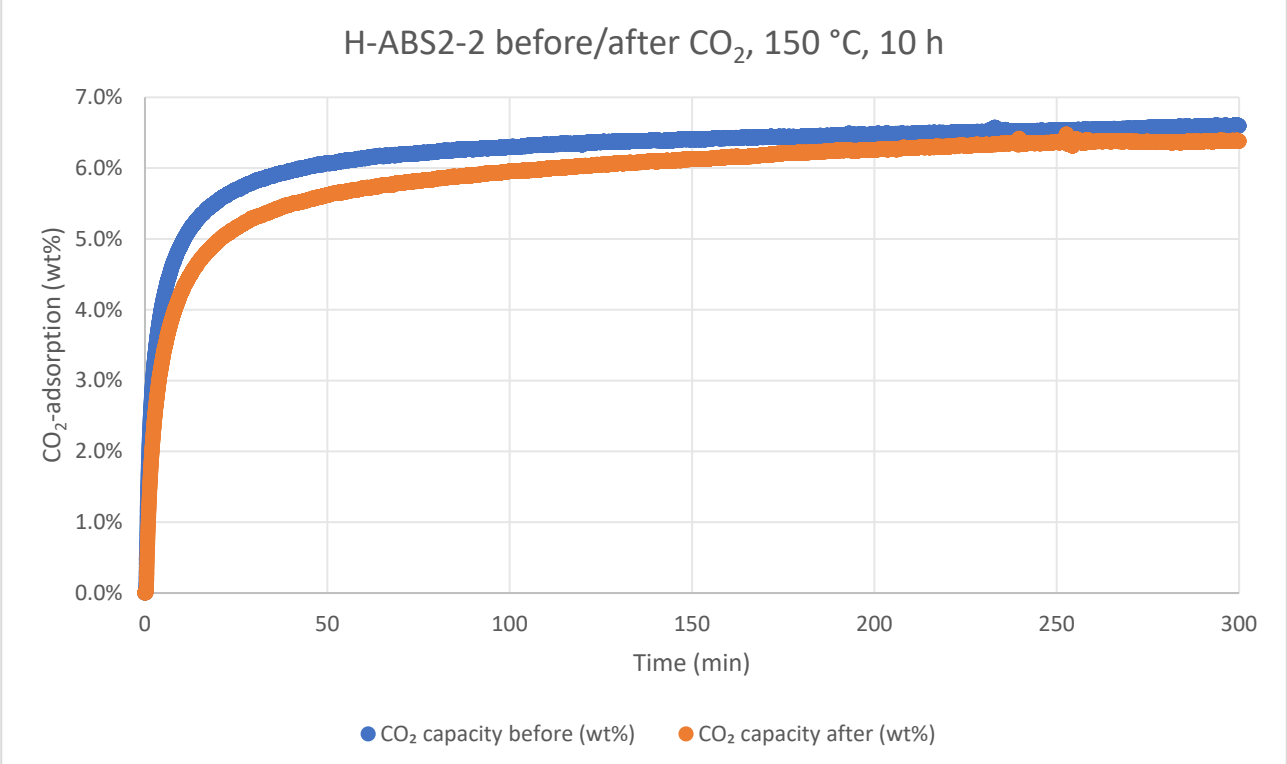

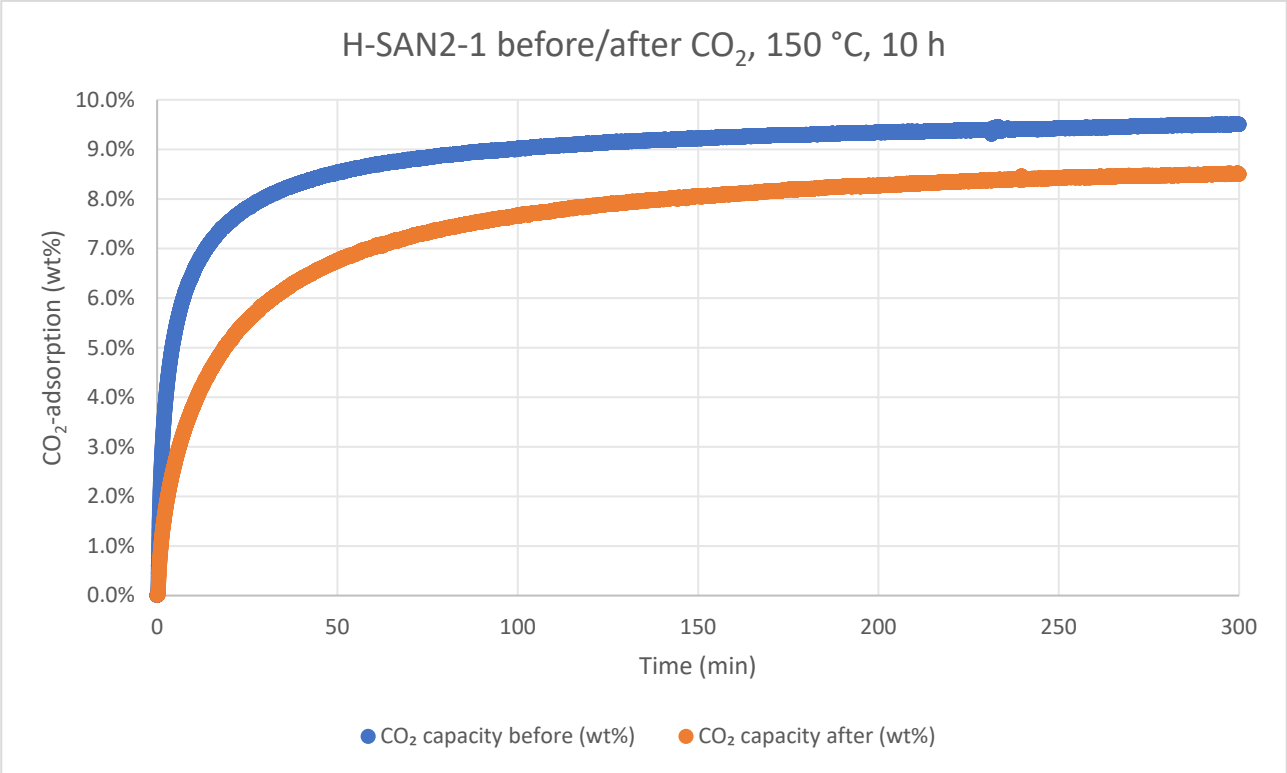

The results show high stability for the adsorbents towards the hot CO_2 as between 89−97% of their 5 h CO_2-capacities are retained after the treatment. TGA also show only 0.3−0.5 wt% weight increases during the 10 hour CO_2-segment at 150 °C, which can be removed by desorption in helium at 130 °C, thus indicating minimal deactivation by urea formation from this treatment. This is supported by FT-IR spectroscopic analysis showing highly identical spectra for the adsorbents before and after the treatment, thus suggesting minimal deactivation. Instead, the likely primary factor contributing to the minor decrease in CO_2-capacity could be particle agglomeration as previously described for the stress test employing helium flow at 150 °C. The capacity retention of Lewatit for this treatment was found to be 92%.

CO_2 (100%), 150 °C, 10 h Stress test	**CO_2-capacity before** (wt%)	**CO_2-capacity after** (wt%)	**Capacity retained** (%)
H-NBR2-3	7.5	7.2	96%
H-ABS2-2	6.6	6.4	97%
H-SAN2-1	9.5	8.5	89%

Table S14. CO_2-adsorption capacities at 25 °C, 5 h, before and after 10 hours of heating at 150 °C in CO_2. In comparison, the capacity retention of Lewatit was found to be 92% (see Lewatit benchmark section, p. S297).

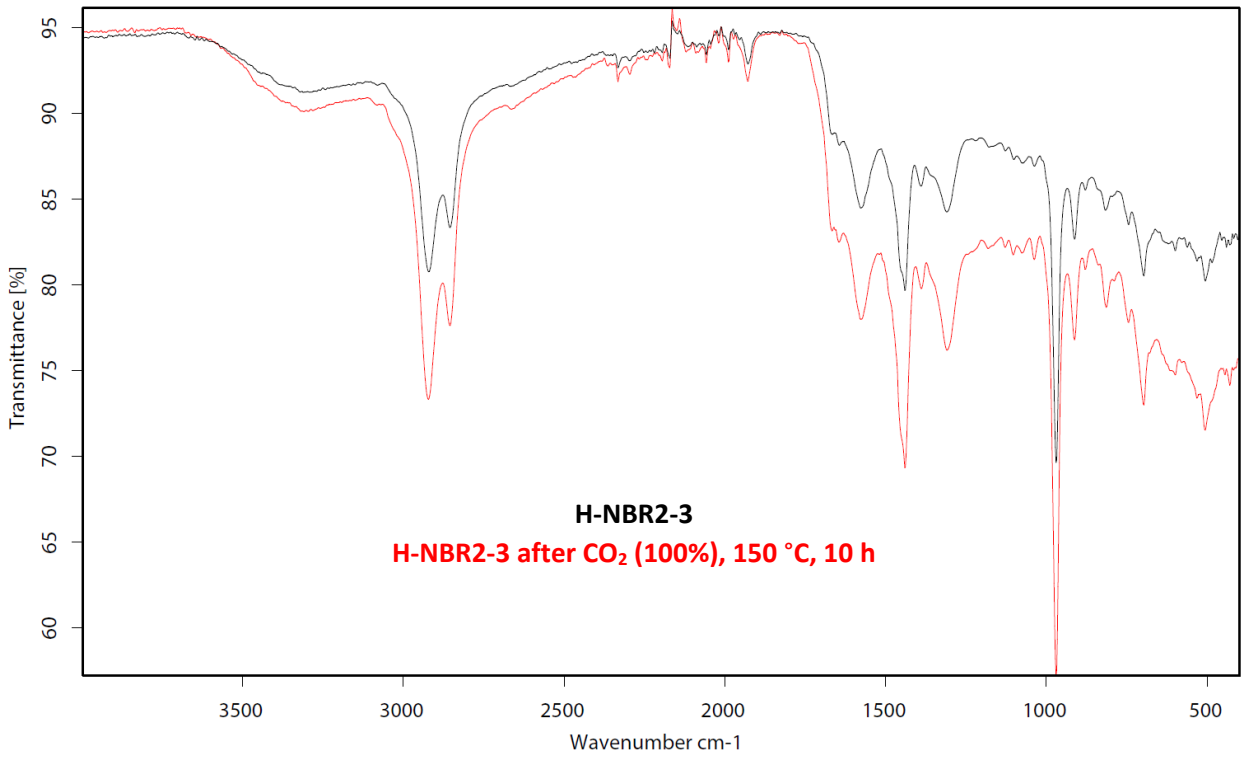
Transmittance [%]
95
90
85
80
75
70
65
60
3500
3000
2500
2000
1500
1000
500
Wavenumber cm-1
H-NBR2-3
H-NBR2-3 after CO2 (100%), 150 °C, 10 h

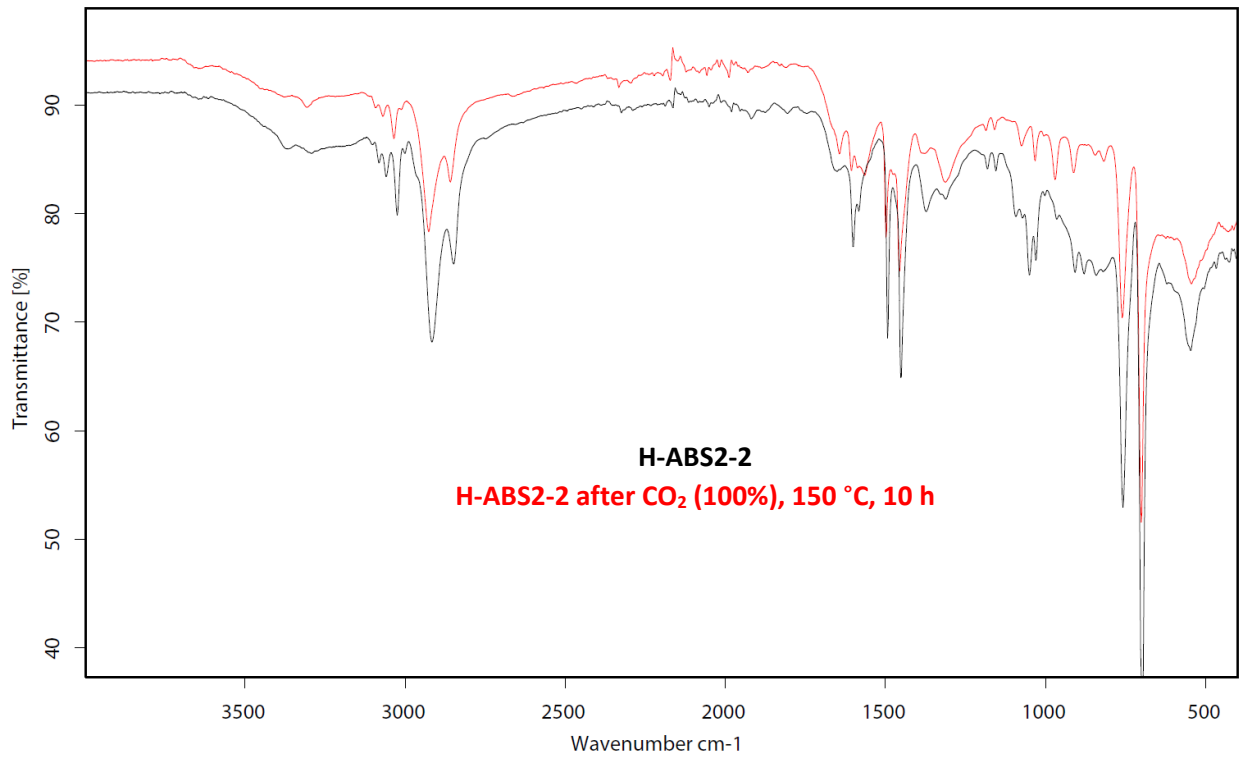
Transmittance [%]
90
80
70
60
50
40
3500
3000
2500
2000
1500
1000
500
Wavenumber cm-1
H-ABS2-2
H-ABS2-2 after CO2 (100%), 150 °C, 10 h

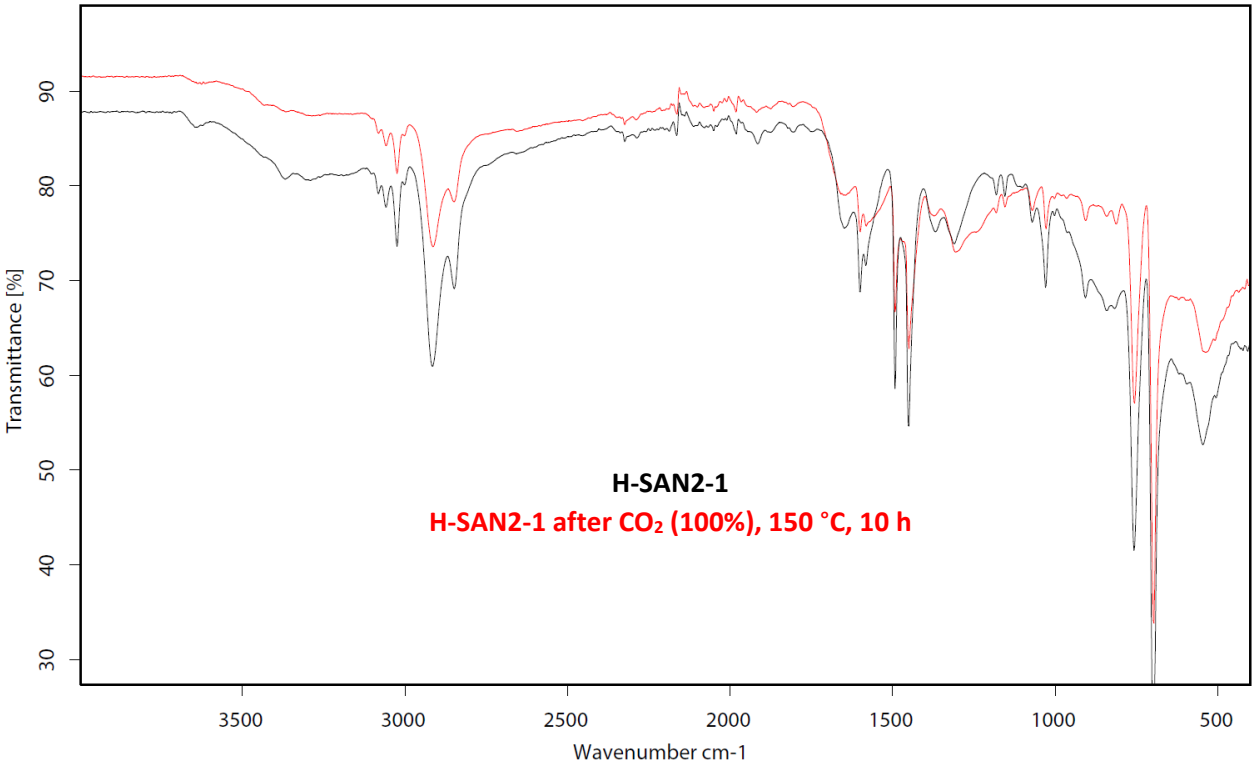
Transmittance [%]
90
80
70
60
50
40
30
3500
3000
2500
2000
1500
1000
500
Wavenumber cm-1
H-SAN2-1
H-SAN2-1 after CO2 (100%), 150 °C, 10 h

CO_2-capacity after boiling water stress test: TGA method 3 was used to measure the weight of adsorbed CO_2 after boiling in water for 7 days, open to air. As a value for CO_2-adsorption before boiling in water, the initial adsorption capacities measured for the hot helium stress test were used (see above). With regards to the procedure, the relevant polymer (50 mg) was suspended in H_2O (20 mL) and heated to 100 °C under stirring and open to air, while using a reflux condenser. After 7 days, the polymer was collected by filtration, rinsed with water (10 mL) and MeOH (10 mL), and finally dried under reduced pressure overnight before being subjected to TGA. Since particles agglomerated during this stress test, a spatula was used to break down agglomerated particles into powders before being subjected to TGA.

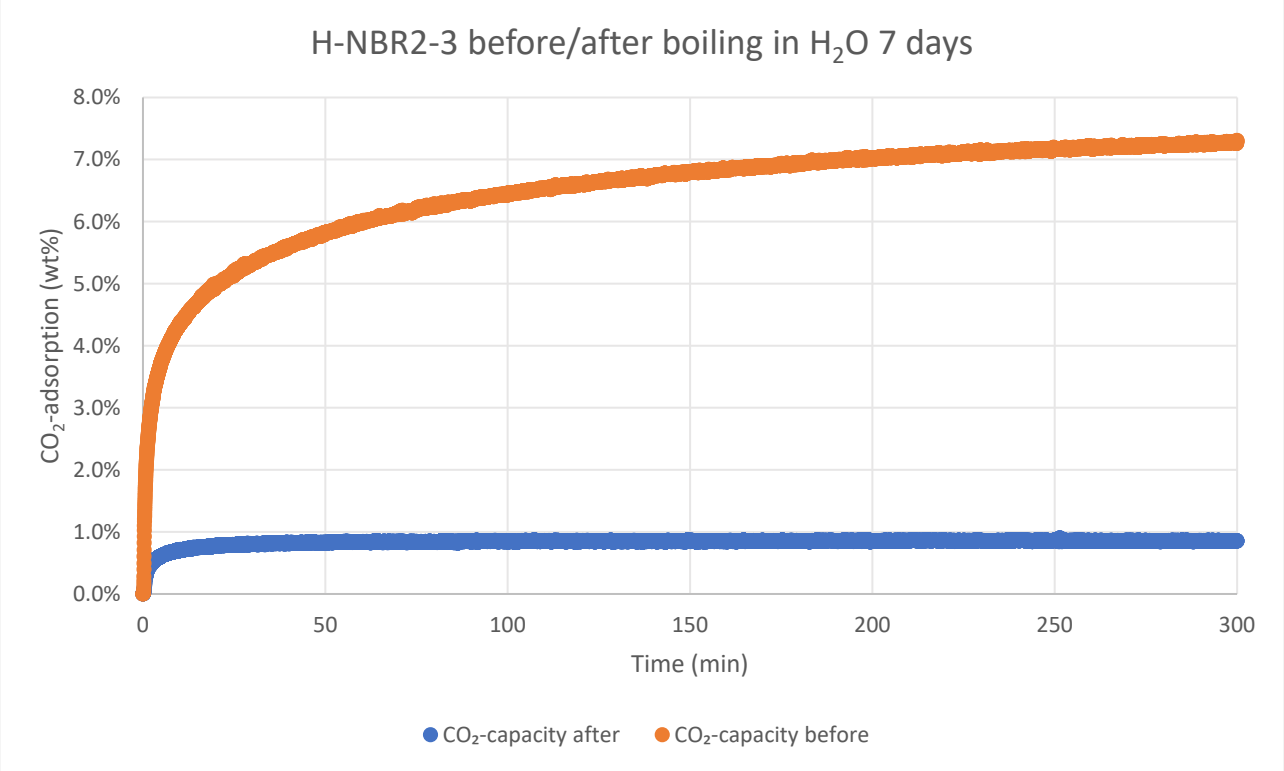

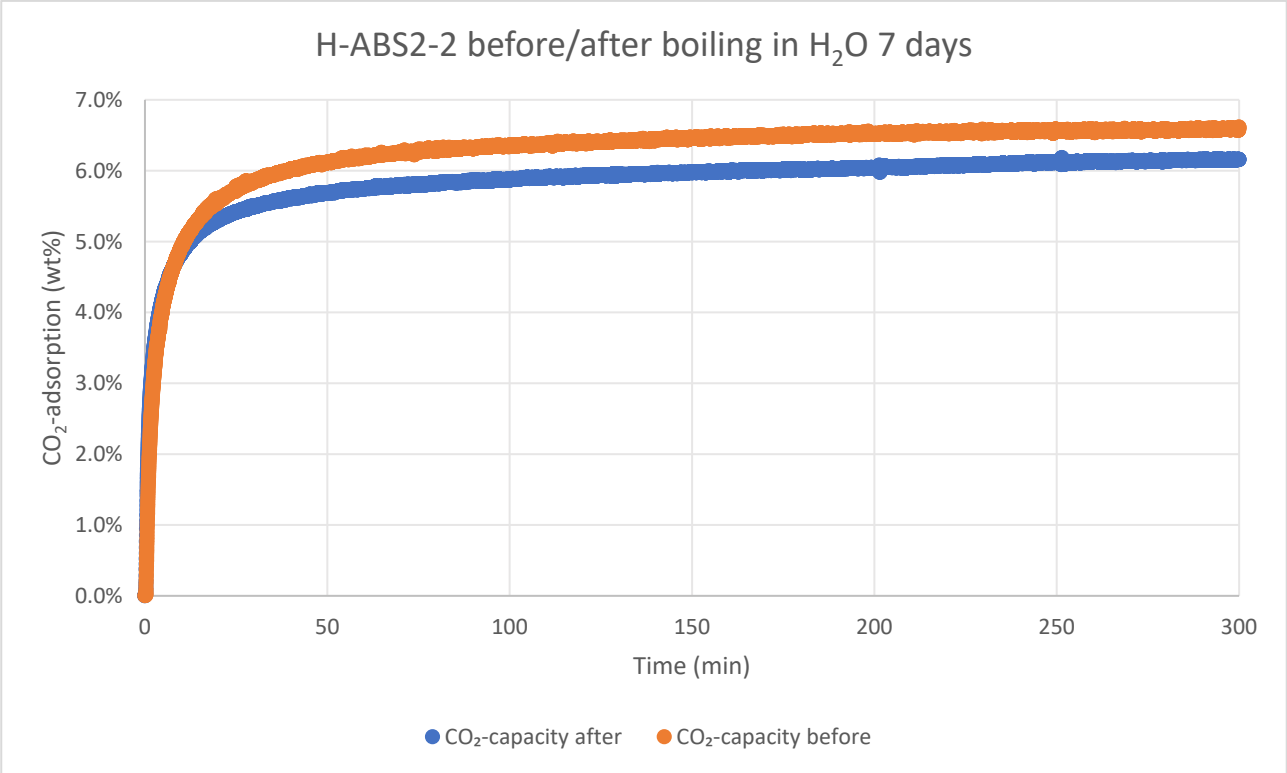

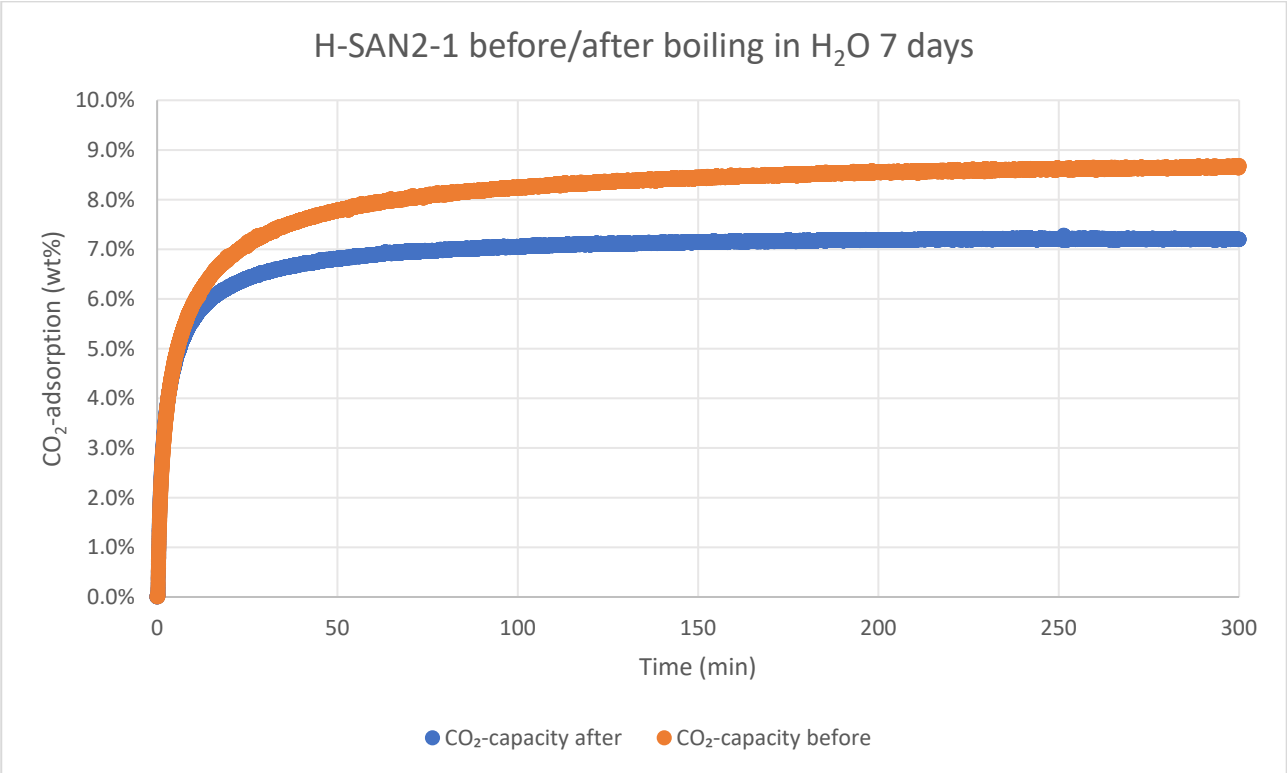

The results show high to excellent stabilities for **H-ABS2-2** and **H-SAN2-1** (83% and 93%, respectively), while **H-NBR2-3** decomposes to give a low CO_2-capacity of 11% after the treatment. FT-IR spectroscopic analysis shows highly similar features for **H-ABS2-2** and **H-SAN2-1** before and after the treatment, while **H-NBR2-3** gives a new C=O stretch band at 1667 cm^{-1} indicative of oxidation. In addition, the decomposition of H-**NBR2-3** is quite visible compared to the more stable **H-ABS2-2** and **H-SAN2-1**, as the green **H-NBR2-3** powder turns

into brown particles, whereas **H-ABS2-2** and **H-SAN2-1** do not visibly change appearance although particle agglomeration occurs. In comparison, the capacity retention of Lewatit was found to be 85%, and this adsorbent did also not visibly change appearance during the treatment.

Boiled in H_2O 7 days Stress test	**CO_2-capacity before** (wt%)	**CO_2-capacity after** (wt%)	**Capacity retained** (%)
H-NBR2-3	7.3	0.9	11%
H-ABS2-2	6.6	6.2	93%
H-SAN2-1	8.7	7.2	83%

Table S15. CO_2-capacities before and after boiling in water for 7 days while open to air. In comparison, the capacity retention of Lewatit was found to be 85% (see Lewatit benchmark section, p. S297). As a value for CO_2-adsorption before boiling in water, the initial adsorption capacities measured for the hot helium stress test were used.

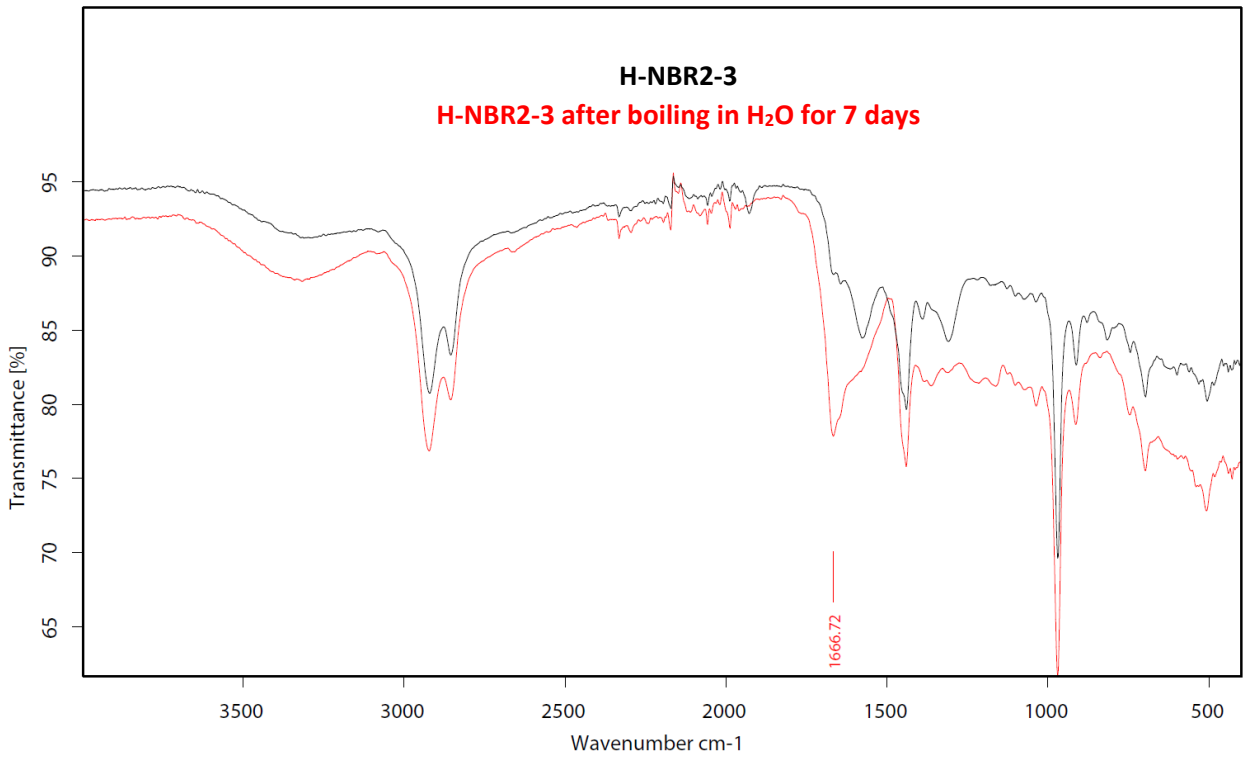

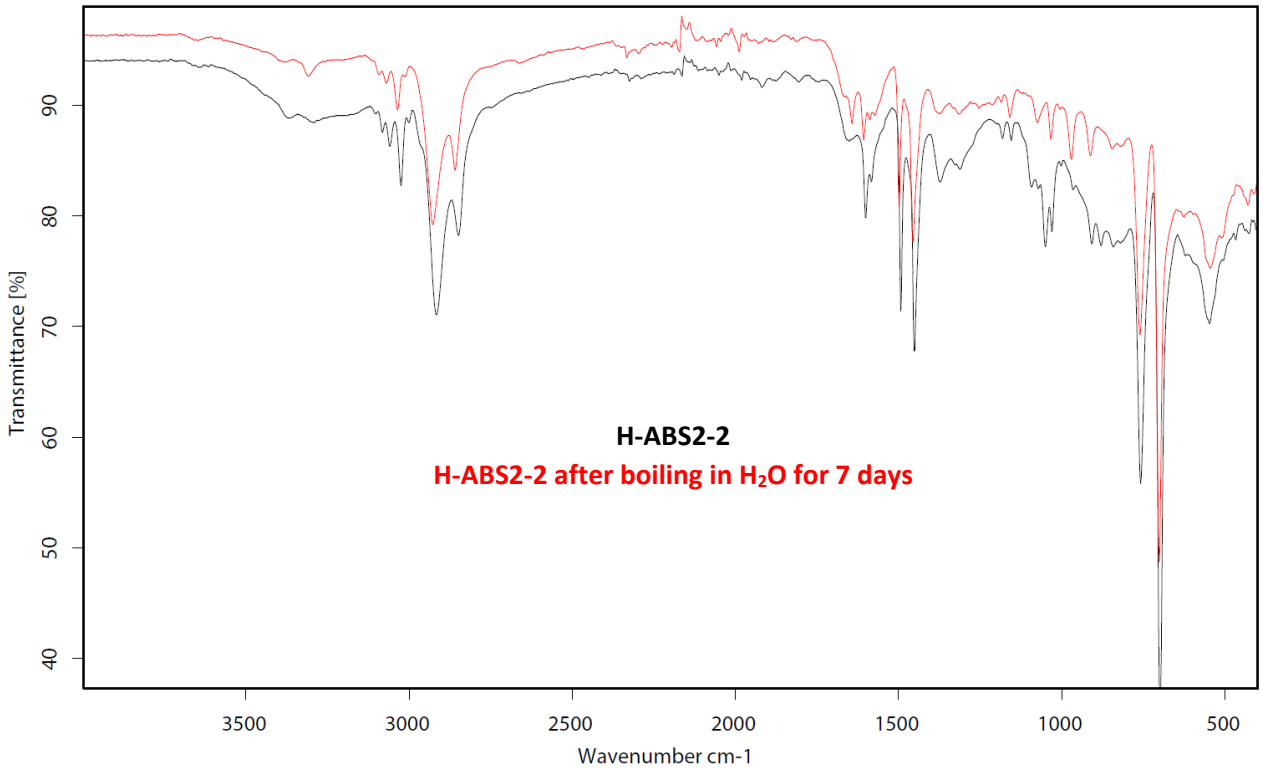
Transmittance [%]
90
80
70
60
50
40
3500
3000
2500
2000
1500
1000
500
Wavenumber cm-1
H-ABS2-2
H-ABS2-2 after boiling in H2O for 7 days

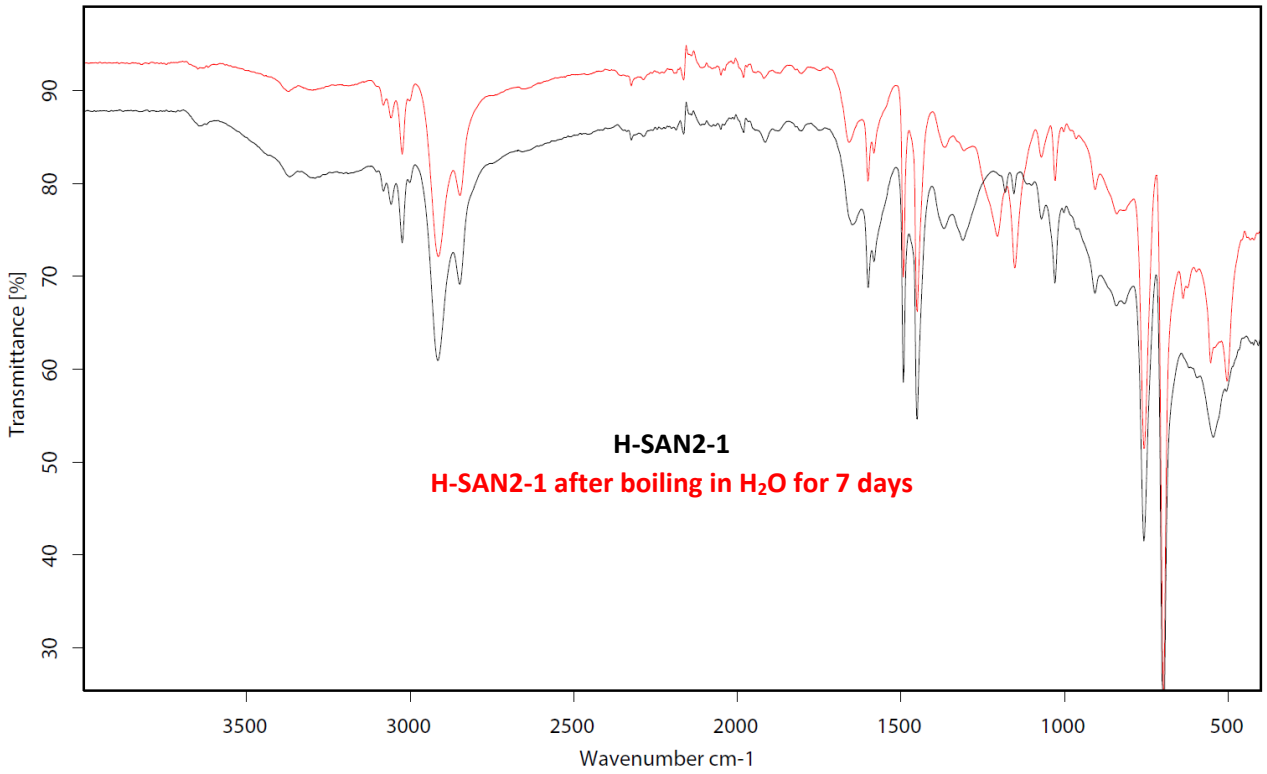
Transmittance [%]
90
80
70
60
50
40
30
3500
3000
2500
2000
1500
1000
500
Wavenumber cm-1
H-SAN2-1
H-SAN2-1 after boiling in H2O for 7 days

CO_2-capacity after NO_2 stress test: TGA method 8 was used to measure the weight of adsorbed CO_2 before and after a 10 h flow of NO_2 (203 ppm balanced by N_2) at 25 °C.

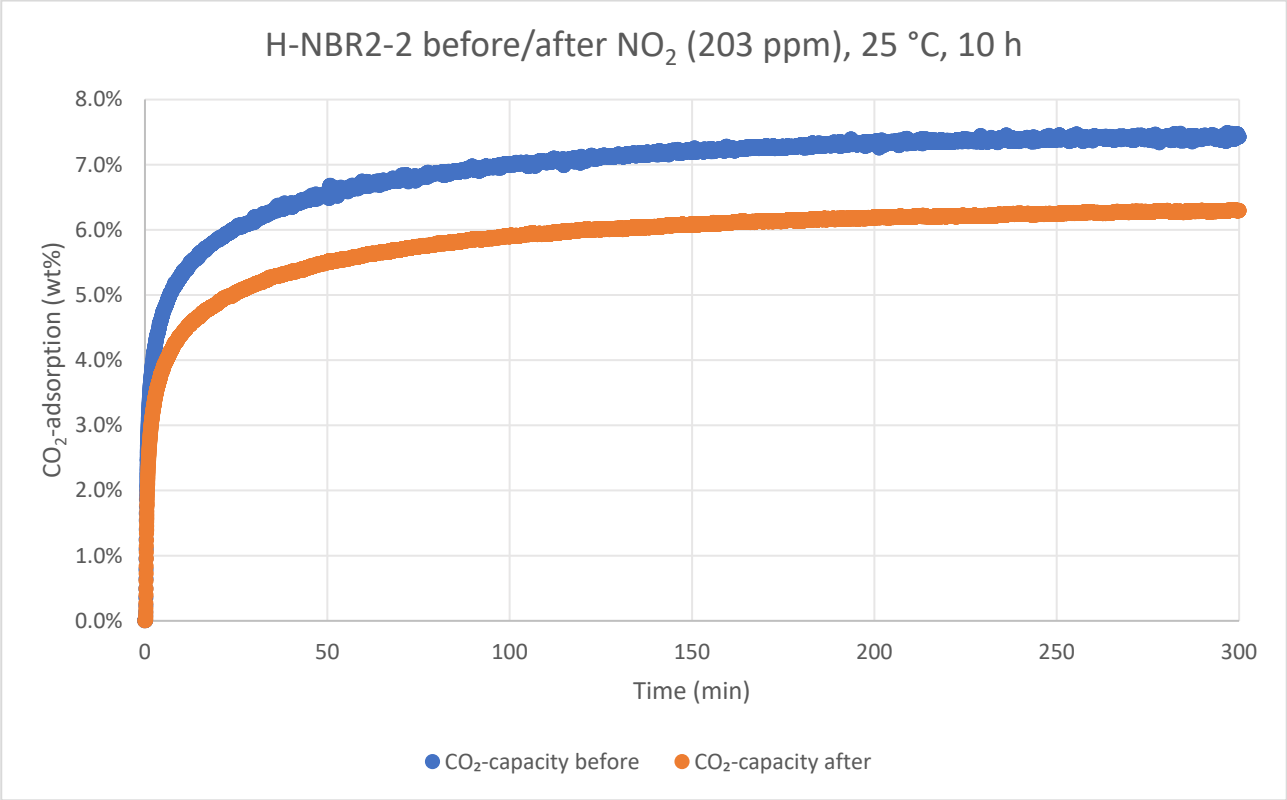

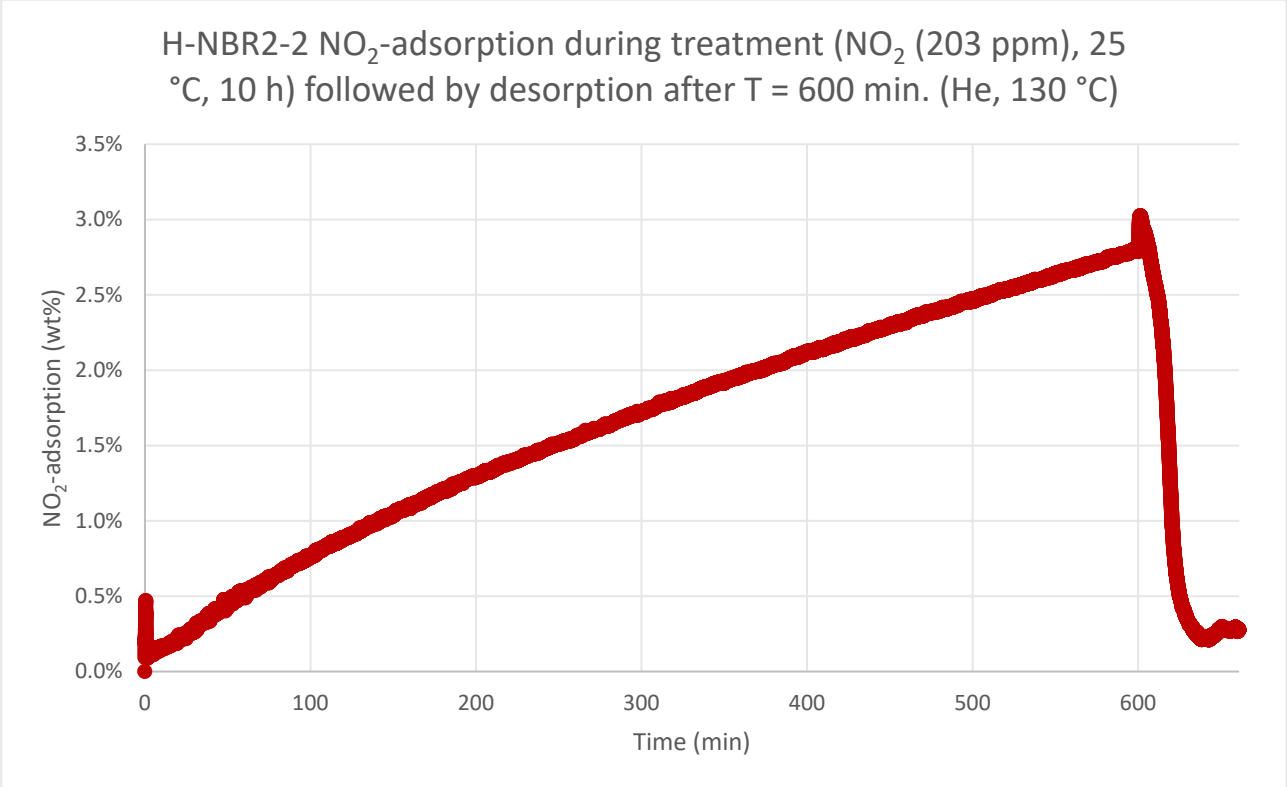

H-NBR2-2 NO_2-capacity (10 h) was 2.8 wt% before and 0.3 wt% after desorption. Note: The sudden

adsorption increase ~ T = 0 min and 600 min are not due to adsorption but a persistent buoyancy TGA effect from switching gasses.

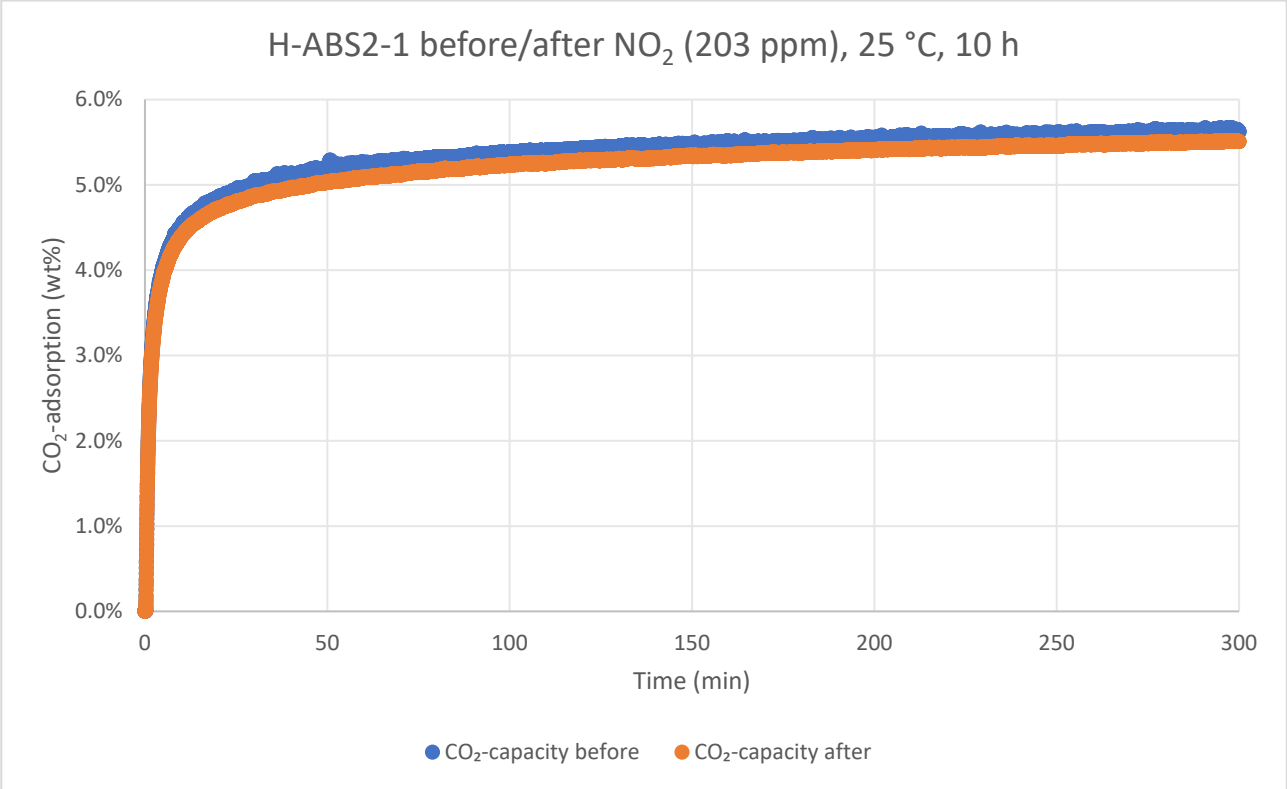

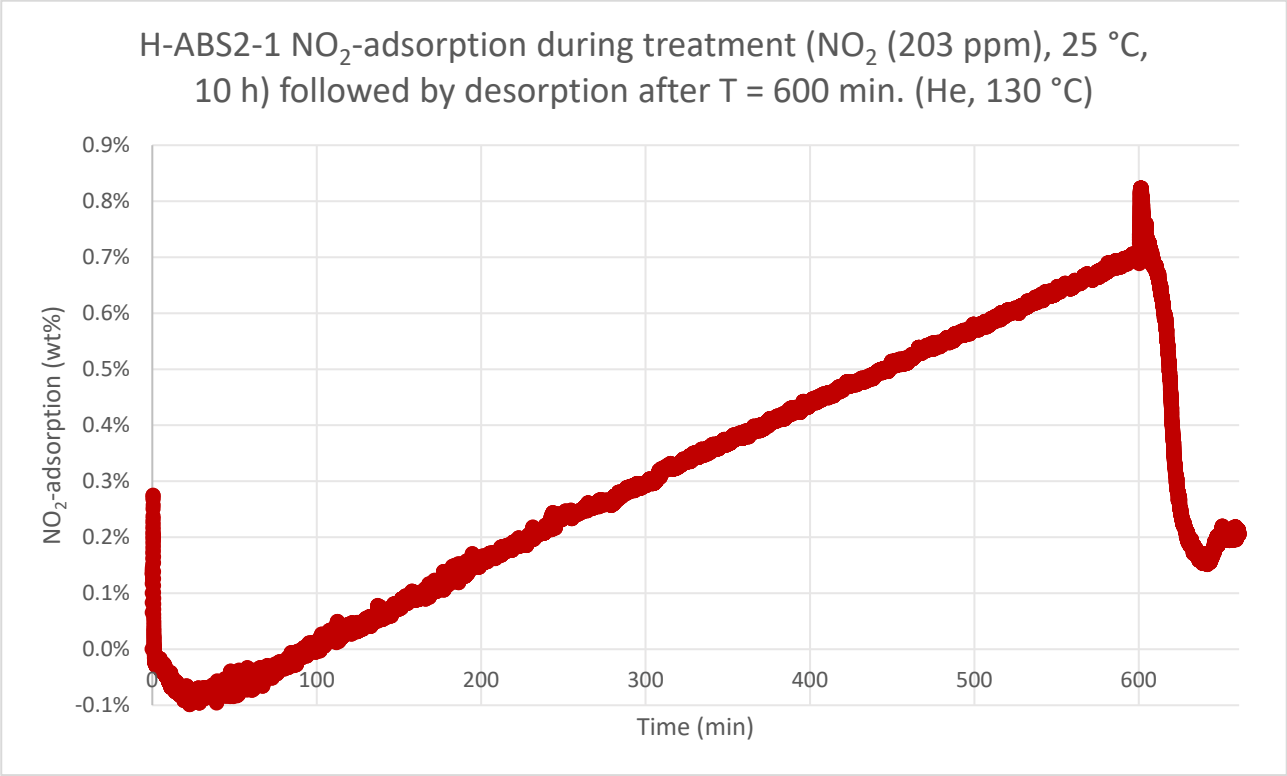

H-ABS2-1 NO_2-capacity (10 h) was 0.7 wt% before and 0.2 wt% after desorption. Note: The sudden adsorption increase ~ T = 0 min and 600 min are not due to adsorption but a persistent buoyancy TGA effect from switching gasses.

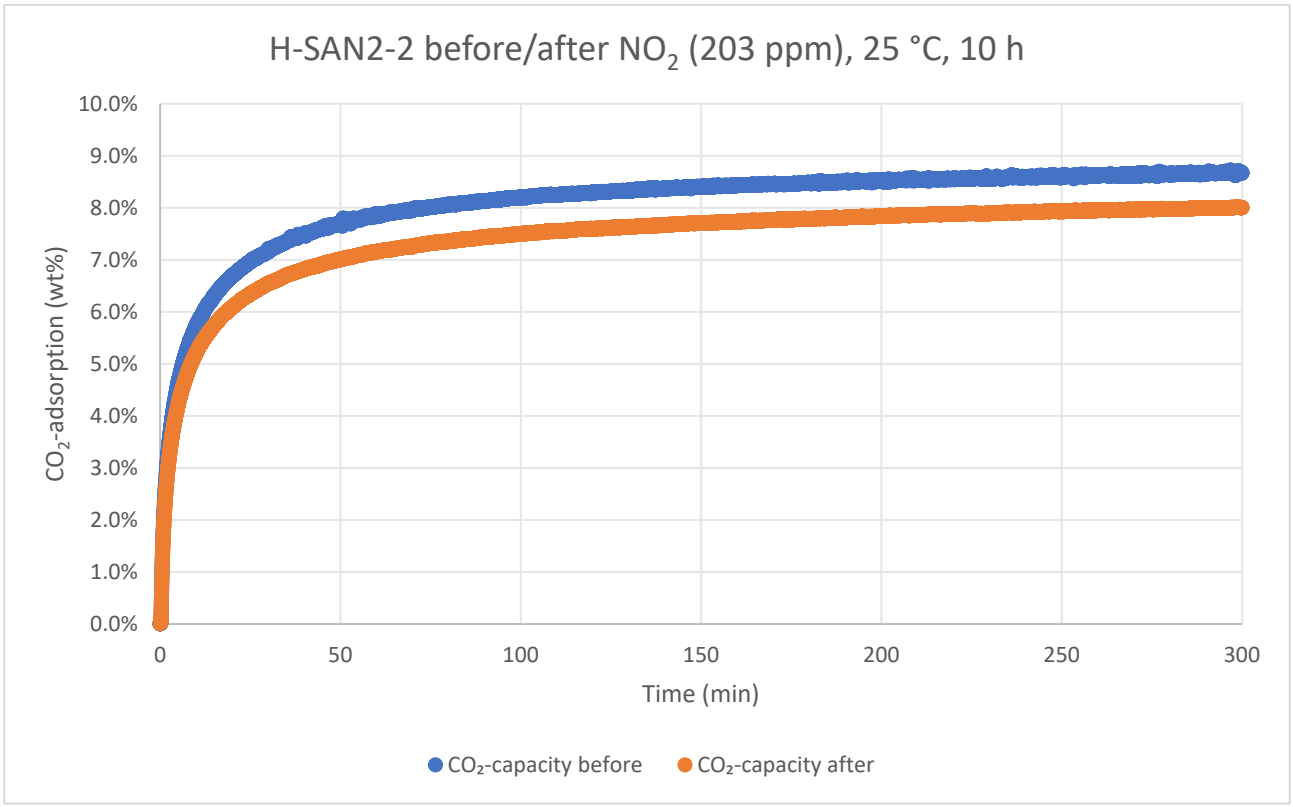

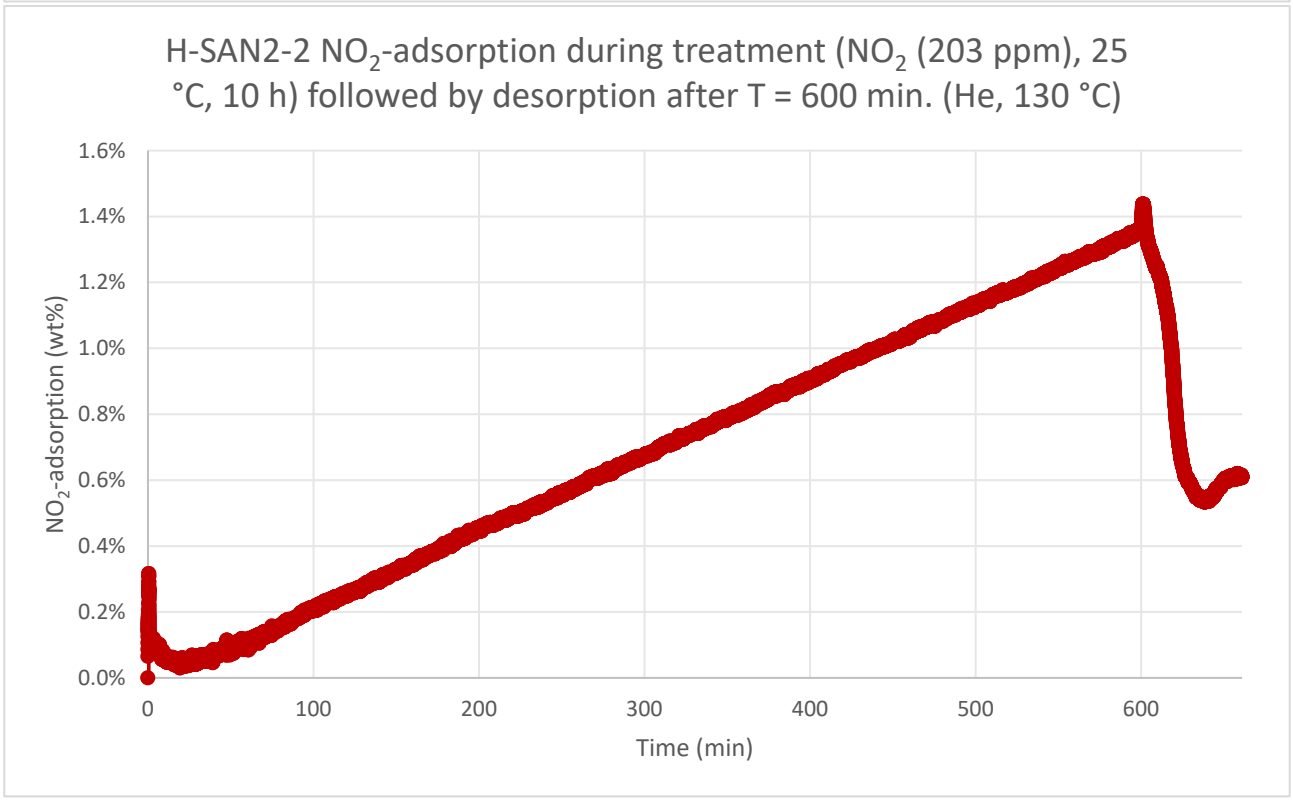

H-SAN2-2 NO_2-capacity (10 h) was 1.4 wt% before and 0.6 wt% after desorption. Note: The sudden adsorption increase ~ T = 0 min and 600 min are not due to adsorption but a persistent buoyancy TGA effect from switching gasses.

The three adsorbents showed high stability towards NO_2 (retentions ranging from 85−98%) compared to the Lewatit benchmark adsorbent (41% retention). This could be explained by less exposed amines in the three adsorbents compared to the macro-porous Lewatit, thus the amine sites are more protected from NO_2. This hypothesis is further supported by the significantly higher NO_2-adsorption of Lewatit (9.9 wt%) compared to the three adsorbents (0.7−2.8 wt%). IR-spectroscopic analysis showed highly similar bands to the IR-spectra of the adsorbents before and after NO_2, supporting the finding of low degrees of deactivation.

NO_2 (203 ppm), 150 °C, 10 h. Stress test	**CO_2-capacity before** (wt%)	**CO_2-capacity after** (wt%)	**Capacity retained** (%)
H-NBR2-2	7.4	6.3	85%
H-ABS2-1	5.6	5.5	98%
H-SAN2-2	8.7	8.0	92%

Table S16. CO_2-adsorption capacities at 25 °C, 5 h, before and after 10 hours of NO_2 (203 ppm in N_2) at 25 °C. In comparison, the capacity retention of Lewatit for the same treatment was found to be 41% (see Lewatit benchmark section, p. S297).

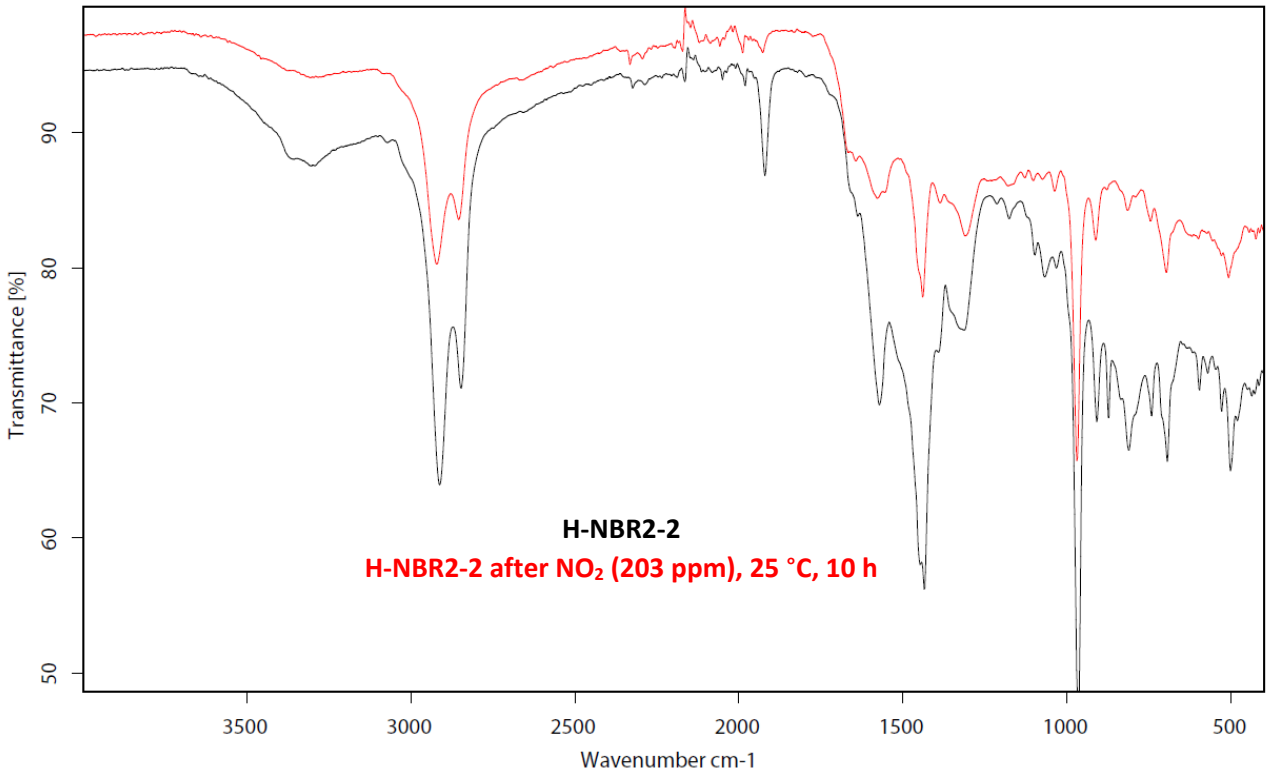

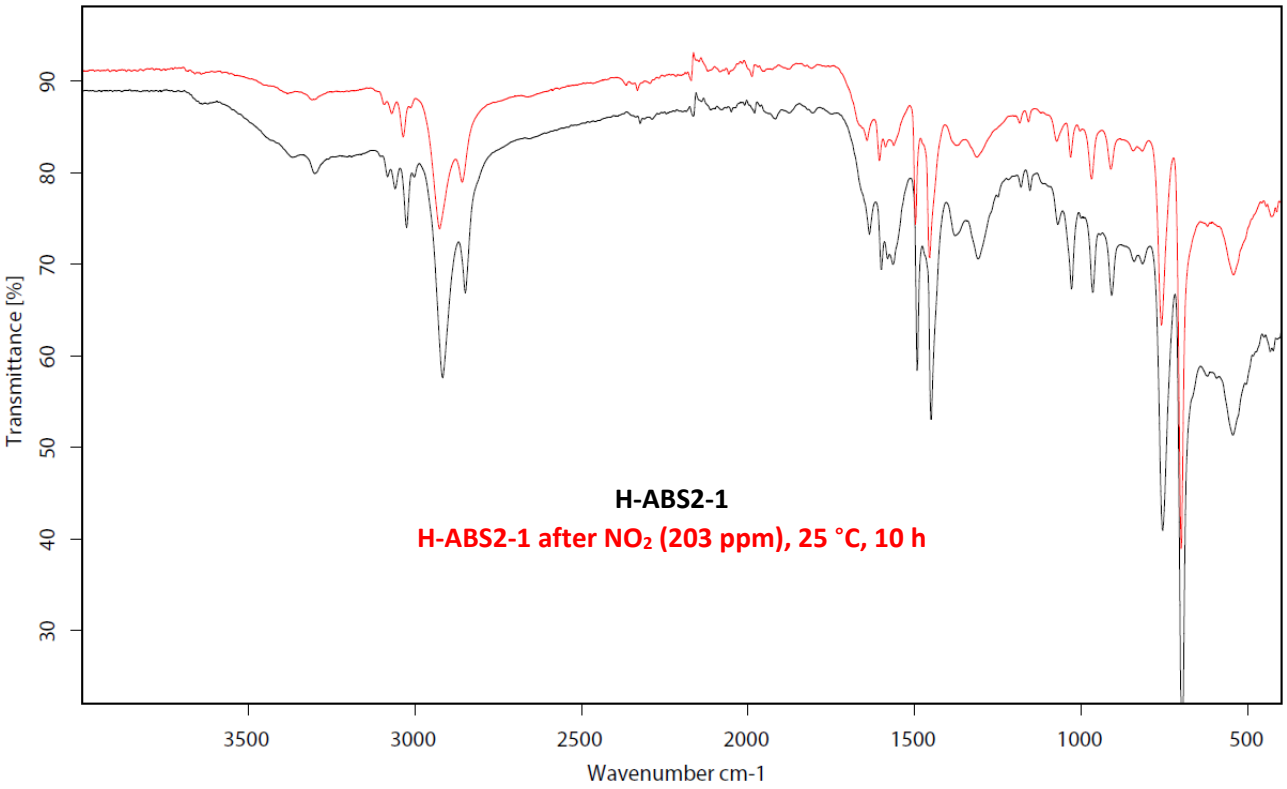
Transmittance [%]
90
80
70
60
50
40
30
3500
3000
2500
2000
1500
1000
500
Wavenumber cm-1
H-ABS2-1
H-ABS2-1 after NO2 (203 ppm), 25 °C, 10 h

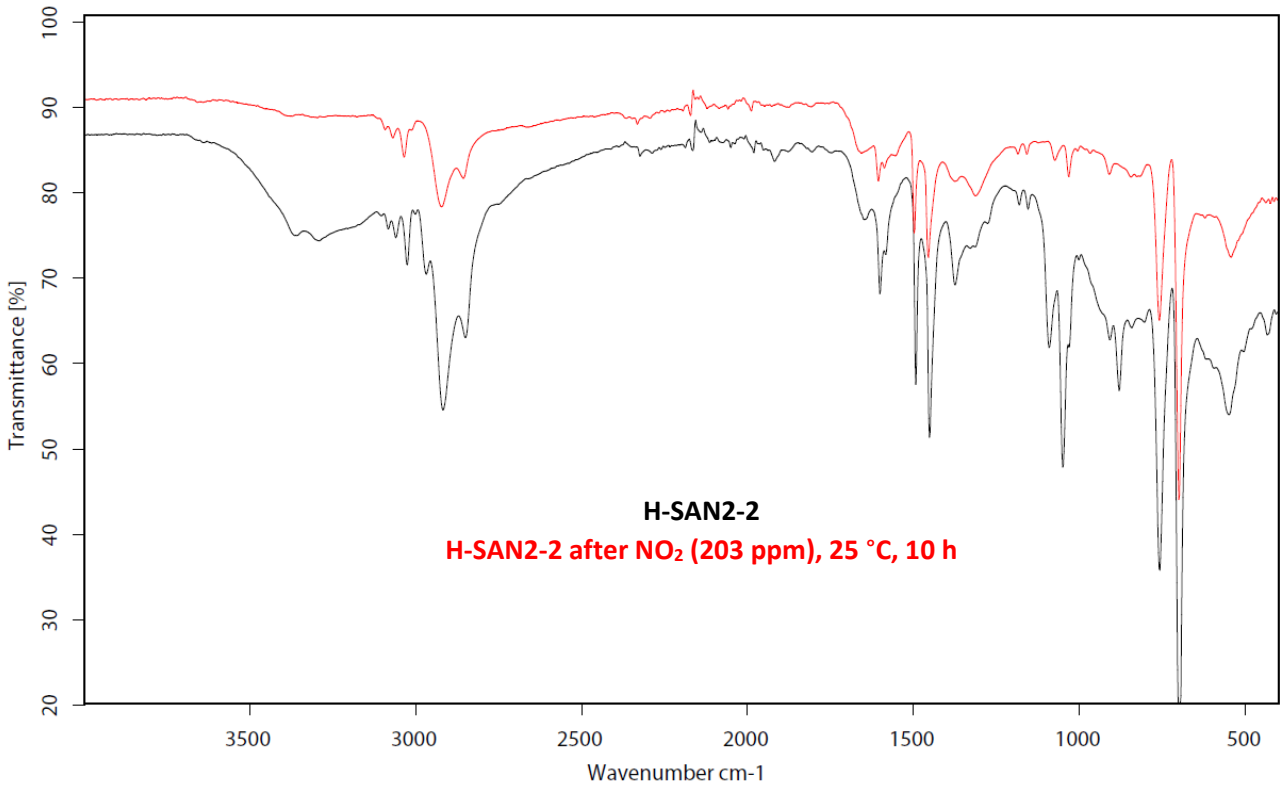
Transmittance [%]
100
90
80
70
60
50
40
30
20
3500
3000
2500
2000
1500
1000
500
Wavenumber cm-1
H-SAN2-2
H-SAN2-2 after NO2 (203 ppm), 25 °C, 10 h

CO_2-capacity after SO_2 stress test: TGA method 9 was used to measure the weight of adsorbed CO_2 before and after a 10 h flow of SO_2 (206 ppm balanced by N_2) at 25 °C.

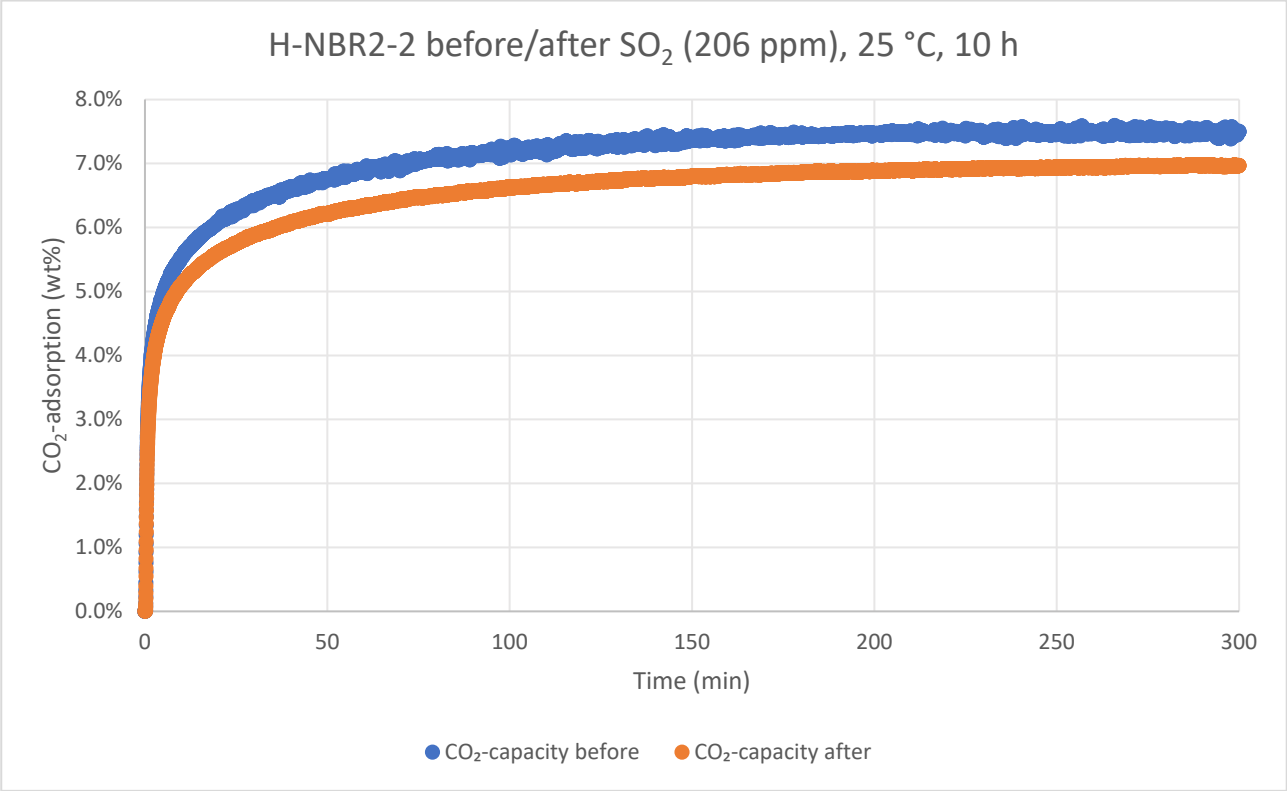

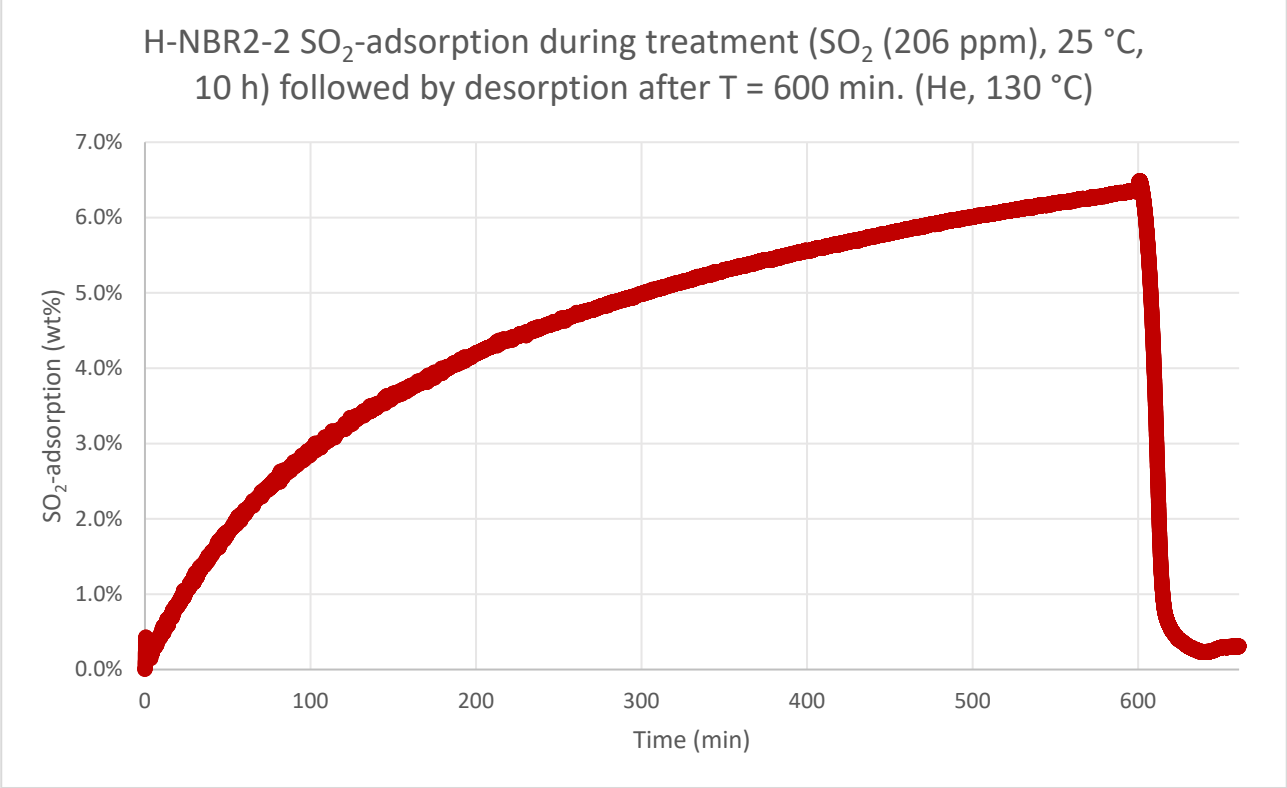

H-NBR2-2 SO_2-capacity (10 h) was 6.4 wt% before and 0.3 wt% after desorption.

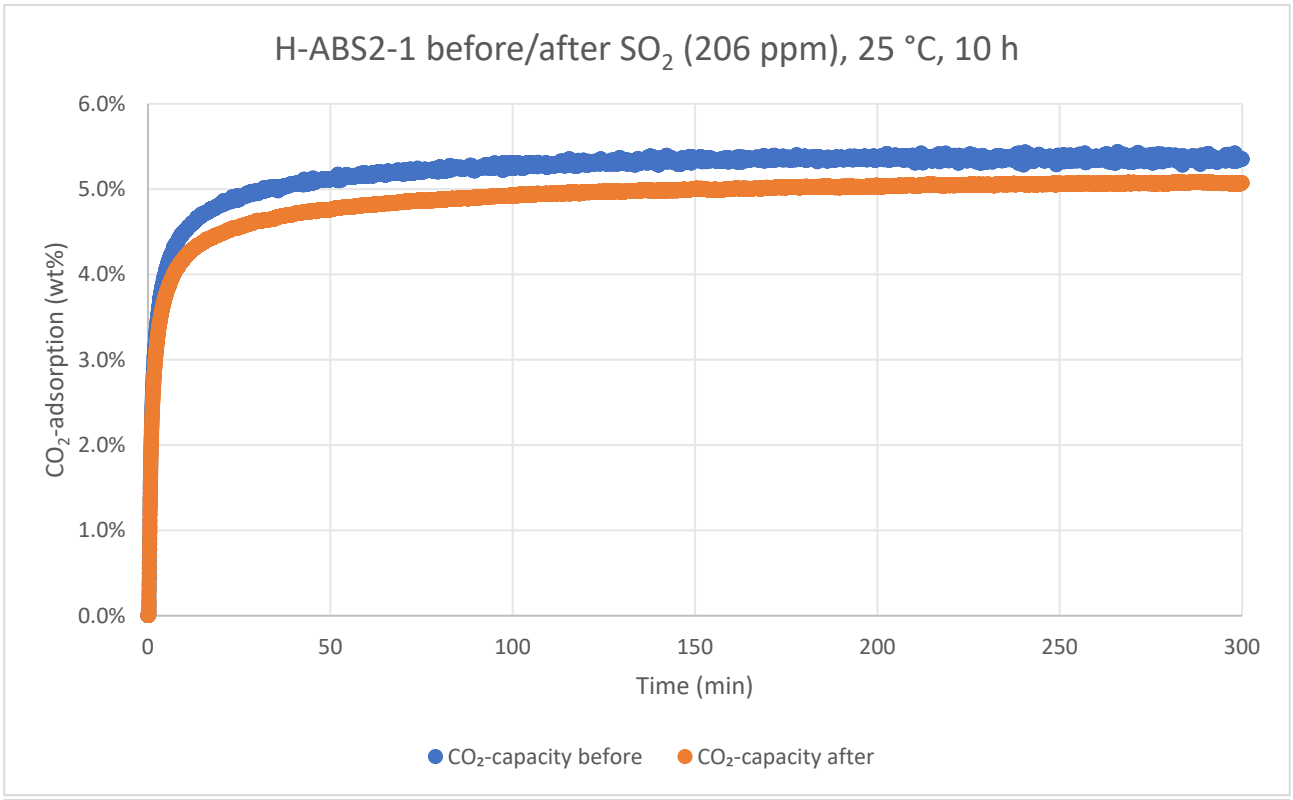

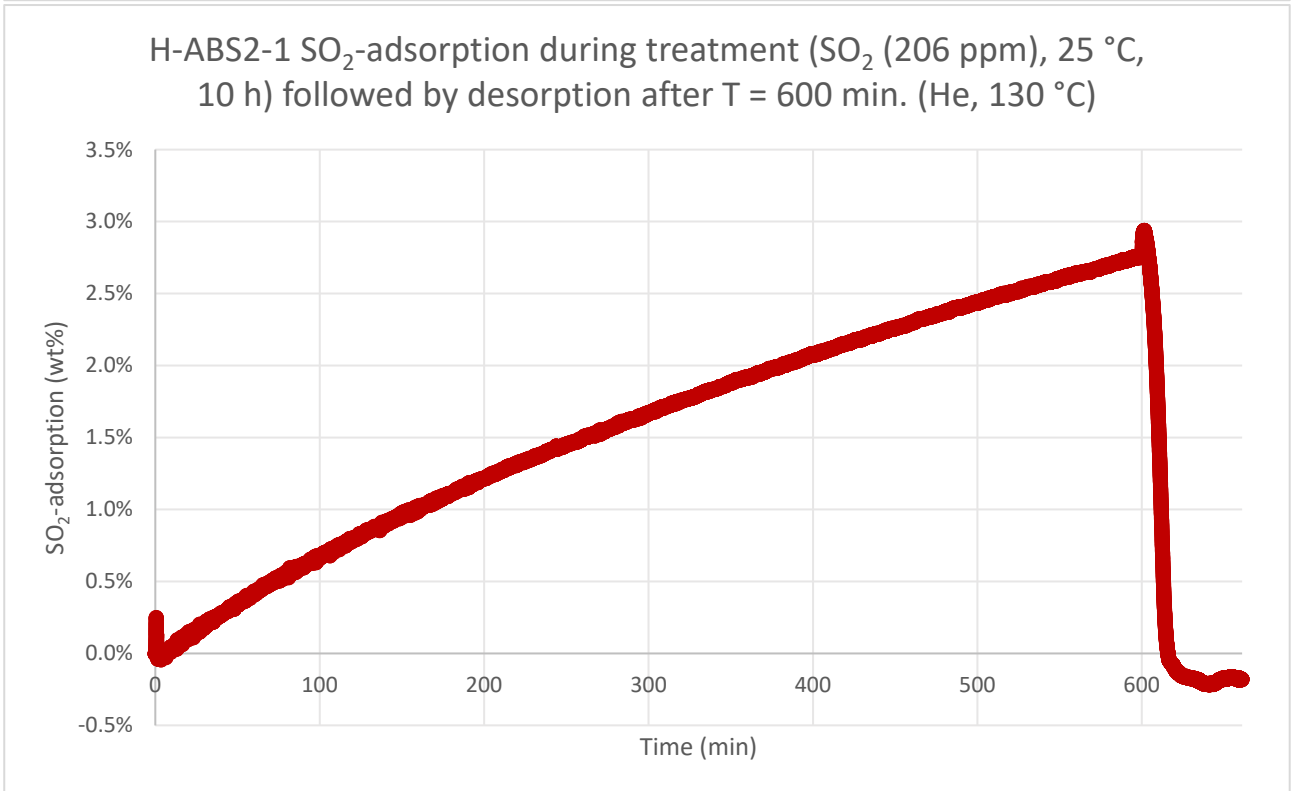

H-ABS2-1 SO_2-capacity (10 h) was 2.8 wt% before and -0.2 wt% after desorption. Note: The negative wt% is likely caused by a minor loss of the material in the 100 mL/min gas flow.

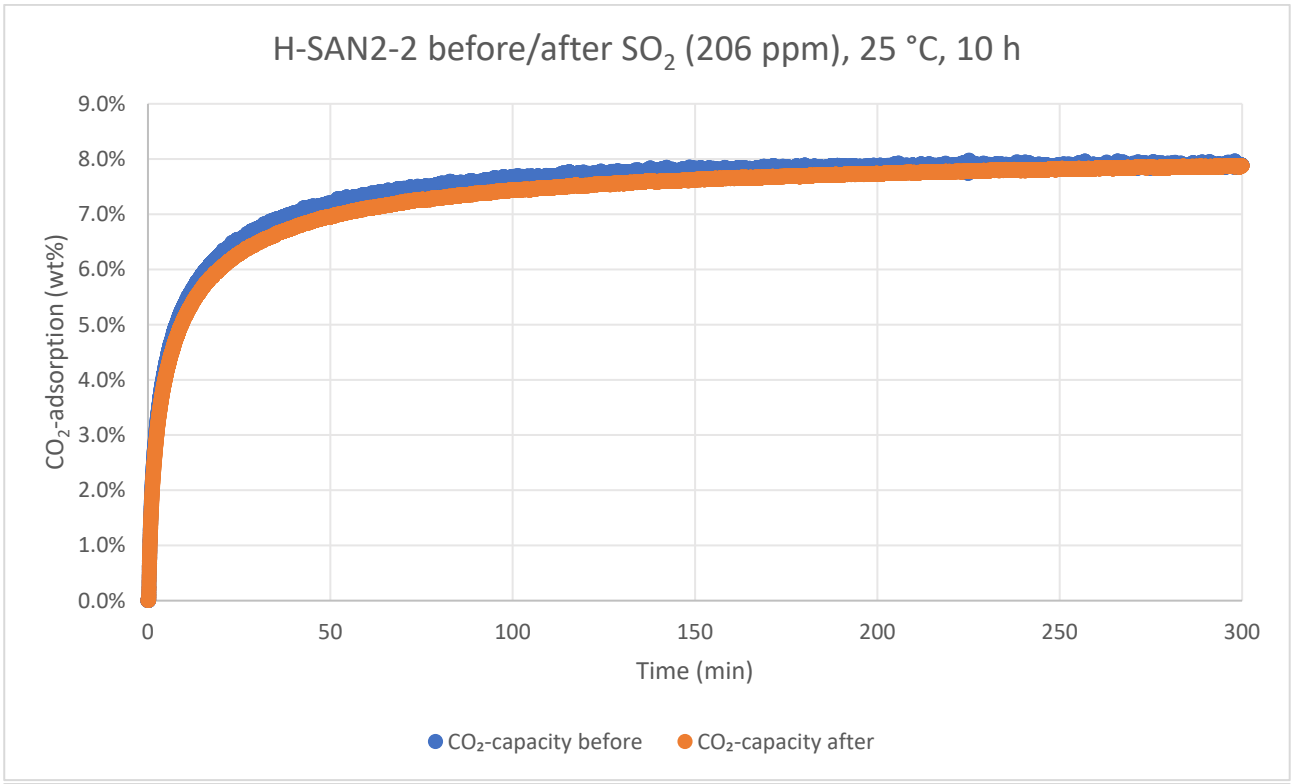

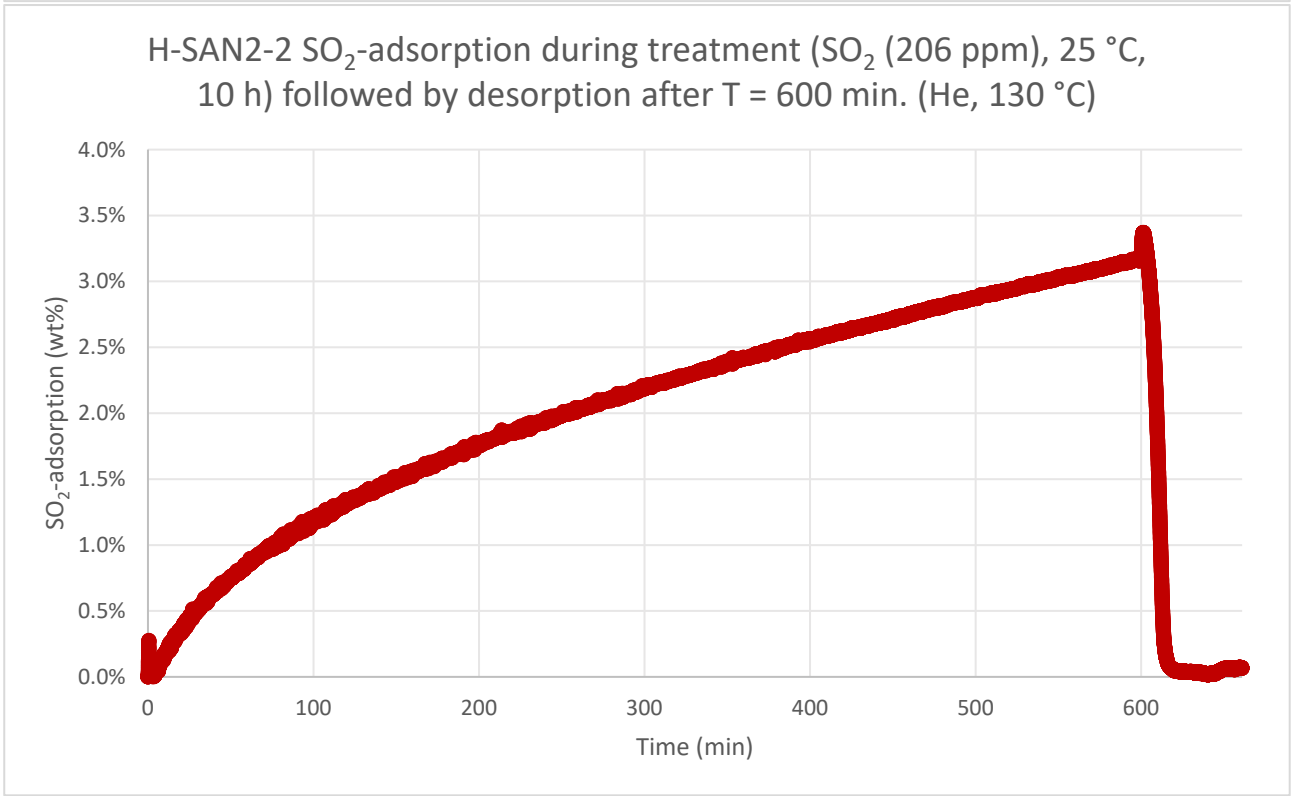

H-SAN2-2 SO_2-capacity (10 h) was 3.2 wt% before and 0.1 wt% after desorption.

The three adsorbents showed high stability towards SO_2 (retentions ranging from 93−100%) compared to the Lewatit benchmark adsorbent (50% retention). This could be explained, as with NO_2 stability (vide supra), by less exposed amines in the three adsorbents compared to the macro-porous Lewatit, thus the amine sites are more protected from SO_2. This hypothesis is further supported by the significantly higher SO_2-adsorption of Lewatit (20 wt%) compared to the three adsorbents (2.8−6.4 wt%). IR-spectroscopic analysis showed highly similar bands to the IR-spectra of the adsorbents before and after SO_2, supporting the finding of low degrees of deactivation.

SO_2 (206 ppm), 25 °C, 10 h. Stress test	**CO_2-capacity before** (wt%)	**CO_2-capacity after** (wt%)	**Capacity retained** (%)
H-NBR2-2	7.5	7.0	93%
H-ABS2-1	5.4	5.1	95%
H-SAN2-2	7.9	7.9	100%

Table S17. CO_2-adsorption capacities at 25 °C, 5 h, before and after 10 hours of SO_2 (206 ppm in N_2) at 25 °C. In comparison, the capacity retention of Lewatit for the same treatment was found to be 50% (see Lewatit benchmark section, p. S297).

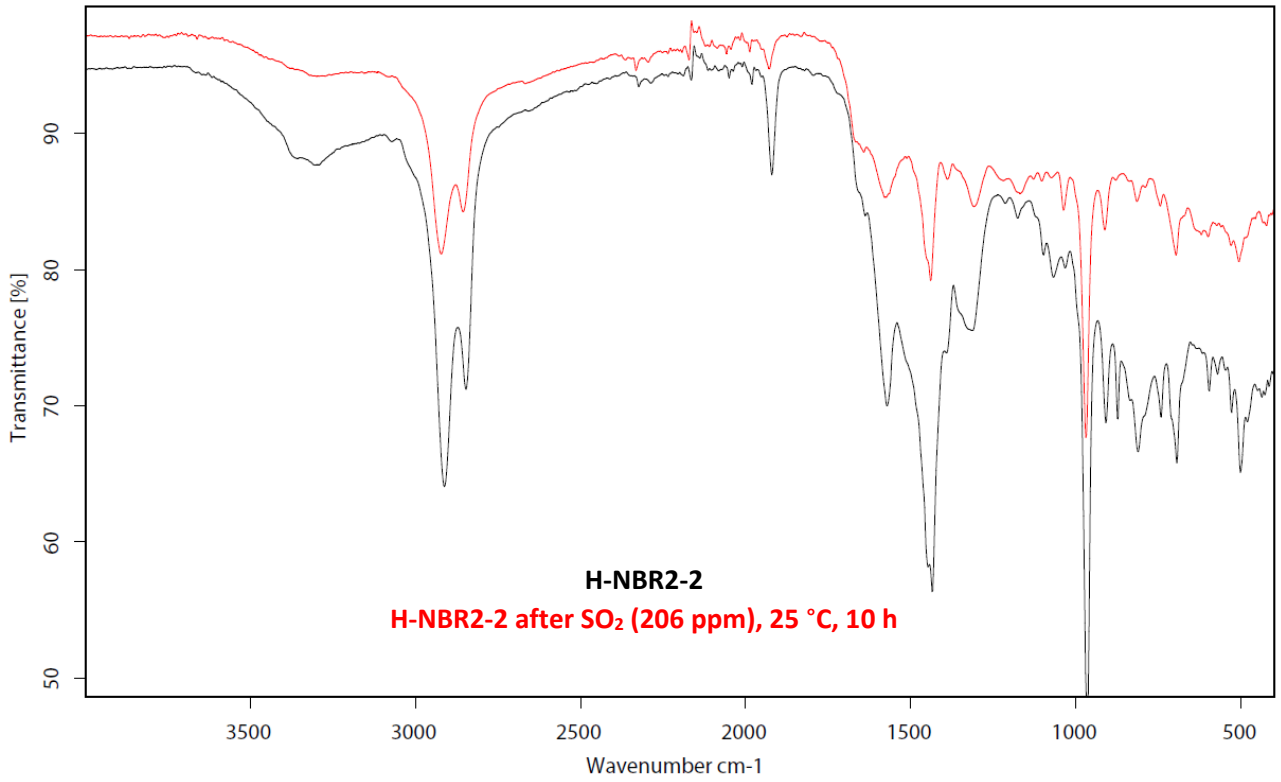

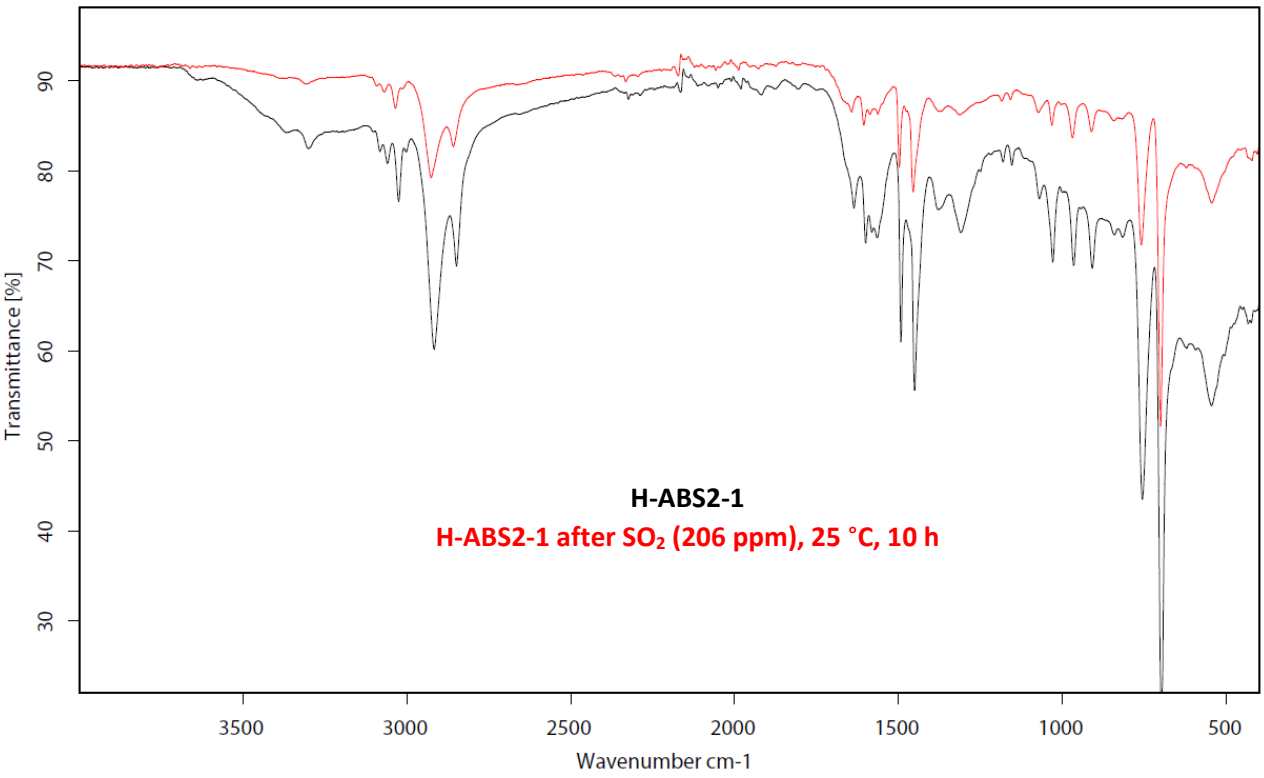
Transmittance [%]
90
80
70
60
50
40
30
3500
3000
2500
2000
1500
1000
500
Wavenumber cm-1
H-ABS2-1
H-ABS2-1 after SO2 (206 ppm), 25 °C, 10 h

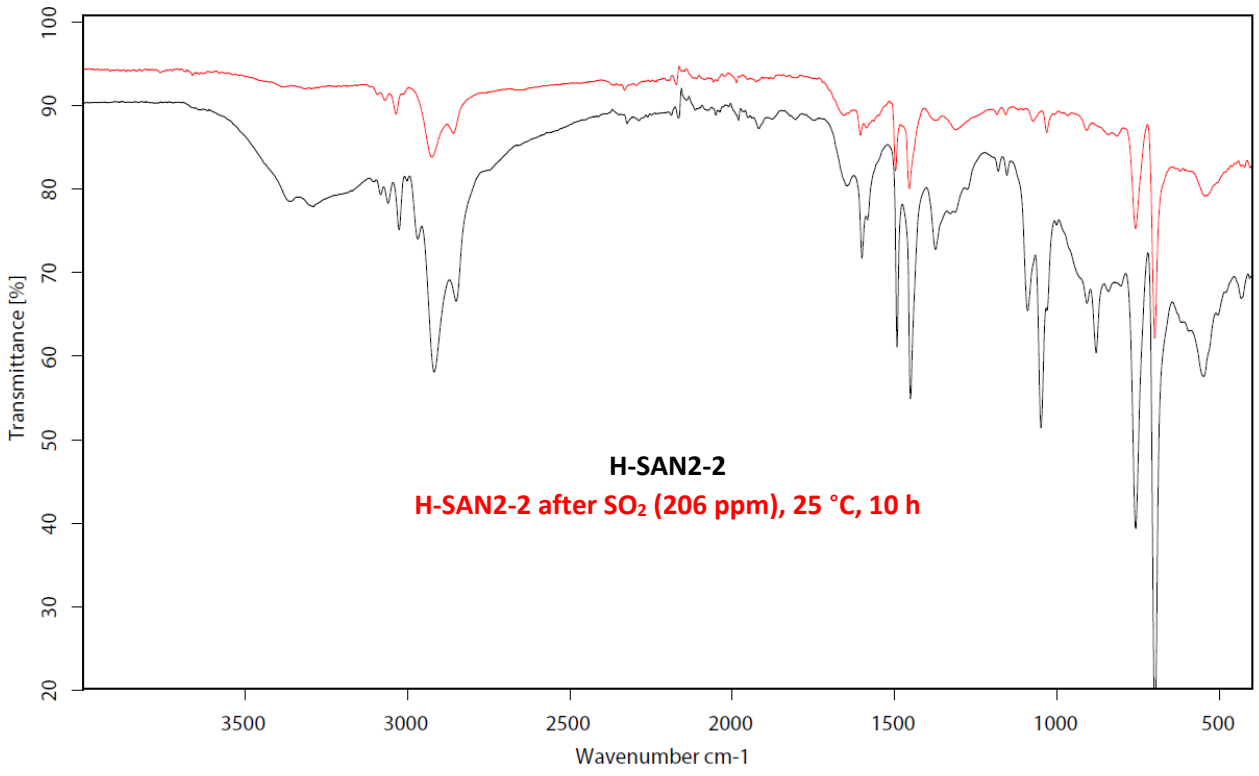
Transmittance [%]
100
90
80
70
60
50
40
30
20
3500
3000
2500
2000
1500
1000
500
Wavenumber cm-1
H-SAN2-2
H-SAN2-2 after SO2 (206 ppm), 25 °C, 10 h

CO_2-working capacity after 40 adsorption-desorption cycles under flue-gas relevant conditions (50 °C / 150 °C): TGA method 10 was used to measure the cycling stability of **H-NBR2**, **H-ABS2**, and **H-SAN2**, using sieved particle size fractions of -140 +500 mesh from batches **H-NBR2-3**, **H-ABS2-2**, and **H-SAN2-1**. As specified in **TGA method 10**, to simulate flue gas conditions, adsorption was conducted under CO_2 (10% balanced by N_2, 50 °C, 15 min.) while desorption was carried out using CO_2 (100%, 150 °C, 15 min.) followed by helium purging to remove non-desorbed CO_2 before the subsequential adsorption step. Working capacities were calculated from the mass difference between the sample mass after adsorption, and the sample mass after desorption in hot CO_2.

HNBR2-3			
Cycle number	Working capacity (wt%)	Working capacity (mmol/g)	Retention of working capacity (%)
1	1.79%	0.41	100%
2	1.73%	0.39	96%
3	1.71%	0.39	95%
4	1.67%	0.38	93%
5	1.67%	0.38	93%
6	1.66%	0.38	92%
7	1.64%	0.37	92%
8	1.64%	0.37	91%
9	1.62%	0.37	90%
10	1.63%	0.37	91%
11	1.62%	0.37	91%
12	1.62%	0.37	90%
13	1.60%	0.36	89%
14	1.61%	0.37	90%
15	1.60%	0.36	89%
16	1.59%	0.36	89%
17	1.59%	0.36	88%
18	1.58%	0.36	88%
19	1.58%	0.36	88%
20	1.56%	0.35	87%
21	1.57%	0.36	87%
22	1.56%	0.35	87%
23	1.56%	0.35	87%
24	1.55%	0.35	87%
25	1.55%	0.35	86%
26	1.55%	0.35	87%
27	1.54%	0.35	86%
28	1.55%	0.35	86%
29	1.54%	0.35	86%
30	1.55%	0.35	86%
31	1.54%	0.35	86%
32	1.53%	0.35	85%
33	1.54%	0.35	86%
34	1.53%	0.35	85%
35	1.53%	0.35	85%
36	1.52%	0.35	85%
37	1.52%	0.34	85%
38	1.52%	0.34	85%
39	1.52%	0.35	85%
40	1.52%	0.34	84%

HABS2-2			
Cycle number	Working capacity (wt%)	Working capacity (mmol/g)	Retention of working capacity (%)
1	1.42%	0.32	100%
2	1.39%	0.32	98%
3	1.36%	0.31	95%
4	1.33%	0.30	93%
5	1.31%	0.30	92%
6	1.30%	0.29	91%
7	1.28%	0.29	90%
8	1.28%	0.29	90%
9	1.27%	0.29	89%
10	1.26%	0.29	89%
11	1.28%	0.29	90%
12	1.27%	0.29	89%
13	1.25%	0.28	88%
14	1.25%	0.28	88%
15	1.25%	0.28	88%
16	1.23%	0.28	86%
17	1.22%	0.28	86%
18	1.23%	0.28	86%
19	1.22%	0.28	86%
20	1.20%	0.27	84%
21	1.21%	0.27	85%
22	1.20%	0.27	84%
23	1.20%	0.27	84%
24	1.21%	0.27	85%
25	1.22%	0.28	86%
26	1.20%	0.27	84%
27	1.20%	0.27	84%
28	1.20%	0.27	84%
29	1.20%	0.27	84%
30	1.20%	0.27	85%
31	1.19%	0.27	84%
32	1.19%	0.27	84%
33	1.20%	0.27	84%
34	1.19%	0.27	84%
35	1.19%	0.27	84%
36	1.18%	0.27	83%
37	1.18%	0.27	83%
38	1.18%	0.27	83%
39	1.18%	0.27	83%
40	1.18%	0.27	83%

HSAN2-1			
Cycle number	Working capacity (wt%)	Working capacity (mmol/g)	Retention of working capacity (%)
1	1.87%	0.43	100%
2	1.63%	0.37	87%
3	1.59%	0.36	85%
4	1.56%	0.35	83%
5	1.52%	0.35	81%
6	1.52%	0.34	81%
7	1.50%	0.34	80%
8	1.48%	0.34	79%
9	1.48%	0.34	79%
10	1.48%	0.34	79%
11	1.47%	0.33	79%
12	1.46%	0.33	78%
13	1.45%	0.33	77%
14	1.46%	0.33	78%
15	1.45%	0.33	77%
16	1.44%	0.33	77%
17	1.44%	0.33	77%
18	1.44%	0.33	77%
19	1.43%	0.33	76%
20	1.41%	0.32	75%
21	1.41%	0.32	76%
22	1.41%	0.32	75%
23	1.41%	0.32	75%
24	1.39%	0.32	74%
25	1.40%	0.32	75%
26	1.40%	0.32	75%
27	1.39%	0.32	74%
28	1.40%	0.32	75%
29	1.39%	0.32	74%
30	1.40%	0.32	75%
31	1.39%	0.32	74%
32	1.38%	0.31	74%
33	1.42%	0.32	76%
34	1.40%	0.32	75%
35	1.40%	0.32	75%
36	1.39%	0.32	74%
37	1.40%	0.32	75%
38	1.39%	0.32	74%
39	1.40%	0.32	75%
40	1.40%	0.32	75%

Lewatit			
Cycle number	Working capacity (wt%)	Working capacity (mmol/g)	Retention of working capacity (%)
1	6.77%	1.54	100%
2	6.70%	1.52	99%
3	6.67%	1.52	99%
4	6.64%	1.51	98%
5	6.62%	1.50	98%
6	6.62%	1.50	98%
7	6.59%	1.50	97%
8	6.58%	1.50	97%
9	6.58%	1.49	97%
10	6.58%	1.49	97%
11	6.58%	1.50	97%
12	6.55%	1.49	97%
13	6.54%	1.49	97%
14	6.55%	1.49	97%
15	6.55%	1.49	97%
16	6.52%	1.48	96%
17	6.51%	1.48	96%
18	6.52%	1.48	96%
19	6.48%	1.47	96%
20	6.45%	1.47	95%
21	6.47%	1.47	96%
22	6.45%	1.47	95%
23	6.43%	1.46	95%
24	6.41%	1.46	95%
25	6.42%	1.46	95%
26	6.39%	1.45	94%
27	6.37%	1.45	94%
28	6.36%	1.45	94%
29	6.36%	1.45	94%
30	6.37%	1.45	94%
31	6.34%	1.44	94%
32	6.32%	1.44	93%
33	6.32%	1.44	93%
34	6.33%	1.44	93%
35	6.30%	1.43	93%
36	6.29%	1.43	93%
37	6.26%	1.42	92%
38	6.27%	1.42	93%
39	6.28%	1.43	93%
40	6.27%	1.42	93%

The 40 adsorption-desorption cycles under flue gas relevant conditions show minor decreases in CO_2-working capacity to give capacity retentions of 75% (**H-SAN2-1**), 84% (**H-NBR2-3**), and 83% (**H-ABS2-2**). In comparison, the capacity retention of the Lewatit benchmark material was 93%. We do, however, observe that the capacity loss is most significant within the first 10 cycles for **H-ABS2-2** and **H-SAN2-1**, after which it stabilises (see Fig. 4b). No significant structural changes were observed by IR-spectroscopic analysis before and after the 40 sorption cycles, however although the corresponding IR-bands are not clearly visible, we suggest urea-formation to be the major cause for loss of CO_2-capacity, as was earlier observed for **H-NBR1**, **H-NBR2**, and **HCN*-NBR2**.

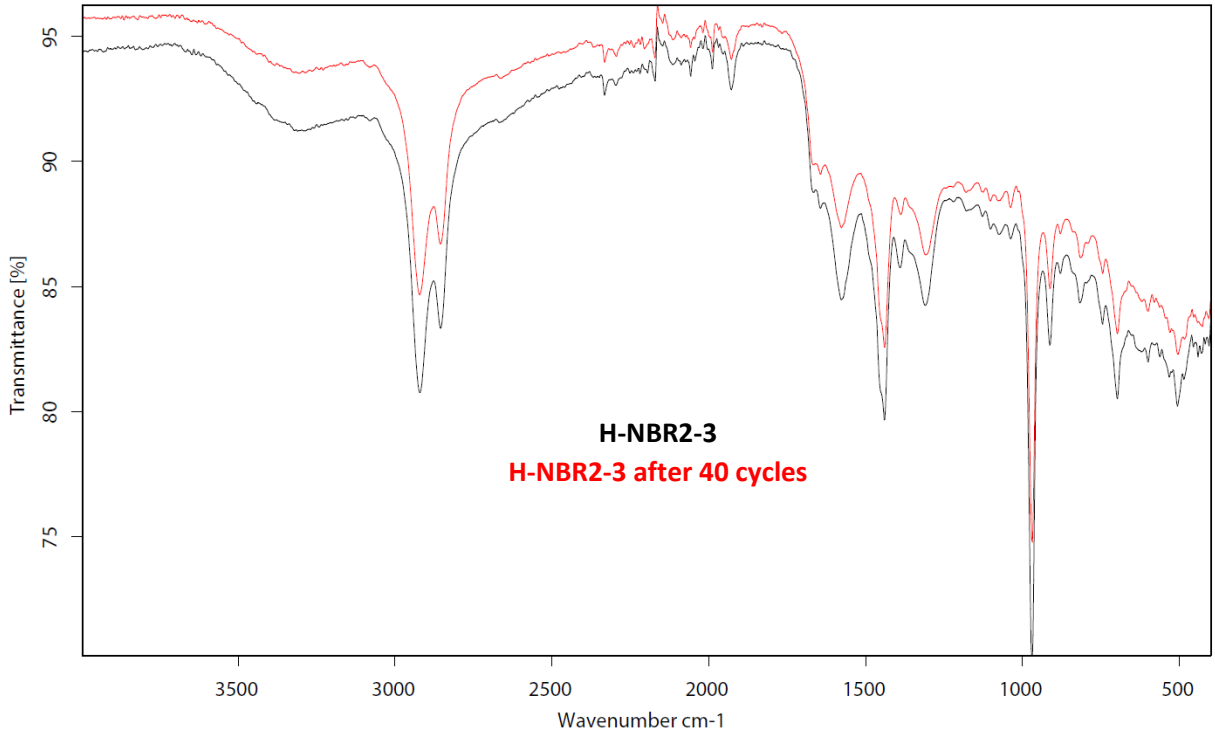

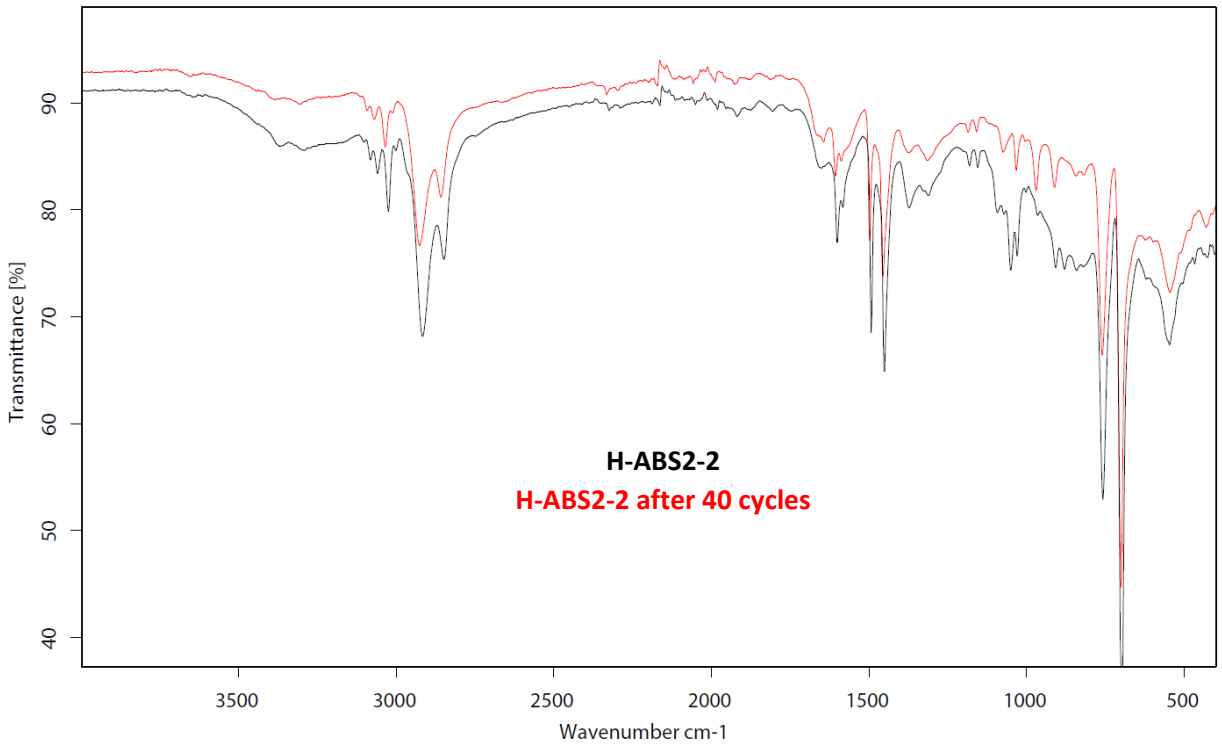
Transmittance [%]
90
80
70
60
50
40
3500
3000
2500
2000
1500
1000
500
Wavenumber cm-1
H-ABS2-2
H-ABS2-2 after 40 cycles

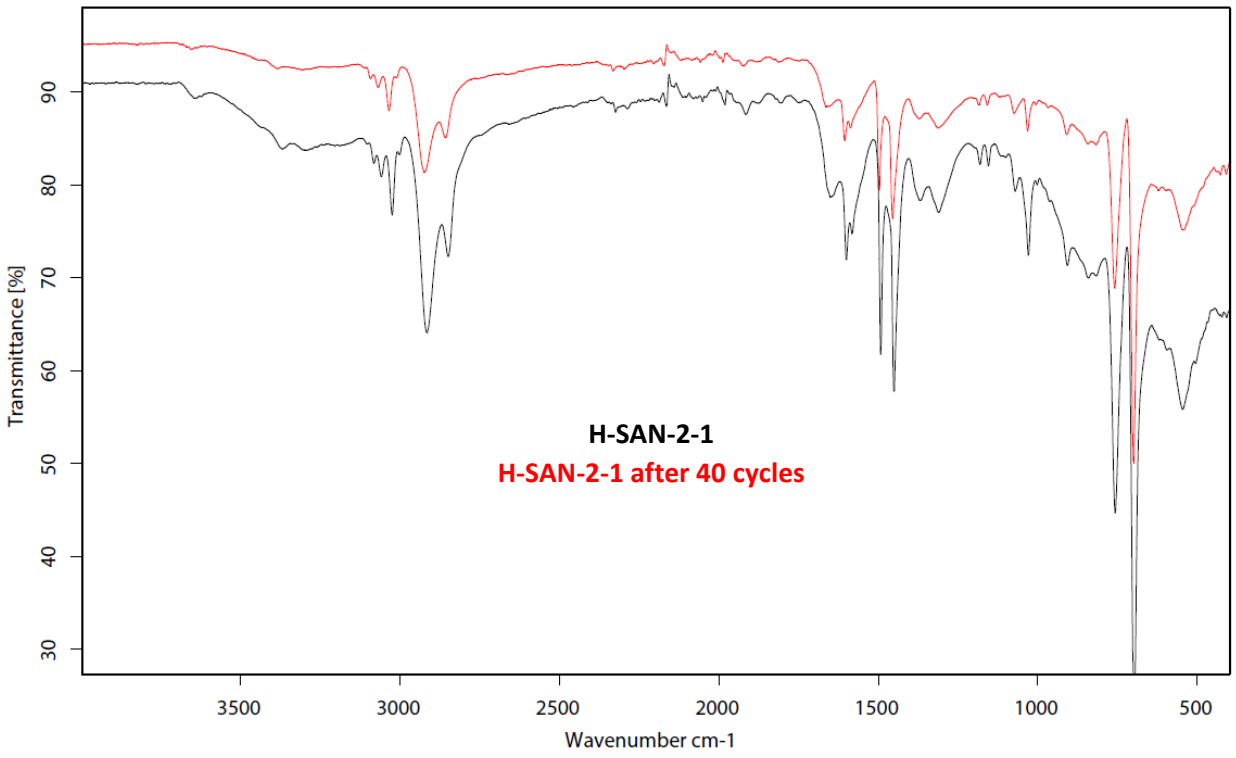
Transmittance [%]
90
80
70
60
50
40
30
3500
3000
2500
2000
1500
1000
500
Wavenumber cm-1
H-SAN-2-1
H-SAN-2-1 after 40 cycles

Desorption study with helium as the purge gas

The desorption degree after a 5 h CO_2-adsorption (100% CO_2, 25 °C, 5 h, **TGA method 11**) was studied using helium as a purge gas at different temperatures, residing at each temperature for 30 min (and finally 12 min at 130 °C). The results are from measurements of **H-NBR2-3**, **HABS2-2**, and **H-SAN2-1**.

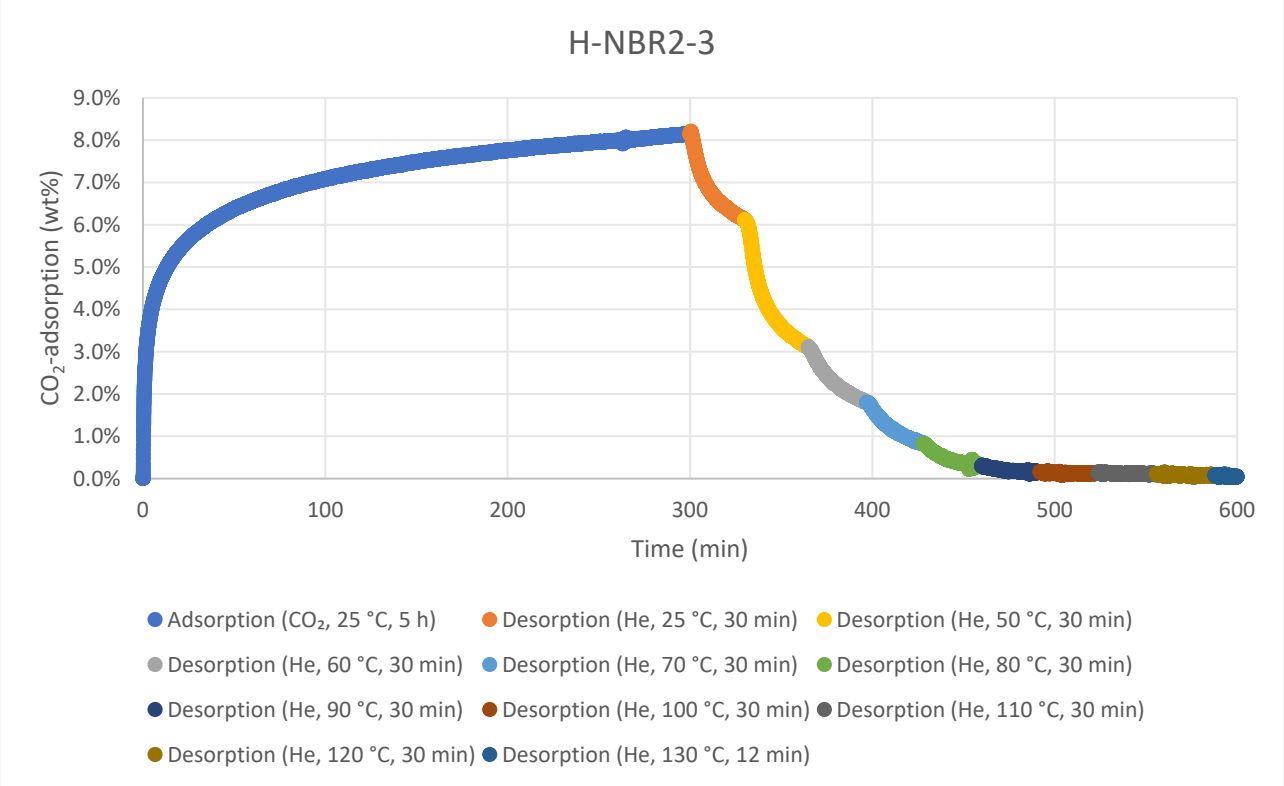

H-NBR2-3	wt%	Desorption degree (%)
CO_2-capacity (5 h)	8.1%	
Capacity after He (30 min, 25 °C)	6.1%	25%
Capacity after He (30 min, 50 °C)	3.1%	62%
Capacity after He (30 min, 60 °C)	1.8%	78%
Capacity after He (30 min, 70 °C)	0.8%	90%
Capacity after He (30 min, 80 °C)	0.3%	96%
Capacity after He (30 min, 90 °C)	0.2%	98%
Capacity after He (30 min, 100 °C)	0.1%	98%
Capacity after He (30 min, 110 °C)	0.1%	99%
Capacity after He (30 min, 120 °C)	0.08%	99%
Capacity after He (12 min, 130 °C)	0.04%	99%

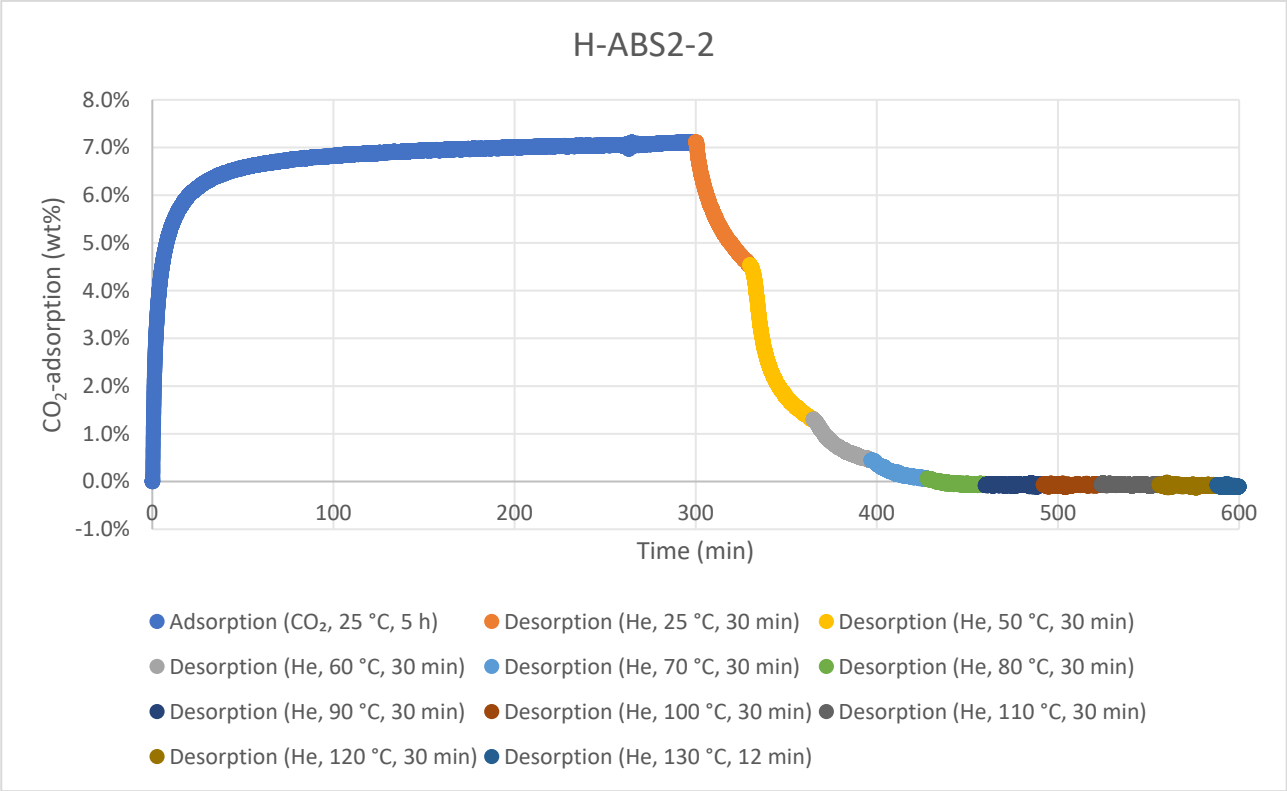

H-ABS2-2	wt%	Desorption degree (%)
CO_2-capacity (5 h)	7.1%	
Capacity after He (30 min, 25 °C)	4.5%	36%
Capacity after He (30 min, 50 °C)	1.3%	82%
Capacity after He (30 min, 60 °C)	0.4%	94%
Capacity after He (30 min, 70 °C)	0.06%	99%
Capacity after He (30 min, 80 °C)	-0.09%	100%
Capacity after He (30 min, 90 °C)	-0.07%	100%
Capacity after He (30 min, 100 °C)	-0.07%	100%
Capacity after He (30 min, 110 °C)	-0.07%	100%
Capacity after He (30 min, 120 °C)	-0.07%	100%
Capacity after He (12 min, 130 °C)	-0.1%	100%

Note: The negative wt% capacity can be attributed to a minor loss of adsorbent powder due to the 100 mL/min gas flow.

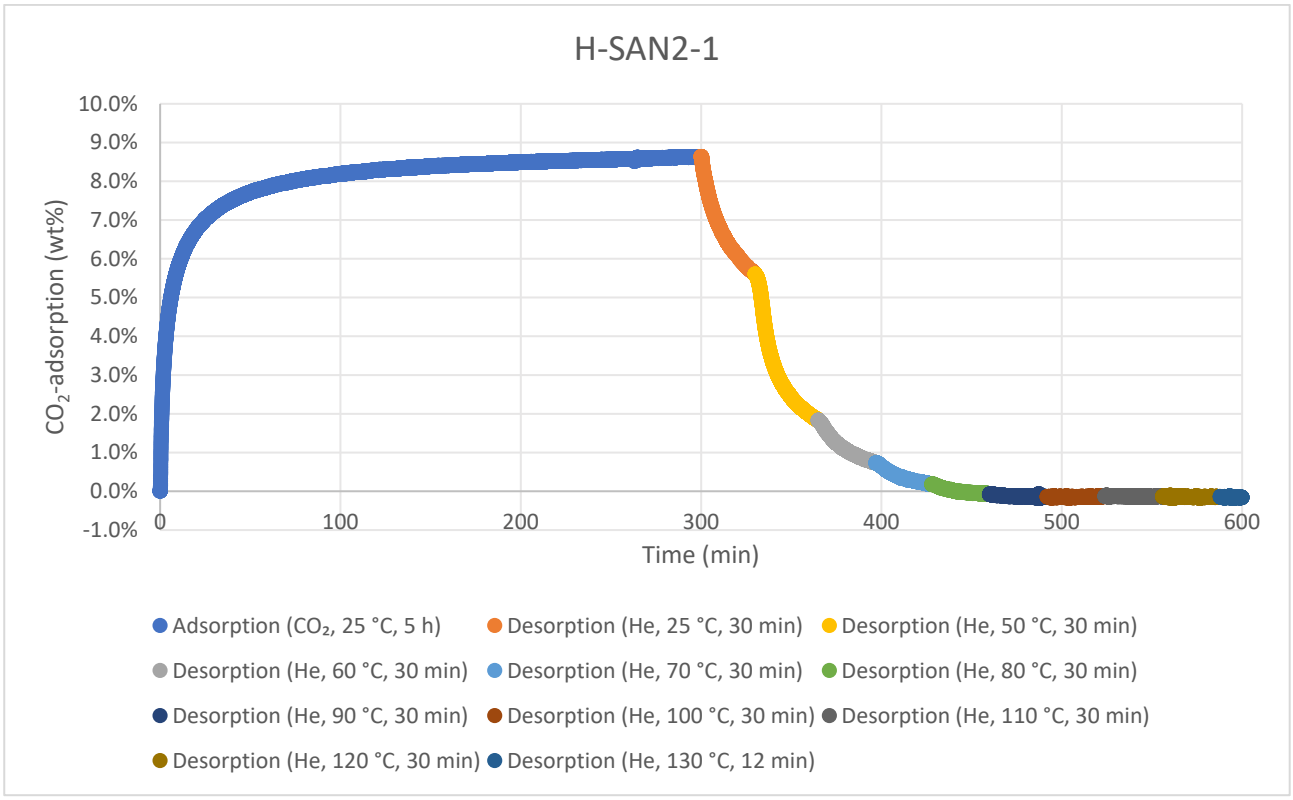

H-SAN2-1	wt%	Desorption degree (%)
CO_2-capacity (5 h)	8.6%	
Capacity after He (30 min, 25 °C)	5.6%	35%
Capacity after He (30 min, 50 °C)	1.8%	79%
Capacity after He (30 min, 60 °C)	0.7%	92%
Capacity after He (30 min, 70 °C)	0.2%	98%
Capacity after He (30 min, 80 °C)	-0.1%	100%
Capacity after He (30 min, 90 °C)	-0.2%	100%
Capacity after He (30 min, 100 °C)	-0.1%	100%
Capacity after He (30 min, 110 °C)	-0.1%	100%
Capacity after He (30 min, 120 °C)	-0.1%	100%
Capacity after He (12 min, 130 °C)	-0.2%	100%

Note: The negative wt% capacity can be attributed to a minor loss of adsorbent powder due to the 100 mL/min gas flow.

Desorption study with CO_2 as the purge gas

The desorption degree after CO_2-adsorption (100% CO_2, 25 °C, 5 h, **TGA method 12**) was studied using CO_2 (100%) as a purge gas at different temperatures, residing at each temperature for 30 min. The results are from measurements of samples sieved to a particle size range of -140 +500 mesh.

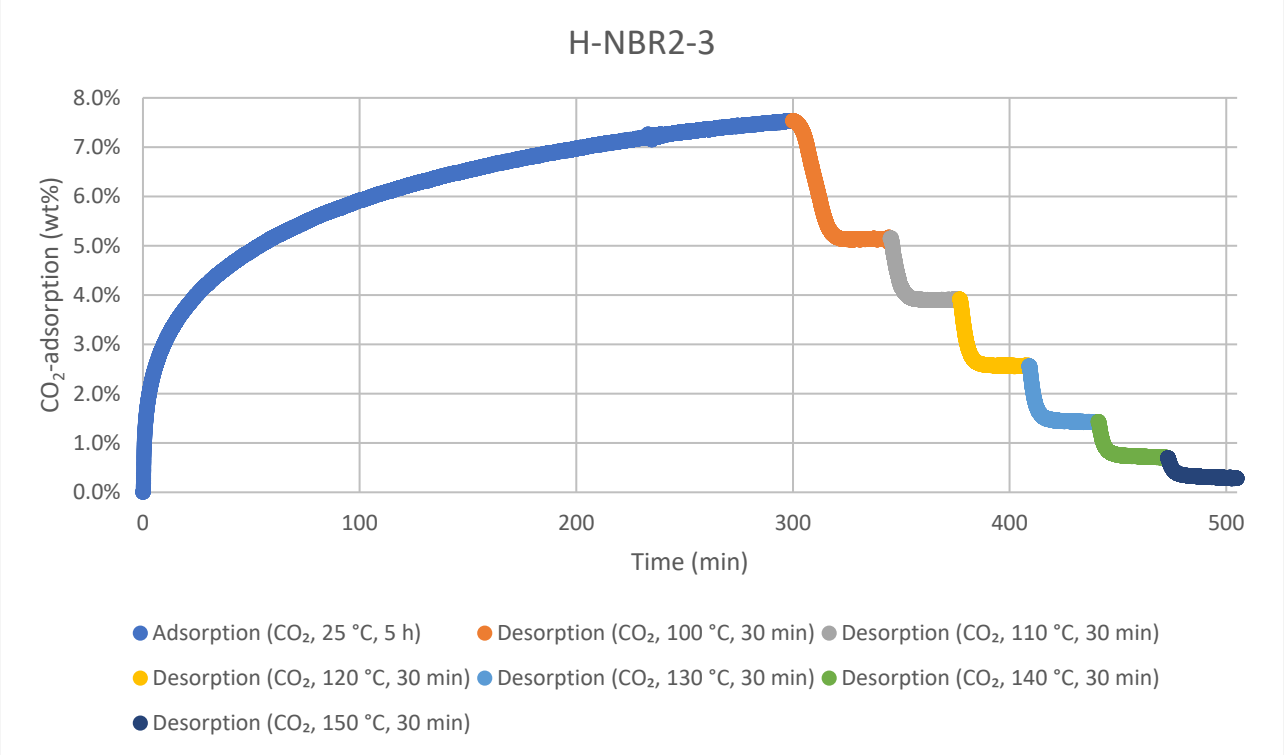

H-NBR2-3	wt%	Desorption degree (%)
CO_2-capacity (5 h)	7.5%	
Capacity after CO_2 (30 min, 100 °C)	5.1%	32%
Capacity after CO_2 (30 min, 110 °C)	3.9%	48%
Capacity after CO_2 (30 min, 120 °C)	2.5%	66%
Capacity after CO_2 (30 min, 130 °C)	1.4%	81%
Capacity after CO_2 (30 min, 140 °C)	0.7%	91%
Capacity after CO_2 (30 min, 150 °C)	0.3%	96%

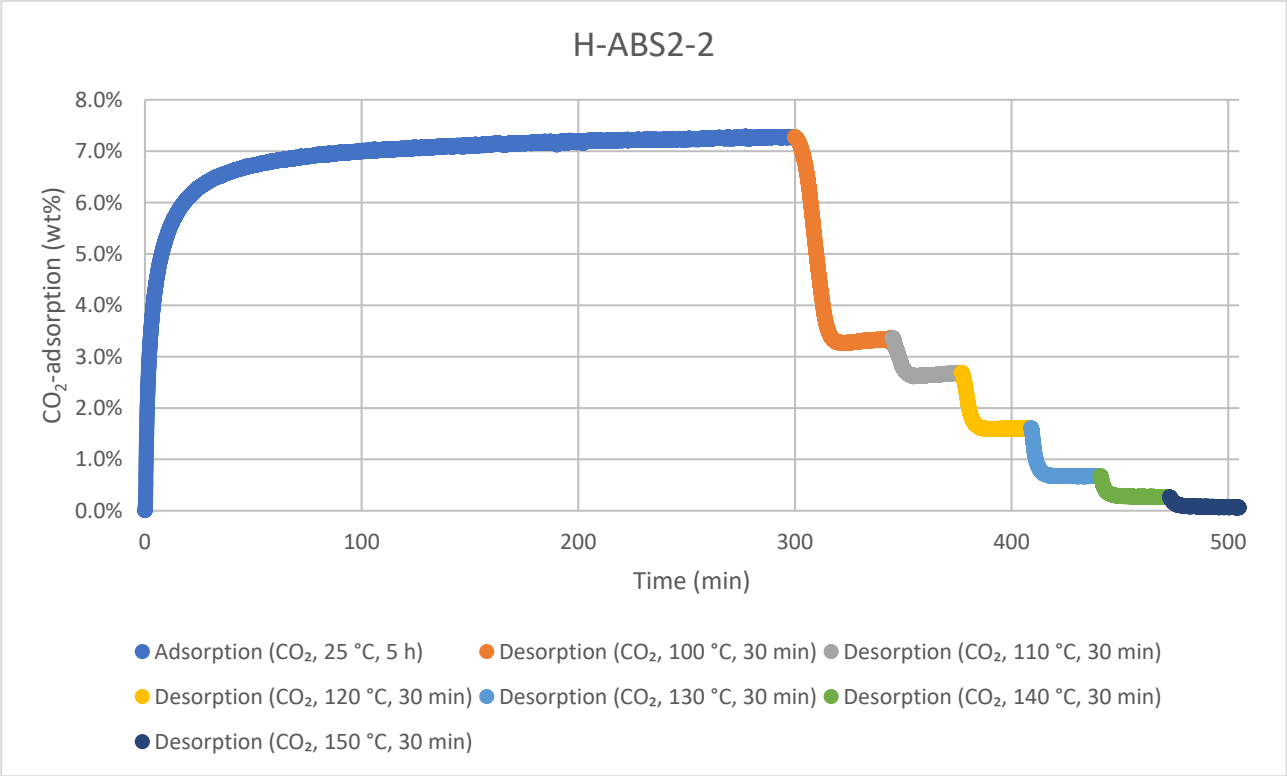

H-ABS2-2	wt%	Desorption degree (%)
CO_2-capacity (5 h)	7.3%	
Capacity after CO_2 (30 min, 100 °C)	3.3%	54%
Capacity after CO_2 (30 min, 110 °C)	2.7%	63%
Capacity after CO_2 (30 min, 120 °C)	1.6%	78%
Capacity after CO_2 (30 min, 130 °C)	0.7%	91%
Capacity after CO_2 (30 min, 140 °C)	0.3%	96%
Capacity after CO_2 (30 min, 150 °C)	0.1%	99%

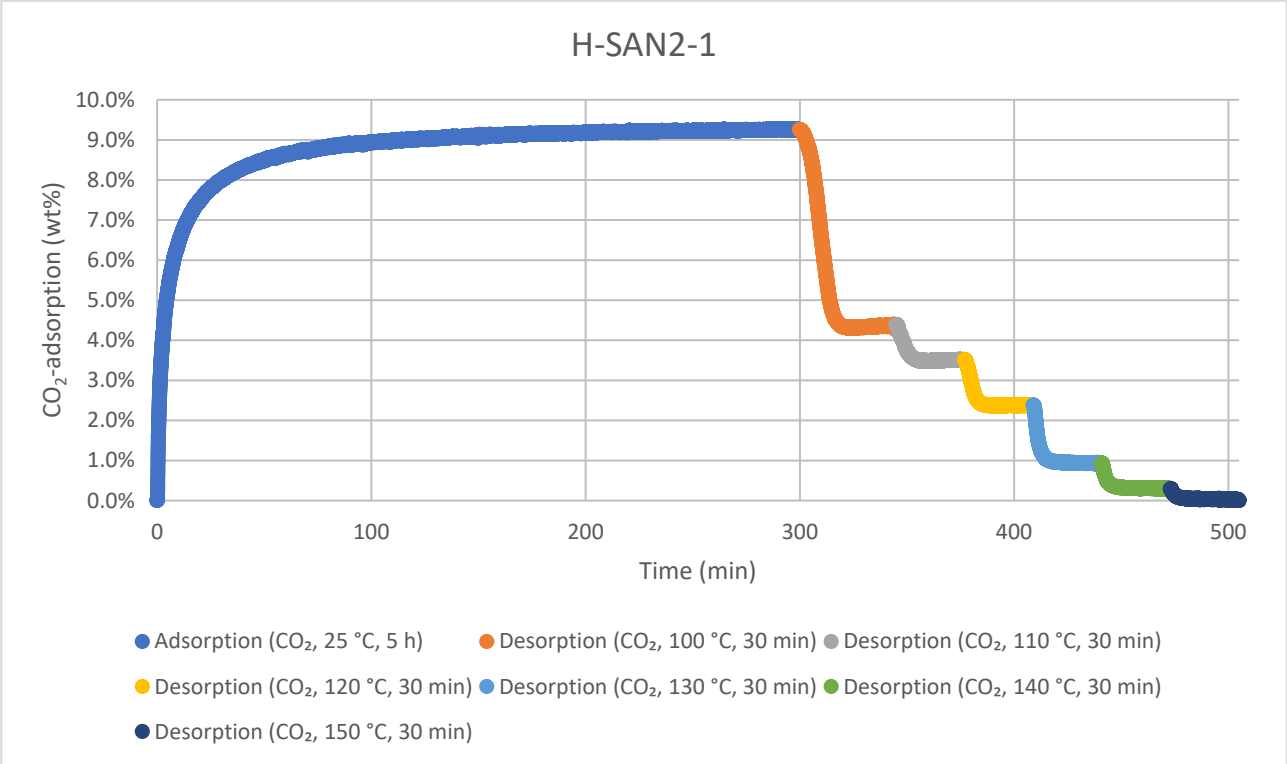

H-SAN2-1	wt%	Desorption degree (%)
CO_2-capacity (5 h)	9.3%	
Capacity after CO_2 (30 min, 100 °C)	4.4%	53%
Capacity after CO_2 (30 min, 110 °C)	3.5%	62%
Capacity after CO_2 (30 min, 120 °C)	2.4%	74%
Capacity after CO_2 (30 min, 130 °C)	0.9%	90%
Capacity after CO_2 (30 min, 140 °C)	0.3%	97%
Capacity after CO_2 (30 min, 150 °C)	0.0%	100%

Slow desorption of CO_2-loaded samples (heating rate of 1K min^{-1} in helium after 5 hours under 100% CO_2 at 25 °C) (TGA method 13):

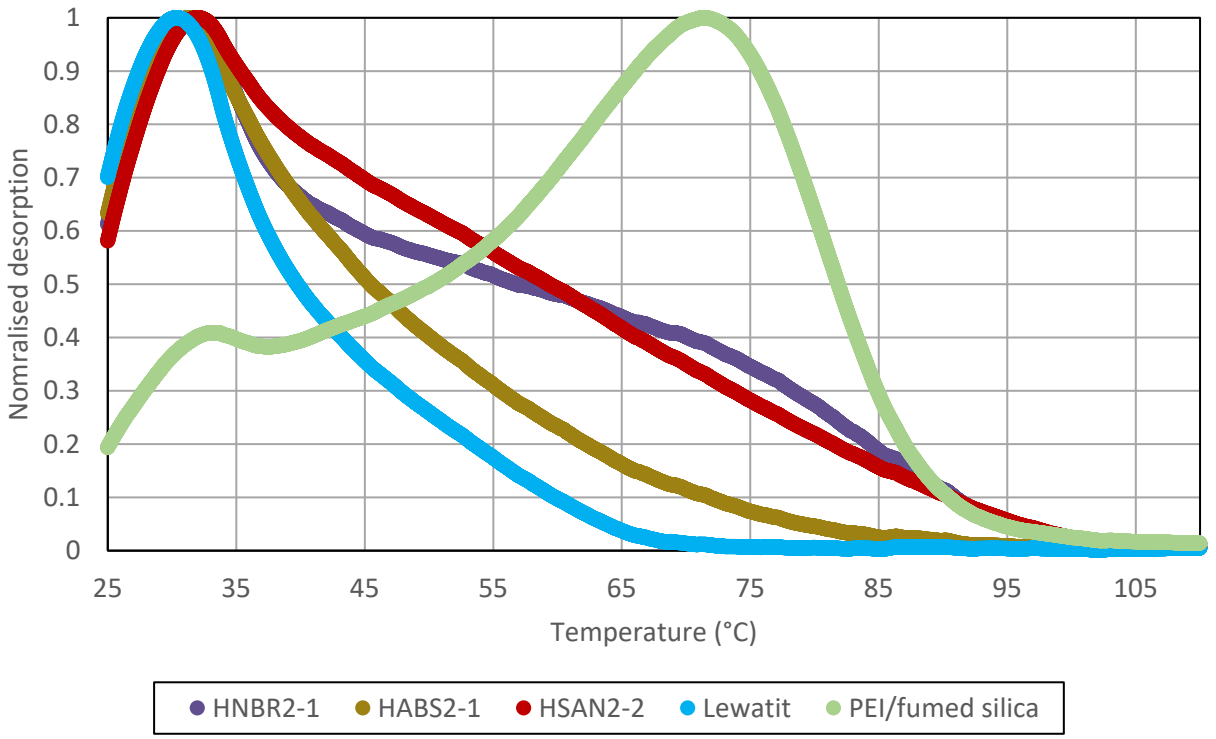

As can be observed from the plot, two CO_2-binding modes are present in the materials as evident from peaks at ~ 31 °C and ~ 72 °C, respectively. The peak at ~ 72 °C increases with **H-ABS2-1** < **H-SAN2-2** < **H-NBR2-1**, which follows the increasing N-content of these three materials, suggesting that this peak corresponds to an amine-chemisorbed CO_2. For an independently synthesised PEI/fumed silica adsorbent (organic loading = 41% from TGA), prepared from a previously reported procedure,[21] we observe an even larger contribution to the ~ 72 °C-peak.

Scanning Electron Microscopy (SEM)

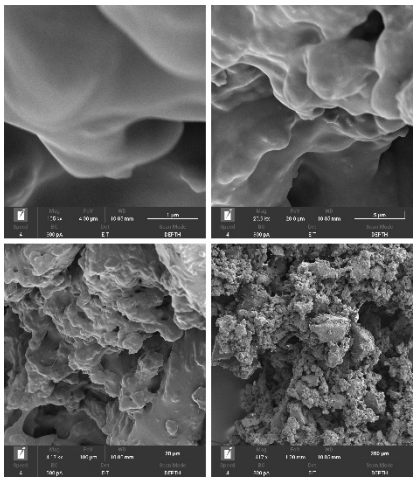

H-NBR1-2

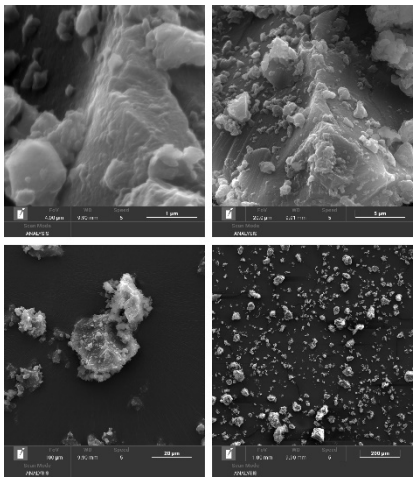

H-NBR2-1

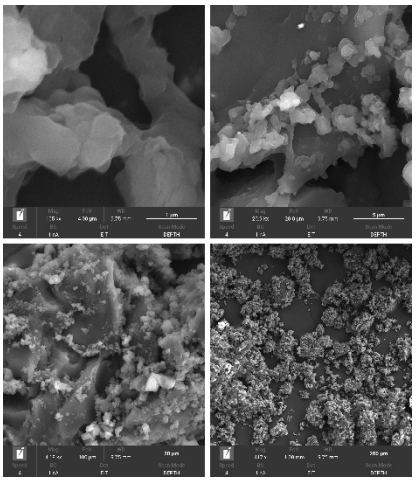

H-NBR2-2

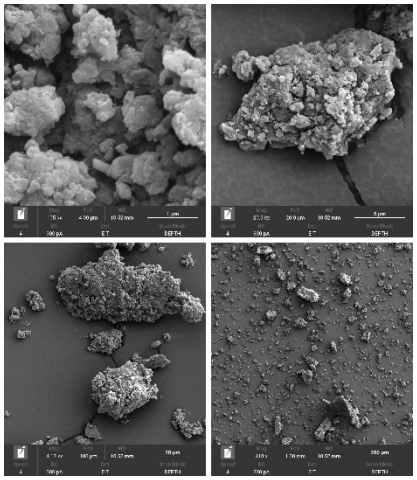

HCN*-NBR2-1

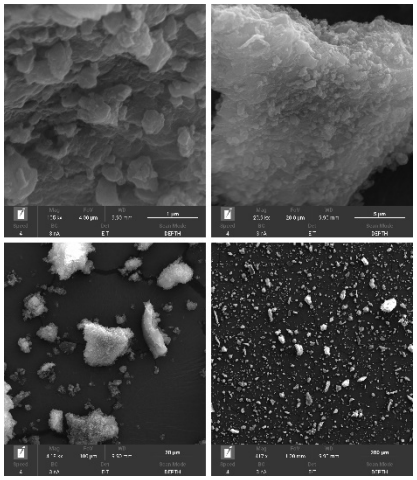

HCN*-NBR2-2

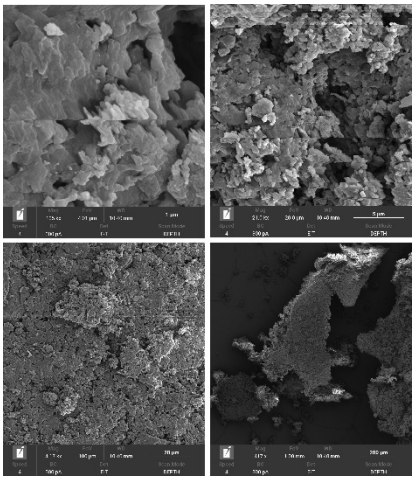

Az-HNBR2-1

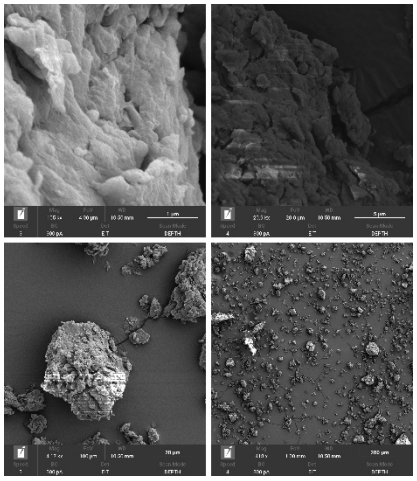

H-ABS2-2

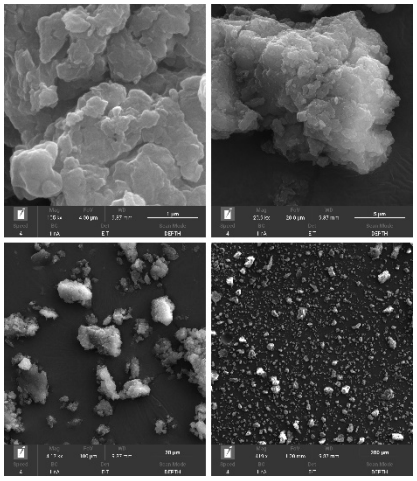

Az-HABS2-2

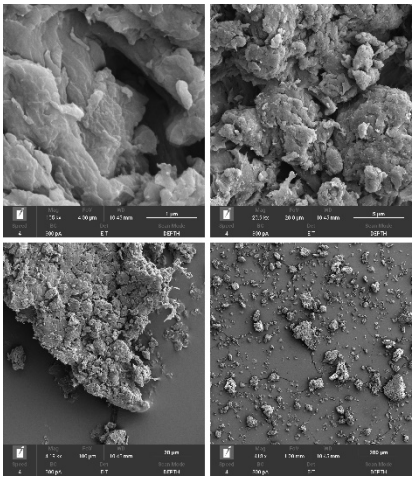

H-SAN2-2

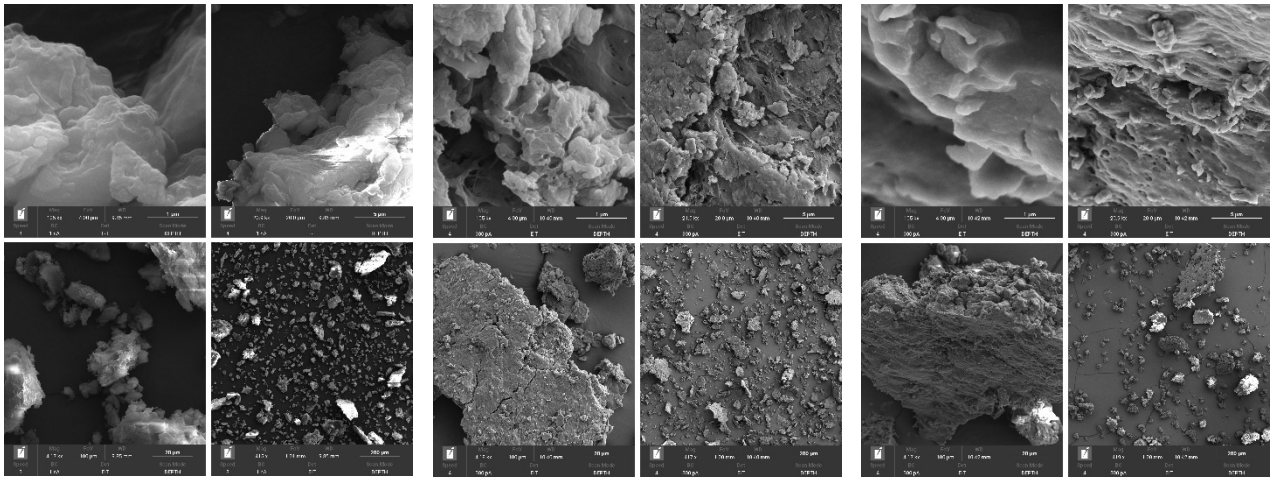

H-TEX2-2 **H-MIX-2** **HCN*-SBR2-2**

Lewatit® VP OC 1065 Benchmark Material

Lewatit® VP OC 1065 was acquired from SigmaAldrich and cryogenically milled similarly to the polymer products of this work before analysis. For certain experiments, an isolated particle size range of -140 +500 mesh, from sieve-shaking, was used, and is indicated for the specific experiments.

CO_2-adsorption (25 °C, 50 °C, and 90 °C, using CO_2 100% or 10% balanced by N_2, TGA method 2):

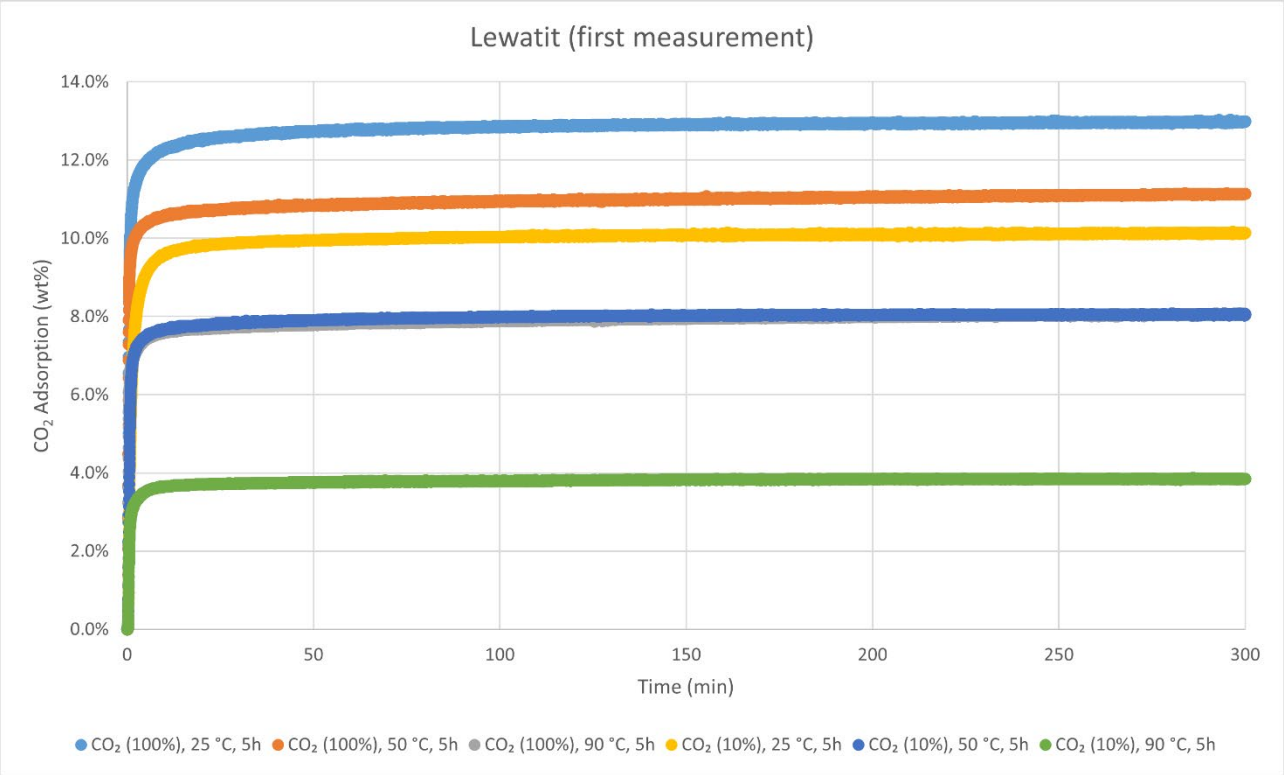

CO_2 adsorption using **TGA method 2** (first measurement).

Lewatit (first measurement)	wt%	mmol/g
CO_2 (100%), 25 °C, 5h	13%	2.95
CO_2 (100%), 50 °C, 5h	11%	2.53
CO_2 (100%), 90 °C, 5h	8.0%	1.83
CO_2 (10%), 25 °C, 5h	10%	2.30
CO_2 (10%), 50 °C, 5h	8.1%	1.83
CO_2 (10%), 90 °C, 5h	3.8%	0.87

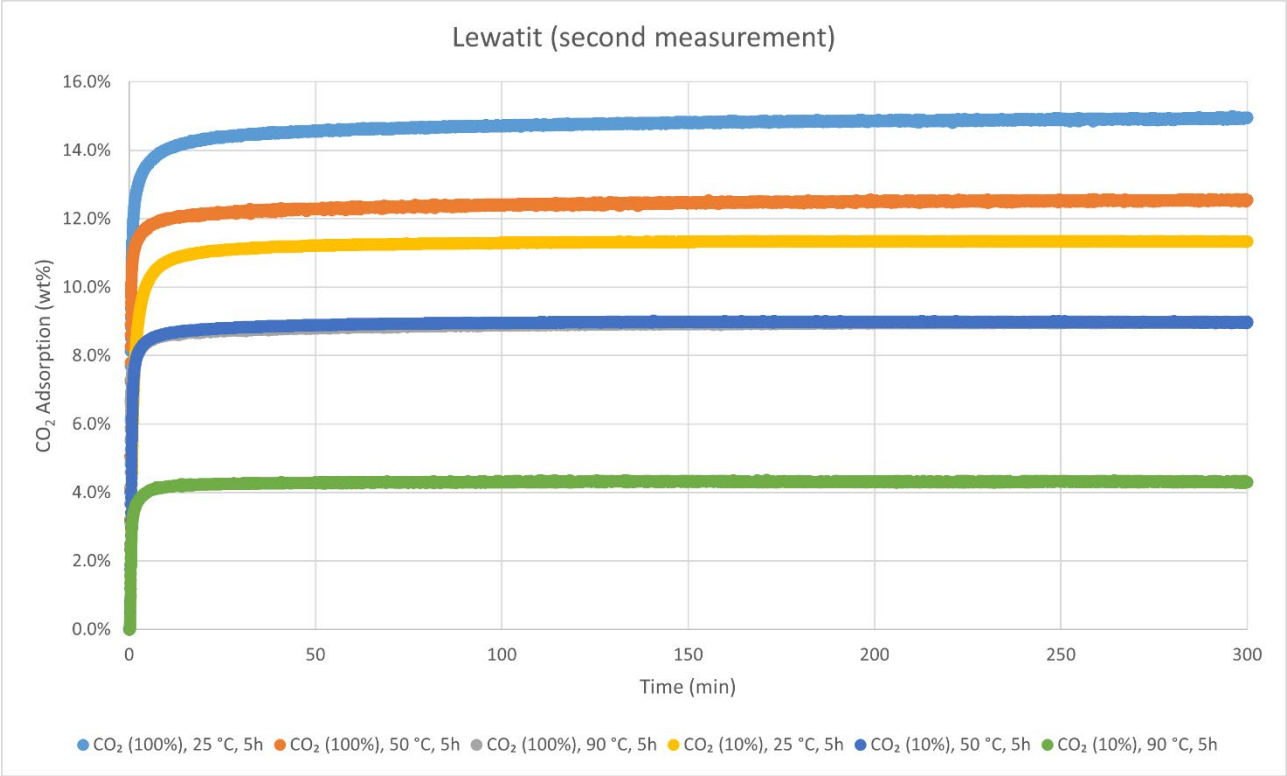

CO_2 adsorption using **TGA method 2** (second measurement).

Lewatit (second measurement)	wt%	mmol/g
CO_2 (100%), 25 °C, 5h	15%	3.40
CO_2 (100%), 50 °C, 5h	13%	2.85
CO_2 (100%), 90 °C, 5h	9.0%	2.04
CO_2 (10%), 25 °C, 5h	11%	2.58
CO_2 (10%), 50 °C, 5h	9.0%	2.04
CO_2 (10%), 90 °C, 5h	4.3%	0.98

Retention of CO_2-capacity after He, 150 °C, 10 h (TGA method 5):

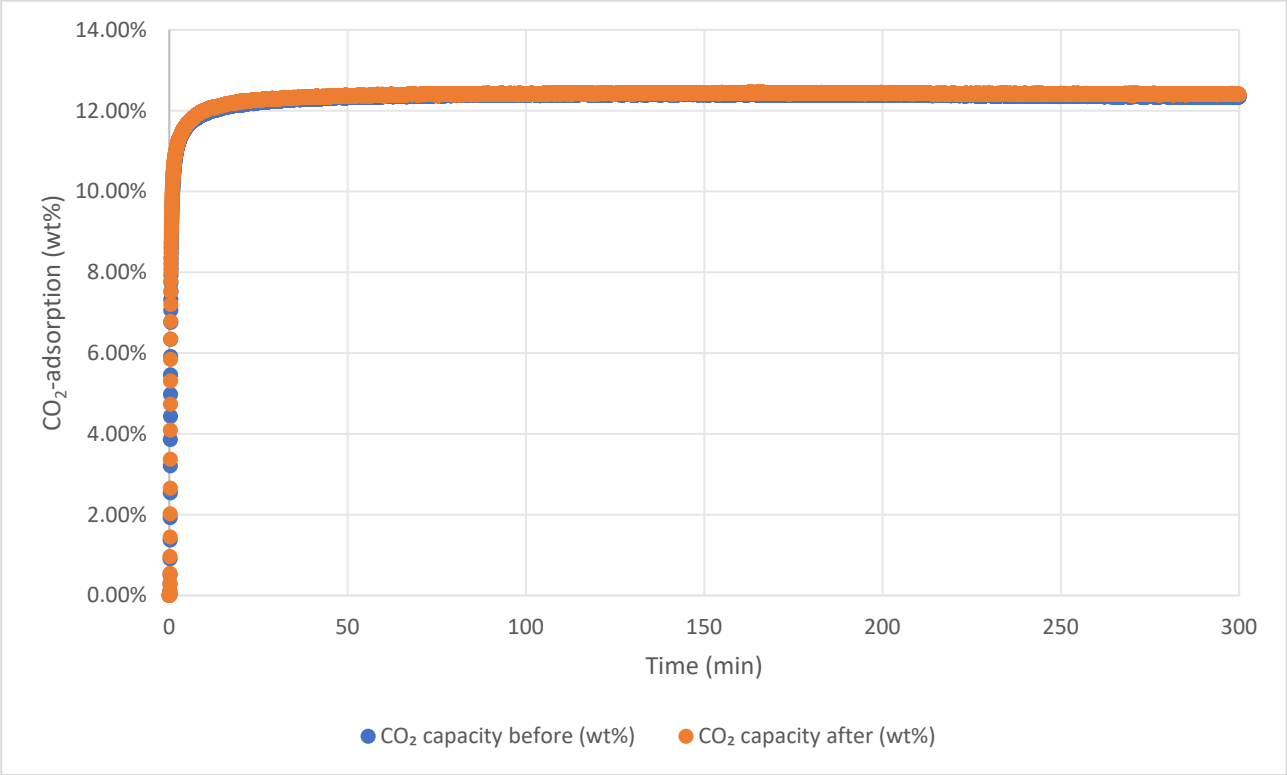

CO_2-capacity before = 12.3 wt%. CO_2-capacity after = 12.4 wt%. The capacity retention after He, 150 °C, 10 h is thus 100%. The +0.1 wt% difference could be due to uncertainty.

Retention of CO_2-capacity after air, 150 °C, 10 h (TGA method 6):

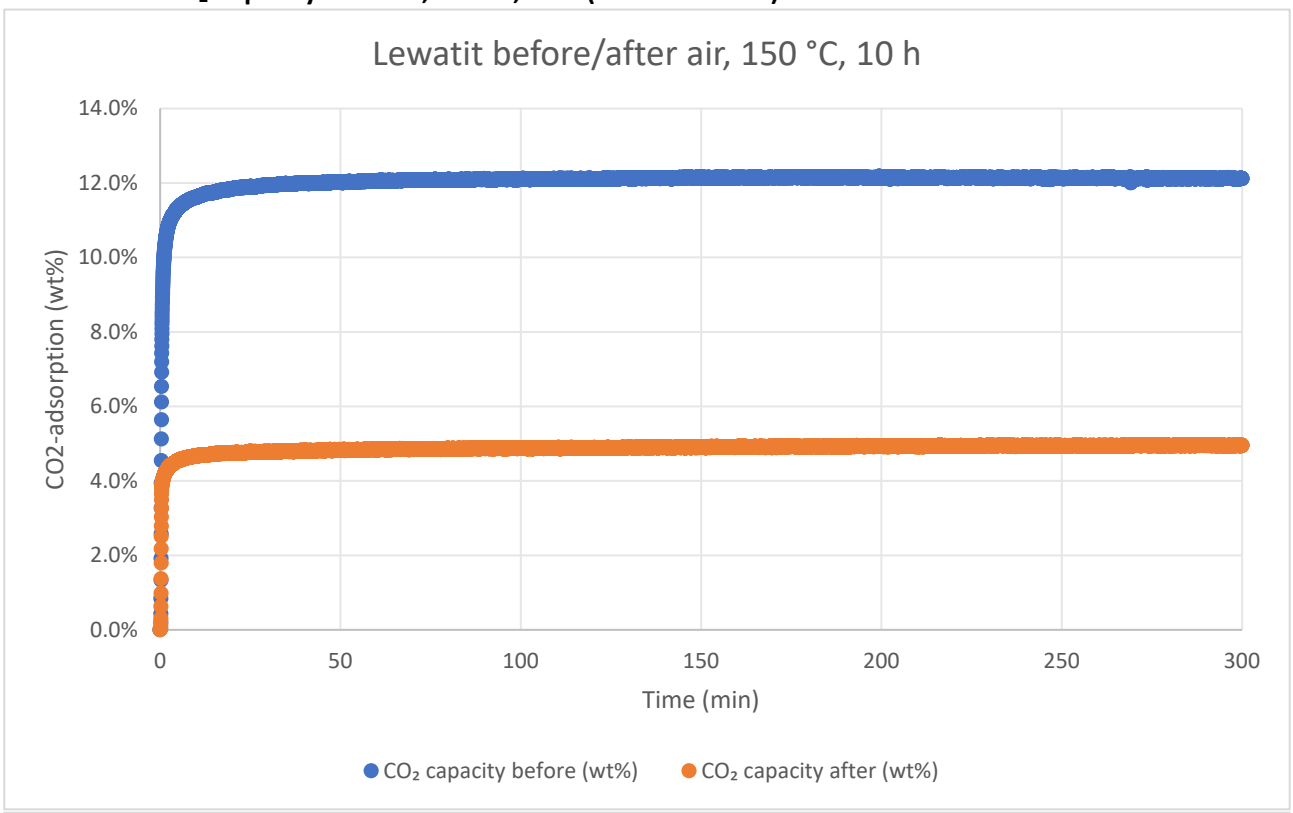

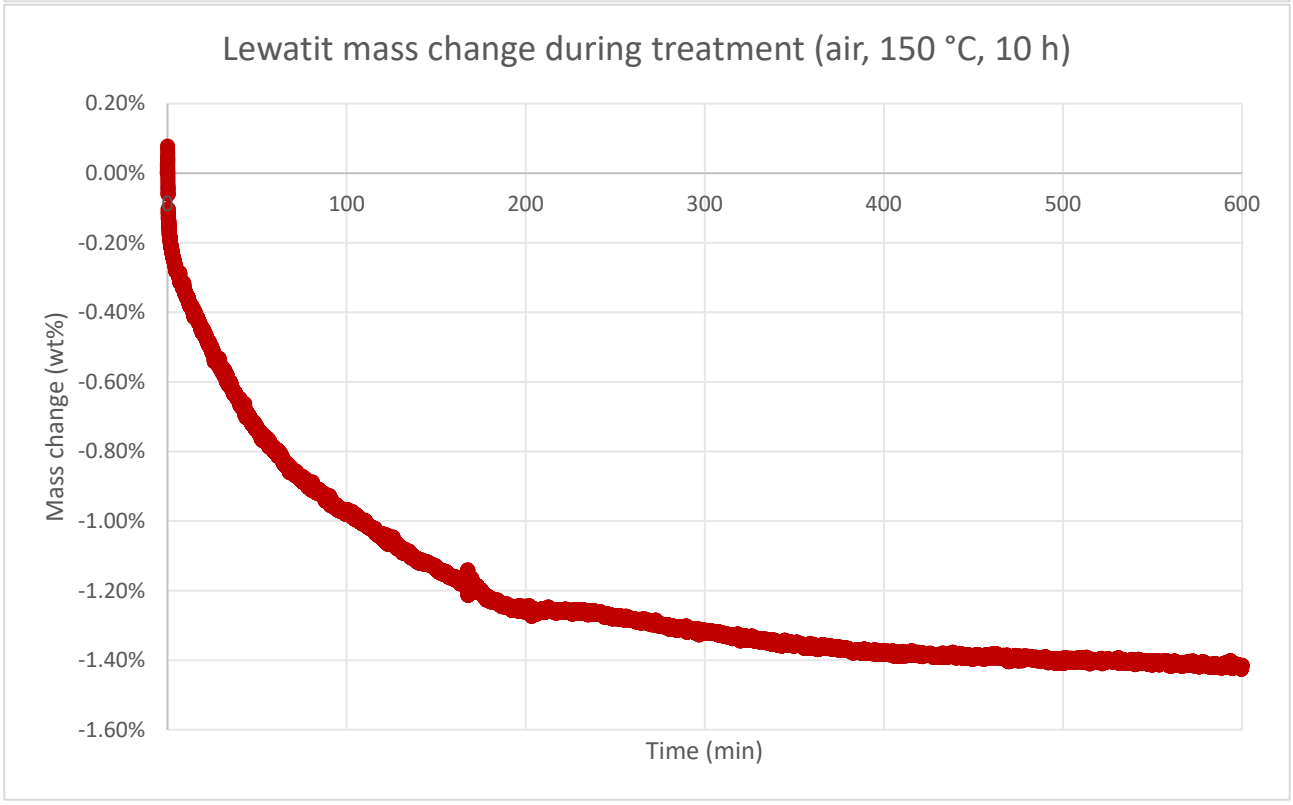

CO_2-capacity before = 12.1 wt%. CO_2-capacity after = 5.0 wt%. The capacity retention after air, 150 °C, 10 h is thus 41%. A decrease in mass of 1.4 wt% is seen during the segment with hot air, indicating oxidative degradation, which has been earlier reported for Lewatit.[22]

Retention of CO_2-capacity after CO_2, 150 °C, 10 h (TGA method 7):

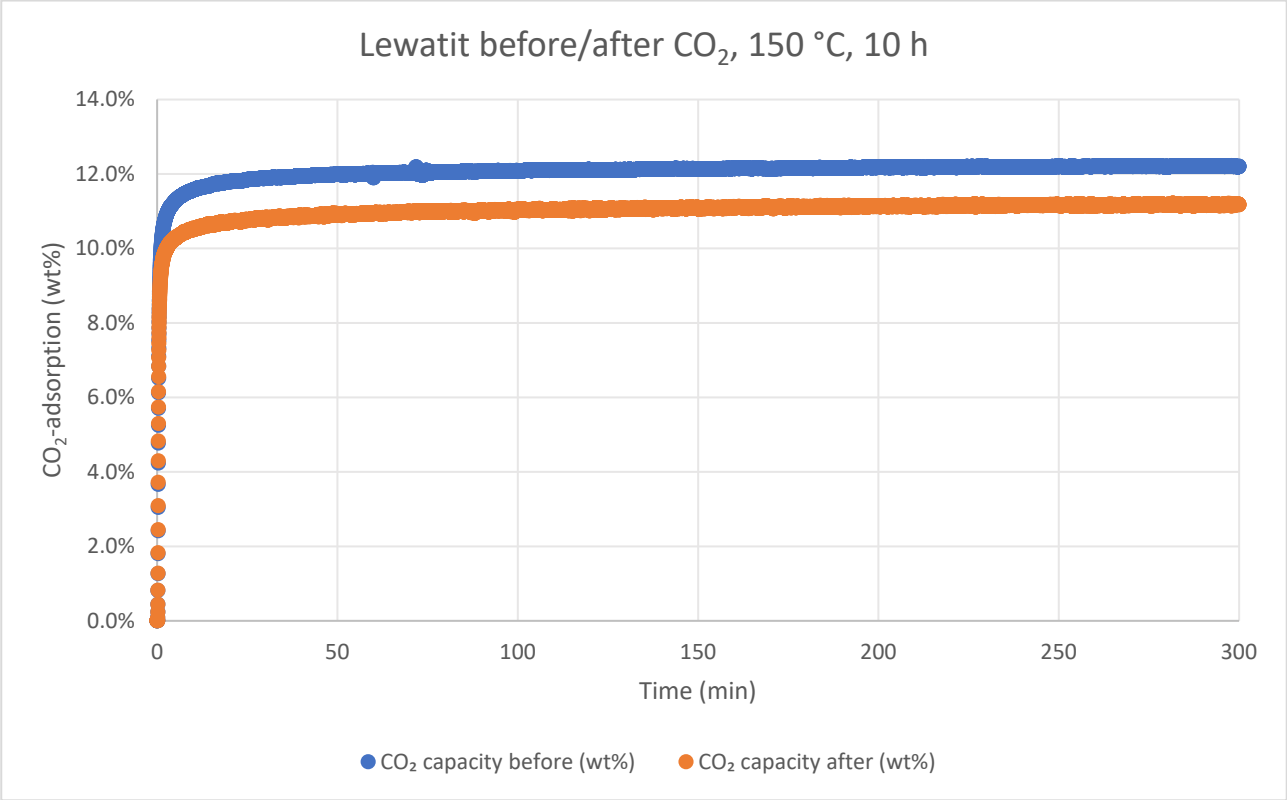

CO_2-capacity before = 12.2 wt%. CO_2-capacity after = 11.2 wt%. The capacity retention after CO_2 (100%), 150 °C, 10 h is thus 92%.

Retention of CO_2-capacity after boiling in H_2O for 7 days (TGA method 3):

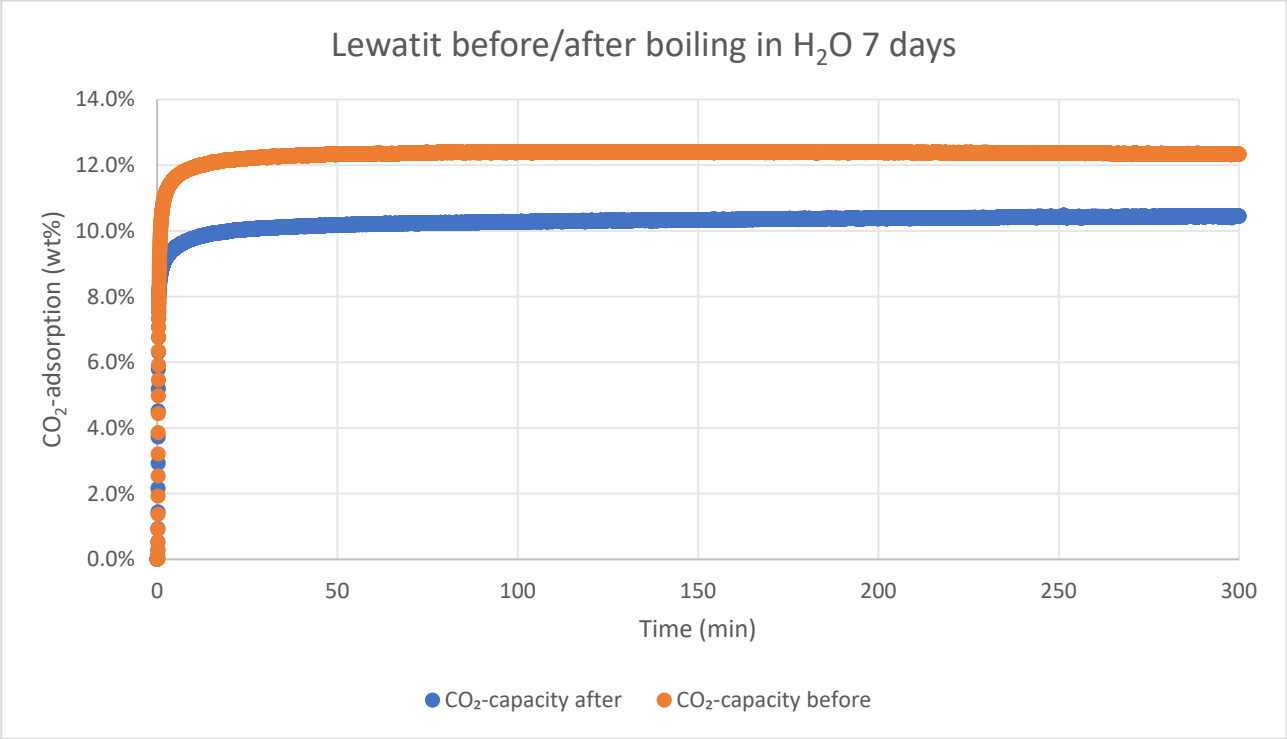

CO_2-capacity before = 12.3 wt%. CO_2-capacity after = 10.5 wt%. The capacity retention boiling in H_2O for 7 days is thus 85%. The adsorption curve before boiling in water is derived from the hot helium stress test.

Retention of CO_2-capacity after NO_2, 25 °C, 10 h (TGA method 8):

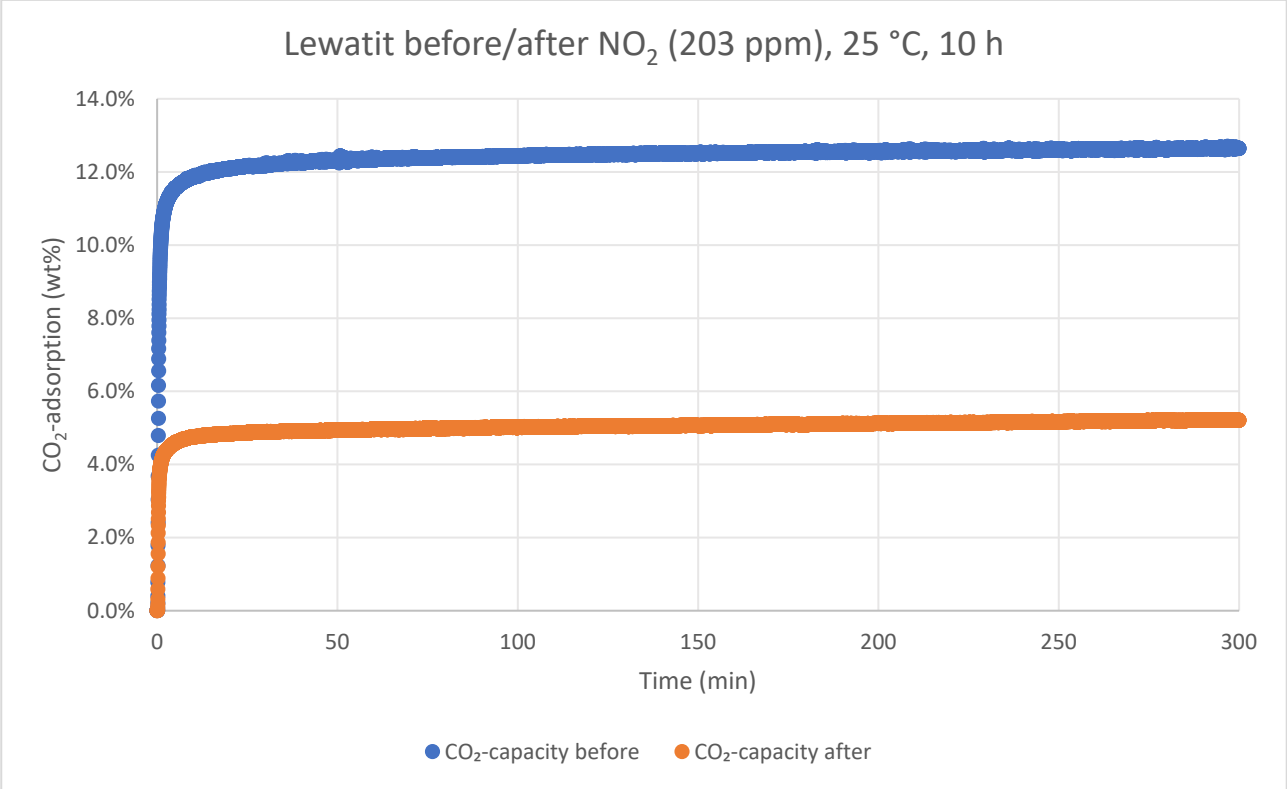

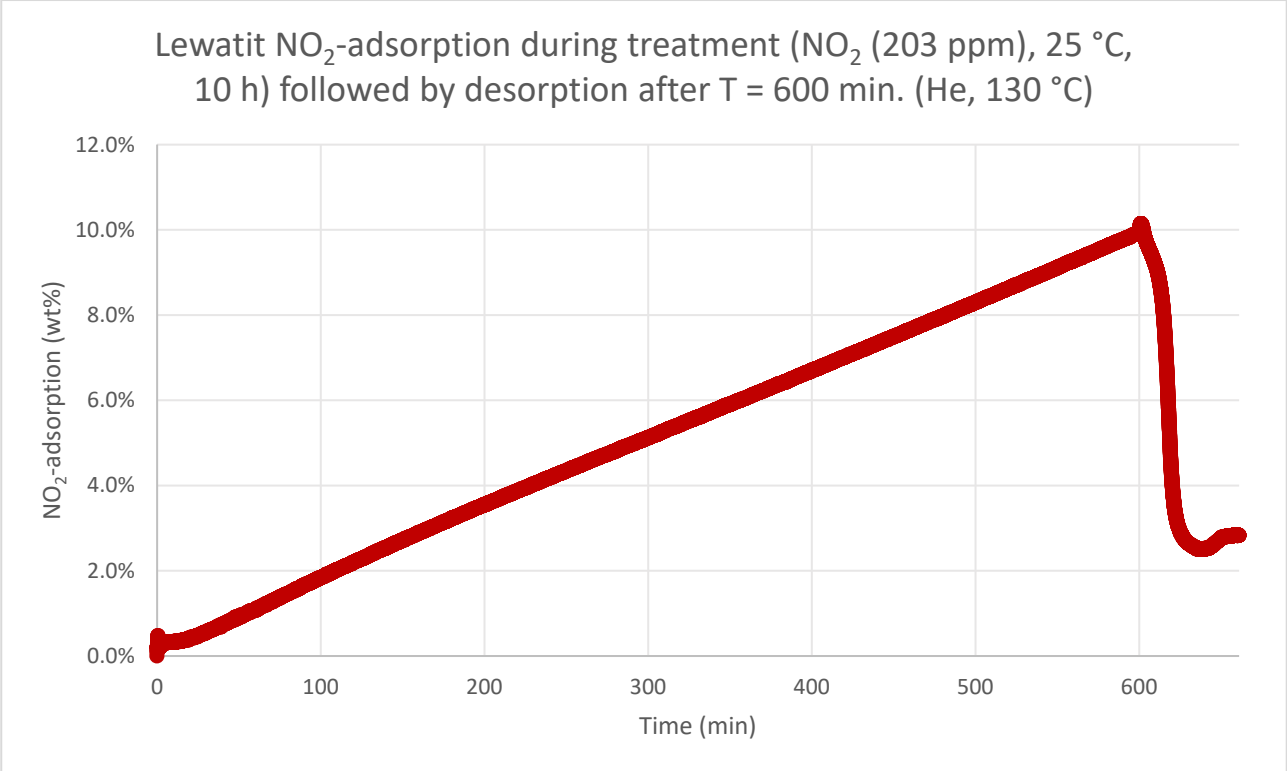

CO_2-capacity before = 12.6 wt%. CO_2-capacity after = 5.2 wt%. The capacity retention after NO_2 (203 ppm), 25 °C, 10 h is thus 41%. An NO_2-adsorption capacity of 9.9 wt% was observed during the 10 h NO_2-segment, while 2.8 wt% was retained after desorption in helium at 130 °C (after T = 600 min.)

Retention of CO_2-capacity after SO_2 (206 ppm in N_2), 25 °C, 10 h (TGA method 9):

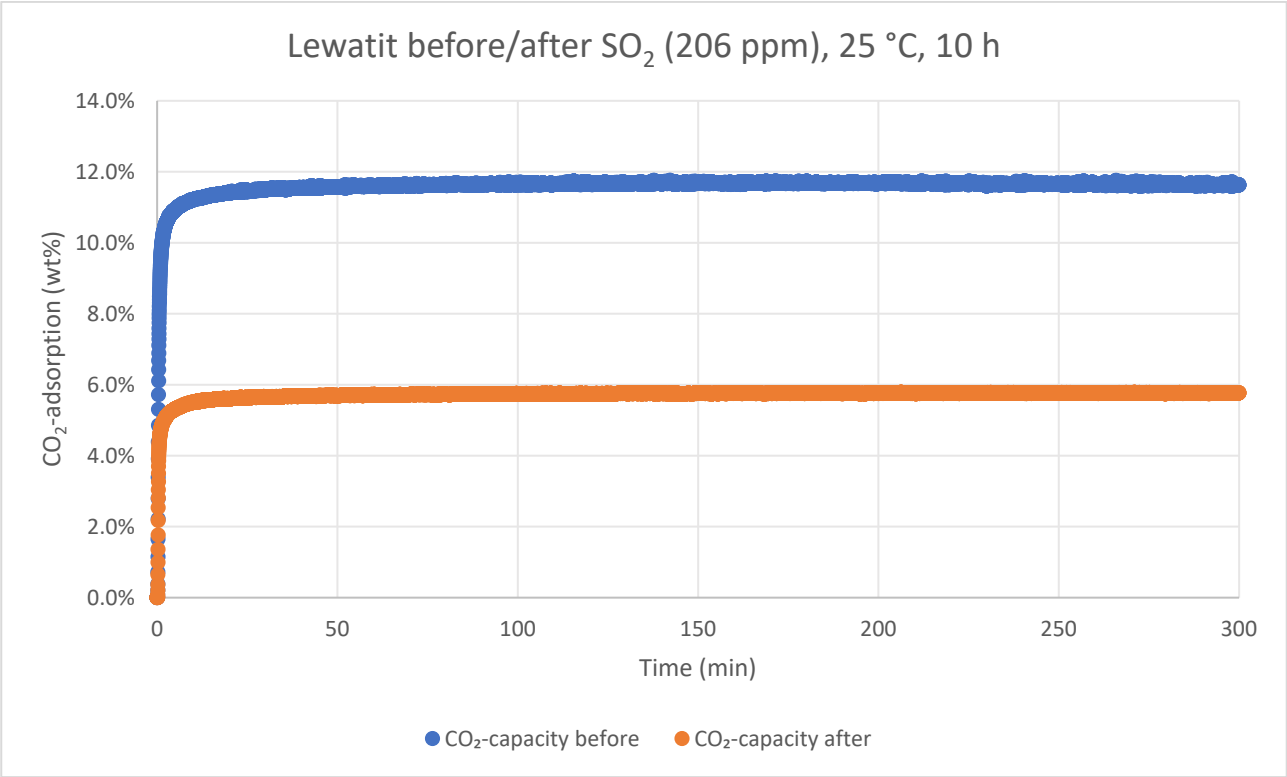

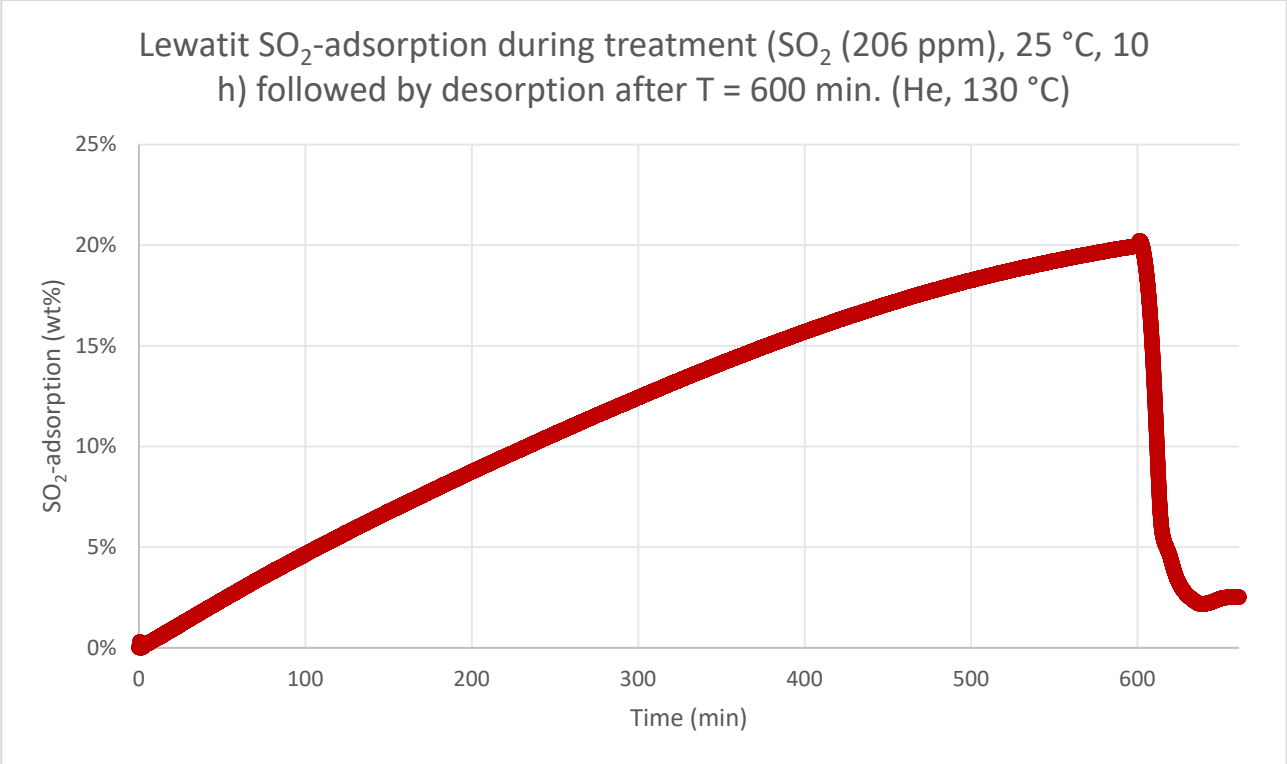

CO_2-capacity before = 11.6 wt%. CO_2-capacity after = 5.8 wt%. The capacity retention after SO_2 (206 ppm), 25 °C, 10 h is thus 50%. An SO_2-adsorption capacity of 20 wt% was observed during the 10 h SO_2-segment, while 2.5 wt% was retained after desorption in helium at 130 °C (after T = 600 min.)

Elemental Analysis

	N [%]	C [%]	H [%]	S [%]	mmol N/g	C/N ratio	C/H ratio
Lewatit VP OC 1065	**2.50**	**7.98**	**74.34**	**Not detected**	**5.70**	**10.86**	**0.80**

References

[1] K. Kristensen, S., Z. Eikeland, E., Taarning, E., T. Lindhardt, A. & Skrydstrup, T. Ex situ generation of stoichiometric HCN and its application in the Pd-catalysed cyanation of aryl bromides: evidence for a transmetallation step between two oxidative addition Pd-complexes. *Chem. Sci.* **8**, 8094–8105 (2017).

[2] Al Musaimi, O., Basso, A., de la Torre, B. G. & Albericio, F. Calculating Resin Functionalization in Solid-Phase Peptide Synthesis Using a Standardized Method based on Fmoc Determination. *ACS Comb. Sci.* **21**, 717–721 (2019).

[3] Akaji, K., Teruya, K., Akaji, M. & Aimoto, S. Synthesis of cyclic RGD derivatives via solid phase macrocyclization using the Heck reaction. *Tetrahedron* **57**, 2293–2303 (2001).

[4] Matsuyama, H., Zhang, X., Terada, M. & Jin, T. Construction of Alkylidene Fluorene Scaffolds Using Pd-Catalyzed Direct Arene/Alkene Coupling Strategy. *Org. Lett.* **25**, 800–804 (2023).

[5] AAPPTEC. Monitoring of Peptide Coupling and Capping; Kaiser Test Solutions. https://www.peptide.com/resources/solid-phase-peptide-synthesis/monitoring-of-peptide-coupling-and-capping/ (2019).

[6] Neumann, J., Bornschein, C., Jiao, H., Junge, K. & Beller, M. Hydrogenation of Aliphatic and Aromatic Nitriles Using a Defined Ruthenium PNP Pincer Catalyst. *Eur. J. Org. Chem.* **2015**, 5944–5948 (2015).

[7] Ni, J., Xia, X., Gu, D. & Wang, Z. Ti-Catalyzed Modular Ketone Synthesis from Carboxylic Derivatives and gem-Dihaloalkanes. *J. Am. Chem. Soc.* **145**, 14884–14893 (2023).

[8] Cabrero-Antonino, J. R., Alberico, E., Drexler, H.-J., Baumann, W., Junge, K., Junge, H., Beller, M. Half-Sandwich Ruthenium Catalyst Bearing an Enantiopure Primary Amine Tethered to an N-Heterocyclic Carbene for Ketone Hydrogenation. *ACS Catal.* **6**, 47−54 (2016).

[9] Yu, R., Rajasekar, S. & Fang, X. Enantioselective Nickel-Catalyzed Migratory Hydrocyanation of Nonconjugated Dienes. *Angew. Chem. Int. Ed.* **59**, 21436–21441 (2020).

[10] Gao, J. *et al.* Nickel-Catalyzed Migratory Hydrocyanation of Internal Alkenes: Unexpected Diastereomeric-Ligand-Controlled Regiodivergence. *Angew. Chem. Int. Ed.* **60**, 1883–1890 (2021).

[11] Gao, J., Ni, J., Yu, R., Cheng, G.-J. & Fang, X. Ni-Catalyzed Isomerization–Hydrocyanation Tandem Reactions: Access to Linear Nitriles from Aliphatic Internal Olefins. *Org. Lett.* **23**, 486–490 (2021).

[12] Mori, M. *et al.* Discovery of 14-3-3 Protein–Protein Interaction Inhibitors that Sensitize Multidrug-Resistant Cancer Cells to Doxorubicin and the Akt Inhibitor GSK690693. *ChemMedChem* **9**, 973–983 (2014).

[13] Redies, K. M., Fallon, T., Oestreich, M. En Route to Stable All-Carbon-Substituted Silylenes: Synthesis and Reactivity of a Bis(α-spirocyclopropyl)silylene. *Organometallics*, **33**, 3235−3238 (2014).

[14] McGouran, J. F. *et al.* Fluorescence-based active site probes for profiling deubiquitinating enzymes. *Org. Biomol. Chem.* **10**, 3379–3383 (2012).

[15] Noji, T., Fujiwara, H., Okano, K. & Tokuyama, H. Synthesis of Substituted Indoline and Carbazole by Benzyne-Mediated Cyclization–Functionalization. *Org. Lett.* **15**, 1946–1949 (2013).

[16] Pinto, M. L., Mafra, L., Guil, J. M., Pires, J., Rocha, J. Adsorption and Activation of CO_2 by Amine-Modified Nanoporous Materials Studied by Solid-State NMR and $^{13}CO_2$ Adsorption. *Chem. Mater.* **23**, 1387−1395 (2011).

[17] Pereira, D., Fonseca, R., Marin-Montesinos, I., Sardo, M., Mafra, L. Understanding CO_2 adsorption mechanisms in porous adsorbents: A solid-state NMR survey. *Curr. Opin. Colloid Interface Sci.* **64**, 101690 (2023).

[18] Ntiamoah, A., Ling, J., Xiao, P., Webley, P. A., Zhai, Y. CO_2 Capture by Temperature Swing Adsorption: Use of Hot CO_2-Rich Gas for Regeneration. *Ind. Eng. Chem. Res.* **55**, 703−713 (2016).

[19] Heydari-Gorji, A. & Sayari, A. Thermal, Oxidative, and CO_2-Induced Degradation of Supported Polyethyleneimine Adsorbents. *Ind. Eng. Chem. Res.* **51**, 6887−6894 (2012).

[20] Sayari, A., Heydari-Gorji, A. & Yang, Y. CO_2-induced Degradation of Amine-Containing Adsorbents: Reaction Products and Pathways. *J. Am. Chem. Soc.* **134**, 13834−13842 (2012).

[21] Kar, S., Goeppert, A., Prakash, G. K. S. Combined CO_2 Capture and Hydrogenation to Methanol: Amine Immobilization Enables Easy Recycling of Active Elements. *ChemSusChem*, **12**, 3172-3177 (2019).

[22] Leenders, S. H. A. M., Pankratova, G., Wijenberg, J., Romanuka, J., Gharavi, F., Tsou, J., Infantino, M., van Haandel, L., van Paasen, S., Just, P.-E. Amine Adsorbents Stability for Post-Combustion CO_2 Capture: Determination and Validation of Laboratory Degradation Rates in a Multi-staged Fluidized Bed Pilot Plant. *ChemSusChem*, **16**, e202300930 (2023).

NMR Spectra

(small molecules)

***O*-Tosyl-*N*-Boc-ethanolamine** (^{1}H−NMR and ^{13}C−NMR)

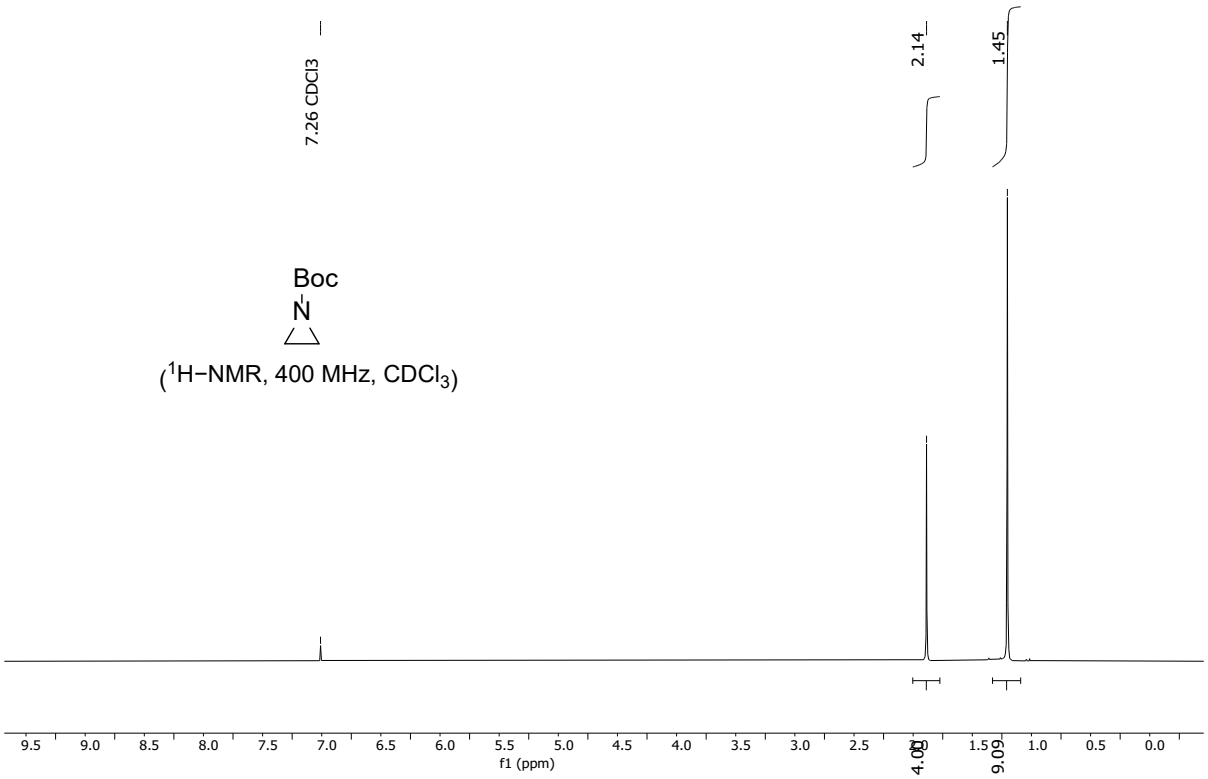

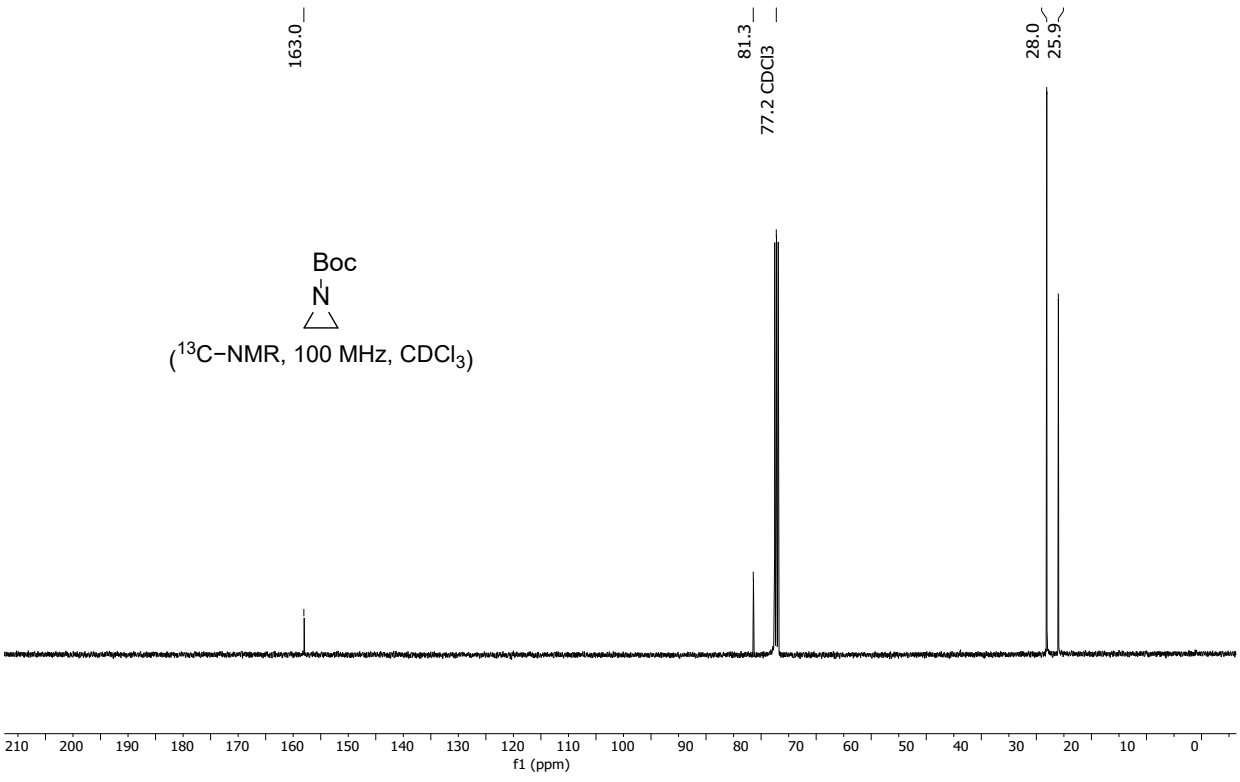

1-((9*H*-fluoren-9-yl)methyl)piperidine (1) and **9-methylene-9*H*-fluorene (2)** mixture after Fmoc-quantification procedure (**Table S1**), entry 30) (^{1}H−NMR and ^{13}C−NMR)

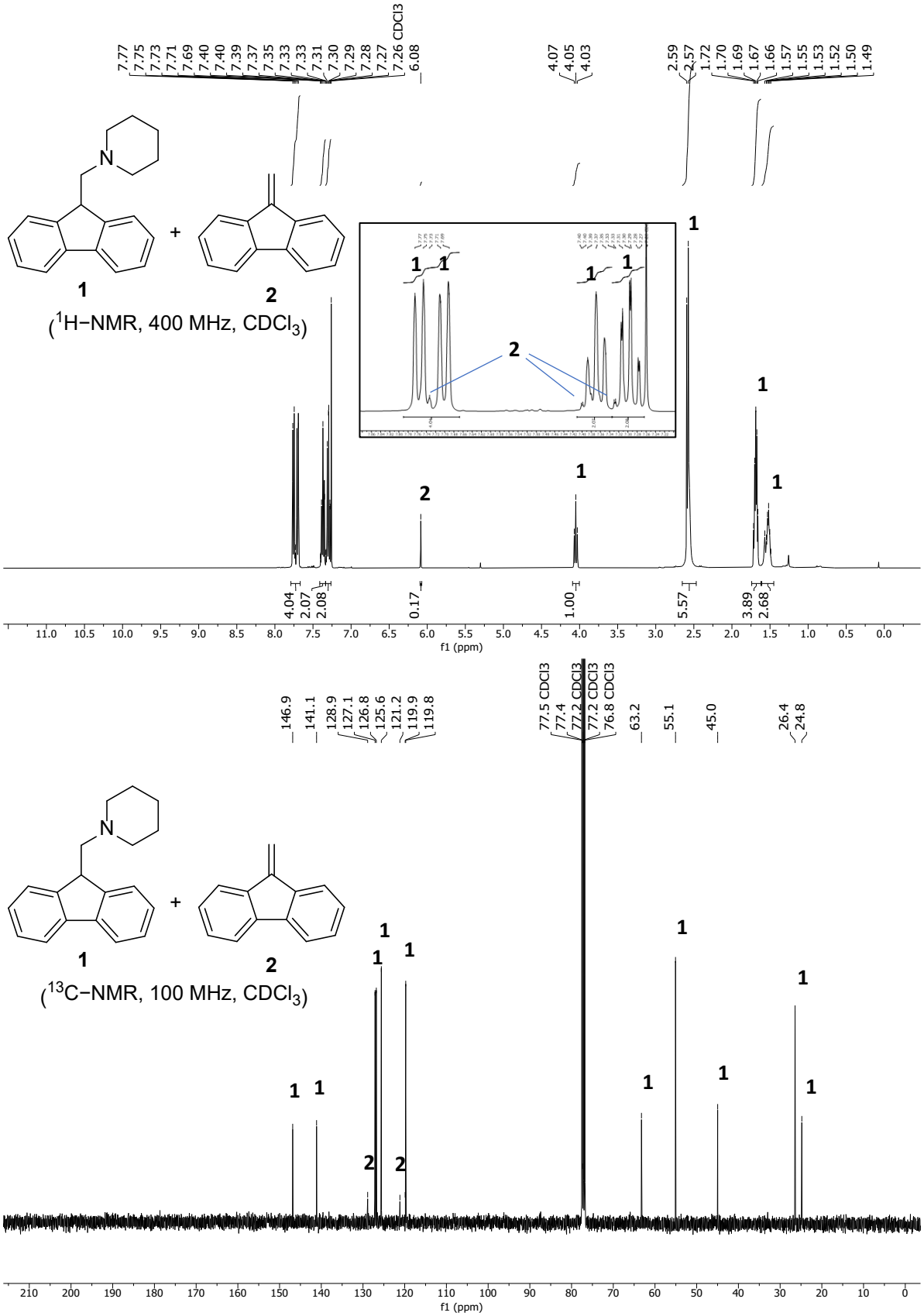

1,6-diphenylhex-3-ene (3) (^{1}H−NMR and ^{13}C−NMR)

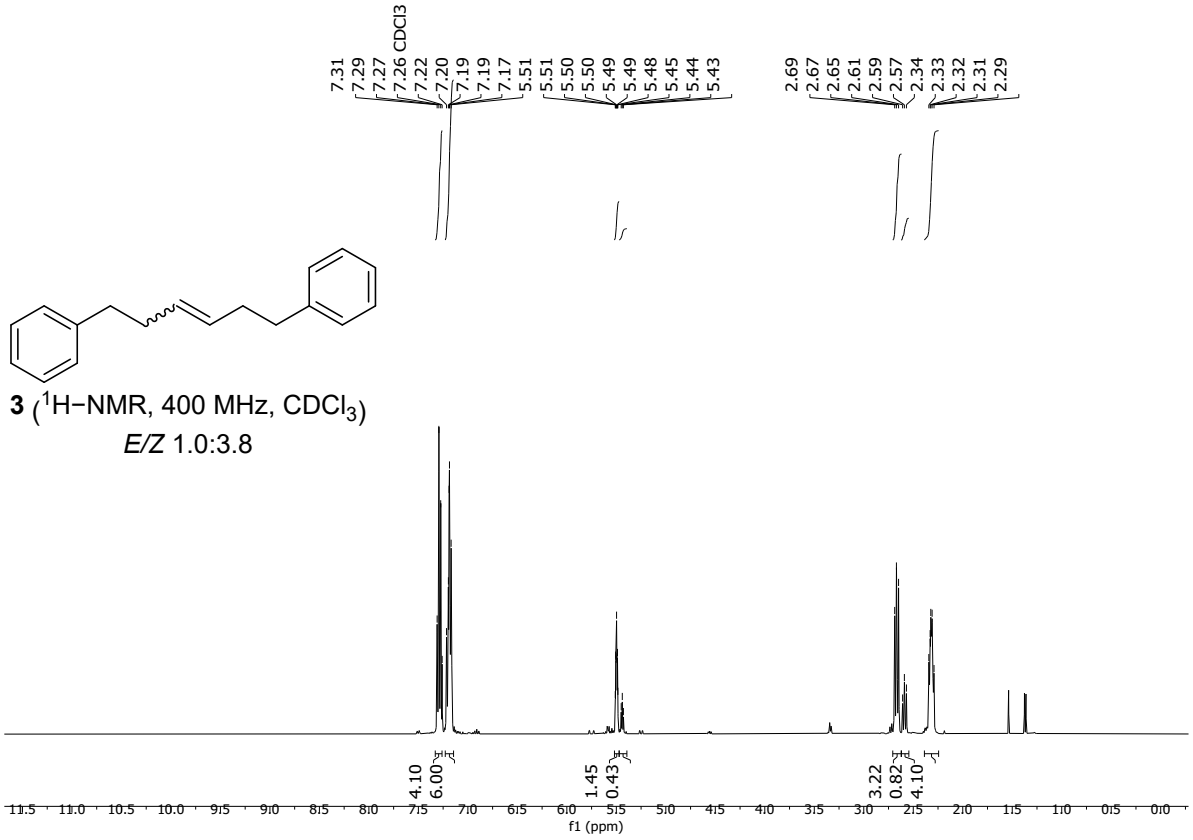

3 (^{1}H−NMR, 400 MHz, $CDCl_3$)
E/Z 1.0:3.8

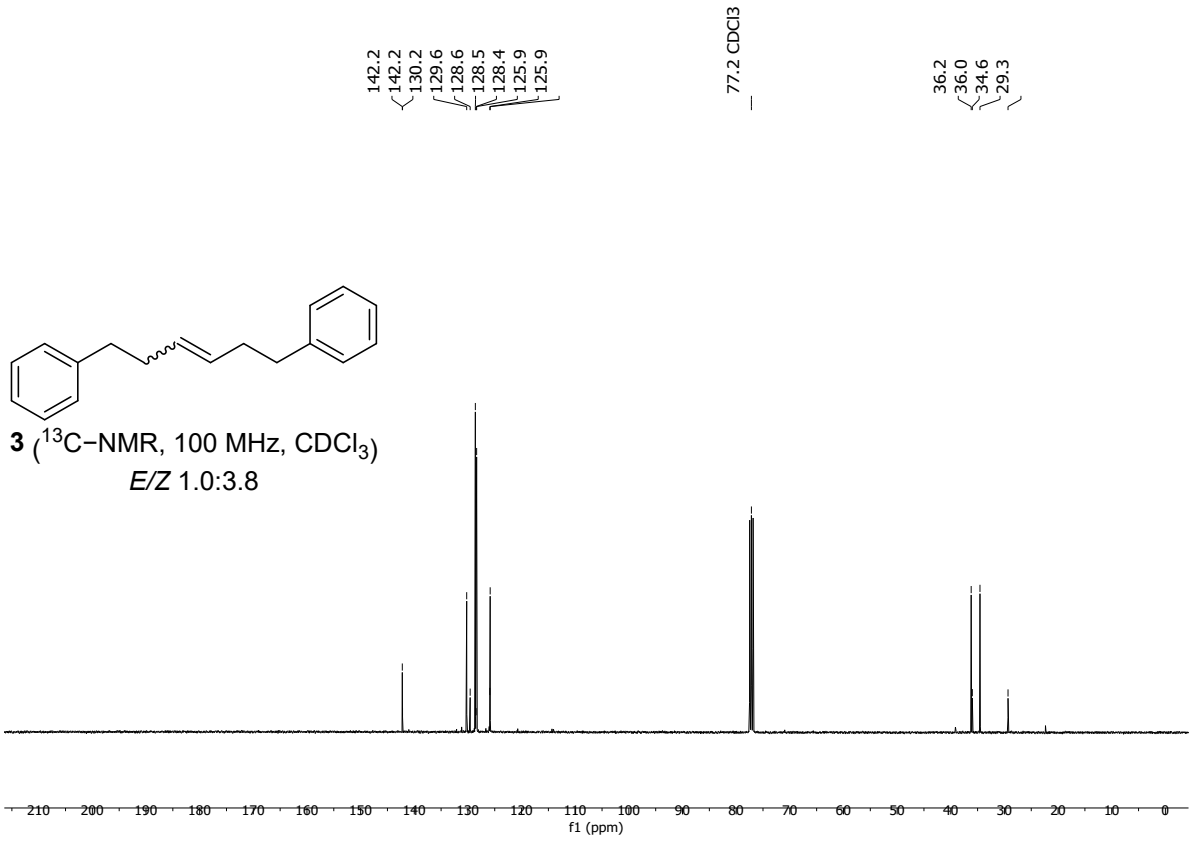

3 (^{13}C−NMR, 100 MHz, $CDCl_3$)
E/Z 1.0:3.8

2,7-diphenylheptanenitrile (4) (^{1}H−NMR and ^{13}C−NMR)

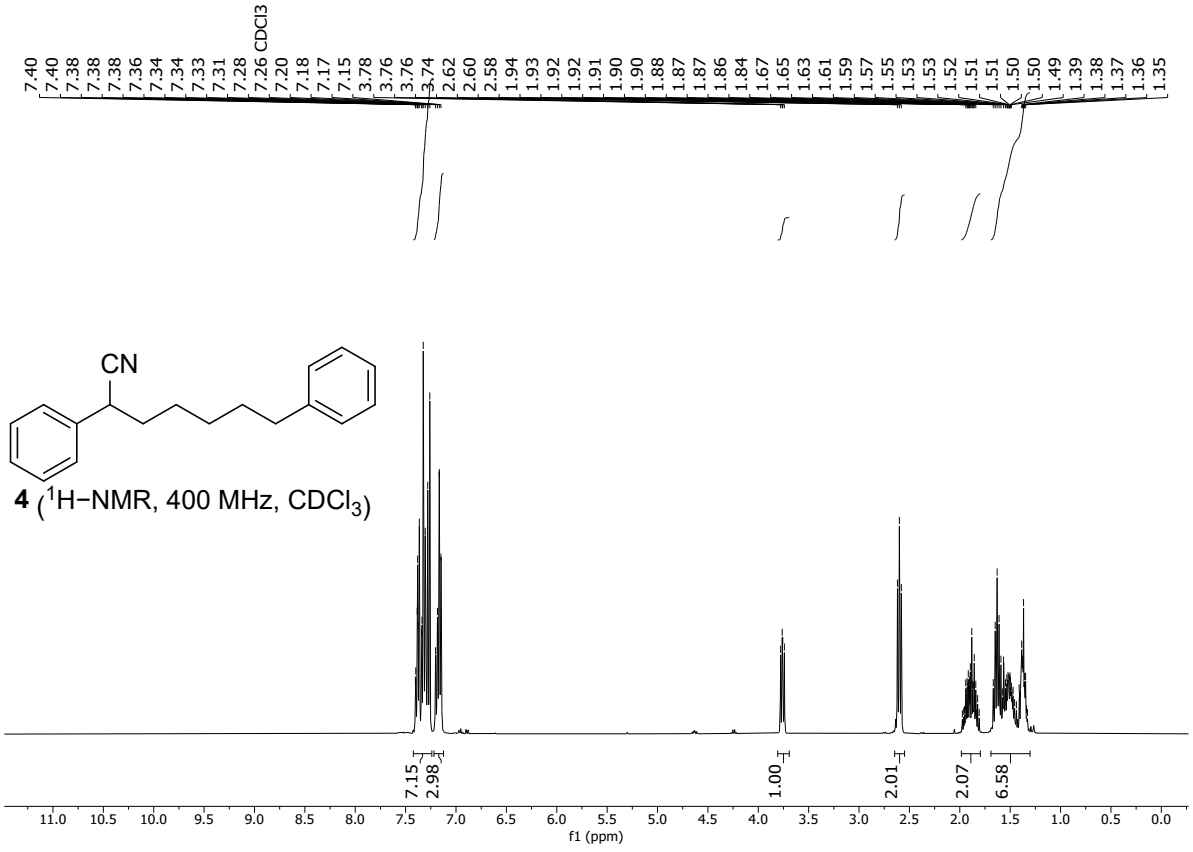

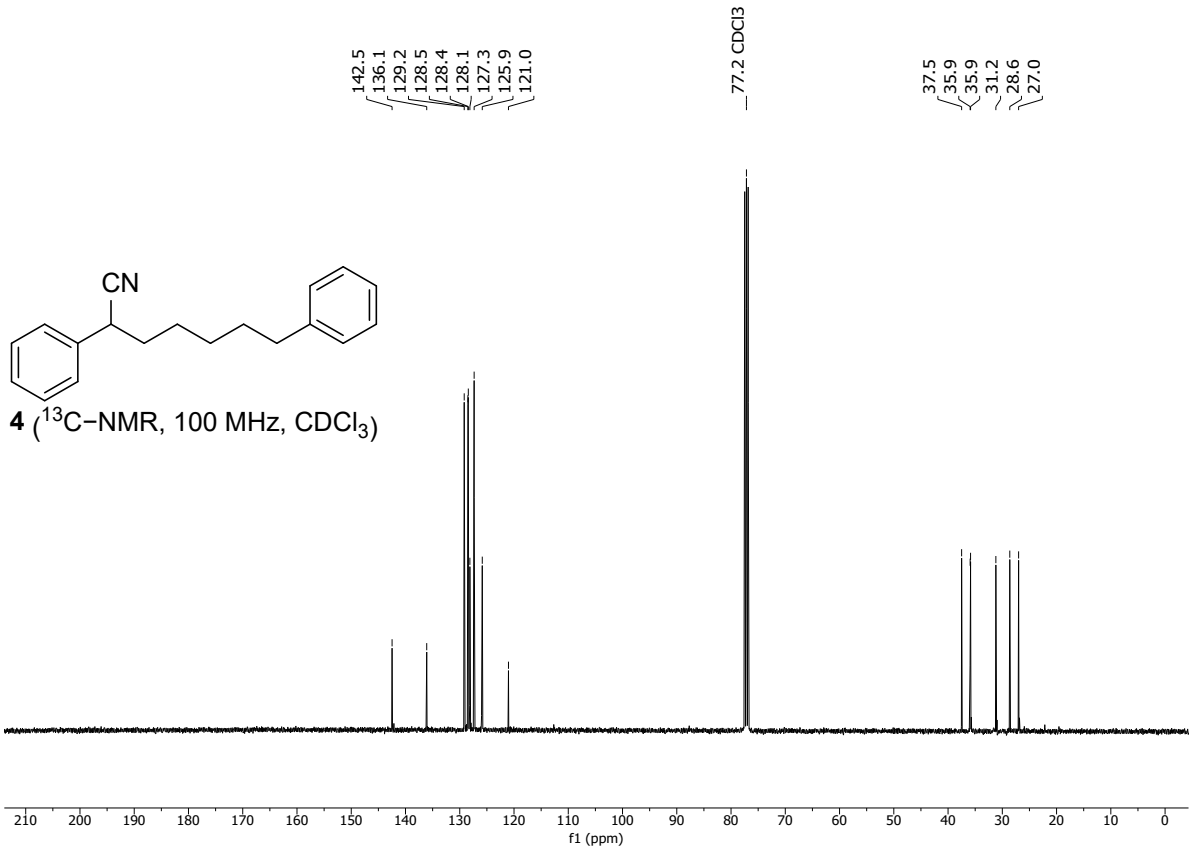

1,4-bis(bromotriphenyl-λ^5-phosphaneyl)butane (5) (^{1}H−NMR, ^{13}C−NMR, and ^{31}P-NMR)

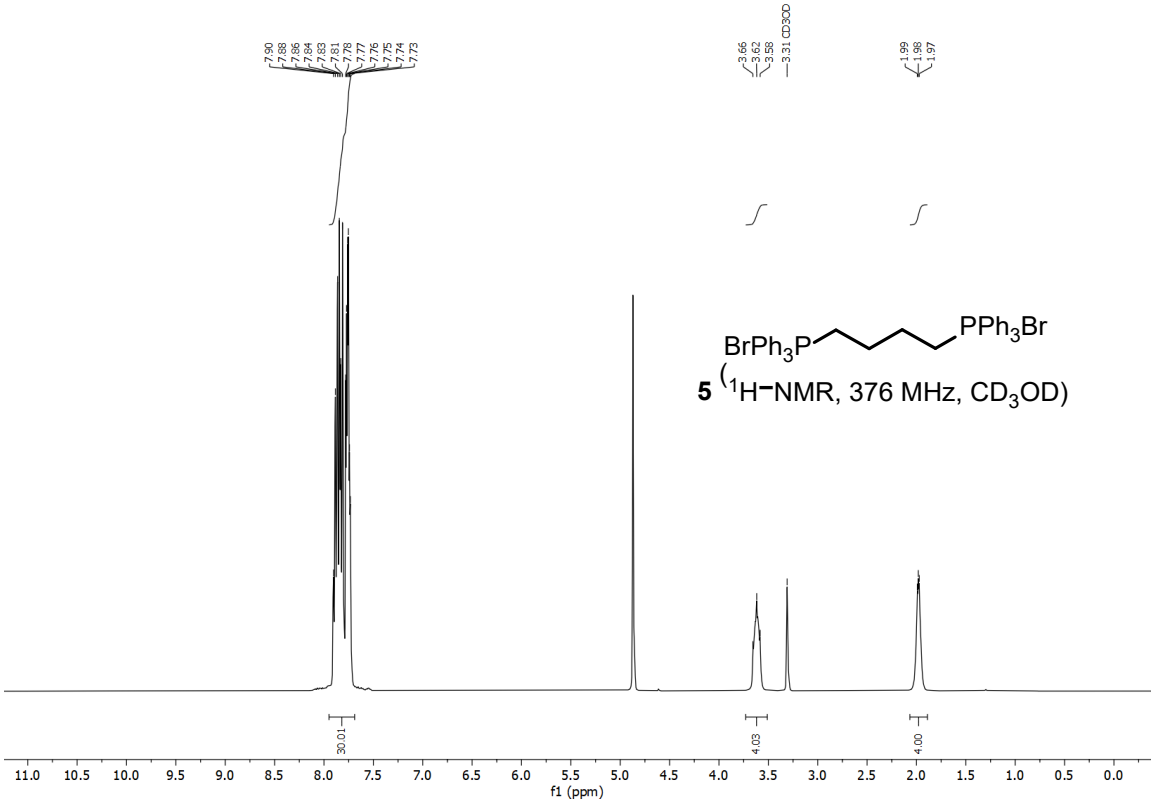

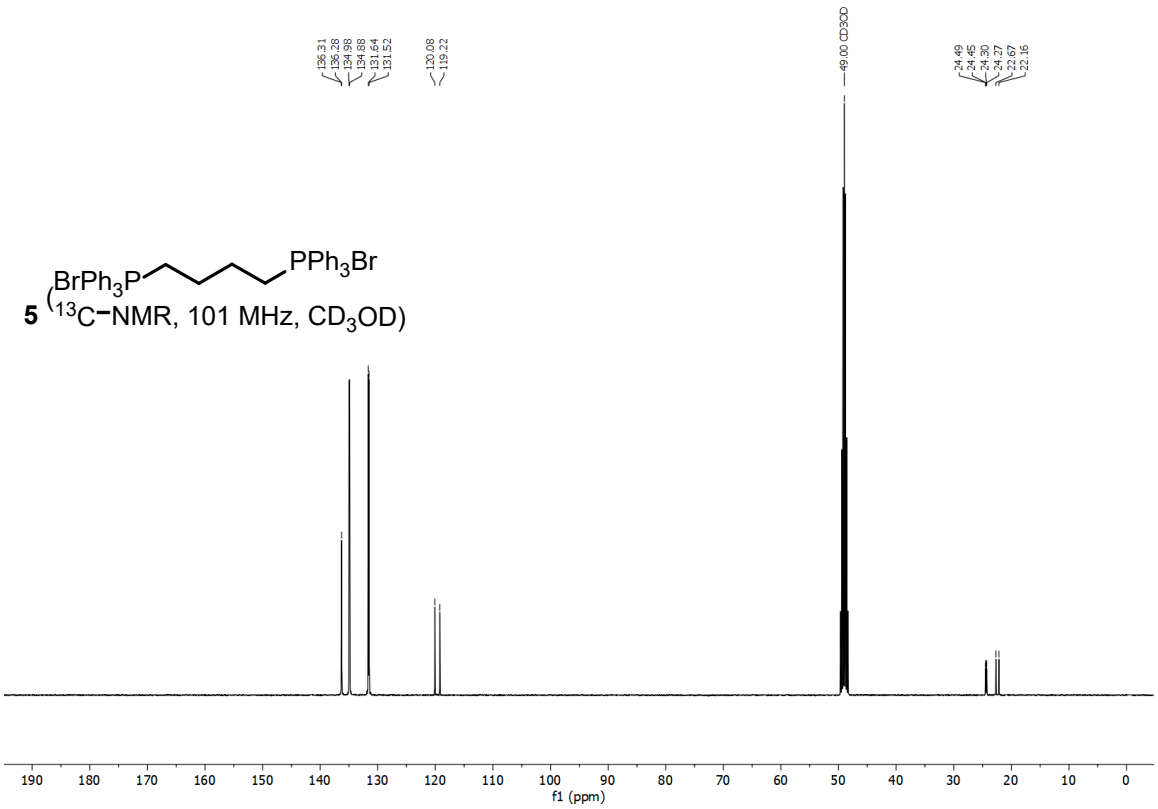

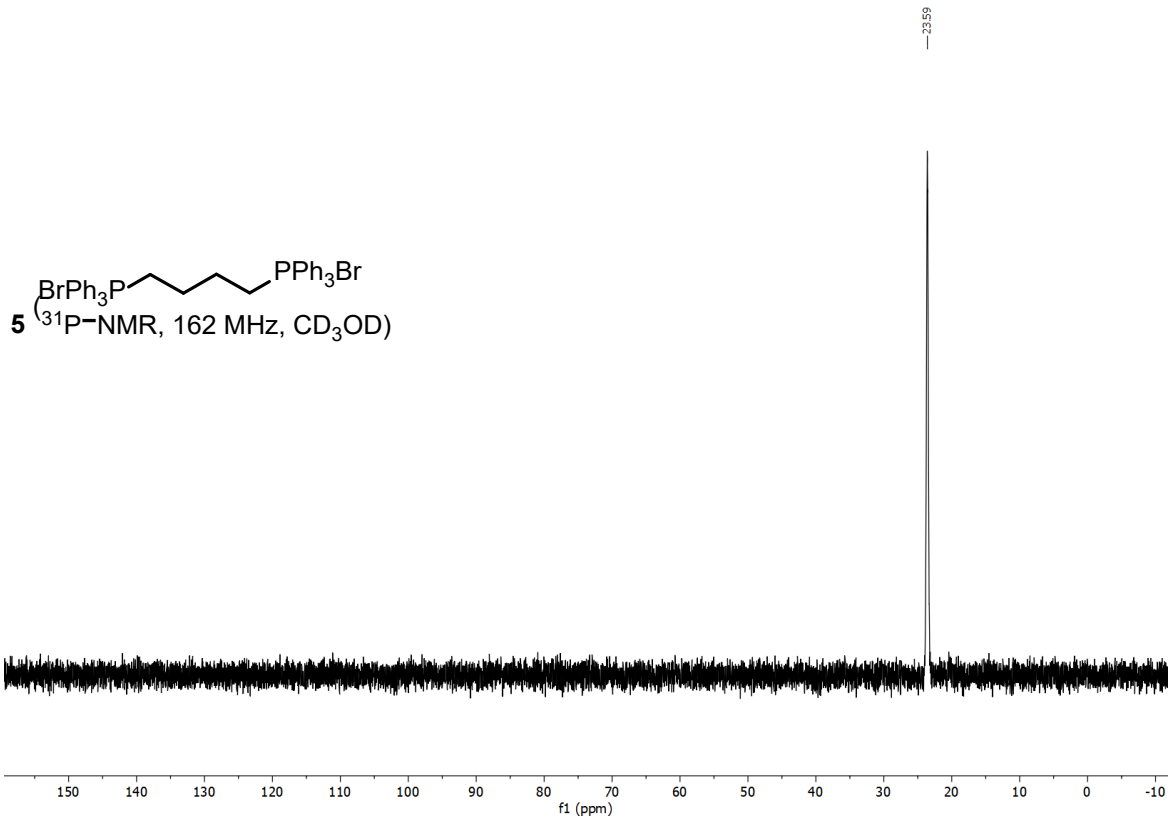

5 (^{31}P−NMR, 162 MHz, CD_3OD)

((4Z,8Z)-dodeca-4,8-diene-2,11-diyl)dibenzene (6) (^{1}H−NMR and ^{13}C−NMR)

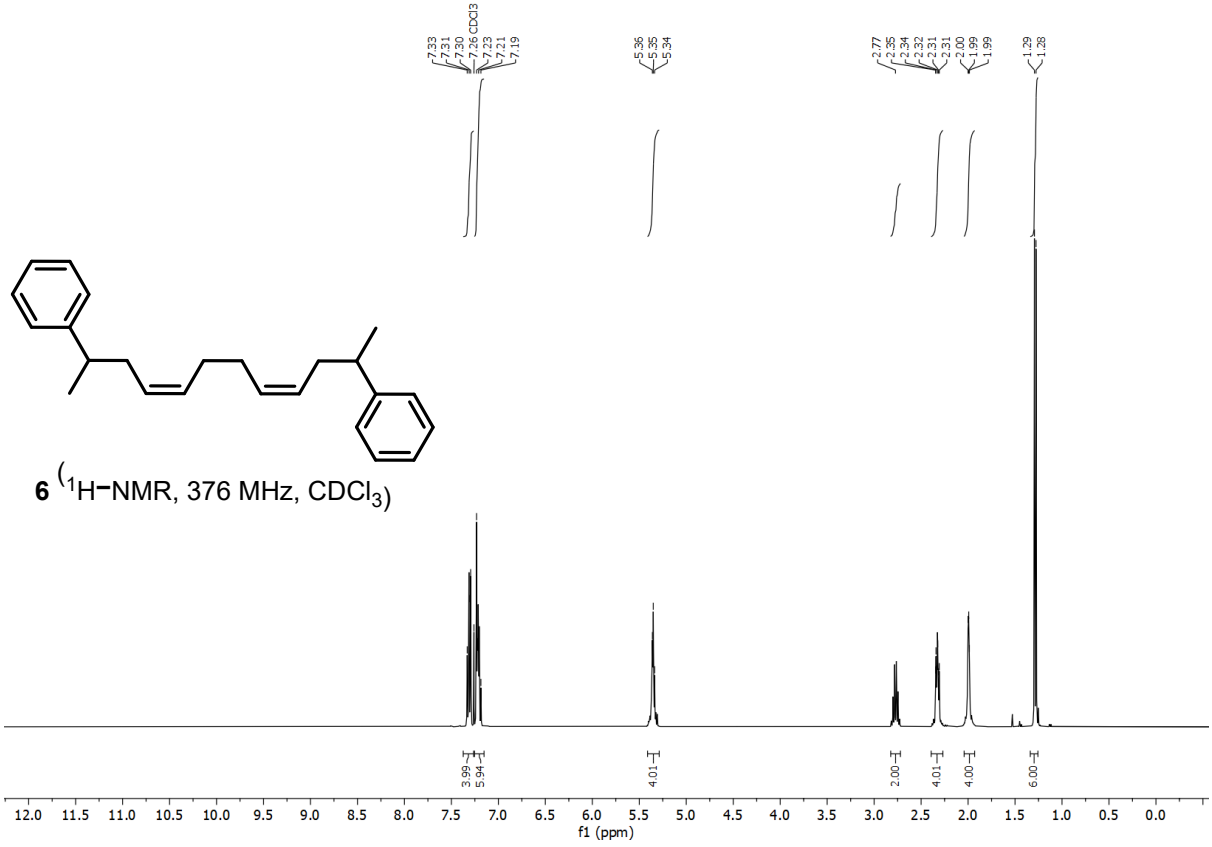

6 (^{1}H−NMR, 376 MHz, $CDCl_3$)

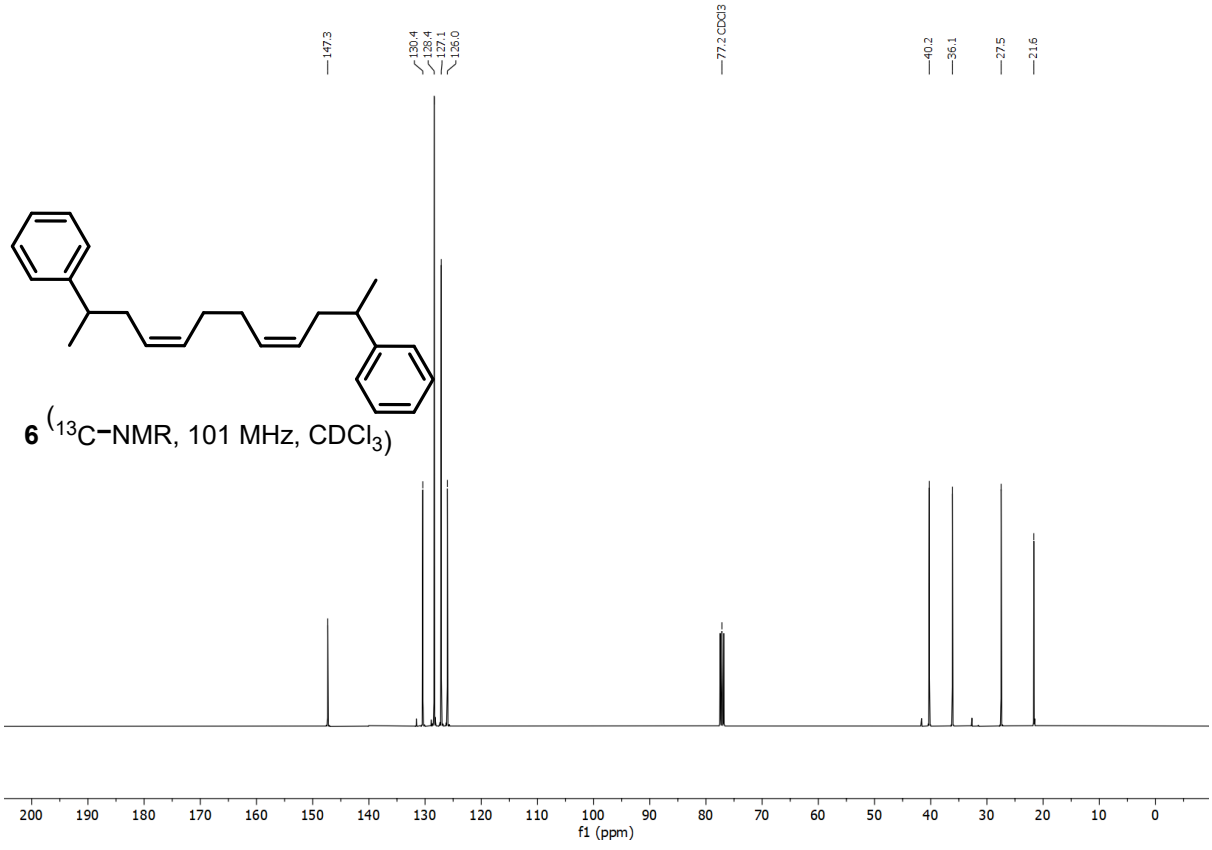

6 (^{13}C−NMR, 101 MHz, $CDCl_3$)